✓MARCH 1971

ANCHAM

ANALYTICAL CHEMISTRY

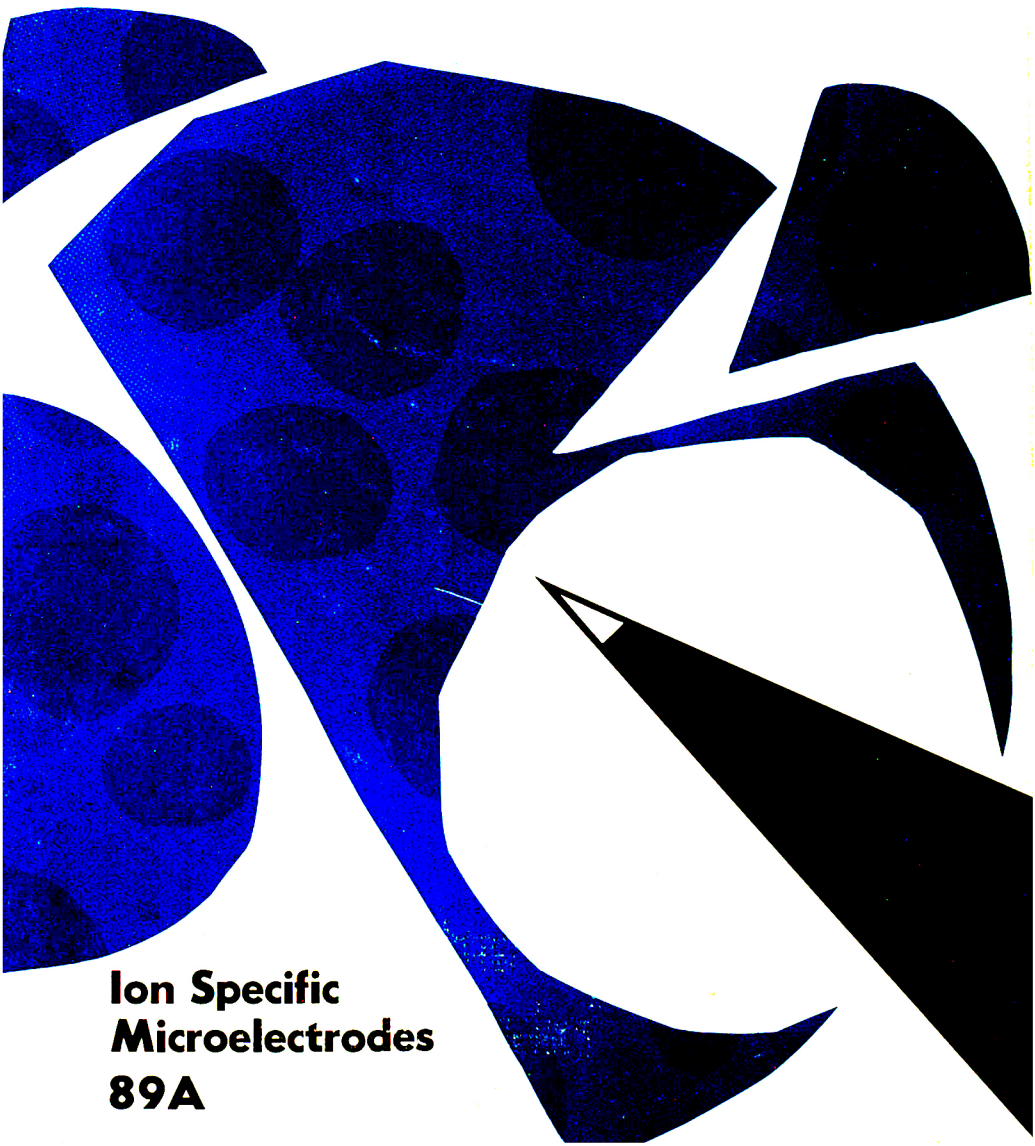

Ion Specific Microelectrodes

89A

technology assessment...

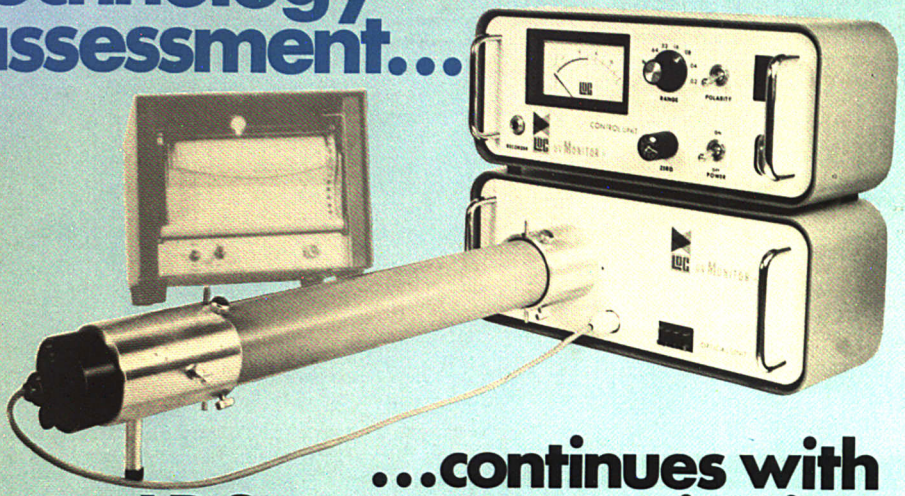

...continues with LDC mercury monitoring

Now — measure mercury contamination in gases, liquids, and solids in concentrations as low as 0.0001 micrograms in a 1 ml sample volume. Ultra-sensitive to mercury, the new LDC mercuryMonitor — an ultra-high-performance uv spectrophotometer — has been designed specifically for the determination of trace mercury contaminants in samples utilizing the cold vapor uv absorption technique.* A cell of unusually long path length (30 cm) and, low internal volume (14 ml), together with high photometric sensitivity (0.0002 O.D.) and excellent photometer stability enables the LDC mercuryMonitor to outperform AA units for a fraction of their cost. Is mercury analysis your business? Then look at the LDC mercuryMonitor. It provides accurate measurements well below the minimum test standards currently recommended by government agencies. It can go as low as 1 part per trillion mercury with samples of 50 ml volume. If you want to stay ahead of an increasingly urgent analytical problem — ask for more information on the LDC mercuryMonitor. It's available now.

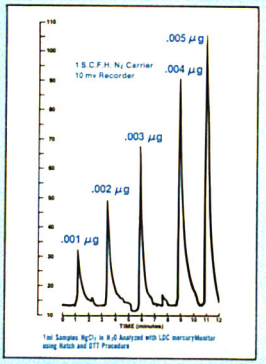

1ml Samples $HgCl_2$ in H_2O Analyzed with LDC mercuryMonitor using Hatch and Ott Procedure

Features:

- High mercury sensitivity — .005 μg full scale; minimum detectable .001 μg
- Dual-beam system — cancels background effects
- Highly stable photometer — drift less than 0.0002 O.D. per hour
- Linear O.D. readout; response directly proportional to concentration
- Control panels are easy to read and operator-oriented
- Low operating cost
- Proven reliability

*December, 1968 — *Analytical Chemistry* — Hatch and Ott

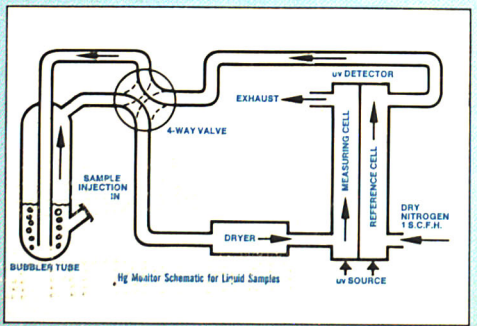

Hg Monitor Schematic for Liquid Samples

LABORATORY DATA CONTROL
P.O. Box 10235 Interstate Industrial Park
Riviera Beach, Florida 33404 (305) 844-5241

Circle No. 109 on Readers' Service Card

NOW, STATE-OF-THE-ART STABILITY

FOR **All present owners of the Aminco-Bowman Spectrophotofluorometer (SPF),** Aminco now offers a new Ratio Attachment to bring the stability of the oldest instrument up to the level of the newest ratio model.

FOR **Anyone contemplating the purchase of a spectrophotofluorometer,** Aminco now makes available a complete Ratio Spectrophotofluorometer providing superior stability and enhanced spectral information.

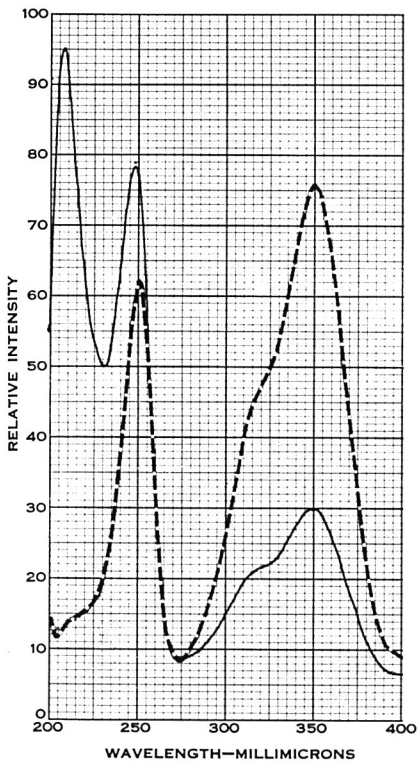

- ☐ **Increase instrument stability** to state-of-the-art levels by compensating for arc wander and electronic drift.
- ☐ **Bring excitation and emission spectra closer to known spectral characteristics.** Note the absorption peak at 208 nm and the ratio of the 250 nm and 350 nm peaks.
- ☐ **Correct for peak shift** due to low intensity in far UV.
- ☐ **Increase signal-to-noise ratio** by automatically subtracting detector dark current.

To receive literature which gives complete information and specifications on the new Ratio Attachment and the new Ratio Spectrophotofluorometer, write to American Instrument Co., Division of Travenol Laboratories, Inc., Silver Spring, Maryland 20910

See the new Aminco Ratio Spectrophotofluorometer in Booths 902-908 at the Pittsburgh Conference.

Curves showing excitation of 1 ppm quinine sulfate in .1 N H_2SO_4 (Emission at 450 nm).

Dotted curve, run in the standard non-ratioing mode, shows peaks at 250 nm and 350 nm. The 250 peak is less than the 350 peak because of decreased UV excitation radiation at 250 nm caused by use of an old lamp. Note the slight shoulder at 313 nm and the absence of peaks below 250 nm.

The solid curve is taken from the same sample run in the same instrument, but operating with the ratio attachment. An absorption peak at 208 nm becomes evident. The peak at 250 nm is now larger than the peak at 350 nm approaching the known ratios of these peaks. The shoulder at 313 nm is now well defined. There is also a slight shift toward the UV in the 250 nm peak. This shift reveals the true absorption peak, unaffected by lamp output.

AMINCO

At the forefront of spectrofluorescence technology from its inception

AMERICAN INSTRUMENT COMPANY
DIVISION OF TRAVENOL LABORATORIES, INC.
8030 Georgia Avenue, Silver Spring, Maryland 20910

Circle No 5 on Readers' Service Card

VOLUME 43, NO. 3 MARCH 1971

Our Cover Design is based on the Instrumentation Column, "Ion Specific Liquid Ion Exchanger Microelectrodes," page 89 A, by John L. Walker, Jr. of the University of Utah College of Medicine. These electrodes are being used to study the intracellular activities of the ions involved. Currently, only the potassium and chloride ion exchanger microelectrodes are of practical use; however, it is expected that ion specific microelectrodes for other ions of interest to biologists, calcium, for instance, will become available.

This month's issue demonstrates the breadth and depth of interest of ANALYTICAL CHEMISTRY from the experiences of an industrial analytical chemist, to environmental measuring problems as illustrated in the Editors' Column, page 81 A, which discusses water resources programs, to the technical program of the Analytical Chemistry Division at the 161st National ACS Meeting, page 51 A, where there will be symposia on air quality and nuclear techniques in environmental sciences (joint with the Divisions of Nuclear Chemistry and Technology and Water, Air, and Waste Chemistry).

Our New Products section this month is divided into major instrumentation, specific detectors and monitoring instruments, recorders and accessories, and miscellaneous items for the laboratory worker.

Next month, the New Products section will focus on some of the instruments and equipment to be exhibited at the Federation of American Societies for Experimental Biology at McCormick Place, Chicago, Ill., Apr. 12 to 17, 1971.

ANCHAM

ANALYTICAL CHEMISTRY

Contents

REPORT FOR ANALYTICAL CHEMISTS

Dr. V. A. Stenger of Dow Chemical Co. discusses the pains and pleasures of industrial analytical chemistry 36 A

SPECIAL REPORT

The organizing committee reports on their workshop on mass spectrometric analysis of solids which was held Nov. 16 and 17, 1970, at the Mellon Institute 45 A

NEWS

The detailed technical program of the Analytical Chemistry Division for the 161st National ACS Meeting, Los Angeles, Calif., Mar. 28 to Apr. 2, 1971, is given. Other technical meetings are scheduled 51 A

BOOK REVIEWS

Books on instrumental analysis, clinical chemistry fundamentals, infrared spectroscopy, and analysis of air pollutants are reviewed by R. L. Pecsok, D. S. Young, B. J. Bulkin, and J. W. Robinson 67 A

EDITORS' COLUMN

Analytical chemists interested in entering the field of water pollution surveillance and control will have many challenging opportunities 81 A

INSTRUMENTATION

Ion specific liquid ion exchanger microelectrodes are being used in single cells to study the intracellular activities of the ions involved. John L. Walker, Jr. discusses some of the programs underway and the possibilities inherent in this type of research 89 A

NEW PRODUCTS

Perkin-Elmer has introduced an automatic gas chromatography system for use with up to eight gc's which does not require the user to know any programming. Other major instruments, detectors, recorders, and lab equipment are presented 99 A

EDITORIAL

Professor Laitinen discusses ANALYTICAL CHEMISTRY'S manuscript review process 297

Author Index 6 A

Briefs 11 A

Calendar of Events 62 A

Future Articles 120 A

Manufacturers' Literature 109 A

New Chemicals 107 A

Product Capsules 113 A

Readers' Information Service 95 A

Scheduled Technical Courses 60 A

Novel Peak Matching Technique by Means of a New and Combined Multiple Ion Detector–Peak Matcher Device. Elemental Analyses of Compounds in Submicrogram Quantities without Prior Isolation. *Carl-Gustaf Hammar and Ronny Hessling* 298

Ion Specific Detection of Internal Standards Labelled with Stable Isotopes. *T. E. Gaffney, Carl-Gustaf Hammar, Bo Holmstedt, and R. E. McMahon* 307

Multivariable Analysis of Quantitative X-Ray Emission Data. The System Zirconium Oxide–Aluminum Oxide–Silicon Oxide–Calcium Oxide–Cerium Oxide. *D. A. Stephenson* 310

Spectrophotometric Determination of Traces of Thallium in Tungsten. The Extraction of Thallium Diethyldithiocarbamate. *Károly Vadasi, Piroska Buxbaum, and Andrá Salamon* 318

Liquid Ion Exchange Electrodes in Mixed Electrolyte Solutions. *J. V. Leyendekkers and Michael Whitfield* 322

Effects of Structure of Peptide Stationary Phases on Gas Chromatographic Separations of Amino Acid Enantiomers. *J. A. Corbin, J. E. Rhoad, and L. B. Rogers* 327

Low Level Sodium Ion Measurement with the Glass Electrode. *E. L. Eckfeldt and W. E. Proctor, Jr.* 332

Spectrophotometric Assay of Ampicillin (α-Aminobenzylpenicillin) Involving Initial Benzoylation of the Side Chain α-Amino Group. *D. E. Tutt and M. A. Schwartz* 338

Application of a Computerized Electrochemical System to Pulse Polarography at a Hanging Mercury Drop Electrode. *H. E. Keller and R. A. Osteryoung* 342

Rapid Analysis for Sub-Nanogram Amounts of Chromium in Blood and Plasma Using Electron Capture Gas Chromatography. *L. C. Hansen, W. G. Scribner, T. W. Gilbert, and R. E. Sievers* 349

Rapid Scan Infrared Spectrometer for Operation with Support Coated Open Tubular or Packed Column Gas Chromatographs. *R. A. Brown, J. M. Kelliher, J. J. Heigl, and C. W. Warren* 353

Simple and Inexpensive Electronic Conductivity Manometer for Monitoring Pressure Changes. Application to Pressuremetric Titrations of Iodate and Ammonium Ions. *D. J. Curran and S. J. Swarin* 358

Near Optimum Computer Searching of Information Files Using Hash Coding. *P. C. Jurs* 364

Teflon, A Noninert Chromatographic Support. *J. R. Conder* 367

Molecular and Unit Sheet Weights of Asphalt Fractions Separated by Gel Permeation Chromatography. *G. A. Haley* 371

Application of Photoelectron Spectrometry to Pesticide Analysis. Photoelectron Spectra of Hydroxy-, and Halo-Alkanes and Halohydrins. *A. D. Baker, D. Betteridge, N. R. Kemp, and R. E. Kirby* 375

Computerized Learning Machine Applied to Qualitative Analysis of Mixtures by Stationary Electrode Polarography. *L. B. Sybrandt and S. P. Perone* 382

Determination of Hydrogen Sulfide, Sulfur Dioxide, Carbonyl Sulfide, Carbon Disulfide, and Carbon Dioxide in a Gas Mixture. *Arthur Schwartz* 389

Simultaneous Determination of Two Electroactive Species by Alternating Current Polarography. *A. M. Bond and J. H. Canterford* 393

A Laboratory-Based Computer System. *Marvin Shapiro and Arthur Schultz* 398

Digital Methods of Photopeak Integration in Activation Analysis. *P. A. Baedecker* 405

Potentiometric Studies with an Ion Permselective Membrane. *Sudarshan Lal and G. D. Christian* 410

Use of Syringaldazine in a Photometric Method for Estimating "Free" Chlorine in Water. *Robert Bauer and C. O. Rupe* 421

Intrinsic End-Point Errors in Precipitation Titrations with Ion Selective Electrodes. *P. W. Carr* 425

Determination of Formation Constants of Iron(III) and Vanadium(V) with β-Isopropyltropolone Using the Extraction Method. *Oscar Menis, B. E. McClellan, and D. S. Bright* 431

Notes

Kinetics and Mechanism of Extraction of Iron(III) with β-Isopropyltropolone. *B. E. McClellan and Oscar Menis* 436

Determination of Nitrogen and Hydrogen at Parts-per-Million Levels in Milligram Steel Samples. *G. L. Hargrove, R. C. Shepard, and Harry Farrar IV* 439

Novel Method of Determining Weak Bases in Small Amounts. *Elio Scarano, Marco Mascini, and Giovanni Gay* 442

Improved Method for Determination of Chlorinated Hydrocarbon Pesticide Residues in Whole Blood. *S. J. Henderson, J. G. DeBoer, and H. M. Stahr* 445

Quantitative Cation Exchange Separation of Zirconium and Hafnium in Formic Acid Media. *Mohsin Qureshi and Khadim Husain* 447

ห้องสมุด กรมวิทยาศาสตร์
6 มิ.ย. 2514

Contributed Articles

Plutonium Determination in Soil by Leaching and Ion-Exchange Separation. *N. Y. Chu* 449

Isothermal Gas Chromatographic Separation of Carbon Dioxide, Carbon Oxysulfide, Hydrogen Sulfide, Carbon Disulfide, and Sulfur Dioxide. *W. L. Thornsberry, Jr.* 452

Optimization of Experimental Conditions for Spectrofluorimetric Determination of Europium, Samarium, and Terbium as Their Hexafluoroacetylacetone–Trioctylphosphine Oxide Complexes. *R. P. Fisher and J. D. Winefordner* 454

Kinetic Study of the Beckmann Rearrangement of 6α-Methyl-17α-Acetoxyprogesterone-1. 3-Oxime by Cathode Ray Polarography. *A. P. Shroff and C. J. Shaw* 455

Spectrophotometric Determination of Cobalt with Benzil Mono-(2-Pyridyl)Hydrazone. *R. T. Pflaum and E. S. Tucker III* 458

Analysis of Polyethylene Terephthalate Prepolymer by Trimethylsilylation and Gas Chromatography. *E. R. Atkinson, Jr., and S. I. Calouche* 460

Gas-Liquid Chromatography of Some Irritants at Various Concentrations. *Samuel Sass, T. L. Fisher, M. J. Jascot, and John Herban* 462

Suppression of Interferences by Sodium Sulfate in Trace Chromium Analyses by Atomic Absorption Spectrometry. *J. A. Hurlbut and C. D. Chriswell* 465

Separation of Perrhenate, Molybdate, and Selenite Ions on Silica Gel. *A. M. Phipps* 467

Fluorometric Determination of Submicrogram Quantities of Zirconium. *T. D. Filer* 469

Liquid–Liquid Extraction of Rhenium(VII) with Mesityl Oxide. *V. M. Shinde and S. M. Khopkar* 473

Emission Spectrochemical Determination of Tantalum in Curium Oxide. *R. H. Gaddy* 475

Novel Technique for Surface Analysis of Solid Metallic Specimens Using Selected Anodic Current-Voltage Characteristics. *George Todd and G. A. Wild* 476

Boron–Polyethylene Irradiation Containers for High Energy Neutron Activation Analysis. *W. A. Jester and K. N. Prasad* 481

Determination of Iron by EDTA Titrimetry of the Thiocyanate Complex. *A. de A. Figueiredo* 484

Confirmation of the High Aromaticity of Anthracite by Broadline Carbon-13 Magnetic Resonance Spectrometry. *H. L. Retcofsky and R. A. Friedel* 485

New Method for Separation of Americium from Curium and Associated Elements in the Zirconium Phosphate–Nitric Acid System. *F. L. Moore* 487

Correction. Determination of Unsaturation by Analytical Hydrogenation and Null Point Pressuremetry. *D. J. Curran and J. L. Driscoll* 435

Aids for Analytical Chemists

Rapid and Efficient Method for Removing Viscous Polymer Solutions from Nuclear Magnetic Resonance (NMR) Sample Tubes. *Alex Jakab* 489

Simple Device for Transferring Thin-Layer Chromatographic Fractions for Spectroscopic Examination. *C. J. Clemett* 490

Modulated Power Unit for Driving Metal Vapor Discharge Lamps. *F. M. Hamm, T. L. Martin, and P. B. Zeeman* 490

Simple Continuous Electronic Readout for Rotameter-Type Fluid Flow Measuring Devices Using a Photoelectric Transducer. *Seymour Lowell and Stewart Karp* 492

Low Cost Parallel-to-Serial Converter for Digital Instrumentation. *Morteza Janghorbani, J. A. Starkovich, and Harry Freund* 493

Ceramic Pressure Device for the Preparation of Known Gas Concentrations at the 100 Parts-per-Million Level. *H. D. Axelrod, R. J. Teck , J. P. Lodge, Jr., and R. H. Allen* 496

© Copyright 1971
by the American Chemical Society

MANUSCRIPT REQUIREMENTS published in December 1970 issue, page 1879, outlines scope and copy requirements to be observed in preparing manuscripts for consideration. Manuscript (4 copies) should be submitted to ANALYTICAL CHEMISTRY, 1155 Sixteenth St., N.W., Washington, D. C. 20036.

The American Chemical Society assumes no responsibility for the statements and opinions advanced by contributors to its publications. Views expressed in the editorials are those of the editors and do not necessarily represent the official position of the American Chemical Society.

1971 Subscription Rates

	1 yr.	2 yr.	3 yr.
Members, domestic and foreign	$ 5.00	$ 9.00	$12.00
Nonmembers, domestic and Canada	7.00	12.00	16.00
Nonmembers, foreign except Canada	15.00	27.50	40.00

Postage: Canada and Pan-American Union, $2.50; foreign, $3.50. Single copies: current, $2.00 except Annual Reviews, $3.00 each. Rates for back issues and volumes are available from Special Issues Sales Dept., 1155 Sixteenth St., N.W., Washington, D. C. Claims for missing numbers will not be allowed if received more than 60 days from date of mailing plus time normally required for postal delivery of journal and claim. No claims allowed because of failure to notify the Subscription Service Department of a change of address or because copy is "missing from files."

Those interested in joining the American Chemical Society should write to Admissions Department at the Washington Office.

Published monthly with Review issue added in April and a Laboratory Guide in August by the American Chemical Society, from 20th and Northampton Sts., Easton, Pa. 18042; Executive Offices, Editorial Headquarters, and Subscription Service Department, 1155 Sixteenth St., N.W., Washington, D. C. 20036; Advertising Office, 142 East Ave., Norwalk, Conn. 06851. ANALYTICAL CHEMISTRY and other ACS periodicals are available on microfilm. For information write to: MICROFILM, Special Issues Sales, American Chemical Society, 1155 Sixteenth St., N.W., Washington, D. C. 20036. Second class postage paid at Easton, Pa.

CHANGE OF ADDRESS: Notify Subscription Service Department, American Chemical Society, 1155 Sixteenth St., N.W., Washington, D. C. 20036. Such notification should include both old and new addresses, with ZIP code numbers, and be accompanied by mailing label from a recent issue. Allow four weeks for change to become effective.

our point of view!

Finding a drop in a bucket is a lead pipe cinch... with AQUATEST

AQUATEST is the only truly automatic Karl Fischer titrator.
Just inject sample... flip switch... step back... read answer!
Digital readout... no standardization... no drying system... no burettes... no measuring... no computations

Accuracy, reproducibility, and sensitivity all within 25 micrograms of water... that's 10 ppm in a 2.5 ml sample!
Our point of view is that "drop in the bucket" water determinations are really a cinch with our AQUATEST. Try one and let us know your point of view.

PHOTOVOLT CORPORATION *1115 Broadway, New York, N.Y. 10010 · (212) 989-2900*

See us at the Pittsburgh Show, Booths 1305–1307

Circle No. 147 on Readers' Service Card

The New Turner Model 430 SPECTROFLUOROMETER

FEATURES OF FLUOROMETRY

Fluorescence involves **two** spectra: the excitation spectrum, corresponding to the absorption spectrum, and the emission spectrum. This second spectrum provides an additional parameter for identification. It also yields increased selectivity, making it possible to use effectively the great sensitivity of fluorescence. **Parts-per-trillion** analyses are common.

FEATURES OF THE TURNER Model 430

Precision monochromators	Automatic blanking*
Digital wavelength display	All solid-state
Jacketed sample compartment	Wide-range light source
Polarization (attachment)	Concentration calculator

*This feature permits setting reagent blank to zero and in **one step** setting a standard to read any desired number (e.g., its concentration), **without having the blank shift from zero.**

FEATURES OF OUR "Aid to Analysts" PROGRAM

Turner Associates has collected over 12,000 references on fluorescent techniques covering quantitative analyses in such fields as **Water Pollution, Pharmacology, Forensic Chemistry, Immunochemistry, Clinical Pathology, Biochemistry, Inorganic Analysis, and many others.** A subscription to TRACES, a technical newsletter abstracting current literature, is free on request, as are bibliographies and review articles on specific compounds. Let us help you with your analytical problems.

Send for descriptive brochure and free subscription to TRACES. Write G. K. Turner Associates, 2524 Pulgas Avenue, Palo Alto, California 94303.

g. k. turner ASSOCIATES
A Subsidiary of
The American Sterilizer Company

Circle No. 178 on Readers' Service Card

AUTHOR INDEX

Allen, R. H. 496
Atkinson, E. R., Jr. 460
Axelrod, H. D. 496

Baedecker, P. A. 405
Baker, A. D. 375
Bauer, R. 421
Betteridge, D. 375
Bond, A. M. 393
Bright, D. S. 431
Brown, R. A. 353
Buxbaum, P. 318

Calouche, S. I. 460
Canterford, J. H. 393
Carr, P. W. 425
Christian, G. D. 410
Chriswell, C. D. 465
Chu, N. Y. 449
Clemett, C. J. 490
Conder, J. R. 367
Corbin, J. A. 327
Curran, D. J. 358

DeBoer, J. G. 445

Eckfeldt, E. L. 332

Farrar, H., IV. 439
Figueriedo, A. de A. 484
Filer, T. D. 469
Fisher, R. P. 454
Fisher, T. L. 462
Freund, H. 493
Friedel, R. A. 485

Gaddy, R. H. 475
Gaffney, T. E. 307
Gay, G. 442
Gilbert, T. W. 349

Haley, G. A. 371
Hamm, F. M. 490
Hammar, C-G. 298, 307
Hansen, L. C. 349
Hargrove, G. L. 439
Heigl, J. J. 353
Henderson, S. J. 445
Herban, J. 462
Hessling, R. 298
Holmstedt, B. 307
Hurlbut, J. A. 465
Husain, K. 447

Jakab, A. 489
Janghorbani, M. 493
Jascot, M. J. 462
Jester, W. A. 481
Jurs, P. C. 364

Karp, S. 492
Keller, H. E. 342
Kelliher, J. M. 353
Kemp, N. R. 375
Khopkar, S. M. 473
Kirby, R. E. 375

Lal, S. 410
Leyendekkers, J. V. 322
Lodge, J. P., Jr. 496
Lowell, S. 492

McClellan, B. E. 431, 436
McMahon, R. E. 307
Martin, T. L. 490
Mascini, M. 442
Menis, O. 431, 436
Moore, F. L. 487

Osteryoung, R. A. 342

Perone, S. P. 382
Pflaum, R. T. 458
Phipps, A. M. 467
Prasad, K. N. 481
Proctor, W. E., Jr. 332

Qureshi, M. 447

Retcofsky, H. L. 485
Rhoad, J. E. 327
Rogers, L. B. 327
Rupe, C. O. 421

Salamon, A. 318
Sass, S. 462
Scarano, E. 442
Schultz, A. 398
Schwartz, A. 389
Schwartz, M. A. 338
Scribner, W. G. 349
Shapiro, M. 398
Shaw, C. J. 455
Shepard, R. C. 439
Shinde, V. M. 473
Shroff, A. P. 455
Sievers, R. E. 349
Stahr, H. M. 445
Starkovich, J. A. 493
Stephenson, D. A. 310
Swarin, S. J. 358
Sybrandt, L. B. 382

Teck, R. J. 496
Thornsberry, W. L., Jr. 452
Todd, G. 476
Tucker, E. S., III 458
Tutt, D. E. 338

Vadasdi, K. 318

Warren, C. W. 353
Whitfield, M. 322
Wild, G. A. 476
Winefordner, J. D. 454

Zeeman, P. B. 490

Most automatic recording titrators aren't. Beckman's is.

The Beckman Automatic Recording Titrator is *truly* automatic...designed to give you maximum ease of operation, precision, repeatability, versatility. Consider these exclusive Beckman features:

All-electronic automatic mode. You can run completely unknown titration curves without adjustment and without overshoot. Slows automatically as the endpoint nears.

Combination mode. The titrator races to a preset critical point and slows to a preset speed while passing through the endpoint. Extremely precise titrations in only 40 to 60 seconds.

Automatic refill. Completely eliminates mechanical buret stopcocks.

Digital display of titrant added. Fast, simplified reading eliminates operator error.

Widest range. Full, calibrated, 0-14 pH range with expansion scales of 1.4, 2.8, 7 and 14 pH (140, 280, 700 and 1400 mv).

Maximum economy. Buy only what you need, single or double column models. Second column can be added when required. Price: $3200, single column model; $3460, double column model.

Write for Data File 25, Scientific Instruments Division, Beckman Instruments, Inc., 2500 Harbor Boulevard, Fullerton, California 92634.

Now Beckman offers a low-cost Endpoint Titrator System for industrial quality control applications. Ask about it.

Beckman® INSTRUMENTS, INC.

HELPING SCIENCE AND INDUSTRY IMPROVE THE QUALITY OF LIFE.

INTERNATIONAL SUBSIDIARIES: AMSTERDAM; CAPE TOWN; GENEVA; GLENROTHES, SCOTLAND; LONDON; MEXICO CITY; MUNICH; PARIS; STOCKHOLM; TOKYO; VIENNA

Circle No. 20 on Readers' Service Card

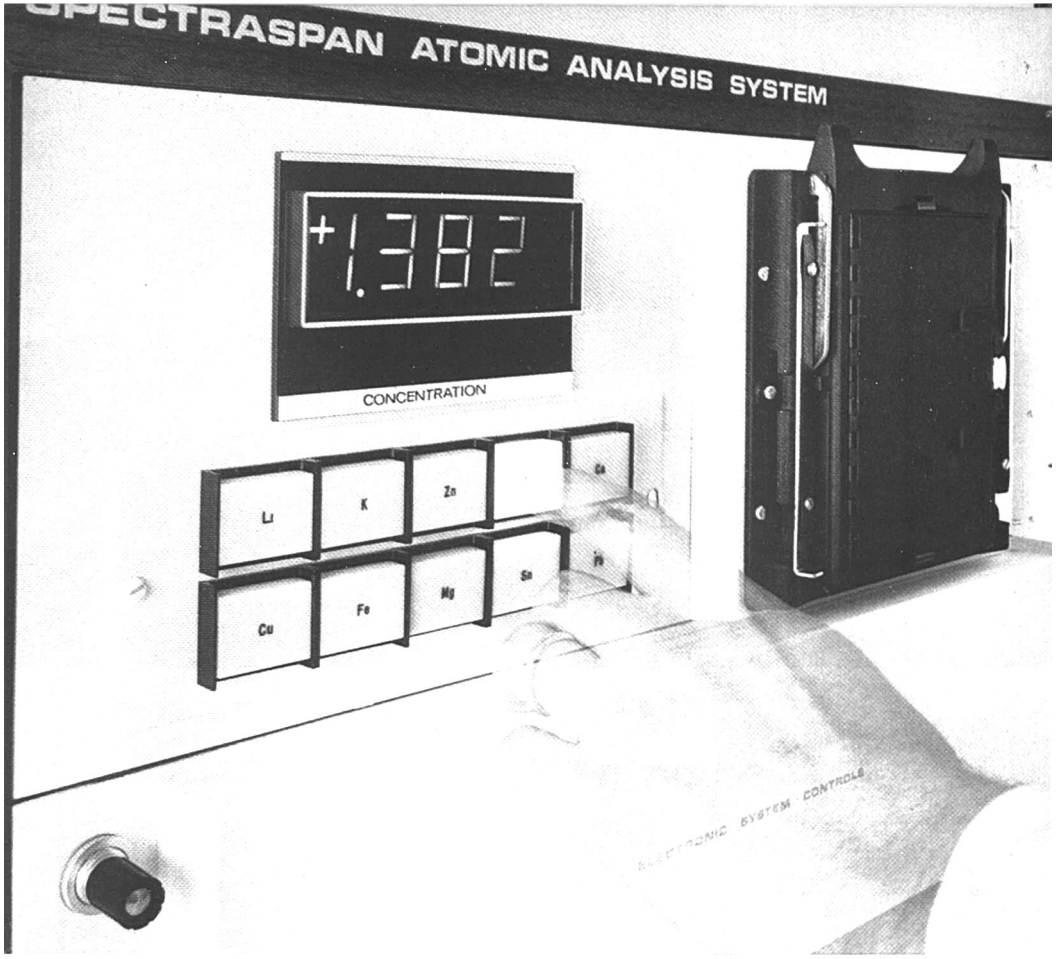

Wanted: Adventurers

... In simultaneous multi-element spectrochemical analysis. To use the SpectraSpan 210 cassette spectrometer for measurement of up to 10 elements at once, with plug-in cassettes for additional 10-element groups.

If you're wedded to AA, you need not apply, because the SpectraSpan is new. It is a quantum jump in spectrochemistry, and one of the major developments in analytical techniques in the last 15 years.

Because the SpectraSpan is new, please don't ask us for bulging "cookbooks" and copious bibliographies. You'll have to write your own papers about new developments. But you'll be aided by a 36-inch bench-top echelle spectrometer with resolution better than that of a three-meter spectrometer occupying an entire special laboratory. SpectraSpan uses a tiny 10,000°K plasma excitation source which eliminates the need for hollow cathode lamps and uses safe, non-explosive argon for "fuel".

The SpectraSpan 210 is an emission spectrometer for use with small liquid samples. Sample preparation and handling techniques are identical to AA. But you'll have to start thinking in new dimensions, because you can make up to 180 10-element determinations per hour from 50 microliter samples.

A core of adventurers have already been using SpectraSpan instruments in clinical, petrochemical, pollution control and astronomical applications for over a year. They have been doing analyses that simply cannot be done with other techniques.

Be an adventurer. While you still can.

SPECTRA METRICS

SpectraMetrics, Inc.
Second Avenue, Northwest Park
Burlington, Mass. 01803
(617) 272-0540

For simultaneous multi-element analysis

Circle No. 167 on Readers' Service Card

Even more versatile: Sargent's new Model XVI Recording Polarograph®

Our new Model XVI Polarograph is a strip chart recording instrument suitable for both research and routine analytical applications. Designed to take advantage of recent developments in the technique of D.C. polarography, it provides facilities for recording the derivative polarogram with or without damping and for compensating the residual current to provide materially improved step definition at low concentrations.

For maximum flexibility in experimental conditions, there are 22 current sensitivities ranging through 3 decades from 0.001 to 1.00 μa/mm; 11 fixed ranges of polarizing voltage, 1, 2, or 3 volts in span; 3 scanning rates; 3 chart speeds; 3 degrees of RC damping; and a total zero displacement range of 11X full scale.

We've priced the Model XVI at $1800.00. That includes electrolysis vessels, electrodes, capillaries, mercury reservoir, chart paper, pens, tubing, connecting cable—everything you'll need.

For complete specifications or a demonstration of this instrument, please call your Sargent man or write directly to us. 7-232 REV-2

Polarograph is a registered trademark of Sargent-Welch Scientific Company

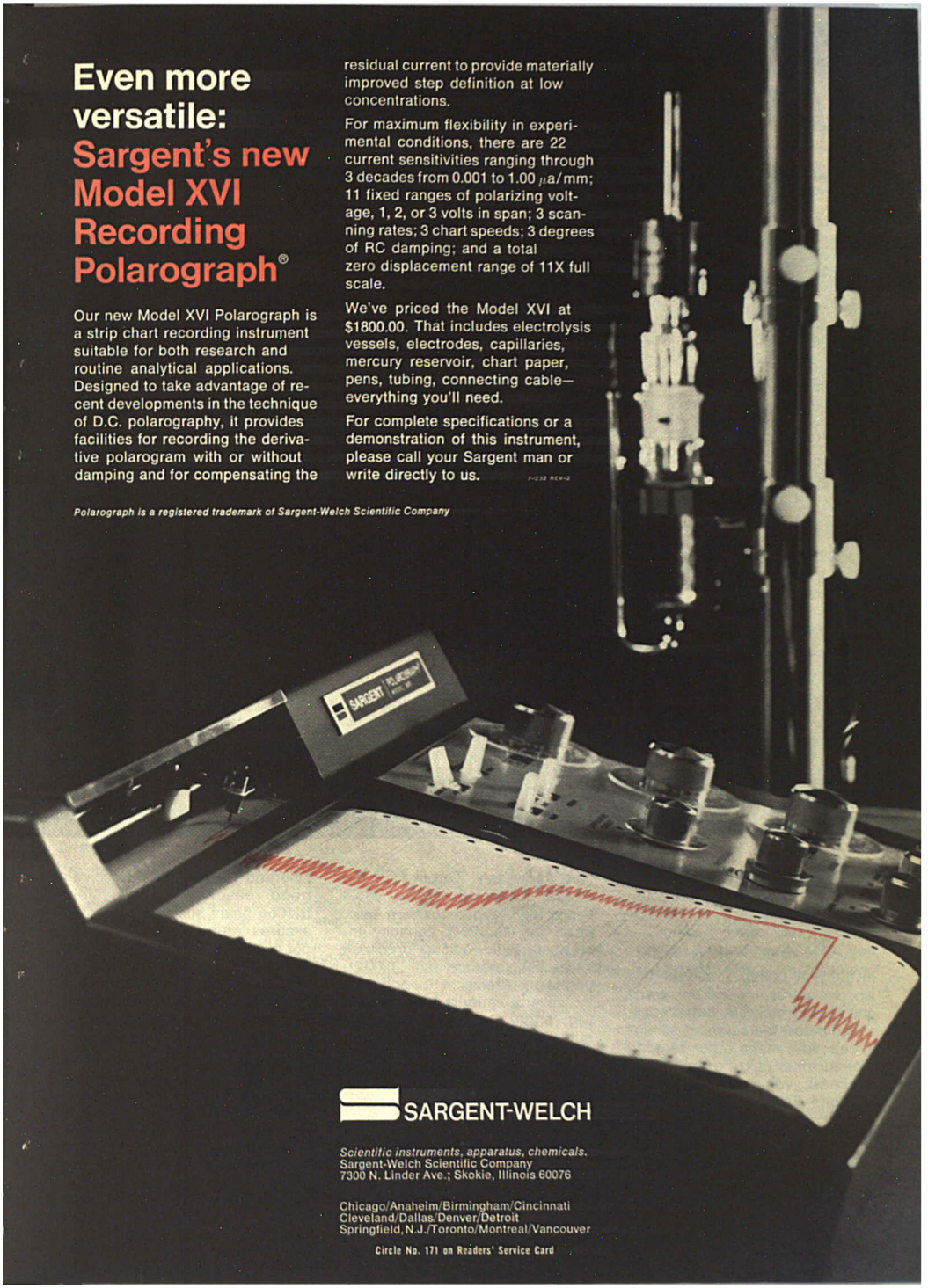

SARGENT-WELCH

Scientific instruments, apparatus, chemicals.
Sargent-Welch Scientific Company
7300 N. Linder Ave.; Skokie, Illinois 60076

Chicago/Anaheim/Birmingham/Cincinnati
Cleveland/Dallas/Denver/Detroit
Springfield, N.J./Toronto/Montreal/Vancouver

Circle No. 171 on Readers' Service Card

When time is in the balance... A Mettler top loader will weigh in seconds to ±0.001 g

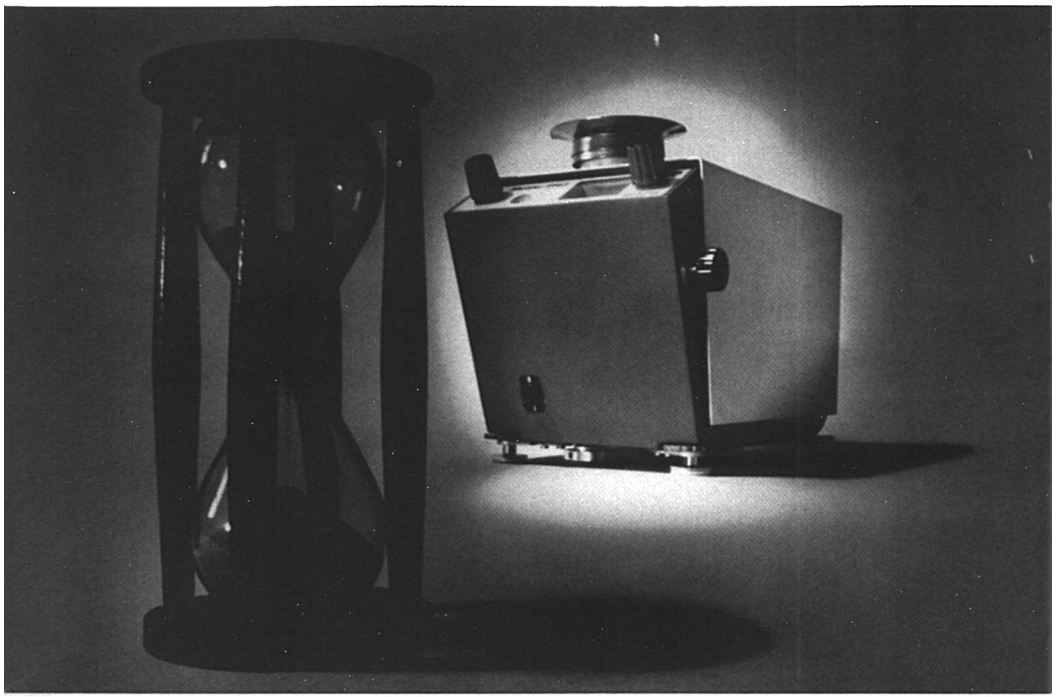

But there is more in the balance than time. If you need accuracy, reproducibility, and application flexibility, no other balance, at any price, gives you as much.

In the R & D lab, quality control lab, or classroom, weigh unknowns, checkweigh, weigh-in, batch weigh, weigh below the balance. All high speed. And make other physical measurements by gravimetry—thickness, volume, area, surface tension.

And accurately. Throughout the Mettler line of 18 models, you'll find a high load-to-precision ratio. From the 11,000-g capacity instrument with ±0.05 g precision to the 170-g balance with ±0.001 g precision. Precision to one part in several hundred thousand. Big, bright, highly visible readouts...depending on model, your choice of digital or analog. Available in metric or other calibrations.

The Mettler top loader is as precise and rugged as it is for very good reasons. Extremely low-friction beam suspension system assures reproducibility throughout the life of the balance. Friction clutches help prevent damage due to forcing. Dust trap keeps foreign matter out. Automatic self-leveling. Rugged construction throughout.

For a catalog, write Mettler Instrument Corporation, Box 100, Princeton, New Jersey 08540, or call 609-448-3000.

Mettler

Circle No. 122 on Readers' Service Card

A C BRIEFS

Highlights
of Articles in
This Issue

Novel Peak Matching Technique by Means of a New and Combined Multiple Ion Detector-Peak Matcher Device. Elemental Analyses of Compounds in Submicrogram Quantities without Prior Isolation

A combined multiple ion detector-peak matcher device for a gas chromatograph-single focusing mass spectrometer allowing elemental analyses of non-isolated compounds in submicrogram quantities during their elution from a GC-column.

CARL-GUSTAF HAMMAR and RONNY HESSLING, Department of Toxicology, Swedish Medical Research Council, Karolinska Institutet, S-104 01 Stockholm 60, Sweden

Anal. Chem., 43, 298 (1971)

Ion Specific Detection of Internal Standards Labelled with Stable Isotopes

Compounds labelled with stable isotopes appear to function as ideal internal standards when the mass-spectrometer is used as the detector for gas chromatographic effluents.

THOMAS E. GAFFNEY, CARL-GUSTAF HAMMAR, BO HOLMSTEDT, and ROBERT E. McMAHON, Department of Toxicology, Swedish Medical Research Council, Karolinska Institutet, 104 01 Stockholm 60, Sweden, and The Lilly Research Laboratories, Indianapolis, Ind.

Anal. Chem., 43, 307 (1971)

Multivariable Analysis of Quantitative X-Ray Emission Data. The System Zirconium Oxide–Aluminum Oxide–Silicon Oxide–Calcium Oxide–Cerum Oxide

A review and discussion of statistical methods for quantitative X-ray emission analysis of multicomponent systems is presented. Application of the techniques to the system ZrO_2-Al_2O_3-SiO_2-CaO-CeO_2 gave results accurate to about ± 1 to 2% relative.

DONALD A. STEPHENSON, Research and Development Laboratories, Corning Glass Works, Corning, N. Y. 14830

Anal. Chem., 43, 310 (1971)

Spectrophotometric Determination of Traces of Thallium in Tungsten. The Extraction of Thallium Diethyldithiocarbamate

The procedure for the determination of 0.1–10 ppm thallium is based on the extraction of thallium as diethyldithiocarbamate complex and on the determination with Methyl Violet with 10–20% relative standard deviation.

KAROLY VADASDI, PIROSKA BUXBAUM, and ANDRAS SALAMON, Research Institute for Technical Physics of the Hungarian Academy of Sciences, Budapest, Hungary

Anal. Chem., 43, 318 (1971)

Liquid Ion Exchange Electrodes in Mixed Electrolyte Solutions

The selectivity characteristics of the Orion Calcium Activity electrode (92-20) in the aqueous systems $CaCl_2$-$MgCl_2$ and $CaCl_2$-$SrCl_2$ are presented together with the Harned coefficients estimated from measurements with this electrode and the Orion Chloride electrode (92-17).

J. V. LEYENDEKKERS and MICHAEL WHITFIELD, Division of Fisheries and Oceanography, CSIRO, Cronulla, Sydney, 2230, Australia

Anal. Chem., 43, 322 (1971)

Effects of Structure of Peptide Stationary Phases on Gas Chromatographic Separations of Amino Acid Enantiomers

Asymmetry at the amide of a dipeptide derivative has been shown to be more important than at the ester end. Structural effects have been examined using a tripeptide and substituents of different types.

J. A. CORBIN, J. E. RHOAD, and L. B. ROGERS, Department of Chemistry, Purdue University, Lafayette, Ind. 47907

Anal. Chem., 43, 327 (1971)

Low Level Sodium Ion Measurement with the Glass Electrode

By using favorable instrumental factors and a selected base reagent, as explained, sodium can be monitored quite satisfactorily down to the 0.1 ppb level.

EDGAR L. ECKFELDT and WILLIAM E. PROCTOR, JR., Corporate Research Department, Leeds & Northrup Company, North Wales, Pa.

Anal. Chem., 43, 332 (1971)

Spectrophotometric Assay of Ampicillin (α-Aminobenzylpenicillin) Involving Initial Benzoylation of the Side Chain α-Amino Group

Ampicillin in assayed at concentrations as low as $4 \times 10^{-5} M$ by benzoylation prior to acid-$HgCl_2$ treatment. The assay is especially useful for following degradation rate of drug.

DAVID E. TUTT and MICHAEL A. SCHWARTZ, Department of Pharmaceutics, School of Pharmacy, State University of New York at Buffalo, Buffalo, N. Y. 14214.

Anal. Chem., 43, 338 (1971)

Application of a Computerized Electrochemical System to Pulse Polarography at a Hanging Mercury Drop Electrode

Results of applying a computerized pulse polarography system to trace analysis are described. Measurements are made at concentrations as low as $4 \times 10^{-8} M$ Cd^{2+}.

H. E. KELLER and R. A. OSTERYOUNG, Department of Chemistry, Colorado State University, Fort Collins, Colo. 80521

Anal. Chem., 43, 342 (1971)

Rapid Analysis for Sub-Nanogram Amounts of Chromium in Blood and Plasma Using Electron Capture Gas Chromatography

Chromium in blood and plasma is simultaneously chelated with 1,1,1-trifluoro-2,4-pentanedione and extracted into hexane by direct reaction in a sealed tube. The chromium is then quantitatively determined by gas chromatography using a tritium detector.

LARRY C. HANSEN and WILLIAM G. SCRIBNER, Monsanto Research Corporation, Dayton, Ohio 45407, T. WILLIAM GILBERT, Department of Chemistry, University of Cincinnati, Cincinnati, Ohio 45221, and ROBERT E. SIEVERS, Aerospace Research Laboratories, Wright-Patterson Air Force Base, Ohio 45433

Anal. Chem., 43, 349 (1971)

FABRI-TEK 1070

...plug-ins make it more than just a signal averager

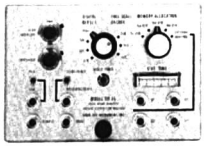

PULSE HEIGHT AND VOLTAGE DISTRIBUTION ANALYZER

Used for applications such as nuclear spectroscopy, particle size distributions, cell size distributions, and vibration analysis the Model SW-75 plug-in digitizes analog signals or signals which occur as amplitude modulated pulses.

The digitized information is stored and displayed as a histogram or distribution function showing the number of times each particular amplitude occurred.

The SW-75 digitizer has a resolution of one part in 1024. Coincidence capabilities are included so that an input signal is analyzed only when a second (coincidence) signal is present at the same time.

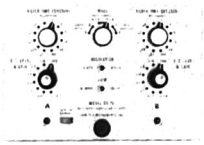

CORRELATION FUNCTION ANALYZER

Typical correlation technique applications include the fields of medicine, seismology, and vibration analysis.

Time-series correlation provides a means for statistically describing random data in the time domain as opposed to either the frequency or amplitude domain. Autocorrelation describes the similarity between a waveform and a time-shifted version of this same waveform. Crosscorrelation describes the similarity between two different waveforms.

The SD-75 when used with the Fabri-Tek Fast Fourier System provides power spectral density computations.

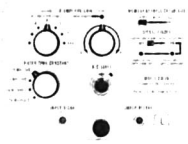

PARAMETRIC SWEEP CONTROL

This plug-in was designed for those traditionally difficult applications where the independent variable changes at an unknown or nonlinear rate. It permits the measurement of the relationship between two variables represented by analog input voltages. The SW-79 plug-in programs the 1070 averager's address advance in accordance with amplitude changes in the independent (X-axis) variable, rather than on a time basis.

Typical applications include averaging temperature as a function of pressure, voltage as a function of current, or absorbed energy as a function of magnetic field intensity.

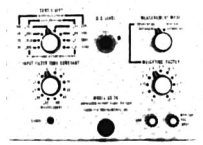

WEIGHTED AVERAGE SIGNAL DIGITIZER

This plug-in offers the option of signal averaging by either the weighted average or normalized average methods.

The weighted average method emphasizes changes in the input signal as they occur. This emphasis is the result of gradually "forgetting" the older accumulated data. Eleven weighting factors are switch selectable.

The normalized averaging method is especially convenient to use, particularly in set-up procedures. Another advantage is that when the numerical display option is used the displayed numbers represent the average number of microvolts per ordinate point.

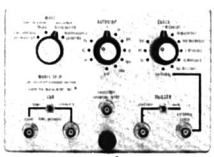

TIME AND FREQUENCY HISTOGRAM ANALYZER

Statistical analysis is a frequently applied technique for describing random data waveforms. Typical examples of these waveforms are the electrical potential of nerve cells, measurements from a quality control application, or the output of a transducer.

The SH-71 plug-in operating modes include time interval distributions between level crossings of voltage waveforms, a plot of successive measurements of time intervals, the distribution of level crossing per unit time, and trend measurements made by plotting the number of events per unit time.

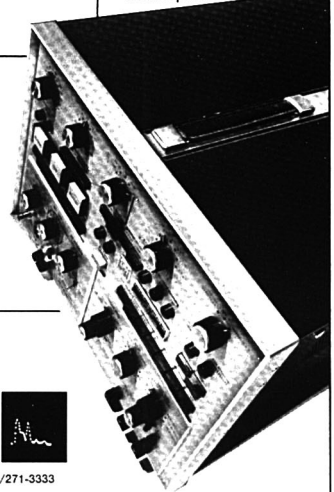

OTHER PLUG-INS . . .

A total of 19 different plug-ins are currently available and include capabilities for high resolution (12 bit), or 1, 2 or 4 input medium resolution (9 bit), or high speed (1 microsecond/address) signal averaging; NMR spectrometer control or signal delay averaging. Call or write to discuss your specific application. For full details request our new 44-page brochure.

FABRI-TEK INSTRUMENTS, INC.

5225 VERONA ROAD • MADISON, WIS. 53711 • PHONE: 608/271-3333

Circle No. 61 on Readers' Service Card

Rapid Scan Infrared Spectrometer for Operation with Support Coated Open Tubular or Packed Column Gas Chromatographs

An infrared spectrometer is described for recording spectra of gas liquid chromatographic fractions from either packed or "SCOT" columns. Good quality spectra are obtained at the twenty microgram level.

R. A. BROWN, J. M. KELLIHER, and J. J. HEIGL, Esso Research and Engineering Co., Linden, N. J., and C.W. WARREN, Instruments & Communications, Inc., Wilton, Conn.

Anal. Chem., 43, 353 (1971)

Simple and Inexpensive Electronic Conductivity Manometer for Monitoring Pressure Changes. Application to Pressuremetric Titrations of Iodate and Ammonium Ions

A pressure transducer system based on electronic monitoring of the liquid level in a manometer is presented. Its use as an end point detection device in volumetric and coulometric titrations is discussed.

D. J. CURRAN and S. J. SWARIN, Department of Chemistry, University of Massachusetts, Amherst, Mass. 01002

Anal. Chem., 43, 358 (1971)

Near Optimum Computer Searching of Information Files Using Hash Coding

Hash coding has been used to develop two algorithms for searching information files similar to those used in spectrometry laboratories. Search speeds up to 2000 spectra per second are obtained.

PETER C. JURS, Department of Chemistry, The Pennsylvania State University, University Park, Pa. 16802

Anal. Chem., 43, 364 (1971)

Teflon, a Noninert Chromatographic Support

Teflon is not an inert support as sometimes supposed. A two-site sorption mechanism describes the substantial sorption of both polar and nonpolar solutes observed with varying loadings of di-*n*-nonyl phthalate.

J. R. CONDER, Chemical Engineering Dept., University College of Swansea, United Kingdom

Anal. Chem., 43, 367 (1971)

Molecular and Unit Sheet Weights of Asphalt Fractions Separated by Gel Permeation Chromatography

Vapor pressure osmometry molecular weight determinations are shown to be solvent dependent. This affects the calibration of gel permeation chromatograms and the correlation of molecular and unit sheet weights.

GRAEME A. HALEY, School of Highway Engineering, University of New South Wales, Box 1, Kensington 2033, N.S.W. Australia

Anal. Chem., 43, 371 (1971)

Application of Photoelectron Spectrometry to Pesticide Analysis. Photoelectron Spectra of Hydroxy-, and Halo-Alkanes and Halohydrins

The photoelectron spectra of several mono- and di-haloalkanes, alcohols, and ethylene halohydrins are reported and their theoretical and analytical significance is discussed.

A. D. BAKER, D. BETTERIDGE, N. R. KEMP, and R. E. KIRBY, Department of Chemistry, University College of Swansea, Singleton Park, Swansea, Glam., U. K.

Anal. Chem., 43, 375 (1971)

Computerized Learning Machine Applied to Qualitative Analysis of Mixtures by Stationary Electrode Polarography

Qualitative resolution of stationary electrode polarographic data by a computerized learning machine has been evaluated. Categorization criteria were optimized by investigation of specific indentification errors made in unbiased training.

L. B. SYBRANDT and S. P. PERONE, Department of Chemistry, Purdue University, Lafayette, Ind. 47907

Anal. Chem., 43, 382 (1971)

Determination of Hydrogen Sulfide, Sulfur Dioxide, Carbonyl Sulfide, Carbon Disulfide, and Carbon Dioxide in a Gas Mixture

The separation and determination of components of a gas mixture absorbed in solutions of copper sulfate and ethanolic potassium hydroxide are presented. Better than 3% accuracy is possible.

ARTHUR SCHWARTZ, Development Center, Chemical Construction Corporation (CHEMICO), New Brunswick, N. J. 08903

Anal. Chem., 43, 389 (1971)

Simultaneous Determination of Two Electroactive Species by Alternating Current Polarography

The possibility of quantitatively determining two species which produce overlapping polarographic waves by the ac technique at the dropping mercury electrode has been examined.

A. M. BOND and J. H. CANTERFORD, Department of Inorganic Chemistry, University of Melbourne, Parkville, Victoria 3052, Australia

Anal. Chem., 43, 393 (1971)

A Laboratory-Based Computer System

A real-time computer system has been implemented in a laboratory research environment. Data are collected by the computer from remotely located instruments simultaneously with other computer processing.

MARVIN SHAPIRO and ARTHUR SCHULTZ, National Institutes of Health, Bethesda, Md.

Anal. Chem., 43, 398 (1971)

Dry detection of SO_2: Out of step, or a step ahead?

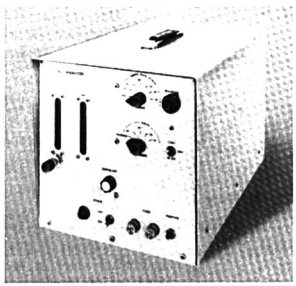

Since dry detection uses no wet chemicals it's out of step with other systems.

But precisely for this reason, it's a giant step ahead of the crowd.

Meloy Laboratories' dry detection sulfur analyzers use a detector which works on the photometric detection of the flame emission of sulfur containing compounds in a hydrogen-air flame.

We use this method not because it's different, but because it's better.

Over 1000 flame photometric systems have been put into service since 1965 for detection and analysis of sulfur and phosphorus compounds and hydrocarbons commonly found in air pollution, pesticides, and petrochemicals.

Get all the facts on dry detection today, call or write to: **Meloy Laboratories** (Mel-Labs Inc.), **Instruments and Systems Division,** 6631 Iron Place, Springfield, Virginia 22151, (703) 354-4450.

Consider these advantages of dry detection:

- ☐ greater detection sensitivity
- ☐ greater detection specificity
- ☐ responds in seconds
- ☐ no leaky valves, corrosion, chemicals
- ☐ lower cost to operate
- ☐ minimum maintenance
- ☐ continuous measurement
- ☐ provides greater repeatability

PRINCIPLES OF OPERATION

Atmospheric pollutants are burned in a hydrogen-rich flame (Flame Photometric Detector). Phosphorus or sulfur compounds burned in this flame give characteristic emissions. Specific detection is achieved by unique geometric arrangement of the burner which shields the primary flame from the photomultiplier and filters.

An ion target included in the burner permits simultaneous operation of the unit as a flame ionization detector for detection of total hydrocarbons with the FPD channel giving simultaneous S or P readout.

Meloy Laboratories

Biosciences · Environmental Sciences · Instruments & Systems

Circle No. 121 on Readers' Service Card

Digital Methods of Photopeak Integration in Activation Analysis

A study has been carried out of the relative precisions which are attainable by seven digital methods of photopeak integration, in activation analysis experiments involving gamma-ray spectrometry.

PHILIP A. BAEDECKER, Department of Chemistry and Institute of Geophysics and Planetary Physics, University of California, Los Angeles, Calif. 90024

Anal. Chem., 43, 405 (1971)

Potentiometric Studies with an Ion Permselective Membrane

A membrane electrode is described that can be used for redox, precipitation, complexometric, acid-base, and nonaqueous potentiometric titrations. It exhibits varying degrees of permselectivity to cations and anions and is stable for several months.

SUDARSHAN LAL and GARY D. CHRISTIAN, Department of Chemistry, University of Kentucky, Lexington, Ky. 40506

Anal. Chem., 43, 410 (1971)

Use of Syringaldazine in a Photometric Method for Estimating "Free" Chlorine in Water

Syringaldazine buffered at pH 7 has been used in a photometric procedure for estimating "free" chlorine. The procedure can detect chlorine in concentrations of 0.05 ± 0.011 ppm and is not affected by chloramines.

ROBERT BAUER and CHAUNCEY O. RUPE, Ames Company, Division of Miles Laboratories, Inc., Elkhart, Ind. 46514

Anal. Chem., 43, 421 (1971)

Intrinsic End-Point Errors in Precipitation Titrations with Ion Selective Electrodes

The effect of finite interference ratios on the analytical precision and accuracy of a variety of potentiometric precipitation titrations is presented. Results are discussed in terms of selectivity and symmetry errors.

PETER W. CARR, Department of Chemistry, University of Georgia, Athens, Ga. 30601

Anal. Chem., 43, 425 (1971)

Determination of the Formation Constants of Iron(III) and Vanadium(V) with β-Isopropyltropolone Using the Extraction Method

Equilibrium constants in the extraction of ferric and vanadyl chelates with β-isopropyltropolone were obtained from graphical and least square calculations of data. An adduct formation of VO_2IPT·HIPT is reported for the first time from the extraction data.

OSCAR MENIS, B. E. McCLELLAN, and DAVID S. BRIGHT, Analytical Chemistry Division, National Bureau of Standards, Washington, D. C. 20234

Anal. Chem., 43, 431 (1971)

Notes

Kinetics and Mechanism of Extraction of Iron(III) with β-Isopropyltropolone

A study of the kinetics and mechanism of the reaction between Fe(III) and β-isopropyltroprolone was made by the extraction method. The reaction orders in metal ion and reagent were found to be unity, and the addition of the first ligand to the Fe(III) is postulated to be rate determining.

B. E. McCLELLAN and OSCAR MENIS, Analytical Chemistry Division, National Bureau of Standards, Washington, D. C. 20234

Anal. Chem., 43, 436 (1971)

Determination of Nitrogen and Hydrogen at Parts-per-Million Levels in Milligram Steel Samples

This micro-inert gas fusion technique yields one σ relative standard deviations of about 10% for the two elements and requires 90 minutes for a complete analysis.

G. L. HARGROVE, R. C. SHEPARD, and HARRY FARRAR IV, Atomics International, A Division of North American Rockwell Corporation, Canoga Park, Calif. 91304

Anal. Chem., 43, 439 (1971)

Novel Method of Determining Weak Bases in Small Amounts

Weak bases (K_b up to 10^{-10}) can be determined in the μmole range by measuring the difference between the quantity of hydrogen chloride added to and that recovered from a saturated aqueous lithium chloride solution.

ELIO SCARANO, MARCO MASCINI, and GIOVANNI GAY, Institute of Analytical Chemistry, Faculty of Pharmacy, University of Genoa, Italy

Anal. Chem., 43, 442 (1971)

Improved Method for Determination of Chlorinated Hydrocarbon Pesticide Residues in Whole Blood

An improved technique is presented that increases the accuracy and precision of the determination of chlorinated hydrocarbon residues in whole blood. The length of time necessary for analysis is also decreased.

S. J. Henderson, J. G. DeBOER, and H. M. STAHR, Veterinary Diagnostic Laboratory, Iowa State University, Ames, Iowa 50010

Anal. Chem., 43, 445 (1971)

Quantitative Cation Exchange Separation of Zirconium and Hafnium in Formic Acid Media

Zirconium has been quantitatively separated from hafnium on Dowex 50 W-X8 column by eluting with 1*M* HCOOH and 4.0*M* HNO_3, respectively. Kd values for these 2 cations have been obtained in (0.1*M*–26*M*) formic acid solutions on this resin.

MOHSIN QURESHI and KHADIM HUSAIN, Chemistry Department, Aligarh Muslim University, Aligarh, India

Anal. Chem., 43, 447 (1971)

ห้องสมุด กรมวิทยาศาสตร์

Noisy Signal?

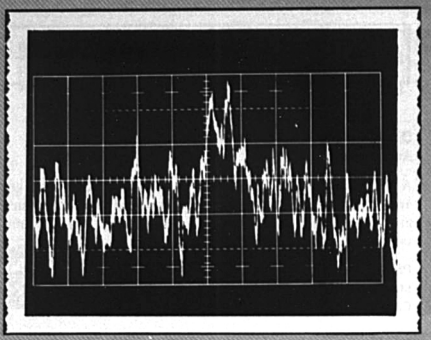

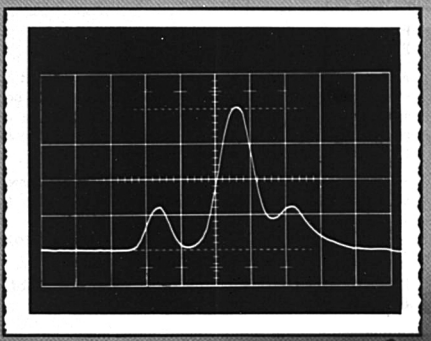

Extract it with a PAR Waveform Eductor™

The Waveform Eductor is a signal averager used to extract repetitive signals from noise. For complete information or to arrange a demonstration of this instrument, write Princeton Applied Research Corporation, P.O. Box 565, Princeton, New Jersey 08540, or call (609) 924-6835.

New Low Price
$3,500

Fifty point version available, $2750. Also, ask about our instrument rental plan.

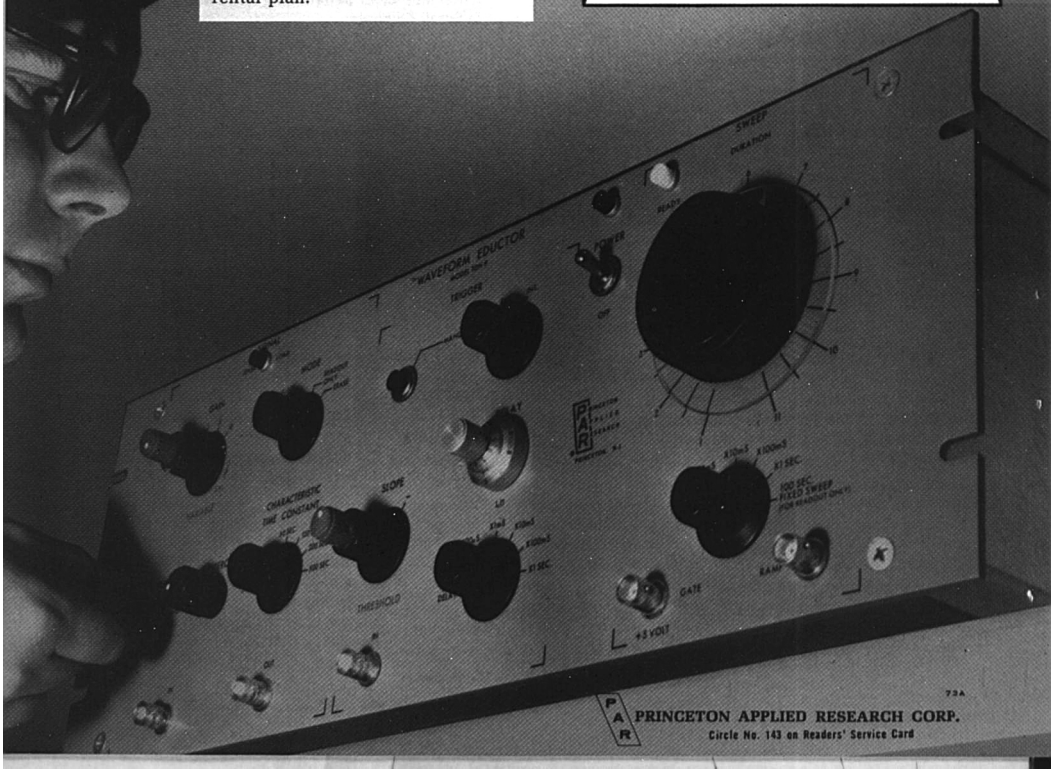

73A

PRINCETON APPLIED RESEARCH CORP.

Circle No. 143 on Readers' Service Card

Plutonium Determination in Soil by Leaching and Ion-Exchange Separation

Plutonium was measured in 100 grams of soil by leaching, ion-exchange, and alpha spectrometry. Average recovery was about 60%, and the results were comparable with complete solution methods.

NORTON Y. CHU, Health and Safety Laboratory, U. S. Atomic Energy Commission, New York, N. Y. 10014

Anal. Chem., 43, 449 (1971)

Isothermal Gas Chromatographic Separation of Carbon Dioxide, Carbon Oxysulfide, Hydrogen Sulfide, Carbon Disulfide, and Sulfur Dioxide

A gas chromatographic column has been developed which enables the simultaneous separation and analysis of sulfur gases. This column was prepared from acid washed "Deactigel."

WILLIS L. THORNSBERRY, JR., Research and Development Laboratory, Freeport Sulphur Company, Belle Chasse, La. 70037

Anal. Chem., 43, 452 (1971)

Optimization of Experimental Conditions for Spectrofluorimetric Determination of Europium, Samarium, and Terbium as Their Hexafluoroacetylacetone–Trioctylphosphine Oxide Complexes

The effect of pH on the fluorescence of the hexafluoroacetylacetone/tri-*n*-octylphosphine oxide complexes of europium, samarium, and terbium was studied and optimum experimental conditions for analysis of these rare earths were determined.

R. P. FISHER and J. D. WINEFORDNER, Department of Chemistry, University of Florida, Gainesville, Fla. 32601

Anal. Chem., 43, 454 (1971)

Kinetic Study of the Beckmann Rearrangement of 6-α-Methyl-17 α-Acetoxyprogesterone-3-Oxime by Cathode Ray Polarography

The kinetic of Beckmann rearrangement was followed by polarography. It was observed that the polarographic method can be used to calculate the syn and anti isomers of steroidal oximes.

ARVIN P. SHROFF and CHARLES J. SHAW, Analytical Research Group, Division of Organic Chemistry, Ortho Research Foundation, Raritan, N. J. 08869

Anal. Chem., 43, 455, (1971)

Spectrophotometric Determination of Cobalt with Benzil Mono-(2-Pyridyl)Hydrazone

A spectrophotometric determination of cobalt, based upon the absorbance of a CoL_2^{+} complex at 535 nm ($\epsilon = 27{,}400$), is described. The method without separation is accurate for traces of cobalt.

RONALD T. PFLAUM and E. SCOTT TUCKER III, Department of Chemistry, University of Iowa, Iowa City, Iowa

Anal. Chem., 43, 458 (1971)

Analysis of Polyethylene Terephthalate Prepolymer by Trimethylsilylation and Gas Chromatography

A method for the determination of ethylene glycol, diethylene glycol, terephthalic acid, and both mono- and bis-(2-hydroxyethyl) terephthalate in polyethylene terephthalate prepolymers was developed. The precision and accuracy were within 10% for each compound.

E. R. ATKINSON, JR., and S. I. CALOUCHE, Analytical and Chemical Section, Firestone Synthetic Fibers Company, Box 450, Hopewell, Va. 23860

Anal. Chem., 43, 460 (1971)

Gas–Liquid Chromatography of Some Irritants at Various Concentrations

Methods are described for determining α-bromobenzylnitrile (CA), *o*-chlorobenzalmalononitrile (CS) and α-chloroacetophenone (CN). For quality control, the accuracy is within ±1%. Vapor concentrations as low as 0.1 mg/m^3 can be measured.

SAMUEL SASS, TIMOTHY L. FISHER, MICHAEL J. JASCOT, and JOHN HERBAN, Chemical Research Laboratory, Research Laboratories, Edgewood Arsenal, Edgewood Arsenal, Md. 21010

Anal. Chem., 43, 462 (1971)

Suppression of Interferences by Sodium Sulfate in Trace Chromium Analyses by Atomic Absorption Spectrometry

The presence of 1% Na_2SO_4 in samples to be analyzed for trace amounts of chromium by atomic absorption spectrophotometry will eliminate the interferences caused by large amounts of contaminants.

J. A. HURLBUT and C. D. CHRISWELL, Department of Chemistry, Metropolitan State College, Denver, Colo. 80204

Anal. Chem., 43, 465 (1971)

Separation of Perrhenate, Molybdate, and Selenite Ions on Silica Gel

The rapid separation of the above anions is described and the influence of solvent system and the TLC medium is presented.

ALAN M. PHIPPS, Raytheon Co., MPT Division, Waltham, Mass.

Anal. Chem., 43, 467 (1971)

Fluorometric Determination of Submicrogram Quantities of Zirconium

A fluorometric method for zirconium using 3,4',7-trihydroxyflavone in a sulfuric acid solution has a detection limit of 0.05 μg, a precision to about 1% on 5 μg, and excellent tolerance to most common elements.

T. D. FILER, Health Services Laboratory, U. S. Atomic Energy Commission, Idaho Falls, Idaho

Anal. Chem., 43, 469 (1971)

Can you pass this test on x-ray spectroscopy?

(1) ☐ True. ☐ False. There are commercially available x-ray spectrometers that can routinely detect Al down to 15 ppm in steel, or Cu in brass with a precision of ±0.15%.

(2) ☐ True. ☐ False. The bugaboo of pulse height analysis is over. Modern spectrometers require PHA settings only once. They need no recalibration for change of 2Θ. And they permit qualitative scans of a selected single order of reflection.

(3) ☐ True. ☐ False. New equipment permits you to discover by visual monitoring, before the analysis is completed, an error in the count caused by interference from an escape peak, high-count rate shifts, or high-order coincident reflections.

(4) ☐ True. ☐ False. There's no need to reconstruct the calibration curve for a given element in a particular matrix. This is because systems are available that provide compensation for source intensity loss due to x-ray tube aging.

If you answered all questions "true," you probably know that only Siemens systems offer all of these advantages. If not, find out about them before spending your company's money on a less effective system.

For technical brochures on Siemens manual and fully automated x-ray spectrometers, contact Dieter Meusel at Siemens Corporation, 186 Wood Ave. So., Iselin, N.J. 08830. (201) 494-1000.

Siemens. A three billion dollar name in quality products.

SIEMENS

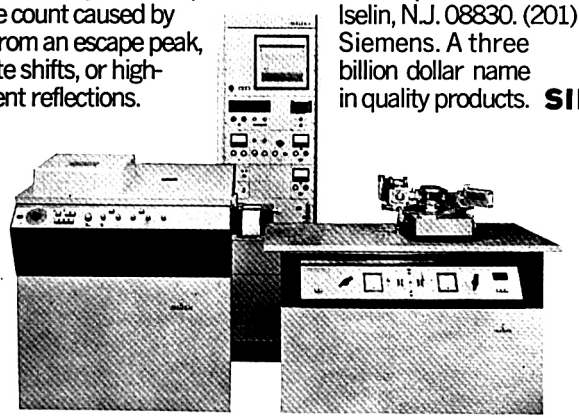

See us at the Cleveland show, booth 525-530.

Circle No. 166 on Readers' Service Card

Liquid–Liquid Extraction of Rhenium(VII) with Mesityl Oxide

About 25 μg was extracted from $1M$ hydrochloric acid and potassium chloride. Rhenium was subsequently determined photometrically as the thiocyanate complex.

V. M. SHINDE and S. M. KHOPKAR, Department of Chemistry, Indian Institute of Technology, Bombay-76, India

Anal. Chem., 43, 473 (1971)

Emission Spectrochemical Determination of Tantalum in Curium Oxide

A spectrochemical method for the determination of tantalum in curium oxide is described. The tantalum is separated from the curium oxide matrix by fusing with potassium carbonate, dissolving the melt in HCl-HF mixture, and isolating the tantalum by solvent extraction.

R. H. GADDY, Savannah River Laboratory, E. I. du Pont de Nemours & Co., Aiken, S. C. 29801

Anal. Chem., 43, 475 (1971)

Novel Technique for Surface Analysis of Solid Metallic Specimens Using Selected Anodic Current–Voltage Characteristics

Corroding alloys exhibit anodic current maxima which can be a function of chemical composition only. Measurement of several such maxima enables an analysis of the alloy surface to be obtained.

GEORGE TODD and G. A. WILD, Royal Armament Research and Development Establishment, Fort Halstead, England

Anal. Chem., 43, 476 (1971)

Boron–Polyethylene Irradiation Containers for High Energy Neutron Activation Analysis

Polyethylene-boron irradiation containers were evaluated for fast neutron activation. Employed with cadmium shielding, they resulted in as much as two orders of magnitude reduction (n,γ) thermal and resonance neutron activation.

W. A. JESTER and K. N. PRASAD, Department of Nuclear Engineering, The Pennsylvania State University, University Park, Pa. 16802

Anal. Chem., 43, 481 (1971)

Determination of Iron by EDTA Titrimetry of the Thiocyanate Complex

A highly selective method for iron is obtained by combining isoamyl alcohol extraction of iron(III)-thiocyanate with EDTA titration at pH 2–3. Good precision is maintained down to 50 μg.

ANTONIO DE A. FIGUEIREDO, Instituto de Tecnologia Alimentar, Rua Jardim Botanico, 1024, ZC-20, Rio de Janeiro, Brasil

Anal. Chem., 43, 484 (1971)

Confirmation of High Aromaticity of Anthracite by Broadline Carbon-13 Magnetic Resonance Spectrometry

Broadline Carbon-13 magnetic resonance spectra of Dorrance anthracite (92.7% carbon) and solid adamantane are presented and discussed in terms of the chemical structure of the former.

H. L. RETCOFSKY and R. A. FRIEDEL, U. S. Department of the Interior, Bureau of Mines, Pittsburgh Energy Research Center, 4800 Forbes Ave., Pittsburgh, Pa. 15213

Anal. Chem., 43, 485 (1971)

New Method for Separation of Americium from Curium and Associated Elements in the Zirconium Phosphate–Nitric Acid System

A new, simple method is described for the rapid separation of americium from curium, other actinide elements, lanthanide elements, and cesium. The method is based on our recent observation of the negligible sorbability of Am(A) on the cation exchanger, zirconium phosphate, from dilute nitric acid.

FLETCHER L. MOORE, Analytical Chemistry Division, Oak Ridge National Laboratory, Oak Ridge, Tenn.

Anal. Chem., 43, 487 (1971)

Aids for Analytical Chemists

Rapid and Efficient Method for Removing Viscous Polymer Solutions from NMR Sample Tubes

ALEX JAKAB, Research Division, Goodyear Tire and Rubber Co., Akron, Ohio 44316

Anal. Chem., 43, 489 (1971)

Simple Device for Transferring Thin-Layer Chromatographic Fractions for Spectroscopic Examination

COLIN J. CLEMETT, Unilever Research, Port Sunlight Laboratory, Port Sunlight, Wirral, Cheshire, L.62 4XN, U. K.

Anal. Chem., 43, 490 (1971)

Modulated Power Unit for Driving Metal Vapor Discharge Lamps

F. M. HAMM, T. L. MARTIN, and P. B. ZEEMAN, Department of Physics, University of Stellenbosch, South Africa

Anal. Chem., 43, 490 (1971)

Simple Continuous Electronic Readout for Rotameter-Type Fluid Flow Measuring Devices Using a Photoelectric Transducer

SEYMOUR LOWELL and STEWART KARP, C. W. Post College, Long Island University, Greenvale, N. Y. 11548

Anal. Chem., 43, 492 (1971)

Low Cost Parallel-to-Serial Converter for Digital Instrumentation

MORTEZA JANGHORBANI, JOHN A. STARKOVICH, and HARRY FREUND, Department of Chemistry, Oregon State University, Corvallis, Ore. 97331

Anal. Chem., 43, 493 (1971)

Ceramic Pressure Device for Preparation of Known Gas Concentrations at the 100 Parts-per-Million Level

HERMAN D. AXELROD, RONALD J. TECK, and JAMES P. LODGE, JR., National Center for Atmospheric Research, Boulder, Colo. 80302 and RAYMOND H. ALLEN, R. H. Allen Co., Boulder, Colo. 80302

Anal. Chem., 43, 496 (1971)

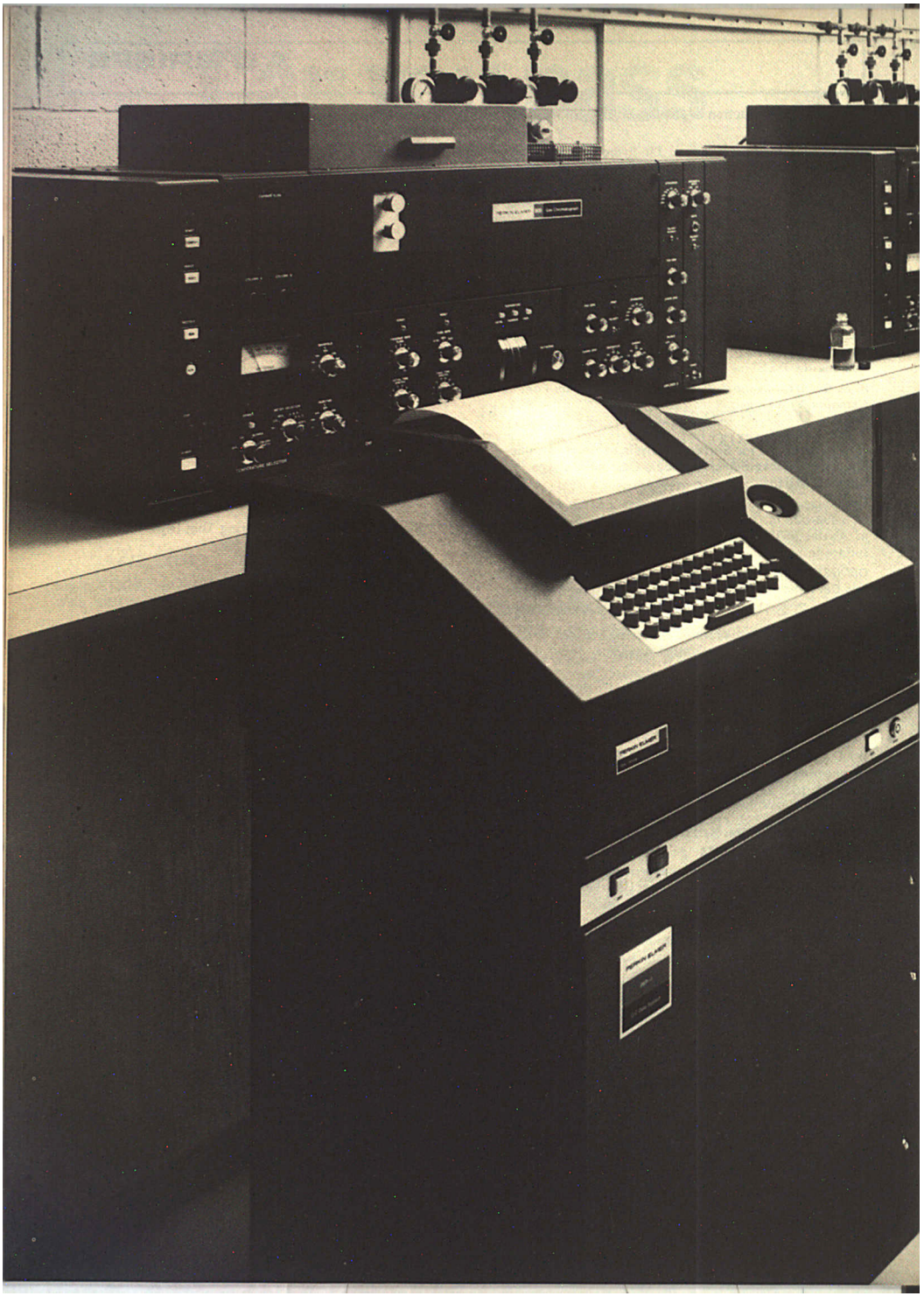

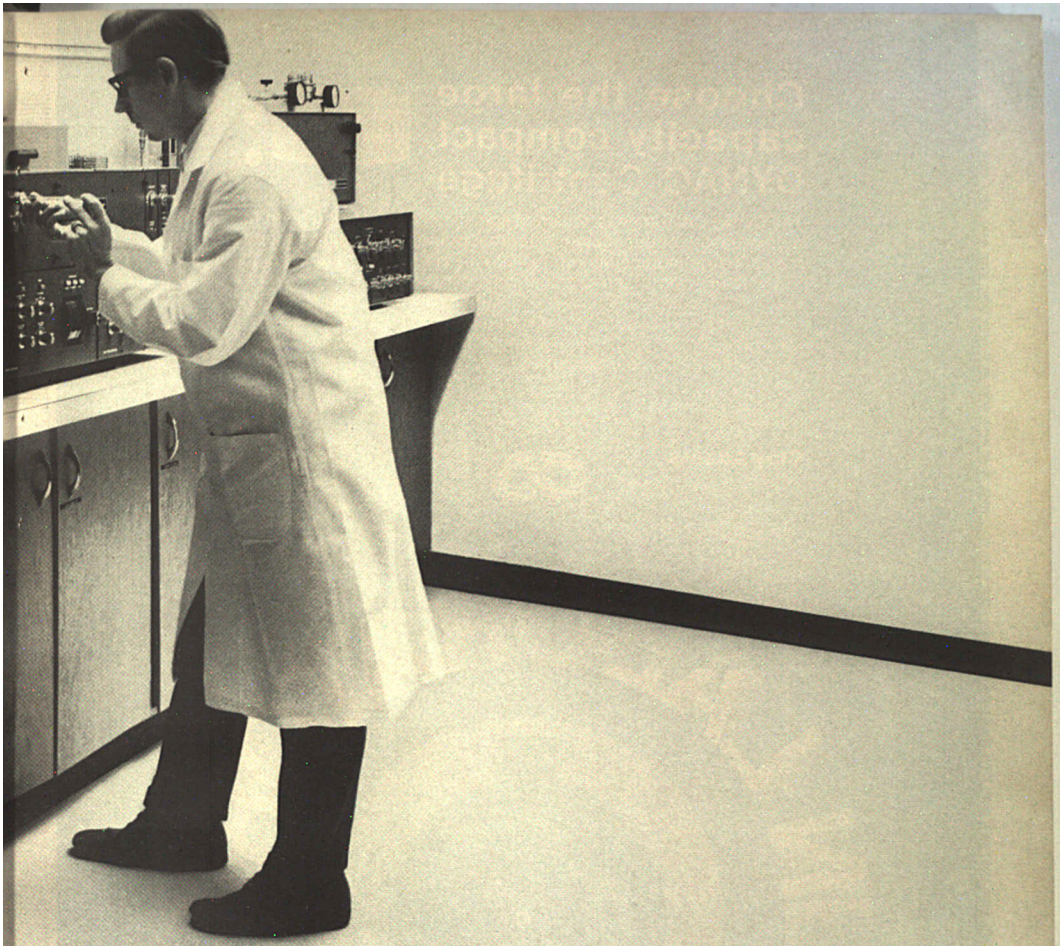

Now there's something better than the computer for gas chromatography.

It's the Perkin-Elmer Gas Chromatography Instrument System. This new system does *automatically* all the calibrations and calculations an educated operator would do. With computer power. At computer speeds and accuracy. At a fraction of computer cost. And gives you a printed analytical report.

If you operate even one or two gas chromatographs, the Perkin-Elmer Instrument System can compete in cost with electronic integrators and yet expand to handle eight gas chromatographs simultaneously.

It is the first data system designed and built by an analytical instrument company, specifically for chromatographers. A dedicated on-line system, it requires no knowledge of computer techniques. Yet you get all the power of the large, on-line or time-sharing computers.

The built-in Perkin-Elmer program allows you complete flexibility in developing your analytical method —using your standard analytical procedures—free of programming responsibility.

Operation is simplicity itself. You simply inject your sample and push the INJECT button. With no further human intervention the typed-out analysis is produced, based on the analytical method you have selected. Because the interface delivers an already digitized signal to the processor, the need for an integrator is eliminated. Retention time, peak area and the correct baseline are determined "post mortem" after the peak has fully emerged rather than "on the fly" as with an integrator.

We deliver it. We put it in operation. We service it. We guarantee it. We can have you using it correctly, all in the same day.

This Perkin-Elmer System is compatible with ours and other gas chromatographs and it is available now.

For a detailed description of this unique new Gas Chromatograph Instrument System write to Instrument Division, Perkin-Elmer Corporation, 702 Main Avenue, Norwalk, Conn. 06852.

PERKIN-ELMER

Circle No. 136 on Readers' Service Card

Choose the large capacity compact DYNAC Centrifuge

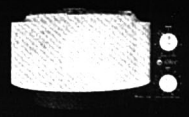

The Dynac Centrifuge is designed specifically to meet the need for a high quality but economical approach to all centrifuge requirements. Large in capacity (up to 400 ml.) but only ten inches high, this versatile centrifuge accommodates over 50 different combinations of tubes (from micro to 100 ml.). It has a wide speed range (up to 5500 RPM) with solid state electronic control, automatic 30 minute timer, electric brake and is available at half the cost of centrifuges with comparable features.

For more information, contact your Clay Adams dealer or write:

Clay Adams
Division of
Becton, Dickinson and Company
Parsippany, N. J. 07054

DYNAC, and are trademarks

IN LABORATORY SEPARATIONS

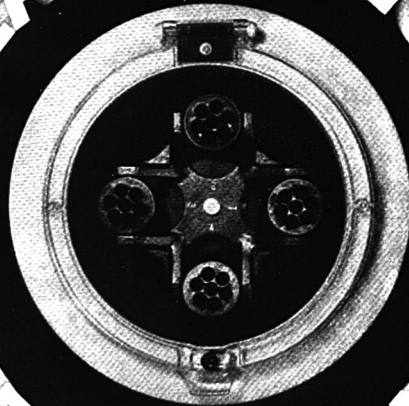

Circle No. 40 on Readers' Service Card

Fill yourself in on supplies for TLC

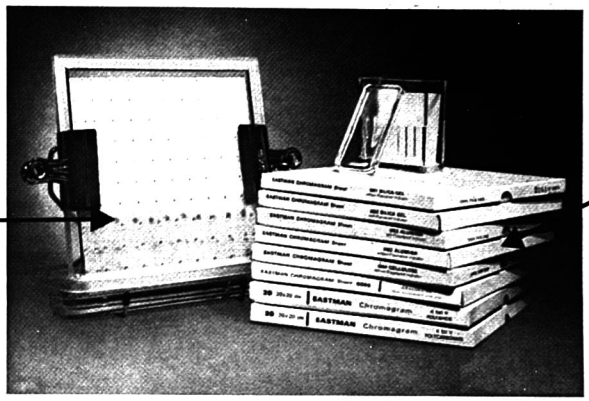

☐ A choice of eight types of precoated EASTMAN CHROMAGRAM Sheet—convenient, uniform, flexible.

☐ A choice of two developing chambers.

- ☐ EASTMAN CHROMAGRAM Developing Apparatus—fast equilibrating, easy to use and store.
- ☐ EASTMAN CHROMAGRAM Developing Jar—small and inexpensive; just right for pretesting and short migrations.

☐ Conveniently located local stocks of these TLC supplies are available from:

Use the coupon below to request information on these specific subjects:

- *TLC Visualization Reagents and Chromatographic Solvents* (Kodak Publication No. JJ-5)
- *TLC with* EASTMAN CHROMAGRAM *Sheet and Developing Apparatus* (Kodak Publication No. JJ-6)
- *Bibliography on the Use of* EASTMAN CHROMAGRAM *Sheet in TLC*, revised August, 1970 (Kodak Publication No. JJ-7)
- *TLC Analysis of Toxic Drugs Using* EASTMAN CHROMAGRAM *Sheet* (Kodak Publication No. JJ-37)

B&A	**HOWE & FRENCH**	**SARGENT-WELCH**
CURTIN	**NORTH-STRONG**	**SCIENTIFIC PRODUCTS**
FISHER	**PREISER**	**WILL/VW&R**

West of the Rockies, your dealer can obtain quick delivery of Eastman Organic Chemicals and Laboratory Supplies from our newly established stock in San Ramon, California.

Thank you for reading this advertisement.

Eastman Kodak Company
Eastman Organic Chemicals
Dept. 412L
Rochester, N.Y. 14650

Please send me: ☐ JJ-5 ☐ JJ-6 ☐ JJ-7 ☐ JJ-37

Name

Address

City

State Zip

3-40

Kodak

Circle No. 56 on Readers' Service Card

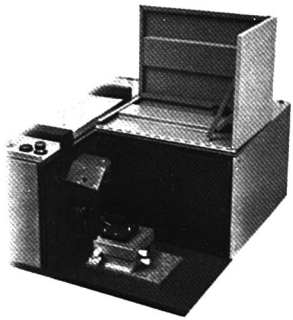

If you're now involved in infrared spectroscopy, it would be worthwhile for you to take a close look at the new Cary 83 laser Raman spectrophotometer. The most obvious advantage is that, complete with A+ laser, the new 83 is still priced under $15,000. But low cost is only the beginning.

RAMAN vs IR

The Raman technique itself, although entirely complementary to infrared, offers several important advantages over IR. Scanning range, for one. Typically, from near 0 to 4000△cm^{-1} (it takes two IR instruments to cover this range). Also, inorganic and biological molecules in aqueous solution can be studied which might be prohibitively difficult, if not impossible, using IR.

Furthermore, many group frequencies, which are either weak or absent in the IR, are strong in the Raman effect. (In general, symmetric vibrations are strong in Raman and weak in IR.)

Finally, sample handling is greatly simplified with Raman because little or no preparation is needed to obtain spectra from liquids, powders, single crystals, gases, polymers and even small single fibers.

COMPACT DESIGN, EASY OPERATION

The solid-state, bench-top Cary 83 is contained in a compact, highly functional housing. Controls are all simple to use and are within easy reach. Scale with the 83 is IR-compatible to facilitate direct comparison between IR and Raman spectra. Also, space has been provided for the mounting of optional pen and scan position encoders for on-line computer interfacing and processing of Raman data. And the 83's flat bed recorder, coupled to the scanning mechanism, presents spectrum in full view.

cary

LARGE SAMPLE COMPARTMENT

The spacious, 9.5″x 12″x 18″ sample area of the new Cary 83 was designed for both convenience and accessibility. Its unique double-hinged cover may be opened just from the front, swung back (above) or completely removed, if desired.

To get the complete story on the new Cary 83, contact Cary Instruments, a Varian subsidiary, 2724 South Peck Road, Monrovia, California 91016. Ask for data file 102.

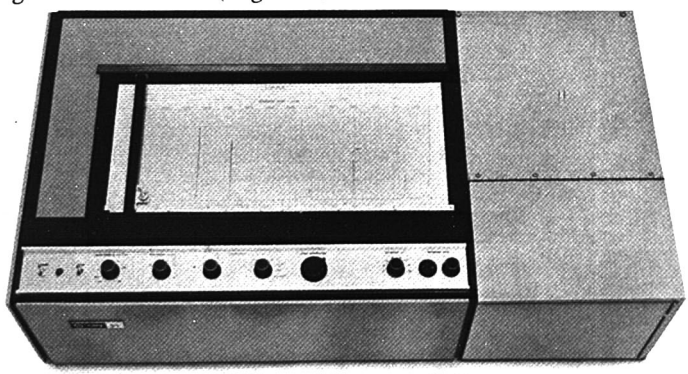

The Cary 83.
A new low in laser Raman spectroscopy.

Circle No. 185 on Readers' Service Card

New, dependable Speedomax XL Recorders from Leeds & Northrup to meet all your research and test requirements

Speedomax XL 600 low-profile recorder

One- or two-channel, fixed- or multi-span. Range spans from 100 μV to 100 V, and degrees C.

Speedomax XL 610 low-profile recorder

One- or two-channel, fixed- or multi-span. Range spans from 1 mV to 1250 mV, and degrees C.

Speedomax XL 680 flat-bed recorder

One- or two-channel, fixed- or multi-span. Range spans from 400 μV to 100 V, and degrees C.

Speedomax XL 683 X-Y plus X-t recorder

Two recorders in one. Fixed- or multi-span; range spans from 400 μV to 100 V, and degrees C.

Speedomax® XL Laboratory Recorders offer the best of two worlds.

They are sensitive, highly-precise null-balance potentiometers that incorporate traditional Leeds & Northrup craftsmanship and reliability.

And they are superbly-styled, solidly-built portables that provide maximum versatility and convenience for a broad spectrum of laboratory applications.

Speedomax XL 600 and XL 610 are low-profile recorders with vertical chart travel. They come equipped with a handle and rubber feet for portability, and can be provided with a swivel base, or modified for rack or wall mounting. A tilt-out writing table facilitates jotting notes on the chart. Case dimensions are approximately 18" wide by 9" high by 11" deep.

Speedomax XL 680 and 683 are flat-bed recorders with horizontal chart travel. They come equipped with retractable tilting bracket in base. Rigid plastic dust cover is standard equipment. Case dimensions are 7¾" deep by 17⅜" wide by 6⅜" high (6¾" high with dust cover in place).

A number of standard and optional features are common to all Speedomax XL recorders. They include:

- All-solid-state guarded circuitry.
- Single- or dual-channel recording with full-scale pen travel.
- Accuracy of ±0.25% of span.
- Single or switch-selected multiple spans.
- ±100% zero adjustment.
- mV or thermocouple calibration.
- Optional zero-left (reverse) range.
- Single, dual or multiple chart speeds.
- 250 mm (Nominal 10") calibrated charts.
- Scuff- and chemical-resistant cases.

Want more information? Contact your L&N Field Representative or write Leeds & Northrup, North Wales, Pa. 19454

Circle No. 110 on Readers' Service Card

Circle No. 111 on Readers' Service Card

Circle No. 112 on Readers' Service Card

Circle No. 113 on Readers' Service Card

LEEDS & NORTHRUP
North Wales, Pa. 19454

The three musketeers said it well: "One for all, and all for one." You can apply that to the Kofler Melting Point Apparatus and Reichert Thermopan Microscope with the Kofler Hot and Cold Stages. All work together for you.

Kofler Melting Point Apparatus can determine melting point in just one minute with a small sample. It's reliable, precise, and easy to operate. Now add the Thermopan Microscope, which is adapted for thermal microscopy, and offers superior quality, convenience and important attachments. The Micro Hot and Cold Stages hold the temperature steady—keep it that way—so you maintain the exact temperature you want throughout your entire observation.

One of the major features of the Thermopan is its convenient coarse and fine focusing with a single control. Another is the polarization equipment: polarizer is mounted below the stage in a swing-out ring mount.

Use the Thermopan to follow and record the behavior of each individual crystal before, during, and after melting and solidification. REICHERT AUSTRIA

Ask your AO Representative for a demonstration.

AMERICAN OPTICAL CORPORATION

SCIENTIFIC INSTRUMENT DIVISION • BUFFALO, N.Y. 14215

Circle No. 4 on Readers' Service Card

ATHOS PORTHOS ARAMIS

When three AO guardsmen join together; melting point determinations, thermal analysis, and purity tests come straight to the point.

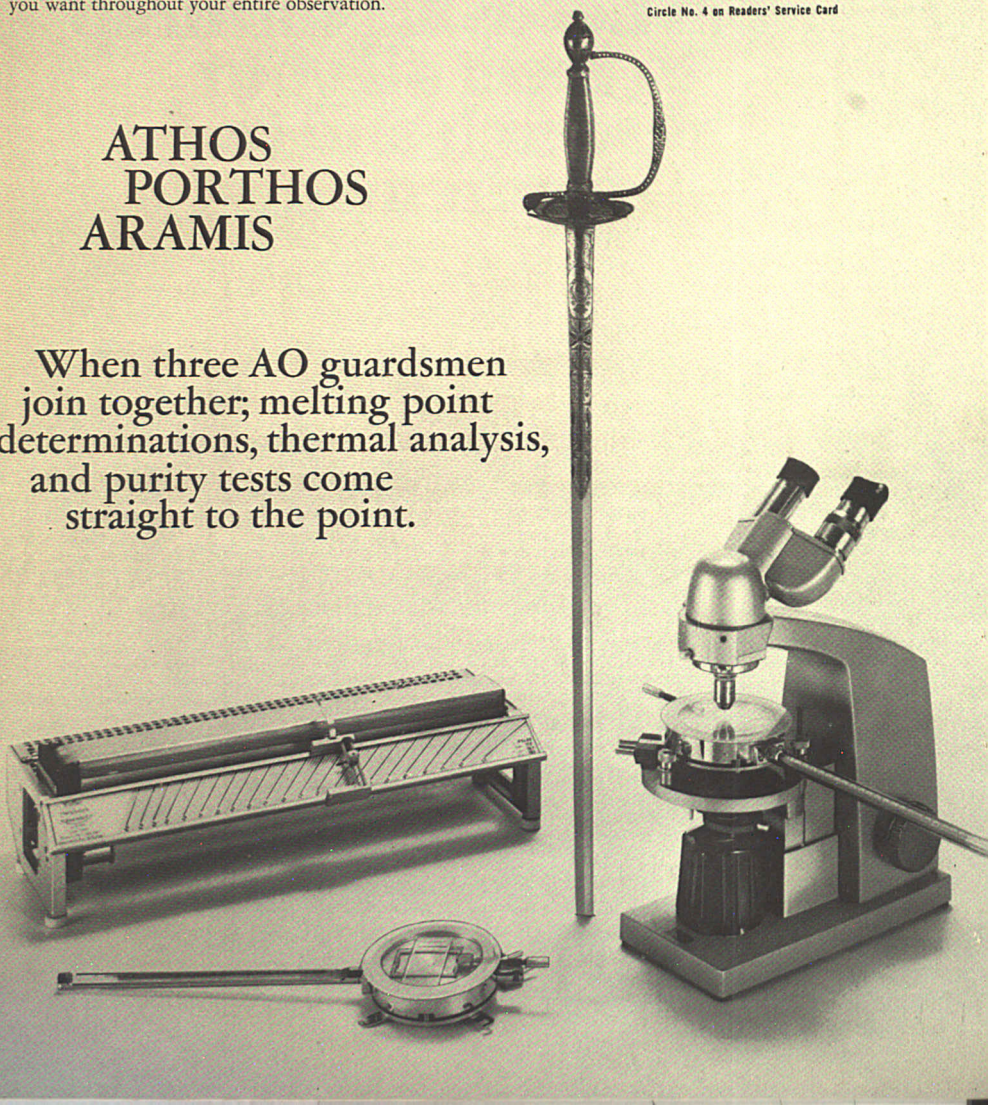

Merck has enough stable isotopes for practically anybody.

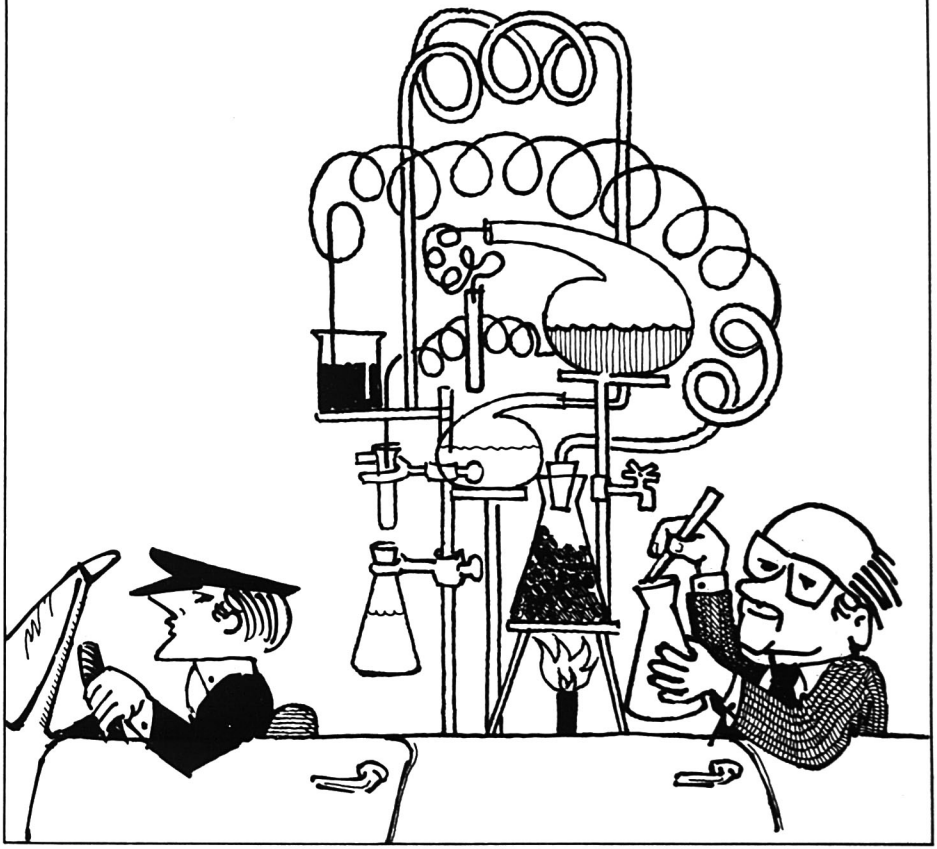

Including the people who want custom synthesis.

With more than fifteen years' experience, we keep almost 600 different isotopically labeled compounds ready to ship from stock.

But maybe you're the exception with a requirement for custom synthesis. That's another specialty of ours, and the most extensive available anywhere. In fact, the compound you want may already have been synthesized, but not kept in stock merely because of limited demand.

And to all our other capabilities in isotopes, we add fast delivery and order-taking by telephone. Talk to your man from Merck about a product list and prices. Merck Chemical Division, Merck & Co., Inc., Rahway, N.J. 07065

We think you should expect something extra

MERCK

Circle No. 125 on Readers' Service Card

Our all-glass U-column GC may well be the established standard in the life sciences.

HERE ARE SOME OF THE REASONS WHY NUCLEAR-CHICAGO'S SERIES 5000 HAS ACHIEVED SUCH WIDE ACCEPTANCE:

Reason No. 1.

The Series 5000 makes great separations. Fatty acids. Drugs. Pesticides. Bile acids. Steroids. Sugars. Vitamins. Even amino acids. And it makes them with minimum sample decomposition. Even the tough ones.

The inlet system is all glass to keep metal away from your samples in this high-temperature zone. (And we've just improved the port for more efficient injection and easier septum replacement.) In fact, sample degradation is minimized throughout the *entire* system.

The system has intake and exhaust dampers for efficient cool-down after each temperature-programmed separation.

The column is re-equilibrated at the *initial* temperature before the next run can start. Peak retention times are routinely reproducible. The electronic temperature programmer gives you oven-temperature reproducibility on a day-to-day basis. The gas flow controllers are insulated *and* isolated for the best stability available today.

Reason No. 2.

The Series 5000 can perform a greater variety of analyses than any other U-column GC. Accessory options such as Radioactivity Monitoring (RAM), Automatic Sample Injection (see below), Automatic Temperature Programming and Cool-Down, Pyrolysis (with better reproducibility than any other pyrolyzer), and Cryogenic Programming are all easily incorporated in this completely modular system.

Reason No. 3.

The Series 5000's low noise levels and excellent reproducibility permit smooth interface with all of the popular computers in laboratory use.

All system modules, including our new solid-state electrometer, are designed to help achieve this interface. The Series 5000 electrometer has unique temperature-controlled FET's, single-point grounds on individual PCB's, and independent outputs for recorder, integrator, and computer. That means exceptional baseline stability, very low noise level, short warmup time, and outstanding computer compatibility.

Our detectors have extremely low S/N ratios and unexcelled sensitivity. Our dual-zone detector oven has independent temperature controls for the successful use of multiple detectors. And it permits servicing of one zone while operating a detector at full sensitivity in the other.

Reason No. 4.

Our Model 5141 Automatic Sample Injection System multiplies your productivity. Permits 24-hour unattended operation for either isothermal or temperature-programmed analyses. Utilizes metal gauzes (to eliminate solvent peak) or "Hot Pop" PTFE capsules (to prevent sample evaporation prior to injection). Up to 72 solid samples, 35 liquid samples.

Reasons No. 5, 6, 7, 8 . . . . .

We maintain a complete inventory of chromatography supplies: Columns, phases, supports, syringes, recorders, detectors, hydrogen generator, et al.

We also maintain more than 30 sales and service offices in major cities from coast to coast.

But we can't tell it *all* here. The *proven* accuracy, the *proven* reliability, the *proven* productivity. All about all Series 5000 features and what they can mean to you.

Our new Series 5000 U-column brochure tells and *shows* it all. Send for it. Then you'll have *all* the facts. 0-228

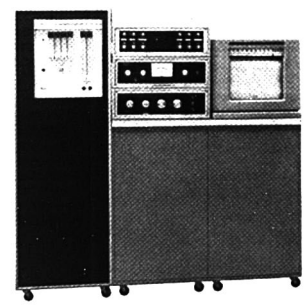

The Series 5000.
From Nuclear-Chicago.
The Up-and-Coming Chromatography People.

NUCLEAR-CHICAGO
A SUBSIDIARY OF G. D. SEARLE & CO.

2000 Nuclear Drive, Des Plaines, Illinois 60018, U.S.A.
Donker Curtiusstraat 7, Amsterdam W. The Netherlands ACS-13

Circle No. 138 on Readers' Service Card

AFS 6™

If this sounds like the most exciting development in flame analysis that you've heard about in recent years you're right. For more information about Technicon's AFS 6 Atomic Fluorescence Spectroscopy system, return this coupon to Technicon Industrial Systems, Dept. 118, Tarrytown, N.Y. 10591. We'll send you a brochure, some recent papers on atomic fluorescence spectroscopy and an application questionnaire.

Name _____

Title _____

Company/Institution _____

Address _____

City _____ State _____ Zip _____

Area Code _____ Phone _____

Ext. _____

Simultaneous multi-element analysis. Technicon® AFS 6 Atomic Fluorescence Spectroscopy System.

- ☐ 6 analytical channels
- ☐ 100 samples/hour...600 analyses
- ☐ Automatic sample handling
- ☐ Easy to operate
- ☐ Fluorescence and/or emission
- ☐ Readout in concentration terms

Technicon Industrial Systems
A Division of Technicon Instruments Corporation
Tarrytown, New York 10591

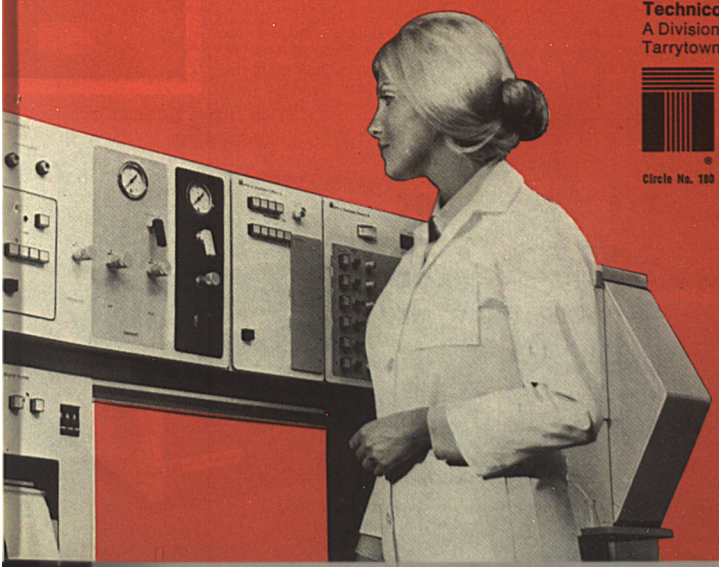

Circle No. 180 on Readers' Service Card

BAUSCH & LOMB
ANALYTICAL SYSTEMS DIVISION

spectronic® system 400

Readings you can trust

Here's why...

■ Greater stability than any other spectrophotometric system—typically, zero drift (T only) less than 0.2%/day. ■ Assured electronic performance—with exclusive, 6-position calibration test switch. ■ Error-proof sampling with automatic sampling and purging. Zero-error micro flow-thru cell prevents sample carry-over and mixing. Sampling and purging times—adjustable. Sampling indicator lights—user always knows whether sample is in the cell, out of cell, or purging. ■ Instant operating mode selection—manual, semi-automatic, fixed or variable time-rate. ■ Positive sample identification and data presentation—identification from 1 to 99, and manual data entry via the keyboard. ■ Direct readings on a four-digit electronic display and paper tape printout—linear absorbance, transmittance, or concentration—with selectable positioning of the decimal point. ■ Over-and-under-range—indicating instantly on both printout and electronic display. ■ Continuous wavelength—precise grating monochromator covers 335-925nm. ■ High optical resolution—with an 8.0nm bandpass. ■ Constant temperature controllable over a wide range for kinetic analyses—with optional temperature-regulated cell.

Later time-and-motion saving modules and computer compatibility provided for. Write for Catalog 34-6032. Better still, see for yourself—with a demonstration why you can *trust the readings*. Analytical Systems Division, Bausch & Lomb, 22 Linden Avenue, Rochester, New York 14625.

Mode, sample identification, time-rate controls.

Micro Flow-thru cell.

Pre-calibration control switch.

```
219  1971
       56
     143
     340
      .30
```
Month, Day, Year
Operator Number
Determination Code
Wavelength
Sample Temperature

Manual Data Entry

```
1   0564
2   0563
3   0563
4   0562
5   0562
6   0561
7   0561
8   0561
9   0560
10  0560
11  0559
```
Change of 5 milliabsorbances for SGOT reaction—one printout every 6 seconds.

Time-Rate Measurements

```
999  9999
```
Sample is over- or-under range

```
219  1971
       57
     144
     440
      30
```
Identification data

```
1   0000
2   0500
```
Set Zero Concentration
Set known Concentration Standard

```
1   0141
2   0201
3   0168
4   0120
5   0133
6   0198
7   0102
8   0109
9   0194
10  0182
11  0149
```
Sample No. 1
Sample No. 2
Analyses of Copper in a solution in Concentration Mode.

Automatic printout in Sequential Mode.

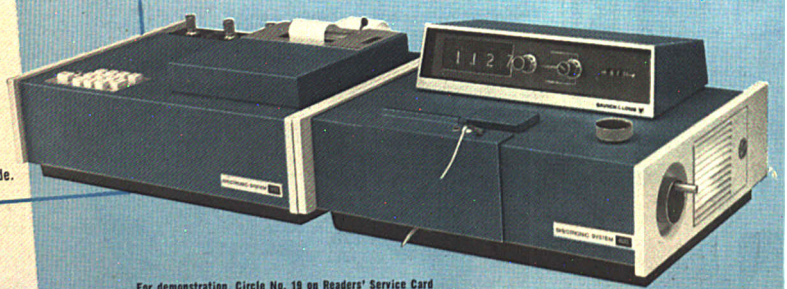

For demonstration, Circle No. 19 on Readers' Service Card
For information, Circle No. 17 on Readers' Service Card

SPECTROSCOPY IN INORGANIC CHEMISTRY

edited by C. N. R. RAO, Department of Chemistry, Indian Institute of Technology, Kanpur, India, **and J. R. FERRARO,** Chemistry Division, Argonne National Laboratory, Argonne, Illinois

CONTENTS OF VOLUME 2: J. A. KONINGSTEIN: Electronic Raman Transitions of Rare Earth Ions and Crystal Field Effects. J. R. FERRARO: High Pressure Vibrational Spectroscopy. A. P. B. SINHA: Fluorescence and Laser Action in Rare Earth Chelates. B. G. RAMSEY: Electronic Spectra of Organometalloids. K. D. J. ROOT and M. T. ROGERS: Electron Spin Resonance Spectra of Inorganic Radicals and Radical Ions. J. M. WILLIAMS and S. W. PETERSON: Molecular Structure Determination by Neutron and X-Ray Diffraction. H. A. KUSKA and M. T. ROGERS: Electron Spin Resonance of Coordination Compounds. Author Index-Subject Index.

April 1971, about 300 pp., $18.00
Volume 1: 1970, 422 pp., $19.50

INTRODUCTION TO MOLECULAR SPECTROSCOPY: Theory and Experiment

by E. F. H. BRITTAIN, W. O. GEORGE and C. H. J. WELLS, all at Kingston Polytechnic, Kingston-upon-Thames, England

Presents a balanced treatment of the principles of molecular spectroscopy and of their use in the determination of molecular structure and in chemical analysis. It also describes commonly available instrumentation and experimental methods. The book describes the principles, instruments and experimental methods of electronic, vibrational, and nuclear magnetic resonance and mass spectroscopy. Each chapter, dealing with one of these branches of spectroscopy, is divided into three sections covering principles, instrumentation and, finally, experiments designed to illustrate the topics discussed in the principles and instruments sections.

1970, 388 pp., $14.50

PAPER CHROMATOGRAPHY AND ELECTROPHORESIS

by GUNTER ZWEIG, Director, Life Sciences Division, Syracuse Univ. Research Corp., Syracuse, N. Y., **and JOHN R. WHITAKER,** Department of Food Science and Technology, College of Agriculture, Univ. of California, Davis, Cal.

VOLUME 2: **PAPER CHROMATOGRAPHY**

by JOSEPH SHERMA, Lafayette College, Easton, Pennsylvania **and GUNTER ZWEIG**

With contributions by **ARTHUR BEVENUE,** University of Hawaii, Honolulu, Hawaii

An up-to-date treatise devoted to the techniques of paper chromatography. It deals briefly with the history and theory of paper chromatography and covers in detail selected techniques and quantitative methods. The literature is surveyed to mid-1970. The remainder of the book describes the separation by paper chromatography of a wide variety of classes of organic and inorganic compounds including amino acids, fatty and organic acids, purines and pyrimidines, sugars, pesticides, vitamins, antibiotics, pigments, steroids, and many other miscellaneous compounds.

1971, 604 pp., $27.50

STANDARD METHODS OF CLINICAL CHEMISTRY

VOLUME 6

By The American Association of Clinical Chemists
Editor-in-Chief: RODERICK MACDONALD, Harper Hospital, Detroit, Mich.
Series Editor: J. STANTON KING, Jr.

This latest volume in a continuing series describes in detail tested and confirmed methods for clinical laboratory determinations. It offers the same features that have made previous volumes into reference works of immediate and lasting practical value. All methods presented are appropriate for general use in the average clinical laboratory, methods are given in enough detail to allow their direct use by any competent laboratory technician, and sources of instruments and chemicals, as well as authors' experience with the methods, are given in detail.

1970, 294 pp., $14.50

THE CHEMISTRY OF NONAQUEOUS SOLVENTS

VOLUME 3: Inert, Aprotic, and Acidic Solvents

edited by J. J. LAGOWSKI, Department of Chemistry, University of Texas, Austin, Texas

CONTENTS: MARION MACLEAN DAVIS: Bronsted Acid-Base Behavior in "Inert" Organic Solvents. D. F. BUROW: Liquid Sulfur Dioxide. RAM CHAND PAUL and SARJIT SINGH SANDHU: Acyl Halides as Nonaqueous Solvents. F. FEHER: Liquid Hydrogen Sulfide. ALEXANDER I. POPOV: Anhydrous Acetic Acid as Nonaqueous Solvent. ALEXANDER I. POPOV: Other Carboxylic Acids. Author Index-Subject Index.

1970, 416 pp., $21.00

ADVANCES IN MAGNETIC RESONANCE

VOLUME 4

edited by JOHN S. WAUGH, Department of Chemistry, Massachusetts Institute of Technology, Cambridge, Mass.

CONTENTS: WESLEY T. HUNTRESS, Jr: The Study of Anisotropic Rotation of Molecules in Liquids by NMR Quadrupolar Relaxation. PAUL D. SULLIVAN and JAMES R. BOLTON: The Alternating Linewidth Effect. RAGNAR A. HOFFMAN: Line Shapes in High-Resolution NMR. JEFF C. DAVIS, Jr. and K. K. DEB: Analysis of Hydrogen Bonding and Related Association Equilibria by Nuclear Magnetic Resonance. B. D. NAGESWARA RAO: Nuclear Spin Relaxation by Double Resonance. Author Index-Subject Index.

1970, 354 pp., $17.50

PHYSICAL PRINCIPLES AND TECHNIQUES OF PROTEIN CHEMISTRY

PART B

edited by SYDNEY J. LEACH, Russell Grimwade School of Biochemistry, University of Melbourne, Parkville, Victoria, Australia

CONTENTS: J. H. COATES: Ultracentrifugal Analysis. J. H. BRADBURY: Viscosity. S. N. TIMASHEFF and R. TOWNEND: Light Scattering. R. D. B. FRASER and E. SUZUKI: Infrared Methods. J. C. METCALFE: Nuclear Magnetic Resonance Spectroscopy. FRANK R. N. GURD: Binding of Protons and Other Ions. H. MORITA: Differential Thermal Analysis. Author Index-Subject Index.

1971, 491 pp., $24.00

AN INTRODUCTION TO GAS-LIQUID CHROMATOGRAPHY

by R. ALAN JONES, School of Chemical Sciences, University of East Anglia, Norwich, England

Provides a basic introduction to the practice of gas-liquid chromatography for organic chemists. Assuming only a basic knowledge of physical chemistry and physics, the book describes the principles of operation of the instrument and the interpretation of the results. An introductory chapter presents sufficient theory for a fundamental understanding of the practical aspects of the technique. The second part of the book comprises tables of reference which will be used for "on the spot" problems during the operation of a gas chromatograph.

1970, 214 pp., $8.00

RESEARCH TECHNIQUES IN NONDESTRUCTIVE TESTING

edited by R. S. SHARPE, Nondestructive Testing Center, Atomic Energy Research Establishment, Harwell, England

CONTENTS: Acoustic Emission. Ultrasonic Spectroscopy. Ultrasound Imaging Systems. Ultrasonic Critical Angle Reflectivity. Ultrasonic Holography. Optical Holography and Coherent Light Techniques. Data Handling Techniques. Direct-View Radiological Systems. Neutron Radiography. A Communication Network Approach to Sub-Millimetric Wave Techniques in Nondestructive Testing. Multiparameter Eddy Current Concepts. Pulsed Eddy Currents. Microwave Techniques. Infrared Techniques. Author Index-Subject Index.

1970, 492 pp., $23.00

ACADEMIC PRESS NEW YORK AND LONDON
111 FIFTH AVENUE, NEW YORK, N.Y. 10003

Circle No. 3 on Readers' Service Card

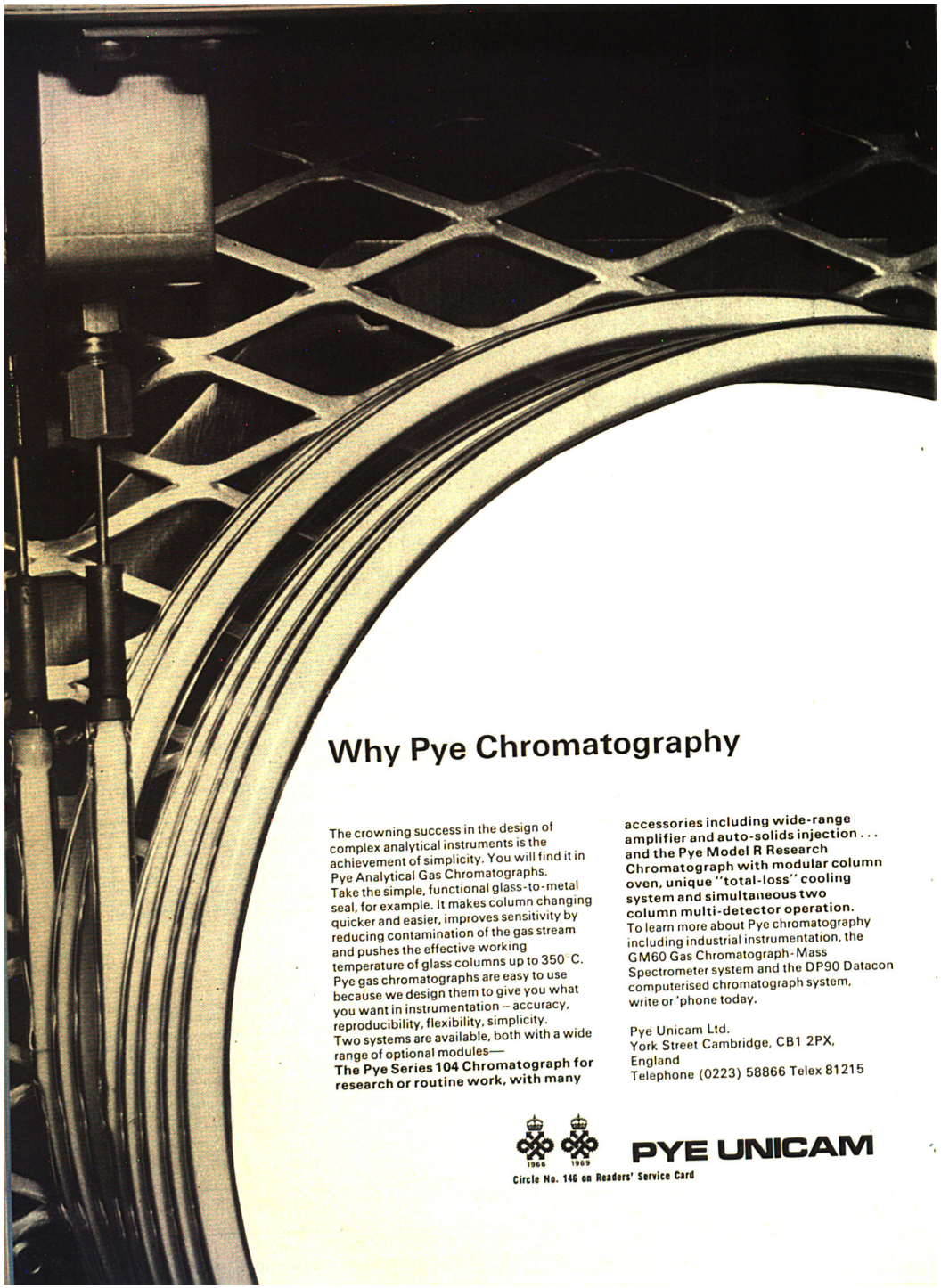

Why Pye Chromatography

The crowning success in the design of complex analytical instruments is the achievement of simplicity. You will find it in Pye Analytical Gas Chromatographs. Take the simple, functional glass-to-metal seal, for example. It makes column changing quicker and easier, improves sensitivity by reducing contamination of the gas stream and pushes the effective working temperature of glass columns up to 350°C. Pye gas chromatographs are easy to use because we design them to give you what you want in instrumentation – accuracy, reproducibility, flexibility, simplicity. Two systems are available, both with a wide range of optional modules—

The Pye Series 104 Chromatograph for research or routine work, with many accessories including wide-range amplifier and auto-solids injection . . . and the Pye Model R Research Chromatograph with modular column oven, unique "total-loss" cooling system and simultaneous two column multi-detector operation.

To learn more about Pye chromatography including industrial instrumentation, the GM60 Gas Chromatograph-Mass Spectrometer system and the DP90 Datacon computerised chromatograph system, write or 'phone today.

Pye Unicam Ltd.
York Street Cambridge, CB1 2PX,
England
Telephone (0223) 58866 Telex 81215

1966 1969 **PYE UNICAM**

Circle No. 146 on Readers' Service Card

The only AA unit with all these extras for $5450.

Corning® Model 240 Atomic Absorption Spectrophotometer

In our Model 240 you get the reliability chemists want for rapid routine determinations. Along with built-in features found only on more expensive research instruments. At considerably lower cost.

Among the advantages of this new, reasonably priced atomic absorption spectrophotometer:

Signal integration. The interpolation of variations in each reading is eliminated, increasing analytical precision. Noise, inherent in some procedures, is eliminated by signal integration. The result is displayed 18 seconds after cycle initiation.

Zero suppression in addition to continuous scale expansion. Scale expansion gives the Model 240 its low-level capabilities. And the unique zero suppression feature allows micro differences to be detected in macro concentrations.

Flame emission. We designed the Model 240 so you can switch rapidly from atomic absorption to flame emission spectroscopy for determinations best done by emission.

Readout. Direct readout appears on a mirrored meter, eliminating parallax. Corning has combined direct meter readout with the integration feature to make your readings even more precise. Other features: built-in recorder outputs, and a digital readout unit that can be plugged in.

The new Model 240 from Corning is the first atomic absorption spectrophotometer to give you all this capability at a reasonable price: $5,450. For full specifications, a convincing demonstration, or both, simply return the coupon.

Corning Glass Works
Scientific Instruments, Dept. AC-3
Medfield, Mass. 02052

☐ Please send complete data on the Corning atomic absorption spectrophotometer.

☐ Have your technical representative call and demonstrate.

Name _____

Title _____

Organization _____

Address _____

City _____ State _____ Zip _____

Area Code _____ Phone No. _____ Ext. _____

CORNING
SCIENTIFIC INSTRUMENTS

Circle No. 38 on Readers' Service Card

The only GC integrator that automatically calculates

The new 3370B Digital Integrator introduces an entirely new and unique automatic tangent baseline capability . . . and sets a new standard for integration accuracy.

The electronic integrator has automated GC calculations and greatly improved the quantitative accuracy of the method. But the fact remains that no integrator has ever been able to base its peak area calculations on anything other than a horizontal baseline. As a result, the best of them can produce serious area count inaccuracies when there is a drifting baseline: area count losses of 10% to as much as 1000% are not uncommon in the case of a peak that appears on the tail of a solvent.

The new 3370B literally puts an end to this problem. Whenever the rear slope of a peak drops below the original baseline, it instantly and automatically performs the necessary mathematical computations that enable it to discover a tangent to the baseline. Since it continues to accumulate the area count until it has established the tangent, it accurately integrates the total area under the peak. No other integrator can do this; no computer can do better.

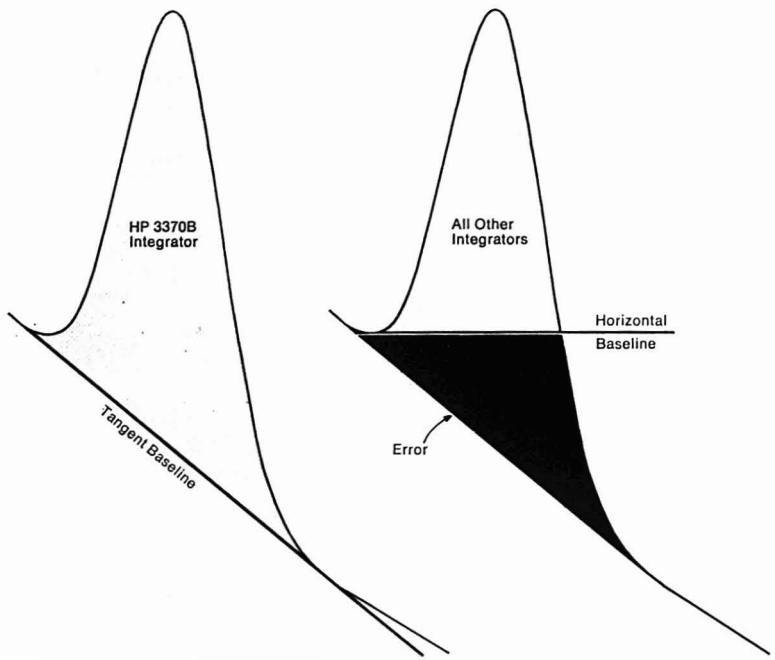

tangent baselines

. . . and accurately tracks the baseline under all drift conditions

The 3370B's ability to integrate peak areas accurately doesn't stop with its unique automatic tangent baseline capability. It is also the only integrator (except for its predecessor, the 3370A) that can track the baseline accurately under all drift conditions . . . because it has separate, independent *up* and *down* slope sensitivity controls.

With upward baseline drift, for example, the only way to start and stop integration accurately—and thus track the baseline accurately—is with low sensitivity for the *up* slope and high for the *down* slope. Precisely the opposite combination is required for downward drift. No integrator with a single slope sensitivity control can do a good job on the *up* slope without compromising its ability to handle the *down* slope properly, and vice-versa. Gross baseline errors

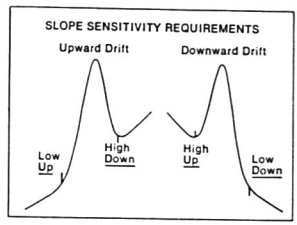

can therefore occur in the one case or the other, except with the 3370B.

In addition, the 3370B has an adjustable area threshold control that automatically eliminates any small peak from 1 to 1000 area counts, without compromising its sensitivity. Its range of noise suppression has been greatly expanded to allow integration even of very noisy detector outputs and of very slow peaks as are found in liquid chromatography and amino acid analysis.

With the 3370B, GC integration enters a new era of quantitative accuracy. Get all the facts from your local HP sales office or write for our new 10-page Bulletin 3370B. Prices start at $5300.
Hewlett-Packard, Route 41, Avondale, Pa. 19311. In Europe: 1217 Meyrin-Geneva, Switzerland.

HEWLETT hp PACKARD

ANALYTICAL INSTRUMENTS

Circle No. 85 on Readers' Service Card

43104

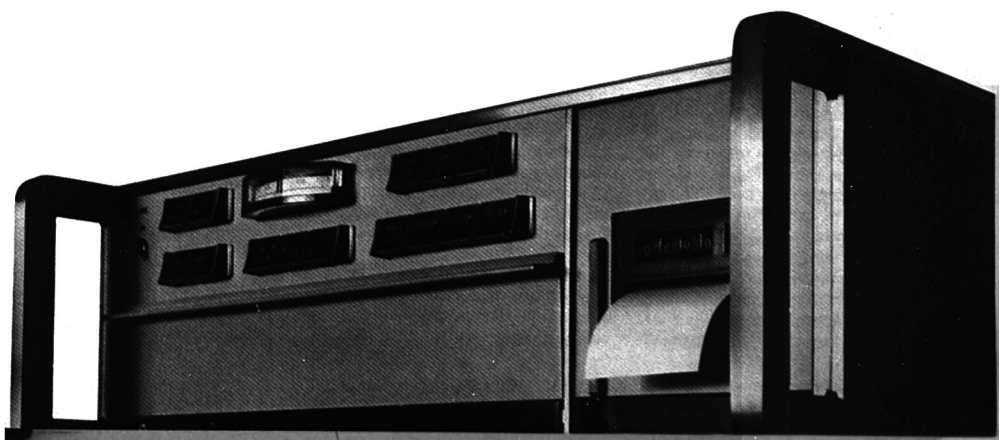

ANACHEM AWARD ADDRESS

The Pains and Pleasures of

The personal reminiscences of Dr. Stenger as related in his Anachem Award Address, October 15, 1970, provide interesting insight into the sort of problems that challenge industrial analytical chemists. The contributions of the analytical chemist are essential in many areas of industry.

THE PURPOSE OF THIS PAPER is twofold. First, I should like to show students of chemistry that industrial analysis is not necessarily a routine, boring occupation. It can be frustrating at times, but it can also be fascinating, instructive, humorous, and even exciting. It is usually pleasant, and it is always worthwhile if one dedicates himself to learning about what goes on in chemical systems. In this usage, perhaps, the term "chemical systems" may also include people. Secondly, I hope to encourage every analytical chemist as to the value of his or her individual efforts. The key to enjoying analytical work lies in knowing that the results will be useful and important.

In industrial chemical analysis there are pleasures to be enjoyed, and pains both to be taken and to be suffered. Hence, the title of the paper. It might have been "Thirty-five Years of Industrial Analytical Chemistry," but nobody would want to hear or read something of that duration. In any case, it is necessary to draw from personal experiences to illustrate my points.

One of the great pleasures of being an analytical chemist is that of being able to associate with exceptionally fine people. We have many in our own organization, our competitors and customers have others, and, of course, there are many in government labs and in the universities. For a person working in an industrial laboratory the opportunities for outside contacts are greatly increased by activity in technical organizations. It has been my privilege to work with the ACS Committee on Analytical Reagents and also to work earlier with the ASTM Committee on Chemical Analysis of Metals. Memories of the distinguished chemists who became my friends in those groups will always be treasured. The list would start with G. E. F. Lundell, W. D. Collins, and Edward Wichers, and would include many of the previous Anachem Award winners. Through the Analytical Division of the ACS I encountered many others. One of these was N. H. Furman of Princeton University. He had translated the first German edition of Kolthoff's "Volumetric Analysis," so we could commiserate on the difficulty of trying to keep Professor Kolthoff satisfied with our slow progress. I got a real lift from Furman's confession that whenever he spent an evening with the *Saturday Evening Post*, he felt guilty knowing that, in the meantime, Kolthoff had probably written three papers.

Initial Challenges

When I first came to the Dow Chemical Co. at Midland, Mich., it was my intention to gain a year of industrial experience and later go into teaching. Several things happened that first year to change my mind. A number of us were hired at about the same time, and the company, still a fairly small organization, arranged for us to tour some of the operating plants and to hear a few lectures on what was being done. In one of the lectures, Ivan Harlow, then chief chemist, spoke about the composition of brines occurring in different geological strata beneath Midland. It was quite interesting to learn that the brines varied in their bromine contents, and also that one could identify the source, independent of dilution, by determining the ratio of calcium to

VERNON A. STENGER
Analytical Laboratories, The Dow Chemical Co.,
Midland, Mich. 48640

Industrial Analytical Chemistry

magnesium. Previously I had been interested in rock analysis and had not thought much about brines.

Later that year I visited a well-known university to apply for a teaching position. During the interview I told the professor about those Midland brines. He did not seem impressed and I did not get the appointment, but he did me quite a favor by asking a simple question which I could not answer. He wanted to know how much fluoride was present in any of the brines. I still do not have an exact answer, but there is less fluoride than we can detect by any sensitive method tried. The reason I appreciated the question is that it opened my eyes to the possibility of learning much more about brines than I then knew, and it gave me an added interest in trace analysis. Subsequently, in about 1938, the company drilled into a deeper stratum yielding brine with a higher bromine content. Walter Kramer and I carried out the first complete analysis of this brine and discovered that it contained about 40 ppm of iodine. Others at Dow developed a process for recovering the iodine, and as a result, Michigan has become the leading state for iodine production in the U. S. We found significant concentrations of strontium and lithium in the brine, too. Later, Robert Goodenough, working in our group, developed processes for the recovery of those elements. The processes have not been used commercially but they are available in case a demand should arise. Needless to say, one of the pleasures of my career has been the opportunity to participate in developments such as these.

During that same first year Willard Dow sent a man over to the laboratory who said he could extract gold from sand. The sand could be taken from a river bank, or almost anyplace. A. W. Beshgetoor, our lab director, asked me to look over the process with him. The man had a big iron bowl, rather flat but rounded, into which he would put the sand, some water, and a little mercury. After stirring the mixture, he would pour off the sand and water, and the mercury remained as a surface layer on the iron. With a rubber spatula he would scrape off the mercury, dissolve it in nitric acid, and end up with a small golden crystal in the acid. We sent a crystal to a spectroscopist, who soon reported back that it was, indeed, gold. Meanwhile, we found that the metal would dissolve only in aqua regia, and that it would give the Cassius purple test. Obviously the man was showing us gold, but was it actually coming from the sand? Mr. Beshgetoor took him out to lunch, and while they were gone I operated the process a little myself. First I found that sand was not necessary. Just putting mercury and water in the bowl would produce gold. Then I found that the bowl, water, and spatula were not necessary either. Our man was using mercury which contained just enough gold to be interesting. When they returned from lunch I reported my findings, much to Mr. Beshgetoor's enjoyment. The promoter packed up his equipment and left, saying, "Here I have a valuable discovery, and you chemists are just too damned skeptical to appreciate it!"

The incident made me wonder why a capable executive like Dr. Dow would allow such a fellow to take up our time. I may have speculated also that chemical company management might occasionally need the aid of a chemist to screen out bad proposals from good ones. Back in Minneapolis I had sought a job with a paper mill, and had been told that they could afford a chemist only in periods of great prosperity. Be that as it may, the gold affair also taught me that an analytical chemist should not be content with carrying out a qualitative or quantitative analysis alone, but should look at the whole problem. Later I had an opportunity to talk with Dr. Dow about the incident. He said that the man had been a company customer, but had evidently taken on some new partners who had involved him in this shady deal. I said, "Then you did know all the time that it was probably a fake?" He laughingly replied, "Yes, but wasn't it fascinating?"

Problem-Solving in Analytical Chemistry

The point about an analytical chemist looking at the whole problem can stand some belaboring; Dr. Laitinen editorialized upon it rather gently in the September 1970 issue

The Nester/Faust 1240 introduces a new concept in high speed analytical liquid chromatography . . . a complete and self-contained precision instrument with features and capabilities that, until now, were only available on more complex and more costly units. To make our point, let's look at the 1240's outstanding features, one by one. First, easy operation and reproducible analyses are due, principally, to an adjustable 1,000 psi pump, with continuous degassing of solvent, and a zero dead-volume, zero back pressure pulse damper. Second, for gradient elution analysis, there's a precision gradient former available. Third, separation is enhanced by a standard, ambient to 125°C forced air oven with nitrogen purge. Fourth, fountain effect is eliminated by the zero dead-volume on-column septum injector. Fifth, we assure highest resolution by designing and manufacturing all our own columns and fittings. Sixth, the 1240 unit is supplied with a 2000 psi, 12 ul U.V. detector, with internal calibration. Ultimate detector sensitivity is 0.0002 O.D. units. In addition, a complete line of column packings is available. All of these features, plus more that we don't have room to discuss here, add up to some of the reasons why the 1240 is a unique analytical L.C. base priced at $4,900 . . . but don't let the price fool you, we haven't sacrificed quality anywhere in this instrument. For more information about the 1240 and its optional accessories, write or call today. NESTER/FAUST MFG. CORP., Instrument Products Division, 2401 Ogletown Road, Newark, Delaware 19711, (302) 737-6330. In Europe, contact: Steinengraben 44, 4000 Basel, Switzerland.

High speed...self contained...easy to operate high resolution...zero dead volume...and more

Circle No. 137 on Readers' Service Card

of ANALYTICAL CHEMISTRY. His points were that an analytical chemist should know enough about existing methodologies to choose the best one for application to a given sample, perhaps modifying it if necessary to fit the particular situation, and that there is also an analytical science which seeks, as its own goal, the improvement of analytical methodologies without regard to specific problems. Years ago, Dr. Lundell wrote about the "analysts" and the "determinators." The analysts were those who could take a sample as it was, apply suitable methods allowing for interferences, and come up with a correct analysis. The determinators were those who preferred to develop methods for single substances. They generally worked with pure solutions and were not concerned about interferences. Nowadays, with more and more instrumental methods in vogue, the analysts and determinators are coming closer together. Some may only be syringe-handlers, button-pushers, or turntable-feeders; the interferences are supposed to be taken care of automatically. Before a determinator can use an automatic system, however, a good analytical chemist has probably been needed to set it up, perhaps with the aid of a computer expert.

I like to think of an industrial analytical chemist taking on a whole problem, in the following sense: A product is found to depart from specifications in some way, perhaps showing an off-color, turbidity, or low melting point, or possibly a foreign peak in a spectrum or chromatogram. The first questions for the chemist are: what is it, and how much? For the production supervisor, though, the questions are: how does it get in, and how can it be kept out or removed? The complete answer requires characterization, measurement, some chemical detective work, and a knowledge of the physical and chemical properties of the impurity and of the rest of the system. That the answer be reached promptly is usually quite urgent; to produce bad material is uneconomical, and to shut a plant down is almost unthinkable. Problems of this kind can be pretty demanding. The analytical chemists who can handle them will be treated with respect.

I am concerned that chemistry students these days may be led to rely too much upon instruments, without learning enough about classical separation methods and the descriptive chemistry that should be taught in analytical courses. These kinds of knowledge are needed to solve our chemical problems. We should face this fact in our technical organizations and in our dealings with colleges and universities. There is an old saying: To be a good chemist one must first be a good analytical chemist. The converse may be even more true—to be a good analytical chemist one must first be a good chemist. We can teach instrumental analysis in industry, but we should not have to teach basic chemistry. Nevertheless, we all must continue to be students of chemistry.

Contributions in Product Development

It should not be thought that industrial chemical analysis deals only with quality control. Often the problem is with the use of a product. Years ago I was asked to participate in the early development of methyl bromide as a fumigant. Methyl bromide was a new and mysterious compound, volatile and quite toxic, and people were afraid to use it. Mr. Beshgetoor may have selected me for the assignment thinking that I was expendable. Questions arose as to how to determine whether, during a fumigation, the vapor would remain in a vault or warehouse long enough to be lethal to insects, whether it might poison someone outside, and how much might remain as a residue in a fumigated food. S. A. Shrader, Mr. Beshgetoor, and I developed methods for use in answering such questions, and published them. The necessary toxicological data were determined in the Biochemical Research Laboratory established somewhat earlier under Don Irish. One of my pleasures during that period consisted in receiving supplies of fine fresh foodstuffs, fumigating them, and preparing samples after periods of airing. I would carry out separations of the organic and inorganic bromide, and Dr. Shrader would determine the bromide in each fraction using Kolthoff and Yutzy's modification of the van der Meulen method. We established that practically any food would lose all of its methyl bromide within two days and that only a trace quantity of inorganic bromide would remain. For a given food, the amount of inorganic bromide remaining would be fairly proportional to the concentration of fumigant and the duration of exposure.

Incidentally, we could also carry home a fair amount of the food. The Stengers and Shraders ate unusually well in those days. At one time we had over 100 lb of fine Wisconsin cheese in the lab. Among other foods tested were hams, dehydrated vegetables, cereals, bakery products, butter, ice cream, chocolate, various kinds of nuts, etc. Thus, we established, not only by analyses, but by practical eating tests, that the foods were suitable for consumption. We, and others, recognized a problem in the fumigation of wheat flour: if an excessive concentration of methyl bromide were used, or if the same flour were fumigated repeatedly, a bad odor might be produced when it was baked into bread or when the bread was toasted. The odor was eventually attributed to the methylation of sulfhydryl groups in the protein, releasing a trace of methyl mercaptan or thio-ether upon heating. We got to be pretty good at recognizing such odors in complaint samples, and could confirm the cause, when it was overfumigation, by determining the bromide residue. My wife took part in this kind of work at home, baking the flour into bread or rolls which we tasted and smelled. Most commercial millers are highly reliable and when presented with our data would accept the fact that the flour had been overexposed. There were a few small outfits, however, that tried to blame fumigation for problems caused by old or moldy wheat. Our testing program thus saved the company considerable money in the early days. It has been continued as a service to fumigators, but whereas we used to determine bromides chemically, now they are done by X-ray fluorescence or by neutron activation, with a

THE NEW ULTRATIP™...

a high power ultrasonic processing horn

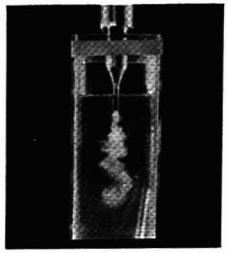

½" Ultratip cavitating oil in a glass pipe.

APPLICATIONS:

- Cell and tissue destruction
- Emulsification
- Accelerated Extraction
- Particle Dispersion
- Catalyst Activation
- Polymerisation and free radicals production
- Degassing, etc.

UNIQUE NEW FEATURES

- Automatic impedance matching with a Q-lock switch
- Maximum probe cooling (no fan) through the use of a magnesium front quarter-wave stub
- Instant and continuous power reading during probe operation
- Electro-acoustic efficiency as high as 85%
- Minimum heating, extended life under heavy duty conditions
- Advanced type solid state generator with integrated circuitry Frequency 23-24 kHz. Average RF power output 200-250 watts
- Computer designed catenoidal Horn
- Numerous accessories available (⅛" Microtip, Lump Mass, etc.)

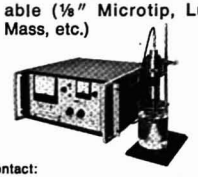

Contact:
WAVE ENERGY SYSTEMS INC.
NEWTOWN COMMONS
NEWTOWN, PA. 18940 (215) 968-3833

Circle No. 195 on Readers' Service Card

saving in time. However, in case of question, we would still rely on the old chemical method.

In one case there was a fatal accident during the fumigation of a flour mill. Two of the fumigators died from methyl bromide exposure and it was later established that they had failed to replace their gas mask canisters following previous fumigations. The charcoal had become saturated with methyl bromide. Nothing could be done for the men, but the milling company was in trouble. A city toxicologist had decided that if methyl bromide killed the men it must also have poisoned the tremendous amount of flour stored in the warehouse. Therefore, he ordered an embargo on shipments. Dow was notified and asked to provide technical assistance. Oscar Daniels and I worked all afternoon getting laboratory equipment packed and preparing bromide-free hydrochloric acid to be used in analysis of the flour. Then, with some other company representatives, we drove most of the night to reach the site of the accident. Part of the evening was taken up at the Canadian border, trying to help customs officials classify our lab apparatus properly; a threatened crisis there was solved by the decision that nickel crucibles, used for alkaline-ashing of the flour, could be classified as kitchenware.

After less than three hours of sleep, we went to work analyzing the flour, at 8 A.M. Fortunately some FDA men had been called in and they were acquainted with our paper on residue determinations. On that basis, they agreed that if the residues did not exceed what we felt to be reasonable for an ordinary fumigation, the flour could be released. This was my first experience demonstrating that a publication might have tangible value. The millers furnished us with samples of flour taken from freight cars that had already been loaded. As we turned out the bromide results and the data were favorable, the car would be hauled away. A vice president of the milling company stood by, and his spirits rose visibly as each car rolled out. We kept working right through until 2 A.M. the next morning, and he stayed with us until the last car was gone. I have seldom seen anyone more appreciative. Ever since then, our company has enjoyed an excellent relationship with his.

Work with Rare Earths

Another pleasure to be enjoyed by an industrial chemist is a very simple one, that of working with chemicals. The larger the company, the greater is the chance of encountering a wide variety of the less common elements and compounds. When alloys of magnesium and the rare earth elements were being studied, our group did much of the analytical work. We began by running total rare earths as oxalates, with ignition to oxides. Different sources of the rare earths were used, so that the individual elements varied in concentration. If I had to do one kind of routine analysis for the rest of my life, it would involve, preferably, the precipitation and filtration of rare earth oxalates. While the precipitates rest in the filter paper they show such beautifully delicate shades of light violet or green, according to the relative amounts of neodymium or praseodymium present. As the work progressed we added a determination of cerium volumetrically, then colorimetric methods for neodymium and praseodymium. Finally, Warren Crummett added spectrophotometric determinations of other elements, applying ultraviolet methods pioneered by H. E. Kremers of the Lindsay Light and Chemical Co. Later a sebacate precipitation was introduced by Wengert, Walker, and Loucks to give more complete recoveries of the rare earths and to allow separations from zirconium and thorium. We might have profited from flame photometry and atomic absorbance in those days, had they been available. Eventually, X-ray fluorescence proved to be of great value, and now, activation analysis is showing tremendous sensitivity for some of the elements. My points are, it was a pleasure to run these analyses and to see how the results could be correlated with the properties of the alloys, it was a challenging task to modify and expand the methods, and it is still

gratifying to learn how newer techniques can be applied.

Pains of Failures and Need for Reliable Data

What about the pains of industrial chemical analysis? There are, to be sure, the actual headaches of the job while a problem remains unsolved, but these arise from its urgency and excitement, and later become subjects of our reminiscences. All good vocations should have some headaches. A more real and undesirable pain is that which comes from failure to do a job correctly. In one of my early assignments, I was given a sample of calcium chloride from an electrolytic cell in which a researcher was trying to prepare calcium metal. The sample contained a dark sludge which interfered seriously with the electrolysis. I diagnosed the sludge as carbon, and thought that a sufficient proof consisted in rinsing and drying it, then igniting to get rid of the combustible part. Only a white residue, high in calcium, remained. The researcher tried to eliminate carbon from the system, but he always produced the sludge, and finally he gave up. Several years later I learned about the effect of boron on the electrolysis of magnesium, and the fact that calcium chloride from brine usually contains some borate impurity. Then I realized that by not actually proving the presence of carbon, and by failing to consider any other element, I had almost single-handedly kept the company out of the calcium business. This may not have been too bad, for an economic evaluator might have done the same with even less evidence, but it was no excuse. The job was done poorly and the memory is painful.

The suffering of pains of that kind can be avoided by taking the proper pains in one's work. Analytical chemists have always been concerned with accuracy. More and more they must become concerned with completeness of analyses and with the total reliability of conclusions, especially in respect to the systems involved in ecology. Traces of substances once thought harmless are now seen to cause problems. Other substances may be blamed, somewhat unjustly, as pol-

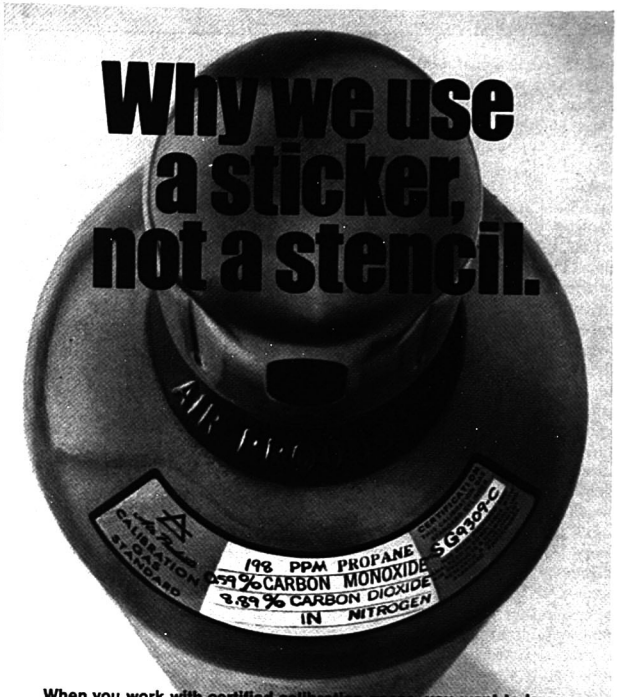

When you work with certified calibration gases, you want to know the exact analysis in the cylinder you're using. No matter whose gas it is, one cylinder's composition can differ from the next by a fraction of a percentage point.

That's why each Air Products cylinder carries a sticker-decal showing the precise figure written in . . . why we don't stencil a row of cylinders all with the same round numbers. Every Air Products cylinder is analyzed individually and carries its individual mark of accuracy.

Not only do we analyze what's in every cylinder but our gas mixtures are the only ones computer-blended. So you can be doubly certain of satisfaction when you order calibration gases from Air Products. Of course, for less demanding uses, we also supply batch-analyzed and unanalyzed mixtures. Contact your nearest Air Products sales office or send in this coupon.

Air Products and Chemicals, Inc.
Specialty Gas Department
733 West Broad Street
Emmaus, Pennsylvania 18049 Telephone (215) 395-8257

☐ Please send additional information on calibration gases.
☐ Send complete catalog of specialty gases and equipment.
☐ Have your representative call.

Name_____ Title_____
Company_____
Address_____
City_____ State_____ Zip_____

Air Products and Chemicals INC. AC-31

Circle No. 1 on Readers' Service Card

lutants; for example, phosphate detergents have taken a beating which a few people, including myself, think should have been administered to organic materials in sewage. Trichlorophenoxy acetic acid (2,4,5-T) and related compounds have been threatened with banishment as herbicides because of reported teratogenic effects on animals. These effects were not caused by the 2,4,5-T, but by an impurity present in the sample that was tested. The active impurity has been identified as a tetrachlorodiphenyldioxin; for a number of years its presence has been held below safe limits by those manufacturers who earlier recognized that the impurity could cause trouble. With pure 2,4,5-T, there is no problem. Another frequently maligned compound is DDT. The presence of DDT has been reported in almost every important living species. However, the gas chromatographic method frequently used for DDT determination has been classed as unacceptable by E. F. McFarren *et al.* who reported in the March 1970 issue of ANALYTICAL CHEMISTRY [ANAL. CHEM. 42, 358 (1970)]. I do not doubt that DDT is a threat to the environment if used improperly or too widely, but it would certainly be desirable to have all judgments made on the basis of completely reliable data. To get at the truth, conscientious analytical chemists, toxicologists, and biochemists must work together. One cannot say enough about the importance of the analytical chemists' contribution. Without it, the others can be completely misled.

Mercury?—Questions and Answers

Some of you may be interested in the question of mercury and its determination in the environment. This is a fascinating question with many aspects. It illustrates, again, the importance of analytical chemists looking at the whole picture. Gunnel Westöö in Sweden had developed a gas chromatographic method for the determination of alkyl and aryl mercuric compounds extracted from fish with benzene and dilute hydrochloric acid. She was interested in those compounds because of their use as slimicides, but it turned out that regardless of what compound was used, the mercury found in fish was present as a monomethylmercuric ion. The determination of mercury in foods in this country generally was being done by the dithizone method, but the digestion procedure used in the analysis would not convert methyl mercury completely to inorganic form, so low results were being obtained on fish. When the discovery of mercury in Great Lakes fish was made by Norvald Fimreite at the University of Western Ontario, it was done by neutron activation analysis. Chemists at the laboratories of Dow Chemical of Canada quickly recognized the importance of using an adequate digestion treatment prior to other types of analysis. They modified a procedure (previously used by others) so that it would give complete recoveries of alkyl mercury. This procedure was then employed in connection with the so-called flameless atomic absorbance method, in which the ultraviolet absorbance of mercury vapor is determined. Cross checks of their procedure between laboratories, and with the neutron activation method, have shown good agreement in analytical results for mercury, both in fish and in bottom sediments.

A number of questions about the behavior of mercury remain to be answered. Several theories have been proposed as to how mercury might go from inorganic form in water or a bottom sediment, into methylated form in a fish. One theory assumes anaerobic conversion in the mud to volatile dimethyl mercury which enters fish *via* the gills. Another assumes aerobic conversion to monomethyl mercury by bacteria, with subsequent transfer up the food chain. Still another assumes that a fish itself can methylate mercury taken in either through the gills as elemental vapor, or *via* the stomach as inorganic ions, or in an adsorbed state on silt particles. There is some evidence for each mechanism. It is desirable to learn which is more important, to know what kinds of methods might be most fruitful for alleviating the situation. Before all the questions can be answered, we need to develop highly sensitive methods for each individual form of mercury. At present the most sensitive methods can go down only to about 0.05 ppb inorganic mercury in water.

At the conference on Environmental Mercury Contamination held in Ann Arbor, Mich., in early October 1970, a number of sources from which mercury may enter the environment were mentioned. Among them, in addition to losses from some segments of the chloro-alkali industry, were the burning of fossil fuels, use of mercurial compounds for slimicides in paper mills and for fungicides both in paints and in agricultural seed treatments, use of elemental mercury in the electrical industry for manufacture of batteries and mercury vapor lamps, use of mercuric catalysts, and the disposal of domestic sewage sludges. It will be up to analytical chemists to evaluate all of the sources and to provide the data on which proper action can be based. This will be true not only for mercury, but for all environmental contaminants. Analytical chemists, especially those in industry, are going to be busy for a long time.

It is interesting that both Finnish and Swedish chemists have found fairly high mercury contents in fish from certain lakes in northern parts of their countries, remote from any known source of pollution. We have encountered some similar cases in northern Michigan and Ontario, and Canadian authorities have found several in various parts of Canada, including Hudson's Bay. The possibility of geological origin remains to be investigated.

Another interesting fact is that mercury will be found in the hair of a person who has been exposed to it. The average person has about one or two ppm in his hair. J. K. Miettinen of the University of Helsinki, Finland, has made a thorough study of data from his own country, Sweden, and Japan. No symptoms of mercury poisoning have been found in any subject whose hair contains less than 60 ppm. R. E. Jervis of the University of Toronto has reported 150 ppm as an upper safe limit. With more than these amounts, a subject may or may not show symptoms, depending, perhaps, upon differences be-

tween individuals as well as upon differences between their exposures. It seems likely that a few severe exposures might produce a greater effect than many very small dosages because the body can more easily handle the smaller quantities. One of the victims in a New Mexico case last winter showed 2500 ppm mercury in the hair. People who have had mild occupational exposures may show from 10 to 30 ppm. By analyzing sections of the hair of a long-haired person and knowing its growth rate, one can approximate the time and intensity of exposure. Most of these analyses have been done by neutron activation, which is advantageous because very small samples can be employed. However, hair can also be analyzed by the atomic absorbance method following the digestion procedure used for fish analysis. A 100-mg sample is sufficient for hair in the range of 1 to 10 ppm.

Economic Pains

I would be remiss if I neglected to recognize the pains that can be felt in an industrial environment during times of economic readjustment. No doubt similar situations occur in government and in academic or institutional life, but industries are likely to react more swiftly. In my experience, management people, especially lab management, do not like these situations any more than do the victims. Also, I believe, that during a period of reorganization, the best chemists, being the most sensitive individuals, usually suffer more mentally than do the poorer ones who may have too high opinions of their own abilities. The good chemist knows he has some weaknesses and can easily see why he might be released. Others may not have such worries. A change is not necessarily bad for the individual, however. At one time when Mr. Beshgetoor and I had to release some people, they took it well and later we were happy to learn that they had found better positions elsewhere.

Professional Pride

The final pain that should be mentioned is one which analytical chemists bring on themselves. Because many chemists and some en-

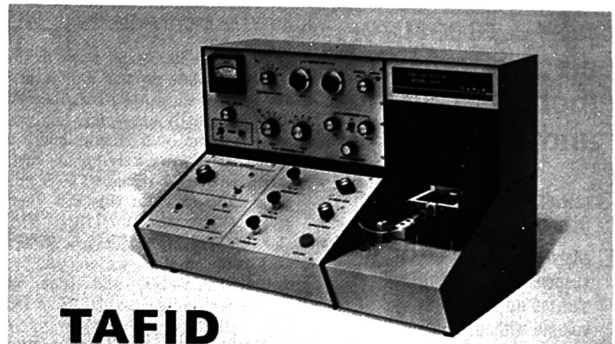

TAFID
A hot new concept that's 100 times more sensitive than TGA.

And that's only the start. Actually, TAFID (Thermal Analysis Flame Ionization Detection) exceeds TGA in six key areas. These were outlined recently by Dr. F. T. Eggertsen and Dr. F. H. Stross in the October issue of THERMOCHIMICA ACTA*. Here is what they said:

Sensitivity: "... is about 100 times greater than ordinarily obtained by thermogravimetric analysis."

Resolution: "Higher resolution is possible than in TGA because of the smaller samples that can be used . . . Effective one-plate resolution is obtainable."

Specificity: ". . . is specific for reduced [organic] carbon and does not respond to water, carbon oxides, nitrogen oxides and other substances normally associated with inorganic materials."

Analysis Time: ". . . capable of high speed of analysis, owing to the small sample requirement and low thermal lag of the furnace . . . an isothermal mode . . . provides especially rapid and convenient measurements."

Data Readout: "is [directly] expressed as rates of evolution or integrated amounts."

Applications: ". . . high sensitivity and wide range of linear response, together with its specificity and uniformity of response to organic carbon, make it uniquely well suited for the quantitative analysis of organic materials."

Write today if you would like a reprint of this paper and a complete technical description of our new Model 3000 Thermal Analysis System . . . the only instrumentation available that incorporates the TAFID concept.

*Eggertsen, F. T., Stross, F. H., *THERMOCHIM. ACTA.*, **1**, 451, (1970).

CARLE
INSTRUMENTS, INC.
1141 EAST ASH AVENUE, FULLERTON, CALIFORNIA 92631 (714) 879-0000

Circle No. 39 on Readers' Service Card

now... measure electrophoretic mobility quickly and accurately

- ☐ calculate zeta potential from mobility data
- ☐ analyze dispersions, suspensions, concentrated slurries up to 50% by volume without dilution
- ☐ for flotation, dispersion, flocculation, coagulation, particle interaction and electrokinetic phenomena studies

Micromeritics' Model 1202 Electrophoretic Mass Transport Analyzer, with its rotating cell, even measures suspensions of particles having appreciable sedimentation velocities and eliminates thermal current effects . . . measures suspensions with conductivities as high as 100,000 micromhos . . . measures particles ranging in size from very small to as large as 1,000 microns . . . maintains constant potential gradient . . . provides excellent repeatability. Aids in determining the stability of lyophobic colloids . . . the flotability of minerals . . . the sedimentation of suspensions . . . the viscosity of slips . . . the structure of soils, etc. Applications include paints, ceramics, industrial wastes and sewage, minerals and ores, pulp and paper coatings, pharmaceuticals, soil mechanics and nutrients, emulsion and purification studies, and many more. Call, wire or write today for complete technical information. Micromeritics Instrument Corporation, 800 Goshen Springs Rd., Norcross, Ga. 30071 (metro Atlanta) phone (404) 448-8282.

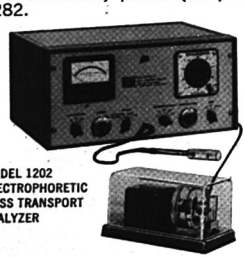

MODEL 1202
ELECTROPHORETIC
MASS TRANSPORT
ANALYZER

micromeritics™

SURVEYORS OF
THE MICROWORLD

8280

Circle No. 127 on Readers' Service Card

gineers start industrial work in the laboratory but do not like it and are anxious to transfer out, the rest of us who really appreciate analytical chemistry and should make a career of it are likely to let their attitudes rub off on us. Dr. Siggia took us to task for this last year, [ANAL. CHEM. 41 (13), 50A, (1969)] pointing out that we should take pride in what we do, that we are indispensable, and that we should feel indispensable. The sad fact is that we are not always so confident, and people in other professions can sense this. To illustrate: I once had to visit a customer on a complaint problem where we faced a possible lawsuit. One of our lawyers cautioned me before I left as to what I should do if the customer brought up the question of a financial settlement. His suggestion was to say, "I am *only* a chemist. If you want to talk about money, you will have to talk with our lawyers." At the time I had no reply to that, but after years of thinking about it, I can now advise on what to say in a similar situation. It is: "Sir, I am a chemist. I am here to help you technically in every way I can. However, if you insist on talking about money, you will have to talk with someone who is *only* a lawyer or an accountant."

In subsequent experiences with lawyers I have had to educate them in technical matters to at least as great an extent as they have had to train me concerning the law. Our professions should be on an equal footing, except that whereas we are always seeking the truth, there are lawyers who sometimes seek to obscure it. Charles Mann, late professor of chemical engineering at Minnesota, handled the matter well in an anecdote he once related at a student gathering. He was serving as an expert witness in a lawsuit and the opposing attorney was browbeating him during cross-examination, but was unable to shake an opinion which Dr. Mann had given in testimony. Finally, in exasperation, the lawyer said, "By what right do you express such an opinion?" Dr. Mann looked the lawyer in the eye and replied, "By the right of being a scientist!" His side won the case.

We base our opinons and conclusions on solid experimental grounds. We are scientists, and we have all the rights and privileges that go with that estate. We are working in the branch of chemistry that has the largest number of members in the American Chemical Society. The results which we obtain are needed. Our work is interesting, honorable, and useful. We can be, and should be, proud of our profession.

To summarize, there are both pains and pleasures in industrial analytical chemistry. I feel that the pleasures we enjoy far outweigh any pains that we have to suffer. The pains that we take are measures of our professional ability, and the means whereby we can render the greatest service to society.

Vernon A. Stenger, *analytical scientist with The Dow Chemical Co., Midland, Mich., received his B.S. in chemical engineering and M.S. in chemistry from the University of Denver in 1929 and 1930, respectively. He earned his Ph.D. degree under I. M. Kolthoff at the University of Minnesota in 1933. He has been with Dow in Midland since 1935. He was honored at Detroit by receiving the Detroit Anachem Award in 1970 for his outstanding contributions to analytical chemistry through research, administration, and other activities advancing this division of chemistry as a profession. Dr. Stenger is a member of the ACS and has served on the Advisory Board of* ANALYTICAL CHEMISTRY.

Workshop on Mass Spectrometric Analysis of Solids

On November 16 and 17, 1970, the American Society for Mass Spectrometry sponsored a Workshop on Mass Spectrometric Analysis of Solids at the Mellon Institute of Carnegie-Mellon University.

As in previous years, the purpose of the Workshop was to provide a forum for the detailed discussion of the state-of-the-art of the mass spectrometric analysis of solids. The program emphasized spark-source mass spectrometry but a full afternoon session was devoted to microanalysis and, in particular, secondary ion mass spectrometry.

The first topic to be discussed, "Gadgets to Assist the Analyst," was moderated by R. J. Guidoboni (Kennecott Copper Corporation). Those items or "tricks of the trade" which were thought to be of practical use to the mass spectroscopist were described during this session. Some of the gadgets discussed included: a cryopump for the spark-source, safety locks for the photoplate drum, an automatic liquid nitrogen filler, disposable insulators, a mask for the removal of the matrix lines and their associated background during long exposures on a photographic plate, developing trays, and a collar and associated flanges for extra entry ports on a spark-source.

A large variety of sample holders and sampling systems were also described at this session. Among these were holders for fragile electrodes, odd shaped samples, micro samples, a sample spinner, and a sample holder for an ion microprobe. The sampling systems included a mini-spark sampler, an auxilliary electrode technique for the analysis of insulators, and a sampling device for small liquid samples.

A group of gadgets which were designed to help improve the accuracy and precision of mass spectrographic results were also discussed under this topic. These included a telescope mount for accurately positioning electrodes within the source, an electrode vibrator, and a rotation system. The latter two of these have been found to be very useful for electrical detection. A movable collector for ion detection was described. This employed dual Faraday cups to monitor two masses simultaneously. A major revision to a Nuclide Graf —2 source was reported. This provided six entry ports to the source for items such as rotary feedthroughs, sample manipulators, and liquid nitrogen feedthroughs.

The session on mass spectrometric microanalysis (discussion leader, E. Berkey, Westinghouse Research) emphasized the rapidly growing activity in the use of ion probe mass spectrometry for the characterization of solids. The interest displayed by both speakers and audience indicated that this topic will require increasing amounts of the Committee's attention in coming years, as more instruments become available and as additional studies continue to be made in this rapidly growing field. Several participants discussed the analytical capabilities and numerous recent applications of commercial ion probe instruments. Of particular analytical importance were thin film analyses, depth profiles, and ion images of element distributions. Problems regarding the generation and interpretation of meaningful data from these instruments in view of the numerous variables inherent in the technique were considered. The relative newness of the instruments, together with the fact that they are analyzing solid microvolumes more comprehensively than ever before possible, means that considerable work remains to be performed. A report on major ion probe activity in Europe was presented, citing several major new instrument developments in progress for the surface analysis of solids. The analytical potential of an instrument capable of simultaneous ion and electron bombardment of a surface that is under development in this country was also discussed.

Several reports on important new applications of the spark source mass spectrometer (SSMS) were also included in the microanalysis session. One report described the use of a continuous laser to excite and ionize nonconducting samples both with and without the presence of auxiliary electrodes. Another report discussed use of the SSMS for the on-line analysis of liquids—*i.e.*, sodium—and gases—*i.e.*, CO_2—and emphasized that the instrument had, in general, reached the point where it could leave the laboratory and begin to make contributions on industrial process and production lines. Finally, a report on interesting SSMS analyses of polywater and a possible fragment from an unidentified flying object was presented, with the results indicating the presence of numerous contaminating elements in the former sample and verifying the terrestrial origin of the latter one.

W. W. Harrison (University of Virginia) moderated a discussion of "The Spark Source—Monitoring and Control." C. W. Kimblin (Westinghouse R & D) discussed his studies on the high ionization yields in a copper arc and noted the possible relevance to arc-like

Unique
Allen-Bradley
sonic-sifting
concept for
dry separation
down to
5 microns
5 microns
5 microns
5 microns
5 microns
5 microns
5 microns

Our Model L3P Sonic Sifter efficiently handles most difficult-to-separate materials—even in the sub-sieve ranges.

Conventional sifters can't do it. They shake and grind your material. Screens quickly blind, resulting in but a marginal analysis.

The L3P is different. It doesn't shake. Instead, an oscillating air column moves the material up and down through stationary screens. This unique concept permits accurate separations down to 5 microns. And there's virtually no screen wear or particle attrition.

Sieves are available in U.S. Standard sizes No. 3½ through No. 400 and in precision sizes from 150 to 5 microns.

For fast, precise dry sifting, try the Model L3P. It's quiet, compact, and portable... weighs only 35 lbs. And it operates on 120-volt, 60 Hz power. For more information write to Lowell Sonderman, Allen-Bradley Company, 205 West Scott Street, Milwaukee, Wisconsin 53204.

AB ALLEN-BRADLEY

FISHER SCIENTIFIC CO.

PS71-1

© Allen-Bradley Company 1971

Circle No. 8 on Readers' Service Card

portions of the spark discharge used in mass spectrometry. Several participants discussed various means of monitoring the spark voltage and relating their observations to the spark discharge. The devices included the use and misuse of a capacitive divider network, a ferrite core current transformer, and a commercially available high voltage oscilloscope probe. The oscilloscope signal from these pickups was shown to be related to electrode gap and oscillator circuit tuning. Several other workers described the effects of spark positioning, spark electrical parameters such as voltage and pulse duration, and instrumental parameters such as Y-deflection and ESA voltages. The gap width and particularly self-shielding or masking of the electrodes were shown to have significant effects. Until techniques are developed to correct for these variations, analytical accuracy and precisions can be maintained only by scrupulous monitoring and control of all instrumental parameters.

Two short discussions presented possible models to explain the effects of electrode positioning and spark gap errors. One worker postulated the existence of elemental inhomogeneity in the spark plasma such that electrode movement would cause greater or lesser amounts of an element to be detected. The other discussion postulated that variations in plasma distribution of charged species and their variable influence on the ion beam monitor measurement could lead to variations in analytical results.

Additional discussions were held on the use of electrical detection systems and special samples such as environmental analyses and the analysis of S and O.

Organizing Committee

F. D. Leipziger,
Kennecott Copper Corp.

C. A. Evans, Jr.,
University of Illinois

H. D. Cook,
Bettis Atomic Power Laboratory

J. McGovern,
Mellon Institute

When OUT OF ORDER ...what good will your next NMR spectrometer be in YOUR lab?

YOU SHOULD THINK ABOUT SERVICE BEFORE YOU BUY!

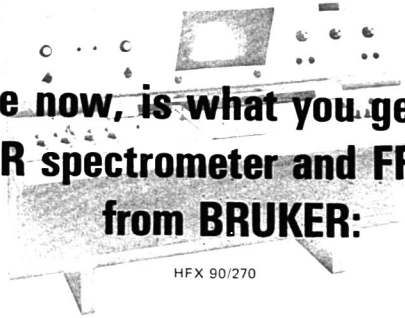

HFX 90/270

Here now, is what you get with an NMR spectrometer and FFT system from BRUKER:

1. Call 914 592-5470 and ask for Werner. (Please call collect).
2. Service comes within 48 hours to anyplace in the U.S.A. and Canada. (Free of charge during the first year after installation).
3. All spare parts are available from our shelf. (Again, free of charge during the first year).
4. The best part of the service at Bruker is – you hardly need it.

A few more good reasons to GO FOR BRUKER

P.S. After our engineer has serviced your instrument, you may even forgive him his Swiss accent.

For details, call or write:

IN U.S.A. – Bruker Scientific Inc.
1 Westchester Plaza, Elmsford, N.Y. 10523
(914) 592-5470

IN CANADA – Bruker Spectrospin Canada Ltd.
797 Don Mills Road, Don Mills, Ontario
(416) 429-2263

ENGLAND
Bruker Spectrospin Ltd.
19, Nordic Drift
Coventry CV 2 2 DE
Tel. (0203) 32 69 45

FRANCE
Bruker Spectrospin SA
7, rue de la Paix
(67) Wissembourg
Tel. (088) 94.02.42

ITALY
Bruker Spectrospin srl.
Via Pasquale Miglioretti, 2
20161 Milano
Tel. (02) 64 64 261

SWITZERLAND
Spectrospin AG
8117 Zurich-Fallanden
Industriestrasse 26
Tel. (051) 85 48 55/85 45 05

W. GERMANY
Bruker-Physik AG
7501 Forcheim
Tel. (0721) 5 80 70, 5 80 76-9
Tx. (07) 826 836

Circle No. 26 on Readers' Service Card

autolab™

The AutoLab 6300...

now a modular family of seven low-cost Digital Integrators...

the first... and only...
full-capability,
truly modular family of
digital integrators
at a reasonable price.

Add all of the flexibility
and convenience features
of high-priced integrators,
even computer time-sharing
— and *still* save money.

The AutoLab 6300 is the new way to full capability in automating your chromatograph. With digital integrator prices starting at $2200, quantitation by manual or mechanical techniques is difficult to justify. No more peak attenuations or measurement of peak areas ... the AutoLab 6300 provides completely automatic, attention-free GC quantitation.

Standard features on all AutoLab 6300's include adjustable peak detector, filtering and noise rejection, a wide 0-1000 mv linear range, and automatic baseline correction. A fully buffered output assures accurate integration of closely spaced or unresolved peaks.

The AutoLab 6300 Accessory Module adds extra convenience and automation to the AutoLab 6300... variable integration delay, self-test mode, selectable digital area rejection to eliminate false peak printout, and function command timer for automatic samplers or valve control. There is even an optional visual display utilizing the new solid-state light-emitting diodes. The Accessory Module may be added at any time.

The AutoLab 6300T with Teletype output, coupled with VIGAS GC data-reduction program for the time-share terminal, provides complete automation comparable to on-line computer systems for even the smallest laboratory. Simple to use and versatile in its calculation modes and output reports, VIGAS comes at no extra cost with the easy-to-justify AutoLab 6300/TTY package.

Match your requirements from seven models. One will suit your particular application better than anything else on the market... at a lower cost. Investigate how AutoLab can help you *now*. For product brochure circle # 188 ... or call for a demonstration.

The lab automation people

VIDAR autolab

77 Ortega Avenue, Mountain View, California 94040, (415) 961-1000

VIDAR offices in Atlanta / Beverly, Mass / Chicago / Houston
Los Angeles / Mountain View / Stirling, N.J. / Washington, D.C.
In Europe: VIDAR AutoLab GmbH, D6233 Kelkheim, Frankfurter Strasse 43

Energy dispersive X-ray analysis goes pushbutton

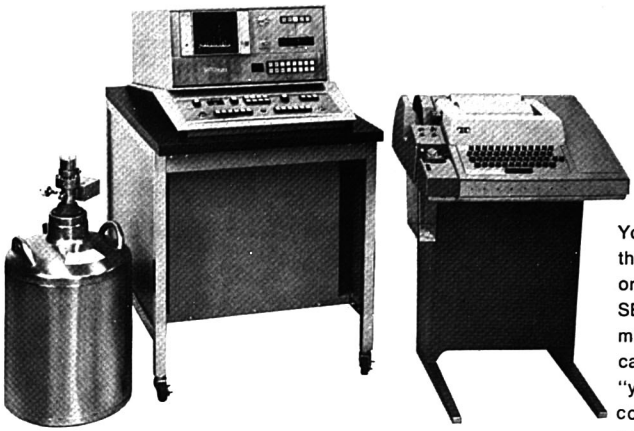

Now, everything you need for completely automatic energy dispersive X-ray analysis—qualitative and quantitative—is available in a single, push-button-controlled system: the Qanta/Metrix EDX/UDS.

The EDX/UDS is more than just a multichannel analyzer hooked up to a detector. For example, besides acquiring and displaying data, the EDX/UDS automatically determines X-ray energies; makes peak area matrix corrections; calculates peak areas; smooths spectra to improve definition; and removes contaminants from spectra of interest.

A complete qualitative, or semi-quantitative analysis usually takes less than a minute; precise quantitative analyses seldom require more than a few minutes.

And, answers are given in your terminology, on the teletypewriter, or on any other device you want to hook up to the system. You can also store spectra in the display, for later comparison or detailed study.

What's more, you can use the EDX/UDS pushbutton panel to vary parameters until you find a sequence that gives you the desired results. Once you're satisfied, just run through the sequence once more and push a single button. Your unique program is then stored in the EDX/UDS for continuous, repetitive analysis while you turn to other work (conversational capability is available, but it's not necessary).

The EDX/UDS is ideal for a wide range of applications: biology, mineralogy, geology, metallurgy, chemistry, medicine—wherever you need immediate, accurate, and complete elemental analysis.

You can also easily adapt the EDX/UDS to complement or extend the capabilities of SEM's, diffractometers, and microprobes. Or, the system can be supplied with a simple "yes/no" panel for quality control and production line use, where you're just looking for a few elements on a repetitive basis.

For more information about the single system, push-button way to automated energy dispersive X-ray analysis, call or write:
Qanta/Metrix Corporation,
120 Industrial Way,
San Carlos, CA 94070.
Phone: (415) 592-7770

QANTA/METRIX

TOTAL PUSHBUTTON OPERATION FOR ELEMENTAL ANALYSIS

Circle No. 155 on Readers' Service Card

THE MODEL RC-18A CONDUCTIVITY BRIDGE is designed exclusively for the measurement of solution conductivity. Accuracy is ± 0.05% and sensitivity exceeds 0.005%. It houses, in one compact unit, an oscillator providing both 1,000 and 3,000 Hz bridge current, decade and ratio resistors that comprise the bridge, decade and continuously variable capacitors that facilitate reactive balance, a Wagner ground circuit, a sharply tuned high-gain amplifier, and a 2" CRT null detector. Range: 0-111,111 ohms and 0-11,111.1 micromhos; Readout: 6 decades in Resistance or Conductance units.

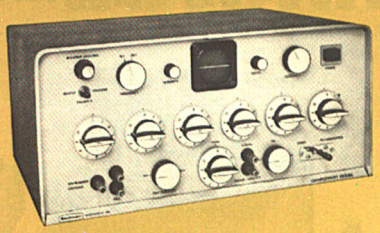

Electrolytic conductivity is our business.

THE MODEL RC-16B2 CONDUCTIVITY BRIDGE is a general purpose unit featuring extremely wide range, high sensitivity, and ± 1% accuracy. This line operated bridge operates from a 120-volt, 50-60 Hz source. It is provided with a dual calibration in resistance and conductance, covering the ranges 0.2 to 2,500,000 ohms, and 0.4 to 5,000,000 micromhos. When used with conductivity cells of appropriate cell constants (low for poorly conductive solutions and high for highly conductive solutions), the entire range of electrolytic conductivity from ultra-pure demineralized water to concentrated strong acids is easily covered.

MODEL RC-19 FIELD & LABORATORY BRIDGE is a small, portable, versatile instrument for measuring solution conductivity. Operating on internal battery supply or standard 115 VAC power, it provides six overlapping ranges for measuring resistance from 1 Ohm to 1.1 Megohms, and six additional overlapping ranges to measure conductance between 0.1 and 110,000 micromhos. Read-out for both measurements is digital, unambiguous and accurate to ± ¼%. The RC-19 also features bridge current frequencies of 100 and 1000 Hz, sensitivity better than 0.05%, solid state electronics and provisions for interchangeable temperature compensators, both manual and automatic. The 10-lb, 11" x 9" x 8" unit makes measurements equally well in grounded or isolated vessels or pipes, in lakes or streams and in the laboratory or plant.

Beckman INSTRUMENTS, INC.

CEDAR GROVE OPERATIONS

89 COMMERCE ROAD
CEDAR GROVE, NEW JERSEY • 07009
(201) 239-6200 • TWX: 710-994-5781

For complete technical specifications on any of our electrolytic conductivity bridges as well as our complete line of cells and associated equipment write to . . .

INTERNATIONAL SUBSIDIARIES: Geneva; Munich; Glenrothes, Scotland; Tokyo; Paris; Capetown; London.

Circle No. 23 on Readers' Service Card

161st National ACS Meeting

Los Angeles, Calif.

March 28 to April 2, 1971

The 161st National American Chemical Society Meeting will be held March 28 to April 2, 1971, in Los Angeles, Calif. The Analytical Chemistry Division has sessions Monday, March 29, through Friday morning, April 2. In addition to general sessions, there will be two special award symposia, other special symposia, and joint symposia with the Divisions of Nuclear Chemistry and Technology, and Water, Air, and Waste Chemistry. A special Chemistry Instrumentation Award Symposium on Monday will honor F. W. McLafferty, Cornell University. This award is sponsored by Sargent-Welch Scientific Co. Dr. McLafferty's Award Address will be given Monday afternoon and is titled "Molecular Information from Mass Spectrometry." Tuesday, the ACS Award in Analytical Chemistry honoring George H. Morrison of Cornell University will be given. The symposium is titled "The Relavance of Trace Analysis in 1971" and Dr. Morrison will give his award address in the afternoon. The Analytical Chemistry Award is sponsored by the Fisher Scientific Co.

Other special symposia will be devoted to Analysis of Microgram (or Less) Quantities of Materials; Standard Radioactive Materials and Their Applications (Joint with the Division of Nuclear Chemistry and Technology); Recent Advances in Flame Spectrometry; Determination of Air Quality; and Nuclear Techniques in Environmental Sciences (Joint with the Divisions of Water, Air, and Waste Chemistry and Nuclear Chemistry and Technology). All of the Analytical Division symposia will be held at the Los Angeles Hilton except for the Symposium on Standard Radioactive Materials and Their Applications which will meet at the Biltmore.

The Analytical Division banquet will be held Wednesday starting at 6:30 and will feature Professor Arie Jan Haagen-Smit who will speak on the current status of the pollution problem.

There will also be a Chemical Exposition with the latest of chemicals, equipment, instrumentation, publications, and services on exhibit.

The detailed technical program of the Analytical Chemistry Division is given below. Complete information on the National Meeting is contained in the February 15th issue of *Chemical & Engineering News*. Further details on Analytical Division activities are available from R. S. Juvet, Jr., Secretary, Dept. of Chemistry, Arizona State University, Tempe, Ariz. 85281.

DIVISION OF ANALYTICAL CHEMISTRY

J. C. White, Chairman — R. S. Juvet, Secretary

PROGRAM

Monday, March 29

Monday Morning

CHEMICAL INSTRUMENTATION AWARD SYMPOSIUM

F. C. Nachod, Presiding

9:10—Applications of ^{13}C Nmr Spectroscopy. J. B. Stothers, University of Western Ontario, London, Ontario, Canada

9:50 Electron Diffraction of Vapors. Jerome Karle, Lab for the Structure of Matter, Naval Research Labs, Washington, D. C. 20390

10:30 Structural Analysis by Mössbauer Spectroscopy. J. J. Zuckerman, State University of New York at Albany, Albany, N. Y. 12203

11:10 Vibrational Spectra and Molecular Structure. P. J. Krueger, University of Calgary, Calgary 44, Alberta, Canada

ANALYSIS OF MICROGRAM (OR LESS) QUANTITIES OF MATERIALS

D. P. Sandoz, Presiding

9:05 Organic Structure and Functional Group Analysis of Microgram Qualities by ^{1}H Nmr. George Levy, Joseph Cargioli, General Electric Research and Development Center, Schenectady, N. Y. 12301; Howard Hill, Vern Burger, Varian Assoc., Palo Alto, Calif. 94303

9:35 An Ultrahigh Vacuum Microbalance and a Study of the Reduction of Nickel Oxide Single Crystals. R. L. Schwoebel, Sandia Labs, Albuquerque, N. M. 87115

10:20 The Use of the Electron Probe Microanalyzer on Returned Lunar Samples. Arden Albee, Arthur Chodos, Div. of Geological Sciences, California Institute of Technology, Pasadena, Calif. 91109

11:00 An On-Line Scanning Electron Microscope/Pseudoelectron Microprobe System. Robert Rogan, Timothy Hartmann, Mark Shulman, Systems Development Div., IBM, Poughkeepsie, N. Y. 12602

11:30 The Atomic Absorption Analysis of Microliter Volumes of Biomedical Samples with the Carbon Rod Atomizer. M. D. Amos, K. G. Brodie, J. P. Matousek, B. Stevens, Varian Techtron Pty., Ltd., Springvale, Australia; D. P. Sandoz, Varian Techtron, 2700 Mitchell Dr., Walnut Creek, Calif. 94598

SYMPOSIUM ON STANDARD RADIOACTIVE MATERIALS AND THEIR APPLICATIONS

(Joint with Division of Nuclear Chemistry and Technology)

W. S. Lyon, Presiding

9:05 Recent Activities of the National Bureau of Standards Radioactivity Section. S. B. Garfinkel, W. B. Mann, National Bureau of Standards, Washington, D. C. 20234

9:30 An Improvement in the Single Crystal Coincidence Counting Method. J. M. R. Hutchinson, Patricia Mullen, National Bureau of Standards, Washington, D. C. 20234

9:55 Problems of Providing a Commercial Supply of Standardized Radioactive Solutions. A. McNair, Physics Dept., Radiochemical Centre, Amersham, England

NEW

chart recorder (only $635) Model 8500 offers quick response (0.5 sec.)

Sturdy construction ensures long operating life... simplicity of design permits easy servicing. The new Matheson Potentiometric Chart Recorder Model 8500 also offers solid state circuitry, superior linearity (0.1%) and resolution (0.2%), four ranges (1, 3, 5, 5000 mv. DC), 2 speeds, (1 & 2"/min.). Here's sensitivity and reliability unequalled by any chart recorder in its price range.

The recorder can be used with the Mass Flowmeter, Dyna-Blender, Chromatograph or any instrument with a 1 to 5000 DC millivolt output. Only Matheson has developed compatible systems for all gases and handling equipment — completely integrated components such as regulators, valves, flow meters, purifiers and generators blended together to form *systems that work.*

For quick response on the "quick responding" Model 8500 chart recorder, send coupon for Engineering Report G-123.

MATHESON GAS PRODUCTS
A Division of Will Ross, Inc.
East Rutherford, N. J.; Cucamonga, Calif.; Gloucester, Mass.; Joliet, Ill.; La Porte, Texas; Morrow, Ga.; Newark, Calif.; Whitby, Ont.

Matheson Gas Products, P.O. Box 85, Dept. AC-371, East Rutherford, N. J. 07073
Send me Engineering Report G-123
Name_____
Firm_____
Address_____
City_____
State_____ Zip_____
1-71G

Circle No. 126 on Readers' Service Card

10:45 Quality Assurance in Nuclear Medicine. Tyra Hutchens, University of Oregon Medical School, Portland, Ore. 97201; Wolfgang Hauser, Brookhaven National Laboratory, Upton, N. Y. 11973; Nilo Herrera, Danbury Hospital, Danbury, Conn. 06813

11:20 Radiochemical Quality Assurance Programs of the AQCS, USPHS. Edmond Baratta, James Hardin, Analytical Quality Control Service, Bureau of Radiological Health, P. O. Box 232, Winchester, Mass. 01890

11:45 Interlaboratory Study of ^{131}I, ^{137}Cs, ^{140}Ba, ^{89}Sr, and ^{90}Sr Measurements in Milk, June 1970. Edmond Baratta, Forrest Knowles, Jr., Analytical Quality Control Service, Bureau of Radiological Health, P. O. Box 232, Winchester, Mass. 01890

CHEMICAL INSTRUMENTATION AWARD SYMPOSIUM

F. C. Nachod, Presiding

2:00 Structure Determination of Natural Products. Koji Nakanishi, Columbia University, New York, N. Y. 10027

2:40 Computer Techniques Applied to Instrumental Methods. R. Venkataraghavan, Cornell University, Ithaca, N. Y. 14850

3:20 AWARD ADDRESS: Molecular Information from Mass Spectrometry. F. W. McLafferty, Cornell University, Ithaca, N. Y. 14850

ANALYSIS OF MICROGRAM (OR LESS) QUANTITIES OF MATERIALS

D. P. Sandoz, Presiding

2:00 The Separation of Microgram Amounts of Lead from a Silicate Matrix by Electrodeposition. T. J. Murphy, I. L. Barnes, K. M. Sappenfield, W. R. Shields, Analytical Chemistry Div., Institute for Materials Research, Washington, D. C. 20236

2:30 The Mass Spectrometric Determination of Subnanogram Samples of Lead. I. L. Barnes, T. J. Murphy, K. M. Sappenfield, W. R. Shields, National Bureau of Standards, Washington, D. C. 20236

3:00 Microminiaturization of Microchemical Tests. W. C. McCrone, McCrone Assoc., Inc., 493 E. 31st St., Chicago, Ill. 60616

3:15 Enzyme Methods for Microanalysis of Biologically Important Substances. G. G. Guilbault, Louisiana State University in New Orleans, New Orleans, La. 70122

SYMPOSIUM ON STANDARD RADIOACTIVE MATERIALS AND THEIR APPLICATIONS

(Joint with Division of Nuclear Chemistry and Technology)

W. S. Lyon, Presiding

2:00 Standards for Low-Level Gamma-Ray Spectrometry of Lunar and Geochemical Samples. J. S. Eldridge, K. J. Northcutt, G. D. O'Kelley, Oak Ridge National Laboratory, Oak Ridge, Tenn. 37830

2:20 A Survey of Needs for Radioactivity Standards. S. A. Reynolds, Oak Ridge National Laboratory, P. O. Box X, Oak Ridge, Tenn. 37830

2:45 National Uses and Needs for Standard Radioactive Materials. Lloyd Zumwalt, Dept. of Nuclear Engineering, North Carolina State University, P. O. Box 5636, Raleigh, N. C. 27607

3:20 Nonpoisson Distributions Observed during Counting of Certain Carbon-14 Labeled Organic (Sub)monolayers. J. L. Anderson, 542 Union Ave., New Providence, N. J. 07974

Tuesday, March 30

Tuesday Morning

THE RELEVANCE OF TRACE ANALYSIS IN 1971

(Fisher Award Symposium in Honor of George H. Morrison)

W. W. Mienke, Presiding

9:00 The Relevance of Trace Analysis in 1971: Introduction. W. W. Meinke

9:05 Trace Analysis in Industry Today. P. F. Kane, Texas Instruments, Inc., P. O. Box 5963, M/S 147, Dallas, Tex. 75222

9:35 The Relevance of Trace Analysis. J. D. Winefordner, University of Florida, Gainesville, Fla. 32601

10:05 Mass Spectrometric Trace Element Analyses. C. A. Evans, Jr., Materials Research Labs, University of Illinois, Urbana, Ill. 61801

10:40 Trace Analyses in Metals by Residual Resistivity Methods. R. L. Powell, Cryogenics Div., NBS-Institute for Basic Standards, Boulder, Colo. 80302

11:10 Trace Analysis by Electrochemical Methods. J. K. Taylor, Analytical Chemistry Div., National Bureau of Standards, Washington D. C. 20234

11:40 The Determination of Trace Elements by High-Flux Activation Analysis. V. P. Guinn, University of California, Irvine, Calif. 92664

Tuesday Afternoon

THE RELEVANCE OF TRACE ANALYSIS IN 1971

W. W. Meinke, Presiding

2:00 The Role of the Spectrophotometer in Modern Trace Analysis. D. F. Boltz, Wayne State University, Detroit, Mich. 48202

2:30 The Analysis of Trace Constituents with the Electron Probe Microanalyzer. K. F. J. Heinrich, Institute for Materials Research, National Bureau of Standards, Washington, D. C. 20234

3:00 The Blank in Trace Analysis—Some Recent Problems and Their Solutions. J. P. Cali, National Bureau of Standards, Washington, D. C. 20234

3:35 Reference Materials for Accurate Trace Measurement. W. W. Meinke, National Bureau of Standards, Washington, D. C. 20234

4:05 Introduction of Fisher Award Winner. H. Freiser

4:15 Fisher Award Address. G. H. Morrison

Wednesday, March 31

Wednesday Morning

RECENT ADVANCES IN FLAME SPECTROMETRY

J. D. Winefordner, Presiding

9:05 Selective Modulation in Flame Spectrometry. V. G. Mossotti, University of Minnesota, Minneapolis, Minn. 55455

9:45 Flame Spectrometric Techniques Utilizing Isolated Droplet Sample Introduction System. G. M. Hieftje, Indiana University, Bloomington, Ind. 47401

10:40 Flame Emission Spectrometry with Optical Scanning. T. C. Rains, Oscar Menis, Analytical Chemistry Div., National Bureau of Standards, Washington, D. C. 20234

11:20 Wavelength Modulation Methods in Atomic Absorption and Atomic Fluorescence Spectrometry. G. Nitis, J. D. Winefordner, University of Florida, Gainesville, Fla. 32601

GENERAL

R. A. Osteryoung, Presiding

9:05 Normal Pulse Polarographic Studies of Halide Depolarization of Mercury in Sodium–Potassium Nitrate Melts. W. O'Deen, R. A. Osteryoung, Colorado State University, Fort Collins, Colo. 80521

9:25 Thin-Layer Electrochemistry in Molten Salts. A. T. Hubbard, L. P. Zajicek, University of Hawaii, Honolulu, Hawaii 96822

9:40 The Electrochemiluminescence Obtained on the Reduction of 9,10-Dichloro-9,10-diphenylanthracene. T. M. Siegel, H. B. Mark, Jr., University of Cincinnati, Cincinnati, Ohio 45221

10:00 Hydration Number of Sodium Ions by Sodium Magnetic Resonance. A. L. Van Geet, State University College at Oswego, Oswego, N. Y. 13126

10:15 Differential Voltammetric Scanning Thermometry of Formic Acid Solution in 1F $HClO_4$. B. B. Graves. Eastern Michigan University, Ypsilanti, Mich. 48197

10:35 Enzyme Electrodes. G. G. Guilbault. Louisiana State University in New Orleans, New Orleans, La. 70122

10:55 Oxidation of Water and Quinones by Silver(II) in Acetonitrile. Byron Kratochvil, Carl Garber, University of Alberta, Edmonton, Alberta, Canada

11:10 Titrimetric Determination of Trace Sulfate Using a Lead Ion-Selective Electrode. R. N. Helstand, C. T. Blake, Sun Oil Co., P. O. Box 426, Marcus Hook, Pa. 19061

Purify solvents in your own laboratory

for
synthesis reactions
biological testing
chromatography
spectroscopy
dehydration

Purify solvents easily and inexpensively by passing them through a column of WOELM Active Alumina Adsorbent. For complete information about this technique, write for Application Note No. 101, "Purification of Solvents by Active Alumina." Waters Associates, Inc., 61 Fountain St., Framingham, Mass. 01701. Phone (617) 879-2000.

WATERS ASSOCIATES

9071

Circle No. 183 on Reader's Service Card

A syringe it's not,

but it injects samples into a gas chromatograph in the volume range of 0.1 μl. In fact, you get high repeatability in sub-micro volumes. There is no liquid hold-up or dead volume since the carrier gas sweeps the sample from the injector. It's all-metal, so it's difficult to break. We call it our Sub-Microliter Liquid Injector and it's used with our inlet systems. Available from authorized dealers or Hamilton Company, P.O. Box 307, Whittier, California 90608.

Repeatable Precision: Hamilton's Sub-Microliter Liquid Injector

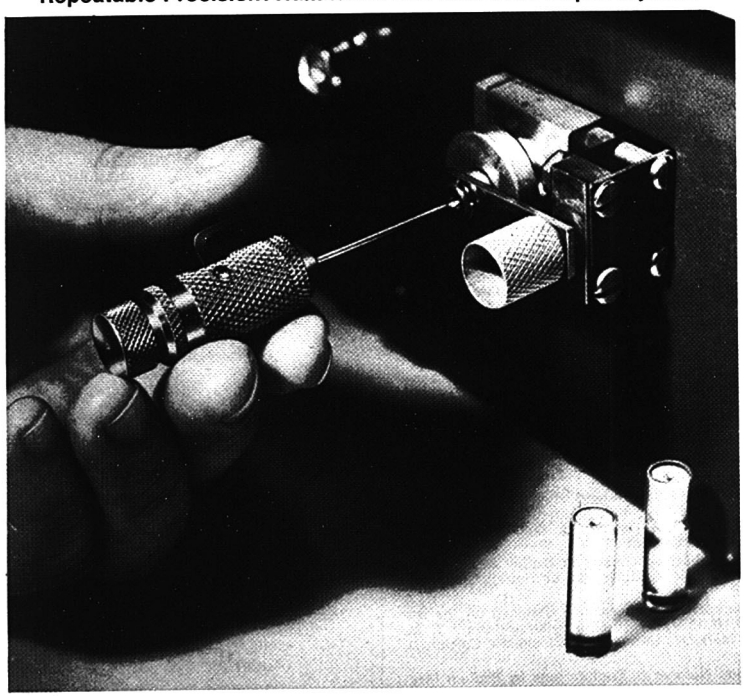

HAMILTON

Circle No. 86 on Readers' Service Card

Wednesday Afternoon

RECENT ADVANCES IN FLAME SPECTROMETRY

J. D. Winefordner, Presiding

2:00 Selective Modulation and Noise in Flame Spectrometry. T. J. Vickers, Florida State University, Tallahassee, Fla. 32306

2:40 An Experimental and Theoretical Evaluation of the Nitrous Oxide–Acetylene Flame as an Atomization Cell for Flame Spectroscopy. J. O. Rasmuson, R. N. Kniseley, V. A. Fassel, Iowa State University, Ames, Iowa 50010

3:35 Recent Advances in the N_2O/C_2H_2 Flame for Emission Analyses. S. R. Koirtyohann, 45 Agriculture Bldg., University of Missouri, Columbia, Mo. 65201

4:15 Recent Advances in Nonflame Cells for Atomic Spectrometry. R. K. Skogerboe, Colorado State University, Fort Collins, Colo. 80521

GENERAL

M. F. Burke, Presiding

2:05 The Influence of Column Material, Configuration, and Type on Efficiency in High Speed Liquid Chromatography. B. L. Karger, Howard Barth, Northeastern University, Boston, Mass. 02115

2:30 A Tandem Thermogravimetric Analyzer-Gas Chromatograph-High Resolution Mass Spectrometer System. T. L. Chang, T. E. Mead, Central Research Labs, American Cyanamid Co., Stamford, Conn. 06904

2:45 An Investigation of Experimental Variables in Frontal Chromatography. C. J. Chen, J. F. Parcher, University of Mississippi, University, Miss. 38677

3:05 Characteristics of Interrupted Elution Gas Chromatography. J. Q. Walker, C. J. Wolf, McDonnell Douglas Research Labs, St. Louis, Mo. 63166

3:25 Predicting Specific Retention Volumes from Relative Retention Data—An Improved Approach. Arleigh Hartkopf, Weber State College, Ogden, Utah 84403

3:35 Gas Chromatographic Studies Utilizing Adsorbents with Partially Filled "d" Orbitals. R. L. Grob, Eugene McGonigle, Villanova University, Villanova, Pa. 19085

3:50 Gas Chromatographic Separation and Determination of Isomeric Methylbenzene Tricarbonylchromium Complexes. J. S. Keller, Hans Veening, B. R. Willeford, Bucknell University, Lewisburg, Pa. 17837

4:10 Gas Chromatographic Study of Electron Donor-Acceptor Complexes. Claude Eon, Northeastern University, Boston, Mass.; Claude Pommier, G. Giuochon, Ecole Polytechnique, Paris, France

4:30 Structural Effects in the Separation of Diastereomeric Silicon Esters in Vapor Phase Chromatograph. S. K. Khetan, G. R. Buell, L. Spialter, Aerospace Research Labs, Wright-Patterson AFB, Dayton, Ohio 45433

6:30 Division Banquet. Speaker: Professor Arie Jan Haagen-Smit. **Current Status of the Pollution Problem**

Thursday, April 1

Thursday Morning

DETERMINATION OF AIR QUALITY

W. D. Shults, Presiding

9:05 Atmospheric Surveillance—Past, Present, and Future. G. B. Morgan, R. J. Thompson, National Air Pollution Control Administration, 1033 Wade Ave., Raleigh, N. C. 27605

9:25 Importance of Air Quality Measurements to Criteria, Standards, and Implementation Plans. D. S. Barth, National Air Pollution Control Administration, 411 W. Chapel Hill St., Durham, N. C. 27701

9:45 Aerometric Data: Needs and Networks. T. R. Mongan, E. L. Keitz, Mitre Corp., 1820 Dolley Madison Blvd., McLean, Va. 22101

10:05 Community Health and Environmental Surveillance Studies (CHESS). C. M. Shy, D. C. Calafiore, W. C. Nelson, F. B. Benson, V. A. Newill, Div. of Health Effects Research, NAPCA, 411 W. Chapel Hill St., Durham, N. C. 27701

10:40 Human Pollutant Burdens. J. F. Finklea, D. I. Hammer, T. A. Hinners, Cecil Pinkerton, Ecological Research Branch, NAPCA, 411 W. Chapel Hill St., Durham, N. C. 27701

11:00 Pesticide Exposure Index. J. E. Keil, S. H. Sandifer, Medical University of South Carolina, Preventive Medicine, 80 Barre St., Charleston, S. C. 29401; J. F. Finklea, Ecological Research Branch, 411 W. Chapel Hill St., Durham, N. C. 27701

11:20 A Combined Pollution Index: Effects of Changing Air Quality Standards. L. R. Babcock, Jr., Dept. of Energy Engineering, University of Illinois, Box 4348, Chicago, Ill. 60680

SYMPOSIUM ON NUCLEAR TECHNIQUES IN ENVIRONMENTAL SCIENCES

(Joint with Divisions of Water, Air, and Waste Chemistry and Nuclear Chemistry and Technology)

J. W. Winchester, Presiding

9:05 Bromine and Chlorine Loss from Lead Halide Aerosol. John Robbins, Great Lakes Research Div., University of Michigan, Ann Arbor, Mich. 48104; John Winchester, Dept. of Oceanography, Florida State University, Tallahassee, Fla. 32306

9:25 Characterization and Tracking of Aerosol Sources with the Use of Aircraft Sampling. G. A. Cowan, T. G. Gregory, Jr., P. R. Guthals, W. A. Sedlacek, H. L. Smith, University of California, Los Alamos Scientific Lab, P. O. Box 1663, Los Alamos, N. M. 87544

9:50 Neutron Activation Analysis of Trace Element Concentration Variations in Northern California. J. J. Wesolowski, K. Rahn, W. John, Lawrence Radiation Lab, Livermore, Calif. 94550

10:30 Source Identification of Atmospheric Aerosols by Neutron Activation Analysis. James Baugh, Irving Russell, Boston College, Chestnut Hill, Mass. 02167

10:55 Size Fractionation of Trace Elements on Urban Aerosols. E. S. Gladney, W. H. Zoller, G. E. Gordon, University of Maryland, College Park, Md. 20742

11:20 Pair and Cluster Correlations among Trace Elements in Air Particulates over the Industrialized Area of Northwest Indiana. Richard Dams, Institute of Nuclear Research, Proeftuinstraat, Ghent, Belgium; John Robbins, Kenneth Rahn, University of Michigan, Ann Arbor, Mich. 48104; John Winchester, Dept. of Oceanography, Florida State University, Tallahassee, Fla. 32306

GENERAL

H. L. Pardue, Presiding

9:05 An Automated Instrumental System for the Fundamental Characterization of Chemical Reactions. H. L. Pardue, Purdue University, Lafayette, Ind. 47907; S. N. Deming, Emory University, Atlanta, Ga. 30300

9:25 Kinetic-Catalytic Titrations. A Titrimetric Adaptation of the Variable Time Procedure for the Kinetic Determination of Traces of Materials. G. L. Heath, H. A. Mottola, Oklahoma State University, Stillwater, Okla. 74074

9:45 Electron Spectroscopy of Some Phosphorus Compounds. W. E. Swartz, D. M. Hercules, University of Georgia, Athens, Ga. 30601

10:00 Electron Spectroscopy of Quaternary Nitrogen Compounds. J. J. Jack, D. M. Hercules, University of Georgia, Athens, Ga. 30601

10:15 Use of Tris(Dipivalomethanato)Europium(III)-Induced Paramagnetic Shifts in Quantitative Analysis by Proton Magnetic Resonance Spectroscopy. D. L. Ravenstein, University of Alberta, Edmonton, Alberta, Canada

10:35 Kinetics and Mechanism of Extraction of Iron(III) with β-Isopropyltropolone. B. E. McClellan, Oscar Menis, Analytical Chemistry Div., National Bureau of Standards, Washington, D. C. 20234

10:50 Optimizing Separations by Countercurrent Distribution. V. G. Martin, R. A. Barford, Eastern Utilization Research and Development Div., USDA, 600 E. Mermaid La., Philadelphia, Pa. 19118

11:10 A Rapid and Selective Extraction of Plutonium with *N*-Benzoyl-*N*-Phenylhydroxylamine. Robert Villarreal, J. O. Young, Argonne National Laboratory, Idaho Facilities, P. O. Box 2528, Idaho Falls, Idaho 83410

NOW... CONVENIENT *PUSH-BUTTON* WEIGHING

●

arrestment and beam release mechanism *fully automatic*

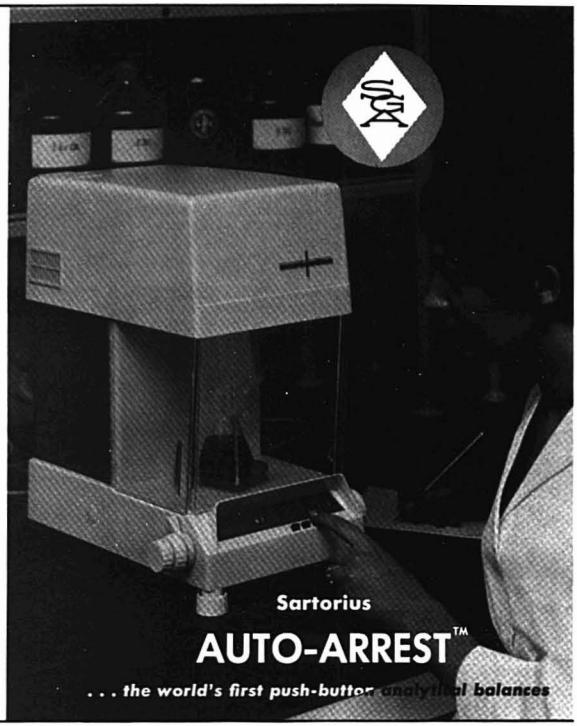

Three new balances have been added to the popular Sartorius Series 2400 line; however, in place of a lever, you arrest and release Models 2472, 2474 and 2492 by pushing a button. This causes a small motor to activate the arrestment system, guaranteeing the smoothest possible weighing technique. Since accidental "jarring" can't occur, chipped knife edges are impossible.

Pre-weighing is also activated by pushing a button. A single optical scale provides both coarse and fine readings — first in grams, then in milligrams. When a sample is placed on the pan, the coarse weight (to the nearest gram) is instantly shown. This completely eliminates trial and error weight dialing, allowing any sample size to be weighed in less than 15 seconds. Result: *weighing time is reduced up to 80%.*

Taramatic, Sartorius' exclusive mechanical taring system, is employed by these new balances, permitting adjustment to zero over the full optical range.

Convenient, push-button weighing is another step forward in automatic weighing. *Ask us for details.*

SPECIFICATIONS AND PRICES

Cat. No.	B-1379XA	B-1379XB	B-1379-10X
Model No.	2472	2474	2492
Type	Analytical	Semi-Micro	Analytical
Weighing Capacity	200 g	160 g	200 g
Taring Ranges:			
Taring in optical range	1 g	100 mg	1 g
Mechanical taring to zero (Separate set of weight counters)	—	—	200 g
Optical Range	1 g	100 mg	1 g
One Optical Division	10 mg	1 mg	10 mg
One Micrometer Division (Digital readability)	0.1 mg	0.01 mg	0.1 mg
Precision (Standard deviation)	±0.05 mg	±0.01 mg	±0.05 mg
Accuracy in Optical Range	±0.05 mg	±0.01 mg	±0.05 mg
Pre-Weighing Ranges:			
Direct	100 g	10 g	100 g
By dialing built-in 100 g weight	200 g	—	200 g
Price	$950.00	$1,050.00	$1,050.00

SCIENTIFIC GLASS APPARATUS CO. INC.
BLOOMFIELD, NEW JERSEY

LABORATORY. . .
♦ APPARATUS
♦ INSTRUMENTS
♦ CHEMICALS
♦ GLASSWARE

Branches: Boston Mass. • Danbury Conn. • Elk Grove Village Ill. • Fullerton Calif. • Philadelphia Penna. • Silver Spring Md. • Syracuse N. Y.

Circle No. 168 on Readers' Service Card

11:30 After Forty Years in the Dithizone Wilderness, Is the Promised Land in Sight? A New Look at an Old Colorimetric Reagent for Heavy Metals. D. G. Hicks, Georgia State University, Atlanta, Ga. 31303

Thursday Afternoon

DETERMINATION OF AIR QUALITY

W. D. Shults, Presiding

2:00 Sulfur Dioxide *vs.* Total Gaseous Sulfur Compounds in Los Angeles—An Evaluation of New Air Pollution Monitors. R. K. Stevens, National Air Pollution Control Administration, Raleigh, N. C.; L. F. Ballard, C. E. Decker, RIT, Research Triangle Park, N. C. 27709

2:35 Ozone-to-Total Oxidants Relationships in Los Angeles—An Evaluation of New Air Pollution Monitors. J. A. Hodgeson, R. K. Stevens, National Air Pollution Control Administration, Raleigh, N. C. 27609

2:55 Comparison of Methods for the Determination of Nitrate through Reduction. C. R. Sawicki, Wing Q, Rm. 301, Research Triangle Park, N. C. 27709; F. Scaringelli, 3820 Merton Dr., Raleigh, N. C. 27609

3:30 Photometric Determination of Polyphenols in Particulate Matter. E. Sawicki, M. Guyer, Wing Q, Rm. 301, Research Triangle Park, N. C. 27709

3:50 The Determination of Trace Metals in Air. P. W. West, Coates Chemical Labs, Louisiana State University, Baton Rouge, La. 70803

4:20 An Evaluation of Atomic Absorption and Flame Emission Spectrometry for Air Pollution Analysis. T. C. Rains, T. A. Rush, Oscar Menis, National Bureau of Standards, Washington, D. C. 20234

SYMPOSIUM ON NUCLEAR TECHNIQUES IN ENVIRONMENTAL SCIENCES

(Joint with Divisions of Water, Air, and Waste Chemistry and Nuclear Chemistry and Technology)

J. W. Winchester, Presiding

2:05 Alpha Backscattering Sensor for Nitrogen and Phosphorus Compounds in Natural and Waste Waters. John Rasmussen, Jr., Yale University, New Haven, Conn. 06520, Richard Rasmussen, Space Vector Corp., 7033 Canoga Ave., Canoga Park, Calif. 91303

2:30 Multielement Analysis of Natural Water by Neutron Activation, Group Chemical Separations, and Gamma-Ray Spectrometric Techniques. T. M. Tanner, L. A. Rancitelli, W. A. Haller, Battelle-Northwest, P. O. Box 999, Richland, Wash. 99352

2:55 The Application of Neutron Activation Analysis to Environmental Problems in the Great Lakes. David Edgington, Morris Wahlgren, Radiological Physics and Chemistry Div., Argonne National Laboratory, Argonne, Ill. 60439

3:30 Nondestructive Neutron Activation Analysis of Environmental Samples. Richard Copeland, Environmental Research Group, P. O. Box 322, Ann Arbor, Mich. 48107

3:55 Elemental Abundances of Streams Exposed to Strip Mine Runoff. James Vogt, David McKown, Michael Kay, University of Missouri, Research Reactor Facility, Columbia, Mo. 65201

4:20 Specific Activity Profiles of Selected Fallout Radionuclides in Whole Trees—Mechanisms of Uptake and Translocation. Irving Russell, Shieh-Lieh Fang, Boston College, Chestnut Hill, Mass. 02167

GENERAL

J. E. Paterson, Presiding

2:05 An Automated Platinum Loop Sampling System for Flameless Atomic Absorption and Atomic Fluorescence Spectroscopy. S. R. Crouch, S. R. Goode, Michigan State University, East Lansing, Mich. 48823

2:25 Precision Analysis of Rhenium by Thermal Activation Analysis. H. A. Braier, E. G. Miller, Gulf Research & Development Co., P. O. Box 2038, Pittsburgh, Pa. 15230

2:35 Neutron Activation Analysis Fingerprinting of Obsidian Artifacts. D. J. R. Evans, AECL-CP, P. O. Box 3100, Station C, Ottawa, Ontario, Canada; R. Wilmeth, National Museum of Man, Archaeology Div., Bells Corners, Ottawa, Ontario, Canada

2:55 Identification by Nmr of Aromatic Acid and Amine Unknowns in Human Urine. Katherine Scott, Dept. of Radiology and Chemistry, University of Florida, Gainesville, Fla. 32601

3:15 X-Ray Microanalysis of Water Using Electrochemical Preconcentration. B. H. Vassos, R. F. Hirsch, Seton Hall University, South Orange, N. J. 07079; Herbert Letterman, Bristol-Myers Products, Hillside, N. J. 07205

3:35 Raman Spectroscopic Analysis of the Cis/Trans Isomer Composition of Edible Vegetable Oils. G. F. Bailey, R. J. Horvat, Western Regional Research Labs, U. S. Department of Agriculture, Albany, Calif. 94710

3:50 Spectrophotometric Determination of Micro Amounts of Ascorbic Acid Using Ferrozine. Bruno Jaselskis, J. Nelapathy, S. J., Loyola University, Chicago, Ill. 60626

4:05 Loss of Gold in Sample Dissolution. H. A. Moore, Jr., R. A. Wessman, Technical Services Dept., Trapelo/West, Div. LFE Corp., 2030 Wright Ave., Richmond, Calif. 94804

Friday April 2

Friday Morning

DETERMINATION OF AIR QUALITY

W. D. Shults, Presiding

9:05 The Activities of the Intersociety Committee on Manual of Methods for Ambient Air Sampling and Analysis. A. C. Stern, Dept. of Environmental Sciences and Engineering, University of North Carolina, Chapel Hill, N. C. 27514

9:35 The Status of Sensory Methods for Ambient Air Monitoring. E. R. Hendrickson, Environmental Engineering, Inc., 2324 S.W. 34th St., Gainesville, Fla. 32601

9:55 Interfacing Chemical and Sensory Sciences in Odorous Pollution Measurements. Andrew Dravnieks, IIT Research Institute, 10 W. 35th St., Chicago, Ill. 60616

10:25 Analysis of the Aerocarcinogen Conglomerate. E. Sawicki, Wing Q, Rm. 301, Research Triangle Park, N. C. 27709

10:55 Studies of Aggressive Chemicals Adsorbed on Smoke Particulates by Photoelectron Spectroscopy. L. D. Hulett, T. A. Carlson, J. L. Durham, B. R. Fish, Oak Ridge National Laboratory, Oak Ridge, Tenn. 37830

11:15 Microwave Spectrometry as an Air Pollutant Analysis Method. E. A. Rinehart, Physics Dept., University of Wyoming, Laramie, Wyo. 82070

11:40 Biological Degradation of Toxic Pollutants. G. G. Guilbault, S. S. Kuan, M. H. Sadar, W. Hussein, S. Hsiung, Louisiana State University, New Orleans, La. 70122

GENERAL

J. S. Juvet, Jr., Presiding

9:05 Determination of the Chromium Content of Lunar Samples by Gas-Liquid Chromatography. W. R. Wolf, R. E. Sievers, Aerospace Research Labs, Wright-Patterson AFB, Ohio 45433; W. D. Ross, Monsanto Research Corp., Dayton, Ohio 45407

9:20 Ultratrace Analysis for Beryllium in Apollo 11 and 12 Lunar Samples by Gas Chromatography. K. J. Eisentraut, D. G. Johnson, M. F. Richardson, R. E. Sievers, Aerospace Research Labs, Wright-Patterson AFB, Ohio 45433

9:35 The Achievement and Measurement of Fast Temperature-Rise Times in Pyrolysis Gas Chromatography (Pgc). R. L. Levy, C. J. Wolf, McDonnell Douglas Research Labs, St. Louis, Mo. 63166

9:55 Factors Affecting the Laser Pyrolysis of Polymers. D. L. Fanter, R. L. Levy, C. J. Wolf, McDonnell Douglas Research Labs, St. Louis, Mo. 63166

10:15 Improved Solid Supports for Gas Chromatography. R. D. Schwartz, R. G. Mathews, Pennzoil United, Inc., Shreveport, La. 71102

10:35 The Mechanical Desulfurization of Coal—Major Considerations for SO_2-Emission Control. L. Hoffman, K. E. Yeager, Mitre Corp., 1820 Dolley Madison Blvd., McLean, Va. 22101

11:05 A Gas Chromatographic Method for the Microdetermination of Iodine. R. A. Hasty, Montana State University, Bozeman, Mont. 59715

AUTOMATIC VISCOSITY TIMER

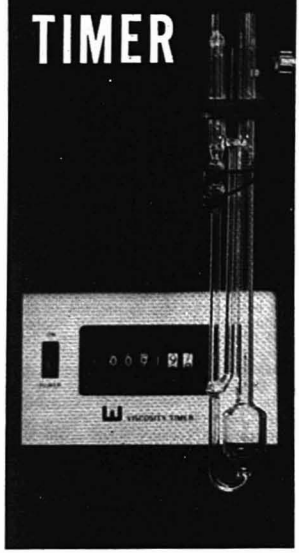

- Starts and stops automatically — whether flow time is 10 seconds or 1000 seconds
- Accurate to .02% ±.01 seconds with both rising and falling-level viscometers

The Wescan Model 220 Automatic Viscosity Timer measures viscosity up to ten times more accurately than manual methods — while freeing the operator for other activity. It measures flow times up to 9999.99 seconds, at temperatures from —75°C to 150°C. Changes in light reflection trigger the timer by means of photosensors.

For details about the way the Model 220 saves time and measures more precisely, write for PB 702.

WESCAN INSTRUMENTS, INC.

WESCAN INSTRUMENTS, INC.
2968 Scott Boulevard
Santa Clara, California 95050

Circle No. 194 on Readers' Service Card

Participants in the January Northeastern ACS Meeting included (left to right): Denis L. Rousseau, Bell Telephone Laboratories, Murray Hill, N. J.; S. Barry Brummer, Tyco Laboratories, Waltham, Mass.; E. F. Levy, Chairman of the Northeastern Section, ACS; and James N. Little, President of the Analytical Group, Waters Assoc. Dr. Rousseau and Dr. Brummer were the speakers on the topic "Polywater or Poly . . . ? A Controversy." Dr. Rousseau took the con side and Dr. Brummer the pro. The Analytical Group was cosponsor of the meeting

JCC Session on Laboratory Automation

Laboratory automation is the topic for a special session planned for the 1971 Fall Joint Computer Conference to be held in Las Vegas, Nev., Nov. 15 to 18, 1971. The primary theme of the conference is the use of computers to improve the quality of life.

Original papers illustrating applications in chemistry and related areas are being solicited for the session, "Systems and Concepts for Laboratory Automation." This session is being designed to provide a forum for the dissemination of methods and techniques now available and to stimulate new developments. Those wishing to submit papers should first contact either of the session cochairmen: Leonard H. Ponder, American Enka, Enka, N. C. 28728, 704-667-6961, or David L. Schroeder, On-Line Systems, 4721 McKnight Rd., Pittsburgh, Pa. 15237, 412-931-7600

The Joint Computer Conferences are held twice a year under the sponsorship of the American Federation of Information Processing Societies (AFIPS) and encompass the entire information processing field. By including this special session, an opportunity is provided to gain an overall view of computer technology as well as specifics in areas of particular interest. Exhibits will portray the impact of modern computer technology in many fields.

Many other sessions are included and one of special interest also to analytical chemists is on environmental control. Prospective authors should request a copy of "Instructions to Authors" from the technical program chairman, Martin Y. Silberberg, P. O. Box 11337, Palo Alto, Calif. 94306. The deadline for papers in all sessions is Apr. 1, 1971.

Symposium on Molelcular Structure and Spectroscopy

The 26th Annual Symposium on Molecular Structure and Spectroscopy will be held June 14 to 18, 1971, at Ohio State University, Columbus, Ohio. Invited papers include the following: Photoionization Studies of Small Molecules by W. A. Chupka, Argonne National Laboratory; Spectra and Intermolecular Forces in Crystals by David Dows, University of Southern California; Molecular Zeeman Effect and the Measurement of Magnetic Susceptibilities and Molecular Quadrupole Moments by W. H. Flygare, University of Illinois; Rotation-Electronic Interaction in the Rydberg States of Simple Molecules by J. W. C. Johns, National Research Council, Canada; Spectroscopic Studies of the Outer Planets by Tobias Owen, State University of New York at Stony Brook; and a paper (title to be announced) by W. Klemperer, Harvard University.

Sessions of contributed papers with the following titles are planned: elec-

tronic spectra (small molecules); electronic spectra (theory); solid state (electronic); solid state (infrared); solid state (low temperature); microwave spectra; astrophysical spectra; lasers; chemical spectroscopy; high resolution infrared, theory and techniques; nmr spectra; vibrational analysis; intensity studies; and others.

Further details on the meeting are available from K. Narahari Rao, Dept. of Physics, Molecular Spectroscopy Symposium, 174 W. 18th Ave., Ohio State University, Columbus, Ohio 43210

Second International Conference on Calorimetry and Thermodynamics

The Second International Conference on Calorimetry and Thermodynamics (26th Annual Calorimetry Conference) will be held at the University of Maine, Orono, Me., July 12 to 14, 1971. This meeting will be sponsored by the Calorimetry Conference (USA) and the Commission on Thermodynamics and Thermochemistry of the International Union of Pure and Applied Chemistry.

The conference will be concerned with all methods and techniques of calorimetry and ancillary measurements, including applications in physics, chemistry, biochemistry, biology, and other fields, and also with noncalorimetric thermodynamic studies: thermochemical quantities obtained from chemical equilibrium studies; vaporization studies (vapor pressures, decomposition pressures, adsorption of gases, effusion measurements); noncalorimetric studies of thermodynamic properties in single and multicomponent systems (pvt data, compressibility, phase studies, solubilities); thermodynamics of systems of biochemical interest; thermodynamics of liquids (mixed liquids, ionic solutions, polyelectrolytes, etc.) For further information write to S. R. Gunn, University of California Radiation Laboratory, Livermore, Calif. 94550

ASTM News

The ASTM infrared spectral data retrieval service (Sirch) is now available on IBM 360 computers. The new system will include the newly completed 14th supplement of 10,000 compounds bringing the total infrared spectral data bank to over 102,000 compounds. Separate tapes for the 14th supplement are also available. Write to R. W. Sherwood, ASTM, 1916 Race St., Philadelphia, Pa. 19103. 215-569-4200

The Unspoiler.

Too bad. Set up a gas chromatography system, develop a proper technique and then spoil it with a leaky system. For as little as $310.00 the GOW-MAC Gas Leak Detector will find the leaks in your system and make your chromatography more accurate. Cordless, portable and equipped with a self-contained rechargeable battery and charger, or line operated, the GOW-MAC pin points leaks of inert, combustible, light or heavy gases in hot or cold pressurized systems and in hard to reach test points through use of a stabilized thermal conductivity cell and a self-contained solid-state amplifier. Signals audibly or visually. Single knob for null balance makes operation simple. Sensitivity is 10^{-8}cc at atmosphere/second of Helium. For Helium or Hydrogen it sees 10ppm of gas in static systems. Selected by the United States Navy for testing underwater equipment, the GOW-MAC Gas Leak Detector can help you stop spoiling your accuracy and eliminate costly and dangerous gas leaks in your lab. For catalog and prices, write or call collect.

GOW MAC **GOW MAC INSTRUMENT CO.**

100 Kings Road ■ Madison, N. J. 07940 U.S.A. ■ Telephone 201/377-3450
Shannon Free Airport, Shannon Ireland

Circle No. 75 on Readers' Service Card

Dial your temperature

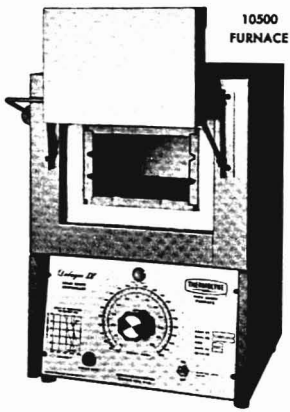

10500 Furnace with Solid-State Control

NEW ORDER OF RELIABILITY

New solid-state controller, Dubuque IV, raises reliability to a new level . . . long life silicon controlled rectifier and transistor establishes positive reliability . . . No tube replacement.

PROPORTIONING BUILT-IN

Automatic proportioning action accurately compensates for temperature lag and overshoot in furnace . . . cyclic temperature variations are minimized.

QUICK RESPONSE HEATING ELEMENTS

Special "low-mass" elements respond quickly to controller demand . . provide balanced heat distribution. New features combine to give highest dollar value in a small furnace

Chamber size—5½" W x 3⅜" H x 6½" D

1093C (2000F) Model——$328.50

1177C (2150F) Model——$339.50

Write for *free* Catalog

THERMOLYNE
SYBRON CORPORATION

2555 KERPER BLVD.
DUBUQUE, IOWA 52001

Circle No. 177 on Readers' Service Card

Scheduled Courses in Analytical Techniques

Information is given in the following order: date, name of course, location of course, professional person(s) in charge of course, and/or sponsoring organizations, and Contact (numbers in parentheses refer to addresses and telephone numbers given at the bottom of the list of scheduled courses).

Mar. 15 to 16—Seminar/Workshop on Specific Ion Electrodes. Cambridge, Mass. *Contact:* Orion Research, Inc., 11 Blackstone St., Cambridge, Mass. 02139. 617-864-5400

Mar. 15 to 19—Industrial Use of the Polarizing Microscope. Chicago, Ill. McCrone Research Institute. *Contact (1)*

Mar. 15 to 19—Laser Applications. Washington University. Includes sessions on laser monitoring of the environment. *Contact:* Div. of Continuing Education, Box 1048, Washington University, St. Louis, Mo. 63130. 314-863-0100, ext. 4530

Mar. 17 to 19—Small Computer Applications and Interfacing. Reston, Va. *Contact:* Donaldson Brown Center for Continuing Education, Virginia Polytechnic Institute and State University, Ext. Div., Blacksburg, Va. 24061. 703-552-8322

Mar. 17 to 19—Thermal Analysis: Differential Scanning Calorimetry, Thermogravimetric Analysis, Thermochemical Analysis. Norwalk, Conn. Perkin-Elmer. *Contact (8)*

Mar. 19 to 20—Atomic Absorption Spectroscopy. New York City. T. C. Rains, J. A. Dean, G. D. Christian. ACS. *Contact (2)*

Mar. 22 to 23—Atomic Absorption Spectroscopy. Norwalk, Conn. Perkin-Elmer. *Contact (8)*

Mar. 22 to 24—Fourier Transform Spectroscopy. Philadelphia, Pa. Sadtler Research. *Contact (3)*

Mar. 22 to 24—Nuclear Magnetic Resonance. Philadelphia, Pa. Sadtler Research. *Contact (3)*

Mar. 25 to 26—Luminescence Spectroscopy. Norwalk, Conn. T. J. Porro, Perkin-Elmer. *Contact (8)*

Mar. 29 to 31—Data Communications Systems. Williamsburg, Va. Introductory seminar to orient a potential user for on-line, real time, or other system. *Contact:* Registrar, The Institute for Advanced Technology, Control Data Corp., 5272 River Rd., Washington, D. C. 20016. 301-652-2268, ext. 245

Mar. 29 to Apr. 1—Electronics for Chemists. Philadelphia, Pa. Sadtler Research. *Contact (3)*

Mar. 29 to Apr. 2—Principles of Color Technology. Rensselaer Polytechnic Institute, Troy, N. Y. F. W. Billmeyer, Jr., Max Saltzman. *Contact (4)*

Mar. 29 to Apr. 2—Photomicrography. London, England. McCrone Research Institute. *Contact (1)*

Apr. 5 to 6—Color Technology. Raleigh, N. C. Diano Corp. *Contact (5)*

Apr. 8 to 9—Color Technology. Washington, D. C. Diano Corp. *Contact (5)*

Apr. 19 to 21—Nmr Workshop. Philadelphia, Pa. Sadtler Research. *Contact (3)*

Apr. 19 to 23—Nondestructive Testing. Metals Park, Ohio. Metals Engineering Institute. *Contact (6)*

Apr. 19 to 23—Industrial Use of the Polarizing Microscope. London, England. McCrone Research Institute. *Contact (1)*

Apr. 19 to 23—Infrared. Chicago, Ill. Philadelphia, Pa. Sadtler Research. *Contact (3)*

Apr. 26 to 27—Thermoanalysis. Philadelphia, Pa. Sadtler Research. *Contact (3)*

Apr. 26 to 30—Gas Chromatography. Philadelphia, Pa. Sadtler Research. *Contact (3)*

Apr. 26 to 30—Metallographic Techniques. Metals Park, Ohio. Metals Engineering Institute. *Contact (6)*

Apr. 27 to 28—Third Symposium on Materials Characterization by Thermal Methods. Wilmington, Del. *Contact:* E. I. du Pont de Nemours & Co., Instrument Products Div., Materials Characterization Symposium, Wilmington, Del. 19898

Electron Microscopy and Analysis Group

The Electron Microscopy and Analysis Group of The Institute of Physics and The Physical Society is arranging a meeting to mark the 25th anniversary of the formation of the Group in Oxford, 1946. The meeting will be held in Cambridge, June 29 through July 1, 1971, and is intended to present the current state of the art in all the subjects of interest to the Group. Both invited speakers and contributed papers will be included. The program will cover the following areas: electron-specimen interaction in transmission, scanning, and probe analysis; electron optical instrumentation; electron lenses and guns; quantitative applications and measurement in electron beam systems; Fourier optics; contrast in both biological and nonbiological specimens imaged under a variety of conditions; ion optics and ion microscopy; applications showing physical principles in metals, materials, biological, and physical investigations. Further information on the meeting is

Apr. 30—Forensic Applications in Scanning Electron Microscopy. Chicago, Ill. *Contact:* Milton E. Nelson, IIT Research Institute, 10 W. 35th St., Chicago, Ill. 60616. 312-225-9630

May 3 to 7—Two Separate Courses: Infrared, Part I; Mass Spectrometry. Philadelphia, Pa. Sadtler Research. *Contact (3)*

May 3 to 7—Metallographic Interpretation. Metals Park, Ohio. Metals Engineering Institute. *Contact (6)*

May 13 to 14—Color Technology. Manchester, England. Diano Corp. *Contact (5)*

May 17 to 18—Color Technology. Milan, Italy. Diano Corp. *Contact (5)*

May 17 to 21—Advanced Microscopy. Chicago, Ill. McCrone Research Institute. *Contact (1)*

May 17 to 21—Two Separate Courses: Thin Layer Chromatography; Laboratory Management. Philadelphia, Pa. Sadtler Research. *Contact (3)*

May 20 to 21—Color Technology. Frankfurt, Germany. Diano Corp. *Contact (5)*

June 7 to 11—Two Separate Courses: Gas Chromatography; Infrared, Part II. Philadelphia, Pa. Sadtler Research. *Contact (3)*

June 7 to 11—Photomicrography. Chicago, Ill. McCrone Research Institute. *Contact (1)*

June 7 to 11—Advanced Electron Microscopy. Philadelphia, Pa. *Contact:* William C. Cohen, Continuing Engineering Studies, University of Pennsylvania, 295 Towne Bldg., Philadelphia, Pa. 19104. 215-594-8574

June 7 to 18—Modern X-Ray Spectrometry. Albany, N. Y. *Contact:* Henry Chessin, State University of New York at Albany, Dept. of Physics, 1400 Washington Ave., Albany, N. Y. 12203

June 9 to 26—Digital Computers in Chemical Instrumentation. Purdue University. *Contact:* S. P. Perone, Chemistry Dept., Purdue University, Lafayette, Ind. 47907. Page 63 A, Jan.

June 14 to 18—Industrial Use of the Polarizing Microscope. Chicago, Ill. McCrone Research Institute. *Contact (1)*

June 17 to 18—Color Technology. Montreal, Canada. Diano Corp. *Contact (5)*

June 21 to 25—Metallographic Techniques. Metals Park, Ohio. Metals Engineering Institute. *Contact (6)*

June 21 to 25—Identification of Small Particles. Chicago, Ill. McCrone Research Institute. *Contact (1)*

June 21 to 25—Two Separate Courses: Infrared, Part I; Nuclear Magnetic Resonance. Philadelphia, Pa. Sadtler Research. *Contact (3)*

June 21 to July 2—Special Summer Program in Infrared Spectroscopy. MIT. R. C. Lord, D. W. Mayo. *Contact (7)*

June 26 to July 17—Digital and Analog Electronics for Scientists. University of Illinois, Urbana, Ill. *Contact:* H. V. Malmstadt, University of Illinois, Urbana, Ill. 61801. 217-333-3120

July 12 to 16—Enzymes and Their Use in Analysis and Clinical Diagnosis. MIT. *Contact (7)*

July 12 to 16—Principles of Color Technology. Rensselaer Polytechnic Institute, Troy, N. Y. F. W. Billmeyer, Jr., Max Saltzman. *Contact (4)*

July 12 to 16—X-Ray Techniques in the Industrial Laboratory. London, England. McCrone Research. *Contact (1)*

(1) Mrs. Miriam Fallert, Registrar, McCrone Research Institute, 451 E. 31st St., Chicago, Ill. 60616. 312-842-7105
(2) Education Office, American Chemical Society, 1155 16th St., N.W., Washington, D. C. 20036. 202-737-3337, ext. 258
(3) Sadtler Educational Div., Sadtler Research Laboratories, Inc., 3316 Spring Garden St., Philadelphia, Pa. 19104. 215-382-7800
(4) Office of Continuing Studies, Rensselaer Polytechnic Institute, Troy, N. Y. 12181
(5) Diano Corp., P. O. Box 231, 132 Central St., Foxboro, Mass. 02035. 617-543-5383
(6) William M. Mueller, Director of Education, ASM, Metals Park, Ohio 44073. 216-338-5151
(7) Director of the Summer Session, Room E19-356, Massachusetts Institute of Technology, Cambridge, Mass. 02139
(8) J. L. Bernard, Supervisor, Customer Training Dept., Mail Station 104, Perkin-Elmer Corp., Norwalk, Conn. 06852. 203-762-4644

available from the Meetings Officer, The Institute of Physics and The Physical Society, 47 Belgrave Sq., London SW1, England. 01-235-6111

Denver Conference on X-Ray Analysis Applications

The 20th Annual Denver Conference on Applications of X-Ray Analysis will be held Aug. 11 to 13, 1971, at the Albany Hotel, Denver, Colo. Technical papers on subjects related to X-rays and their applications will be presented during the 3-day meeting. The emphasis this year will be on instrumentation as applied to diffraction, fluorescence, microprobe, and other related techniques, including developments in automation. Also, general papers on other aspects of X-ray analysis are invited. Abstracts of papers (three copies, about 300 words) should be sent before Apr. 15, 1971, to C. O. Ruud, Conference Cochairman, Dept. of Metallurgy and Materials Science, University of Denver, Denver, Colo. 80210. Final manuscripts are due July 16, 1971.

this instrument can make the gradient

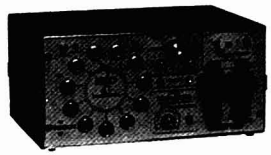

FOR
CHROMATOGRAPHIC ELUTION
OR FILLING ZONAL ROTORS

With a capacity of 3200 ml/hr, the Model 380 DIALAGRAD Programmed Gradient Pump is especially suited for filling zonal rotors as well as forming liquid chromatographic elution gradients and similar applications. Almost any two component gradient can be formed by simply setting a series of dials. There are no cams to cut or multiple solutions to mix at estimated concentrations. The shape of the curve is determined by setting eleven 0 to 100% dials which represent the initial, final, and nine evenly spaced intermediate ratios. This gives 10 program intervals, each of which are automatically subdivided by five linear interpolations to produce a smooth gradient.

Calibrated flow rates from 1 to 3200 ml/hr and program durations from 5 minutes to 16 days are set with positive stop switches. The DIALAGRAD will produce linear or curved gradients with equal accuracy and the program will be perfectly reproducible run after run. The instrument takes but a few minutes to program and requires no attention during a program run.

For more information, please request Brochure DP31.

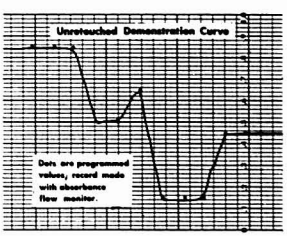

INSTRUMENTATION SPECIALTIES COMPANY

4700 SUPERIOR LINCOLN, NEBRASKA 68504
PHONE (402) 434-0231 TELEX 48-6453

Circle No. 91 on Readers' Service Card

Directory of Graduate Research 1969

Biennial publication of the ACS Committee on Professional Training

Covers the universities and colleges in the United States and Canada known to offer an organized curriculum leading to the doctoral degree in chemistry, biochemistry, chemical engineering, and pharmaceutical or medicinal chemistry.

The guide to graduate schools, research, and personnel in these areas.

201 Departments of Chemistry
165 Departments offering Biochemistry
106 Departments of Chemical Engineering
29 Departments of Pharmaceutical or Medicinal Chemistry

Lists 2807 full- and part-time staff members, each with outline of career, teaching and research specialties, and list of publications for the past two or five years.

Statistical data on departments include number of Ph.D. degrees conferred during the previous two years, number of staff members, and number of postdoctoral appointments.

Other listings include interdisciplinary programs and doctoral theses accepted during previous two years.

1213 pp. with index of names paper bound (1970) $10.00 postpaid in U.S., plus 50 cents Canada and Pan America, plus 75 cents foreign.

Order from:
Special Issue Sales
American Chemical Society
1155 Sixteenth St., N.W.
Washington, D. C. 20036

CALENDAR OF EVENTS

Mar. 9 to 13	**Fifth International Exhibition of Industrial Electronics.** Basel, Switzerland. Includes special group display for medical science. *Contact:* Sekretariat INEL71, CH-4000, Basel, Switzerland. Page 72 A, Nov.
Mar. 11 to 12	**Symposium on Advanced Analytical Concepts for the Clinical Laboratory.** Oak Ridge, Tenn. *Contact:* Dr. Charles D. Scott, ORNL, P. O. Box X, Oak Ridge, Tenn. 37830. 615-483-8611, ext. 3-6265. Page 73 A, Nov.
Mar. 16 to 17	**Conference on Effectiveness of On-Line Biomedical Computing.** International Hotel, Los Angeles. Includes session relating to clinical laboratories. *Contact:* M. J. Miller, AAMI, 9650 Rockville Pike, Bethesda, Md. 20014. 201-530-2800. Page 72 A, Dec.
Mar. 18	**American Microchemical Society Meeting.** Ramada Inn, Rte. 18, Exit 9, N. J. Turnpike. Speaker: Roland S. Yunghans, "Pollution Control." *Contact:* Louis M. Brancone, Lederle Laboratories Div., American Cyanamid Co., Pearl River, N. Y. 10965. 914-735-5000
Mar. 28 to Apr. 2	**161st National ACS Meeting.** Los Angeles, Calif. Includes Analytical Chemistry Division sessions. *Contact:* J. C. White, Analytical Chemistry Div., ORNL, Oak Ridge, Tenn. 37830. 615-483-8611, ext. 3-1472. Page 51 A, Mar.
Mar. 29 to Apr. 2	**Labex International 1971.** Earls Court, London, England. *Contact:* Bevan M. Gilpin, U.T.P. Exhibitions, Ltd., 36–7 Furnival St., London, EC4A, England. 01-405-4886. Page 86 A, Feb.
Mar. 30 to Apr. 3	**The Chemical Society and Royal Institute of Chemistry Joint Annual Meeting.** Brighton, England. *Contact:* John F. Gibson, The Chemical Society, Burlington House, London, W1V OBN, England

Coming Events

Apr. 5 to 7—Ninth Annual Vacuum Technology Seminar. Palo Alto, Calif. *Contact:* William Mills, Varian, Vacuum Div., Palo Alto, Calif. 415-326-4000

Apr. 12 to 17—Federation of American Societies for Experimental Biology. McCormick Place, Chicago, Ill. *Contact:* Steven K. Herlitz, Inc., 850 Third Ave., New York, N. Y. 10022. 212-421-6900

Apr. 14 to 16—National Pollution Control Conference & Exposition. Cobo Hall, Detroit, Mich. *Contact:* Bill Reeves, 1107 S. Loop West, Houston, Tex. 77021

Apr. 19 to 21—17th ISA Analysis Instrumentation Symposium. Marriott Motor Hotel, Houston, Tex. *Contact:* G. A. McNeill, Monsanto Co., 730 Worcester Ave., Springfield, Mass. 01107

Apr. 19 to 23—International Solvent Extraction Conference, SCI. The Hague, The Netherlands. *Contact:* ISEC '71, 14 Belgrave Sq., London, W.W.1, England

Apr. 21 to 23—7th Annual Symposium on Vacuum Science. Albuquerque, N. M. *Contact:* D. G. Schreiner, P. O. Box 11451, Albuquerque, N. M. 87112

Apr. 26 to 28—Advanced Thin Layer Chromatography and Electrophoresis Symposium. Cherry Hill Inn, Cherry Hill, N. J. *Contact:* Camag, Inc., 2855 S. 163rd St., New Berlin, Wis. 53151

Apr. 26 to 30—17th Annual Meeting and Equipment Exposition of the Institute of Environmental Sciences. Biltmore Hotel, Los Angeles, Calif. Includes topics on data acquisition and reduction and instruments for environmental measurements. *Contact:* Institute of Environmental Sciences, 940 E. Northwest Hwy., Mt. Prospect, Ill. 60056. 312-255-1561. Page 74 A, Nov.

Apr. 27 to 29—Fourth Annual Scanning Electron Microscopy Symposium. Chicago, Ill. *Contact:* Dr. Om Johari, Metals Div., IIT Research Institute, 10 W. 35th St., Chicago, Ill. 60616. 312-225-9630, ext. 4843. Page 73 A, Nov.

Apr. 30 to May 3—Metro Chem '71. San Juan, Puerto Rico. *Contact:* Dr. G. Ewing, Dept. of Chemistry, Seton Hall University, South Orange, N. J. 07079. Page 67 A, Oct.

May 2 to 7—19th Annual Conference on Mass Spectrometry and Allied Topics. Regency Hyatt House Hotel, Atlanta, Ga. *Contact:* F. E. Saalfeld, Naval Research Laboratory, Code 6110, Washington, D. C. 20390. Page 72 A, Dec.

May 9 to 14—Electrochemical Society National Meeting. Sheraton-Park Hotel, Washington, D. C. *Contact:* Electrochemical Society, 30 E. 42nd St., New York, N. Y. 10017. 212-867-4430

May 12 to 14—Dialogues in Microscopy 1971. Hotel New Yorker, New York, N. Y. *Contact:* John A. Reffner/NYMS, Institute of Material Science, University of Connecticut, Storrs, Conn. 06268. Page 67 A, Oct.

May 25 to 26—5th IMEKO: Symposium on Photon Detectors. Varna, Bulgaria. *Contact:* IMEKO Photon Detectors Subcommittee, Dr. H. C. P. Gorlich, Chairman, 69 Jena, Carl Zeiss Platz 1, East Germany

May 31 to June 4—Biological Aspects of Electrochemistry. Rome, Italy. Sponsors: CITCE; IUPAC. *Contact:* Prof. G. Milazzo, Istituto Superiore di Sanita, Viale Regina Elena, 299, 00161, Roma, Italy. Page 72 A, Nov.

June 2 to 3—Second All-Industry Conference on Pollution Control. Pick Carter Hotel, Cleveland, Ohio. *Contact:* William M. Mueller, Director of Education, ASM, Metals Park, Ohio 44073

June 4 to 5—Third Gas Chromatography Symposium. Hueston Woods Lodge, near Oxford, Ohio. Sponsor: Ohio Valley Gas Chromatography Discussion Group. *Contact:* Robert Lemieux, P. O. Box 125, Dayton, Ohio 45402

June 7 to 8—ACS Central Regional Meeting. University of Cincinnati, *Contact:* Joseph Cantrell, Dept. of Chemistry, Miami University, Oxford, Ohio 45056. 513-529-3013

June 10 to 11—ACS Great Lakes Regional Meeting. Bradley University, Peoria, Ill. *Contact:* James Van Lanen, Hiram Walker & Sons, Inc., Peoria, Ill. 61601

June 14 to 17—International Symposium on Identification and Measurement of Environmental Pollutants. Ottawa, Ont., Canada. *Contact:* M. K. Ward, National Research Council of Canada, Ottawa 7, Ontario. 613-993-1421. Page 71 A, Nov.

June 14 to 18—62nd Annual Meeting of the American Society of Biological Chemists. San Francisco, Calif. *Contact:* Robert A. Harte, ASBC, 9650 Rockville Pike, Bethesda, Md. 20014. Page 88 A, Feb.

June 14 to 18—26th Annual Symposium on Molecular Structure and Spectroscopy. Ohio State University. *Contact:* K. Narahari Rao, Dept. of Physics, 174 W. 18th Ave., Ohio State University, Columbus, Ohio. Page 58 A, Mar.

June 16 to 18—24th Annual Summer Symposium, Division of Analytical Chemistry, ACS. NBS, Gaithersburg, Md. Topic: Analytical Chemistry: The Key to Progress in National Problem Areas. *Contact:* W. W. Meinke, National Bureau of Standards, Washington, D. C. 20234. Page 84 A, Feb.

June 21 to 24—5th Symposium on Temperature, Its Measurement and Control in Science and Industry. Washington, D. C. *Contact:* Vincent J. Giardina, Instrument Society of America, 530 William Penn Pl., Pittsburgh, Pa. 15219. Page 71 A, Nov.

June 27 to July 1—Air Pollution Control Association Annual Meeting. Hotel Traymore, Atlantic City, N. J. *Contact:* Nicholas Post, Water Pollution Controls Inc., 160 Broadway, New York, N. Y. 10038. 212-349-7282

June 27 to July 2—ASTM 74th Annual Meeting and Exposition. Chalfonte-Haddon Hall, Atlantic City, N. J. *Contact:* American Society for Testing and Materials, 1916 Race St., Philadelphia, Pa. 19103. 215-569-4200

New Becker 407 Series Gas Chromatographs

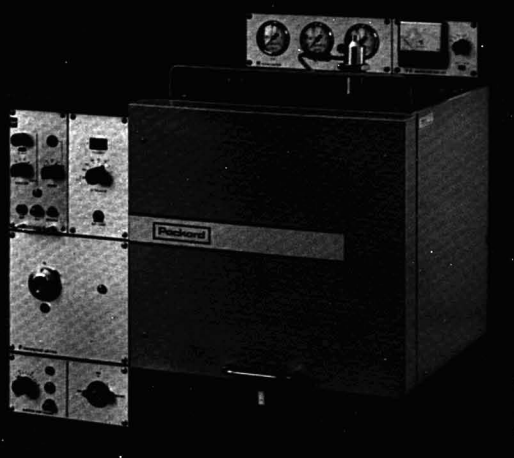

Unique research instruments priced from only $2,175.00

- **True Computer-Compatibility**—A separate output direct from the chromatograph provides a full-range signal for integration.
- **Built-in Flow Controls**—An exclusive, pressure-regulating flow controller is part of the instrument, not an option. Provides accuracy better than 0.1%.
- **Research-Quality Oven**—A full size (7⅞ x 7⅞ x 8¾") oven with a temperature range of 30 to 400°C and stability within 0.1°C.
- **Wide-Range Electrometer**—Low system noise, linear dynamic range of more than 200,000, and a time constant of 50 milliseconds produce clean signals which allow full use of electronic integrators and computers.

The low cost of Series 407 Chromatographs was achieved by limiting their versatility, not by compromising quality. That makes them an ideal purchase for the research lab with an urgent need to add capacity, but a limited budget. 407 Series instruments can be used to implement techniques developed on more sophisticated chromatographs, without loss of data comparability.

Clip and mail the coupon for 16-page Catalog 1124 B

Please send me a copy of Catalog 1124 B

NAME_____ TITLE_____

COMPANY/INSTITUTION_____

ADDRESS_____

CITY_____ STATE_____ ZIP_____

Packard

PACKARD INSTRUMENT COMPANY, INC.
PACKARD INSTRUMENT INTERNATIONAL S.A. LTD.
2200 WARRENVILLE ROAD • DOWNERS GROVE, ILLINOIS 60515
SUBSIDIARIES OF AMBAC INDUSTRIES, INC.

Circle No. 135 on Readers' Service Card

Here's Perkin-Elmer's new Model 710 Infrared Spectrophotometer.

It's a Super 700.

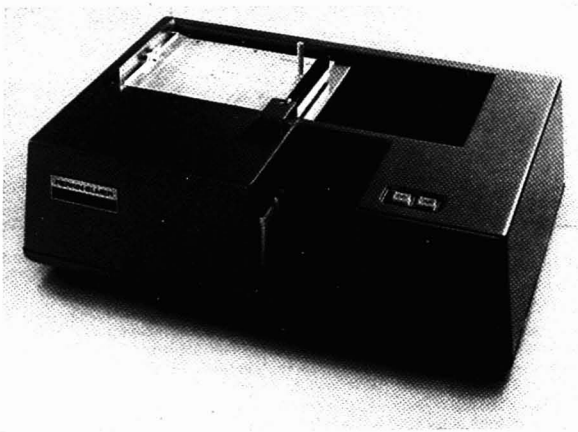

The spectrum below shows the difference.

Resolution at 3000 cm^{-1} is now better than 10 cm^{-1}. Resolution at 1000 cm^{-1} is better than 5 cm^{-1}. In other respects, the Model 710 is the same proven 700 you see everywhere in colleges and universities, in industrial research and control laboratories. Same push-button simplicity, compactness and reliability. Same choice of scan speeds. Same unbroken chart presentation, linear frequency recording from 4000-650 cm^{-1} (2.5 to 15.4 microns).

Now, get the Model 710 at $3,150.00 or the Model 700 at $2,760.00. You get outstanding performance both ways. Write for our new brochure. Instrument Division, Perkin-Elmer Corporation, 702 Main Avenue, Norwalk, Conn. 06852.

PERKIN-ELMER

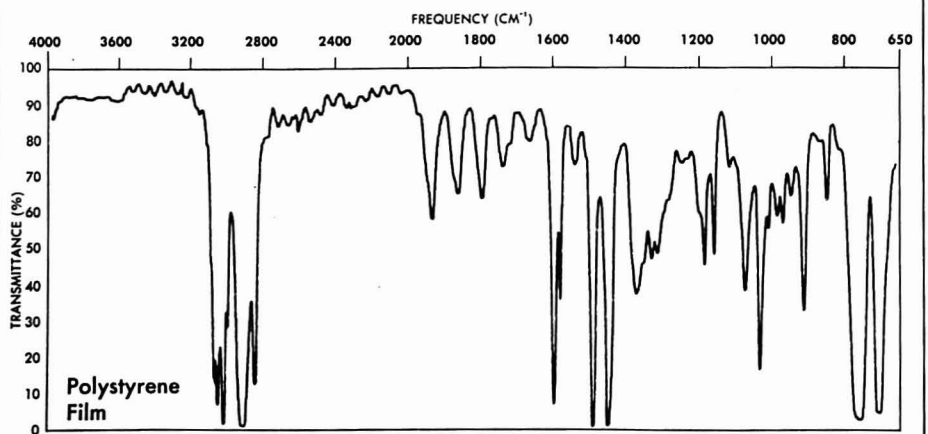

Circle No. 141 on Readers' Service Card

Industry Items

Sadtler Research Laboratories, Inc., 3316 Spring Garden St., Philadelphia, Pa. 19104, 215-382-7800, is now marketing a line of audio-visual instructional aids relating to laboratory instrumentation. The first in the series is on basic infrared spectroscopy.

Laboratory Instrument Exchange, Inc., 625 N. Michigan Ave., Chicago, Ill. 60611, 312-787-0800, has created a **Labex Appraisal Division** to provide low-cost appraisals of reconditioned laboratory equipment or computers.

Sadtler Research Laboratories, Inc., 3316 Spring Garden St., Philadelphia, Pa. 19104, 215-382-7800, is now marketing a data-retrieval system called IRIS. This infrared information system (produced in conjunction with the **University Computing Co.**) offers a fast, economical way to identify spectral unknowns. There are about 100,000 coded spectra in the data base which will be added to as other spectra collected are coded. Multiple searches, up to 25 at one time are permitted, helping reduce costs.

Bendix Corp., Southfield, Mich. 48075, 313-352-6233, has purchased substantially all of the assets of **Unico Environmental Instruments, Inc.,** a wholly-owned subsidiary of the **Gelman Instrument Co.** In addition, certain other products, property, and assets of Gelman related to the Unico product line have been bought. The products are related to environmental health and include instruments for the detection, analysis, and measurement of gases, vapors, and particulates, as well as devices for the sampling and monitoring of large volumes of air.

The Swedish scientific instrument manufacturer, **LKB-Produkter,** which is known in the U. S. through its subsidiary, **LKB Instruments, Inc.,** of Washington, D. C., has acquired the Finnish instrument company, **Wallac OY.** The latter firm makes automatic liquid scintillation counters and automatic gamma counters, as well as other instruments connected with isotope analysis and radioactivity measurements. Also, a new LKB subsidiary has been established in France.

A new program called **HELP (Honeywell Equipment Leasing Plan)** provides for the lease or rental of electronic testing, measuring, and recording products marketed by Honeywell's Test Instruments Division in Denver. Honeywell has also announced a 20% reduction in repair and calibration costs for electronic test instruments. This service is called Honeywell Plus-20.

Circle No. 6 on Readers' Service Card

Circle No. 144 on Readers' Service Card

The Chopper.

Introducing the most versatile, yet inexpensive chopper in America.

Designed for photometric and radiometric applications in conjunction with a lock-in amplifier, this is the lowest priced chopper on the market.

Features? The Chopper has them all.

Variable speed motor/tachometer drive controlled by a solid state speed control unit (not shown). 0.5Hz to 3KHz.

Blades are fastened directly to drive shaft, eliminating belt and gear drive problems. Quick disconnect blade fasteners.

Your choice of single and dual frequency blades with from one to sixty apertures. Dual frequency blades simultaneously modulate two light beams at different frequencies . . . use with a ratiometric lock-in system (we recommend Ithaco's Model 353RA Lock-in, naturally) to form a double-beam spectrophotometer.

Light emitting diodes used to generate dual reference signals (no light bulbs to burn out here). Identical reference signals with single frequency blades, separate reference signals with dual frequency blades.

Interested? Write today for specs and application information.

Ithaco, Inc.,
Box 818-1, Ithaca, New York 14850.
Or call 607 · 272·7640.

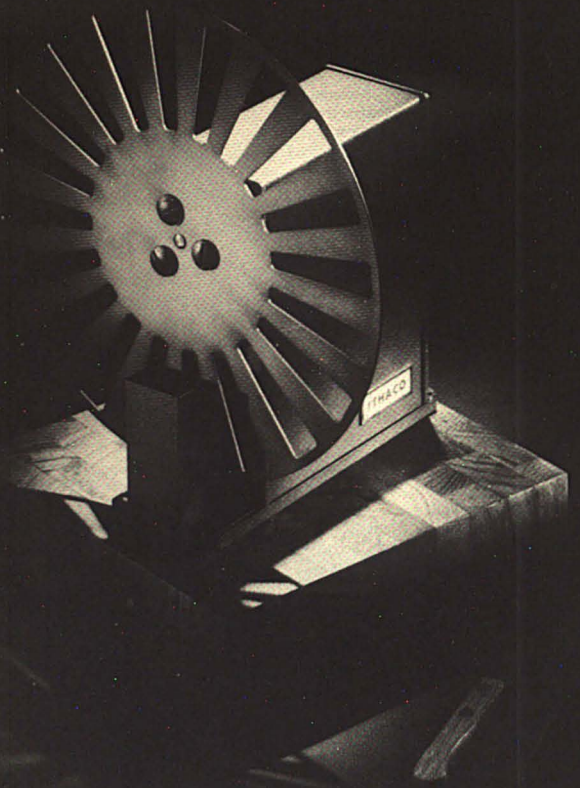

ITHACO

Circle No. 94 on Readers' Service Card

BOOK REVIEWS

Undergraduate Instrumental Analysis. James W. Robinson. xvii + 379 pages. Marcel Dekker, Inc., 95 Madison Ave., New York, N. Y. 10016. 1970. $11.50

Reviewed by Robert L. Pecsok, Department of Chemistry, University of California, Los Angeles, Calif. 90024

With the trend to introduce instrumental techniques earlier in the curriculum (often in courses for nonmajors), a new instrumental text at this level is most welcome. This book "presents a bird's eye view of the recent innovations in analytical chemistry" in simple language. Numerous applications are mentioned (without specific references) and suggested experiments are listed at the ends of most chapters. However, a lab manual would be a necessity.

Three-fifths of the book covers spectrometry with the remaining devoted to chromatography, thermal analysis, mass spectrometry, and electrochemistry. Because of the extensive coverage and the anticipation that each instructor would choose among the topics, each chapter is intended to stand alone. By and large this plan is successful, although some topics are discussed repeatedly—*e.g.*, prisms are discussed in Chapters 3, 4, 6, 7, 8, and 9, but it is not until Chapter 10 that we learn that quartz is birefringent and that prisms consist of both right- and left-handed quartz. (The Littrow prism is not mentioned.) Incidentally, Figure 3.2, which is also featured on the dust jacket, gives an erroneous explanation of dispersion by a prism—the incident beam is not collimated. Nor will the grating shown in Figure 3.4 produce a spectrum—a single groove will not suffice (dispersion is confused with reflection).

Serious errors of this sort begin on page 2—if quantitative analysis has been responsible for advances in inorganic chemistry, it can't be true that "NaCl was always found to contain 26.14% Na!" On page 83, the mole ratio is confused with the mole %. All ir absorption bands are given in microns; although wave numbers are shown on spectra, they are never mentioned. On page 242 the equation for the number of theoretical plates is based on the wrong retention time. The section on the Van Deemter (misspelled throughout) Equation is simple but erroneous—flow rate and velocity are confused, two figures and several statements are incorrect. The explanation given for frontal chromatography is actually for displacement chromatography. Skipping to the last topic, polarography, we read on page 358 and page 362 that $E_{1/2} = E^\circ$ for metal ions reduced to the metal. This reviewer found at least 50 similar objections including: poor, misleading diagrams, confusing explanations, incorrect derivations, incorrect facts, unconventional symbols, misspelled names, irrelevant bibliography for Chapter 1—not counting numerous typographical errors.

Because of these shortcomings, this book cannot be recommended in its present version. Nevertheless, the style, scope, and level of this book make it attractive, and we can hope that the author will produce an early revision.

Infrared Spectroscopy: Experimental Methods and Techniques. James E. Stewart. xiii + 636 pages. Marcel Dekker, Inc., 95 Madison Ave., New York, N. Y. 10016. 1970. $36.50

Reviewed by Bernard J. Bulkin, Department of Chemistry, Hunter College, New York, N. Y. 10021

"Infrared Spectroscopy" is a valuable analytical tool because one does not need to know very much of the material in James Stewart's book to obtain good results. For most routine laboratory applications of a qualitative nature the commercial instrument is virtually foolproof. This consideration aside, some users of instruments will always want to know the design principles, how the instrument works, and how it can distort spectra.

For many years, such lore of experimental infrared spectroscopy was revealed only in a few articles and books, and in a fragmented way. Thus, a comprehensive volume which is exclusively devoted to electronic and optical considerations in infrared spectrometers, containing information about sampling as well, is a welcome addition to the literature.

Written for readers at a variety of levels, the book attempts to be self-contained. It introduces basic concepts in geometrical and physical optics which are needed for understanding the design and operation of infrared instruments, then carries through the discussion to a high level. A similar plan is followed with the material on electronics. Scientists with considerable formal training in electronics and optics will thus find a large portion of the text superfluous, although the sections on infrared spectroscopy will still be informative.

In writing this volume on infrared instrumentation and techniques, the author has wisely devoted only limited space to a description of currently available commercial instruments. These are likely to disappear, while the basic principles will still be of importance. Because of this approach, this book will probably be read after many of its recent competitors are no longer of any use.

Although this volume purports to be of interest to advanced undergraduates, beginning graduate students, and practicing spectroscopists, it will probably find almost all its readers in the latter category. Each subject treated is done in considerable depth, and this is very likely of interest only to those working in the field. Unless one is involved with infrared instrumentation on an almost daily basis, either as operator, analyst, salesman, or instrument designer, the detailed discussions of instrument design and performance contained in Stewart's book will not warrant attention.

For those who do have this concern, however, the book is a gold mine of important information, literature references, helpful hints, etc. Particularly valuable are the discussions of photometric accuracy, transfer functions, and spectrum distortion by instrumental factors. A detailed study of this material should be required reading for anyone interested in carrying out quantitative work using commercial infrared instrumentation.

A weakness of the discussion of instrument parameters is the fact that the author has drawn rather heavily on his experience with a particular instrument company in his discussion. Readers using other instruments will find it difficult to set their instruments according to the scheme proposed in this text, although the scheme itself is sound.

A minor criticism of this book is the extensive use of wavelengths, in mi-

Analytical & Preparative
GEL ELECTROPHORESIS

Buchler provides these important, temperature controlled instruments for separating proteins, hemoglobin, albumin, enzymes and other compounds using polyacrylamide or another supporting medium. For complete information and prices, write for appropriate bulletin.

POLYANALYST
Basic analytical unit for separation and destaining. Migration takes place in 12 sample columns. Request Bulletin #3-1750.

POLY-PREP® "100"
Preparative instrument for continuous fractionation and elution. Request Bulletin #3-1700.

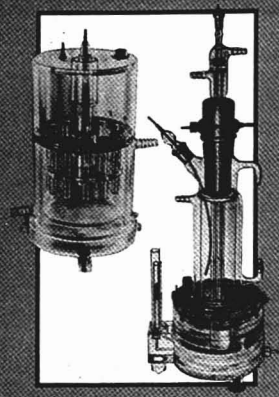

BUCHLER INSTRUMENTS

BUCHLER INSTRUMENTS DIVISION
NUCLEAR-CHICAGO CORP.
A SUBSIDIARY OF G.D. SEARLE & CO.
1307 SEVENTH STREET, FORT LEE, NEW JERSEY, 07024

Circle No. 21 on Readers' Service Card

ANALYZE
THESE BOOKS FROM
HRW

PRINCIPLES OF INSTRUMENTAL ANALYSIS
By Douglas A. Skoog, Stanford Univ., and Donald M. West, San Jose State College
This text, designed for undergraduate students, provides an introduction to the instrumental methods basic to modern scientific research and technology. Throughout the text, the emphasis is on the kinds of information offered by each type of instrument, its scope and limitations, and the fundamental physical and chemical principles upon which its use is based. Instrumental methods commonly encountered by the practicing chemist, biochemist, or chemical engineer are treated.
May 1971/640 pages/$15.00 (tent.)

FUNDAMENTALS OF ANALYTIC CHEMISTRY, Second Edition
By Douglas A. Skoog and Donald M. West
Emphasis throughout is on chemical principles as they apply to the problems of modern analytical chemistry. The authors' purpose is to provide a reasonable balance between classical and instrumental analysis and to show the unifying principles associated with both types of analysis.
1969/845 pages/14.75 Instructor's Manual and Solutions Manual

EQUILIBRIUM: A Chemistry of Solutions
By Thomas R. Blackburn, Hobart and William Smith Colleges
This text is a logically integrated treatment of acid-base, coordination, solubility, solvent extraction, redox, and electrochemical equilibrium. Graphical solutions to equilibrium systems are presented side-by-side with algebraic treatments which begin with mass and charge balance and the equilibrium constant. Included are exercises and problems.
1969/208 pages/$4.15 paper $6.75 cloth

Holt, Rinehart and Winston, Inc.
383 Madison Avenue, New York 10017

Circle No. 83 on Readers' Service Card

crons, for discussion of various regions of the infrared spectrum. Almost all commercial instruments now in production feature linear wave number display.

Very little space is devoted to modern, computer-interfaced interferometry, though this is destined for a major role in infrared instrumentation, in this reviewer's opinion. The basic theory of interferometry is presented in the text, however, and this material is clear and thorough.

This book will undoubtedly find a place in many analytical spectroscopy laboratories, although the high price will not encourage many individuals to purchase it. As such it will be a valuable reference book, and one which can be highly recommended.

Fundamentals of Clinical Chemistry. Norbert W. Tietz, Ed. xxi + 983 pages. W. B. Saunders Co., W. Washington Sq., Philadelphia Pa. 19105. 1970. $26

Reviewed by Donald S. Young, National Institutes of Health, Bethesda, Md. 20014

The field of clinical chemistry has now grown to such an extent that neither a single author, nor textbook, can cover it in depth. Tietz attempts to discuss only the basic principles of clinical chemistry in this book and has assembled a distinguished panel of experts to do this. Throughout the book he emphasizes the interaction of the biological sciences with the different branches of chemistry—the foundation of clinical chemistry. In most chapters a discussion of the biochemistry and clinical significance of compounds is included with the methods for measuring them.

The first three chapters are concerned with the basic principles of measurement which are equally applicable in analytical and clinical laboratories. For analytical chemists entering clinical chemistry this will remind them of the importance of sound analytical principles, and for people with different backgrounds these chapters will provide a sound introduction. As with other chapters, a list of comprehensive, relevant texts is included to facilitate greater study. Unlike the editor of many textbooks on clinical chemistry, Tietz has recognized the impact of mechanization of procedures in the clinical laboratory and Evenson describes the principles of the equipment which is used to perform the majority

(*Continued on page 72A*)

An unprecedented offer from Johnston Laboratories!

The only particle-photon detector you can lease!

The MM-1 Electron Multiplier

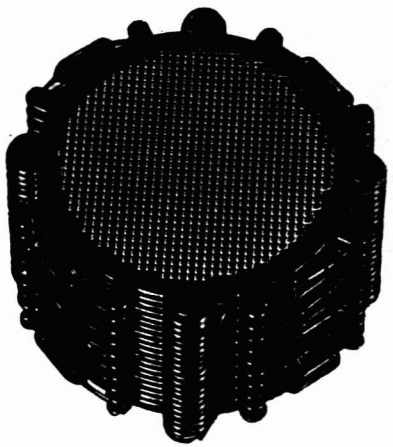

For pulse counting or current measurement of electrons, ions, UV or x-ray photons, and energetic neutral atoms or molecules. Guaranteed reactivateable. Delivered gain: 10^4 to 10^8. Noise less than 1 count-minute at 10^7 gain. Gain stability at count rates in excess of 10^6/second. Bakeable at 350° C. No ion feedback. Non-magnetic. 1.5 sq. in. active surface area.

SHOULD YOU LEASE OR BUY?

If budget limitations force you to buy electron multipliers that must be discarded when they lose gain, you'll be better off leasing the MM-1.

If you need the superior performance of the MM-1, but for only a limited time, then leasing will be more economical than buying.

If you require the dependable performance of the MM-1 in a long term project, you'll do better if you buy it.

If you're not sure how long you are going to need the MM-1, lease it now and pay only for the time you actually need it. You will always have the option to buy the MM-1 with a large amount of the leasing cost credited toward the purchase price.

Write for complete leasing data, specifications, and application notes.

THESE ELECTRONIC COMPONENTS AVAILABLE FOR YOUR COMPLETE MATCHED SYSTEM.

All Solid State High Voltage Power Supply (HV-4R). Ultra low noise for operating electron multipliers, photo multipliers, proportional counters, and ionization chambers. Small, lightweight, 500 to 6,100 volts DC range, reversible polarity, highly filtered noise, less than 300 microvolts. Drift less than .01% / hour, .02% / day.

Preamplifier-amplifier-discriminator (PAD-1). For use with electron multipliers and photo multipliers in mass spectrometers and fast counting systems. Charge sensitive; rise time: 3 nsec, output: 4 volts into 50 ohms. Adjustable discriminator: 20:1 range. Rugged, miniature.

MM-2: miniature version of MM-1. Also available on lease plan.

Johnston Laboratories, Inc.

3 Industry Lane,
Cockeysville, Maryland USA 21030

Circle No. 183 on Readers' Service Card

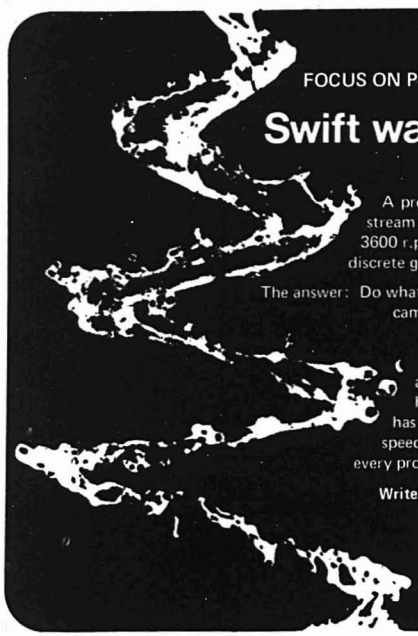

FOCUS ON PROFITS:

Swift water watching made easy

A problem: You want to observe the breakup characteristics of a stream of water shot from a ½" diameter tube oscillating at a rate of 3600 r.p.m. You are particularly interested in seeing the formation of discrete globules – closeup and super sharp.

The answer: Do what Dow Chemical did. Using a Redlake HYCAM rotating prism camera, Dow "stopped" the action at 5,000 pictures per second.

Result? Dow and many other chemical and industrial leaders have turned to Redlake to solve a wide variety of production and research problems. From the formation of synthetics, how media mix, to explosion and plasma studies. Redlake has the answers because it is the world's largest maker of high-speed photo analysis cameras, with speed to spare to solve almost every problem – 8 to 60,000,000 pps.

Write today for a free, four-color brochure, The Unseen World.

2991 CORVIN DRIVE
SANTA CLARA, CALIFORNIA 95051
TELEPHONE (408) 739-3034

REDLAKE LABS., INC.

Circle No. 158 on Readers' Service Card

The following spectrum is brought to you by the new EM-600, a medium resolution mass spectrometer system that costs a mere $6925:*

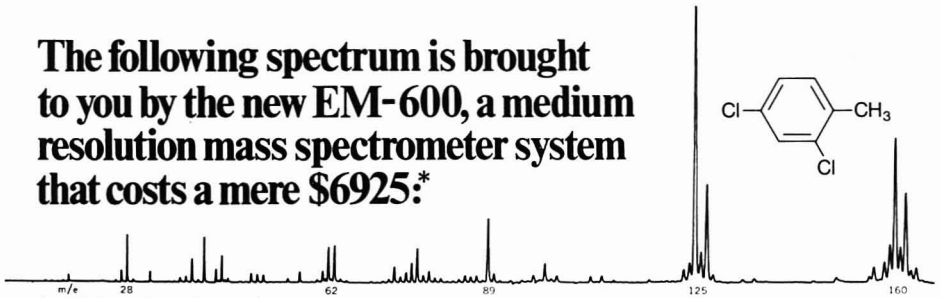

(2, 4-Dichlorotoluene Spectrum)

Before leaving, we might mention that the 60° sector, magnetically scanned EM-600 is a complete, easy-to-use system which also features a heated inlet for volatile organic compounds up to mass 330 or higher and linear mass readout.

For complete details or a demonstration, call (415) 326-4000 Ext. 2207. Or write Varian Anaspect, 611 Hansen Way, Palo Alto, California 94303.

*$6210 without recorder

varian anaspect

Visit us at the Spring ACS Show in Los Angeles.

Circle No. 184 on Readers' Service Card

STOPCOCK CONTAMINATION PROBLEMS?

Never again with High-Vacuum Stopcocks from WESTEF!®

Ground glass stopcocks require lubricants. Lubricants carry contamination! Avoid the problem with new WESTEF Stopcocks of Teflon, Viton, and Pyrex.

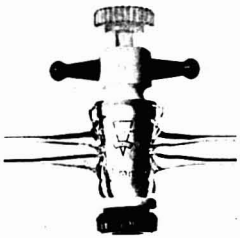

W-1710-T*

STOPCOCK, Straight Bore, TEFLON Plug, with Metering Valve. The metering valve needle which regulates bore opening for fine flow control is threaded from the top of the TEFLON plug for easy access and adjustment.

Bore, mm	1	2	3	4
Side Arm, O.D., mm	8	8	10	10
Price, Each	12.00	12.00	14.00	14.25

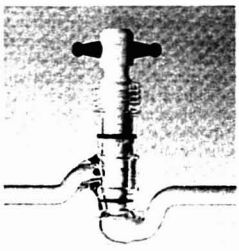

W-1831

STOPCOCKS, Westef, High-Vacuum, straight sidearms.

Bore, mm	2	4	6	8
Side Arm, O.D., mm	9	10	12	14
Price, Each	11.00	11.30	17.80	18.85

Bore, mm	10	15	20
Side Arm, O.D., mm	16	22	26
Price, Each	19.95	61.90	69.85

Bore, mm	2
Capillary Side Arm, O.D., mm	2
Price, Each	11.50

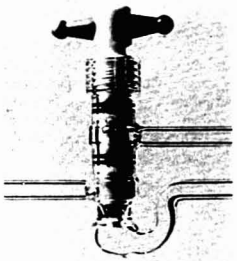

W-1846

WESTEF STOPCOCK, High-Vacuum, Three-Way.

Size, mm	0-4
Side Arm, O.D., mm	10
Price, Each	39.00

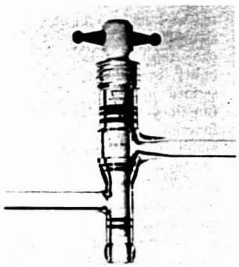

W-1848

WESTEF STOPCOCK, Ultra-High Vacuum. Straight Bore Stopcock with a vacuum connection on bottom.

Size, mm	0-6
Price, Each	25.25

***W-1712-T**

Same as W-1710-T except with capillary side arms with the same bore as the hole in the plug.

Vacuum and positive pressure WESTEF Stopcocks can be used with liquids or gases and are easily serviced and cleaned. The body of the WESTEF Stopcock is tooled on heavy-wall Pyrex glass, and features the "ACME" thread for added strength and easy regulation of the valve. The Teflon plug has two Viton O-Rings at top protected by a Teflon ridge.

Dependable, versatile, economical WESTEF Stopcocks are guaranteed to conform to published specifications or will be replaced free of charge with any stopcock of comparable value of your choice. Call or write...

SciChemCo P. O. Box 23616, Los Angeles, Calif. 90023 Phone (213) 263-1181

SciChemCo. Frese Division Los Angeles, Calif.

SciChemCo. Howe & French Division Boston, Massachusetts

SciChemCo. Durham Division Durham, North Carolina

Circle No. 172 on Readers' Service Card

of present-day analyses. However, no specific procedures are discussed.

Separate chapters on carbohydrates, proteins, porphyrins, lipids, and enzymes are included. Usually only one procedure for each important serum constituent is described in detail, and unlike Henry's textbook there is often inadequate justification for the choice of the method. It is disheartening to find that kinetic procedures are not advocated universally for the measurement of enzyme activity. The chapter on endocrinology is particularly thorough and includes a general introduction to radioimmunoassay, although the technique is not described in detail.

Several calcium procedures are described, but a laboratory director would be left with a lack of information to aid him in the selection of the best method to use on a routine basis. In a new textbook one would like to see no mention of archaic tests like the cephalin–cholesterol flocculation and thymol-turbidity procedures, but these are described in detail. Chapters on renal function, gastric analysis, pancreatic function, and the analysis of calculi maintain the high standard set by the editor. Chapters on toxicology and amniotic fluid analysis will be very useful for today's clinical chemist, because, until the advent of this book, there was no simple and authoritative text to assist the chemist in these areas. Many tables providing practical information for the technician or clinical chemist are included in an appendix. The volume is completed by a list of normal values and a comprehensive index.

This is a good book. Both trainees and laboratory directors will benefit from reading it. It combines (in a readable manner) much of the detailed description of test procedures of Henry's book with some of the background chemical pathology of Thompson and King's test. An up-to-date American book of this type was long overdue.

The Analysis of Air Pollutants. W. Leithe. x + 304 pages. Ann Arbor-Humphrey Science Publishers, Inc., Drawer No. 1425, Ann Arbor, Mich. 48106. 1970. $18.75

Reviewed by J. W. Robinson, Department of Chemistry, Louisiana State University, Baton Rouge, La. 70803

This book is 304 pages long and is divided into six major sections. The first section is concerned with the general background of air pollution including a summary of the European historical events in the field, particularly those involving loss of life; the major sources of air pollution; background levels before pollution; the identity of major pollutants in our atmosphere and their significance.

The second section deals with definitions of concentration levels (a necessary item in such a book), analytical accuracy, and precision, also requirements for acceptable analytical procedures. Air-sampling techniques, scrubbing methods, and methods for concentrating dilute pollutants are also described.

The third section discusses fields of research currently being pursued in air control, such as the labeling of air masses.

The fourth section deals with special analytical techniques, such as those used in photometric analysis and automatic continuous analysis devices.

The fifth and sixth sections are devoted to special topics such as dust analysis, precipitators, inert gases, O_2, O_3, sulfur compounds, organic pollutants, and carcinogens to name a few.

The book is well-conceived and gives a good summary of the present state-of-the-art of the determination of pollutants in the air. It is written with authority and reveals considerable experience on the part of the author. The translation is very good and permits easy reading of the book. The book's major shortcoming is that it does not devote much time to instrumental methods currently in use or in process of being developed. An example is the field of atomic absorption spectrometry which is now widely used throughout the world. However, it should be stated that it is impossible for a text to be completely current in all areas.

In summary, for those involved in the determination of air pollutants, this is a useful book and will provide a good reference in many related fields. Furthermore, it is written with sufficient detail to use directly in the routine analytical laboratory or the research laboratory.

New Books

Quantitative Analysis: Elementary Principles and Practice. Harvey Diehl. vii + 454 pages. Oakland St. Science Press, 409 Douglas Ave., Ames, Iowa 50010. 1970. $12.50

This is an introductory text, presenting the fundamental theory, descriptive chemistry, and laboratory techniques of titrimetric, spectrophotometric, gravimetric, and fluorometric methods of analysis. The theory introduced is that which bears directly on practice. In addition to the usual descriptive material on each method of analysis (inherent errors, interferences, basic reactions, and applications), supplementary material on the chemistry of the general area has been included. Laboratory procedures have been tested and have been written in sufficient detail to be readily followed by beginning chemists. Emphasis was placed on the attention to detail necessary to secure accurate and reliable results, and attention is called to the evaluation of errors. A fair amount of the history of chemistry has been incorporated into this text, thereby placing this book in the forefront of the trend in undergraduate education away from the premature presentation of advanced technical material and toward a more humanistic and cultural approach. The appearance and quality of this book in regard to the binding, paper, and layout of pages is above average.

Practical X-Ray Spectrometry. R. Jenkins and J. L. DeVries. x + 190 pages. Springer-Verlag, New York, Inc., 175 Fifth Ave., New York, N. Y. 10010. 1970. $7.80

This book is the revised and corrected edition. It is a reference book which covers all of the more usual practical difficulties experienced in the application of X-ray spectrometry. The latest developments in this relatively new field of analysis such as the expansion of the spectral range into the ultrasoft X-ray and vacuum ultraviolet region, the wavelength shift and absorption edge fine structure measurements are covered in this edition. Other topics include: physics of X-rays, dispersion, detection, pulse height selection, counting statistics, matrix effects, quantitative analysis, sample preparation, and trace analysis. Worked examples are used to illustrate specific points, particularly in the sections on counting statistics and quantitative analysis.

Proceedings of the Apollo 11 Lunar Science Conference. 3 Vols. A. A. Levinson, Ed. xxii + 2492 pages. Pergamon Press, Inc., Maxwell House, Fairview Park, Elmsford, N. Y. 10523. 1970. $40 (3 Vol. Set)

These volumes feature papers written by the 150 principal investigators and their associates who participated

in the three-month lunar science conference, which was held in Houston, January 5–8, 1970. The articles were divided as follows: Vol. 1: Mineralogy and Petrology; Vol. 2: Chemical and Isotope Analyses (including the organic geochemistry papers); and Vol. 3: Physical Properties. The information found in this set cannot be found as complete in any other form. They represent a rich and accurate sourcebook for everyone involved in forging new advancements in all of the various fields of scientific endeavor.

The Determination of Hydrazino-Hydrazide Groups. Hugh E. Malone. xv + 393 pages. Pergamon Press, Inc., Maxwell House, Fairview Park, Elmsford, N. Y. 10523. 1970. $18.75

This book presents a complete digest of the essential experimental details and applications of the methods available for the analysis of hydrazine, its derivatives, and, in general, the hydrazino-hydrazide functional group. This text is unique in its comprehensive coverage of the available methods, ranging from the classical oxidative, gasometric, and acid-base methods to modern instrumental methods, including spectrophotometry, chromatography, colorimetry, polarography, and coulometry. Although this book is primarily a text or guidebook for analytical chemists, it should also be of value to fuel cell and rocket propulsion technologists, as well as research, development, and production chemists engaged in modern chemical industry.

Man's Impact on the Global Environment. C. L. Wilson, SCEP Director, and W. H. Matthews, Assoc. Director. xxii + 319 pages. MIT Press, 50 Ames St., Cambridge, Mass. 02142. 1970. $2.95

This is the report of the one-month, interdisciplinary Study of Critical Environmental Problems (SCEP). It presents an assessment of the existing state of scientific knowledge on these and related global environmental problems and contains specific recommendations for action which would reduce the harmful effects of the pollution or would provide the information required to understand the impact of man on the global environment. Topics covered include: climatic effects of man's activities—*e.g.*, carbon dioxide from fossil fuels; ecological effects of man's activities—*e.g.*, mercury and other toxic heavy metals; and implications of change and remedial action. The reports of the Work Groups include topics such as climatic effects, ecological effects, monitoring, implication of change, industrial products and pollutants, domestic and agricultural wastes, and energy products.

Electrochemistry. J. Koryta, J. Dvorak, and V. Bohackova. xv + 350 pages. Barnes & Noble, Inc., 105 Fifth Ave., New York, N. Y. 10003. 1970. $16.75

This is the English edition of the Czech textbook, "Elektrochemie," which was published in 1966. The aim of this book is to provide the reader with the principles of modern electrochemistry which may enable him to read original papers and more advanced monographs. This text gives a comprehensive account of the principles of electrochemistry and encompasses both the classical theories and their modern extensions, emphasizing particularly the processes of electrochemical kinetics. The book is divided into four main parts: equilibria in electrolyte solutions; transport phenomena in electrolyte solutions; equilibria in heterogeneous electrochemical systems; and processes in heterogeneous electrochemical systems.

Chemistry: Man and Matter. E. Russell Hardwick and Charles M. Knobler. xi + 531 pages. Ginn & Co., 6900 E. 30th St., Indianapolis, Ind. 46218. 1970. $11.95

This is a textbook for a course in chemistry for nonmajors. It does not attempt to make an exhaustive survey of chemistry while at the same time penetrating deeply into the fundamentals. This text concentrates on the fundamentals, since the authors feel that if a student is to have only one or two courses in the field, he should understand the great conceptual accomplishments of science rather than memorize specific reaction data and detailed lists of properties. There are three major divisions: Chapters 1 to 14 deal with matter, energy, and the fundamentals of atoms, molecules, and chemical reactions; Chapters 15 to 20 deal with the chemical properties of the families of elements; and Chapters 21 to 27 introduce the student to a new way of viewing his world. This last section applies the complexes introduced in Chapters 1 to 14 to the physical world, to the interaction of science and society, and to life itself.

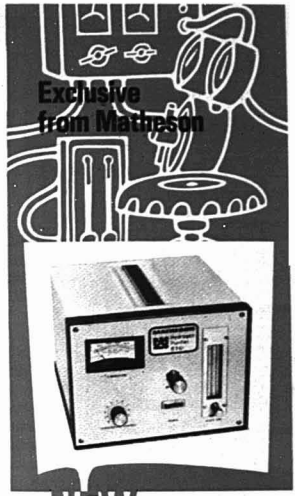

NEW

hydrogen purifiers produce ultra-pure hydrogen at low cost

If you have a need for ultra-pure hydrogen with total impurity levels lower than 0.5 ppm, these compact instruments (4 sizes: 1, 5, 12 and 24 liters per minute) are your answer. Savings start immediately because you can buy low cost commercial hydrogen. Starting with this crude hydrogen, these units will deliver ultra high purity hydrogen by breaking down H_2 into two hydrogen atoms, which diffuse through the walls of palladium tubes. No other atom will pass through these walls.

Because Matheson offers compatible gas handling systems, these Hydrogen Purifiers work at top efficiency with other Matheson regulating and manifolding components. Send coupon for Engineering Report G-125. It contains all the facts on these new purifiers plus other Matheson "work together" system compatibles.

MATHESON GAS PRODUCTS
A Division of Will Ross, Inc.
East Rutherford, N. J.; Cucamonga, Calif.; Gloucester, Mass.; Joliet, Ill.; La Porte, Texas; Morrow, Ga.; Newark, Calif.; Whitby, Ont.

Matheson Gas Products, P.O. Box 85,
Dept. AC-371, East Rutherford, N. J. 07073
Send me Report G-125.

Name_____

Title_____

Address_____

City_____

State_____ Zip_____

4-71G

Circle No. 128 on Readers' Service Card

POLLUTION
is right up our street....

Pollution is now a major threat to all forms of life. To track and determine impurity levels rapidly and precisely there is no instrument to equal the MS702R spark source mass spectrometer.
The MS702R is available with a unique electrical detection system giving increased precision, higher speed and high sensitivity in quantitative analysis.
The MS702R will detect:-
ALL air and water pollution particulates
The amounts of pesticides in foods
The trace element levels in human beings
Send for literature and find out in detail how the MS702R can help you to keep a closer check on pollution. The wide range of accessories enables the MS702R to be used in many other applications including geology, forensic science, metallurgy and biology.

MS702R mass spectrometer

The only spark source instrument available with an electrical detection system

AEI Scientific Apparatus Limited, Barton Dock Road, Urmston, Manchester, M31 2LD
Telephone: 061-865 4466 Telex: 668482 Telegrams: Sciapp Manchester
In the U.S.A.
AEI Scientific Apparatus Inc., 500 Executive Boulevard, Cross Westchester Executive Park, Elmsford, New York 10523

AEI scientific apparatus

A14052

Circle No. 2 on Readers' Service Card

For your chemical library..

these Advances in Chemistry Series books from the A C S

PATENTS FOR CHEMICAL INVENTIONS (No. 46)
Patentability problems: nature of invention, ownership, signatory formalities during prosecution, priority. Patentability requirements: novelty, utility, unobviousness. Situations related to chemical patents: prior art, new use, patentability of natural products, foreign patent protection.
117 pages with index.
Cloth bound. $5.50 per copy.

ENGINEERING PLASTICS AND THEIR COMMERCIAL DEVELOPMENT (No. 96)
A "how-to-do-it" book with discussion and case histories on developing plastics to profitable commercial products. Topics include use research, marketing research, process and processing development, and patent and legal aspects including clear warnings on contributory infringement.
128 pages with index.
Cloth bound. $7.50 per copy.

CHEMICAL MARKETING: THE CHALLENGES OF THE SEVENTIES (No. 83)
Twenty-one articles discuss the challenges in four chemical markets, in organizing for marketing, in market research and development, in domestic and international sales, in technical service and application research, in distribution, and in computer applications in marketing.
199 pages with index.
Cloth bound. $9.50 per copy.

EQUILIBRIUM CONCEPTS IN NATURAL WATER SYSTEMS (No. 67)
Sixteen papers represent the collaboration of aquatic chemists, analytical chemists, geologists, oceanographers, limnologists, and sanitary engineers, working with simplified models to produce fruitful generalizations and valuable insights into the factors that control the chemistry of natural systems.
344 pages with index.
Cloth bound. $11.00 per copy.

PLASTICIZATION AND PLASTICIZER PROCESSES (No. 48)
Plasticization principles, glass transition, plasticizer mobility, antiplasticizers.
Other topics include three processes for phthalate esters, developments in phosphate plasticizers, chromatographic analysis of plasticizers.
200 pages with index.
Cloth bound. $8.00 per copy.

EPOXY RESINS (No. 92)
Discusses formulation and performance of epoxy resins. Properties such as improved flexural strength, moisture resistance, adhesion, rigidity, light weight, and mechanical, electrical, and chemical resistance are explored. Also discussed are processes and reactions including condensation reactions, gelation, synthesis, electro-deposition, curing, reactivity.
230 pages with index.
Cloth bound. $10.50 per copy.

TRACE INORGANICS IN WATER (No. 73)
Research reports; analytical developments including atomic absorption, flame emission, and neutron activation; and broad reviews, such as effects of trace inorganics on the ice-water system and the role of hydrous manganese and iron oxides on fixing metals in soils and sediments.
396 pages with index.
Cloth bound. $12.50 per copy.

PLEASE PRINT OR TYPE

I propose for ACS Membership:

Name_____

Address_____

City_____ State_____ Zip_____

Name_____

Address_____

City_____ State_____ Zip_____

Name_____

Address_____

City_____ State_____ Zip_____

Name_____

Address_____

City_____ State_____ Zip_____

An ACS membership application will be sent to each of the above proposed names.

Special Issues Sales
American Chemical Society
1155 - 16th Street, N.W., Washington, D.C. 20036

Please send me the following
ADVANCES IN CHEMISTRY SERIES books.

1._____
2._____
3._____
4._____
5._____
6._____
7._____
8._____

NOTE: If ordering more than one book, please indicate quantity.

Payment enclosed (Payable to ☐ American Chemical Society) ☐ Please bill

Name_____

Mailing address_____

City_____ State_____ Zip_____

Signature_____

IRRADIATION OF POLYMERS (No. 66)

Eighteen papers survey radiation mechanics in polymers, the chemical nature of reactive species produced, crosslinking and scission, homopolymerization, graft copolymerization, and the effects of ultraviolet light radiation.
275 pages with index.
Cloth bound. $10.00 per copy.

ORGANIC PESTICIDES IN THE ENVIRONMENT (No. 60)

Gives a clear perspective of environmental hazards in soil, water, and air; surveys effects of mammal enzyme systems, residues in human body tissues, effects of chronic poisoning by organophosphorous insecticides.
309 pages with index.
Cloth bound. $10.50 per copy.

LITERATURE OF CHEMICAL TECHNOLOGY (No. 78)

Forty articles discuss the literature of many aspects of chemical technology. Nine of these are related to polymers, including resources for resins and plastics, photographic chemistry, cellulose, pulp, and paper, printing inks, coatings, synthetic rubber, rocket construction materials, textiles, and waxes and polishes.
732 pages with index.
Cloth bound. $17.50 per copy.

ADDITION AND CONDENSATION POLYMERIZATION PROCESSES (No. 91)

"Molecular engineering" demands an understanding of the relationship between molecular structure, process kinetics, and performance characteristics. The first 26 chapters are devoted to process improvements and the polymerization kinetics of common monomers. The last 22 chapters deal with new and improved polymers designed for specific uses or properties.
767 pages with index.
Cloth bound. $19.50 per copy.

POLYMERIZATION AND POLYCONDENSATION PROCESSES (No. 34)

An I & EC Division symposium with emphasis on unit processes. Twenty-one papers on addition polymerization, polycondensation reactions, commercial polymerization processes, and equipment design.
260 pages with index.
Paper bound. $10.00 per copy.

CHEMICAL NOMENCLATURE (No. 8)

Concerns nomenclature in organic, inorganic, and biological chemistry as well as coding, indexing and classifying, with some attention to nomenclature in industry. International aspects are also covered.
112 pages with index.
Paper bound. $5.00 per copy.

SALINE WATER CONVERSION — II (No. 38)

Fourteen papers from two symposia; includes recovery of minerals from sea water, minimizing scale formation, wiped thin-film distillation, diffusion still, solar flash evaporation, osmosis, electrodialysis (3 papers), research in Israel, hydrate process.
199 pages with index.
Paper bound. $8.00 per copy.

STABILIZATION OF POLYMERS AND STABILIZER PROCESSES (No. 85)

Twenty-two papers survey progress and report recent work on a variety of stabilization problems – thermal stabilization, antioxidants and antiozonants for polyolefins, rubbers, and rubbers containing polymers. Other topics include microbial stabilization, ultraviolet light absorbers, and fire retardants.
332 pages with index.
Cloth bound. $12.00 per copy.

PESTICIDAL FORMULATIONS RESEARCH. PHYSICAL AND COLLOIDAL CHEMICAL ASPECTS (No. 86)

Fifteen papers survey contact angle of surface-active agents, transport through a membrane, vapor pressure of pesticides, role of surfactants in sprays, biological activity, evaporation, spray formation and drift, and several studies on specific pests and pesticides.
212 pages with index.
Cloth bound. $9.50 per copy.

FIRST CLASS
Permit No. 1411-R
Washington, D. C.

BUSINESS REPLY MAIL
No postage stamp necessary if mailed in the United States

Postage will be paid by

AMERICAN CHEMICAL SOCIETY
1155 Sixteenth Street, N.W.
Washington, D.C. 20036

Admissions Department

FIRST CLASS
Permit No. 1411-R
Washington, D. C.

BUSINESS REPLY MAIL
No postage stamp necessary if mailed in the United States

Postage will be paid by

AMERICAN CHEMICAL SOCIETY
1155 Sixteenth Street, N.W.
Washington, D.C. 20036

Keep Pace With The New!

Discover New Horizons, New Interests, Valuable Information through Internationally Respected ACS Journals

Twenty-one ACS Journals cover each of the disciplines of Chemistry in depth, or range across the field on an interdisciplinary basis, offer news of chemistry, and cover special skills helpful to any professional chemist.

No one can read 21 professional journals, but the ACS is pleased to offer you an opportunity to subscribe to many which will benefit you, in addition to the journal of your special professional interest.

Chemical Technology

The American Chemical Society's newest publication. Designed to impart immediate, authoritative and relevant data of a pragmatic nature, particularly for chemists and chemical engineers in industry. All ACS members will have an opportunity to receive complimentary copies through June 1971. Monthly.

Nonmember
U.S. $18.00
Canada, PUAS $20.50
Other Nations $21.50

Analytical Chemistry

The only complete, authoritative source of technical information covering all fields of analysis, both fundamental and applied. Covers research, news, new products, new chemicals, and exchanges of comments between authors and readers. Monthly.

ACS Member	Nonmember
U.S. $5.00	U.S. $7.00
Canada, PUAS $7.50	Canada $9.50 PUAS $17.50
Other Nations $8.50	Other Nations $18.50

Environmental Science & Technology

Fundamental research and technology in water, air and waste chemistry—plus news, interpretive reports and commentary on political and industrial aspects of environmental management. Monthly.

ACS Member	Nonmember
U.S. $5.00	U.S. $7.00
Canada, PUAS $8.00	Canada, PUAS $10.00
Other Nations $8.50	Other Nations $10.50

The Journal of the American Chemical Society

If you had to choose one publication in chemistry, *Journal of the American Chemical Society* would be the most valuable. Since 1879, it has offered subscribers original research that cuts across *all* disciplines of chemistry. (With 8100 pages published in 1970 it costs subscribers less per page than any other major journal in the world). Biweekly.

ACS Member	Nonmember
U.S. $22.00	U.S. $44.00
Canada, PUAS $26.50	Canada, PUAS $48.50
Other Nations $27.50	Other Nations $49.50

Biochemistry

Reflects the strong relationship among chemistry, biochemistry and other biological sciences. Covers enzymes, proteins, carbohydrates, lipids, nucleic acids and their metabolism, genetics, other expanding fields. Biweekly.

ACS Member	Nonmember
U.S. $20.00	U.S. $40.00
Canada, PUAS $23.00	Canada, PUAS $43.00
Other Nations $23.50	Other Nations $43.50

The Journal of Medicinal Chemistry

Journal of Medicinal Chemistry emphasizes papers on the biological and pharmacological effects of medical agents on basic body processes. Covers chemical-biological relationships, chemistry of compounds, and pharmacology of compounds Monthly.

ACS Members	Nonmember
U.S. $15.00	U.S. $30.00
Canada, PUAS $18.00	Canada, PUAS $33.00
Other Nations $18.50	Other Nations $33.50

Single Article Announcement Service

This twice monthly current awareness service reproduces contents pages from current editions of all ACS primary journals, except Chemical & Engineering News, Chemistry, Chemical Technology, Chemical Reviews and Accounts of Chemical Research.

You can scan these tables of contents, thus gaining wider insight into developments in major fields of chemical research. Articles of specific interest may be ordered through a form provided.

ACS Member	Nonmember
U.S. $8.00	U.S. $16.00
Canada, PUAS $11.00	Canada, PUAS $19.00
Other Nations $11.50	Other Nations $19.50

AMERICAN CHEMICAL SOCIETY, 1155 16th St., N.W., Washington, D.C. 20036

Please enter a one-year subscription for the following publications:

1. _____ 2. _____
3. _____ 4. _____
5. _____ 6. _____

Name _____ Position _____

Company _____ Address _____

City _____ State/Country _____ Zip _____

Nature of Your Employer's Business:

☐ Manufacturing or Processing ☐ Government ☐ University

☐ Other (Please Indicate) _____

If Manufacturing,

Type of Products Produced _____

☐ I am ☐ am not an ACS member.

☐ I enclose $_____ (payable to American Chemical Society) ☐ Bill me.

☐ Please send me information on how to become an ACS member.

Payment must be made in U.S. currency, by international money order, UNESCO coupons, or U.S. bank draft; or order through your book dealer. Subscriptions at ACS member rates are for personal use only.

A-12

Inorganic Chemistry

Articles may range from the borders of organic chemistry to the borders of theoretical physics. Authoritative information. Monthly.

ACS Member	Nonmember
U.S. $18.00	U.S. $36.00
Canada, PUAS $21.00	Canada, PUAS $39.00
Other Nations $21.50	Other Nations $39.50

Journal of Organic Chemistry

Emphasizes organic reactions, natural products, studies of mechanism, theoretical organic chemistry, aspects of spectroscopy. Biweekly.

ACS Member	Nonmember
U.S. $20.00	U.S. $40.00
Canada, PUAS $24.50	Canada, PUAS $44.50
Other Nations $25.50	Other Nations $45.50

Chemical & Engineering News

Official organ of the ACS. Covers news of current developments in all phases of chemistry for readers in Industry, Government, Consulting and Education. Weekly.

ACS Member.	Nonmember
Receive C&EN as part of dues.	U.S. $7.00
	Canada $11.00
	PUAS $19.00
	Other Nations $20.00

Journal of Agricultural & Food Chemistry

Covers a growing, important field, with emphasis on pesticides, fertilizers, plant growth regulators, and chemistry of food processing. Bimonthly.

ACS Member	Nonmember
U.S. $10.00	U.S. $20.00
Canada, PUAS $13.00	Canada, PUAS $23.00
Other Nations $13.50	Other Nations $23.50

Journal of Chemical & Engineering Data

Articles are primarily concerned with presentation of data of permanent value, available in journal form. Today's new instrumentation makes this current information especially valuable. Quarterly.

ACS Member	Nonmember
U.S. $15.00	U.S. $30.00
Canada, PUAS $18.00	Canada, PUAS $33.00
Other Nations $18.50	Other Nations $33.50

Macromolecules

Results of original research on all fundamental aspects of polymer chemistry. Vital information for an expanding field. Bimonthly.

ACS Member	Nonmember
U.S. $12.00	U.S. $24.00
Canada, PUAS $15.00	Canada, PUAS $27.00
Other Nations $15.50	Other Nations $27.50

Accounts of Chemical Research

Short, critical reviews of current research in all areas of chemistry, normally by investigators active in the field reviewed. Monthly.

ACS Member	Nonmember
U.S. $5.00	U.S. $10.00
Canada, PUAS $8.00	Canada, PUAS $13.00
Other Nations $8.50	Other Nations $13.50

Chemical Reviews

Authoritative, critical, comprehensive reviews of recent research in the various fields of chemistry, not reviewed in readily available publications for previous five years. Bimonthly.

ACS Member	Nonmember
U.S. $13.00	U.S. $26.00
Canada, PUAS $16.00	Canada, PUAS $29.00
Other Nations $16.50	Other Nations $29.50

The Journal of Physical Chemistry

Editorially balanced between classical areas of chemistry and modern structural quantum mechanical areas. Special emphasis on papers dealing with fundamental aspects of atomic and molecular phenomena. Biweekly.

ACS Member	Nonmember
U.S. $20.00	U.S. $40.00
Canada, PUAS $24.00	Canada, PUAS $44.00
Other Nations $25.00	Other Nations $45.00

Journal of Chemical Documentation

For those who use and work with chemical literature. Covers communications skills, data systems, technical writing, linguistics, nomenclature. Quarterly.

ACS Member	Nonmember
U.S. $7.00	U.S. $14.00
Canada, PUAS $10.00	Canada, PUAS $17.00
Other Nations $10.50	Other Nations $17.50

Chemistry

For the high school chemistry student and teacher, and science-oriented college student and faculty. Interprets basic chemical concepts and reports on new developments. Imaginatively illustrated. Monthly.

All Subscribers

U.S. $6.00—Canada, PUAS $7.00
Other Nations $7.50

I & EC Fundamentals

Publishes original scientific papers dealing with the very frontiers of chemical engineering understanding. Quarterly.

I & EC Process Design & Development

Theoretical and experimental results related to process development—translatable to other systems and process steps. Quarterly.

I & EC Product R & D

Original research dealing with factors influencing product properties and performance. "Plenary Accounts" feature updates state of the science for selected subjects. Quarterly.

Fundamentals, Process Design & Development, Product R&D, EACH:

ACS Member	Nonmember
U.S. $7.00	U.S. $14.00
Canada, PUAS $9.50	Canada, PUAS $16.50
Other Nations $10.00	Other Nations $17.00

FIRST CLASS
Permit No. 1411-R
Washington, D.C.

BUSINESS REPLY MAIL

No Postage Stamp Necessary if Mailed in the United States

Postage Will Be Paid by

AMERICAN CHEMICAL SOCIETY
1155 SIXTEENTH STREET, N.W.
WASHINGTON, D.C. 20036

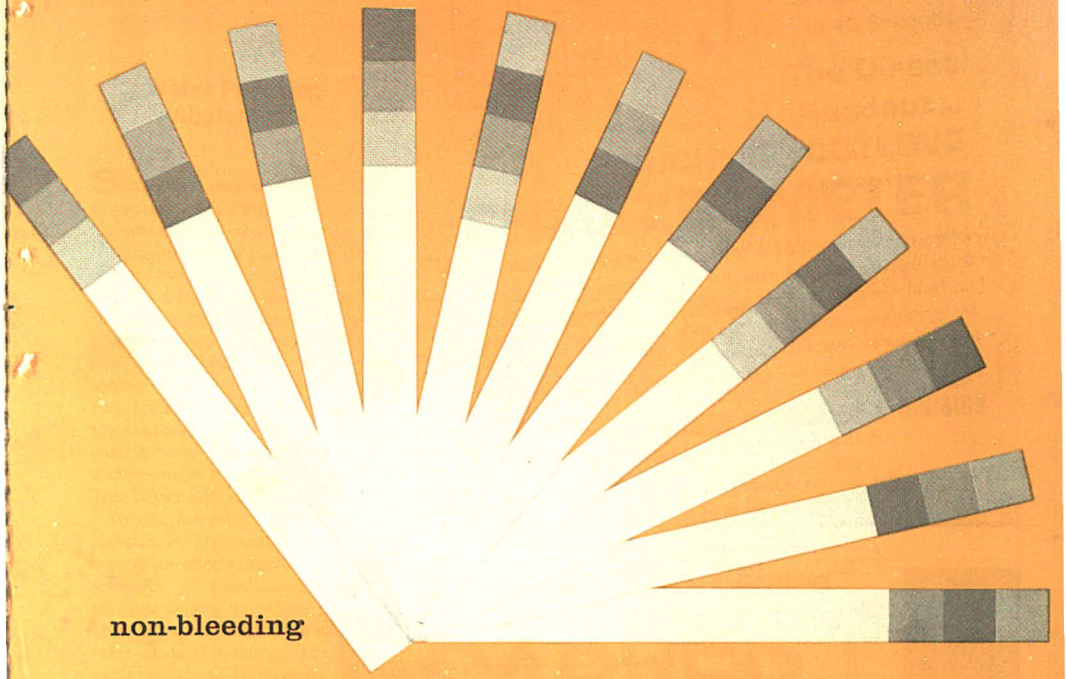

non-bleeding

Universal Indicator Strips: pH 0–14
Special Indicator Strips: pH 0–2.5
pH 2.5–4.5 pH 4.0–7.0 pH 6.5–10.0 pH 11.0–13.0
Neutralit® pH 5–10 Acilit® pH 0–6
Alkalit® pH 7.5–14

Special advantages:

Reactive zones sealed onto plastic strips

Non-bleeding

Prolonged immersion possible

Weakly buffered or unbuffered and even coloured solutions may be measured

Distinctive colour differences

Highly stable to light

Please request our special brochure

E. Merck, Darmstadt Germany

317-EO

Circle No. 131 on Readers' Service Card

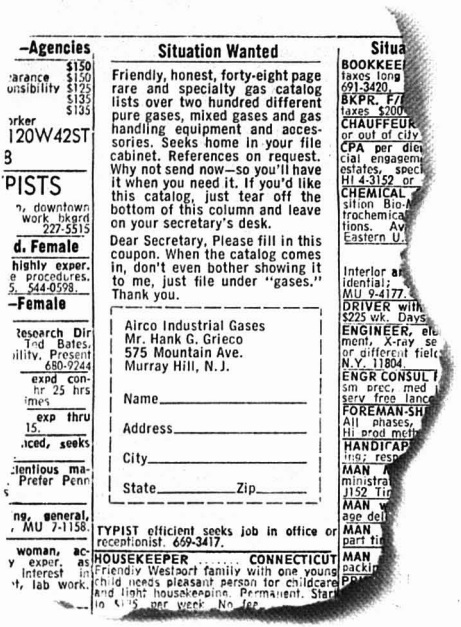

Circle No. 11 on Readers' Service Card

EDITORS' COLUMN

Water Pollution Abatement

SCIENTISTS, POLITICIANS, and the news media have directed increasing attention in recent months to the urgent need for pollution abatement of our domestic lakes and rivers. As a result, the lion's share of the budget for the recently formed Environmental Protection Agency has been allocated to the fight against water pollution. Many private industries have also accepted the challenge and are beginning to contribute to the nationwide clean waters program proposed by President Nixon last year.

Indeed, domestic water pollution surveillance and control promise to occupy the efforts of more and more research scientists—analytical chemists among them—as the nation gears up in its battle to improve environmental quality. For those analytical chemists interested in entering the field of water pollution abatement, this year's national meetings of the American Water Resources Association, listed below, will offer valuable background information.

The AWRA Research Conference, "Planning for Water Quality and Standards," will be held June 14–18 at the University of Wisconsin-Milwaukee. For more information, contact Dr. G. Karadi, General Chairman and Professor, Department of Applied Science and Engineering, University of Wisconsin-Milwaukee, Milwaukee, Wis. 53201. Telephone: 414-228-4964.

The National Symposium on "Social and Economic Aspects of Water Resources Development" will convene June 21–23 at Cornell University. For more information, contact Professor Leonard B. Dworsky, Director, Water Resources and

Determine Serum Chloride in 40 Seconds

The Direct Readout...

BUCHLER-COTLOVE

CHLORIDOMETER

Fast, direct readout in seconds and mEq/L • Sensitivity better than 1 ppm • Accuracy ± 0.5% in wide range of concentrations • High reproducibility with only 10 lambda sample • Ideal for sweat chloride determination in pediatric and clinical applications • Recognized method for standardizing automatic analyzers and for individual or multiple chloride determinations

BUCHLER INSTRUMENTS

BUCHLER INSTRUMENTS DIVISION
NUCLEAR-CHICAGO CORP.
A SUBSIDIARY OF G. D. SEARLE & CO.
1327 SIXTEENTH STREET, FORT LEE, NEW JERSEY, 07024

Request Bulletin AC4-2000C
Circle No. 24 on Readers' Service Card

Convert your hand operated laboratory press to automatic

CARVER®

MOTORIZATION PACKAGE

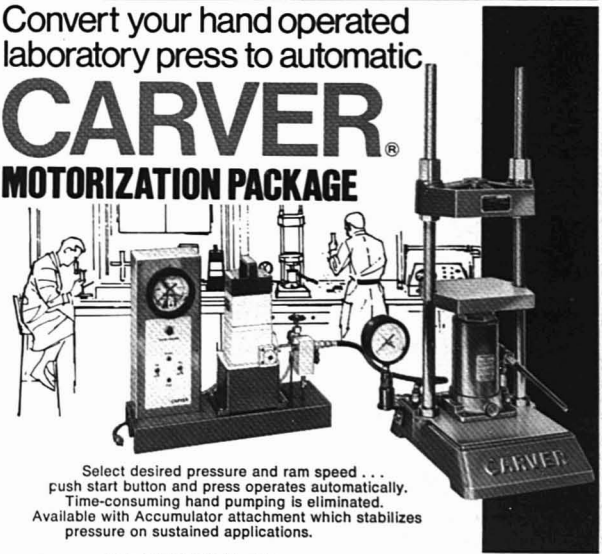

Select desired pressure and ram speed . . . push start button and press operates automatically. Time-consuming hand pumping is eliminated. Available with Accumulator attachment which stabilizes pressure on sustained applications.

Write for Bulletin No. 120

FRED S. CARVER, INC.
One Chatham Road
Summit, New Jersey 07901

a subsidiary of Sterling, Inc.
Milwaukee, Wisconsin

Circle No. 32 on Readers' Service Card

What do you want in atomic absorption?

To zip through hundreds of routine analyses?

The Jarrell-Ash Dial-Atom II is just the thing for rigorous, routine, day-in day-out use. It's as big in performance as it is easy on

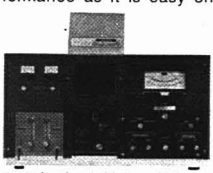

your budget. Note all these traditionally "expensive" features you'll find on the low-cost Dial-Atom II: Direct concentration readout. Fast dial-an-element wavelength selector. Built-in hollow cathode lamp warmup. Scale expansion to 10X. Flame emission capability.

Multi-element analyses without lamp warm-up?

The hollow cathode lamp turret on the Jarrell-Ash Atomsorb holds up to six lamps on warm-up. To switch lamps, just rotate the turret. No waiting. Switching oxidants and lighting the burner, moreover, are just a matter of turning a control and pushing a button. More pluses: Direct concentration readout. Two switch-selectable gratings. Corrosion-resistant laminar flow burner. Scale expansion to 10X. Flame emission capability.

Simultaneous analyses of two metals? And compensation for matrix interferences?

You'll find analytical capabilities like that only with the Jarrell-Ash Model 800. Its unique dual-channel double-beam design makes it the most advanced instrument of its kind. Consider, too, its other high performance features: Digital readout. Signal integration. Scale expansion to 25X. Flame emission.

Equal efficiency in flame emission and atomic absorption?

That calls for the Jarrell-Ash Model 500. Its exceptional versatility and superb

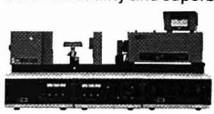

optics will especially please the researcher. Reasons why: a high resolution monochromator. Selection of eight wavelength scanning speeds. Interchangeable gratings. Unobstructed burner area.

For a product bulletin on each Jarrell-Ash atomic absorption instrument, circle the number given below on the readers' service card.

F-905

Jarrell-Ash

Division of Fisher Scientific Co.

Circle No. 63 on Readers' Service Card

Reprints from Chemical & Engineering News

Keeping broadly informed challenges every person today. If you missed these features from recent issues of C&EN, you can still get copies by filling in the coupon at the bottom of the page.

Chemical Mutagens

Howard J. Sanders, C&EN
May 19, 1969 & June 2, 1969, 36 pp. **75¢**

Geneticists, physicians, chemists, and growing segments of the public at large are becoming intensely aware of the possibility that drugs of all sorts, as well as pesticides, food ingredients and additives, industrial chemicals, and other substances, may be causing genetic damage in human general-body cells (somatic cells) and in germinal (sex cells). **05199**

Pollution Causes, Costs, Controls

Arnold Levitt, C&EN
June 9, 1969, 20 pp. **50¢**

No one has to make a case anymore for the need for pollution control or for the related concept of environmental management. Open the window, go boating, drive along the highway—that should provide recognition enough that a real pollution problem exists. **06969**

Microwave Spectroscopy

Dr. William H. Kirchoff
National Bureau of Standards
Washington, D.C.
March 24, 1969, 12 pp. **50¢**

The recent availability of commercial microwave spectrometers has caused renewed interest in microwave spectroscopy as a tool for chemical analysis. **03249**

Infrared Spectroscopy

Dr. Kermit Whetsel,
Tennessee Eastman Co.
Feb. 5, 1968, 14 pp. **50¢**

The usefulness of ir spectroscopy is widening. Dr. Whetsel examines the developments in instrumentation, data handling, technique, and applications, that promise greater utility in the future. **02058**

1 to 49 copies—single copy price
50 to 299 copies—20% discount

Prices for larger quantities available on request

☐ 05199 ☐ 06969 ☐ 02058 ☐ 03249

TO: REPRINT DEPARTMENT

ACS Publications
1155 Sixteenth St., N.W.
Washington, D.C. 20036

FROM:

Name

Street

City

State ZIP Code

Amount enclosed $

Marine Sciences Center, Cornell University, Ithaca, N. Y. 14950. Telephone: 607-256-1000.

The Seventh Annual American Water Resources Conference will meet October 25–28 at the Statler Hilton Hotel, Washington, D. C. For more information, contact F. E. McJunkin, Deputy Director, Department of Environmental Sciences and Engineering, University of North Carolina, Chapel Hill, N. C. 27514. Telephone: 919-966-2129.

Pollution of the Seas

In most countries, water quality standards applying to inland waters are also extended to coastal waters. Outside territorial waters, however, no standards currently exist. The immensity of the oceans, and the tremendous mass of seawater, could lead one to believe that all contaminants would disappear eventually. However, tides and currents can return waste and garbage unbelievably quickly to the coastal areas. The havoc caused by recent offshore oil spills is well-known. Last year's discoveries of DDT contamination in ocean fish fat and severe mercury contamination (in excess of 0.5 ppm) in tuna and swordfish should further alert the public to the problem of the pollution of the seas.

In the case of mercury contamination, no one is positive yet how much of the mercury comes from natural geological sources and how much from man's pollution. Clearly, this is a pressing goal for study, and one which the efforts of analytical chemists can help meet. Governmental agencies participating in studies of the pollution of the seas will include the National Oceanic and Atmospheric Administration, the Environmental Protection Agency, the Food and Drug Administration, and the National Science Foundation, which is sponsoring a long-range cooperative program described in detail below.

This year marks the beginning of the National Science Foundation's International Decade of Ocean Ex-

INTRODUCING:

The Superior $^3He/^4He$ Dilution Refrigerator System!

Pardon our pride, but it *does* sometimes take the aggressive efforts of a young, established domestic equipment manufacturer to produce a truly superior cryogenic system. Cryogenic Associates has done just that with the introduction of its Dilution Refrigerator . . . another step beyond its sophisticated research dewar lines and system accessories.

This complete modular system delivers continuous operation at externally measured sample temperatures of 0.020°K. Heat extraction capability (also measured externally) is as large as 1000 erg/sec. at 0.1°K and 120 erg/sec. at 0.040°K.

One more point: The versatility of design allows individual components to be matched to specific needs. Further: Several optional devices make it even more interesting to the scientist*.

But get the full story. Complete specifications are available for you . . . by return mail!

*Some Experimental Applications: Mossbauer Effect Spectroscopy/Polarized Targets for Nuclear and Elementary Particle Physics/Quantum Liquids/Superconductivity/Thermal Transport Properties of Solids/Kondo Effect/Nuclear Demagnetization

CRYOGENIC ASSOCIATES INC.

". . . for the finest in Cryogenic Systems".

1718 North Luett Avenue
Indianapolis, Indiana 46222
Phone: (317) 632-2515

Catalog Available On Request

Circle No. 33 on Readers' Service Card

Inspect this new Spectroquality Solvents Book

Then send for it! It's FREE

This unique 56 page reference was designed to assist the Spectroscopist and researcher in selecting the right solvent for each application. This book obviates the need to consult several references as it contains complete information on usage, transmittance, absorbance, physical properties and MC&B specifications with over 300 charts and graphs. Do we pass inspection? If so, fill out the handy coupon and mail.

MC/B MANUFACTURING CHEMISTS

Norwood, Ohio; Baton Rouge, La.; Raleigh, N.C.; East Rutherford, N.J.; Los Angeles, Calif.

MC&B MANUFACTURING CHEMISTS
2909 Highland Avenue
Norwood, Ohio 45212

You've passed inspection. Send me your Spectroquality Solvents Book

NAME _____
COMPANY _____
ADDRESS _____
CITY _____
STATE _____ ZIP _____
10-70 MCB

Circle No. 129 on Readers' Service Card

ploration, a multidisciplinary program for the support of scientific research projects whose long-range goals are: (1) to increase opportunities for international sharing of responsibilities and costs for ocean exploration and to assure more equitable use of limited resources; (2) to begin long-range efforts to protect the marine environment by accelerating scientific observation of the natural state of the ocean and its interactions with the continental margins; (3) to develop and improve an ocean forecasting and monitoring system, to facilitate the prediction of oceanographic and atmospheric conditions, and to reduce hazards to life and property and permit more effective use of marine resources; (4) to expand seabed assessment activities, to provide scientific information needed to permit better management of ocean mineral exploration and utilization; (5) to improve worldwide oceanographic data exchange.

Rapid availability and accessibility of data and intercalibration of instruments will be emphasized for the fiscal year 1971. Resources will be concentrated on three main themes: (1) environmental quality—studies to provide comprehensive "baselines" of the chemical and biological characteristics of the entire ocean, with particular application to pollution monitoring and control; (2) environmental forecasting—studies with emphasis on modeling and oceanic variability, air-sea interaction, upwelling, and the flow of energy, nutrients, and other substances through the food web; (3) seabed assessment—studies with emphasis on the topography, structure, and dynamic properties of the continental margin and deep ocean floor, including the general character and stratigraphy of ocean sediments. For further information about the program or to submit a proposal for support, write to: Head, Office for the International Decade of Ocean Exploration, National Science Foundation, Washington, D. C. 20550.

Alan J. Senzel

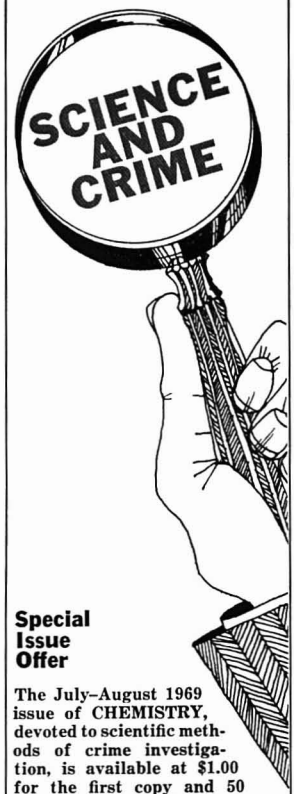

Special Issue Offer

The July–August 1969 issue of CHEMISTRY, devoted to scientific methods of crime investigation, is available at $1.00 for the first copy and 50 cents for each additional copy.

Feature articles include "Dimensions of Crime Today", "Origin of Modern Criminology", "Scientific Methods of Crime Investigation", and "Chromosomes and Crime". Also included: the story of how the lie detector was developed; how cause of an airplane crash was deduced from a single seat cushion; and a comprehensive reading list on crime and scientific methods used in crime investigation.

Some readers' comments: comprehensive; fun-reading; a fascinating issue; a work of art in make-up and content.

Send your order to:

Reprint Department
American Chemical Society
1155 16th St. N.W.
Washington, D.C. 20036

Amount Enclosed _____

New. Perkin-Elmer goes atomic absorption 6 better.

Perkin-Elmer is introducing four new atomic absorption spectrophotometers and two high-sensitivity sampling systems. This spring six Perkin-Elmer product specialists will tour North America to demonstrate them to you. For time and place, contact your nearest Perkin-Elmer office. For data, write Instrument Division, Perkin-Elmer Corporation, 702 Main Avenue, Norwalk, Conn. 06852.

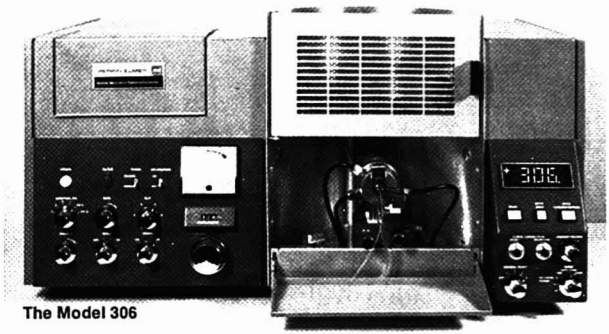

The Model 306

1. New: The Model 103
A compact, low-cost instrument which does absorption and emission analyses with equal ease. To light the flame, push a lever and actuate an "electric match." To set zero on the 12-cm meter, push the AUTO-ZERO button. To go from absorption to emission, flip a switch. To read out results, select between three damping times and two INTEGRATION modes. With meter integration, the needle rises to a stable reading; it doesn't quiver. The same stable signals can be read on a laboratory recorder.

2. New: The Model 107
To many, it's worth a little extra to read concentration on electronic digits. In the 107, the meter of the 103 is replaced by a four-digit readout with adjustable decimal point. To set concentration, use the integration mode, then "unlock" the digits and set them to any value you want. Both instruments have a 0-1 absorbance range, and 50X scale expansion; 0.02 absorbance unit can be set to read full-scale on the digits. Both instruments have all-mirror optics to cover all the wavelengths from arsenic to cesium (1900-9000 A).

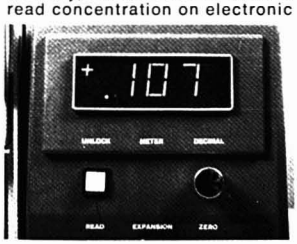

3. New: The Model 306
A double-beam instrument which reads concentration, in absorption or emission, on four electronic digits. An electric match is standard; fully automatic ignition is a little extra. To set zero, push the button. Then, use AUTO-CONCENTRATION. Just dial the concentration of the standard, aspirate the standard solution, and push the button. Calibration is now completed. Is the working curve non-linear? Straighten it with two controls, each used only once. The 306, too, has integration on both digits and recorder; the recorder traces appear noise free, and are easy to read. Conventional damping can also be used.

Circle No. 140 on Readers' Service Card

4. New: The Model 305A
The 305A has built-in flame emission, a new burner, a phase switch to improve the effectiveness of the Deuterium Background Corrector, and a metal instrument cover which gives easy access to optics and electronics. Result: proved reliability, improved performance.

5. New: The HGA-70 Graphite Furnace
A flameless system which gives far better detection limits than the burner-nebulizer. A small amount of sample is pipetted into a hollow graphite cylinder. The cylinder is then electrically heated as high as 2700° C in an inert atmosphere. Many metals are detected in amounts down to 10^{-12} grams.

6. New: The Delves Microsampling Cup™ System

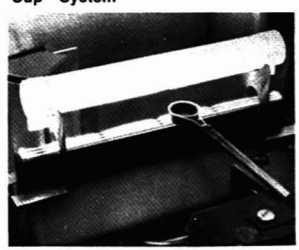

A modification of the Sampling Boat™ system, developed to determine lead in 10 μl of blood. The Delves system can also determine other volatile metals including cadmium, arsenic, selenium, and mercury.

PERKIN-ELMER

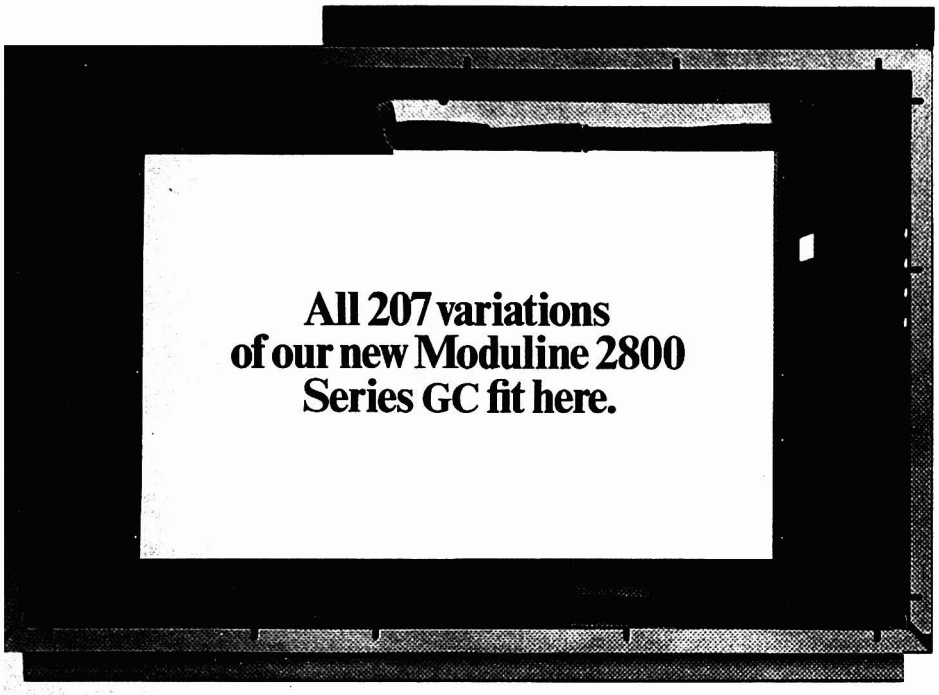
All 207 variations
of our new Moduline 2800
Series GC fit here.

At last count, we came up with 207 different versions of our new 2800 Series Gas Chromatograph. Each able to do a very specific GC job reliably well. With remarkable reproducibility.

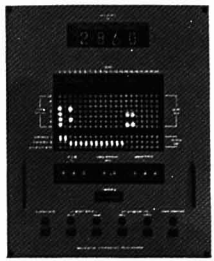

MULTILINEAR TEMPERATURE PROGRAMMER

Built around a truly modular mainframe (left), the entire 2800 Series shares an impressive list of standard features. Among them are a newly redesigned electrical system that's not only compatible with any commonly used voltage in the world, but which also produces the cleanest signal ever to come out of a GC. A unique all solid state dual/differential electrometer (above right). A greatly simplified flow control system. A spacious 1090 cubic inch column oven. And dual column, dual detector capability.

But that's just the beginning.

You can choose from four different temperature programmers, plus four versions of our computer-compatible MultiLinear Temperature Programmer (MLTP) pictured above on the left.

We currently have five detectors–four ionization and one TC–from which a variety of combinations can be made. Significantly, all four ionization detectors fit on a common base for speed and ease of interchangeability.

In the end, regardless of versatility, a GC is only as good as the results it produces.

The automobile exhaust emission analysis, below, is just one example of the tough jobs the 2800 handles with authority. This particular analysis is the result of four different capabilities working at once. Cryogenic operation. Capillary capability. Multi-linear temperature programming. And computer controlled operation. The results speak for themselves. (We might also note that in 18 runs of similar samples over a period of 48 hours, the *worst* cumulative retention time error was less than two seconds over a retention time of 1100 seconds.)

DUAL/DIFFERENTIAL ELECTROMETER

We've published a booklet detailing all 207 variations of the new Moduline 2800 Series GC. For your copy, simply write on your letterhead to Varian Aerograph, Walnut Creek, California 94598; Tokyo, Japan; Malton, Ontario, Canada; Crows Nest, N.W.S., Australia; or Zug, Switzerland.

And, if you find 207 combinations aren't enough, we'll be glad to sit down with you and work out Number 208.

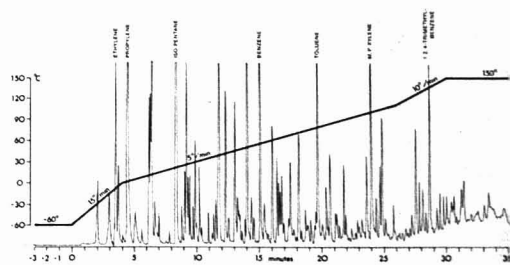

AUTOMOBILE EXHAUST ANALYSIS FOR HYDROCARBONS
Conditions: Flame ionization detector; 200' x 0.020" i.d. capillary column with DC 200 (50CS) liquid phase; He carrier gas at 7 ml/min; temperature program as shown.

varian aerograph

Circle No. 186 on Readers' Service Card

Contact us or your representative:

U.S.A.
I MASS
Box 134 - Accord,
Mass. 02018
Tel. (617) 749-5728

GREAT BRITAIN
Wanted

CANADA
TECHNEUROP
20060 ouest GOUIN west
Pierrefonds P.Q.
Tel. (514) 626-2020

ITALY
HENRY COE et CLERICI
Ramo Technico
Via M.A.Colonna 12
20149 Milano Tél 31.32.51

BELGIUM
VAN ERMENGEN
19 Penitentienenstraat
Leuven
Tel. 016/25106

HOLLAND
MEYVIS EN CO
Pergolesilaan 4
Bergen Op Zoom
Tel. 01640-6922

GERMANY
Klaus Schaefer
Darmstadter Strasse 62
6079 Sprendlingen bei
Frankfurt
Tel. (06 103) 67-361)

U.R.S.S.
Eastern Countries
COMEF
57, Av. d'Iena - Paris 16e
Tel. 553.24.90

JAPAN
SHINTO JITSUGYO K.K
Futsugin Building
1/2 Akasaka 1-Chome
Minato-Ku
107 Tokyo - Tel. 582-0871

ISRAEL
ELINA
Pob 1020
Ramat-Gan - Tel. 720715

ARGENTINA
V. TOKATLIAN
Casilla de Correro 4322
Buenos-Aires
Tel. 89.5801

SPAIN
ELVIRIO
Plaza del Marquès de
Salamanca 9
Madrid 6
Tel. 225-60-68

havas/lyon

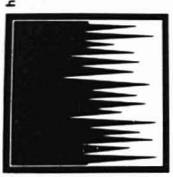

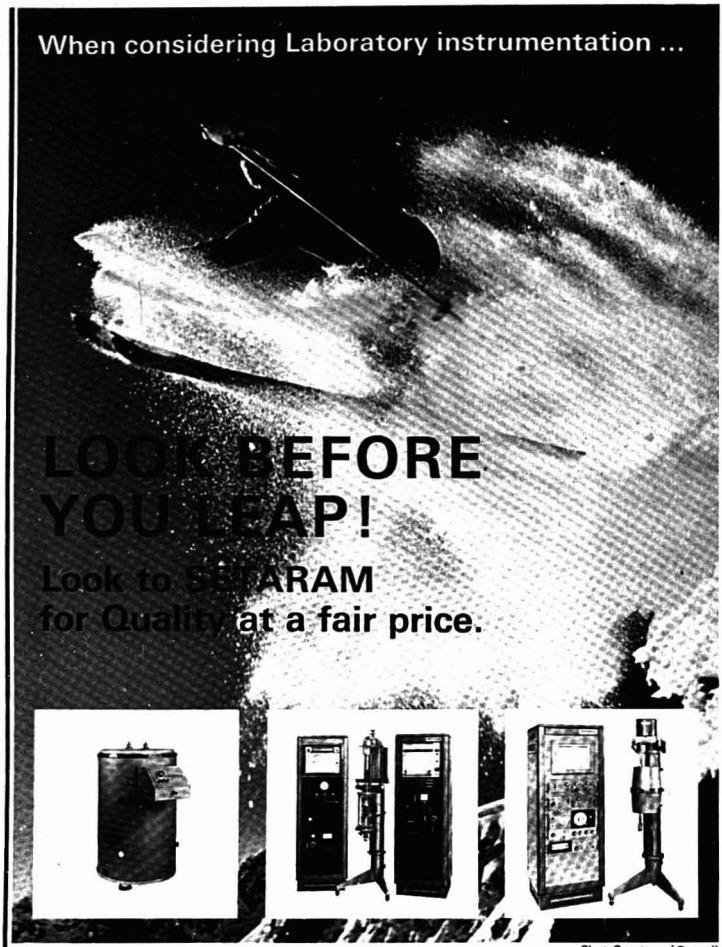

Phot. Courtesy J.Durnell

CALORIMETRY

... CALVET MICROCALORIMETER
One of the most sensitive calorimeters known. Based on thermal flow principle which approaches isothermal microcalorimetry. Available in 2-cell or 4-cell models of 15 ml or 100 ml capacity. Also available in two temperature ranges ambient to 200° C or 1000° C. Can measure as little as 0.001 calories per hour. A cryogenic model is under development.

... CRMT CALORIMETERS
Can measure 0.1 calories per hour. A single-cell model with detection system based on Calvet principle. Fast operation - as little as 20 minutes per run. Accessories for mixing studies and microbomb calorimetry. Temperature range ambient to 80° C. Available in 15 ml or 100 ml models.

THERMOGRAVIMETRY

... A symmetrical system employing the MTB 10-8 Microbalance which detects 0.4 µg on a 10 g sample. The symmetrical beam and twin furnace are designed to minimize disturbances from convection currents, Archimeadian bouyancy, and radiometric effects. Especially for TGA and DTG experiments at a high level of sensitivity.

...A system which provides TGA, DTG, DTA and Gas Analysis all in one run. Employs a B. 70 Balance which can detect 10 µg on a 100 g sample.

Furnaces available on both systems for 1000° C - 1600° C - 2200° C. Also, a microfurnace for magnetic studies from - 150° C to 1000° C.

GAS AND LIQUID FLOWMETERS

Based on thermal principle with measurement by Wheatstone bridge unbalance. No moving parts. Can handle corrosive or non-corrosive materials.

For Gas... measures with 0.5 % accuracy as little as 10 cc/hr. with no significant pressure loss.

For Liquids... measures flows from a few cc per hour up to 50 liters per hour. Not affected by variations in viscosity. Operation to 40° C. with special versions for high temperature.

SETARAM

SOCIÉTÉ D'ÉTUDES D'AUTOMATISATION DE RÉGULATION ET D'APPAREILS DE MESURES
101-103, rue de Sèze - 69 / Lyon 6e - France - B.P. 510 Lyon RP - Tél. 78/24.17.41 - Télex SETARAM 33 560

Circle No. 169 on Readers' Service Card

Advisory Panel

Jonathan W. Amy
Jack W. Frazer
G. Phillip Hicks
Donald R. Johnson
Charles E. Klopfenstein
Marvin Margoshes
Harry L. Pardue
Ralph E. Thiers
William F. Ulrich

Ion Specific Liquid Ion Exchanger Microelectrodes

Miniature ion specific electrodes with liquid ion exchanger membranes provide a convenient means of measuring intracellular ionic activities in living cells

JOHN L. WALKER, JR., Department of Physiology,
University of Utah College of Medicine,
Salt Lake City, Utah 84112

NERVE CELLS convey information to other nerve cells and to effector organs by means of electrical impulses propagated along the cell membrane. In many types of muscle cells, an electrical impulse propagated over the cell membrane is a necessary prerequisite to mechanical contraction. These electrical events are dependent upon an asymmetrical distribution of inorganic ions between the extracellular and intracellular spaces. In addition, the electrical-mechanical coupling in muscle involves changes in the intracellular activity of calcium. To understand the electrical and mechanical activities of nerves and muscles, an accurate knowledge of the intracellular activities of the ions involved is necessary.

To measure the intracellular activities of ions is a difficult technical problem for two reasons. First, the cells and, therefore, the intracellular volumes are very small. Table I contains the dimensions and volumes of some cells of interest. The first two entries in the table represent the upper size limit, with few exceptions, while the third is approaching the lower size limit. Second, the measurements must be made without appreciable damage to the cell membrane. If the membrane is damaged to the extent that the membrane potential is not normal, the intracellular ionic activities are certain to be different from their normal values.

It is possible to make estimates of the intracellular concentrations by measuring the amount of an ion in whole tissue, the whole tissue volume, the extracellular space concentration, and the extracellular volume. However, in addition to the uncertainties of the method, it gives only concentrations, which are not very meaningful (*1–3*). One needs to know the intracellular activities of the ions.

Since the development of ion specific glasses for hydrogen and the alkali cations, microelectrodes have been fabricated from these glasses (*4, 5*). Chloride microelectrodes have been made by coating a platinum wire protruding from the end of a glass micropipet with Ag–AgCl (*4*) or by depositing silver chloride inside the tip of a micropipet (*6*). These electrodes all have the drawback of having a large ion sensitive surface which must be entirely within the cell and their use is, therefore, limited to cells the size of skeletal muscle or larger. While these electrodes may have a tip diameter of one micron or less, the sensitive area is on the order of ten microns in length with a diameter of five microns or more at the top of this area. In addition to the problem of size, they are difficult to fabricate.

Liquid Ion Exchangers

Liquid ion exchangers have been used in liquid-liquid ion extraction processes in industry for some time and, from time to time, as models for biological membranes (*7, 8*). In the past decade, there was renewed interest in liquid ion exchangers on the part of biologists, and the theory of their behavior as ion selective membranes was developed (*9, 10*). At the same time, a practical calcium electrode was developed which utilizes a liquid ion exchanger membrane as the sensitive element of the electrode (*11*). Since then, several other ion specific liquid ion exchanger electrodes have become commercially available. This paper discusses the miniaturization of these electrodes for the express purpose of measuring intracellular ionic activities in living cells.

A liquid ion exchanger is composed of an organic electrolyte dissolved in a water-immiscible solvent, usually an organic solvent with a low dielectric constant. The organic ion should have a low water solubility and is often highly branched to prevent micelle formation (*12*). Owing to the low dielectric constant of the exchanger, inorganic ions have a very low solubility in the exchanger and, consequently, a membrane made of a liquid ion exchanger is much more permeable to ions whose valence sign is opposite to that of the organic ion than to ions of the same valence sign because of ion pair formation with the organic ion. For example, negatively charged phosphate esters are cation exchangers while positively charged amines are anion exchangers. Furthermore, some exchangers exhibit marked selectivity within a group of ions of the same valence sign, the selectivity being a function of the strength of interaction between the organic and inorganic ions.

An ion specific electrode is made by forming a liquid ion exchanger membrane in a suitable holder so that one side of the membrane is in contact with an aqueous reference solution of con-

Table I. Dimensions and Volumes of Some Electrically Excitable Cells

Kind of cell	Cell shape	Diameter	Length	Volume
Molluscan neuron	Spherical	1 mm		0.52 μl
Frog skeletal muscle	Cylindrical	0.1 mm	30 mm	0.25 μl
Frog ventricle	Cylindrical	0.01 mm	0.13 mm	1×10^{-6} μl

stant composition while the other side can be brought into contact with the solution to be analyzed. Electrical contact is made with the internal reference solution by means of an electrode which is reversible to one of the ions in the reference solution. The electrical potential difference across the membrane changes in proportion to the activity in the test solution of the ion(s) for which the liquid ion exchanger is selective.

A quantitative theory has been developed (*9, 10*) which describes the electrode potential, but it is cumbersome and contains parameters which are difficult to measure. It is, therefore, more convenient to use the following empirical equation:

$$E = E_o + \frac{nRT}{F} \log_e (a_i + K_{ij} a_j^{z_i/z_j}) \quad (1)$$

E is the electric potential (volts); E_o is a constant (volts); R is the gas constant (8.3 joules deg^{-1}mole^{-1}); T is the temperature (°K); F is Faraday's number (96,500 coulomb equivalent^{-1}); n is an empirical constant (dimensionless) chosen so that nRT/F is the slope of the line when E is plotted as a function of $\log_e a_i$ when $K_{ij}a_j = 0$; z_i and z_j are the valences of the ith and jth ions, respectively; a_i is the activity (arbitrary concentration units) of the ion the electrode is expected to measure; the a_j's are the activities (same units as a_i) of interfering ions whose valence sign is the same as that of the principal ion and the K_{ij}'s are the selectivity constants for the jth ions with respect to the ith ion. When $K_{ij} < 1$ the electrode has a higher selectivity for the ith ion than for the jth ion. K_{ij} is an empirical number and should not be assigned a strict physical interpretation.

The problem, then, is to form a liquid ion exchanger membrane in a holder small enough to insert into a cell so that one surface of the membrane is in contact with the intracellular fluid.

Electrode Fabrication

A standard technique for making intracellular electric potential measurements has been to pull a glass micropipet with a tip diameter of about 0.5 micron and fill it with 3*M* KCl. Extensive research with this technique has shown that when the tip of such a pipet is inserted into a cell, it does not disrupt the normal functioning of the cell (*13*) and, therefore, if a liquid ion exchanger membrane could be formed in the tip of such a pipet, the problem would be solved.

The primary difficulty is that a clean glass surface is hydrophilic, so an organic liquid membrane will not remain in place in the tip of the pipet. Instead, it will be displaced by one of the aqueous phases with which it is in contact. To prevent this, it is necessary to render hydrophobic the portion of the pipet which is to contain the organic liquid. The method used to do this is to apply an organic silicone compound to the terminal 200 microns of the pipet tip.

A successful method for making potassium and chloride microelectrodes involves the following steps. Borosilicate glass capillary tubing (1.2 mm od, 0.3-mm thick wall) is cleaned with hot ethanol vapor and dried. Pipets are pulled from the clean tubing with a commercially available pipet puller and have a tip diameter of 0.5 to 1.0 micron. Immediately after pulling, the pipet tips are dipped in a fresh solution of 1% Siliclad (Clay-Adams) in 1-chloronaphthalene until there is a column of the solution about 200 microns long inside the tip. This takes approximately 15 sec. The pipets are then placed tip up in a metal block and when the desired number (one to two dozen) have been prepared, they are placed in a 250°C oven for one hour. After being removed from the oven and allowed to cool, the pipets are ready for filling but can be held in this condition for at least one week before being filled.

To fill a pipet, the tip is dipped into the ion exchanger (Corning code 477317 potassium exchanger or Corning code 477315 chloride exchanger) until the terminal 200 microns (approximately) of the tip is filled with the exchanger (one to two minutes). One-half molar KCl is then injected as far down into the top of the pipet as possible using a three-in., 30-gauge needle attached to a syringe. The pipet is placed horizontally on the movable stage of a compound microscope and a hand-drawn, solid glass needle mounted on a micromanipulator is advanced down the inside of the pipet while viewing under 100× magnification. The tip of the glass needle is brought to the center of the field and the microscope stage is carefully moved until the tip of the needle touches the meniscus of the ion exchanger. The KCl solution flows down to the liquid ion exchanger, displacing the air toward the top of the pipet where it can be flushed out using the 30-gauge needle. Air bubbles of 100 microns or less in length may be disregarded since they will be quickly absorbed. With practice, electrodes can be dipped and filled in an average of five min. A small amount of mineral oil is then injected into the top of the pipet to prevent water evaporation, and the pipet is stored with the tip in a solution of 0.5*M* KCl. Best results are obtained when the filled electrodes are allowed to stand for at least two hr before being used. Figure 1 shows a schematic diagram of an electrode ready for use, and Figure 2 is a photograph of a potassium microelectrode with 125 microns of liquid ion exchanger in the tip.

Two difficulties have been encountered with these electrodes. Sometimes the tips of the electrodes will not fill with the ion exchanger, or take it up very slowly. This is owing, presumably, to the tips being plugged by the Siliclad. If a pipet does not take up the desired amount of exchanger within two min, it is discarded. An alternative to this is to break the tip slightly, but this is only useful if a tip diameter of two microns or larger can be tolerated. The other difficulty is that the electrodes will sometimes lose the exchanger within two to three hr after being filled. The cause for this difficulty has not been determined. To alleviate these problems, other siliconizing procedures using a variety of organic chlorosilanes in different solvents are being investigated.

Although both kinds of electrodes can be made in the same way, there is another method of siliconizing which

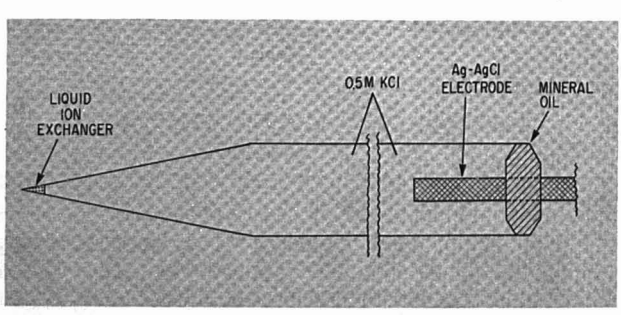

Figure 1. Schematic diagram of an ion specific liquid ion exchanger microelectrode

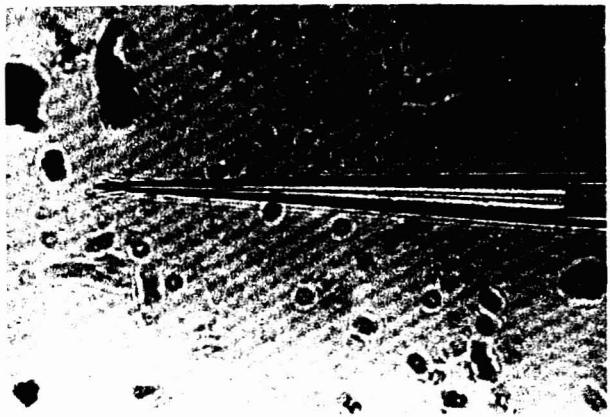

Figure 2. Photograph of a potassium liquid ion exchanger microelectrode with 125 microns of ion exchanger inside the tip. Magnification, 400×

works better for the potassium electrodes but is not satisfactory for the chloride electrodes. After being pulled, the pipet tip is dipped in a 5% solution of tri-*n*-butylchlorosilane in 1-chloronaphthalene until there is a column about 200 microns long inside the tip (about 15 sec). The pipet is then allowed to air dry for at least 24 hr before being filled as described above. The tips of pipets siliconized in this way do not plug up as they sometimes do with the Silielad solution.

Electrode Resistance and Selectivity

Because of the small size of the tip of the electrodes and the low conductivity of the liquid ion exchangers, the resistance of the electrodes is high and a voltage measuring device with an input impedance of at least 10^{13} ohms is required. A satisfactory solution has been to use a varactor bridge operational amplifier (Analog Devices, model 311K) which has an input impedance of 10^{14} ohms with an input capacitance of two picofarads. The microelectrode is connected to the input of the amplifier *via* a chloridized silver wire inserted into its top, and the amplifier output is connected to a digital voltmeter. The resistance of the microelectrodes, as measured from the charging time of the input of the operational amplifier, is in the range of 10^9 to 10^{10} ohms.

The response time of the electrodes when the concentration of potassium or chloride is changed has not yet been measured carefully because of the technical problems involved. However, when one of the electrodes is dipped into a solution and the amplifier input is opened as rapidly as possible, the new steady-state potential is reached within five sec, which indicates that the time constant of the response is not more than one sec. Once the steady-state potential is attained, it remains constant to within ± 1 mV for several hours. In Table II, some data from experiments with *Aplysia* neurons (*14*) are presented showing the long-term stability of both the potassium and chloride electrodes.

The selectivities of the electrodes for interfering ions with respect to the principal ion has been determined for some interfering ions commonly found in biological preparations. These have been determined by measuring the electrode potentials in mixtures of constant ionic strength and finding the K_{ij} which makes the data fit Equation 1. The results of these measurements are presented in Table III for the chloride electrode and for potassium electrodes made by both of the methods described above.

Making Intracellular Measurements

Immediately before making an intracellular measurement with one of the electrodes, the electrode must be calibrated. This is done by measuring its potential with respect to a 3*M* KCl-filled micropipet in a series of KCl solutions of known concentrations. The KCl concentrations used should bracket the expected concentration of the unknown solution. The electrode is then moved to the solution bathing the cell in which the measurement is to be made, which normally contains some of the ion to be measured, potassium and/or chloride. The potential of the electrode in that solution should agree with the potential predicted for the electrode from the calibration curve, taking into account any interfering ions which may be present in the solution. The tip of the electrode is then inserted into the cell. Since it is not possible to see the tip of the electrode enter the cell, the criterion used to determine cell entry is an abrupt shift in the potential of the electrode as it is slowly advanced toward the cell. This shift in potential is due to two factors: (1) the difference in activity of the ion being measured between the extracellular and intracellular fluids; and (2) the cell membrane potential. The shift of the electric potential as the electrode tip enters the cell can be written as:

$$\Delta E = E_m + \frac{nRT}{z_iF} \log_e \left[\frac{a_i^e + K_{ij}a_j^e}{a_i^i + K_{ij}a_j^i} \right] \quad (2)$$

where ΔE (volts) is the difference in electric potential between the inside and the outside of the cell; E_m (volts) is the cell membrane potential; the

Table II. Data from Experiments on *Aplysia* Neurons with Chloride and Potassium Microelectrodes[1] (*14*)

Slope, mV		Potential in artificial seawater, mV		Time in cell(s), min
Before[2]	After[2]	Before[2]	After[2]	
58	58	34	34	335
58	58	31	30	486
58	58	48	48	137
58	58	44	44	118
58	58	35	36	347
54	54	46	44	495
56	56	50	51	140
54	54	49	49	380
52	52	42	40	144
52	52	40	40	384

[1]First five measurements are with potassium electrodes and last five are with chloride electrodes. In most experiments, more than one cell penetration was made with the electrode during the indicated time. [2]Before and after intracellular measurement(s).

Only Jeolco's new laser Raman spectrophotometer records depolarization ratio automatically and simultaneously with the normal Raman spectra. ☐ Jeolco's compact, table-top JRS-S1 is the first unit to give you this important advantage. The first to record depolarization ratio throughout the measured range, automatically and simultaneously, to aid in the assignment of the Raman band. This all-digital model offers the following high performance features: better than 1 cm^{-1} resolution, less than 10^{-10} scattered light at 25 cm^{-1} shift, 10,000 cm^{-1} spectrometer cover range, with 30mW He-Ne laser as standard equipment and the ability to adopt any available cw laser source. ☐ High sensitivity benefits include: special low-noise photomultiplier with extended S-20 photocathode, thermoelectric photomultiplier cooling, low-noise photon counting system, optimum sample chamber system, and double-monochromator (f/6.7). ☐ Push-button selection of operating conditions, with warning lamps for mis-selection, large sample chamber, two-pen recorder with automatic adjustment of wave scale to monochromator sweep range, safety circuit for photomultiplier protection, and automatic attenuation of laser – to protect operator's vision. ☐ The unit's monochromator drive is linked to the recorder drive. With automatic setting of repeated recording. Half of the recording scale is above 2,000 cm^{-1} to match the infrared spectra. ☐ For full details call or write Jeolco, 235 Birchwood Avenue, Cranford, N.J. 07016; Tel. (201) 272-8820.

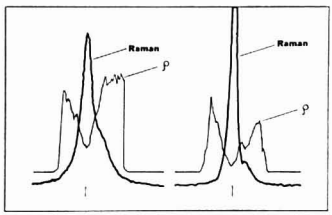

Jeolco.

Putting the 70's into focus.

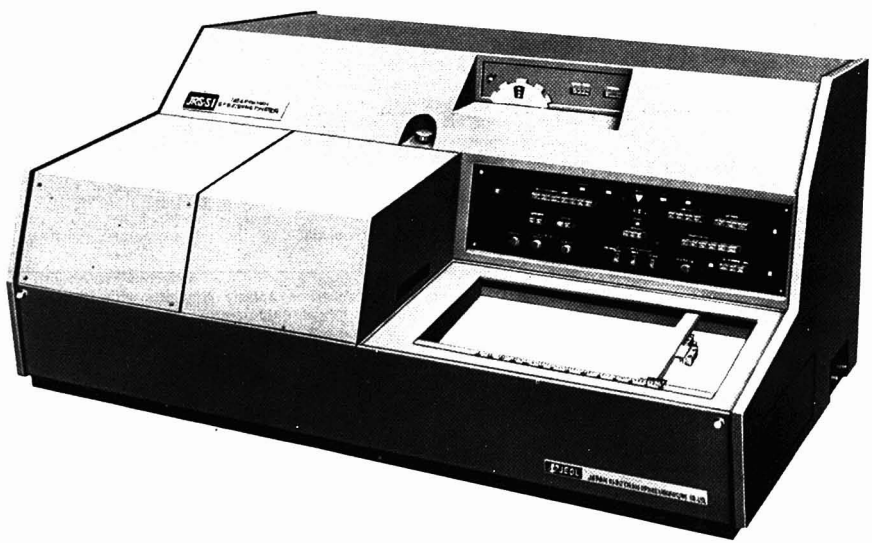

Mass Spectrometers/Amino Acid Analyzers/Nuclear Magnetic Resonance Spectrometers/Scanning Electron Microscopes/Electron Microscopes/Electron Spin Resonance Spectrometers/X-ray Diffractometers/Laboratory Computers

Circle No. 102 on Readers' Service Card

Table III. Selectivities for Interfering Ions with Respect to Principal Ion for Chloride and Potassium Microelectrodes

Interfering ion	K_{ij}		
	0.1M[1]		1.0M[1]
Bicarbonate[2]	0.05		0.05
Isethionate[2]	0.2		0.2
Propionate[2]	0.5		0.7
Calcium[2]	0.002	a[4]	0.03
	0.002	b	0.03
Hydrogen[3]	0.02	a	0.03
	0.025	b	0.016
Sodium[3]	0.02	a	0.02
	0.02	b	0.014

[1] Ionic strength. [2] Ions interfering with chloride. [3] Ions interfering with potassium. [4] a and b refer to Siliclad and tri-n-butylchlorosilane potassium microelectrodes, respectively.

superscripts on the activities, o and i, refer to outside and inside of the cell; and n, determined from the calibration curve for each electrode, is 1.0 for the potassium electrodes and in the range of 0.90 to 0.97 for the chloride electrodes. While n varies from one chloride electrode to another, it is constant for any one electrode and constant over the range of at least $1.0 \times 10^{-3} M$ KCl to $1.0 M$ KCl for both potassium and chloride electrodes. E_m is measured by impaling the cell with a $3M$ KCl-filled micropipet.

When Equation 2 is solved for the denominator of the logarithmic term, it takes the form of Equation 3.

$$a_i^i + K_{ij}a_j^i = (a_i^o + K_{ij}a_j^o)\exp\left[\frac{(\Delta E - E_m)z_iF}{nRT}\right] \quad (3)$$

It is now a simple matter, knowing all the factors on the right side of Equation 3, to calculate a numerical value for the left side. The only remaining problem is to determine the value of the term, $K_{ij}a_j^i$. If microelectrodes specific for the interfering ions are available, the a_j^i's can be measured directly. Unfortunately, this is not usually possible and, therefore, it is necessary to use estimates arrived at by other means. When whole tissue analyses have been done, the values of the concentrations can be used by assuming values for the intracellular activity coefficients (*2*). Intracellular sodium activity can be estimated from the overshoot of the action potential (*15*), and in the case of ions which appear to be passively distributed across the cell membrane, the intracellular activity can be calculated by using the extracellular activity of that ion and assuming a Donnan distribution (*2*).

When the cells are large, as in the case of *Aplysia* neurons or frog skeletal muscle, the KCl-filled micropipet can be seen in the same cell as the ion specific electrode, but with smaller cells this is not possible. When the cells are too small to see if both electrodes are in the same cell, the membrane potential and ion specific electrode measurements can be made separately in several cells and the average values of the measurements used to calculate intracellular activity. A better solution to the problem is to make double-barrel electrodes where one barrel is the ion specific electrode and the other barrel is the reference electrode. Attempts to fabricate such electrodes are currently being made.

As shown in Table II, both the potassium and chloride microelectrodes are stable over a period of several hours even when several cell penetrations are made with the same electrode. When an electrode has shown a DC drift, it has usually been traced to a change in the potential of the Ag–AgCl electrode making contact with the internal reference solution of the electrode. Most important is the fact that the slopes of the electrodes do not change during the course of the experiments. Since the intracellular measurements are made with respect to the extracellular solution, which is of known composition, a slow DC drift is of little consequence as long as the slope of the response curve remains constant.

As is the case with any new technique, it is necessary to establish that the data obtained with the technique are valid. In measuring intracellular activities with ion specific electrodes, this is not easy to do because of the lack of accurate information concerning intracellular activities of ions, both organic and inorganic, which may interfere with the measurement. This is especially true of the chloride electrode because of the presence of organic anions in the intracellular fluid. Some experimental results bearing on this point have been presented and discussed by Cornwall *et al.* (*16*).

At the present time, only the potassium and chloride ion exchanger microelectrodes are of practical use. Attempts to make a calcium microelectrode have not been completely successful, although some progress has been made. They can be made to exhibit a Nernst slope in solutions of $CaCl_2$ from $1.0 \times 10^{-4} M$ to $1.0 M$ with a time constant and stability comparable to the potassium and chloride microelectrodes. However, when potassium, in concentrations approximating those found inside cells, is added to the $CaCl_2$ solutions, it reduces the calcium response drastically. Work is continuing on the calcium microelectrode and as liquid ion exchangers for other ions of interest to biologists become available, they will be used to make ion specific microelectrodes of the type described above.

References

(1) J. A. Johnson, *Amer. J. Physiol.* **181**, 263 (1955).
(2) E. J. Conway, *Physiol. Rev.* **37**, 84 (1957).
(3) E. Page, *J. Gen. Physiol.* **46**, 201 (1962).
(4) J. A. M. Hinke in "Glass Microelectrodes," Lavalee *et al.*, Eds., Wiley, New York, N. Y. 1969.
(5) N. W. Carter, F. C. Rector, Jr., D. E. Campion, and D. W. Seldin, *J. Clin. Invest.* **46**, 920 (1967).
(6) G. A. Kerkut and R. W. Meech, *Life Sci.* **5**, 453 (1966).
(7) R. Beutner, *Amer. J. Physiol.* **31**, 343 (1913).
(8) G. Eisenman, J. P. Sandblom, and J. L. Walker, Jr., *Science* **155**, 965 (1967).
(9) J. P. Sandblom, G. Eisenman, and J. L. Walker, Jr., *J. Phys. Chem.* **71**, 3862 (1967).
(10) J. P. Sandblom, G. Eisenman, and J. L. Walker, Jr., *J. Phys. Chem.* **71**, 3871 (1967).
(11) J. Ross, *Science* **156**, 1378 (1967).
(12) R. Kunin and A. G. Winger, *Angew. Chem., Int. Ed. Engl.* **1**, 149 (1962).
(13) W. L. Nastuk and A. L. Hodgkin, *J. Cell. Comp. Physiol.* **35**, 39 (1950).
(14) D. L. Kunze and A. M. Brown, unpublished results, 1970.
(15) A. L. Hodgkin and B. Katz, *J. Physiol.* **108**, 37 (1949).
(16) M. C. Cornwall, D. F. Peterson, D. L. Kunze, J. L. Walker, Jr., and A. M. Brown, *Brain Res.* **23**, 433 (1970).

This work was supported by American Heart Association Grant #70 837, Utah Heart Association Grant 1T, and the United States Public Health Service Grant GM 14328.

Thomas offers a complete, self-contained system for determination of mercury.

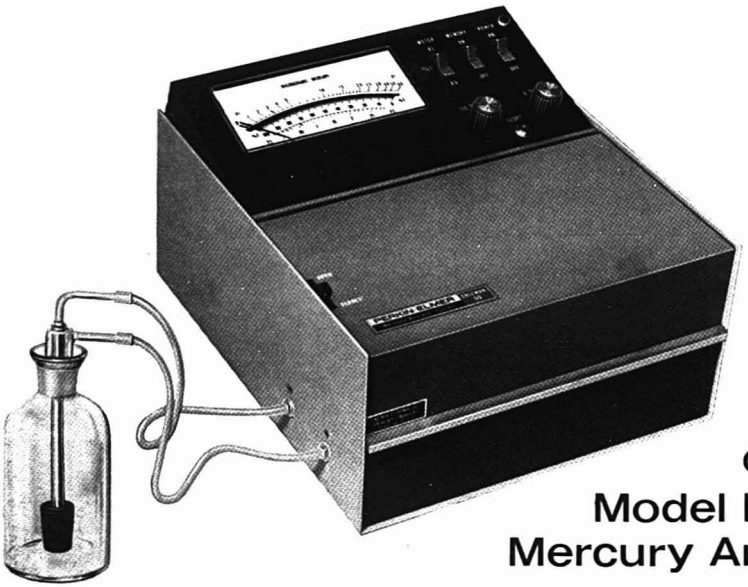

Coleman
Model MAS-50
Mercury Analyzer

APPLICATIONS

This compact system can be used in many scientific fields.

Pollution:
air, water, food, soil, tissue.

Clinical:
urine, blood, tissue.

Industrial Control:
food, metal, soil, fertilizer.

In stock for immediate shipment.

Call or write for Bulletin B-350.

This easy-to-operate unit displays mercury content of sample directly in micrograms. Dual ranges are 0-9 micrograms and 0-0.28 microgram full scale. Sensitivity is 0.01 microgram of mercury and reproducibility is better than 3%.

Features simple sample preparation utilizing Hatch and Ott stannous chloride reduction and subsequent bubbling of mercury vapor through a closed system for detection by "cold atomic absorption" technique.

Instrument has rapid response with "memory" system to hold peak reading until released. Other features include simple 5-step procedure of reagent addition. A mercury-free reagent kit is available.

Inexpensive and complete, the Coleman MAS-50 can release more expensive atomic absorption instrumentation for other uses and provides a higher degree of accuracy.

Thomas **ARTHUR H. THOMAS COMPANY**

Scientific Apparatus and Reagents

VINE STREET AT 3RD • P.O. BOX 779 • PHILADELPHIA, PA. 19105, U.S.A.

Circle No. 176 on Readers' Service Card

Enter your personal subscription to

Environmental Science and Technology

First journal in its field. Provides monthly information on research and technology involved in water, air and waste chemistry, as well as news of political and industrial aspects of environmental management.

Analytical Chemistry

Foremost monthly publication in the vital fields of chemical analysis. Treats both theoretical and applied aspects of analysis. Subscription includes special "ANNUAL REVIEWS" and "LAB GUIDE" issues.

Chemical Technology

The Society's newest publication. Serves chemists and chemical engineers charged with industrial innovation. Imparts immediate information of a pragmatic nature.

Please enter my subscription to the publications I have checked below at the indicated one year rates.

☐ **ENVIRONMENTAL SCIENCE AND TECHNOLOGY**	*ACS members	☐ U.S. $5.00	☐ Canada, PUAS ** $8.00	☐ Other Nations ** $8.50
	Nonmembers	☐ U.S. $7.00	☐ Canada, PUAS ** $10.00	☐ Other Nations ** $10.50
☐ **ANALYTICAL CHEMISTRY**	*ACS members	☐ U.S. $5.00	☐ Canada, PUAS ** $7.50	☐ Other Nations ** $8.50
	Nonmembers	☐ U.S. $7.00	☐ Canada ** $9.50 ☐ PUAS ** $17.50	☐ Other Nations ** $18.50
☐ **CHEMICAL TECHNOLOGY**	*ACS members	☐ U.S. $9.00	☐ Canada, PUAS ** $11.50	☐ Other Nations ** $12.50
	Nonmembers	☐ U.S. $18.00	☐ Canada, PUAS ** $20.50	☐ Other Nations ** $21.50

☐ Payment enclosed *(payable to American Chemical Society).* ☐ Bill me. ☐ I am an ACS member.

NAME_____ POSITION_____

YOUR EMPLOYER_____

ADDRESS ☐ Home ☐ Business _____

CITY_____ STATE_____ ZIP_____

Nature of Your Employer's Business: ☐ Manufacturing or Processing ☐ Government ☐ Academic ☐ Other _____

If Manufacturer, Type of Products Produced _____

*NOTE: Subscriptions at ACS member rates are for personal use only. **Payment must be made in U.S. currency, by international money order, UNESCO coupons, or U.S. bank draft; or order through your book dealer.

FIRST CLASS
Permit No. 1411-R
Washington, D. C.

BUSINESS REPLY MAIL
No postage stamp necessary if mailed in the United States

Postage will be paid by

AMERICAN CHEMICAL SOCIETY
1155 Sixteenth Street, N.W.
Washington, D. C. 20036

Attn: H. C. Spencer

ANALYTICAL CHEMISTRY

March 1971, Vol. 43, No. 3

Editor: HERBERT A. LAITINEN

EDITORIAL HEADQUARTERS
Washington, D.C. 20036
1155 Sixteenth St., N.W.
Phone: 202-737-3337 Teletype: WA 23

Managing Editor: John K. Crum

Associate Editor: Virginia E. Stewart

Assistant Editor: Alan J. Senzel

Editorial Assistant: Sylvia Crawford

PRODUCTION STAFF

Direction of Design: Joseph Jacobs

Production Manager: Bacil Guiley

Art Director: Norman W. Favin

Associate Production Manager: Charlotte C. Sayre

Editorial Assistant: Patricia W. Kener

NEW YORK OFFICE
733 Third Avenue
New York, N.Y. 10017
212-867-3161

Associate Editor: Josephine M. Petruzzi

EDITORIAL PRODUCTION OFFICE, EASTON, PA.

Assistant Editor: Elizabeth R. Rufe

ADVISORY BOARD: Norman G. Anderson, Klaus Biemann, C. G. Enke, James S. Fritz, John Funkhouser, Walter E. Harris, W. Wayne Meinke, Edwin P. Przybylowicz, William C. Purdy, Eugene M. Sallee, Donald T. Sawyer, A. Lee Smith, Lloyd R. Snyder, Samuel M. Tuthill, James D. Winefordner

AMERICAN CHEMICAL SOCIETY PUBLICATIONS DIVISION

Director of Publications, Richard L. Kenyon

Director of Business Operations, Joseph H. Kuney

Group Manager, Journals, John K. Crum

Assistant to the Director, Publications Division, William Q. Hull

REGIONAL EDITORIAL BUREAUS

CHICAGO, Ill. 60603
36 South Wabash Ave.

SAN FRANCISCO, Calif. 94104
57 Post St.

LOS ANGELES, Calif. 90005
422 South Western Ave.

HOUSTON, Texas 77002
514 Main Bldg.
1212 Main St.

FRANKFURT/MAIN, West Germany
32 Grosse Bockenheimerstrasse

LONDON, W. C. 2, England
27 John Adam St.

TOKYO, Japan
Iikura Central Building, 4th Floor
12 Iikura Kata-machi, Azabu
Minato-ku, Tokyo

Advertising Management
CENTURY COMMUNICATIONS CORP.
(for Branch Offices, see page 119 A)

For submission of manuscripts, see page 4 A.

The Manuscript Review

It is a popular misconception that the sole or principal purpose in subjecting manuscripts to review is to reach a decision as to whether the manuscript is to be accepted or rejected. To be sure, the reviewer is asked to recommend whether in his judgment the manuscript should be published with minor or major revision, or at all. However, in the end, the main function of the review process is to improve the manuscript through criticism and revision.

Statistical data support this conclusion. Of each 100 manuscripts received, on the average, we reject about 10 on the basis of preliminary evaluation by the editorial staff, some on the basis of quality, and some on the basis of inappropriateness of medium. Of the remainder, about 25 are rejected after review and 65 are published. Of these, the vast majority undergo some revision of content beyond minor corrections of spelling, punctuation, usage, and the like. According to recent records, only 20 per cent of the manuscripts are published essentially as received.

Of the manuscripts listed as rejected, some are actually withdrawn by the author who refuses to accept rather drastic revision (and usually condensation) imposed by the editors as a condition for publication. Many of these manuscripts are eventually published in another journal, and of course it is the privilege of the author to seek another outlet if he feels that the editorial decision is unwarranted.

The purpose of this editorial is to point out, first of all, that authors are encouraged to offer rebuttal arguments against criticisms they regard as incorrect or unfair, and secondly, that most manuscripts can be, and actually are, improved by revision. The most important function of the reviewers is to serve as an unusually well-informed microcosm of the readership, and, as such, to help the author present his work in the best light.

H. A. Laitinen

Novel Peak Matching Technique by Means of a New and Combined Multiple Ion Detector–Peak Matcher Device

Elemental Analyses of Compounds in Submicrogram Quantities without Prior Isolation

Carl-Gustaf Hammar[1] and Ronny Hessling

Department of Toxicology, Swedish Medical Research Council, Karolinska Institutet, S-104 01 Stockholm 60, Sweden

The multiple ion detector (MID), built as an accessory to a combined gas chromatograph–single focusing mass spectrometer, allows simultaneous recordings of three different masses within a mass range of 20%. The recorded mass traces are continuous. The intensities of the different masses may be individually amplified. The interference of the column bleed is overcome by individual bucking controls. The different accelerating voltages required are obtained by adding voltages (0 to +700 V) to the basic accelerating voltage (3500 V). Fast switching between the selected voltages allows simultaneous recording of the total ion current. The MID accessory is easily converted to a peak matcher device by addition of a sweep voltage generator. This allows a novel peak matching technique to perform elemental analyses of nonisolated compounds in submicrogram quantities during their elution from a GC column using a single focusing mass spectrometer. The compounds are matched afterward using the recorded peaks of the respective compounds. This allows a statistical treatment of all the data obtained from the records of multiple sweep cycles. Knowing the sweep voltage constant and the accelerating voltages used, the accurate mass of an unknown compound may be calculated and its empirical formula deduced. Performed mass determinations of either isolated or nonisolated compounds had a mean error of a few ppm at a static resolution of only 500–600, which favors the sensitivity. The dynamic resolution was about 70,000.

COMBINED GAS CHROMATOGRAPHY–MASS SPECTROMETRY (GC-MS) offers several important and well documented advantages—e.g., mass spectra can be obtained of small quantities of organic compounds, even in complex mixtures, if the compounds can be volatilized and eluted as single components by the GC column.

Even if the GC procedure fails to separate the compounds in the mixture, it may still be possible to resolve the components by recording the changing intensities of two selected, characteristic ion fragments or mass numbers simultaneously during the elution of the mixture from the GC column (*1*, *2*).

If, in addition to being incompletely resolved by the GC column, the amounts of compounds present are too small to allow interpretable mass spectra to be recorded, it is possible to use a technique which has tentatively been called mass fragmentography (*3*, *4*).

In this latter technique the mass spectrometer is utilized as a uniquely selective GC detector, which is capable of detecting multiple ionic species simultaneously and with great sensitivity. At least two mass numbers characteristic of the compound(s) in question are chosen, and the ratio of the intensities of these selected masses is used to characterize the components of the effluent. Further confirmation of molecular identity can be obtained by refocusing upon additional characteristic fragments and molecular ion(s). By this technique as little as 100–1 picograms of drug (10^{-10}–10^{-12} gram) have been detected and identified in unresolved gas chromatographic effluents (*3*).

The new multiple ion detector (MID) offers a new way of recording the selected masses, an expanded mass range (20%), great sensitivity in that each channel has individual base-line and gain controls and efficient filtration of the signals, and fast switching of the accelerating voltage which allows simultaneous recording of the selected masses and total ion current.

In line with these improvements and developments, made to facilitate analyses of small amounts of components present in complex mixtures of particularly biological origin, we have also created possibilities to perform elemental analyses of nonisolated compounds present in submicrogram amounts.

Elemental analyses as performed by mass spectrometry, especially when the peak matching technique is employed, is generally thought to require prior isolation of the compound and the use of a high resolution instrument (*5*). When the only instrumental facility available is a low resolution mass spectrometer, the peak matching technique is the only alternative by which elemental analyses can be performed.

By means of a combined gas chromatograph–low resolution mass spectrometer, the new peak matcher device and the technique reported in this article, we are now able to perform accurate mass determinations of compounds during their elution from a GC column. The device is identical to the MID accessory with the exception of the addition of a sweep voltage generator.

EXPERIMENTAL

Instrumentation. The combined gas chromatograph–single focusing mass spectrometer used is the LKB 9000 equipped with mass marker, direct inlet, and heated inlet system (LKB Produkter AB, Stockholm, Sweden), a direct recording oscillograph, ABEM Ultralette (Svenska Diamantbergborrnings AB, Stockholm, Sweden) and a potentiometric microvoltmeter, Medistor model A-75A (Seattle, Wash., USA).

Schematic diagrams of the MID-accessory (Patent pending) and its conversion to the peak matcher device (Patent pending) are shown in Figure 1*A* and 1*B*, respectively.

[1] Present address, Research Department of the Kabi Group, S-104 25 Stockholm 30, Sweden

(1) C. C. Sweeley, W. H. Elliott, I. Fries, and R. Ryhage, ANAL. CHEM., **38**, 1549 (1966).
(2) L. P. Lindeman and J. L. Annis, *ibid.*, **32**, 1742 (1960).
(3) C.-G. Hammar, B. Holmstedt, and R. Ryhage, *Anal. Biochem.*, **25**, 532 (1968).
(4) C.-G. Hammar, B. Alexanderson, B. Holmstedt, and F. Sjöqvist, *Clin. Pharmacol. Ther.*, **11**, in press (1971).
(5) W. J. McMurray, B. N. Greene, and S. R. Lipsky, ANAL. CHEM., **38**, 1194 (1966).

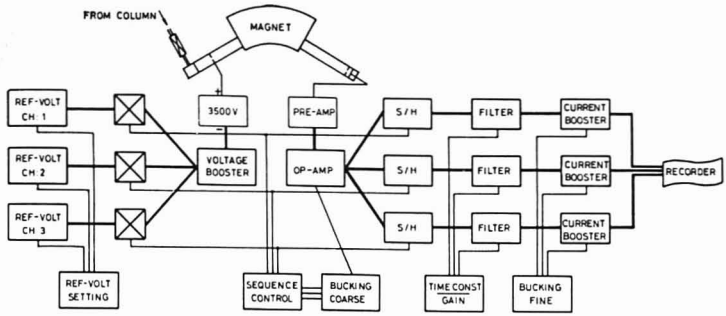

Figure 1A. Schematic diagram of the new multiple ion detector (MID)

RESULTS AND DISCUSSION

Principle and Description of the Multiple Ion Detector. The relationship $m/e = R^2H^2/2\ V$ (m = mass of the ion with the charge = e, usually $e = 1$; R = radius of the ion beam; H = magnetic field, and V = accelerating voltage) indicates that, if the magnetic field is kept constant, a decreased accelerating voltage will bring a higher mass into focus, and vice versa (*1*, *2*). A schematic diagram of the new multiple ion detector (MID) based upon this principle is shown in Figure 1*A*. Three different accelerating voltages can be applied, alternating between the three channels. This allows three different masses to be monitored continuously.

The basic accelerating voltage (V_o = 3500 volts) is unaltered while each channel, when in action, adds a certain, preset voltage (V_n) to provide the different accelerating voltages ($V_n + V_o \geq 3500$ volts). Between 0 and +700 volts of extra voltage can be added to each channel. This allows focusing upon masses which may differ by as much as 20% from each other (20% of the lower mass or 16.7% of the higher mass).

The sequence-control brings the channels into action by alternating sequentially between them. Each channel in turn is activated for 25 msec, resulting in a switching frequency of 40 Hz. This means that during these 25 msec the voltage of the channel (V_n) plus the basic accelerating voltage (V_o) act upon the ions formed in the ion source. Ions, whose mass is appropriate for this accelerating voltage and magnetic field, will hit the collector and give rise to signals.

Each channel has its own S/H circuit, bucking unit (coarse and fine), filters, and gain control. The connection of the coarse-bucking as well as the S/H circuit are timed by the sequence control to coincide with the addition of the voltage to the basic accelerating voltage. The bucking current is fed together with the signals to the S/H circuit, and from there through the selected filter (0.01, 0.1, 0.5, 1, 5, or 10 Hz) to still another amplifier with an adjustable gain (0 to 10 times). Finally, the signals are passed to the current booster. Here they can again be combined with an additional small positive or negative bucking current from the fine bucking unit before they reach the UV recorder and cause the galvanometer for the channel to be deflected.

When the sequence control switches to the second channel, the first and the third channel are disconnected, but the S/H circuits of these channels maintain the levels of the last signals and thus the same galvanometer deflections until the circuits receive new signals from the operational amplifiers. As each channel has its own galvanometer, the recorded curves, representing different masses, will be continuous and make the records easily interpretable.

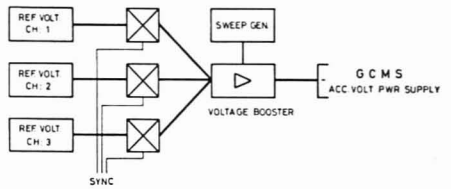

Figure 1B. Schematic diagram of how a sweep voltage generator converts the MID-accessory to a peak matcher device

Separate and Variable Amplification Systems for Each Channel. The usefulness of the tenfold amplification system can be illustrated by recording three different fragment ions, *e.g.*, m/e 204, 219, and 232, of trifluoroacetylated nortriptyline, 5-(γ-monomethylaminopropylidene)-5*H*-dibenzo[*a*,*d*] [1,4]-cycloheptadiene (NT-TFA). A plotted mass spectrum of NT-TFA is shown in Figure 2, upper panel.

If these masses are recorded with the same gain on each channel, the result shown in Figure 2, lower left panel, will be obtained. Mass number 204 is almost lost and its intensity cannot be amplified by increasing the multiplier voltage, without m/e 232 becoming too intense, and thus lost. If instead, the gain of each channel is adjusted to compensate for the differences in the intensities of these ions, the recording looks like that in Figure 2, lower right panel. The true relative intensities of these ions may be calculated from the gain settings. The application of variable amplification thus allows a more accurate determination of the ratios between the intensities or peak heights, of the selected mass numbers (compare the two figures). This allows compounds to be identified from the relative intensities of the chosen mass numbers, as well as from the retention time. By comparing these two figures, it is obvious that the adjustable gain controls create the possibility of a greater dynamic range of recording. Another aspect of the usefulness of separate gains is that if two compounds are present in an extract in quite different amounts, this difference can be compensated in the recording by using appropriate gain settings and thus allowing determination of both substances during the same analysis.

Bucking Unit. The bucking unit makes it possible to balance out the signals caused by column bleed and thus to

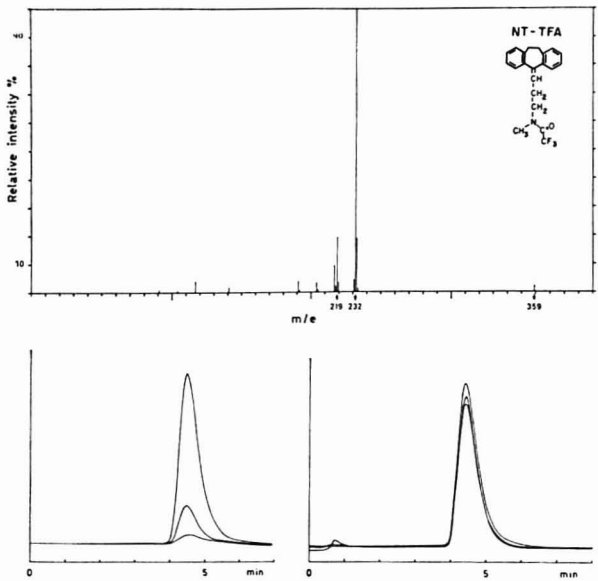

Figure 2. Upper panel. Mass spectrum of trifluoroacetylated nortriptyline (NT-TFA)

Lower panels. Ion specific recordings of 50 ng of trifluoroacetylated nortriptyline

GC conditions: coiled glass column, 1.1 m × 1.5 mm i.d., packed with 0.75% OV-17 on Chromosorb G (100–120 M). Column temperature: 220 °C. Carrier gas (He) flow: 20 ml/min. Paper speed: 2.5 cm/min. Focused mass numbers are 204, 219, and 232. Ionization energy: 18 eV. *y*-axes represent ion intensities

Lower left panel. Recording obtained with the same gain-setting on all channels. *m/e* 204 is the smallest peak and *m/e* 232 is the largest one

Lower right panel. Recording obtained with different gain-settings, *m/e* = 204–gain = 10; *m/e* = 219–gain = 2; and *m/e* 232–gain = 0.5

bring the base lines of the channels to the same level. This unit eliminates, under isothermal conditions, the potentially deleterious effect of column bleed upon sensitivity. As the masses, present in the column bleed, all the time will give rise to different base lines at different levels, they will also affect the dynamic recording range. Such a limitation becomes worse, if the gain sensitivity is increased. Without a bucking unit, the column bleed may even exclude certain mass numbers from study.

Filters. Electronic noise as well as other instabilities of not too low frequency may be efficiently removed by employing appropriate filters, and thus improving the signal to noise ratio. An efficient filtration of the signals is achieved by using sample-hold circuits and six different filter settings: 0.05, 0.1, 0.5, 1, 5, and 10 Hz. The filter requirement depends upon the expected rate of the galvanometer deflection.

Channel Identification. The recorded curves are identified by electronically generated spikes. Channel I has no marking, II has spikes upward, III has spikes downward. Spike frequencies can be generated at 2 Hz, 0.25 Hz, or 0.05 Hz to allow appropriate marking at different recording speeds.

Simultaneous Selective and Nonselective Ion Current Recording. The high switching frequency of the accelerating voltage allows the total ion current (TIC) to be recorded at the same time as the ion current of the selected mass numbers—a simultaneous nonselective and highly selective recording. Such a simultaneous recording (Figure 3) may, for example, help select TIC peaks which belong to a certain group of compounds, and mass spectra can then be obtained for the peaks of greatest interest.

Principles of Common and Novel Peak Matching Techniques. The common way of visualizing ions of a certain mass is to sweep the beam of the ion over the collector slit, while the change in the ion current is recorded on an oscilloscope screen. The distribution of the ions, as presented on the screen, will be a Gaussian-shaped curve. A small external, continuously variable magnetic field may be applied to produce this sweep of the ion beam.

In the usual technique of peak matching, the Gaussian curves representing the respective ions of the unknown and the known compound are superimposed on an oscilloscope screen by adjusting the accelerating voltage by means of a precision decade. This decade is calibrated to read the ratio (r) of the masses of the two ions. The setting of the decade, when both curves are superimposed, or "matched," is used to calculate the accurate value of the unknown mass according to:

$$r = \frac{M_{unknown}}{M_{known}} \text{ if } M_{unknown} > M_{known} \text{ (or vice versa), } r \text{ being}$$

always greater than 1.0 because of the design of the instruments. It is only the curve representing the higher mass which can be moved by changing the decade setting. This means that the position of the curve of the lower mass (adjustable with the magnetic field) is the reference point—the matching position. In this position the precision decade may be calibrated, *e.g.*, by using known substances. The accelerating voltage enters the expression for the mass ratio as follows:

$$r = \frac{V_{\text{nonred}}}{V_{\text{red}}} = \frac{M_{\text{high}}}{M_{\text{low}}}$$

but the value of the accelerating voltages need not be known.

Contrary to this method, our technique consists of sweeping the ion beam by continuously varying the accelerating voltage over a small range (Figure 1*B*) while recording each sweep cycle on paper. Knowing the exact value of the accelerating voltage at every point in the sweep cycle, the peak matching is done afterward from these permanent records. Several alternative matching positions can be chosen as each sweep cycle is recorded, and the results may be treated statistically. Either the sweep constant or the actual accelerating voltage at the selected matching position may be determined simultaneously with the mass of an unknown compound. The selected masses are recorded simultaneously during the sweep cycle, thus improving the accuracy of the mass determination.

Sweep Voltage and Determination of Sweep Constant, k. In this technique the accelerating voltage may be regarded as the sum of three different potentials: (1) the basic accelerating voltage (V_o = 3.5 kV) which is always kept unchanged; (2) the applied channel voltage (V_n) which is added to V_o to bring a certain mass into focus; V_n can be varied individually from 0 to +700 volts; and (3) the sweep voltage is a linear function of time and is thus a dynamic potential, in contrast to the above mentioned potentials which are fixed.

The sweep voltage starts at about +7 volts, passes zero volts and ends at about −7 volts. After the end point of the sweep is reached, the sweep starts automatically again. The sweep time is about 3 seconds. Neither the start nor the end points of the sweep must be known exactly. The linearity and the short-time reproducibility of the sweep are the important parameters. At the moment the linearity is not satisfactory. It is, however, possible to compensate partly for the nonlinearity in an empirical way and still perform accurate mass determinations. (We intend to make another sweep generator based upon other principles to eliminate the nonlinearity of the existing one and to achieve some other advantages which should lead to still better accuracy.) The reproducibility may vary slightly with changes in room temperature. However, this may easily be overcome by determining the sweep constant just before, or simultaneously with, the peak matching.

The voltage which is added to ($V_o + V_n$) at a certain moment by the sweep may be expressed by the sweep constant k (volts/sec) times the time-distance t (sec) measured from the zero-volt-point of the sweep. Thus, the active accelerating voltage (V_{act}) at any time during the sweep is given by the expression: $V_{\text{act}} = V_o + V_n \pm k \cdot t$. As the sweep goes from plus to minus, k becomes negative. By definition, t is negative before the zero-volt-point of the sweep and becomes positive after passing this point. The sweep adds to ($V_o + V_n$) positive voltages between the starting point and the zero point of the sweep [(−k)·(−t) = +k·t)] and negative voltages between the zero point to the end of the sweep [(−k)·(+t) = −$k \cdot t$)].

The sweep constant (k) is determined by focusing upon ions of an arbitrary mass. The ions may be molecular ions, fragments, or ions formed from the GC column bleed. The ions of the same mass are focused in the second channel but are brought slightly out of focus in the first and third channels.

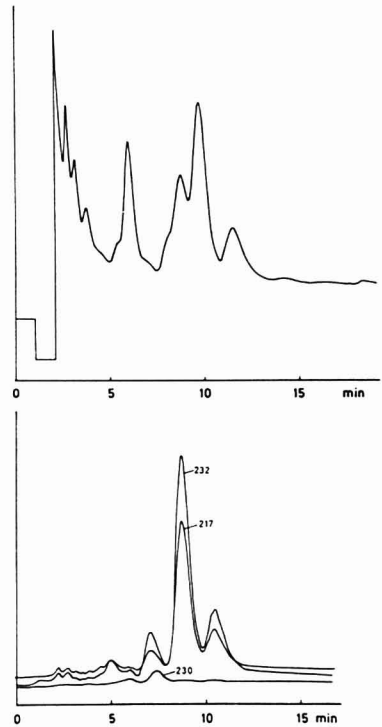

Figure 3. Simultaneous ion specific and total ion current recordings of an extract of urine from a patient receiving nortriptyline

Extract treated with trifluoroacetic anhydride. GC conditions as in Figure 2 except for lower column temp. Paper speed: 1 cm/min

Upper panel. Total ion current recording

Lower panel. Simultaneous recording of focused mass numbers 21, 230, and 232. Equal gain-settings on all channels. Ionization energy: 35 eV

This means that the applied voltage on the first channel is a few volts too high (V_1) and on the third one is a few volts too low (V_3) but correct for optimum focus (V_2) on the second channel. In symbols this can be written as ($V_o + V_1$) > ($V_o + V_2$) > ($V_o + V_3$).

The defocused ions are brought into focus by the sweep voltage, first on the third channel, last on the first one, as the sweep goes from plus to minus. At the midpoint, when the sweep voltage is zero, the focused ions will appear on channel two. In symbols this may be expressed as $V_{\text{act}} = V_o + V_3 + k \cdot t_3 = V_o + V_2 + 0 = V_o + V_1 - k \cdot t_1$.

The appearance of the ions on the different channels is recorded by means of a UV recorder. Such a recording is

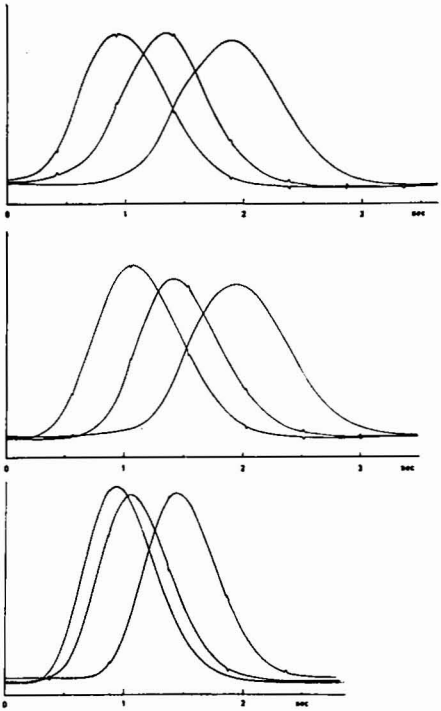

Figure 4. Recordings of single sweep cycles. The three peaks represent different molecular ions. The small spikes on two of the peaks are for channel identification. The *y*-axes represent ion intensities

Upper panel. The shoulder on the right-hand peak is from an unresolved compound and interferes with the interpretation of this record

Middle panel. The width of the right-hand peak also indicates interference

Lower panel. Suitable recording for peak matching. This record shows a higher resolution (narrower peaks) than the above panels, because of a narrower slit width. One of the compounds used above was replaced

shown in Figure 4. In spite of the switching of the accelerating voltage, the curves presented are continuous and smooth. This is achieved by using the sample-hold circuits and appropriate filters (f_o = 1 Hz). The recording goes from left to right, from positive to negative sweep voltage. The sweep of the ion beam over the collector slit is thus recorded as a Gaussian-shaped curve, where each increment of the curve corresponds to a certain accelerating voltage. Regarding the curve produced by one channel, there is only one part of its active accelerating voltage which is not constant—*vis.*, the applied sweep voltage.

The active accelerating voltage (V_{act}) at the center of the curve, the peak center, has to have exactly that value which is equal to the ratio of the strength of the applied magnetic field (H) and the accurate mass value (m) of the selected ions ($V_{act} = R^2H^2 \cdot e/2\,m$ where R = mean radius of the ion beam and e = charge of the ion, usually 1).

If the same mass is recorded on all three channels, as mentioned earlier, the distances between the peak centers have to be equivalent to the change of the sweep voltage, as well as to the differences in the applied voltages which are kept constant during the run. It is only V_{act} which is the same for all these channels according to the above mentioned equations.

As V_o (=3.5 kV) is constant and does not enter into the calculation of the sweep constant (k), we are for the moment not interested in its exact value. The only voltages we have to know are the applied ones, which are measured immediately after a run by means of a potentiometric microvoltmeter (Medistor) with an accuracy of about ±2–3 mV. Thus, the values of $V_1 > V_2 > V_3$ are known.

The calculations for finding the peak centers and the distances between them are done by measuring the peak width at approximately half the peak height, using an ordinary ruler. A point on the increasing part of the first, for example the peak shown on the left in Figure 4, lower panel, is chosen as the zero point of a coordinate system. From this point, the positions of the peak centers and the distances between them can be measured.

Usually, 10 to 12 successive runs or sweep cycles are recorded which takes about 30 seconds to perform. It is always the mean values of the distances between the peak centers which are used in the further calculations. The standard deviation is astonishingly small (about ±0.5 mm at a paper speed of 100 mm/sec,) particularly when taking into account the inaccurate measurements of the distances and that all instabilities of the entire system are included in this value.

When both the applied voltages and the distances between the corresponding peak centers are known, it is possible to determine the sweep constant, k, as the following relationship has to be valid:

$$k = \frac{V_1 - V_2}{c_1 - c_2} = \frac{V_1 - V_3}{c_1 - c_3} = \frac{V_2 - V_3}{c_2 - c_3}$$

where c_1, c_2, and c_3, respectively, are the positions of the peak centers in the arbitrarily chosen coordinate system. Thus, k will become negative and express volts/mm. Of course, the value of k is related to the paper speed used. We are using a paper speed of 100 mm/sec. From the relationship above, it is obvious that it is not necessary to utilize all three channels. Repeated determinations of k have given a value of 0.04664 volt/mm or approximately 47 mV/mm at an accelerating voltage of 3847(= $V_o + V_n$) volts. When this k value is used at other accelerating voltages, it has to be corrected to fit these potentials. This correction factor will be discussed in connection with the expression of the mass ratio as a function of the active accelerating voltages.

Selection of Matching Position. We have to define a position in the sweep at which we are going to match an unknown mass with a known. Three alternative definitions have been tested.

A. Matching position where the sweep voltage is zero: The reference mass is focused by the magnetic field when the sweep voltage is grounded and thus zero. At this position the active accelerating voltage is the sum of the basic accelerating voltage (V_o) and the applied voltage (V_n). The latter voltage has to be measured from one case to another, while the former has to be calculated prior to or simultaneously with the peak matching. In practice, difficulties were encountered in exact and thus reproducible focusing and with small variations in

V_o (estimated to some hundred millivolts) if this was determined beforehand.

B. In order to eliminate the focusing difficulties we introduced on one of the channels a very fast spike, generated and controlled by the sweep. This spike serves as indicator for the matching position which means that both the unknown and the reference peak have to be "moved" to this position in order to be matched. Even if the position of the spike is not at sweep zero, it is at a constant distance from zero. Thus the calculated V_o at this spike will become the sum of the basic accelerating voltage and a constant contribution of the sweep voltage, which value depends upon the spike's position within the sweep. The variations in V_o are, however, not eliminated.

C. Any peak related to a known mass anywhere in the sweep may serve as matching position if V_o (including the contribution of the sweep voltage at the selected position) can be determined by using two different reference substances together with the unknown. This is a way of including the variations in V_o in the calculations, as well as of avoiding the necessity of exact focusing. The disadvantage of this alternative may perhaps be the need of two different reference compounds with masses rather close to that of the unknown, and an increased risk of interference by the produced fragments.

When using alternative B, it is possible to check the sweep constant for each run but not V_o, which has to be assumed constant, while for alternative C, it is the reverse. Alternative A allows simultaneous determination of either k or V_o. This limitation can be eliminated by adding a fourth channel, which will allow a simultaneous determination of k, V_o, and the unknown mass.

Determination of the Basic Accelerating Voltage, V_o, at the Selected Matching Position. V_o at the chosen matching position is determined by matching two compounds with known masses. The sweep constant, k, is determined simultaneously with V_o, if V_o is determined prior to matching an unknown substance.

In this technique, the expression of the mass ratio as a function of the active accelerating voltages used to calculate V_o at the selected matching position, as well as the accurate mass of an unknown compound, is as follows:

$$\frac{m_1}{m_2} = \frac{V_o + V_2 \pm k \cdot d_2 \dfrac{V_o + V_k}{V_o + V_2}}{V_o + V_1 \pm k \cdot d_1 \dfrac{V_o + V_k}{V_o + V_1}}$$

V_1 and V_2 are the applied channel voltages. The matching factor, k times the distance, d, between the peak and the matching position, brings the respective peaks to superimpose each other at the selected matching position. V_k is the applied channel voltage used at the determination of k. The expression

$$\frac{V_o + V_k}{V_o + V_n}$$

is a correction factor for the matching factor, $k \cdot d$, to adapt it to the actual accelerating voltage ($V_o + V_n$). If the peak center of m_1 or m_2 represents the matching position, $k \cdot d_1$ and $k \cdot d_2$, respectively, becomes zero. As mentioned earlier, the sign is dependent upon the direction in which the peak has to be "moved." A peak appearing before the selected matching position has a lower static accelerating voltage than that at the matching position and vice versa as the sweep goes from plus to minus. The matching factor ($k \cdot d$) is thus positive before the matching position and negative after.

Peak Matching of Isolated Compounds. The m/e value of the molecular ion of the unknown compound to be matched is assumed to be known, *e.g.*, from a previously scanned mass spectrum. The reference should theoretically be chosen so that its molecular ion will be as close as possible to that of the unknown. In spite of this requirement, as illustrated in the example below, mass differences of 14 (amu), corresponding to about 6% of the whole mass, have been acceptable.

An example of the set-up procedure is as follows:

The matching position is chosen according to alternative C which means that a peak representing a known mass is selected. V_o has now to be determined at this position and, simultaneously, k can be determined. In order to simplify the procedure, the unknown together with the two references is introduced at the same time into the ion source by means of the direct inlet system. An appropriate voltage is applied to one of the channels (*e.g.*, No. 1) and the magnetic field is used to bring into focus the molecular ion of that reference substance which is going to serve as the matching compound. The same ions are slightly defocused in the second channel by applying a suboptimal accelerating voltage. This produces a recording which shows two separated peaks. This separation of peaks increases the accuracy with which the distance between the peak centers is measured. By means of a suboptimal voltage applied to the third channel, the molecular ions of the second reference are also slightly defocused, preferably on the same side of the matching position as the other defocused ions. This is done to decrease the influence of a nonlinear sweep.

After this focusing procedure, the switching between the three channels and the sweep are started. The reference peaks are then adjusted by means of the individual channel gains to give approximately the same height, after which the recording can be started. Immediately after a recording is finished, *e.g.*, 10–15 sweep cycles, the applied voltages are read by the potentiometric microvoltmeter (Medistor) with the sweep grounded. The distances between the peaks are then measured as described earlier.

The information obtained from the recording, together with the measured channel voltages and the known masses, allows determination of k (first and second channel) and V_o (first and third channel) for the peak produced by the first channel.

The peak matching of the unknown compound may now be performed by only applying the required voltage either on the second channel which allows simultaneous determination of V_o, or on the third channel which allows simultaneous determination of k. The applied channel voltage required to focus the molecular ion of the unknown by the second or third channel is estimated from the following expression:

$$V = \left(\frac{m_{\text{known}}}{m_{\text{unknown}}}\right)(V_o + V_1) - V_o$$

where m represents whole mass numbers and V_1 is the applied voltage on the first channel chosen for the matching position. This estimated voltage is sufficient to bring the unknown ion into focus by the sweep, as the sweep covers several volts. This approach is necessary when nonisolated compounds are to be peak matched during their elution from a GC column, as there is no time to adjust this voltage.

The accurate molecular weight of the unknown compound is calculated by means of the same formula used to calculate V_o (see above). It is just to substitute m_2 with m_x and the corresponding voltage (V_x) and peak distance (d_x).

Table I. Determination of Molecular Weights of Isolated Compounds

Correct molecular weights = 252.1626, 266.1783, and 280.1939

Calculated mass	Mass deviation	Error in ppm
252.1639	+0.0013	+5
252.1634	+0.0008	+3
252.1624	−0.0002	−0.9
252.1641	+0.0015	+6
252.1628	+0.0002	+0.7
252.1616	−0.0010	−4
252.1630	±0.0008	±3
266.1778	−0.0005	−2
266.1794	+0.0011	+4
266.1799	+0.0016	+6
266.1783	+0.00002	+0.08
266.1794	+0.0011	+4
266.1775	−0.0008	−3
266.1782	−0.0001	−0.45
266.1796	+0.0013	+5
266.1762	−0.0021	−8
266.1788	+0.0005	+2
266.1775	−0.0008	−3
266.1784	±0.0011	±4
280.1954	+0.0025	+9
280.1928	−0.0011	−4
280.1931	−0.0008	−3
280.1928	−0.0011	−4
280.1935	±0.0011	±4

About 20 test determinations of molecular weights have been performed using this technique, including the substances imipramine, 5-(γ-dimethylaminopropyl)-10,11-dihydro-5*H*-dibenz[*b*,*f*]azepine (M^+ = 280.1939), desmethylimipramine (M^+ = 266.1783) and didesmethylimipramine (M^+ = 252.1626). Most of these tests were done by using a previously determined V_o and simultaneously determining k and the unknown mass. The deviations from the true values varied from 0.08 ppm to about 10 ppm. The slit widths used varied between 0.01–0.08 mm (ion source) and 0.05–0.2 mm (collector) but these variations affected the accuracy of the mass determination very little. Generally, the static resolution (10% valley) was about 500–600, while the dynamic resolution obtained by this sweep voltage technique was about 70,000, or even more (depending upon the actual stability of the system). About 20% of the measurements had an error of 1 ppm and less but most were in the range 2 to 6 ppm.

The mean values of the calculated masses (Table I), obtained from runs at different occasions, deviate +1.6 ppm (n = 6), +0.4 ppm (n = 11), respectively, −1.4 ppm (n = 4) from the true ones. The same increase of the accuracy cannot be achieved by increasing the number of recorded sweep cycles because the errors in the measurements of the applied voltages will not cancel each other.

Peak Matching of a Compound, in Submicrogram Quantity during Its Elution from a GC Column. The setting of the applied voltage of the channel which will be used to record the unknown ion has to be calculated in advance. This, as well as the set-up procedure, is described above. After selection of an appropriate sensitivity (multiplier voltage), the column bleed is led into the ion source together with the reference(s), and each channel is balanced to the same base line while the accelerating voltage is switching and the sweep is in operation.

When the sample is injected into the GC column, the separation procedure may be followed in ordinary way by recording the so-called total ion current (TIC) even though the repetitive sweep is being applied. The accelerating voltage is not switched but is kept at the calculated and preset voltage, which will bring the ions of the unknown compound into focus with the aid of the sweep voltage. By watching the galvanometer deflection, the right moment is found to start switching the accelerating voltage and to begin recording from all three channels. To decide if it is the ions of the unknown compound which have been recorded, we have to rely upon the retention time determined from the TIC recording. It may very well happen that other compounds in a complex mixture give rise to the same mass number and thus will become recorded. This constitutes a limitation of this technique, when a low resolution machine is used, since interference may be expected if two compounds giving rise to the same mass number cannot be satisfactorily separated by the GC procedure. However, this may be overcome by changing GC conditions and derivative formation used. Whether interference exists or not may be observed by the shape of the ion peak (see "Sources of error" and Figure 4).

When testing this part of the peak matching technique we selected an unfavorable compound. This substance, nortriptyline, 5-(γ-monomethylaminopropylidene)-5*H*-dibenzo-[*a*,*d*][1,4]cycloheptadiene (NT), a secondary amine, has its molecular ion at mass number 263 with a relative intensity of about 0.4% (Figure 5). Nonderivatized NT chromatographs rather badly with a pronounced tailing under the conditions used. About 500 nanograms (5×10^{-7} g) of this substance were injected and nine measurable recordings of the sweep cycle were obtained. The parent ion of didesmethylimipramine, 252.1626, was used as reference. The width of the slits was 0.05 mm and 0.15 mm, respectively. The matching position was chosen according to alternative A. The calculations based upon these nine recordings, with varying ion intensities, gave a value of the molecular weight which differed 8 ppm from the exact one. Repetition of this test on different days gave deviations from the true value ranging from 2 to 10 ppm. By injecting greater amounts, a greater number of recordings of the sweep cycle could be measured and thus a slight increase in accuracy could be obtained.

The mean value calculated from eleven separate runs (Table II) differs from the true value only with 0.0001 amu equalling an error of +0.4 ppm.

Sources of Error. Instabilities in the basic accelerating voltage, the applied voltages, the sweep voltage, and the magnetic field, as well as the measurements of voltages and distances between the respective peak centers, are some of the sources of error. Mechanical vibrations of the analyzer tube including the collector slit and the ratio between the sampling time on each channel and the sweeping rate are other examples.

The requirements for stability, etc., may be illustrated by the following example. Three compounds, M^+ = 252, 266, and 280, respectively, were used. M^+ = 280 was assumed to be the unknown. By using the true mass values of M^+ = 252 and 266, V_o was calculated at a matching position equal to the peak center of M^+ = 266 (alternative C). A previously determined value of k was used and was assumed to be unchanged. Table III shows the measured values of the peak distances.

In the first column, 3 out of 12 values are outside the standard deviation, one (two stars) markedly, and in the second one 5 out of 12 values are outside, again one markedly. Using these mean values, the calculated mass of 280 differed 9 ppm from the true one. Instead of using the measured distance

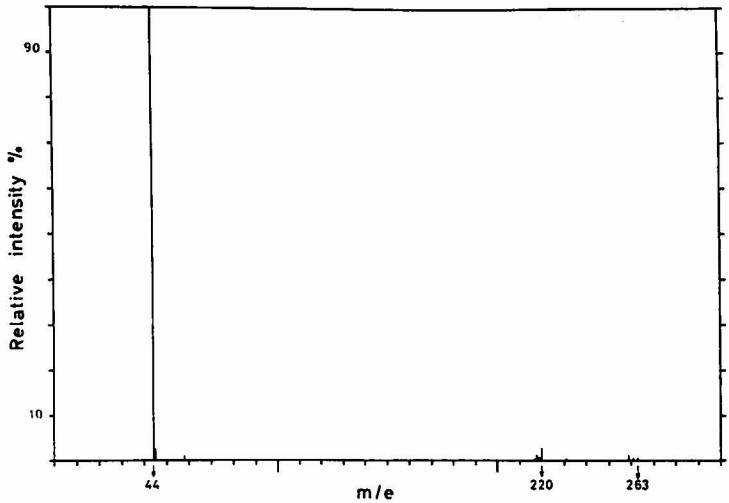

Figure 5. Normalized mass spectrum of nortriptyline. Molecular ion = 263 with a relative intensity of 0.4%

between the peak centers of 50.88 mm, this distance was reduced by the amount of the standard deviation to 50.0 mm and the calculation was repeated. The error in the mass determination now became 0.6 ppm. For the usual value of 0.047 volt/mm, 0.88 will correspond to 40 mV.

The sum of all errors, instabilities, readings of the applied voltages, distance measurements etc., if expressed in mV, may thus not exceed more than some 10 mV (compare this to *e.g.*, the voltages we are dealing with, 4 kV = 4.10^6 mV) in order to obtain a deviation of a few ppm from the true value of the mass.

Another source of error is the sampling time *vs.* the sweeping rate. The sampling time will be 25 msec, as the switching frequency is 40 Hz and during this time the sweep voltage will be changed about 120 mV, as k is roughly 47 mV/mm at paper speed 100 mm/sec. During these 25 msec the paper has moved 2.5 mm. This means that the sampling time of each channel is about five times longer than the estimated resolution on the paper, if this is expressed in msec.

The reason that, in spite of this, such good results can be achieved is because of the 1-Hz filters which are used. These filters smooth and idealize the curves. Theoretically, it would be desirable to have a sampling time which is at least equal to the resolution time, and an increased switching frequency.

Still another source of error may arise from a phase difference between the individual filters of each channel. These have to be matched as exactly as possible.

A serious source of error is the present lack of a linear sweep. This may, however, be partly overcome, *e.g.*, by focusing both the known mass (used to determine either k or V_o) and the unknown at the same side of the matching position. If then a second peak matching can be performed, the influence of the nonlinearity of the sweep can be diminished by using the values obtained from the first one to bring all peaks as close as possible to the matching position. On the other hand, this means that measuring the distance between the peak centers will become more difficult, and probably also less

Table II. Determination of Molecular Weight of Nonisolated Compound

(Molecular weights of NT (M^+ = 263.1674) obtained from eleven different injections of 0.5–0.8 μg of the substance)

Calculated mass	Mass deviation	Error in ppm
263.1652	−0.0022	−8
263.1654	−0.0020	−8
263.1686	+0.0012	+5
263.1679	+0.0005	+2
263.1647	−0.0027	−10
263.1689	+0.0015	+6
263.1694	+0.0020	+8
263.1690	+0.0016	+6
263.1682	+0.0008	+3
263.1660	−0.0014	−5
263.1692	+0.0018	+7
263.1675	±0.0017	±6.5 ppm

Table III. Distances in mm between M^+ = 280 and M^+ = 266, and M^+ = 252 Obtained from Twelve Successive Sweep Cycles

280/266	266/252
51.15	46.25
49.90*	46.40
50.90	45.65
50.20	46.20
50.80	45.45
51.70	45.45
51.60	44.05**
52.80**	44.85*
51.20	46.50
49.75*	46.70*
50.25	46.90*
50.30	44.85*
50.88 ± 0.88 mm	45.77 ± 0.87 mm

accurate. The results presented in this paper are all obtained by single peak matching.

Nonresolved peaks may be another source of error. As we are working usually with very low resolution, peaks from adjacent masses may very well interfere. The peak width and the peak shape may serve as indication of such interference as is shown in Figure 4.

Indications, that the errors in manually measured peak distances contribute very little to the overall error in mass determination, have been obtained by having a computer working "on-line" to perform these measurements. In spite of its better resolution (about 3 mV/unit) compared to that (about 47 mV/mm) obtained by using a ruler, the accuracy of mass determination was not improved.

The Potential Use of This Peak Matching Technique with High Resolution Instruments. As we do not have access to a double focusing mass spectrometer, we have not been able to test this technique with such an instrument, but we believe that it is possible to adapt this MID-PM accessory, in a modified form, to these types of machines. Quisenberry, Scolman, and Nier showed in 1956 (6) that, by keeping the ratio between the potential of the electrostatic analyzer (V_e) and the accelerating voltage (V_a) constant while these potentials were simultaneously changed between two different values, it was possible to compare two masses. The mass difference was deduced from the setting of that resistor which caused the change of the potential of the electrostatic analyzer. Instead of reducing the potentials, we should provide the electrostatic analyzer and the ion source with additional positive or negative voltages to bring the desired masses into focus. These voltages, including the sweep voltage, should be applied in a ratio equal to the optimum of V_e/V_a in order to maintain this ratio. This could be performed by means of a voltage divider placed between the device and the instrument. This divider could be made adjustable in order to be able to optimize the ratio. There is also the possibility of employing one device to regulate V_e and the high voltage part of a second device to regulate V_a. These two are synchronized by the sequence control (compare Figure 1A). As the potential of V_e is usually about a tenth of that of V_a, V_e becomes easier to accurately regulate and measure than V_a. This fact emphasizes the advantage of using the V_e voltages in the calculation of the mass as well as indicating a better accuracy of the mass determination than that obtainable by means of a low resolution machine using the accelerating voltages. In addition to this, there is the availability of high enough static resolution, offered by a double focusing instrument.

Possibilities of Performing Peak Matching by Aid of Computer. The way in which the signals, produced by the ions, are handled by this MID–PM accessory, as well as the peak matching technique itself, makes them well suited for further treatments by a computer. To be able to calculate the peak centers and the differences between them is mainly a question of software. It is also possible to use the computer to control the device, which then requires more sophisticated hardwares, and at the same time to take care of the signals produced. The computer can be programmed so that, upon order to focus certain mass numbers, the device will be provided with the required voltages. Information about the magnet setting, expressed in mass number at a given accelerating voltage, has of course to be given to the computer, which also will control the sweep voltage. The computer will thus be able to do the necessary calculations to control the whole system, and also to treat the data received and present them as the accurate mass of the unknown compound in a form of a mean value, calculated from the repetitive sweep cycles and with the standard deviation. A number of possible empirical formulas which are deduced from the obtained mean value and its standard deviation will also be shown. Elemental analyses will become possible to perform, within a minimum of time, by means of this peak matching technique and by aid of a computer.

(6) K. S. Quisenberry, T. T. Scolman, and A. O. Nier, *Phys. Rev.*, **102**, 1071 (1956).

ACKNOWLEDGMENT

This work could not have been done without the encouragement and support of Bo Holmstedt. We appreciate the freedom with which he entrusted us to pursue this work and his guidance regarding the application of these methods to medical problems.

RECEIVED for review June 8, 1970. Accepted December 1, 1970. This project has been supported by the Swedish Medical Research Council, Grant No. B70-40X-2629-01-02, and Riksbankens Jubileumsfond Grant No. 68/53 and Wallenberg Foundation.

Ion Specific Detection of Internal Standards Labelled with Stable Isotopes

Thomas E. Gaffney,[1] Carl-Gustaf Hammar,[2] Bo Holmstedt, and Robert E. McMahon[3]

Department of Toxicology, Swedish Medical Research Council, Karolinska Institutet, 104 01 Stockholm 60, Sweden, and The Lilly Reseach Laboratories, Indianapolis, Ind.

The purpose of an internal standard in quantitative analytical techniques is to permit the analyst to correct for losses of the compound under study. This requires chemical similarity between the internal standard and the compound in question. When conventional gas chromatographic detector systems are used, there must at the same time be sufficient dissimilarity so that the peaks from the compound and the standard can be resolved. However, in the study described in which the mass spectrometer is used as the detector for a gas chromatographic effluent, there is no need for any chemical differences, and mass differences alone are sufficient to discriminate between the compound being analyzed and the standard. This allows the use of the ideal internal standard, namely the actual compound under study modified to contain an increased mass by the introduction of stable isotopes. Examples of the use of ^{15}N and/or deuterium labelled compounds as internal standards are given.

THE TECHNIQUE in which a mass spectrometer is used as an ion-specific detector for a gas chromatographic effluent has been used for the qualitative identification of drugs and drug metabolites in biological fluids (*1*). The sensitivity, 10^{-12} gram, and ion-specificity of this technique and the need for sensitive, specific, and quantitative methods for studies in the biology and medical sciences have encouraged us to consider innovations which may help this technique serve in a quantitative as well as qualitative manner.

Since internal standards provide the greatest accuracy in quantitative gas chromatography, we have tested the use of isotopically labelled internal standards (stable isotopes). Our reasoning was that the best internal standard might be the actual molecule under study modified to contain an increased mass. For example, the substitution of ^{15}N for ^{14}N and/or deuterium for hydrogen in a molecule should not change its chemical characteristics but the increase in mass would allow the molecule to be easily distinguished from its nonisotopic counterpart.

We have studied two possible internal standards for nortriptyline (NT), *i.e.* deuterated nortriptyline (M + 2 AMU) and deuterated and ^{15}N labelled (M + 3 AMU) nortriptyline. An increase of two AMU enabled us to avoid interference from the natural ^{13}C present in the unlabelled NT. For comparison with isotopically labelled internal standards, we have used what has to date been our best unlabelled internal standard for NT, namely IBD 78.

[1] Present addresses, Division of Clinical Pharmacology, Departments of Pharmacology and Internal Medicine, University of Cincinnati, College of Medicine, Cincinnati, Ohio.

[2] Present address, Research Department of the KABI Group, S-104 25 Stockholm 30, Sweden.

[3] Present address, The Lilly Research Laboratories, Eli Lilly and Co., Indianapolis, Ind. 46206.

(1) C.-G. Hammar, B. Holmstedt, and R. Ryhage, *Anal. Biochem.*, 25, 532 (1968).

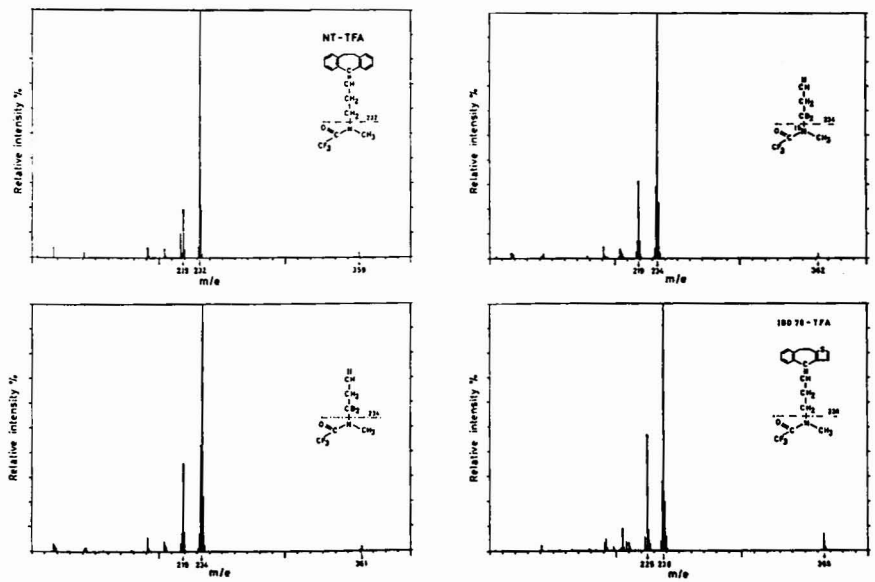

Figure 1. Mass spectra of nortriptyline-trifluoroacetylated (NT-TFA) deuterated, ^{15}N-labelled NT-TFA and IBD-18-TFA

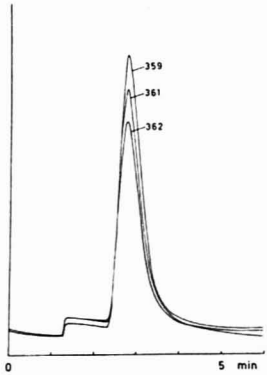

Figure 2. Recording of the molecular ions of nortriptyline – trifluoroacetylated (NT-TFA), M 359, doubly-deuterated NT-TFA, M 361, and deuterated and ^{15}N-labelled NT-TFA, *M* 362

Two-hundred nanograms of each compound were injected at zero time

EXPERIMENTAL

Materials and Methods. The study was performed using the basic technique originally described by Hammar, Holmstedt, and Ryhage (*1*). The actual recordings were made, however, using the recently developed Multiple Ion Detector Accessory (MID) described by Hammar and Hessling (*2*).

(2) C.-G. Hammar and R. Hessling, ANAL. CHEM., **43**, 298 (1971).

The focusing of individual channels of single ions was achieved by first focusing with the manual magnetic field control on a reference ion introduced *via* the direct inlet probe. The remaining ions were then brought into focus on the other channels by the addition or subtraction of accelerating voltages while the magnetic field was held constant. The accuracy of focusing was confirmed during the elution of the compounds from the column.

An all glass chromatographic column was used containing 0.5% XE 60 and 0.25% DC LSX on silanized Chromosorb G; the internal diameter was 1.5 mm and the length about 1.2 meters. The flash heater and column were held at 220 and 190 °C, respectively. Helium flow was about 20 ml/minute.

Conditions included an ion source temperature of 310 °C and a separator temperature of 250 °C. All recordings were made at an ionization energy of 20 electron volts.

Chemicals Used. NT was obtained as the hydrochloride salt from the Lilly Company, U.S.A. Deuterium and ^{15}N labelled NT were synthesized and provided as the hydrochloride salts by Dr. Fred Marshall and Dr. Bill Lacefiled of the Lilly Research Laboratories, Indianapolis, Ind. The side-chains were labeled as $-CHCH_2CD_2NHCH_3$, (the M + 2 compound) and $=CHCH_2CH_2{}^{15}NHCH_3$ (the M + 3 compound). IBD 78, whose formula is shown in Figure 1, was provided by Sandoz Laboratories in Switzerland. Derivatives were prepared with trifluoroacetic anhydride as the reagent and dimethylformamide as the catalyst.

RESULTS AND DISCUSSION

Mass spectra confirmed the chemical identity, Figure 1, of each compound studied. The simultaneous but easily resolved elution of an equimolar mixture of the nortriptylines,

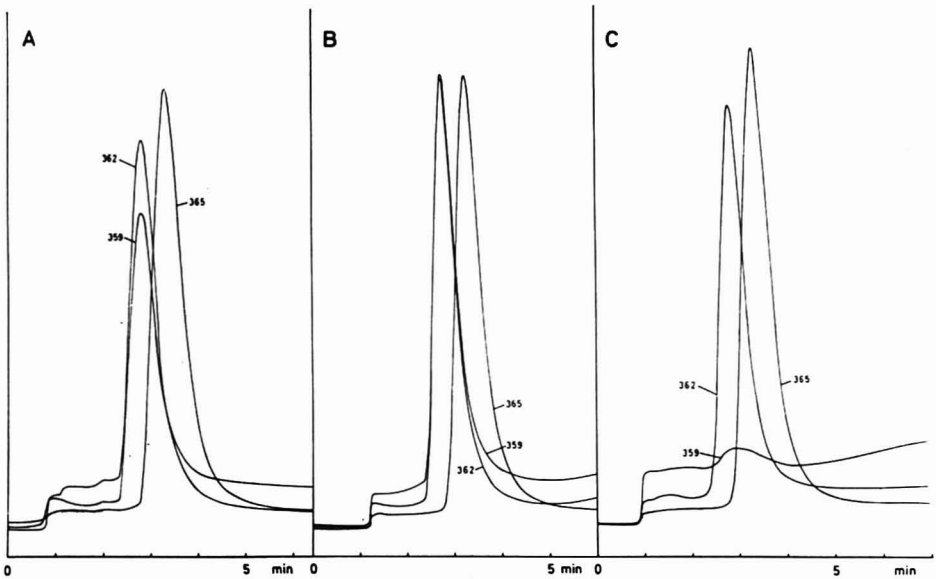

Figure 3. Recordings of M 359, M 362, and IBD-18-TFA, M 365

Two-hundred nanograms of specified compounds were injected at zero time. All three compounds were injected in 3 *A* and 3 *B*, but M 359, NT-TFA, was omitted from the injection shown in 3 *C*. The capacity of individual channel amplication systems to normalize peak heights is shown by a comparison of 3 *A* and 3 *B*. The specificity of the technique is emphasized by comparison of 3 *A* with 3 *C*

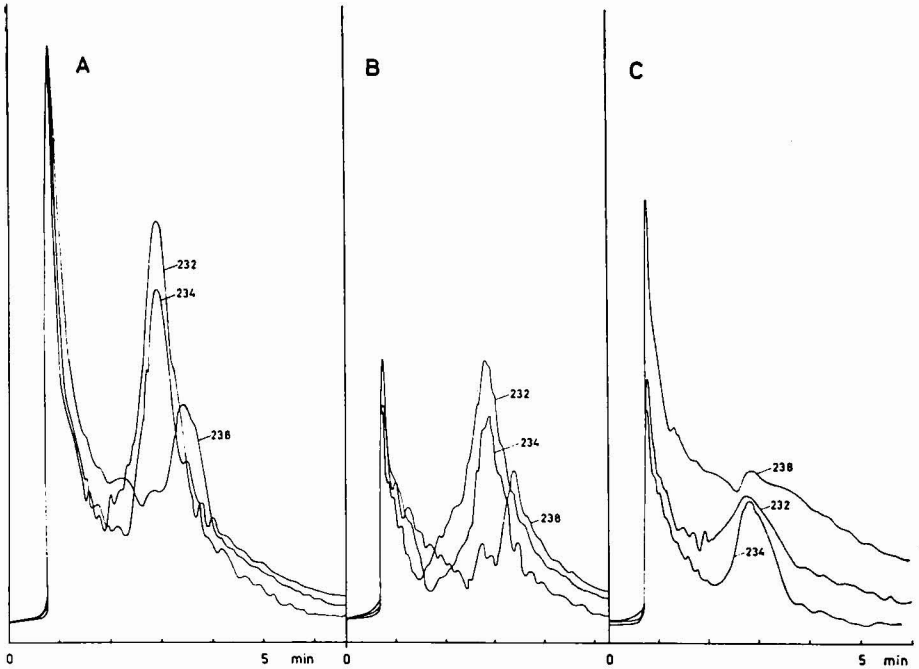

Figure 4. Base peak fragmentograms of 100 picograms (*A*) and 50 picograms (*B*) of NT-TFA, M-232, deuterated NT-TFA, M 234, and IBD 18, M 238

Minimal disorption produced by the injection of solvent is shown in panel *C*. Notice the reduced signals from IBD 18-TFA compared to that produced by the same concentrations of the nortriptylines, M 232 and M 234

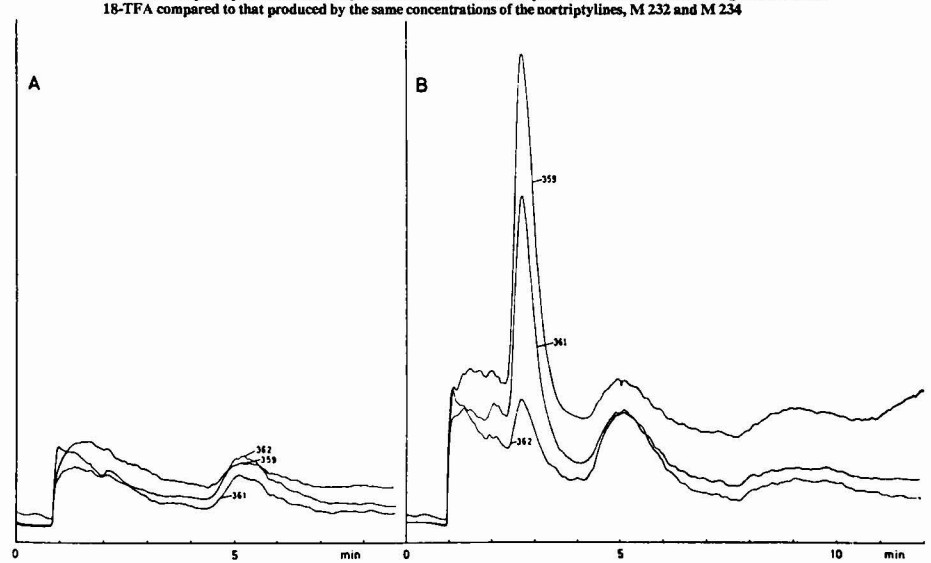

Figure 5. Mass fragmentograms of trifluoroacetylated extracts of human plasma without (*A*) and with (*B*) NT, M 359, and its deuterated counterpart M 361. Injection is marked as zero time

i.e. M, M+2 and M+3, is shown in Figures 2 and 3. The elution characteristics of the three molecular ions emphasize the chemical similarity between NT and its labelled counterparts, either one of which could function as an internal standard for NT. The impressive resolving power of the technique as compared to the more commonly used chromatographic detection systems is also evident. The chromatographic characteristics of IBD 78 as compared to NT and M+3 is also shown in Figure 3. IBD 78 has different chromatographic characteristics.

Performance of Internal Standards Near the Limits of Sensitivity. It is apparent that the use of the base peak offers the highest sensitivity. For example, the elution of 100 and even 50 picograms of NT-TFA is easily distinguished as the base peak from the same concentrations of its isotopically labelled counterpart, Figure 4. Even at this concentration, the chromatographic characteristics of NT-TFA and M+2 are indistinguishable. In contrast, 100 and 50 picograms of IBD 78-TFA produce much lower signals than the same concentrations of NT-TFA or M+2. This difference between IBD 78-TFA and the nortriptylines suggest that more IBD 78-TFA is lost by column absorption.

Such a difference in column absorption between a compound and the substance serving as its internal standard is only one example of how the measured recovery of most internal standards probably does not reflect the recovery of the compound under study. In the example shown in Figure 4, the differential loss of IBD 78-TFA over NT-TFA would result in an overestimation of the concentration of NT that is present.

Drugs and Internal Standards in Biological Materials. Biological samples present problems in that they must be shown to be free of the substance or in this case, the mass which is chosen as the "marker" for the internal standard.

Figure 5 shows a study of plasma before and after the addition of NT and a possible internal standard—*i.e.*, M+3. The plasma is first shown to be free of NT and M+3, and other substances with comparable retention times containing the same masses. Figure 5, *A* and *B* demonstrate the elution and resolution of the two substances after their addition to the plasma. Notice that even though the background recorded from plasma (Figure 5) is greater than is seen with the injection of methanolic solutions of reference material (Figures 2–4), the quality of the resolution of the two nortriptylines is adequate. Notice that had IBD 78-TFA been used as the internal standard for this plasma sample, the broad peaks present in the plasma extract, which represent the same masses as are found in IBD 78-TFA, could have interfered with the resolution of IBD-78-TFA. This example of the potential interference by non-drug substances in biological samples emphasize the usefulness of internal standards which have a retention time identical to the substance under study.

RECEIVED for review June 8, 1970. Accepted December 1, 1970. This research was supported by the Clinical Pharmacology Fund of Cincinnati, Ohio, NIH-USPHS Grants HE 07392, GM13 978, NIH3RoI MH, 12007-03Sl, and by a grant from the Wallenberg Foundation and Riksbankens Jubileumsfoud, Stockholm, Sweden, Swedish Medical Research Council No. B70-40X-2629-01-02.

Multivariable Analysis of Quantitative X-Ray Emission Data

The System Zirconium Oxide–Aluminum Oxide–Silicon Oxide–Calcium Oxide–Cerium Oxide

Donald A. Stephenson

Research and Development Laboratories, Corning Glass Works, Corning, N. Y. 14830

Guidelines for the correct use of statistical methods for quantitative X-ray emission analysis of multicomponent systems are set forth, and a general review and discussion of the technique is presented. The regression model first proposed by Alley and Myers is the only model, among many, that seems both physically and statistically adequate for general application, and its use is recommended before more elaborate models are tried. A new procedure for the selection of synthetic reference standards covering any region of interest in any *n*-component system in a homogeneous fashion is described and applied to the standardization of part of the system ZrO_2 (35–85 wt %)-Al_2O_3 (5–55 wt %)-SiO_2 (1–10 wt %)-CaO (5–15 wt %)-CeO_2 (5–15 wt %). The residual error in the prediction of the composition of the synthetic standards is around 1 to 2% relative, which compares favorably with other methods of analysis.

THE MATHEMATICAL INTERPRETATION of quantitative X-ray emission data has steadily gained popularity during the last decade. The spate of activity in this area is due largely to the widespread availability of large-scale computing facilities necessary to perform the complex calculations associated with various techniques for treating the data. Numerous authors have proposed equations that relate the concentration of a particular component in an unknown sample to the observed intensity of characteristic X-rays of that and/or other components through coefficients obtained from known standards by either regression analysis—Lucas-Tooth and Price (*1*), Sugimoto (*2*, *3*), Lamborn and Sorenson (*4*), Lucas-Tooth and Pyne (*5*), Alley and Myers (*6*, *7*), Miller and Galletta (*8*),

(1) H. J. Lucas-Tooth and B. J. Price, *Metallurgia*, **64**, 149 (1961).
(2) M. Sugimoto, *Bunseki-Kagaku*, **11**, 1168 (1962).
(3) *Ibid.*, **12**, 475 (1963).
(4) R. E. Lamborn and F. J. Sorenson, *Adcan. X-Ray Anal.*, **6**, 422 (1963).
(5) H. J. Lucas-Tooth and C. Pyne, *ibid.*, **7**, 523 (1964).
(6) B. J. Alley and R. H. Myers, ANAL. CHEM., **37**, 1685 (1965).
(7) B. J. Alley and R. H. Myers, *Norelco Rep.*, XV, 87 (1968).
(8) L. D. Miller and F. A. Galletta, "Application of Computer Techniques in the X-Ray Fluorescence Analysis of Iron Ore Sinters," Denver Conference on the Applications of X-Ray Analysis, Denver, Colo., 1967.

Mitchell (*9*)—or the solution of simultaneous equations—Beattie and Brissey (*10*), Criss and Birks (*11*). While all these equations probably apply well enough to narrow ranges of compositional variation encountered in such areas as quality control or the routine analysis of very similar samples, only the method outlined by Alley and Myers (*6, 7*) is sufficiently general to reliably include very large compositional variation.

The aim of this paper is to demonstrate that the methods proposed by Alley and Myers are indeed physically and statistically applicable to a general n-component system, to simplify the procedure for selecting reference standards, and to demonstrate the optimization of the regression equations relating the concentrations of individual components to observed X-ray intensities.

EXPERIMENTAL

The General Regression Equation. First consider any general binary system A–B. The observed relative intensity of characteristic X-rays from component A, as A varies from 0 to 100%, can generate a curve of three possible types (Figure 1), depending upon whether A X-rays are unaffected, absorbed, or enhanced by the presence of B.

Any ternary, quaternary, or higher-component system will always have bounding intensity *vs.* composition curves similar to one of the three possibilities. These binary curves extend into the n-component system as n-dimensional surfaces that are continuous. As such, they may be represented by an analytic function of either concentrations or intensities, *viz.*,

$$Y_i = f(X_i), \qquad i = 1,n \tag{1}$$

where the Y_i and X_i may be either concentrations or intensities of the individual components. Since the bounding binary curves are of a simple nature, easily expressed by second degree polynomials of the general form

$$Y_i = \alpha_0 + \alpha_1 X_1 + \alpha_2 X_2 + \alpha_3 X_1^2 + \alpha_4 X_2^2 + \alpha_5 X_1 X_2 \tag{2}$$

a linear combination of n such equations to form an n-dimensional surface should also be expressible by an equation of the second degree, thus

$$Y_i = \alpha_0 + \sum_{i=1}^{n} \alpha_i X_i + \sum_{i=1}^{n} \alpha_{ii} X_i^2 + \sum_{\substack{i=1 \\ i<j\leq n}}^{n-1} \alpha_{ij} X_i X_j \tag{3}$$

By determining the coefficients α, the n-dimensional intensity *vs.* composition surface may be specified for each component. To apply conventional regression analysis to Equation 3 in hopes of predicting the concentrations of the individual components from a knowledge of measured X-ray intensities of unknowns, the X_i are required to be known concentrations and the Y_i measured X-ray intensities. Furthermore, in the absence of replication, any error is assumed to fall upon the dependent variate Y_i and be symmetrically and independently distributed. Clearly, there are errors associated with the X_i, since no chemical analysis is perfect nor can the preparation of synthetic reference standards be perfect. The error associated with obtaining X-ray intensities is quasi-normal for high count rates, because Poisson counting statistics approach the normal distribution. Strictly speaking, the application of conventional regression techniques to this problem is mathematically invalid. Advanced statistical methods have been developed for treating the case where all variates carry errors that are symmetrically and independently distributed and can be assigned a probability density function—Hey (*12*), Smith, Stephenson, Howie, and Hey (*13*). Even if all the sources of random and systematic error could be estimated, the procedures involved in the correct statistical treatment of the data probably offer no substantial improvement in the accuracy in which the concentrations of the individual components may be estimated, so for practical purposes the regression equation of choice becomes

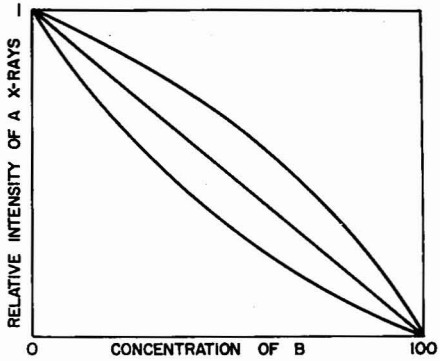

Figure 1. Illustration of possible variation of X-ray intensity observed from component A in a hypothetical binary system A–B

Top curve represents enhancement by component B, middle curve shows no effect by the addition of B, and bottom curve indicates absorption of A X-rays by B

$$\hat{Y}_i = \hat{\alpha}_0 + \sum_{i=1}^{n} \hat{\alpha}_i X_i + \sum_{i=1}^{n} \hat{\alpha}_{ii} X_i^2 + \sum_{\substack{i=1 \\ i<j\leq n}}^{n-1} \hat{\alpha}_{ij} X_i X_j + \epsilon_i \tag{4}$$

The fact that the concentrations are subject to the constraint

$$\sum_{i=1}^{n} X_i = 1 \tag{5}$$

leads to a simplification of Equation 3, whereby fewer coefficients α are required to specify the Y_i. This will be shown for the ternary case.

It follows from Equation 5 that

$$\alpha_0(X_1 + X_2 + X_3) = \alpha_0 = \alpha_0 X_1 + \alpha_0 X_2 + \alpha_0 X_3 \tag{6}$$

Substituting 6 into 3 gives

$$Y_i = (\alpha_0 + \alpha_1)X_1 + (\alpha_0 + \alpha_2)X_2 + (\alpha_0 + \alpha_3)X_3 + (\alpha_{12}X_1X_2) + (\alpha_{13}X_1X_3) + (\alpha_{23}X_2X_3) + \alpha_{11}X_1^2 + \alpha_{22}X_2^2 + \alpha_{33}X_3^2 \tag{7}$$

Equation 5 can be multiplied by X_1, X_2, and X_3 in turn to give

$$X_1^2 = X_1 - X_1X_2 - X_1X_3 \tag{8a}$$

$$X_2^2 = X_2 - X_1X_2 - X_2X_3 \tag{8b}$$

$$X_3^2 = X_3 - X_1X_3 - X_2X_3 \tag{8c}$$

(9) B. J. Mitchell, *Advan. X-Ray Anal.*, **11**, 129 (1968).
(10) H. J. Beattie and R. M. Brissey, ANAL. CHEM., **26**, 981 (1954).
(11) J. W. Criss and L. S. Birks, *ibid.*, **40**, 1080 (1968).
(12) M. H. Hey, *Mineral. Mag.*, **37**, 83 (1969).
(13) J. V. Smith, D. A. Stephenson, R. A. Howie, and M. H. Hey, *ibid.*, p 90.

Substituting these into 7 results in

$$Y_i = (\alpha_0 + \alpha_1 + \alpha_{11})X_1 + (\alpha_0 + \alpha_2 + \alpha_{22})X_2 + (\alpha_0 + \alpha_3 + \alpha_{33})X_3 + (\alpha_{12} - \alpha_{11} - \alpha_{22})X_1X_2 + (\alpha_{13} - \alpha_{11} - \alpha_{33})X_1X_3 + (\alpha_{23} - \alpha_{22} - \alpha_{33})X_2X_3 \quad (9)$$

and letting $\alpha_0 + \alpha_1 + \alpha_{11} = \beta_1$, etc., we arrive at

$$Y_i = \beta_1X_1 + \beta_2X_2 + \beta_3X_3 + \beta_4X_1X_2 + \beta_5X_1X_3 + \beta_6X_2X_3 \quad (10)$$

Or for the general n-component system

$$Y_i = \sum_{i=1}^{n} \beta_iX_i + \sum_{\substack{i=1 \\ i<j\leq n}}^{n-1} \beta_{ij}X_iX_j \quad (11)$$

This is Scheffe's (*14*) "canonical" polynomial for second-degree equations. Hence, only $(n + n^2)/2$ coefficients need to be determined to completely specify an n-dimensional intensity *vs.* composition surface.

The problem that now arises is that the n equations relating intensities to concentrations cannot be inverted for the estimation of the concentrations since the matrix of coefficients is not square, and in addition a singular linear relation (Equation 1) exists between the independent variates so that no conventional regression analysis program is competent to handle the inversion of the full general model given in Equation 11. Consequently, there is no alternative except changing the roles of the Y_i and X_i to arrive at the preliminary model of the intensity *vs.* composition surface. This now forces all error upon the concentrations of the individual components of the standards. To ensure that the sum of the observed X-ray intensities for each reference standard is as near 1.0 as possible (so that the arguments given by Equations 5 through 11 also *on the average* apply to intensities), the observed number of X-ray counts from each component should be divided by the number of counts obtained from end-member (pure oxide) primary reference standards. This, or some similar procedure, is normally done anyway to eliminate instrumental drift. Changing notation now, the preliminary regression model is

$$\hat{C}_i = \sum_{i=1}^{n} \hat{\beta}_iI_i + \sum_{\substack{i=1 \\ i<j\leq n}}^{n-1} \hat{\beta}_{ij}I_iI_j + \epsilon_i \quad (12)$$

where $\hat{C}$ stands for the estimated weight fraction of the ith component, I_i is the observed X-ray intensity of the ith component relative to the pure end-member, and the $\hat{\beta}$ are regression coefficients to be estimated by ordinary least-squares techniques. Equation 12 was first proposed by Alley and Myers (*7*).

Selection of Reference Standards. Womeldorph (*15*) and Alley and Myers (*7*) introduced the concept of simplex lattices to the field of X-ray emission spectrometry to simplify solving for the coefficients of Equation 11 and to rigorously test the applicability of the model. Further references to simplex lattices are given by Thompson and Myers (*16*). When Equation 12 is used to estimate concentrations directly from intensities, the rigid requirements on the selection of reference standards on a simplex lattice need no longer apply. What is now required is the selection of an adequate number of standards, hopefully covering the compositional region of interest in some homogeneous fashion. For limited ranges of variation—say no more than 10 to 20% relative—a representative selection of standards around twice the number required is usually sufficient to obtain good estimates of the coefficients. Wide compositional variation in multicomponent systems poses problems if only chemically analyzed reference standards are available, in that it may become rather difficult to secure standards covering the required range of variation, and, even if a good selection of standards were available, it is difficult to avoid clustering them in one or more subregions within the main region of interest. To aid in the preparation of synthetic standards that cover the region of interest in a systematic manner, a Fortran computer program, NPOINTS (*17*), was written. The program calculates the composition of a specified number of points to be distributed on an n-dimensional hypercubic lattice bound by selectable upper and lower limits on the end-member components. The constraints imposed by the use of simplex lattices with pseudocomponent end-members are thereby eliminated and homogeneity of points in the composition space of interest is ensured.

Table I. Ranges of Variation of End-Member Components in Weight Fraction

Component	Range of variation in weight fraction: Required range	Range for NPOINTS[a]
ZrO_2	0.35–0.85	0.30–1.00
Al_2O_3	0.05–0.55	0.00–0.65
SiO_2	0.01–0.10	0.00–0.20
CaO	0.05–0.15	0.00–0.15
CeO_2	0.05–0.15	0.00–0.20

[a] Since NPOINTS places all calculated points within the specified range required, limits of variation frequently need to be widened to obtain the necessary spread.

In this investigation, a region of the five-component system ZrO_2–Al_2O_3–SiO_2–CaO–CeO_2 was standardized so that Equation 12 could be used to predict the composition of unknowns. The minimum number of standards required is 15. Increasing the number of standards by a factor of two or three enhances the least-squares estimation of the coefficients, permits easy identification of outliers, and the chances of obtaining an artifically good fit to the data are reduced. Utilizing only as many standards as coefficients to be determined is especially dangerous when simultaneous equation techniques are used. Table I shows the ranges of end-member variation over which standardization was required, and Table II lists the calculated composition of the hypercubic points in composition space. Thirty-six standards, roughly two and a half times the minimum, were called for in the standardization procedure.

Preparation and Measurement of the Standards. The first postulate for the successful implementation of Equation 12 is that both standards and unknowns be physically and chemically homogeneous. There are many ways to achieve this, *i.e.*, fine grinding and briquetting, solution techniques, preparation of thin films, etc. The technique of choice here is flux-fusion as outlined by Stephenson (*18*). A total of 2.0 grams of each of the standards listed in Table II was prepared by weighing the requisite amount of reagent grade ZrO_2, Al_2O_3, SiO_2, $CaCO_3$, and CeO_2. The mixtures were ground in a tungsten carbide mill for 10 minutes to provide thorough mixing. Three-tenths gram of each standard was then blended with 2.7 grams of Stephenson's flux A (90 wt % $Li_2B_4O_7$, 10 wt % Li_2CO_3) and melted in graphite crucibles at 1100 °C for a total of 15 minutes with constant agitation. The resulting glass disks were then ground and polished on diamond-embedded wheels to assure a flat, scratch-free surface for presentation to the X-ray spectrometer. A Phillips Uni-

(14) H. Scheffe, *J. Roy. Statistical Soc., Series B*, **20**, 344 (1958).
(15) D. E. Womeldorph, Jr., "Estimation in the Use of X-Ray Fluorescence Method and Use of Reference Components in Mixture Experimental Designs," Doctorate Thesis, Virginia Polytechnic Institute, Blacksburg, Va., 1966.
(16) W. O. Thompson and R. H. Myers, *Technometrics*, **10**, 739 (1968).
(17) W. M. Buehl and D. A. Stephenson, unpublished data, 1970.
(18) D. A. Stephenson, ANAL. CHEM., **41**, 9661 (1969).

Table II. Composition of Thirty-Six Standards Calculated by NPOINTS

Standard	ZrO_2	Al_2O_3	SiO_2	CaO	CeO_2
1	0.3493	0.4436	0.1085	0.0493	0.0493
2	0.3493	0.5422	0.0099	0.0493	0.0493
3	0.3493	0.3450	0.1085	0.0493	0.1479
4	0.3493	0.4436	0.0099	0.0493	0.1479
5	0.3493	0.3450	0.1085	0.1479	0.0493
6	0.3493	0.4436	0.0099	0.1479	0.0493
7	0.3493	0.2464	0.1085	0.1479	0.1479
8	0.3493	0.3450	0.0099	0.1479	0.1479
9	0.4479	0.3450	0.1085	0.0493	0.0493
10	0.4479	0.4436	0.0099	0.0493	0.0493
11	0.4479	0.2464	0.1085	0.0493	0.1479
12	0.4479	0.3450	0.0099	0.0493	0.1479
13	0.4479	0.2464	0.1085	0.1479	0.0493
14	0.4479	0.3450	0.0099	0.1479	0.0493
15	0.4479	0.1479	0.1085	0.1479	0.1479
16	0.4479	0.2464	0.0099	0.1479	0.1479
17	0.5464	0.2464	0.1085	0.0493	0.0493
18	0.5464	0.3450	0.0099	0.0493	0.0493
19	0.5464	0.1479	0.1085	0.0493	0.1479
20	0.5464	0.2464	0.0099	0.0493	0.1479
21	0.5464	0.1479	0.1085	0.1479	0.0493
22	0.5464	0.2464	0.0099	0.1479	0.0493
23	0.5464	0.0493	0.1085	0.1479	0.1479
24	0.5464	0.1479	0.0099	0.1479	0.1479
25	0.6450	0.1479	0.1085	0.0493	0.0493
26	0.6450	0.2464	0.0099	0.0493	0.0493
27	0.6450	0.0493	0.1085	0.0493	0.1479
28	0.6450	0.1479	0.0099	0.0493	0.1479
29	0.6450	0.0493	0.1085	0.1479	0.0493
30	0.6450	0.1479	0.0099	0.1479	0.0493
31	0.6450	0.0493	0.0099	0.1479	0.1479
32	0.7432	0.0493	0.1085	0.0493	0.0493
33	0.7436	0.1479	0.0099	0.0493	0.0493
34	0.7436	0.0493	0.0099	0.0493	0.1479
35	0.7436	0.0493	0.0099	0.1479	0.0493
36	0.8422	0.0493	0.0099	0.0493	0.0493

Table III. Observed Relative Intensities of the X-Ray Emission Lines

Standard	I_{Zr}	I_{Al}	I_{Si}	I_{Ca}	I_{Ce}
1	0.3206	0.4401	0.1072	0.1013	0.1208
2	0.3217	0.5334	0.0195	0.1001	0.1178
3	0.3137	0.3226	0.0975	0.0988	0.3221
4	0.3194	0.4135	0.0172	0.1020	0.3311
5	0.3010	0.3224	0.1022	0.2822	0.1091
6	0.3065	0.4001	0.0139	0.2851	0.1068
7	0.3040	0.2300	0.1030	0.2800	0.3000
8	0.3006	0.3165	0.0183	0.2757	0.2930
9	0.4060	0.3334	0.1009	0.0957	0.1130
10	0.4159	0.4334	0.0149	0.0984	0.1163
11	0.4146	0.2306	0.1027	0.0976	0.3160
12	0.4012	0.3329	0.0165	0.0958	0.3157
13	0.3879	0.2347	0.1018	0.2782	0.1057
14	0.3901	0.3218	0.0199	0.2751	0.1030
15	0.3828	0.1364	0.1044	0.2681	0.2849
16	0.4014	0.2187	0.0135	0.2769	0.2932
17	0.5136	0.2421	0.1081	0.0942	0.1102
18	0.4942	0.3349	0.0176	0.0924	0.1085
19	0.5103	0.1455	0.1011	0.0937	0.3051
20	0.5003	0.2342	0.0183	0.0928	0.3023
21	0.4775	0.1389	0.1015	0.2584	0.0985
22	0.4895	0.2416	0.0157	0.2668	0.1014
23	0.4746	0.0473	0.0976	0.2570	0.2720
24	0.4902	0.1324	0.0162	0.2544	0.2737
25	0.6124	0.1506	0.1136	0.0895	0.1072
26	0.6047	0.2479	0.0196	0.0905	0.1050
27	0.6062	0.0483	0.1050	0.0867	0.2802
28	0.6158	0.1422	0.0150	0.0900	0.2926
29	0.5838	0.0500	0.1067	0.2560	0.0971
30	0.5719	0.1354	0.0173	0.2520	0.0964
31	0.5875	0.0489	0.0154	0.2540	0.2740
32	0.7110	0.0544	0.1100	0.0874	0.1022
33	0.7054	0.1445	0.0178	0.0868	0.1016
34	0.7147	0.0499	0.0163	0.0885	0.2853
35	0.6877	0.0521	0.0204	0.2499	0.0974
36	0.8033	0.0521	0.0176	0.0848	0.0997

versal Vacuum X-ray Spectrometer employing a chromium target X-ray tube, flow proportional counter, and pulse height selection was employed for the measurement of the X-ray intensities. An LIF crystal was used to measure Ca Kα, and the Lα, Kα, Kα, and Lα lines of Zr, Al, Si, and Ce, respectively, were measured with an EDDT crystal. Although a fixed-count mode is preferable from the standpoint of obtaining a constant variance of measured X-ray intensities, its use was precluded by the practical limitation of counting times to around 100 seconds per element. Therefore, all measurements were carried out in a fixed-time mode of 100 seconds. Measurements were made in duplicate to guard against outliers introduced by missetting instrumental parameters. The resulting mean intensities relative to end-member components are presented in Table III.

Regression Analysis of the Data. Equation 12, is as derived, the most general second-order model of the intensity *vs.* composition surface. It is not, however, parsimonious—the simplest model yielding as good a fit statistically to the data as any other. Indeed if only as many standards are used as coefficients to be determined, it is possible to obtain what appears to be an extremely good fit, even if one or more data points were somehow grossly in error. This is the main reason for using two to three times the required number of standards for calibration. All the coefficients are seldom necessary to obtain satisfactory regression equations and the null hypothesis H_0:$\beta_i = 0$ should always be tested. This point is commonly overlooked.

The first step in the analysis of the data is a thorough examination of the correlation matrix of all the variates. This provides good insight into which independent variates are contributing to the regression as well as indicating in a qualitative way the effect of individual X-ray intensities upon the concentration of the component being estimated. Table IV shows the correlation matrix for the regression of weight fraction ZrO_2 on the individual intensities, their cross products, and also the squares of the intensities corresponding to using the full quadric Equation 4 instead of Equation 12. Correlations of the squares of intensities are shown in order to make an important point. Regression equations become increasingly unstable in proportion to the degree of correlation between independent variates included in the regression. Squared intensity terms will always be highly positively correlated with their corresponding nonsquared intensities. While this is not so serious as a high inverse (negative) correlation between independent variates, it is nevertheless dangerous. In binary systems, the observed intensities of the two components will always be highly inversely correlated, so that the only the X-ray intensity corresponding to the component being estimated, and its cross product with the other component's intensity should be used in the model. Regression coefficients obtained from few data using equations with highly correlated variates may lead to small residuals for the particular data employed in the regression, but additional data might significantly alter them. Several of the proposed regression equations include squared terms and persons using them should be cognizant of their consequences. The suggestion that the squared term can account for dead-time counting losses, Lucas-Tooth and Pyne (*5*), is inaccurate, since errors can be corrected systematically only if there is some direct or indirect estimate of them. It is true that background and dead-time are absorbed by the regression coefficients, but this is in a completely vicarious way.

The remaining correlation coefficients between independent

Table IV. Correlation Matrix for the Regression of Weight Fraction ZrO_2 on Intensities, Cross-Products, and Squares of Intensities

	I_{Zr}	I_{Al}	I_{Si}	I_{Ca}	I_{Co}	C_{Zr}	$I_{Zr}I_{Al}$
I_{Zr}	1.000	−0.417	−0.310	−0.269	−0.224	0.997	0.019
I_{Al}		1.000	−0.212	−0.207	−0.194	−0.414	0.497
I_{Si}			1.000	−0.181	−0.191	−0.321	−0.244
I_{Ca}				1.000	−0.200	−0.243	−0.166
I_{Co}					1.000	−0.222	−0.114
C_{Zr}						1.000	0.043
$I_{Zr}I_{Al}$							1.000

	$I_{Zr}I_{Si}$	$I_{Zr}I_{Ca}$	$I_{Zr}I_{Co}$	$I_{Al}I_{Si}$	$I_{Al}I_{Ca}$	$I_{Al}O_{Co}$	$I_{Si}I_{Ca}$
I_{Zr}	0.264	0.343	0.387	−0.160	−0.237	−0.205	−0.020
I_{Al}	−0.223	−0.264	−0.244	0.271	0.397	0.409	−0.113
I_{Si}	0.104	−0.199	−0.196	0.074	−0.165	−0.164	0.089
I_{Ca}	−0.086	0.309	−0.132	−0.066	0.242	−0.098	0.216
I_{Co}	−0.065	−0.097	0.363	−0.050	−0.077	0.285	−0.035
C_{Zr}	0.281	0.408	0.405	−0.146	−0.193	−0.188	0.027
$I_{Zr}I_{Al}$	−0.069	−0.037	0.017	0.400	0.557	0.600	−0.089
$I_{Zr}I_{Si}$	1.000	0.172	0.183	0.486	−0.150	−0.136	0.645
$I_{Zr}I_{Ca}$		1.000	0.248	−0.104	0.319	−0.146	0.435
$I_{Zr}I_{Co}$			1.000	−0.092	−0.151	0.330	0.016
$I_{Al}I_{Si}$				1.000	0.325	0.328	0.522
$I_{Al}I_{Ca}$					1.000	0.456	0.266
$I_{Al}I_{Co}$						1.000	−0.031
$I_{Si}I_{Ca}$							1.000

	$I_{Si}I_{Co}$	$I_{Ca}I_{Co}$	$I_{Zr}I_{Zr}$	$I_{Al}I_{Al}$	$I_{Si}I_{Si}$	$I_{Ca}I_{Ca}$	$I_{Co}I_{Co}$
I_{Zr}	0.007	−0.016	0.931	−0.430	−0.335	−0.344	−0.330
I_{Al}	−0.103	−0.087	−0.468	0.897	−0.188	−0.200	−0.196
I_{Si}	0.089	−0.141	−0.221	−0.135	0.967	−0.102	−0.109
I_{Ca}	−0.043	0.268	−0.276	−0.206	−0.172	0.908	−0.187
I_{Co}	0.239	0.296	−0.242	−0.208	−0.184	−0.194	0.903
C_{Zr}	0.028	0.036	0.904	−0.444	−0.352	−0.349	−0.344
$I_{Zr}I_{Al}$	−0.054	−0.022	−0.224	0.095	−0.256	−0.259	−0.241
$I_{Zr}I_{Si}$	0.647	0.027	0.127	−0.240	−0.133	−0.160	−0.154
$I_{Zr}I_{Ca}$	0.044	0.567	0.140	−0.319	−0.239	−0.070	−0.228
$I_{Zr}I_{Co}$	0.426	0.520	0.200	−0.302	−0.232	−0.232	−0.021
$I_{Al}I_{Si}$	0.536	0.031	−0.300	0.038	−0.114	−0.131	−0.126
$I_{Al}I_{Ca}$	−0.018	0.412	−0.415	0.081	−0.177	−0.040	−0.168
$I_{Al}I_{Co}$	0.226	0.390	−0.381	0.094	−0.175	−0.172	−0.001
$I_{Si}I_{Ca}$	0.610	0.404	−0.159	−0.175	−0.114	−0.024	−0.123
$I_{Si}I_{Co}$	1.000	0.393	−0.133	−0.171	−0.116	−0.125	−0.002
$I_{Ca}I_{Co}$		1.000	−0.195	−0.195	−0.181	−0.039	−0.013
$I_{Zr}I_{Zr}$			1.000	−0.359	−0.204	−0.241	−0.234
$I_{Al}I_{Al}$				1.000	−0.087	−0.117	−0.121
$I_{Si}I_{Si}$					1.000	−0.063	−0.071
$I_{Ca}I_{Ca}$						1.000	−0.097
$I_{Co}I_{Co}$							1.000

variates follow a predictable pattern, *i.e.*, the individual components are inversely correlated with each other, and cross products are inversely correlated with the components not included in them. While no variates are so unusually correlated as to warrant immediate exclusion from the regression, data over smaller ranges of compositional variation and data from systems known to exhibit strong interelement effects should always be checked for such interactions.

Having established that there are no serious interactions between the independent variates, the next step is to identify those variates which contribute most to the regression (H_0:$\beta_i = 0$ is false). This is most conveniently accomplished by a forward selection stepwise regression analysis program. It is important to note here that, while many multiple linear regression analysis programs are available, the program of choice should probably be the most comprehensive one obtainable that has been tested and approved by someone thoroughly familiar with regression analysis techniques. Some programs, although frequently used and accepted with little or no question, are quite inadequate when dealing with these X-ray data. Longley (*19*) compared a dozen or so different multiple regression programs in use throughout the country, and reached the conclusion that, for his test data, no program was very good, and some were so inaccurate that they yielded no correct significant digits for the regression coefficients of the model. Programs oriented toward "minicomputers" should be approached with caution. The small word length associated with them can introduce serious rounding errors, and core limitations may drastically reduce the level of statistical sophistication necessary for the optimum treatment of the data.

The program utilized in this study, Dixon (*20*), first calculates F-ratios for each of the coefficients of Equation 12, one at a time, to identify the independent variate whose coefficient has the maximum effect of lowering the sums of squares of residuals. This variate is then the first to be incorporated into the regression. The program proceeds in subsequent steps to calculate F-ratios for the variates not included in the regression, to again identify that variate whose coefficient leads to the maximum reduction of the sums of squares of

(19) J. W. Longley, *J. Amer. Statis. Ass.*, 61, 819 (1967).

(20) W. J. Dixon, "BMDO2R-Stepwise Regression," Univ. Calif. Publications in Automatic Computation, No. 2, Biomedical Computer Programs, Univ. Calif. Press, 1967.

Table V. Forward Selection Regression Analysis of Weight Fraction ZrO_2 on Individual Intensities and Cross Products

Step 1

Variable entered: I_{Zr}
Correlation coefficient: 0.9965
Std error of estimate ($S_{\hat{Y}}$): 0.0187
Overall F ratio: 5588.8
Variables in equation

Variable	Coefficient	Std error	F
const	0.0267		
I_{Zr}	1.0295	0.0138	5588.8

Step 2

Variable entered: $I_{Zr}I_{Ca}$
Correlation coefficient: 0.9990
Std error of estimate ($S_{\hat{Y}}$): 0.0101
Overall F ratio: 9668.7
Variables in equation

Variable	Coefficient	Std error	F
const	0.0136		
I_{Zr}	1.0029	0.0079	16117.7
$I_{Zr}I_{Ca}$	0.3624	0.0369	96.2

Step 3

Variable entered: $I_{Zr}I_{A1}$
Correlation coefficient: 0.9994

Step 3 (*Continued*)

Std error of estimate ($S_{\hat{Y}}$): 0.0081
Overall F ratio: 9902.5
Variables in equation

Variable	Coefficient	Std error	F
const	0.0042		
I_{Zr}	1.0019	0.0064	24664.9
$I_{Zr}I_{Ca}$	0.3688	0.0298	152.7
$I_{Zr}I_{A1}$	0.1160	0.0251	21.3

Step 4

Variable entered: $I_{Si}I_{Ca}$
Correlation coefficient: 0.9996
Std error of estimate ($S_{\hat{Y}}$): 0.0069
Overall F ratio: 10284.1
Variables in equation

Variable	Coefficient	Std error	F
Const	0.0003		
I_{Zr}	1.0020	0.0054	34149.5
$I_{Zr}I_{Ca}$	0.3646	0.0254	206.3
$I_{Zr}I_{A1}$	0.1203	0.0214	31.7
$I_{Si}I_{Ca}$	0.4100	0.1051	15.2

F level of all remaining variates is less than 2.0

residuals and to include it in the regression. This continues until either all variates are included in the regression or until none of the remaining variates possess coefficients which contribute significantly. The user may, if desired, specify F-levels for inclusion and deletion of variates, so that if at any time a variate included in the regression becomes nonsignificant through the inclusion of subsequent variates it will be deleted. This option serves mainly to limit the number of steps taken by the program (*i.e.*, increase its operating efficiency). The optimum regression model could also be determined by examining the pertinent statistical details output at the end of each step as the program includes variates in order of their decreasing contribution. Again, the object of the regression analysis is to include only those variates that contribute significantly as determined by the F-ratio test statistic. Including nonsignificant variates will always decrease the sum of squares of residuals so that what appears to be a better fit is obtained; however, the overall F-ratio of the regression will be lower than that of the most efficient and certainly sufficient equation.

Regression programs that attempt to arrive at an optimum equation by deleting variates one at a time from the full general Equation 12 frequently run into trouble (*e.g.*, they will delete the X-ray intensity of the component being estimated). This is because the "independent" variates are not at all independent in a mathematical way as required by conventional regression theory, but rather interdependent. In fact, the order in which highly correlated variates appear in Equation 12 according to some computer programs can influence their rank (partial correlation) in the overall regression, which is absurd. The use of this type program is discouraged when dealing with nearly all kinds of composition data.

Table V shows the steps taken by the program for the regression of weight fraction ZrO_2 on the intensity data. The F-level for inclusion and deletion of variates was set at 2.0 (for $\alpha = 0.05$ with one degree of freedom for the coefficients and around 35 degrees of freedom for the residuals, depending upon how many variates are included at any one time, the critical F-level is about 4). [The F-level is calculated by the formula $F = SSR_{K+1} - SSR_K/s^2_{y \cdot x}$ given by Anderson and Bancroft (*21*).] The regression coefficients obtained for all five components are shown in Table VI along with pertinent

(21) R. L. Anderson and T. A. Bancroft, "Statistical Theory in Research," McGraw-Hill, New York, N. Y., 1952.

Table VI. Final Regression Coefficients Obtained for Individual Components and Pertinent Statistical Measures

1. ZrO_2

Correlation coefficient 0.9996
Std error of estimate ($S_{\hat{Y}}$) 0.0069
Analysis of variance

	d.f.	Sum of squares	Mean square	F ratio
Regression	4	1.966	0.492	10284.1
Residual	31	0.002	0.000	

Regression coefficients

Variable	Coefficient	Std error	F
const	0.0003		
I_{Zr}	1.0020	0.0054	34149.4
$I_{Zr}I_{A1}$	0.1203	0.0214	31.7
$I_{Zr}I_{Ca}$	0.3646	0.0254	206.3
$I_{Si}I_{Ca}$	0.4100	0.1051	15.2

2. Al_2O_3

Correlation coefficient 0.9998
Std error of estimate ($S_{\hat{Y}}$) 0.0046
Analysis of variance

	d.f.	Sum of squares	Mean square	F ratio
Regression	5	1.493	0.299	14114.9
Residual	30	0.001	0.000	

Regression coefficients

Variable	Coefficient	Std error	F
const	−0.00007		
I_{A1}	0.9993	0.0046	47299.2
$I_{Zr}I_{A1}$	−0.0612	0.0205	8.9
$I_{A1}I_{Ca}$	0.3071	0.0343	80.3
$I_{A1}I_{Co}$	0.1620	0.0283	32.5
$I_{Si}I_{Ca}$	−0.1616	0.0844	3.6

(*Continued on next page*)

Table VI. (*Continued*)

3. SiO_2

Correlation coefficient 0.9998
Std error of estimate (S_y) 0.0032
Analysis of variance

	d.f.	Sum of squares	Mean square	F ratio
Regression	5	0.980	0.196	19069.7
Residual	30	0.000	0.000	

Regression coefficients

Variable	Coefficient	Std error	F
const	−0.0011		
I_{Si}	1.0013	0.0035	81312.1
$I_{Zr}I_{Al}$	−0.0476	0.0125	14.5
$I_{Zr}I_{Ce}$	−0.0277	0.0124	4.9
$I_{Al}I_{Si}$	0.2069	0.0709	8.5
$I_{Si}I_{Ce}$	0.3624	0.0790	21.1

4. CaO

Correlation coefficient 1.0000
Std error of estimate (S_y) 0.0016
Analysis of variance

	d.f.	Sum of squares	Mean square	F ratio
Regression	7	0.936	0.134	49717.7
Residual	28	0.000	0.000	

Regression coefficients

Variable	Coefficient	Std error	F
const	0.0009		
I_{Ca}	0.9990	0.0018	306822.1

4. CaO (*Continued*)

Regression coefficients

Variable	Coefficient	Std error	F
$I_{Zr}I_{Al}$	0.0419	0.0072	33.7
$I_{Zr}I_{Si}$	0.0507	0.0184	7.6
$I_{Zr}I_{Ca}$	−0.4961	0.0073	4649.6
$I_{Al}I_{Ca}$	−0.7497	0.0151	2451.3
$I_{Si}I_{Ca}$	−0.7908	0.0481	240.9
$I_{Ca}I_{Ce}$	−0.3104	0.0142	480.2

5. CeO_2

Correlation coefficient 1.0000
Std error of estimate (S_y) 0.0017
Analysis of variance

		Sum of squares	Mean square	F ratio
Regression	8	0.936	0.117	45580.5
Residual	27	0.000	0.000	

Regression coefficients

Variable	Coefficient	Std error	F
const	0.0003		
I_{Ce}	0.9996	0.0018	320947.7
$I_{Zr}I_{Al}$	0.0302	0.0088	11.9
$I_{Zr}I_{Si}$	0.0453	0.0187	5.8
$I_{Zr}I_{Ce}$	−0.5725	0.0074	6048.6
$I_{Al}I_{Ca}$	0.0288	0.0160	3.2
$I_{Al}I_{Ce}$	−0.8279	0.0134	3821.8
$I_{Si}I_{Ce}$	−0.8482	0.0443	367.4
$I_{Ca}I_{Ce}$	−0.2847	0.0188	229.6

Table VII. Predicted Concentrations of Individual Components Using Equations Shown in Table VI

Standard	Composition in weight fraction ZrO_2	Al_2O_3	SiO_2	CaO	CeO_2
1	0.3557	0.4516	0.1129	0.0478	0.0475
2	0.3560	0.5487	0.0121	0.0472	0.0460
3	0.3510	0.3412	0.1068	0.0486	0.1481
4	0.3505	0.4399	0.0104	0.0489	0.1484
5	0.3491	0.3451	0.1065	0.1457	0.0502
6	0.3547	0.4436	0.0077	0.1496	0.0502
7	0.3570	0.2518	0.1122	0.1457	0.1461
8	0.3454	0.3514	0.0134	0.1450	0.1441
9	0.4423	0.3392	0.1033	0.0500	0.0499
10	0.4544	0.4430	0.0058	0.0501	0.0494
11	0.4553	0.2416	0.1102	0.0501	0.1500
12	0.4445	0.3510	0.0085	0.0489	0.1486
13	0.4437	0.2484	0.1042	0.1506	0.0509
14	0.4463	0.3455	0.0138	0.1486	0.0497
15	0.4398	0.1460	0.1116	0.1487	0.1479
16	0.4552	0.2415	0.0070	0.1528	0.1511
17	0.5524	0.2439	0.1093	0.0506	0.0498
18	0.5429	0.3396	0.0090	0.0503	0.0498
19	0.5507	0.1506	0.1065	0.0499	0.1501
20	0.5349	0.2447	0.0103	0.0496	0.1492
21	0.5358	0.1437	0.1026	0.1475	0.0500
22	0.5533	0.2472	0.0089	0.1479	0.0497
23	0.5439	0.0476	0.1025	0.1497	0.1483
24	0.5466	0.1438	0.0103	0.1461	0.1468
25	0.6500	0.1499	0.1143	0.0494	0.0498
26	0.6451	0.2493	0.0113	0.0498	0.0486
27	0.6425	0.0484	0.1096	0.0480	0.1440
28	0.6499	0.1471	0.0067	0.0486	0.1474
29	0.6475	0.0484	0.1076	0.1479	0.0491
30	0.6359	0.1424	0.0121	0.1483	0.0497
31	0.6486	0.0524	0.0101	0.1482	0.1492
32	0.7447	0.0527	0.1105	0.0490	0.0490
33	0.7425	0.1441	0.0110	0.0488	0.0486
34	0.7457	0.0510	0.0097	0.0477	0.1476
35	0.7472	0.0538	0.0167	0.1461	0.0486
36	0.8358	0.0514	0.0131	0.0471	0.0479

statistical details. Table VII summarizes the predicted concentrations of the standards (*cf.* Table II).

The equations indicated by Table VI are the simplest representation of the data yielding nearly as good a fit as any other. Nearly as good a fit here implies within the mean square residual error. The equations, *in sensu stricto*, permit prediction of X-ray intensities from a knowledge of composition and not *vice versa*. As Alley and Myers (*6*) emphasize, the equations are *statistically* meaningless if used to predict concentrations other than those included in the regression data. This does not mean, however, that the equations are incapable of predicting unknown concentrations, nor are they *physically* meaningless, as witnessed by the widespread successful application of similar equations. What is now assumed is that the estimated coefficients are sufficiently close to the "true" values of similar coefficients equating concentrations and intensities *via* a functional relationship (Equation 1) that we *assume* to be of the form indicated in Table VI for each component. This implicitly requires that additional data will not significantly alter the coefficients. The implied and expressed statistical risks of doing this must be borne by the investigator, and this usually amounts to little more than never attempting to extend the equations beyond the calibration range. Demanding that the equations be kept as simple as possible and employing more standards than are absolutely necessary lends confidence to the above assumptions, provided the overall accuracy attained in the prediction of the composition of the standards meets requirements. Attainable accuracy is frequently limited to around ±1 to 2% relative, since, when all sources of random and systematic error in the chemical analysis of standards or the preparation of synthetic standards are considered, the original data are seldom better than ±1 to 2% relative.

As a final check on the stability of the equations, the co-

Table VIII. Comparison of Theoretical and Calculated Compositions of Five Test Samples and End-Member Primary Reference Standards

	Composition in weight fraction									
	Theoretical					Calculated				
Sample	ZrO_2	Al_2O_3	SiO_2	CaO	CeO_2	ZrO_2	Al_2O_3	SiO_2	CaO	CeO_2
1	0.500	0.250	0.050	0.100	0.100	0.5014	0.2487	0.0509	0.1012	0.1020
2	0.700	0.100	0.100	0.050	0.050	0.7033	0.0987	0.1029	0.0513	0.0487
3	0.300	0.300	0.100	0.150	0.150	0.3023	0.2950	0.1021	0.1488	0.1511
4	0.400	0.400	0.050	0.075	0.075	0.3975	0.3985	0.0478	0.0739	0.0765
5	0.600	0.050	0.050	0.150	0.150	0.6034	0.0513	0.0490	0.1466	0.1527
6	1.000	0.000	0.000	0.000	0.000	1.0023	−0.0001	−0.0011	0.0009	0.0003
7	0.000	1.000	0.000	0.000	0.000	0.0003	0.9992	−0.0011	0.0009	0.0003
8	0.000	0.000	1.000	0.000	0.000	0.0003	−0.0001	1.0001	0.0009	0.0003
9	0.000	0.000	0.000	1.000	0.000	0.0003	−0.0001	−0.0011	0.9999	0.0003
10	0.000	0.000	0.000	0.000	1.000	0.0003	−0.0001	−0.0001	0.0009	0.9999

Table IX. Observed Relative Intensities of Five Test Samples

	Observed relative intensity				
Sample	I_{Zr}	I_{Al}	I_{Si}	I_{Ca}	I_{Ce}
1	0.451	0.235	0.053	0.193	0.215
2	0.667	0.100	0.103	0.092	0.102
3	0.225	0.267	0.093	0.286	0.308
4	0.357	0.380	0.050	0.150	0.176
5	0.543	0.049	0.050	0.253	0.281

variance matrix for the regression coefficients can be calculated, although marked covariance between coefficients is usually eliminated by selecting independent variables with the least degree of correlation. The coefficients given in Table VI can now be incorporated into the appropriate equations to solve for the concentrations of individual components using measured relative intensities of unknowns.

RESULTS

To test the applicability of the final regression equations, five samples not included in the original regression data were prepared and measured in duplicate. Table VIII lists the theoretical and calculated composition of each sample, and Table IX shows the observed mean intensities. Data for each of the end-member primary reference standards are also shown in Table VIII, although they are far outside the range of calibration. The errors in all cases are comparable with the standard errors of estimate given in Table V. The equations have been used to analyze several hundred actual unknowns over a period of a year with good success.

DISCUSSION AND CONCLUSIONS

The application of statistical techniques to the solution of absorption and enhancement effects in quantitative X-ray emission analysis should, if properly applied, permit quite accurate prediction of the concentrations of individual components in unknowns through a knowledge of their associated X-ray intensities. To obtain equations relating concentrations to intensities that are reliable throughout the range of standardization, careful attention must be paid to all pertinent statistical details of the regression analysis. It is possible to invent, derive, guess, or in general vicariously arrive at many different equations that, from the same data, permit more or less accurate prediction of unknown concentrations. The question quite simply is: Which regression is best? The answer is summarized by the following:

1. The best equation is the simplest one yielding nearly as good a fit to the data as any other.

2. Equations which involve variates that are highly correlated (positively or negatively) are less stable than equations with smaller correlations between the independent variates.

3. Equations that show a marked degree of covariance between two regression coefficients can usually be improved by deleting one of the variates without adversely affecting the regression.

4. The assumption that the response (intensity *vs.* composition) surface is quadric in all *n*-component systems, while unproved, appears to be the best choice for the preliminary model. Equation 12 ought to be tried before more elaborate models are considered.

5. The acronym GIGO (garbage in, garbage out), although a bit overworked lately, should always be borne in mind. Equations that predict the concentrations of individual components in reference standards more accurately than they are actually known should be viewed with considerable skepticism. The variance of predicted concentrations can at best equal the true variance of the original data.

The philosophy underlying the use of multiple linear regression analysis is to account for as much of the variation in the concentrations of individual components in reference standards as possible with the fewest number of independent variates (X-ray intensities and their transformations) that are necessary. The fact that a good fit to the data employed in the regression is obtained can in no way be construed to imply that equally good accuracy will be attained in the prediction of unknowns. This is the risk involved in the method. The more reference standards that are used to estimate the regression coefficients, the more confident one can be in assuming the resulting equations accurately predict the composition of unknowns. McKinney and Rosenberg (*22*) found that a twenty-eight-term polynomial suggested by Mitchell (*9*) gave less accurate results than a simpler expression, although the residual standard deviations were on the average a factor of two less than those for their model. This is easily explained by the fact that the coefficients of the most significant variates were so diluted by the effect of nonsignificant variates that the equations collapsed when small errors in the measurement of X-ray intensities were encountered. The principle of parsimony can indeed govern the success of multiple regression methods of analysis.

Several "semitheoretical" approaches to the solution of absorption and enhancement effects have been suggested, notably by Beattie and Brissey (*10*), Traill and Lachance

(22) C. N. McKinney and A. S. Rosenberg, *Advan. X-Ray Anal.*, 13, 230 (1970).

(23–25), Andermann (26), Holland and Brindle (27), Claisse and Quintin (28), and McKinney and Rosenberg (22). The proposed equations all ultimately reduce, after substantial peregrination, to equations similar to Equation 12 or functionally like those of Criss and Birks (11), the main difference being that the coefficients are deduced from absorption coefficients rather than estimated by regression techniques or found by the simultaneous equation method. The statistical ability to decide which variates are really important is, of course, lost in the process, and the increased complexity of these techniques greatly enhances the possibility of obtaining an artificially good fit to the data. Before resorting to such procedures, it is wise to determine if ordinary regression analysis might yield sufficiently accurate results since, in principle, regression techniques will suffice if the data are both accurate and sufficiently numerous. In any case, quantitative measures do exist to help decide between the alternatives. The clear distinction between empirical and theoretical methods of X-ray emission analysis made by Criss and Birks (11) seems entirely justified. The method of choice is naturally the one that yields correct answers the majority of the time in the actual analysis of unknowns, and any equation that fulfills this, whether physically or statistically realistic or not, may be used.

The regression technique described here is oriented toward minimizing the variance of predicted concentrations. The possibility does exist that the equations may be biased. The most serious bias error likely to arise is that the assumed quadric model is really cubic. Since variance, in almost all cases, is the overriding source of imperfection in the models, the choice of an all-variance design is the most logical, and the least-squares minimization of the residuals between theoretical and calculated concentrations should give satisfactory equations. If we also postulate normality for all the errors, the least-squares method is also equivalent to maximum likelihood methods. The greatest source of difficulty is the confounding correlations between the independent variates. While substantially more accurate results might obtain by eliminating such correlations through a linear transformation of the variates *via* component or canonical analysis of the data according to the principles nicely described by Kendall (29), the added effort probably should be directed toward seeking a solution to the absorption and enhancement problem through first physical principles, although advanced statistical analysis of the data is not intractable.

RECEIVED for review October 5, 1970. Accepted November 25, 1970.

(23) R. J. Traill and G. R. Lachance, *Geol. Survey Can., Pap.* 64–57 (1964).
(24) G. R. Lachance and R. J. Traill, *ibid.*, **11**, 43 (1966).
(25) R. J. Traill and G. R. Lachance, *ibid.*, p 63.
(26) G. Andermann, ANAL. CHEM., **38**, 82 (1966).
(27) J. G. Holland and D. W. Brindle, *Spectrochim. Acta*, **22**, 2083 (1966).
(28) F. Claisse and M. Quintin, *Can. Spectrosc.*, **12**, 129 (1967).
(29) M. G. Kendall, "A Course in Multivariate Analysis," Charles Griffin and Co., Ltd., London (1957).

Spectrophotometric Determination of Traces of Thallium in Tungsten

The Extraction of Thallium Diethyldithiocarbamate

Károly Vadasdi, Piroska Buxbaum, and András Salamon
Research Institute for Technical Physics of the Hungarian Academy of Sciences, Budapest, Ujpest 1., Pf. 76, Hungary

A spectrophotometric method is presented for the determination of thallium in tungsten metal. The samples are dissolved in the mixture of hydrofluoric and nitric acids. The thallium is separated from tungsten by extraction with sodium diethyldithiocarbamate into chloroform between pH 8–11 and the Methyl Violet method was used for its determination at 605 nm. Interference effects of some diverse ions are reported. Iron(III) interference is prevented with EDTA. The method is suitable for the determination of 0.1–10 ppm thallium in tungsten metal with a precision of 10–20%. The equilibrium constants in the Tl(I)–diethyldithiocarbamate–chloroform system have also been determined by means of EDTA competition as well as the stability constant of Tl(I)–EDTA complex by potentiometric methods.

A GREAT NUMBER of methods have been described in the literature for the determination of different impurities and doping materials in tungsten. One of the recently introduced doping materials is thallium (1). For this reason a sensitive method has been needed for the determination of small quantities of thallium in tungsten metal.

For the separation and determination of thallium from different elements, sensitive and accurate methods are known (2, 3). Thallium can be determined with the highest sensitivity by means of inverse polarography. Among the colorimetric methods, the Rhodamine B and Methyl Violet methods are well known (4–6).

The main problem which occurs during the determination of different ions in tungsten is the selection of a suitable separation method because the tungstate ion may form heteropoly-acid complexes with the considerable part of the elements of the periodic table. These complexes usually are much more

(1) T. Millner and J. Neugebauer, Hungarian Patent 155.352 (1969); French Patent 1.536.155 (1969).
(2) E. B. Sandell, "Colorimetric Determination of Traces of Metals," Interscience, New York, N. Y., 1959.
(3) O. G. Koch, Koch, and G. A. Dedic, "Handbuch der Spurenanalyse," Springer, Heidelberg, Germany, 1964.
(4) H. Onishi, *Bull. Chem. Soc. Japan*, **29**, 943 (1956).
(5) N. T. Voskresenskaya, *J. Anal. Chem. USSR*, **11**, 585 (1956).
(6) M. E. Campbell, C. Millingan, and A. Lindsay, *Amer. Ind. Hyg. Ass. J.*, **20**, 23 (1959).

stable than the customary metallic ion–organic reagent complexes and can only be destroyed in alkaline medium.

For the determination of thallium in the presence of tungsten or for the separation of thallium from tungsten, no method can be found in the literature. No data are available about the existence of heteropolyacid complexes formed either thallium(I) or thallium (III) and tungsten, like aluminium and gallium (*7*, *8*).

EXPERIMENTAL

Apparatus and Reagents. All absorbance measurements were made with a Beckman DU spectrophotometer in matched 1.000-cm cuvettes.

The pH measurements were made with a Radelkisz OP-205 and Radiometer pHM 26 precision pH meters. The pH standards were 0.05*M* potassium acid phthalate and 0.05*M* borax.

SODIUM DIETHYLDITHIOCARBAMATE (NaDDTC). Reagent grade (98.5% min) $NaDDTC \cdot 3H_2O$ was used to prepare a 2% aqueous solution which was adjusted to about pH 9–10 with alkali.

METHYL VIOLET (Standard Fluka, C.I. 69710). A 0.1% aqueous solution was mixed with diluted sulfuric acid to prepare fresh daily a 0.05% working solution (0.05*N* in sulfuric acid).

ETHYLENEDIAMINETETRAACETIC ACID AND DISODIUM SALT (EDTA), reagent grade.

CHLOROFORM, reagent grade with 1% ethanol content was used without further purification.

BENZENE, reagent grade.

GLYCINE BUFFER. From reagent grade material, a 0.1*M* solution of glycine was prepared adjusting its pH to 10 ± 0.2 with alkali.

BORATE BUFFER. Reagent grade borax ($Na_2B_4O_7 \cdot 10H_2O$) was twice recrystallized from water. A 0.2*M* solution was prepared adjusting its pH with alkali to the desired value.

PHOSPHATE BUFFER. A 0.2*M* solution was prepared from reagent grade KH_2PO_4 and $Na_2HPO_4 \cdot 2H_2O$.

THALLIUM(I) NITRATE AND THALLIUM(III) CHLORIDE solutions were prepared from reagent grade salts and the metal content was determined complexometrically by the thorium nitrate–xylenol orange methanol (*9*). Other materials used in this work were reagent grade.

Preparation of the Calibration Curve. Add 0, 1, 2, 4, 7, 10 μg Tl(I)- or Tl(III)-containing solution into a 150-ml beaker, add 1.8 ml concentrated sulfuric acid and 20 ml of 30% hydrogen peroxide and evaporate to sulfuric acid fumes. (After cooling down, wash down the sides of the beaker with a little water and evaporate again.) Dilute with 20 ml of water, add 2 ml of 1:9 hydrobromic acid and 10 drops of bromine water. Boil the solution for a few minutes to expel the excess bromine. After cooling down, complete the volume to 49 ml, pour the solution into a separatory funnel.

Add to the solution 5.0 ml of benzene and 1.0 ml of diluted working Methyl Violet solution, and immediately after shake for 1 minute. Allow the layers to separate completely, discard the aqueous layer, and obtain the transmittance of the organic layer at 605 nm in 1-cm cuvette. Pure benzene is used in the reference cells.

Recommended Procedure for the Determination of 0.1–10 ppm Thallium. IF 1–10 PPM THALLIUM PRESENT. Add 2 ml of 38% hydrofluoric acid in a Teflon (Du Pont) vessel to 1 gram of powdered tungsten metal and add dropwise 65% nitric acid until the complete dissolution of the sample.

Table I. Summarization of Extraction Data

(pH; log *Q*)

	Tl(I)	
C_{NaDDTC}	$1 \times 10^{-1}M$	5.2; −2.87, 6.1; −1.60,
C_{Tl}	$1 \times 10^{-6}M$	7.2; −0.46, 8.1; 0.79,
Medium	$1 \times 10^{-1}M$ $NaClO_4$	8.9; 1.81, 9.7; 2.44,
Temperature	20 °C	10.1; 2.53, 10.5; 2.49,
Time of extr.	24 hours	11.5; 2.48, 12.1; 1.82,
Method	Isotope	12.6; 1.31
Author	Schweitzer–Norton (*12*)	
	Tl (I)	
C_{NaDDTC}	$1 \times 10^{-2}M$	3.8; 1.18, 4.8; 1.84, 5.8;
C_{Tl}	$2.5 \times 10^{-4}M$	2.29, 7.0; 2.22, 7.2; 2.32,
Medium	$2 \times 10^{-1}M$, W as Na_2WO_4 $2 \times 10^{-1}M$ tartaric acid	7.6; 2.34, 8.2; 2.33
Temperature	25 ± 2 °C	
Time of extr.	3 minutes	
Method	Isotope, ^{204}Tl, 3.56 years	
Author	This work	
	Tl(III)	
C_{NaDDTC}	$1 \times 10^{-1}M$	2.7; −1.07, 3.2; −0.49,
C_{Tl}	$2.5 \times 10^{-4}M$	3.8; 0.31, 4.8; 1.78, 5.8;
Medium	$2 \times 10^{-1}M$, W as Na_2WO_4 $2 \times 10^{-1}M$ tartaric acid	2.11, 7.0; 2.48, 7.3; 2.70, 8.2; 2.94, 10.5; 3.16, 12.5; 3.24
Temperature	25 ± 2 °C	
Time of extr.	3 minutes	
Method	Isotope, ^{204}Tl, 3.56 years	
Author	This work	

After this add 4 ml of 30% tartaric acid and adjust the pH of the solution between 8–11 with 20% potassium hydroxide. Add 1 ml of 2% NaDDTC solution (and EDTA solution if necessary calculating the amount according to Equation 11). Pour the solution which has a volume of about 25–30 ml into a separatory funnel and shake twice with 20 ml of chloroform for 2 minutes. Wash the combined chloroform layers twice with 2–3 ml of 10 pH glycine buffer. Discard the aqueous layers. Evaporate the chloroform on a water bath and destroy the organic residue with 1.8 ml of sulfuric acid and 20 ml of hydrogen peroxide evaporating to sulfuric acid fumes and determine the thallium as described under the preparation of the calibration graph.

IF 0.1–1.0 PPM THALLIUM PRESENT. Add 25 ml of 38% hydrofluoric acid in a Teflon vessel to 10 grams of finely powdered tungsten sample and dropwise 65% nitric acid until the sample completely dissolves. Add 40 ml of 30% tartaric acid, 2 ml of 0.05*N* EDTA solution, and adjust the pH between 8–11 with 60% potassium hydroxide. After cooling down, add 10 ml of 2% NaDDTC and pour the solution which has a volume between 200–300 ml into a 500-ml separatory funnel and shake four times with 20 ml of chloroform for 2 minutes. Wash the combined organic phases with 10 pH glycine buffer; evaporate it on a water bath, destroy the residue, and determine the thallium as described above.

RESULTS AND DISCUSSION

Extraction of Thallium(I) and Thallium(III) Diethyldithiocarbamates. Bode carried out the first systematic study on the extraction of thallium diethyldithiocarbamates (*10*, *11*).

(7) T. Millner and J. Neugebauer, *Magy. Kem. Foly.*, **57**, 321 (1951).
(8) K. G. Vadasdi, *Chem. Anal.* (*Warsaw*), **14**, 733 (1969).
(9) J. Kinnunen and B. Wennestrand, *Chemist-Analyst*, **46**, 92 (1957).
(10) H. Bode, *Z. Anal. Chem.*, **142**, 414 (1954).
(11) *Ibid.*, **144**, 165 (1955).

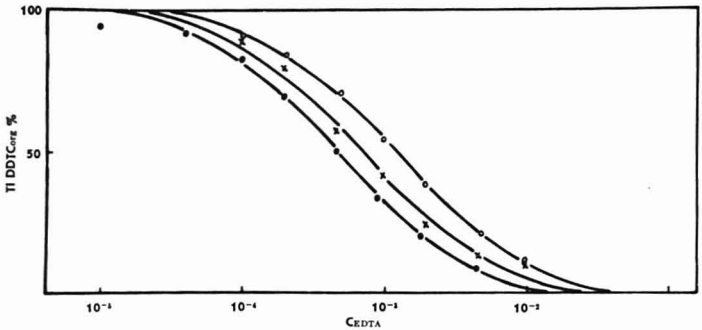

Figure 1. Equilibrium concentration of the TlDDTC in the chloroform phase as the function of EDTA concentration at different pH values

○ **pH 9.30 ± 0.03 (0.1*M* borate buffer)**
× **pH 9.88 ± 0.03 (0.1*M* borate buffer)**
● **pH 10.14 ± 0.03 (0.1*M* glycine buffer)**
$C_{Tl[I]} = 4.9 \times 10^{-6} M$; $C_{NaDDTC} = 1.0 \times 10^{-4} M$; $t = 25 \pm 2$ °C; **extraction time 10 minutes**

He stated that the extraction of $Tl(DDTC)_2$ was not interfered with by tartarate, citrate, phosphate, borate, glycine, cyanide, or EDTA between pH 8–11, whereas that of TlDDTC was hindered by EDTA. Later Schweitzer and Norton investigated the extraction of TlDDTC into chloroform and they gave the pH function of the distribution constant (*12*).

Since no data are available for the extraction of TlDDTC and $Tl(DDTC)_2$ in the presence of tungstate and fluoride ions, we have investigated their influence. Results in the case of tungstate ion were summarized in Table I. (Tartaric acid was added to prevent the precipitation of tungstic acid in lower pH regions.) No remarkable effect of these ions was observed.

In the following, the influence of EDTA on the extraction of TlDDTC was investigated in order that its hindering effect could be minimized, because it was found that the presence of EDTA was needed to mask iron.

Determination of Extraction Equilibrium Constant of TlDDTC Complex by EDTA Competition. Figure 1 shows the effect of EDTA concentration on the extraction of TlDDTC at different pH values from 0.1*M* borate or 0.1*M* glycine buffers. Ten-minute extraction periods were used at 25 ± 2 °C. The concentration of TlDDTC in the chloroform phase was determined by spectrophotometric measurements at 245 nm.

Since from the literature is known the formation constant of [Tl (I)-EDTA]$^{3-}$ complex (*13*)—in the following denoted as TlY^{3-}—the calculation of extraction equilibrium constant of TlDDTC became possible, with the help of the following relations:

$$TlY^{3-} + (HDDTC)_{org} \rightleftharpoons (TlDDTC)_{org} + HY^{3-}$$

$$K_1 = \frac{[TlDDTC_{org}]\,[HY^{3-}]}{[TlY^{3-}][HDDTC_{org}]} \qquad (1)$$

The two phase formation constant of TlDDTC:

$$Tl^{+} + DDTC^{-} \rightleftharpoons (TlDDTC)_{org}$$

$$K_2 = \frac{[TlDDTC_{org}]}{[Tl^{+}][DDTC^{-}]} \qquad (2)$$

where the three times and four times ionized fractions of EDTA were denoted as HY^{3-}, Y^{4-}; the diethyldithiocarbaminic acid as HDDTC and its anion as $DDTC^{-}$; the thallium (I) diethyldithiocarbamate and EDTA complexes as TlDDTC and TlY^{3-}.

The following equilibriums also were needed, the constants of which are known from the literature: (*13–15*).

$$Tl^{+} + Y^{4-} \rightleftharpoons TlY^{3-}$$

$$K_3 = \frac{[TlY^{3-}]}{[Tl^{+}][Y^{4-}]} \qquad (3)$$

$$HY^{3-} \rightleftharpoons Y^{4-} + H^{+}$$

$$K_{d_4} = \frac{[H^{+}][Y^{4-}]}{[HY^{3-}]} \qquad (4)$$

Here it should be mentioned that the formation constant of TlY^{3-}, K_3, was determined formerly by a polarographic method by Bouten, Verbeek, and Eckaut who found log K = 5.81 ± 0.05 in 0.2*M* sulfate medium at 20 °C (*13*), and recently by Koch and Kupsch with extraction method log K = 6.1 ± 0.2 (*15*). During this work we redetermined this value by a pH titration method with KOH in 0.1*N* KNO_3 at 25 °C, and the so-called stoichiometric constant was found log K = 6.38 ± 0.02. The ionization constants of EDTA measured under these conditions are in agreement with the values reported in the literature, $pK_3 = 6.15$; $pK_4 = 10.24$ (*14*).

The two-phase ionization constant of diethyldithiocarbamic acid was also needed.

$$H^{+} + DDTC^{-} \rightleftharpoons (HDDTC)_{org}$$

$$K' = \frac{[HDDTC_{org}]}{[H^{+}][DDTC^{-}]} \qquad (5)$$

The K′ was determined by Bode in the case of carbon tetrachloride. We have also determined this constant by the method of Bode for chloroform at 25 ± 2 °C from 0.1*M* phosphate buffer (*11*).

(12) G. K. Schweitzer and A. D. Norton, *Anal. Chim. Acta.*, **30**, 119 (1964).

(13) J. Bouten, F. Verbeek, and J. Eckaut, *Anal. Chim. Acta.*, **17**, 339 (1957).
(14) R. Shockdopole and S. Chaberek, *J. Inorg. Nucl. Chem.*, **11**, 222 (1959).
(15) H. Koch and H. Kupsch, *Z. Naturforsch. B.*, **24**, 398 (1969).

Table II. Summarization of Used or Calculated Equilibriums and Constants

Process	Equilibrium constant	Reference
$TlY^{2-} + (HDDTC)_{org} = (TlDDTC)_{org} + HY^{2-}$	$K_1 = (4.0 \pm 0.9) \times 10^3$	This work; 25 ± 2 °C 0.1 *M* glycine or borate
$Tl^+ + DDTC^- = (TlDDTC)_{org}$	$K_3 = K_1K'K_2K_{d_4} = (5.2 \pm 1.1) \times 10^6$	
$Tl^+ + Y^{4-} = TlY^{2-}$	$K_2 = (2.4 \pm 0.1) \times 10^6$	This work; 25 °C 0.1 *M* KNO_3
$HY^{3-} = Y^{4-} + H^+$	$K_{d_4} = (5.37 \pm \quad) \times 10^{-11}$	(*14*)
$H^+ + DDTC^- = (HDDTC)_{org}$	$K' = (1.0 \pm 0.1) \times 10^7$	This work; 25 ± 2 °C $CHCl_3$ 0.1 *M* phosphate
	$K' = (1.6 \pm \quad) \times 10^6$	Bode (*10*); CCl_4 18–20 °C

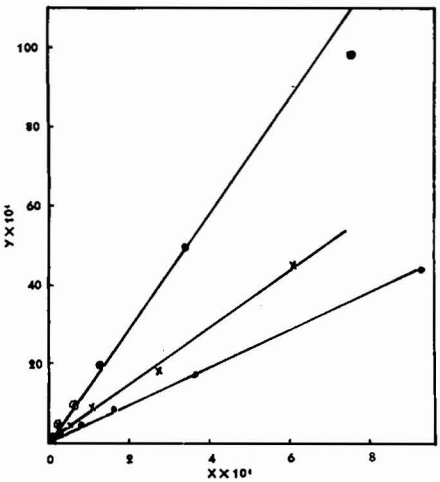

Figure 2. Determination of $K_1K'(K_{d_4} + [H^+])$ at different pH values. Calculated from the data of Figure 1

○ pH 9.30
× pH 9.88
● pH 10.14

The distribution of thallium between the aqueous and organic phases:

$$D = \frac{[Tl_{org}]}{[Tl_{aq}]} \approx \frac{[TlDDTC_{org}]}{[TlY^{2-}]} \quad (6)$$

The following approaching equations can also be described which are valid only under the experimental circumstances (between pH 8–11):

$$C_{Tl} \approx [TlDDTC_{org}] + [TlY^{2-}] \quad (7)$$

$$C_{NaDDTC} \approx [TlDDTC_{org}] + [DDTC^-] \quad (8)$$

$$C_{EDTA} \approx [TlY^{2-}] + [Y^{4-}] + [HY^{3-}] \quad (9)$$

Combining Equations 1, 4–6, 8, and 9, the following simple connection can be derived giving us the possibility for the calculation of K_1 from experimental data.

$$C_{EDTA} - \frac{[TlDDTC_{org}]}{D} = K_1K'(K_{d_4} + [H^+])\frac{C_{NaDDTC} - [TlDDTC_{org}]}{D} \quad (10)$$

Table III. Accuracy of Method

Thallium added, μg	Diverse ions added, μg	Thallium found, μg: Procedure 1–10 ppm (1 g W)	Thallium found, μg: Procedure 0.1–1.0 ppm (10 g W)
0	...	0	0
2.0	...	1.9	1.7 ± 0.4 (std dev)
5.0	...	5.6	5.0 ± 0.7 (std dev)
10.0	...	10.1	...
5.0	As(V), Sb(III), Sn(IV) 100 μg each	5.0	...
		5.6	...
5.0	Fe(III), Co(II), Ni(II), Bi(III) 100 μg each	8.8[a] 4.3[b]	...
		17.5[a] 4.7[b]	...
5.0	Bi(III) 100 μg	4.7[a] 4.5[b]	...
		5.0[a] 4.9[b]	...

[a] Without EDTA.
[b] With addition of 5.0 ml 0.01 *M* EDTA.

where C_{Tl}, C_{NaDDTC}, C_{EDTA} are the total analytical concentrations of thallium, sodium diethyldithiocarbamate, and EDTA.

From extraction experiments at constant pH values, the Y *vs.* X function gives straight lines with different slopes, where the

$$Y = C_{EDTA} - \frac{[TlDDTC_{org}]}{D}$$

$$X = \frac{C_{NaDDTC} - [TlDDTC_{org}]}{D}$$

Figure 2 displays the Y *vs.* X at three different pH values. In Table II the measured and those constants were summarized which were taken from the literature for the calculations.

In that case, when the concentration of sodium diethyldithiocarbamate and EDTA is considerably higher than that of thallium, the distribution ratio of the thallium between chloroform and aqueous phases can be calculated from the following equation at given pH values (between pH 8–11):

$$\frac{1}{D} = \frac{1}{Q} + \frac{1}{K_1K'(K_{d_4} + [H^+])} \times \frac{C_{EDTA}}{C_{NaDDTC}} \quad (11)$$

where Q is the distribution constant of TlDDTC in the absence of EDTA.

Interfering Effect of Different Ions. According to the literature the color reaction between Tl(III) and Methyl Violet is interfered by the following ions: Au(III), B(III), Fe(III), Bi(III), Sb(III), Sn(II), Cd(II), Hg(II), and Cr(VI). From these ions, the boron cannot be extracted by diethyldithiocarbamate, and the Au, Sb, Fe, Cd, Hg can be masked with EDTA and cyanide between pH 8–11 (*2*, *3*). The in-

terfering effect of Bi cannot be eliminated in such a way but according to our experiences the interfering effect of 100/μg of Bi may be neglected for 5/μg of Tl (Table III).

Precision of the Method. Table III shows the accuracy of our method both for 1–10 ppm and for 0.1–1.0 ppm ranges. Even in the lower range, the relative standard deviation doesn't exceed 20% which is general at the determination of such a small amount of impurities.

ACKNOWLEDGMENT

The authors are indebted to Prof. Dr. T. Millner and Dr. L. Bartha for encouraging and helpful advice in the course of this work.

RECEIVED for review April 27, 1970. Accepted August 10, 1970.

Liquid Ion Exchange Electrodes in Mixed Electrolyte Solutions

J. V. Leyendekkers and Michael Whitfield

Division of Fisheries and Oceanography, CSIRO, Cronulla, Sydney, 2230, Australia

Two liquid ion exchange electrodes (Orion Calcium 92-20 and Chloride 92-17) were used to monitor changes in the activity coefficient of calcium chloride in the two aqueous systems $CaCl_2$–$MgCl_2$ and $CaCl_2$–$SrCl_2$ over the ionic strength range 0.1–6 molal at 25 °C. On the basis of comparison with isopiestic data, it is considered that useful estimates of Harned's coefficients can be made with these electrodes provided the selectivity characteristics are not too unfavorable and depending on the complexity of the ionic interactions. Experimental selectivity isotherms are presented for both systems. Parameters are derived, on the basis of simple ion exchange theory and regular solution theory, which facilitate interpolation over the experimental range.

A THOROUGH AND VERY USEFUL review of ion-selective electrodes has recently become available (*1*). Among the important points discussed are two which are relevant here. The first concerns the need for more thermodynamic studies made on a basis of comparison with other, unrelated, methods. For example, how useful are electrodes of the liquid-ion exchange type for measuring activities in mixed electrolyte solutions as compared with isopiestic studies? The second point concerns electrode selectivity. This is of general interest, as many natural systems contain appreciable concentrations of different counterions. Even in the analysis of single electrolyte solutions, complexing reagents and buffers can introduce significant levels of interfering ions. In short, the behavior of the electrode in a mixed electrolyte solution is often the main concern. Since the electrode measures activities, data on the activity coefficients of the electrolytes in mixed solutions will be needed. Data for around 30 two-electrolyte systems are available (*2*, *3*), and a number of theories and empirical relationships (*2–6*) enable reasonable estimates of activity coefficients in multicomponent systems to be made; however, many more experimental data are needed.

In this paper, results are given of measurements of activity coefficients of calcium chloride in the presence of strontium(II) or magnesium(II) over the ionic-strength range 0.1–6 molal. Isopiestic data are available for these two systems and these are used as a guide to the usefulness of the electrodes for such measurements.

The selectivity characteristics of the Orion calcium activity electrode in these systems are also given. This electrode has an acidic organophosphorus exchanger, and from the considerable amount of study on this type of extractant over the past few years (*7*), it has been shown that in general the cation exchange reactions are more complicated than those of exchange resins. However, even though the actual mechanism of the reaction is unknown, the distribution can always be described in terms of a convenient chemical reaction through which meaningful and useful information can be obtained concerning the system studied. We adopted this attitude in a previous paper (*8*) where, by means of a simple theory, the composition of an exchange site was derived. This enabled an estimate to be made of the parameters A and B in the equation

$$\log (a^{m}_{Ca}{}^{2+}/a^{n}_{M}{}^{z+})[(1 - y)/y] = A - B(2y - 1) \qquad (1)$$

where a represents the activity of the ion in the aqueous phase, M the interfering counterion (of charge z), y the mole fraction of exchange sites occupied by calcium(II), and m and n are integers related to the exchange reaction [A and B were formerly represented by log K_t and B', respectively (*8*)]. This facilitated interpolation so that the ionic strength range 0–6 molal was completely covered. The same procedure is adopted here, with some limited extrapolation to extend the range to an ionic strength of 7.5 molal.

EXPERIMENTAL

The same equipment and technique were used as described previously (*8*). The additional reagents used were AR grade

(1) "Ion-Selective Electrodes," Richard A. Durst, Ed., *Nat. Bur. Stand. (U.S.) Spec. Publ.*, **314**, 474 pp (1969).
(2) H. S. Harned and R. A. Robinson, "Multicomponent Electrolyte Solutions," in The International Encyclopedia of Physical Chemistry and Chemical Physics, Topic 15, Vol. 2, Pergamon Press, London, 1968.
(3) R. M. Rush, Oak Ridge National Laboratory Report ORNL-4402, UC-4-Chemistry, 1969.
(4) G. Scatchard, *J. Amer. Chem. Soc.*, **90**, 3124 (1968).
(5) J. Leyendekkers, *J. Phys. Chem.*, **74**, 2225 (1970).
(6) Y. C. Wu, R. M. Rush, and G. Scatchard, *ibid.*, **73**, 2047 (1969).
(7) Y. Marcus and A. S. Kertes, "Ion Exchange and Solvent Extraction of Metal Complexes," Wiley-Interscience, London, 1969.
(8) Michael Whitfield and J. V. Leyendekkers, ANAL. CHEM., **42**, 444 (1970).

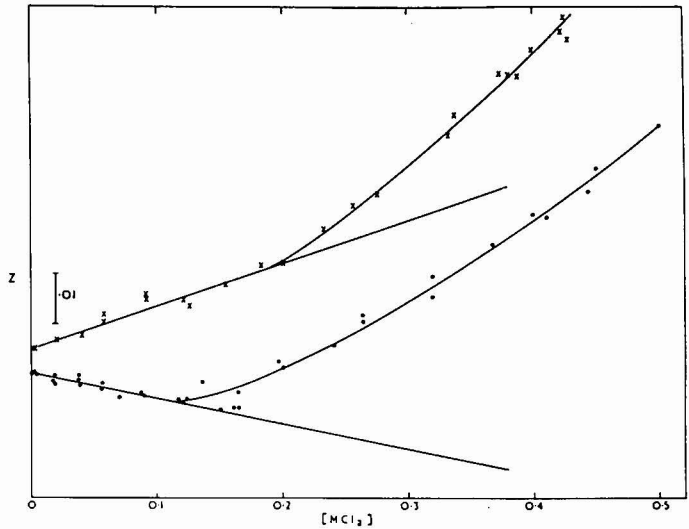

Figure 1. Titration curves for ionic strength 3 molal

$Z = 3 \log \gamma_{\pm CaCl_2} + \text{const} - \log y$, slope $= -9\alpha_{12}$ for linear section (Equations 2 and 3)
Z is dimensionless, 0.01 unit represents a change in ΔE of ~2 mV
Upper curve: $CaCl_2$–$MgCl_2$
Lower curve: $CaCl_2$–$SrCl_2$

strontium chloride ($SrCl_2 \cdot 6H_2O$) and magnesium metal which was neutralized with hydrochloric acid. Stock solutions were prepared and standardized by titrating with DCTA, using calcium chloride (prepared from Mallinckrodt calcium carbonate) as the primary standard and the Orion divalent electrode (92–32) to monitor the end point. The stock solutions were diluted on a weight basis. Temperature was maintained at 25.0 ± 0.1 °C and pH at 7.5–8.

RESULTS AND DISCUSSION

Activity Coefficients. The analysis of the results was carried out as described previously (*8*). The Harned slopes (α_{12}) were determined on the basis of the relationships

$$\Delta E/S - \log [Ca][Cl]^2 = 3 \log \gamma_{\pm CaCl_2} + \text{constant} - \log y \quad (2)$$

where ΔE is the difference in potential between the calcium and chloride electrodes, the square brackets denote concentrations, S represents $2.303RT/2F$ and has the value 29.58 mV at 25°, y is defined above, and

$$\log \gamma_{\pm CaCl_2} = \text{constant} - \alpha_{12} I_{MCl_2} \quad (3)$$

where I_{MCl_2} is the ionic strength of either strontium or magnesium chloride. Provided y is close to 1.00 and Harned's rule is obeyed, the lefthand side of Equation 2 *vs.* $[MCl_2]$ should give a linear plot of slope $-9\alpha_{12}$. Figure 1 shows representative plots for the two systems.

Linearity holds only for 10% (strontium chloride) to 20% (magnesium chloride) of the curve, after which the term (log y) becomes significant. This represents a maximum change in ΔE of only 1–3 mV as the ion interactions in the alkaline earth systems are small. Nevertheless, it was possible to estimate α_{12} from a least-squares fit of the points along the linear section (Table I). On the basis of comparison with the isopiestic data (*9*, *10*) the results at the higher concentrations are surprisingly good in view of the severe limitations imposed by the nonspecificity of the electrode for calcium. The assump-

Table I. Values of α_{12} Estimated from Activity Measurements (Reciprocal ionic strength units)

	Ionic strength	This work	Mean	Isopiestic
$CaCl_2$–$MgCl_2$	0.1	−0.047	−0.038	
		−0.029		
	0.3	−0.017	−0.022	
		−0.028		
	0.7	−0.012	−0.010	
		−0.009		
	3	−0.0107	−0.0100	−0.0096 (*9*)
		−0.0093		
	6	−0.0117	−0.0114	−0.0111
		−0.0110		
$CaCl_2$–$SrCl_2$	0.06	0.028	0.022	
		0.017		
	0.3	0.003	0.0035	0.0055 (*10*)
		0.004		
	3	0.0060	0.0054	0.0055
		0.0047		
	6	0.0047	0.0044	0.0061
		0.0040		

(9) R. A. Robinson and V. E. Bower, *J. Res. Nat. Bur. Stand.*, *A*, 70, 305 (1966).
(10) Souheng Wu, University of Kansas, Ph.D. Thesis, 66–6062 University Microfilms, Inc., Ann Arbor, Michigan, 1965.

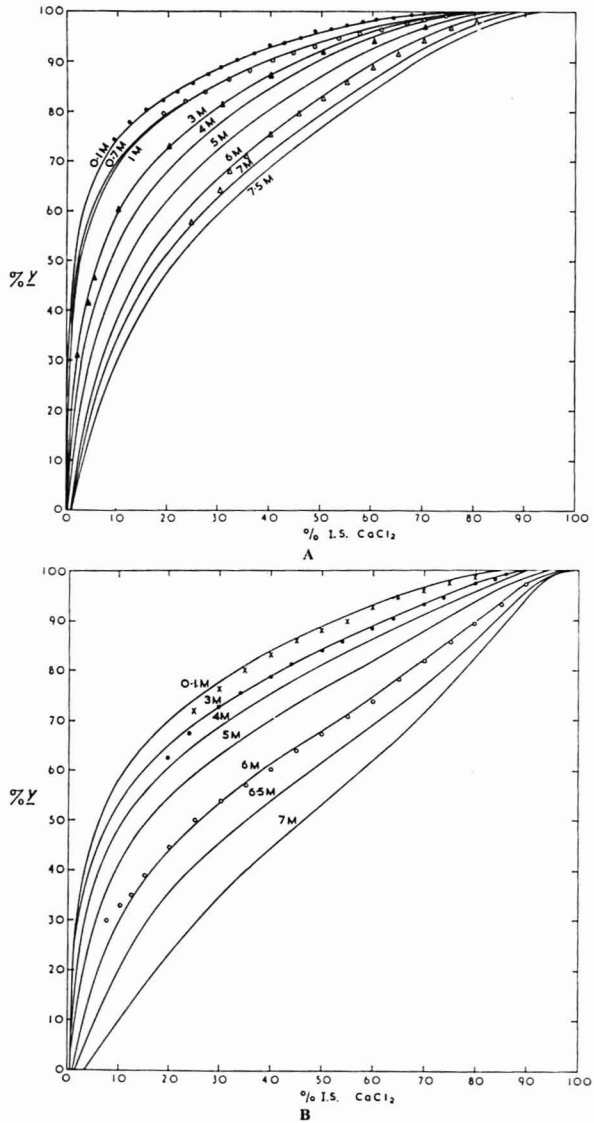

Figure 2. Selectivity isotherms for the Orion calcium activity electrode at constant ionic strength at 25 °C and pH ~7.5. Symbols represent experimental points

(A) Aqueous $CaCl_2$–$MgCl_2$; ● 0.1 molal; ○ 0.7 molal; ▲ 3 molal; △ 6 molal
(B) Aqueous $CaCl_2$–$SrCl_2$; × 0.3 molal; ● 3 molal; ○ 6 molal. —— curves derived from Equation 1 and Table II

tion that the electrode behavior is Nernstian [ref. *(8)* and implied in our use of Equation 2] seems justified, even though deviations could be expected at these concentrations *(11)*. The low values of α_{12} for the system with strontium chloride at 6 molal may be due to such deviations. As far as we know, there are no comparative data at the lower concentrations so that no firm conclusions can be made regarding the accuracy of these data.

The overall results suggest that the electrodes should be useful for estimating changes in activity coefficients in two-electrolyte systems provided the selectivity does not exceed that shown here. Results for the NaCl–$CaCl_2$ system at an ionic strength of 3.15*m*, using the Orion (98-20-02) exchanger, showed that the selectivity for sodium was too high at this ionic strength for an accurate estimate of α_{21} to be made *(12)*.

(11) Rima Huston and J. N. Butler, ANAL. CHEM., **41**, 200 (1969).

(12) "Ion-Selective Electrodes," Richard A. Durst, Ed., *Nat. Bur. Stand. Spec. Publ.*, **314**, 184 (1969).

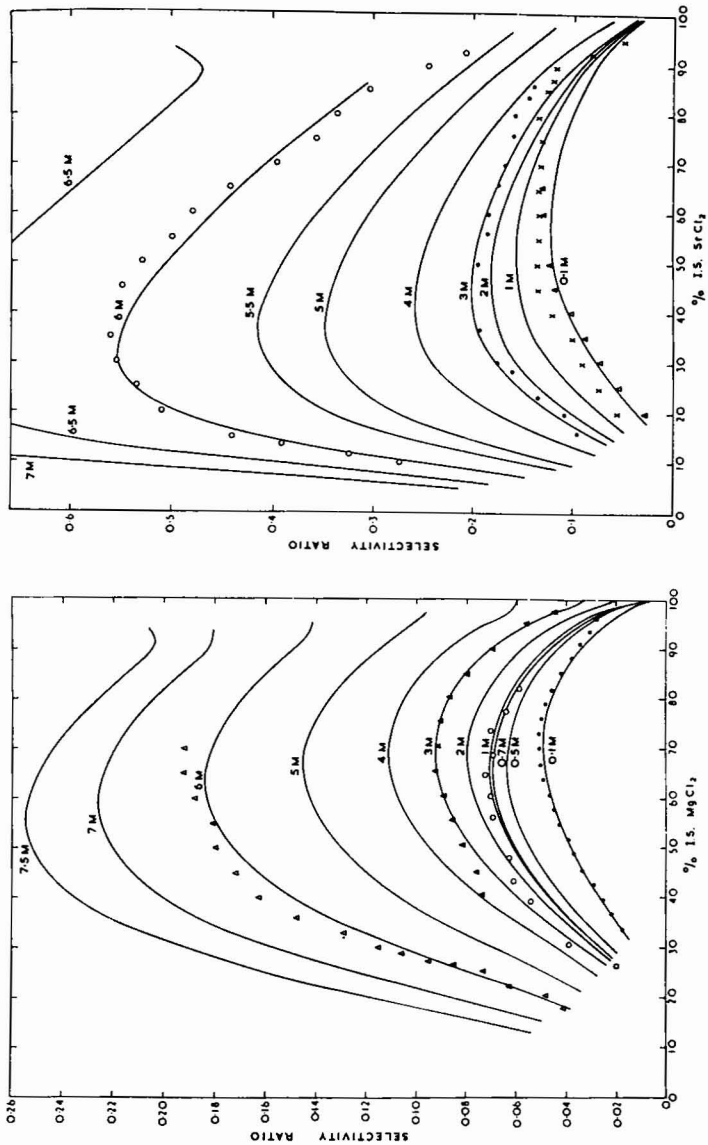

Figure 3. Selectivity curves based on estimates of K' at ionic strengths shown (molal)
Symbols represent experimental values of K'
(*A*) Aqueous $CaCl_2$–$MgCl_2$, ● 0.1 molal; ○ 0.7 molal; ▲ 3 molal; △ 6 molal
(*B*) Aqueous $CaCl_2$–$SrCl_2$, △ 0.06 molal; × 0.3 molal; ● 3 molal; ○ 6 molal

Even so, a tangent drawn to the first part of the curve gives a value of around -0.027 compared with -0.0165 for the isopiestic method, which shows that at least a reasonable estimate can be made in a case as unfavorable as this. However, it is difficult to generalize, since apart from selectivity, the magnitude and complexity of the ion interactions will influence the results. For instance, if Harned's rule is not obeyed, this would greatly complicate the analysis. On the other hand, if the alpha coefficients are relatively large and Harned's rule is obeyed, the accuracy should be higher.

Selectivity. The values of y were estimated from the deviations of the smoothed curve from the Harned slope (Figure 1). The experimental isotherms could then be constructed (Figure 2) and the selectivity ratio K' (Figure 3)

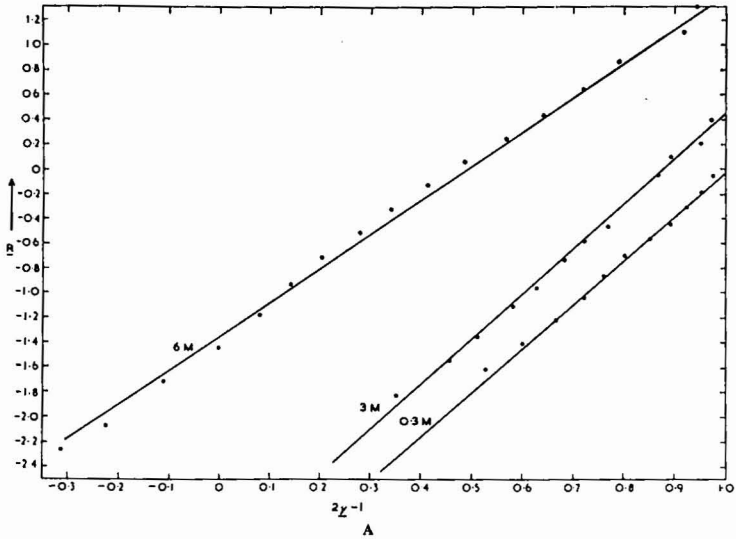

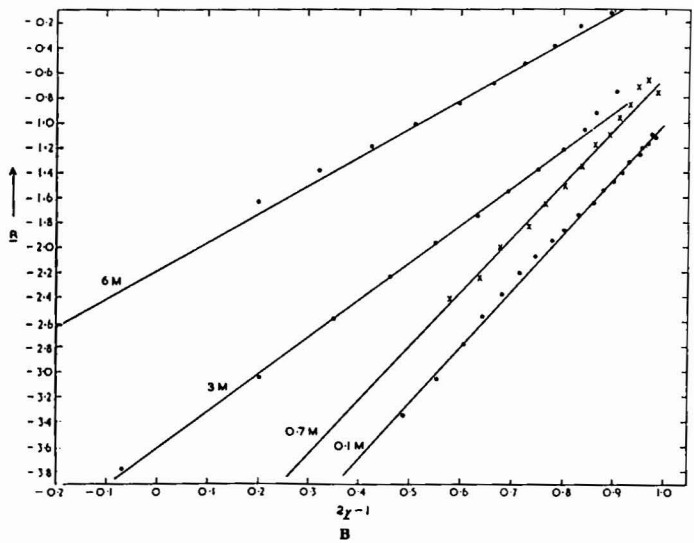

Figure 4. Linear fit of the data on the basis of three divalent ions occupying an exchange site, $m = n = 3$ in Equation 1

R represents 3 log $(a_{Ca^{2+}}/a_{M^{2+}}) + \log(1 - y)/y - 3 \log (\gamma_{Ca^{2+}}/\gamma_{M^{2+}})$
(*A*) M^{2+} represents Mg^{2+}
(*B*) M^{2+} represents Sr^{2+}

calculated from the relationship

$$a_{Ca^{2+}}/a_{M^{2+}} = K'[y/(1 - y)] \quad (4)$$

On the basis of regular solution theory and simple ion exchange concepts (*8*), the results indicate that three divalent ions (M^{2+}) occupy an exchange site so that $m = n = 3$ in Equation 1. The fit is illustrated in Figure 4, where the concentrations have been used for simplicity. This will not affect the closeness of the fit very much since log $\gamma_{Ca^{2+}}/\gamma_{M^{2+}}$ (equivalent to log $\gamma_{\pm CaCl_2}/\gamma_{\pm MCl_2}$) is approximately constant at a given ionic strength. The activities were used in all other cases (*e.g.*, Equation 4 and Table II). Values of the mean molal activity coefficients for the single electrolyte solutions were obtained from references (*13*) and (*14*). The

(13) Roger Parsons, "Handbook of Electrochemical Constants," Butterworths, London, 1959.
(14) H. S. Harned and B. B. Owen, "The Physical Chemistry of Electrolytic Solutions," 3rd ed., ACS Monograph 137, Reinhold Publishing Corp., New York, N. Y., 1958.

Table II. Selectivity Parameters of Equation 1 (with $m = n = 3$)

Ionic strength	$CaCl_2$–$MgCl_2$		$CaCl_2$–$SrCl_2$	
	$-A$	$-B$	$-A$	$-B$
0.1	5.60	4.50	3.52[a]	3.40[a]
0.3			3.52	3.50
0.7	4.99	4.20[b]	3.50[a]	3.60[a]
1.0[a]	4.78	4.02	3.47	3.66
2.0[a]	4.19	3.46	3.36	3.76
3.0	3.71	3.02	3.14	3.66
4.0[a]	3.24	2.66	2.66	3.44
5.0[a]	2.78	2.42	2.10	3.20
6.0	2.37	2.25	1.24	2.80
7.0[a]	2.09	2.20	0.08	2.10

[a] Interpolated values.
[b] Smoothed value.

Harned coefficients of references (*9*) and (*10*) were used as far as possible, otherwise our experimental values or estimates (interpolations) were used. The variations of A and B with ionic strength were obtained by drawing smooth curves through the experimental data in Table II. Values of these parameters at other ionic strengths could then be estimated and the corresponding isotherms and selectivity curves constructed (Figures 2 and 3).

The experimental points fit the predicted curves reasonably well, although not over the whole composition range. Deviations are greatest for the low ionic strengths where the smoothed and experimental values of the parameters A and B differed by 2–3%. The change of selectivity with solution composition is similar to that found for the calcium chloride–sodium chloride systems (*8*) and, as expected from the manufacturer's handbook, the interference from the alkaline earth cations (listed as $K'_{Sr} = 0.017$, $K'_{Mg} = 0.014$) is greater at lower concentrations than that of the sodium ion ($K'_{Na} = 0.001$), the magnesium effect being less than that of strontium. The effect of ionic strength is relatively much smaller, however, so that sodium interference exceeds that of the alkaline earths at higher concentrations.

In the simple chloride systems studied so far it does not appear that the anion plays a major role in the ion exchange process; however, other anions (*e.g.*, the nitrate ion) may be extracted with the cation at the higher concentrations so that mixed complexes are formed in the organic phase. In extreme cases, the extraction may occur *via* a solvation mechanism characteristic of non-ionic phosphorylated extractants (*7*). It is not known, therefore, whether the selectivity data given here will apply generally to alkaline earth salts at high ionic strengths.

Received for review September 14, 1970. Accepted December 7, 1970.

Effects of Structure of Peptide Stationary Phases on Gas Chromatographic Separations of Amino Acid Enantiomers

J. A. Corbin,[1] J. E. Rhoad,[2] and L. B. Rogers
Department of Chemistry, Purdue University, Lafayette, Ind. 47907

The gas chromatographic behavior is described for a series of systematically-substituted, optically-active, peptide derivatives used as stationary phases. Results with pairs of phases containing one racemic center indicated that the major part of the separation occurred at the amide end of the dipeptide. Nevertheless, α values were sensitive to changes in the structure of the side group at the ester end. A steady decrease in α occurred as the bulkiness of the peptide side groups decreased. A tripeptide derivative produced α values nearly as large as the corresponding dipeptide and showed a small, but significant, increase in chromatographic temperature stability. However, underivatized solid peptides used as stationary phases did not show enantiomer separations. An increase in the bulkiness of the solute ester group produced an increase in α on all phases studied. An increase in bulkiness at the solute α carbon atom produced a consistent, but not straightforward, effect.

The compound *N*-TFA(trifluoroacetyl)-L-valyl-L-valine cyclohexyl ester (vv) has been shown to be an excellent stationary phase for the separation of the enantiomers of a wide variety of amino-acid derivatives (*1–3*). Recently, a second dipeptide phase, *N*-TFA-L-phenylalanine-L-leucine cyclohexyl ester, was synthesized which also gave good enantiomer separations and could be used at higher operating temperatures (*4*). The particular ease of separability associated with the dipeptide phase was attributed to the possibility of formation of three hydrogen bonds in a diastereomeric bridged association complex between the solute and solvent.

While there have been detailed studies of solute behavior on the above stationary phases, there has been no study of systematic changes in the peptide stationary phase itself. The main purpose of this study was, therefore, to investigate those factors which were most important in leading to an enantiomer separation with peptide phases so that, hopefully, new and better stationary phases, suitable for specific applications, could be prepared. First, a study was done to

[1] Present address, Celanese Fibers Co., Charlotte, N. C. 28201
[2] Present address, Department of Chemistry, Vanderbilt University Nashville, Tenn. 37203

(1) E. Gil-Av, B. Feibush, and R. Charles-Sigler in "Gas Chromatography 1966," A. B. Littlewood, Ed., The Institute of Petroleum, London, England, 1967, p 227.
(2) E. Gil-Av and B. Feibush, *Tetrahedron Lett.*, 35, 3345 (1967).
(3) S. Nakaparksin, P. Birrell, E. Gil-Av, and J. Oro, *J. Chromatogr. Sci.*, 8, 177 (1970).
(4) W. A. Koenig, W. Parr, H. A. Lichtenstein, E. Bayer, and J. Oro, *ibid.*, p 183.

determine which end of the stationary phase was more significant in bringing about the separation and whether two asymmetric centers were necessary for resolution. Then, the effects of systematic changes in the side chains of the peptide were determined. Specifically, we were interested in determining if the two amino acid portions of the peptide acted independently of one another and the significance of a change on the amide end relative to a similar change in the ester portion. Also, since *N*-PFP (pentafluoropropionyl) solutes have been shown to be more stable and, in some cases, to give larger α values than the corresponding *N*-TFA derivatives, it was of interest to compare the chromatographic behavior of the *N*-PFP and *N*-TFA stationary phases with respect to *N*-PFP and *N*-TFA solutes (*5*, *6*).

Previous investigators have worked only with dipeptide stationary phases. Since it was thought that higher polymer peptides might have better chromatographic temperature stability, a tripeptide was derivatized for comparison with the corresponding dipeptide derivative. Also, since enantiomers have recently been separated on an optically active solid adsorbent, insoluble, solid, underivatized peptides, stable to above 200 °C, were investigated (*7*).

EXPERIMENTAL

Reagents. The *N-tert*-BOC (tertiary-butyloxycarbonyl) derivatives of L-valine, L-leucine, and glycine, *N*-CBZ (carbobenzoxy) derivative of DL-valine, L-valine, L-leucine, DL-alanine ethylester hydrochloride DL-alanine methylester hydrochloride, and DL-valine methylester hydrochloride were purchased from Mann Research Laboratories, New York, N.Y. The glycine, DL-alanine, and trifluoroacetic acid were obtained from Matheson, Coleman and Bell, Norwood, Ohio. The poly-L-phenylalanine, and *N*-TFA-*L*-valyl-L-valine cyclohexyl ester were from Miles Laboratories, Elkhart, Ind. The 30% HBr in glacial acetic acid and dicyclohexylcarbodiimide were from Eastman Organic Chemicals, Rochester, N.Y. The L-leucyl-L-leucyl-L-leucine was obtained from Schwarz BioResearch, Orangeburg, N.Y., and the L-valyl-L-leucine from Nutritional Biochemicals Corp., Cleveland, Ohio. The trifluoroacetic anhydride was from Aldrich Chemical Co., Milwaukee, Wis., and the pentafluoropropionyl anhydride from K and K Laboratories, Plainview, N.Y. All chemicals were used without further purification.

The individual peptide stationary phases were prepared in one of two ways. Either the free peptide was esterified and trifluoroacetylated or an amino acid ester was coupled to a *tert*-BOC or CBZ-protected amino acid followed by trifluoroacetylation.

The *N*-PFP-L-valyl-L-leucine cyclohexyl ester (p-vl), *N*-TFA-L-valyl-L-leucine cyclohexyl ester (vl) and N-TFA-L-leucyl-L-leucine cyclohexyl ester (lll) phases were prepared by the direct esterification procedure which consisted of the following. One gram of the peptide was mixed with 100 ml of reagent grade cyclohexanol. The mixture was heated to 100 °C and dry HCl bubbled in for 60 minutes to produce a clear solution. The reaction mixture was then maintained at 100 °C for 10 hours with occasional addition of HCl. At the end of this period, the cyclohexanol was removed by vacuum distillation to produce a clear gum. In the vl case, the peptide ester hydrochloride was precipitated by addition of dry ether to produce a white solid. (However, the lll derivative could not be precipitated in that way. So the next step was carried out on the entire solution.) The peptide ester was dissolved in 50 ml of CH_2Cl_2, cooled in an ice bath, and reacted with a fivefold excess of anhydride for 1 hour. The solvent, excess anhydride, and by-products were removed with a rotary evaporator producing an oil which was taken up in approximately 5 ml of dry ether.

The product was then purified by preparative gas chromatography using SE-30 as a stationary phase. In general, the reaction mixtures contained 3–5 impurity peaks. The product was always the last compound to emerge and was well separated from the other components (peptide derivative peak $k \simeq 4$). Final product yield was 50–75%.

The *N*-TFA-L-leucyl-L-valine cyclohexyl ester (lv), *N*-TFA-L-leucyl-L-leucine cyclohexyl ester (ll), *N*-TFA-glycyl-L-valine cyclohexyl ester (gv), *N*-TFA-L-valyl-glycine cyclohexyl ester (vg), *N*-TFA-DL-valyl-L-valine cyclohexyl ester (DL-L) and *N*-TFA-L-valyl-DL-valine cyclohexyl ester (L-DL) phases were prepared by a coupling procedure similar to that described by Koenig *et al.* with the following minor modifications (*4*). The amino acid ester reaction mixtures were heated to 100 °C, rather than leaving them at room temperature, so as to achieve solution. The crude amino acid ester products were precipitated with $CHCl_3$ prior to recrystallization from CH_2Cl_2 and ether.

In the DL-L case, the CBZ derivative of DL-valine was used rather than the *tert*-BOC derivative. The CBZ protecting group was removed by treatment with 25 ml of 30% HBr in glacial acetic acid at 35 °C for 30 minutes. The free peptide ester was then precipitated by addition of 500 ml of dry ether. The rest of the procedure was the same.

The peptide trifluoroacetylation procedure for all phases was the same as described above. Unlike the procedure of Koenig *et al.* (*4*), we were unable to find a suitable recrystallization method for these phases. Therefore, the phases were purified by preparative-scale gas chromatography in the same manner as with the direct esterification products.

The identity and chemical purity of the stationary phases were carefully considered. The preparative-scale gas chromatographic purification procedure afforded a high degree of purity not possible by most other purification methods. However, as a check, a microanalysis was run on the lv phase. The results showed that it was the desired product and was indeed of very high purity. The identities of all products were checked by IR and mass spectrometry using the Miles vv phase as a reference. There was no question that the phases were the desired compounds.

Optical purity was also of prime concern. It is generally accepted that no racemization takes place during esterification under acid conditions (*8*). However, as a check, the *N*-TFA derivatives of the L- and DL-valine cyclohexyl esters were put through a vv column, and they produced a single peak and two peaks in a ratio of 1:1, respectively. The stationary phases prepared by the direct peptide esterification method were assumed to be optically pure since the starting peptides were optically pure and the process did not involve any steps which would have led to racemization. Also, the coupling process, performed under the given conditions, should not have produced racemization (*9*). Therefore, all stationary phases were assumed to be pure ones of the desired optical composition.

The amino acid derivatives used as solutes in the study were prepared from commercial or laboratory-prepared ester hydrochlorides by a previously described method (*7*). The identity and chemical purities of the amino acid derivatives were confirmed by NMR and mass spectrometry.

Apparatus. For all work with capillary columns, an Aerograph 660 gas chromatograph, modified to minimize the dead volume in the system and equipped with a Hamilton

(5) W. Parr, C. Yang, J. Pleterski, and E. Bayer, *J. Chromatogr.*, **50**, 510 (1970).
(6) E. Anggard and G. Sedvall, ANAL. CHEM., **41**, 1250 (1969).
(7) J. A. Corbin and L. B. Rogers, *ibid.*, **42**, 974 (1970).
(8) M. Bodanszky and M. A. Ondetti, "Peptide Synthesis," Interscience Publishers, New York, N. Y., 1966, p 145.
(9) D. T. Bessette, Mann Research Laboratories, Orangeburg, N. Y., private communication, April 17, 1970.

inlet splitter, was used. The chromatograph was operated at a detector temperature of 180 °C, an injection temperature of 200 °C, and at different column temperatures. During studies of the effect of temperature change, fifteen minutes were allowed for equilibration after each new temperature had been reached, unless otherwise stated. A flow rate of approximately 2 ml/min of nitrogen, dried using 5A molecular sieve traps at ambient temperatures, was usually used. An Esterline-Angus Speed Servo recorder recorded the chromatograms.

Open tubular, borosilicate glass columns were used throughout the study of enantiomer separations. The 40 m by 0.25 mm columns were cleaned, drawn, and conditioned as previously described (7). They were coated using 20% w/v solutions in dry ether (*10*) except the poly-L-phenylalanine and solid tripeptide columns which were prepared from saturated solutions of these compounds (≃3% w/v) in dichloracetic acid and water, respectively.

For preparative-scale purification of the stationary phases, an Aerograph 202 gas chromatograph equipped with a thermoconductivity detector was used. The stainless steel columns were 3.1 m by 4 mm packed with 5% SE-30 on DMCS-treated, acid-washed, 80/100 mesh Chromosorb G. The column was maintained at 285 °C, the injection port at 310 °C, and the detector at 310 °C with a helium flow rate of approximately 40 ml/min. The sample concentrations were adjusted so that a 50-μl injection produced 2–3 mg of product upon collection.

Capacity ratio, k, separation factor, α, and resolution, R, were calculated in the same way as before (7). The k and α values were reproducible within ±0.003. Values for R could be reproduced within 0.1 unit.

RESULTS

Effect of Individual Asymmetric Centers. To determine the relative contribution to the overall enantiomer separation of each of the two centers in the dipeptide, two pairs of compounds, L-DL/DL/L *N*-TFA-valyl-valine cyclohexyl ester and vg/gv, were synthesized. It was assumed that, in the *L*-DL and DL-L cases, the L and D fractions of the racemic center would contribute equal and opposite interactions and, thus, cancel out the enantiomer separating ability of that center. Because glycine is not optically active, the vg and gv dipeptides made with that amino acid contained only one asymmetric center.

As shown in Table I, the L-DL phase gave excellent enantiomer separations with α values for the isopropyl alanine derivative which were only approximately 0.1 unit less than the vv phase. Surprisingly, the DL-L compound gave no detectable enantiomer separations. These results suggested that the amide end of the stationary phase made a far greater contribution to the separation than the ester end.

Unfortunately, the gv and vg stationary phases had quite different physical properties so that a completely comparable study could not be made. Although the gv phase behaved similarly to the other dipeptide phases (mp ≃90 °C), the vg phase was a high-melting white solid (mp = 155 °C) which made it unsuitable as a stationary phase. Like the DL-L valyl-valine which produced no observable separation of the enantiomers of the isopropyl alanine derivative, the gv produced only a very small separation. The k values at 100 °C were 10.46 and 10.57, respectively, which represented an α value of approximately 1.01. Again, these results suggested that the differential interaction at the ester end of the stationary phase produced only a small enantiomer separation.

(10) L. S. Ettre, "Open Tubular Columns in Gas Chromatography," Plenum Press, New York, N. Y., 1965, p 82.

Table I. k_1, α, and R Values for Enantiomers of *N*-TFA-DL-Alanine Isopropyl Ester as a Function of Temperature on Dipeptide Stationary Phases Containing Only One Asymmetric Center

Stationary phase	90 °C			110 °C		
	k_1	α	R	k_1	α	R
N-TFA-L-valyl-DL-valine cyclohexyl ester	9.56	1.102	1.39	3.89	1.073	0.83
N-TFA-DL-valyl-L-valine cyclohexyl ester	3.53	[a]	[a]	2.16	[a]	[a]

[a] No enantiomer separation was observed.

Effects of Systematic Changes in the Amino Acid Composition of Peptide Stationary Phases. To determine the effects on the α values of enantiomers of the side groups on a dipeptide, comparisons were made of isobutyl (leucyl) and isopropyl (valyl) derivatives, In all cases, $\ln k$ *vs.* $1/T$ plots were essentially straight lines between 90 and 110 °C so Table II shows only the results at the temperature extremes. When valine was replaced by leucine in a series of dipeptide stationary phases, α for the isopropyl and ethyl alanine derivatives was always less by nearly the same amount, regardless of whether the substitution was at the amide end or ester end. However, the ethyl valine derivative was an exception on both mixed phases (vl, lv), the α value for lv being greater than that for vv.

Apparently, the larger α values associated with the valine-containing phases were the result of greater steric interaction with the isopropyl group, where the branching is closer to the asymmetric carbon, than with the isobutyl group of leucine. However, the results with the ethyl valine solute indicated that this was not a rigid rule and depended on the specific solute involved. In any case, the nearly equal effects on α of substituents at the amide and ester ends of the dipeptide indicated that important secondary steric contributions were made by the ester end of the dipeptide, even though the primary bonding interaction occurred at the amide end.

The stationary phases showed similar abilities to separate the individual amino acid derivatives (the compounds themselves, not their enantiomers). For example, using the data in Table II to calculate an α_1 value from the k_1 value for each of two compounds, one finds that the α_1 values for the ethyl valine derivative relative to the isopropyl alanine derivative ranged between 1.51 and 1.57 at 90 °C. This behavior was not unexpected considering that the only difference between a leucine moiety and a valine moiety was an additional CH_2 group in the former.

Surprisingly, in light of the virtually identical α_1 values, Table III shows that the various peptide phases differed greatly in their relative abilities to resolve different pairs of enantiomers. In other words, the relative widths of the peaks were greatly different even though the ratio of k_1 (and k_2) values were nearly the same. To minimize the effect of column instability, the pairs of compounds shown in Table III were chromatographed immediately after one another in as short a time-span as possible. Because the resolving abilities of the columns were changing slowly with time and the sample sizes were not exactly the same, the reported values were precise only within ±0.1. However, some of the observed differences were well outside this range of experimental error. Apparently, the band broadening for the otherwise symmetrical peaks depended strongly on the individual solute and differed from phase to phase. This

Table II. k, α, and R Values for Enantiomers of a Series of Amino Acid Derivatives on a Series of Peptide Stationary Phases as a Function of Temperature

	Amino acid derivative																		
	N-TFA-DL-alanine isopropyl ester						*N*-TFA-DL-valine ethyl ester						*N*-TFA-DL-alanine ethyl ester						
	90 °C			110 °C			90 °C			110 °C			90 °C			110 °C			Methane
Stationary phase	k_1	α	R	k_1	α	R	k_1	α	R	k_1	α	R	k_1	α	R	k_1	α	R	
N-TFA-L-valyl-L-valine cyclohexyl ester	9.27	1.126	2.40	4.18	1.112	1.23	14.57	1.080	1.51	6.18	1.064	0.80	8.30	1.107	1.79	3.70	1.079	1.00	111
N-TFA-L-valyl-L-leucine cyclohexyl ester	8.71	1.118	2.75	3.65	1.095	1.17	13.85	1.061	1.44	5.33	1.043	0.60	7.83	1.095	2.07	3.24	1.075	1.00	114
N-TFA-L-leucyl-L-valine cyclohexyl ester	13.04	1.114	2.52	5.95	1.090	1.23	19.59	1.087	2.14	8.55	1.066	0.76	11.37	1.095	2.31	5.35	1.075	1.05	110
N-TFA-L-leucyl-L-leucine cyclohexyl ester	9.88	1.103	1.91	4.21	1.076	1.01	14.77	1.062	1.22	6.00	1.049	0.70	8.70	1.081	1.40	3.77	1.064	0.85	114
N-TFA-L-leucyl-L-leucyl-L-leucine cyclohexyl ester	6.67	1.096	2.15	2.59	1.072	1.11	10.07	1.061	1.60	3.81	1.045	1.00	5.73	1.076	1.75	2.32	1.058	1.09	110

Table III. Ratios of Resolutions of Enantiomers of Amino Acid Derivatives as a Function of Temperature for a Series of Peptide Stationary Phases

	90 °C		110 °C	
Stationary phase	R_1[a]/R_2	R_1/R_3	R_1/R_2	R_1/R_3
N-TFA-L-valyl-L-valine cyclohexyl ester	1.4	1.2	1.5	1.2
N-TFA-L-valyl-L-leucine cyclohexyl ester	1.9	1.3	1.9	1.2
N-TFA-L-leucyl-L-valine cyclohexyl ester	1.2	1.1	1.6	1.2
N-TFA-L-leucyl-L-leucine cyclohexyl ester	1.5	1.3	1.4	1.2
N-TFA-L-leucyl-L-leucyl-L-leucine cyclohexyl ester	1.3	1.2	1.1	1.0
N-PFP-L-valyl-L-leucine cyclohexyl ester	1.6	1.2	1.6	1.0

[a] R_1 = Resolution of enantiomers of *N*-TFA-DL-alanine isopropyl ester. R_2 = Resolution of enantiomers of *N*-TFA-DL-valine ethyl ester. R_3 = Resolution of enantiomers of *N*-TFA-DL-alanine ethyl ester.

latter aspect should be considered in any future attempts to tailor individual phases for special applications.

Dipeptide Phases *vs.* Larger Polymers. Table II also presents a comparison of α values on a tripeptide derivative (III) and its corresponding dipeptide derivative (II). This particular pair was chosen because the starting materials were readily available. All solutes gave slightly smaller α values on the tripeptide phase than on the corresponding dipeptide phase. However, the absolute differences were quite small and, for many practical applications, the tripeptide could be substituted for the dipeptide.

The fact that the tripeptide produced a separation indicated that the ester and amide ends of the molecule did not need to be in close proximity so as to cause a differential steric interaction. Apparently, the mechanism does not necessarily involve a joint interaction with both ends of the phase since the distance between the amide and ester portions was too great to be spanned by the solutes, assuming a linear tripeptide conformation.

One reason for preparing the tripeptide phase was to investigate its chromatographic temperature stability relative to the corresponding dipeptide. It was thought that, since it was a larger molecule with a higher boiling point (as evidenced by a longer retention time on the SE-30 column), the tripeptide phase might be more suitable for use at high temperatures than the more volatile dipeptide phase. This was indeed the case. The rate of loss of resolution was much less at 120 °C for the tripeptide than the dipeptide phase. Operation at 120 °C for 60 minutes produced losses in R of 0.3 and 0.1 unit for the dipeptide and tripeptide, respectively. In general, the tripeptide phase, at approximately 10 C° higher termperature than the correrponding dipeptide, had the same rate of loss of resolution. Attempts to use the tripeptide phase at 130 °C showed that the rate of degradation was so great that the column was essentially useless after 30 minutes.

Another interesting point was that each of the three tripeptide columns used always produced k values which were approximately 30% smaller than the dipeptide phases, even though the coating solutions were the same weight/volume per cent. Since there was no way of accurately measuring the amount of stationary phase in the column, smaller k values may have been the result of a smaller quantity of stationary phase retained in the column or of a smaller effective fraction of active sites.

Since enantiomer separations have been done by adsorption on a solid stationary phase (7), attempts were made to use solid poly-L-phenylalanine (molecular weight range 3000–5000) and the solid underivatized L-leucyl-L-leucyl-L-leucine tripeptide. These materials were solids which decomposed without melting at temperatures in excess of 200 °C. Columns coated with these compounds were quite difficult to prepare since both were nearly insoluble in most common solvents.

As adsorbents, both of the solid peptides produced very small k values and no detectable enantiomer separations. Representative k values at 70 °C for the isopropyl alanine derivative were 1.74 and 0.29 for poly-L-phenylalanine and for the tripeptide, respectively. The fact that the k values were small and the peaks were sharp indicated that there was little or no exposed glass. Hence, adsorption on the solid underivatized peptide appears to hold little promise.

***N*-PFP *vs.* *N*-TFA Stationary Phases.** *N*-PFP derivatives produced larger α values than the corresponding *N*-TFA derivative on a solid ureide stationary phase (7). Parr *et al.* reported a larger α value for the enantiomers of some *N*-PEP-DL derivatives than for the corresponding *N*-TFA

Table IV. k, α, and R Values for Enantiomers of a Series of Amino Acid Derivatives on *N*-PFP and *N*-TFA Peptide Stationary Phases at 110 °C

Stationary phase	Amino acid derivatives: *N*-TFA-DL-alanine isopropyl ester k_1	α	R	*N*-TFA-DL-alanine ethyl ester k_1	α	R	*N*-PFP-DL-alanine ethyl ester k_1	α	R	Methane, sec
N-TFA-L-valyl-L-leucine cyclohexyl ester	3.65	1.095	1.17	3.24	1.075	1.00	2.73	1.068	0.79	112
N-PFP-L-valyl-L-leucine cyclohexyl ester	4.90	1.088	0.78	4.31	1.069	0.76	3.79	1.063	0.51	114

derivative (*5*, *11*). Also, in a study of catecholamine metabolites, *N*-PFP derivatives were shown to be more stable than *N*-TFA derivatives (*6*). Therefore, it was of interest to compare the chromatographic properties of an *N*-PFP phase with its corresponding *N*-TFA derivative. We were particularly interested in determining if the *N*-PFP phase produced larger α values with *N*-PFP solutes.

Table IV shows that for the p-vl and vl phases used for this study, the *N*-PFP solute gave only slightly smaller α values but much smaller k values and R values than the corresponding *N*-TFA derivative on both phases. The same was true at all temperatures. The ratio of α values on both stationary phases was quite temperature sensitive, those on the *N*-PFP changing somewhat more. For example, at 90 °C, the α values of *N*-PFP and *N*-TFA DL-alanine ethyl ester were virtually equal (1.087 *vs.* 1.089), while at 110 °C the former were somewhat smaller (1.063 *vs.* 1.069). The same was true for the corresponding α values for the *N*-TFA stationary phase.

In summary, *N*-PFP stationary phases can be readily synthesized and did produce reasonably good enantiomer separations. However, no advantages over the *N*-TFA derivatives were apparent.

Solute Effects. A complete evaluation of solute behavior was beyond the scope of this study. However, as shown in Table II, an increase in bulkiness of the solute ester group produced larger α values on all the stationary phases studied. Nevertheless, an increase in bulkiness at the α carbon atom produced a consistent but poorly understood effect. For instance, the ethyl alanine derivative (methyl side group) produce smaller k values, larger α values, and better resolution on all phases at all temperatures than the ethyl valine derivative (isopropyl side group). It is clear from these results, as well as from those of Nakaparksin *et al.* (*3*), that more work is needed before the effects of individual solutes will be completely understood.

(11) W. Parr, C. Yang, E. Bayer, and E. Gil-Av, *J. Chromatogr. Sci.*, 8, 591 (1970).

Discussion. A variety of optically-active, dipeptide (and higher polymeric) stationary phases can be obtained in high chemical and optical purity in the laboratory. Good yields are possible and purification is simple by preparative-scale gas chromatography. Hence, it should be possible to tailor the individual phase to the experimenter's needs.

This study indicated that the best separations of enantiomers of amino acid derivatives, using peptide stationary phases, would be achieved using a dipeptide stationary phase possessing an *N*-TFA group, bulky side groups, and a similarly bulky ester group, with a column operated at the lowest feasible temperature. A stationary phase containing more sterically hindered side groups, such as *tert*-butyl, might or might not produce better separations than existing phases, depending upon the effect of added crowding. However, the results with poly-L-phenylalanine indicated that an adsorption mechanism or an underivatized polypeptide will not work and suggested that there was a practical limit on the length of the peptide chain.

The derivatives of the volatile solutes should also possess a bulky ester group (such as *tert*-butyl or isopropyl) and an *N*-TFA group. Somewhat greater chromatographic temperature-stability can be achieved, with a small sacrifice in α, by going to derivatized tri- or higher peptides.

Since the amide end of a dipeptide appeared to make the primary contribution to the separation, and since only one end of the peptide molecule had to be derivatized, it should be possible to produce a high-temperature stationary phase by derivatizing the amide end and attaching the carboxylic acid group to a stable, non-volatile optically-inactive substrate. However, since the substrate would not contribute to the enantiomer separation, care would have to be taken to maintain a high concentration of active sites.

RECEIVED for review October 5, 1970. Accepted December 2, 1970. This work was supported, in part, by funds from the U. S. Atomic Energy Commission under contract AT (11-1)-1222.

Low Level Sodium Ion Measurement with the Glass Electrode

Edgar L. Eckfeldt and William E. Proctor, Jr.

Corporate Research Department, Leeds & Northrup Company, North Wales, Pa.

Power plants and other industries need continuous measurement of sodium ion, both at higher concentrations and also in the range from 0.1 to 1.0 ppb, to determine quality of process water. Laboratory and field studies have shown that sodium, even at the lower level, can be successfully monitored over long periods of time if attention is given to several conventionally overlooked factors. A strong base is preferred to economically reach the high pH of sample (11.0–11.6) needed for adequate suppression of hydrogen ion; also preferred is one that produces a cation (dimethylamine, or better, diisopropylamine) that exerts minimal electrode interference. Other troublesome interferences and ways to avoid them are discussed, including potassium and silver ion interference from the reference electrode solution during both normal and stopped flow sample conditions and electrical noise originating at the liquid junction.

SOME AREAS OF MODERN industry require very high purity of materials to support the advanced technology achieved. Examples are the semiconductor industry and electric power generation. Process water used in these industries may exceed in purity, for example, the distilled water commonly used in many laboratories. To meet the purity requirements, industry needs sensitive, convenient, and reliable analytical techniques.

The ubiquitous character of sodium in our environment makes sodium an effective telltale to reveal the condition of a high purity water system and to signal trouble when contamination enters. Flame photometry can serve to determine sodium at rather low concentrations, but the measurements involved are not easy to carry out, nor is the method easily and inexpensively adaptable to continuous monitoring instrumentation. The sodium selective glass electrode offers an attractive alternative. Although many people have contributed, Eisenman (*1*) has contributed outstandingly to theoretical and experimental knowledge of the electrochemistry of cation-sensitive glass electrodes (see Reference *1* for a comprehensive discussion). Gurney (*2*) pioneered the use of the glass electrode for measuring sodium in process water of power plants. In contrast to flame photometry, glass electrode measurements are easy to carry out, and a successful monitor of this type offers considerable practical advantage. Accordingly, this electrode measurement has generated much interest and is the basis of several commercial instruments now on the market.

Two careful recent studies have shown the current status of low-level sodium ion measurement with the glass electrode. Following usual practice, ammonia was used in those investigations as the base agent to raise pH. In one of the studies, Hawthorn and Ray (*3*) concluded that the electrode follows the Nernst equation over concentrations ranging from 25 ppb to 25 ppm. Below 25 ppb, corrections to compensate for background sodium in the water used to prepare solutions are said to be needed in order to allow use of the electrode to measure down to 1 ppb with a maximum uncertainty of 1.8 ppb. Sodium concentration changes at lower levels than this, however, are said to be discernible. In the other study, Webber and Wilson (*4*) claim that the electrode can be made to follow the Nernst equation down to about 1 ppb by controlling the pH of the sample and by using continuously flowing samples. They found standard deviations of 0.4 to 1.2 ppb in measuring low concentrations of sodium.

The present authors, along with W. A. Lower and W. D. Howie of Duquesne Light Company, published results of an extensive field study of the glass electrode for measuring sodium ion in various power plant applications (*5*). The work featured several innovations, including the use of base agents other than ammonia. It was concluded that measurement of sodium ion, even in the low range of 0.1 to 1.0 ppb, should be no more difficult to carry out than conventional pH measurement. A measurement as low as 0.07 ppb was reported on one specially purified sample.

Those results represent a sensitivity increase over results reported by others, corresponding to at least one order of magnitude lower in sodium ion measurement. Capability of measuring at such low levels is important, because good deionizer effluents and much of the hot well condensate water of high-pressure steam plants contain sodium in the 0.1 to 1.0 ppb range.

A novel calibration technique was used which circumvented a problem that has confronted other workers who have attempted to measure very low levels of sodium ion—namely, the problem of knowing the background sodium content of reagent water used to prepare standard sodium solutions. The method determines background sodium content by introducing a known sodium concentration increment and calculating the initial solution concentration using the known logarithmic (Nernstian) response characteristic of the electrode. Adherence of the electrode to theoretical Nernstian response can be checked down to very low sodium ion levels by using small increments in conjunction with larger increments. Details of the calibration technique have been described (*5*, *6*). Although that method of calibration adds greatly to overall measurement confidence, the improvements in electrode reliability and sensitivity are attributable to other factors.

The purpose of the present paper is to describe laboratory studies that elucidate the fundamentals involved and to explain preferred operating conditions. Early sections of the paper deal with problems of hydrogen ion and base ion interference; the later sections discuss instrumental considerations, including equipment design factors and other conditions that lead to good performance.

HYDROGEN-ION, BASE-ION INTERFERENCE

Glass electrodes are not perfect sensors for sodium ion measurement and, depending on selectivity considerations, may respond to other ions present in the sample water (*1*).

(1) G. Eisenman, "Advances in Analytical Chemistry and Instrumentation," C. N. Reilley, Ed., Wiley, New York, N. Y., 4, 213 (1965).
(2) W. B. Gurney, *Elec. World*, March 23, 1964, p 125.
(3) D. Hawthorn and N. J. Ray, *Analyst*, 93, 158 (1968).
(4) H. M. Webber and A. L. Wilson, *Analyst*, 94, 209 (1969).
(5) E. L. Eckfeldt, W. E. Proctor, Jr., W. D. Howie, and W. A. Lower, *Proc. 29th Inter. Water Conf.*, Engineers Society of Western Pennsylvania, Pittsburgh, November 19–21, 1968, p 109.
(6) E. L. Eckfeldt, *ISA Trans.*, 9, 37 (1970).

Some of the substances commonly present in power plant sample water might be expected to exert little or no interference effect, and this has been confirmed by experimental evidence (see the rather extensive studies of interferences reported in References *4* and *5*). Electrode theory indicates, however, that monovalent cations might be troublesome (*1*), and certain important ones have heretofore been overlooked.

For low level sodium ion measurement, sample pH must be raised by addition of a base, as already noted, to avoid hydrogen ion interference. A satisfactory value for the ratio of H^+ to Na^+ is often quoted at 10^{-3}, and even 10^{-4} has been advocated (*7*).

Not generally appreciated is the interfering effect arising from the cation that comes from the base agent used to raise pH. If a hydrolyzable base, B, is added to water, it reacts to produce hydroxyl ion:

$$B + HOH \rightleftharpoons BHOH \overset{K_B}{\rightleftharpoons} BH^+ OH^- \qquad (1)$$

For every hydroxyl ion produced, a corresponding base cation, BH^+, is generated. The situation may be even worse if the sample water initially contains some acid, such as HCl. With a sample of this kind, a reaction of the base with the acid must first take place, as follows, before Reaction 1 can occur:

$$B + H^+ + Cl^- \rightarrow BH^+ + Cl^- \qquad (2)$$

In this case a surplus of base cations over hydroxyl ions will result. In any case a rather high base cation activity will exist in the sample solution at the high pH value needed for low-level sodium ion measurement. Whether or not this constituent will interfere will depend on its activity level and on the selectivity characteristics of the electrode.

Eisenman (*1*) has described the response of cation-sensitive electrodes to ammonium ion, as well as to a number of substituted ammonium ions. Rechnitz and coworkers investigated the response of a general cation-sensitive electrode to ammonium ion (*8*) and to various alkyl-substituted ammonium ions (*9*). They used neutralized hydrochloride salts in a THAM buffer for their measurements. The cations present were the same as those which would have been formed at lower concentration by adding the corresponding bases to water. They found that the electrode did respond to ammonium ion and several alkyl-substituted ammonium ions.

These observations do not pertain directly to the problem of sodium ion measurement, because for sodium ion measurement one would normally choose an electrode that had good selectivity for sodium, rather than one of general cation response. Also, the solution conditions were quite different. Nevertheless, it was clear that the base cation interference must be considered, and experimental evidence in the laboratory and field has amply confirmed this view.

EXPERIMENTAL

Substances of moderate price which would produce strongly basic aqueous solutions were sought. A number of organic amines appeared quite suitable for the purpose and certain of these were studied experimentally. These substances were added in gaseous or vapor form, thereby forestalling possible contamination from dissolved sodium compounds as might occur if the base were added directly in liquid form. Experimentation focused attention on the base cation effect, but hydrogen ion was not overlooked. Special efforts were exerted to keep sodium in the reagent water at the lowest possible level in order to avoid its effect.

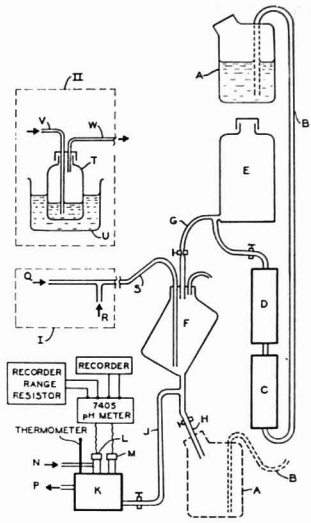

Figure 1. Experimental arrangement

The equipment is illustrated in Figure 1. The vessels and lines were of polyethylene construction throughout, and the interior of the system was kept closed from the ambient. The flow cell *K* contained the sodium ion sensor *M* (LN 117,201 glass electrode). The lithium alumino silicate glass of the electrode bulb was especially developed for the purpose. This electrode has good selectivity for sodium ion and will give many months of satisfactory field service with little or no maintenance. The reference electrode *L* of saturated calomel type had a fused-in porous ceramic junction and was internally pressurized through line *N* by means of air pressure kept at 5 lb/in^2. The range resistor was selected to provide 500 mV full scale on a Speedomax G recorder readout device. In most of the work the zero adjuster of the pH meter was set to give a recorder scale of +50 to −450 mV.

The chemical bases studied were used as received from suppliers. Matheson Company supplied the gaseous bases in pressurized cylinders, monomethylamine (98.0%), monoethylamine (98.5%), dimethylamine (99.0%), and trimethylamine (99.0%). Pennsalt Chemicals supplied anhydrous ammonia. Liquid bases in the laboratory work were supplied as follows: Eastman Organic Chemicals, 1396 diisopropylamine, 616 triethylamine, and P6760 *N*-methylmorpholine; Fisher Scientific Company, D-46 diethylamine. In the field work the liquid bases (diethylamine and diisopropylamine) were the usual commercial grade supplied by Union Carbide Chemicals in 5-gal containers; the dimethylamine was the same as in the laboratory work.

Reagent water was prepared by starting with distilled and deionized water in the elevated 5-gal bottle *A* (Figure 1). The water was passed in series through the ion exchange columns *C* and *D* and into the 5-gal bottle *E*. Next, the water completely filled the mixing flask *F* and flowed through tube *H* back into bottle *A*, which was now located in the indicated lower position. The water was circulated at least twice through the ion exchangers in this manner before being

(7) M. Hanss, M. de Heaulme, and P. Morin, *Bull. Soc. Chim. France*, **1963**, 2658.
(8) S. A. Katz and G. A. Rechnitz, *Z. Anal. Chem.*, **196**, 248 (1963).
(9) G. A. Rechnitz and G. Kugler, *ibid.*, **210**, 174 (1965).

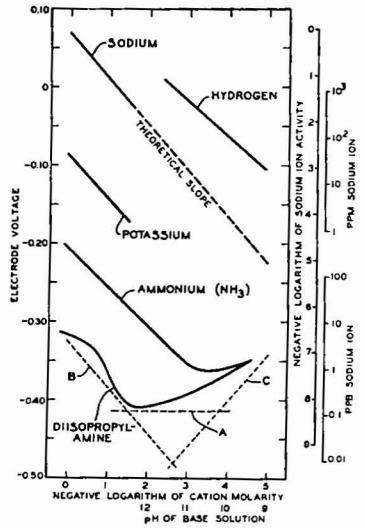

Figure 2. Electrode response to various cations

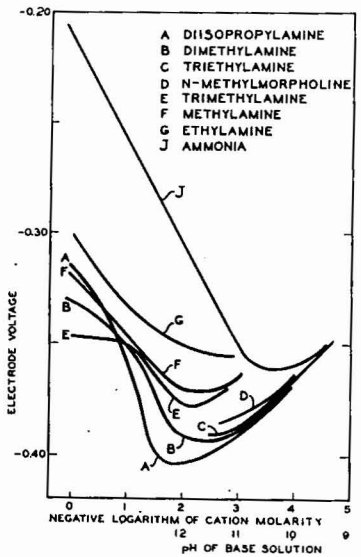

Figure 3. Electrode response with different base reagents

retained in bottle *E*, preparatory to making test solutions. The treatment rinsed the system and lowered the sodium content of the water to the vicinity of 0.1 ppb.

In preparing a base solution, a portion of the water in *E* was run into the flask *F*. A flow of cylinder nitrogen gas entered through tube *R* and passed into flask *F* (transport system I). Gaseous base entered through tube *Q* and mixed with the flow of nitrogen entering flask *F*. In the case of liquid bases, transport system II was used; the base was put into vessel *T* and nitrogen flow through tubes *V*, *W*, and *S* carried vapor of the base into flask *F*. The hot water bath *U* accelerated the rate of transport of base. Nitrogen gas flow promoted mixing in flask *F* and prevented backflow into tube *S*. The ion concentrations of individual batches of base in water thus prepared were determined after passing the solution through the measurement cell *K* by measuring the pH of the effluent at *P*. For electrode measurements, solutions flowed at a rate of about 100 ml/min and were at room temperature (approximately 25 °C).

Higher concentrations of base cation, between 0.1 and 1.0 molar, were prepared by a somewhat different procedure, also designed to avoid contamination from sodium ion. Multiply-deionized, distilled water contained in a 5-gal polyethylene bottle was acidified by passing HCl cylinder gas over the surface of the water, while keeping the water briskly stirred with a magnetic stirrer. A portion of the hydrochloric acid solution thus prepared was run into flask *F*, where it was treated with excess base, by means of transport system I or II until its pH was in excess of 10.5. Small samples were withdrawn to carry out the pH test. Also, samples of the original HCl solution were withdrawn for titration with standardized base in order to determine the HCl concentration and, therefore, the approximate base cation concentration in the respective final solutions. The base cation solutions thus prepared were passed in turn through the cell for electrode measurement, but in each instance enough solution was retained in flask *F* to allow making up a quantitatively diluted solution, using deionized water. The diluted solutions were likewise submitted to electrode measurement.

Additionally, electrode response measurements were made on several solutions of sodium chloride and potassium chloride which had been rendered basic with amine. Response to hydrogen ion was obtained on solutions of measured pH containing ammonium chloride and different amounts of acetic acid. To check calibration stability of the electrode, voltage measurements were made at the beginning and/or end of each working period using a basic 0.075*M* sodium chloride solution.

RESULTS AND DISCUSSION

Results of Tests. Response characteristics of the electrode are summarized in Figures 2 and 3. Electrode potential values are referred to the saturated calomel electrode throughout and the IUPAC sign convention is used. Figure 2 portrays the electrode response situation in general and will help to explain the nature of the interference problem and what can be done to achieve low level sodium ion measurement. The approximate way in which the electrode responds in the presence of each of a number of different bases is shown in Figure 3, and this information will be helpful in choosing a suitable base.

Discussion of Amine Tests. In all but the tests specifically on sodium solutions, the experimental precautions precluded sodium ion as a factor except for the unavoidable low background level. A background of 0.1 ppb corresponds to a voltage somewhat more negative than −0.400 volt. The voltage value corresponding to dotted line *A* of Figure 2 serves to represent a postulated low concentration of sodium ion which one may wish to measure.

Since the electrode is more responsive to hydrogen ions than to sodium ions, the hydrogen ion content of even a rather high pH sample solution may introduce interference. The dotted line *C* of Figure 2 (relating to the pH abscissa) was arbitrarily drawn to represent hypothetical response to hydrogen ion concentration, which at each voltage point is

1/100 that of the competitive sodium ion concentration determined by extrapolation of the theoretical sodium ion line.

Although actual slope values are in some disagreement, the right-hand branches of the diisopropylamine and ammonia curves of Figure 2 nevertheless correlated with the hypothetical hydrogen response line *C*. The experimental results of Figure 3 substantiate the existence of a region of hydrogen ion dominance—namely, on the right-hand side where a number of the curves with upward slope lie nearly on top of each other.

The dotted line *C* lies a short distance from the hydrogen ion-dominated portion of the experimental curves. For satisfactory sodium ion measurement, one needs a hydrogen-to-sodium ion ratio closer to 1/1000 than to the 1/100 used in plotting line *C*.

These results demonstrate that solution pH is an important factor, if really low level sodium ion measurement is to be achieved. Solution pH must be elevated into the region of pH 11.0 to 12.2. The 117,201 electrode satisfactorily withstands protracted exposure to such strongly basic solution.

In general each base of Figure 3 produces a unique curve. The differences presumably arise from individuality of the respective base cations. The straight line portion of the ammonia line, with a nearly theoretical Nernstian slope, definitely demonstrates an ammonium ion response of the electrode. Although exhibiting more random behavior, the curves for the other bases nevertheless indicate corresponding base cation response.

The dotted line *B* has been arbitrarily inserted in Figure 2 to illustrate the hypothetical base cation effect. The line has Nernstian slope and is placed close to the cation response branch of the diisopropylamine curve. If the intersection of the hypothetical dotted lines *B* and *C* lies below the postulated sodium ion line *A*, then sample conditions can theoretically be found to enable measurement of that presumed sodium ion concentration. On the other hand, if the sodium ion concentration lies below the intersection point, then conditions satisfactory for the measurement will theoretically not be attainable. As Figure 3 shows, the selection of the particular compound to be used as base reagent will markedly influence the position of the electrode response line arising from the base cation, and hence along with the pH factor will determine the lowest sodium ion level that can be measured. Intersection of line *C* with an extrapolated ammonium line, for example, will take place at a much higher level than that obtained by extrapolating the cation branch of the diisopropyl line. This explains why diisopropylamine has proved in practice to be an efficient base for low level sodium ion measurement. The other bases tested (Figure 3) show cation response lines at somewhat less negative voltages than the diisopropylamine curve and hence might be expected to be inferior base agents. The difference, however, in the case of dimethylamine is not great.

Sodium ion measurements were made in the field on a series of sample solutions, each of which was separately tested with diisopropylamine and dimethylamine. The results are summarized in Figure 4. At low sodium ion levels an appreciable difference exists in the performance of the two bases, which disappears at concentrations above 1 ppb. These tests likewise show the superiority of diisopropylamine for making very low sodium ion measurements.

Individuality in behavior of the various bases undoubtedly is related to differences in molecular properties. In the study of alkyl-substituted ammonium ions referred to earlier (*9*), cation size was considered the important factor—the larger

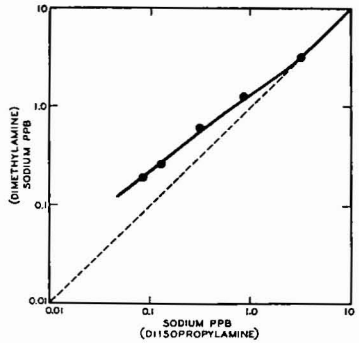

Figure 4. Comparative measurements with dimethylamine and diisopropylamine on common samples

the cation, the less its effect in producing an electrode response. Recently, Rechnitz has suggested that adsorption phenomena may be more important than size (*10*). Although some exceptions may be noted, the present study nevertheless confirms the merit of having a base cation of large size (a base of large molecular weight) to avoid interference in low level sodium ion measurement.

Matheson Company has furnished analytical information on the identity and approximate concentration of impurities typically present in their amines (*11*). They give the ammonia impurity in respective bases as follows: methylamine, 0.0%; ethylamine, 0.6%; dimethylamine, 0.0%; trimethylamine, 0.0%. The appreciable amount of ammonia in ethylamine, contrasted with its indicated absence in the three other amines, may account for the poor showing of ethylamine in the present study. In the absence of ammonia impurity, the ethylamine curve *G* might have appeared lower on the graph, possibly below the methylamine curve *F*, in which case its position would have agreed with the cation size principle. No special attempt was made in the study to purify the bases (gas or liquid) prior to testing. Although a preliminary purification step would not be acceptable in practical situations, the manner of introducing the bases in practice (*5*), particularly in the case of liquids, should result in progressive purification of the supply through fractional distillation of the more volatile ammonia impurity.

It should be noted that electrode response to low-level hydrogen ion and cations of the organic amines studied was somewhat less definite and less reproducible than in the case of the ammonium, potassium, and sodium ions. The electrode takes time to equilibrate. Also, the undissociated base molecules may or may not exert a complicating influence. Furthermore, some of the observed curvature and non-Nernstian character of the data may be attributable to mixed response of the electrode, which is trying to adjust its potential, for example, to the competing influences of sodium ion (line *A*), base cation (line *B*), and hydrogen ion (line *C*). Other work has shown satisfactory electrode response to changes in

(10) G. A. Rechnitz, discussion following presentation of the present paper at the Pittsburgh Conference, Cleveland, Ohio, March 5, 1970.

(11) Matheson Gas Products, East Rutherford, N. J., Data Sheets on monomethylamine, dimethylamine, trimethylamine, and monoethylamine, communication received May 5, 1970.

Table I. Value of Dissociation Constant and Consumption of Base

Base reagent	Dissociation constant, 25 °C ($\times 10^6$)	Mol wt	Quantities calculated at solution pH of 11.3: Degree of dissociation of base	Solution molarity	Grams of base per liter	Pounds of base used per month[a]
Morpholine	0.244[b]	87.1	0.0012	1.64	143	1360
Ammonia	1.79[c]	17.0	0.0088	0.23	3.9	37
Trimethylamine	5.45[c]	59.1	0.027	0.075	4.4	42
Dimethylamine	52[c]	45.1	0.21	0.0097	0.44	4.3
Diisopropylamine	112[d]	101.2	0.36	0.0056	0.57	5.4

[a] At assumed sample flow rate of 100 ml per min (1.6 gal per hour).
[b] A. R. Ingram and W. F. Luder, *J. Amer. Chem. Soc.*, **64**, 3043 (1942).
[c] H. S. Harned and B. B. Owen, *ibid.*, **52**, 5079 (1930).
[d] N. F. Hall and M. R. Sprinkle, *ibid.*, **54**, 3469 (1932).

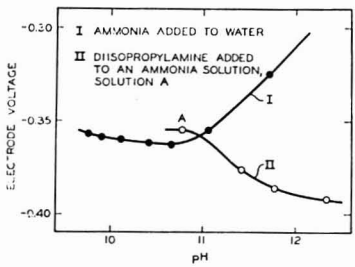

Figure 5. Ammonium ion suppression by addition of diisopropylamine

sodium ion concentration at low levels, when pH and the amine concentration are kept constant (*5*).

Advantages of a Strong Base. A large dissociation constant of the base reagent will be helpful in producing the desired high pH of the sample solution. A greater degree of dissociation results from a constant of larger value. The situation is illustrated by the approximate data of Table I. These data were calculated assuming that the listed base reagents were added to water in each case in amounts to produce a solution pH of 11.3, an arbitrary value within the recommended pH range. Bases at the bottom of the table with large dissociation constants exhibit a much greater degree of dissociation than the bases at the top of the table. Accordingly, as the table shows, a much lower solution molarity is needed to produce the specified pH. Needed amounts of base expressed on a weight basis will reflect the molecular weight, but this factor is not as important as the dissociation constant.

The last column of Table I presents base consumption rates for a sample flow rate that might be reasonably established in practice. The amount of morpholine needed to keep equipment running is prohibitively large, thus ruling out the use of this base and any other base with a correspondingly low dissociation constant. If ammonia were not excluded for other reasons, its dissociation constant might be regarded as sufficiently large to make this a practical base, especially in view of its low molecular weight. To avoid base cation interference, as previously described, a base of larger molecular weight is needed and a dissociation constant larger than that of ammonia will be desirable. The constant for trimethylamine (5×10^{-5}) might be regarded as minimal. The advantage of using a much stronger base is illustrated by the tabulated data for dimethylamine and diisopropylamine. For these bases, only a relatively small amount of each compound is needed to reach the specified pH, thus making these compounds economical to use as base reagents.

As pointed out previously, ammonium ion is an interference in measuring sodium at low levels. Ammonium ion often is present in process sample water, and its concentration may be several orders of magnitude higher than that of the sodium ion to be measured. A high hydroxyl ion concentration, resulting from the use of a strong base reagent, will substantially remove ammonium ion from the solution, making it go into the form of undissociated ammonium hydroxide. Calculation indicates that of the total ammonium (NH_4^+ and NH_4OH) present in a solution of pH 10.5, only about 6% will be in the ionized form. At 11.0, the ionized fraction drops to about 2%, while at pH 11.5 the ionization further diminishes to about 0.6% (*12*). Experimental evidence of the beneficial effect of the strong base diisopropylamine in suppressing ammonium ion concentration is shown in Figure 5.

PREFERRED OPERATING CONDITIONS

Several factors in addition to the choice of base reagent are important in achieving good performance. Some of these are related directly or indirectly to the flow of sample solution.

Cell. In a flow cell of conventional type, we have observed interference arising from potassium ion coming from the reference electrode, even though the reference electrode was located downstream from the sensor electrode. The explanation appears to be turbulence generated in the flowing sample stream by electrodes that are mounted at right angles to the flow path. The turbulence causes some regions of the flowing solution to move in a direction opposite to the nominal flow direction. If potassium chloride solution leaking from the reference junction is caught in one of these eddies, it may be carried upstream to the bulb of the sodium electrode, where it can generate a significant interference voltage of a sporadic or cyclic nature.

This type of potassium ion interference was eliminated by using the cell illustrated in Figure 6. Sample water enters pipe *A* at the bottom of the sodium electrode compartment, promptly contacts the sensor bulb, and rises through the annular space surrounding the electrode stem. At the cross-aperture *B* the solution flows into the reference electrode compartment and descends to the bottom of the annular space, where it contacts the junction of the reference electrode. The solution then passes into the temperature compensator compartment, where it rises through the annular

(12) D. S. McKinney, *ASTM Proc.*, **41**, 1285 (1941).

space and discharges from outlet *C*. (In the present study, a thermometer replaced the temperature compensator shown.) It will be noted that the advancing flow of solution through the nonturbulent annular spaces adjacent to the electrodes will prevent the backward passage of potassium chloride solution. The more dense potassium chloride solution will not flow upward against the current and is carried away with the discharge.

When solution flows through the cell, its level is determined by the height of outlet *C*, thereby assuring sufficient liquid in aperture *B* to maintain satisfactory electrical conductance between the electrodes. If the sample flow stops, as sometimes happens in plant practice, the solution in the reference electrode compartment leaks through the small opening *D*, until the level drops to that point. When this happens, the tips of both electrodes remain immersed in solution, but solution continuity between them is broken. Consequently, potassium chloride from the reference electrode cannot reach the sodium electrode, as it otherwise could by diffusion through the quiescent solution bridging between them. This feature of the cell provided automatic indication of down time, because with the meter used, the indication went off scale when the solution circuit opened. Furthermore, reliable measurement begins immediately when sample flow resumes, because the electrode is already adjusted to sample conditions and does not need time to dispel the effect of potassium ions. A calomel rather than a silver reference electrode is used to avoid any possibility of interference from silver ion.

The electrolytic conductivity of the amine-treated sample water is relatively high. Therefore, no trouble was encountered with streaming potential effects, which probably would be encountered with this cell in measuring pH of high purity water.

Liquid Junction. In sodium ion measurement, the liquid junction can be a source of serious trouble unless this item is properly designed and operated. The high pH of the sample solution, combined with flow-induced head fluctuations that result in transport variations of potassium chloride away from the junction, can make a poor junction produce electrical noise. Many of the erratic electrode flow effects in pH and specific ion measurements reported from the field are undoubtedly related to faulty liquid junctions. Bad conditions are illustrated at *A*, *B*, and *C* of Figure 7. These are traces of actual sodium ion chart records. As shown, a poor junction can cause excursions of the trace of 5 or 10 mV or more, occurring sporadically or in rapid succession. The seriousness of an erratic junction is illustrated by scale *E*, which indicates the percentage error introduced into the measurement by excursions in traces *A*, *B*, and *C*.

Two factors were found to be important in greatly improving the operation of the liquid junction. The solution pressure difference across the junction should be much greater than that usually employed. Instead of the usual 5- or 10-cm head differential, the head difference should be approximately 300 cm. Since it was inconvenient to elevate the reference solution reservoir this much, the desired condition was achieved by applying 5 lb/in.^{2} gas pressure to the reservoir, using a cylinder of compressed inert gas, equipped with a regulator set at the desired pressure.

The other important factor is the construction of the junction itself. A small porous plug of ceramic sealed into the reference electrode tube is preferred. The porosity is chosen to give a solution flow under operating pressure of about 2 ml per day. At this flow rate, a 500-ml supply of solution will last in the field more than 6 months before needing replenishment. With the junction described, very satisfactory field performance was observed over a period of many months. The trace shown at *D*, Figure 7, is typical of the entire period.

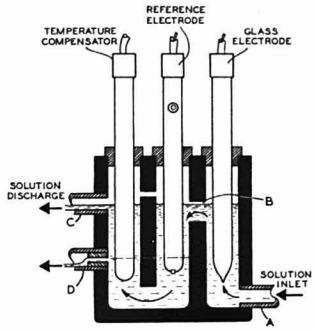

Figure 6. Cell arrangement

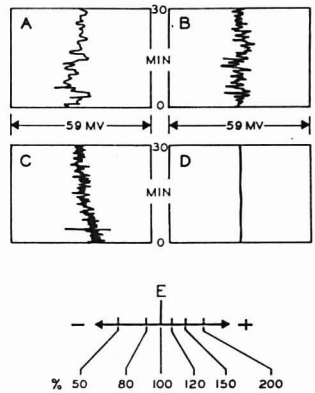

Figure 7. Liquid junction effect on output record

ACKNOWLEDGMENT

Some of the information reported, particularly that of Figures 4 and 7, is based on field experience gained at Duquesne Light Company. Expressions of appreciation go to Walter A. Lower, who was in charge of the field work, and to his associates.

RECEIVED August 31, 1970. Accepted December 2, 1970. Paper presented at the Twenty-first Pittsburgh Conference on Analytical Chemistry and Applied Spectroscopy, Cleveland, Ohio, March 5, 1970.

Spectrophotometric Assay of Ampicillin (α-Aminobenzylpenicillin) Involving Initial Benzoylation of the Side Chain α-Amino Group

David E. Tutt[1] and Michael A. Schwartz[2]

Department of Pharmaceutics, School of Pharmacy, State University of New York at Buffalo, Buffalo, N. Y. 14214

The rate of formation of α-aminobenzylpenicillenic acid, 2, from ampicillin (α-aminobenzylpenicillin, 1) under strongly acidic conditions in the presence of mercuric chloride at 50 °C is very slow owing to stabilization of the penicillin by the side chain α-amino group. Consequently, ampicillin may not be readily assayed spectrophotometrically under these conditions. However, treatment of an aqueous solution of sodium ampicillin with benzoyl chloride in dioxane under mildly alkaline conditions produces a new, acid-unstable penicillin, α-benzamidobenzylpenicillin, 3, which on treatment with mercuric chloride in acid solution rearranges rapidly to form α-benzamidobenzylpenicillenic acid, 4, which may be assayed spectrophotometrically at 322 nm after only 48 minutes. Optimum conditions are reported for the benzoylation procedure and the subsequent spectrophotometric analysis. The overall assay, which may be used for concentrations as low as 4×10^{-5} M ampicillin, is shown to be very reproducible and to yield accurate results for the rate of alkaline hydrolysis of ampicillin when compared to a titrimetric method. A novel use for this assay is suggested, involving analysis of mixtures of ampicillin and other penicillins.

SEVERAL PROCEDURES have been described for the assay of penicillins, involving either of two general chemical modifications of the penicillin nucleus. Initial nucleophilic cleavage of the β-lactam of penicillins under alkaline conditions is the basis of titrimetric (*1*), iodometric (*1*), and hydroxamic acid (*2*) assays. Treatment of penicillin under acidic conditions (pH 1–5) in the presence of heavy metal ions (mercuric or cupric) produces the corresponding penicillenic acid (*3*, *4*) which contains a chromophore (oxazolone) with an absorption maximum at 320–360 nm, depending on the side chain. Since intact penicillin is required for oxazolone formation and the presence of penicilloyl derivatives does not interfere with the procedure, the penicillenic acid assay is specific for penicillin and has been used extensively for the spectrometric analysis of penicillins. The method described originally by Herriott (*5*) involved treatment of penicillin solutions at pH 4.6 and 100 °C. This was modified by Brandriss and coworkers (*3*) for analysis of aqueous and protein-containing solutions of penicillins at ambient temperature using mercuric chloride and pH 1–3.

The procedure described by Brandriss *et al.* has been used extensively in our laboratory for analysis of aqueous solutions of a variety of penicillins. However, acid-stable penicillins, such as ampicillin (α-aminobenzylpenicillin, **1**), cannot be analyzed readily by this method since the rate of formation of penicillenic acid, **2**, is extremely slow at ambient temperature. Smith and coworkers (*6*) used a modification (*7*) of the original assay procedure, in which solutions of sodium ampicillin, **1**, containing copper sulfate were heated at 75 °C and pH 5.2 for 30 minutes. Attempts to use their procedure in our laboratory for the assay of ampicillin in kinetic reaction solutions yielded unsatisfactory results, and another assay procedure was sought.

It has been recognized (*8*) that the nature of the side chain is important in determining acid stability of penicillins. Thus, α-methoxy, α-chloro-, and α-aminobenzylpenicillin are increasingly more acid-stable than benzylpenicillin (*9*), and this effect has been rationalized in terms of the inductive effect of the α-substituent decreasing the nucleophilicity of the side chain amide carbonyl oxygen, which is involved in oxazolone formation. It seemed likely that removal of this inductive effect by suitable chemical modification of the side chain amino group would yield a new, acid-unstable penicillin which could be assayed readily at low pH. One possible procedure involves benzoylation of the amino group under very mildly alkaline conditions (*ca.* pH 9) using benzoyl chloride to give α-benzamidobenzylpenicillin, **3**. (A review points out that although it is reasonable to assume that only benzoylation is taking place we have not isolated and identified the reaction product.) Under such conditions, alkaline hydrolysis of the β-lactam would be negligible, although benzoylation would be fairly rapid.

We now describe an analytical procedure for ampicillin involving initial benzoylation of the side chain amino group and subsequent spectrophotometric assay for penicillin of the resulting solution using a modification of the method of Brandriss and coworkers (*3*).

EXPERIMENTAL

Materials. Sodium ampicillin was provided by Bristol Laboratories. Benzoyl chloride was purified by distillation [lit. (*10*) bp 197 °C at 760 mm Hg]. Commercially available 95% ethanol, *n*-propanol, and 1,4-dioxane were used without further purification. Water was deionized and distilled under nitrogen in all-glass apparatus.

Benzoylation Procedure. One milliliter of a solution of benzoyl chloride in dioxane was added from a syringe to 40 ml of the appropriate solution of sodium ampicillin in water at pH 9.0 stirred in a reaction cell thermostated at 31.5 °C. pH was maintained at 9.0 ± 0.5 during this procedure by the addition of titrant (1.0*N* NaOH) by the pH-stat. The mixture

[1] Present address, Dept. of Chemistry, University of Sussex, Sussex, England.

[2] To whom correspondence should be addressed.

(1) J. V. Scudi and H. B. Woodruff, "The Chemistry of Penicillin," H. T. Clarke, J. R. Johnson, and R. Robinson, Ed., Princeton University Press, Princeton, N. J., 1949, p 1025.
(2) J. H. Ford, IND. ENG. CHEM., ANAL. ED., **19**, 1004 (1947).
(3) M. W. Brandriss, E. L. Denny, M. A. Huber, and H. G. Steinman, "Antimicrobial Agents, and Chemotherapy—1962," American Society for Microbiology, Ann Arbor, Mich., p 626.
(4) A. Holbrook, *J. Pharm. Pharmacol*, **10**, 762 (1958).
(5) R. M. Herriott, *J. Biol. Chem.*, **164**, 725 (1946).
(6) J. W. G. Smith, G. E. DeGrey, and V. J. Patel, *Analyst (London)*, **92**, 247 (1967).
(7) F. G. Stock, *ibid.*, **79**, 662 (1954), and reference (*5*).
(8) F. P. Doyle and J. H. C. Nayler, "Advances in Drug Research," Vol. 1, N. J. Harper and A. B. Simmonds, Ed., Academic Press, London, England, 1964, p 26.
(9) F. P. Doyle, J. H. C. Nayler, H. Smith, and E. R. Stove, *Nature*, **191**, 1091 (1961).
(10) "Dictionary of Organic Compounds," Vol. I, I. Heilbron, A. H. Cook, H. M. Bunbury, and D. H. Hey, Ed., Eyre and Spottiswoode Ltd., London, England, 4th ed., 1965, p 358.

was stirred for a further period at pH 9.0 and 31.5 °C until liberation of benzoic acid in the system was complete (determined by the addition of titrant). It was important to maintain rapid mixing throughout this procedure because addition of dioxane solution to the aqueous solution of ampicillin produced a dispersion of fine droplets of benzoyl chloride which dissolved completely within about 5 minutes. An aliquot of the reaction solution was then removed and analyzed for penicillin (α-benzamidobenzylpenicillin, 3) by the method of Brandriss and coworkers (*3*). The appropriate concentrations of benzoyl chloride (0.80*M*) and ampicillin ($2.0 \times 10^{-3}M$) solutions, the rate of addition of benzoyl chloride (1 ml, 0.5 ml/min), and time of mixing of the reaction solution (12 min) were kept constant except in studies to determine a particular effect upon the maximum absorbance (A_{max}) in the penicillenic acid assay. The absorbance values reported have been corrected for the effect of dilution of the initial ampicillin solution by the dioxane and titrant except the spectra in Figure 1 and curves in Figure 2.

Assay for Penicillin. The basic procedures for this assay have been described previously (*3*), and only the specific conditions employed for the spectrophotometric assay for α-benzamidobenzylpenicillin are given here. An aliquot of the benzoylated ampicillin solution was diluted (20-fold) with the appropriate buffer solution preequilibrated at 50 °C and assayed spectrophotometrically by conversion of the α-benzamidobenzylpenicillin to the corresponding penicillenic acid in the presence of mercuric chloride at pH 1.8 (preliminary investigation), pH 0.9–2.3 (assay pH dependence), and pH 1.71 ± 0.03 (all other studies) in 19% ethanol–water at 50 °C. A glycine–hydrochloric acid buffer (0.2*M*) was used for pH 2.3 and hydrochloric acid was used for pH 0.9–2.0.

Apparatus. A Radiometer pH-stat system, consisting of a TTT-1c pH-stat, SBR 2c titrigraph, and SBU 1c syringe buret fitted with a jacketed reaction cell, was used for maintenance of pH during benzoylation of ampicillin, for measurement of pH at 31.5 °C, and for maintenance and measurement of pH at 31.9 °C in a study to compare the benzoylation assay procedure with a titrimetric method used to obtain kinetic data for alkaline hydrolysis of ampicillin. Ultraviolet spectrometric measurements were made using a Beckman–Gilford recording quartz spectrophotometer fitted with a thermostated block (50 °C) and a Beckman DB-G double-beam spectrophotometer fitted with a Sargent SR recorder. Since the DB-G spectrophotometer was not equipped with a thermostated block, the absorption spectra shown in Figure 1 were obtained by transferring an aliquot of penicillin assay solution (stored at 50 °C) to a silica cell and immediately measuring the absorption spectrum in the region 290–355 nm. Fresh aliquots were taken for each spectrum recorded. Stoppered silica cells (1 cm) were used for all spectral measurements. A Radiometer pH meter 26 was used for measurement of pH values of assay solutions at 50 °C. Constant temperatures (31.5 ± 0.1, 31.9 ± 0.1, or 50 ± 0.5 °C) were maintained using Bronwill circulating water pumps.

RESULTS

Preliminary Investigation. A solution of sodium ampicillin (40 ml, $2.0 \times 10^{-3}M$) was treated with a solution of benzoyl chloride in dioxane (1 ml, 0.80*M*; concentration after dilution with ampicillin solution, $20 \times 10^{-3}M$) under the reaction conditions described in the Experimental section. An aliquot of this solution was assayed spectrophotometrically for penicillin. The presence of a new, acid-unstable penicillin was revealed by the development of a chromophore in the region 320–330 nm [characteristic of an oxazolone structure (*3*) which attained a maximum absorbance of 0.7 at 322 nm after 50 minutes under the assay conditions (See Experimental section)]. In contrast, treatment of a solution of sodium ampicillin with dioxane alone and subsequent spectrophotometric

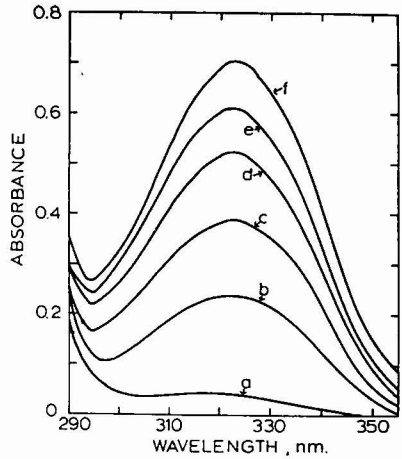

Figure 1. Absorption spectra showing formation of α-benzamidobenzyl-penicillenic acid after addition of excess benzoyl chloride and acid treatment

a. 2 min
b. 8 min
c. 14 min
d. 18 min
e. 27 min
f. 50 min

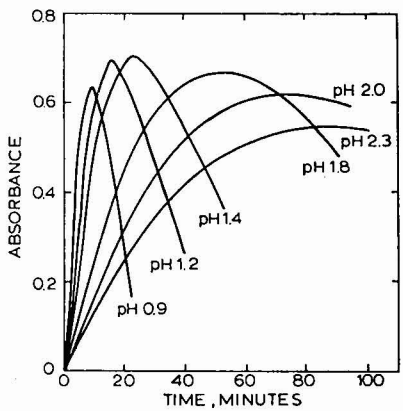

Figure 2. Effect of pH on time course of α-benzamidobenzylpenicillenic acid in presence of mercuric chloride at 50 °C in 19% aqueous ethanol

assay of the solution under the same conditions revealed the much slower development of a chromophore (corresponding to 2) in the region 320–330 nm. The absorbance of this solution was only 0.05 at 322 nm after 54 minutes and was still rising after 7 hr (A = 0.34 at 322 nm). It should be emphasized that, since the penicillenic acid (2 or 4) is an intermediate in a series first-order reaction, only the maximum absorbance of the chromophore corresponding to the intermediate (2 or 4) is proportional to the initial concentration of penicillin (1 or 3, respectively) assayed by this method

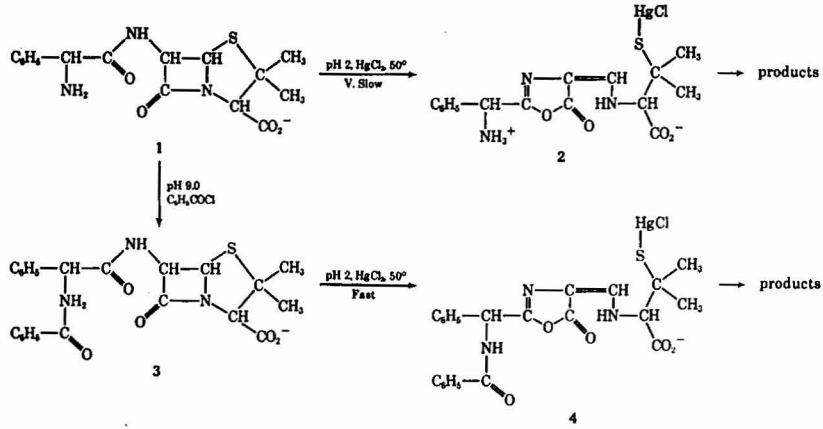

Scheme I

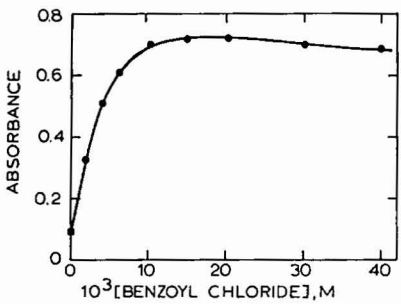

Figure 3. Absorbance as a function of benzoyl chloride concentration (see text for details)

(*4*, *11*). Thus, a considerably longer time would be required to reach the maximum absorbance for α-aminobenzylpenicillenic acid, 2, than for the benzoylated penicillenic acid, 4 (see Scheme). Spectrometric analysis of a sample of water treated with benzoyl chloride under the reaction conditions showed a negligible absorbance at 322 nm even after 3 hr, demonstrating that excess benzoic acid (formed by hydrolysis of benzoyl chloride) does not interfere with the assay procedure.

We concluded that sodium ampicillin, an acid-stable penicillin, had been benzoylated under mildly alkaline conditions to yield α-benzamidobenzylpenicillin, 3, an acid-unstable penicillin, which was readily converted into the corresponding penicillenic acid on treatment with acid (see Scheme). Subsequent investigations were concerned primarily with the determination of a suitable solvent and the optimum pH and wavelength for the penicillin assay; and the optimum molar excess and rate of addition of benzoyl chloride solution, and time of sampling from the benzoylation mixture.

Penicillin Assay. The method of Brandriss and coworkers (*3*) was used to assay for α-benzamidobenzylpenicillin by its conversion to α-benzamidobenzylpenicillenic acid. As solvent, 19% ethanol–water was used rather than water (determined by the solubility of 4). The variation of absorbance as a function of wavelength in the region 280–360 nm for a benzoylated solution of ampicillin (assayed at pH 1.74) showed an absorption maximum at 322 nm after about 48 minutes (Figure 1). The curves in Figure 1 represent the experimentally measured spectra of the assay solution during the formation of α-benzamidobenzylpenicillenic acid after benzoylation with 1 ml of 0.80*M* benzoyl chloride and treatment at pH 1.8 at 50 °C.

Sodium ampicillin was treated with a constant molar excess of benzoyl chloride (see Experimental section for conditions) and the mixture was assayed for penicillin at a variety of pH. The variation of absorbance at 322 nm as a function of time for pH 0.9–2.3 is shown in Figure 2. The choice of a suitable pH value for the penicillin assay rests on three considerations: the time (t_{max}) taken to attain maximum absorbance, the absorbance (A_{max}) at t_{max}, and the period of time (Δt) during which A_{max} is maintained. Using these criteria *ca.* pH 1.7 was considered suitable (t_{max} = 48 min, A_{max} = 0.7, and Δt = 9 min) for the α-benzamidobenzylpenicillin assay. The effect of variation of mercuric chloride concentration upon A_{max} was constant (0.715 ± 0.005) within the reproducibility of the overall procedure for the range 4.0–12.1 × $10^{-3}M$ $HgCl_2$, and as a result, a constant concentration of mercuric chloride (8.0 × $10^{-3}M$) was used for subsequent assays.

Benzoylation Procedure. A solution of sodium ampicillin in water was treated with increasing concentrations of benzoyl chloride in dioxane (1 ml, 0–1.6*M*; 0–40 × $10^{-3}M$ after addition to ampicillin solution under the benzoylation conditions, see Experimental) and assayed spectrophotometrically at 322 nm in pH 1.7 buffer at 50 °C. Figure 3 shows the variation of absorbance (A_{max}) as a function of initial concentration of benzoyl chloride after addition to the ampicillin solution. The full circles represent experimentally determined absorbance (corrected for dilution of the benzoylation solution by dioxane and titrant) and the intercept on the absorbance axis (square) represents the absorbance measured at 322 nm after 48 minutes (corresponding to t_{max} for the α-benzamidobenzylpenicillin assay at pH 1.7) of a solution of sodium ampicillin treated under the reaction conditions in the absence of benzoyl chloride. An essentially constant absorbance was observed for assay solutions which were treated with benzoyl chloride at initial concentrations (after addition to the aqueous

(11) A. A. Frost and R. G. Pearson, "Kinetics and Mechanism," J. Wiley and Sons, Inc., New York, N. Y., 2nd ed., 1961, p 166.

solution of ampicillin) 7.4–10 times that of ampicillin ($2.0 \times 10^{-3}M$) and, in subsequent procedures, a constant initial concentration of benzoyl chloride ($20 \times 10^{-3}M$) was employed.

Variation of the rate of addition of benzoyl chloride solution (1 ml, 0.1–1.0 ml/min) to sodium ampicillin solution under the reaction condition produced a negligible change in absorbance ($A_{max} = 0.716 \pm 0.004$) at 322 nm in the spectrophotometric assay for penicillin. In subsequent assays, the benzoyl chloride solution was added to the sodium ampicillin solution during a period of 2 min (0.5 ml/min).

The addition of titrant (NaOH) was usually complete after about 10 min, corresponding to complete hydrolysis of excess benzoyl chloride. In experiments to investigate the effect of the sampling time on A_{max}, aliquots were removed at subsequent times (12–20 min after addition of benzoyl chloride) and assayed spectrophotometrically at 322 nm. The results indicated that A_{max} (0.716 ± 0.008) was independent of sampling time within the period studied, and, for convenience, aliquots were removed for assay 12 minutes after the addition of benzoyl chloride.

In order to estimate the reproducibility of the overall benzoylation and penicillin assay procedures, two series of four solutions of sodium ampicillin ($1.0 \times 10^{-3}M$ and $2.0 \times 10^{-3}M$) were benzoylated under optimum conditions and assayed spectrophotometrically at 322 nm. The absorbances (A_{max}) for each series of experiments ($1.0 \times 10^{-3}M$: $A_{max} = 0.356 \pm 0.005$; $2.0 \times 10^{-3}M$: $A_{max} = 0.715 \pm 0.005$) are reported as mean ± standard deviation, and demonstrate the method to be very reproducible.

A series of sodium ampicillin solutions of increasing concentration was benzoylated under optimum conditions and assayed spectrophotometrically. The variation of A_{max} as a function of initial sodium ampicillin concentration is shown in Figure 4, and demonstrates that Beer's law is obeyed by α-benzamidobenzylpenicillenic acid in the concentration range studied.

Comparison with Titrimetric Assay. A solution of sodium ampicillin in water was treated under mildly alkaline conditions ($4.0 \times 10^{-1}M$ ampicillin, pH 10.66, $\mu = 0.2M$, 31.9 °C) and aliquots assayed periodically using the benzoylation procedure and subsequent spectrophotometric analysis at pH 1.7. The apparent first-order rate constant for loss of penicillin β-lactam ($k_{obs} = 1.03 \times 10^{-2}$ min^{-1}; $k_{obs}/(OH^-) = 12.7$ l. mol^{-1} min^{-1}) was in agreement with the rate constant for formation of penicilloic acid under the same conditions ($k_{obs} = 1.10 \times 10^{-2}$ min^{-1}; $k_{obs}/(OH^-) = 13.2$ l. mol^{-1}) measured titrimetrically by the pH-stat system. Moreover, the second-order rate constant for alkaline hydrolysis of ampicillin was in good agreement with the previously reported (*12*) rate constant ($k = 12.3$ l. mol^{-1} min^{-1}) determined titrimetrically at 31.5 °C.

DISCUSSION

Treatment of a solution of sodium ampicillin under acidic conditions (*e.g.*, $1.0 \times 10^{-4}M$ ampicillin, $8.0 \times 10^{-3}M$ $HgCl_2$, pH 1.7, 50 °C 19% ethanol–water) and spectrophotometric analysis at 322 nm using the method of Brandriss and coworkers (*3*) revealed the slow development of a chromophore (oxazolone) corresponding to α-aminobenzylpenicillenic acid ($A = 0.34$ and rising after 7 hr). Since only the absorbance (A_{max}) corresponding to the maximum concentration of penicillenic acid is directly proportioned to the initial concentration of penicillin (*3*, *11*), this method is unsatisfactory for the analysis of ampicillin and other acid-stable penicillins. However, when a solution of benzoyl chloride in dioxane was added to an aqueous solution of sodium ampicillin under very mildly alkaline conditions (*e.g.*, $2.0 \times 10^{-3}M$ ampicillin, $20 \times 10^{-3}M$ benzoyl chloride, pH 9.0, 31.5 °C) a new penicillin, α-benzamidobenzylpenicillin was produced within 10 minutes. Spectrophotometric observation of the resultant solution under acidic conditions revealed the rapid formation of a chromophore ($\lambda_{max} = 322$ nm), corresponding to α-benzamidobenzylpenicillenic acid, which attained a maximum absorbance ($A_{max} = 0.7$) after only 50 minutes. Thus, benzoylation of the side chain amino group of ampicillin, which had conferred acid stability on the penicillin, afforded a new, acid-unstable penicillin, (α-benzamidobenzylpenicillin) which could be assayed readily under acidic conditions.

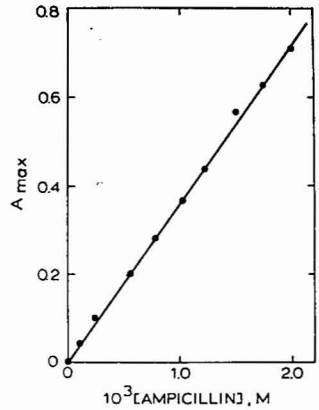

Figure 4. Absorbance as a function of ampicillin concentration, assayed under optimum conditions

The benzoylation procedure was shown to be insensitive to large changes in either the rate of addition of benzoyl chloride solution (0.1–1.0 ml/min) to the ampicillin solution or the time of sampling (12–20 min) for the spectrophotometric analysis. An initial concentration of benzoyl chloride in the assay solution of 7–10 times the initial concentration of ampicillin ($2.0 \times 10^{-3}M$) produced the highest A_{max} values (see Figure 3) corresponding to the maximum conversion of ampicillin to α-benzamidobenzylpenicillin in the benzoylation procedure. The assay of ampicillin using this modified procedure was shown to be very reproducible (±1%) and in good agreement with the titrimetric analysis for penicillin in the alkaline hydrolysis of ampicillin. Although ampicillin concentrations as high as $2.0 \times 10^{-2}M$ were used to investigate the dependence of A_{max} in the spectrophotometric assay upon the initial concentration of ampicillin in the benzoylation solution (Beer's law, see Figure 4), solutions containing as low as $4 \times 10^{-5}M$ ampicillin may be assayed using the benzoylation procedure by employing suitable variations in the experimental conditions (spectrophotometer absorbance scale, assay dilutions, cell path length). Thus, treatment of a solution of ampicillin ($4 \times 10^{-5}M$) with a 10-fold molar excess of benzoyl chloride at pH 9.0 and 31.5 °C and subsequent spectrophotometric analysis at 322 nm of an aliquot of the reaction mixture

(12) R. D. Kinget and M. A. Schwartz, *J. Pharm. Sci.*, 58, 1102 (1969).

(diluted 5-fold with pH 1.7 buffer containing $HgCl_2$ at 50 °C) would produce an absorbance (A_{max} = 0.06 after 48 minutes) which could be measured accurately using the Beckman–Gilford spectrophotometer.

Since benzoylation of the side chain amino group and subsequent rearrangement of α-benzamidobenzylpenicillin to form α-benzamidobenzylpenicillenic acid is specific for intact ampicillin (*6*), the overall procedure could be employed for the spectrophotometric assay of ampicillin both in kinetic reaction solutions and presumably in solutions containing a mixture of ampicillin and another penicillin. For example, treatment of an aliquot of an aqueous solution of benzylpenicillin and ampicillin at pH 2.1 in water at ambient temperature would yield benzylpenicillenic acid only after *ca.* 30 minutes (*3*) (measured spectrophotometrically at 322 nm) since the rate of degradation of ampicillin under such conditions is negligible (*9*). Benzoylation of another aliquot of the mixture and treatment of an aliquot of the resultant solution at pH 1.7 and 50 °C in 19% ethanol–water would yield both benzylpenicillenic acid and α-benzamidobenzylpenicillenic acid (from ampicillin). However, an absorbance measured at 322 nm after 48 minutes would correspond almost entirely to α-benzamidobenzylpenicillenic acid since the benzylpenicillenic would have decomposed completely under these conditions.

ACKNOWLEDGMENT

The authors thank Bristol Laboratories for the gift of sodium ampicillin.

RECEIVED for review August 3, 1970. Accepted December 2, 1970.

Application of a Computerized Electrochemical System to Pulse Polarography at a Hanging Mercury Drop Electrode

H. E. Keller[1] and R. A. Osteryoung

Department of Chemistry, Colorado State University, Fort Collins, Colo. 80521

Application of computerized pulse polarography on a hanging drop to analysis of extremely dilute solutions is demonstrated. An approximate theory is developed which shows that for reversible systems functionally identical behavior can be expected on the dropping and hanging drop mercury electrodes. A decrease in sensitivity for irreversible reactions would be observed under otherwise identical conditions with the stationary electrode. Ensemble averaging and digital smoothing are described and their effect on signal-to-noise ratio is demonstrated. Variations of pulse height, pulse width, and time between pulses are briefly discussed. Response obtained on $4 \times 10^{-8}M$ Cd^{2+} solution indicates that usable data can be obtained at this level while a precision of 10% is indicated on $4 \times 10^{-7}M$ Cd^{2+}.

DERIVATIVE MODE PULSE POLAROGRAPHY has been shown to be a very sensitive analytical technique (*1–4*). When performed on a stationary electrode, additional advantages may accrue such as increased electrode area (*5*), increased speed of analysis, and ensemble-averaging (*6, 7*) undisturbed by drop area uncertainty.

Computerization of chemical analysis is becoming very popular today, a fact occasioned by utility and by novelty. In electrochemical analysis, several workers have been engaged in demonstrating the utility of an on-line computer system (*6, 8–10*). By employing a computer to take measurements, control the experiment, and analyze the resulting data, maximum use is made of the advantages of derivative pulse polarography at a stationary electrode. Other capabilities such as convolution of the current response to increase the signal-to-noise ratio and automatic determination of peak positions and heights by a real-time successive approximation technique can be developed readily on a computer system.

In this paper the characteristics of a computerized electrochemical system are described and demonstrated in an application to pulse polarography at a stationary electrode. Some of the advantages of the computer system over conventional systems are developed; some further potential advantages are mentioned.

The realizable sensitivity of the system as an analytical tool seems, at present, to be limited by background. Instrumental artifacts and oxygen appear to be the primary contributors. With the problems, however, measurable response is obtained with $4 \times 10^{-8}M$ Cd^{2+}. Reducing the concentration of supporting electrolyte to below $10^{-3}M$ is an important factor in this achievement. This sensitivity compares with stripping analysis where sensitivities as low as $6 \times 10^{-11}M$ (*11*) have been reported. More normally, values of $10^{-9}M$ are seen with respect to this technique. It does require that the species determined be concentrated into another phase, a fact which limits its general utility. Potential sweep voltammetry has a reported sensitivity of $\sim 10^{-6}M$ (*12*)

[1] Present address, Department of Chemistry, Northeastern University, Boston, Mass. 02115

(1) E. Temmerman and F. Verbeek, *J. Electroanal. Chem.*, **12**, 158 (1966).
(2) A. Lagrou and F. Verbeek, *ibid.*, **19**, 413 (1968).
(3) E. P. Parry and R. A. Osteryoung, ANAL. CHEM., **36**, 1366 (1964).
(4) C. Peker, M. Herlem, and J. Badoz-Lambling, *Fresenius' Z. Anal. Chem.*, **224**, 204 (1967).
(5) G. D. Christian, *J. Electroanal. Chem.*, **22**, 333 (1969).
(6) S. P. Perone, J. E. Harrar, F. B. Stevens, and R. E. Anderson, ANAL. CHEM., **40**, 899 (1968).
(7) V. W. Lee, T. P. Cheatham, Jr., and J. B. Wiesner, *Proc. I.R.E.*, **38** 1165 (1950).
(8) G. Lauer and R. A. Osteryoung, ANAL. CHEM., **40** (10), 30A (1968).
(9) G. P. Hicks, A. A. Eggert, and E. C. Toren, Jr., *ibid.*, **42**, 729 (1970).
(10) G. Lauer, R. Abel, and F. C. Anson, *ibid.*, **39**, 765 (1967).
(11) S. P. Perone and J. R. Birk, *ibid.*, **37**, 9 (1965).
(12) J. W. Ross, R. D. DeMars, and I. Shain, *ibid.*, **28**, 1768 (1956).

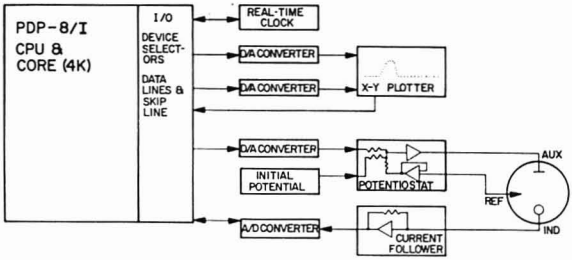

Figure 1. System block diagram

and can be extended by an order of magnitude by analog differentiation (*13*). For a discussion of these and other electroanalytical techniques, the reader is referred to reference (*14*).

EXPERIMENTAL

A PDP-8/I computer (Digital Equipment Corp.) was used for all computing, control, and measurement functions except for the use of a potentiostat and current amplifier, which employed Philbrick-Nexus SP656 and P65AU operational amplifiers. A more complete description of the digital system is given in the next section.

All chemicals were reagent grade and used without further purification. The water was twice-distilled, the first distillation being from alkaline permanganate solution.

A spoutless 100-ml beaker was used as the electrochemical cell. A commercial cover (Beckman Instruments) was adapted to use in this experiment, and prepurified nitrogen was always kept flowing over or through the solution. No frits were used in the apparatus.

The indicating electrode was a Brinkmann microburet hanging mercury drop electrode. The capillary was dewetted with dichlorodimethylsilane prior to use and the end broken off. The reference was a Sargent SCE. The auxiliary electrode was a platinum wire separated from the solution by a pinhole in the end of a piece of glass tubing.

All deaerations were performed for at least 15 minutes. A glass tube with a small hole in the end was used as the nitrogen inlet.

SYSTEM DESCRIPTION

The system, Figure 1, consists of a PDP-8/I computer interfaced with a real-time clock, and X-Y plotter, and a potentiostat plus current follower system based on operational amplifiers. All operations are under computer control.

The real time clock can be set under program control to turn on a flag after the passage of from 1 to 4096 clock pulses or "ticks." This flag is connected to computer skip line so that it may be interrogated by an I/O command. Normally the program uses the skip instruction in a wait loop. The clock can also be read at any time to determine the elapsed time, and it will provide a computer interrupt when the flag is set if the interrupt is enabled. For a more complete description of the clock, see reference (*15*). Further information on the interface is contained in the article by Lauer and Osteryoung (*8*).

The plotter is a Hewlett-Packard X-Y plotter with a digital plotting accessory. The two axes are driven by 10-bit D/A converters. Completion of the plotting of a point is signalled to the computer from the plotter.

(13) S. P. Perone and T. M. Mueller, *Anal. Chem.*, **37**, 2 (1965).
(14) H. A. Laitinen, in "Trace Characterization, Chemical and Physical," W. W. Meinke and B. F. Scribner, Ed., *Nat. Bur. Stand. U.S. Monogr.* **100**, 1967.

(15) D. M. Mohilner and P. R. Mohilner, *O.N.R. Tech. Report No. 1*, Project **NR359-493** (July 1969).

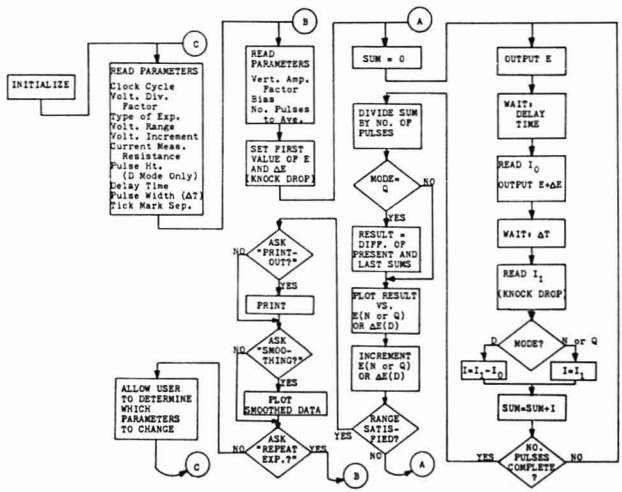

Figure 2. Program block diagram

The electrochemical circuitry is conventional. Input to the potentiostat comes from a variable voltage source and from a 12-bit D/A converter interfaced with the computer. This converter, when properly connected, has a resolution of 0.5 mV for a 2-volt scan. It is run with a single digital buffer into which information is input from the computer by a jam-transfer method. This method of transfer eliminates the need to clear the buffer before it can receive an input and, therefore, prevents spurious signals during transfer. Switching time of the converter is about 3 μsec.

The current output from the cell is converted to a voltage through a current follower. The output from this follower is input to a 12-bit A/D converter. This converter has a sample and hold accessory which is activated by program command. The aperture time is 150 nsec while the track time is 12 μsec. The converter begins conversion on command and gives a conversion complete signal. Conversion time is 35 μsec. The conversion complete signal may also produce an interrupt if activated.

PROGRAM DESCRIPTION

A block diagram of the program is given in Figure 2. A description of the terms used and certain processes not obvious in the diagram follows.

The experimental parameters are read in a question-answer mode. The clock cycle, voltage division factor, and current measuring resistor values allow time, voltage, and current parameters to be communicated in engineering units rather than in computer internal representation. The voltage division factor is an attenuation between the appropriate D/A converter and the potentiostat. The full 12-bit precision of the D/A converter is realized only if its full scale output of 10 volts can be utilized. Therefore the 10-volt output is divided to result in a control voltage slightly greater than the desired scan range. This division is accomplished by utilizing the fact that the input to the potentiostat is a summing network. Appropriate choice of summing resistor for the D/A input results in the desired scaling.

There are three types of pulse polarography that may be performed. The first, designated N (for normal or integral mode), is produced by maintaining the potential between pulses at a constant value. Each successive pulse is of greater magnitude than the preceding one, and the current response at a fixed time after the application of a pulse is plotted against pulse height. In the D (for derivative) mode, all pulses are of equal height. However, the potential between pulses is stepped to a greater value after each pulse. The current is plotted against the potential prior to application of the pulse. A third mode, Q, has been incorporated to allow the difference between successive pairs of current responses output in the N mode to be plotted. This mode is termed the difference mode. Although the D and Q modes give functionally identical behavior when used on reversible systems, the fact that the waiting period between pulses is spent at different potentials can produce marked differences in behavior for systems with complications. An example might be a system exhibiting absorption where desorption would be observed at some potential in the D mode, but since the Q mode would always begin each pulse in the same state it would give no indication of the desorption.

Only in the derivative mode (D), is it necessary to give the value of the pulse height in addition to the other parameters required for all modes.

Delay time is the time between pulses. If a dropping mercury electrode were to be used, the drop would be dislodged at the end of each pulse prior to the delay time. For plotting, provision is made to input horizontal and vertical tick mark spacings.

During the experiment, the current is measured before and at the end of each pulse voltage which is applied to the electrode. After completion of the requisite number of averaging cycles (pulses) at one potential, the calculated point is plotted and the appropriate digital representation of the potential is incremented.

When the experiment is completed, the stored results may be printed. Also, a digitally smoothed plot may be obtained. If a repeat is desired, it can be made with a change of the plotter vertical amplification factor (a program calculation), the plotter bias (also programmed), and/or the number of averaging cycles simply by answering "Y" (Yes) to the computer's query. For other alterations, the answer must be "N" (No). In the latter case the computer switches are set to indicate the changes desired. The computer will ask for only the parameters selected.

THEORY

Pulse Polarography. An approximate theory of differential pulse polarography is developed here for stationary electrodes. For details, see Appendix II. The results are essentially the same as those derived for derivative pulse polarography at a dropping electrode, and the reader is referred to the original papersfor details (*16–19*). The approximate model used here is the application of a potential step from a region of no Faradaic reaction to the potential of interest followed at a time τ by a pulse of height ΔE and duration t. The concentration gradient near the electrode is assumed to be linear when necessary. This assumption should be good for $\tau \gg t$.

For "totally reversible" systems, the concentrations of reactant, C_r, and product, C_p, at the electrode surface are determined by the electrode potential, the bulk concentrations, and the diffusion coefficients, D_r and D_p. They are time invariant at any fixed potential. When the Fick's law equations are solved, the concentration gradient prior to pulse application is found to be missing from the expression for Δi.

$$\Delta i = \frac{nFAD_p^{1/2}C_r^{\circ}\gamma^{\circ}}{\pi^{1/2}t^{1/2}} \frac{1-\beta}{(\beta\gamma^{\circ}+\delta)(\gamma^{\circ}+\delta)} \quad (1)$$

See appendix I for notation. Note that this expression also does not depend on τ and, further, that it is symmetrical about $E_{1/2} + {}^1/_2\Delta E$, where $E_{1/2}$ is the polarographic half-wave potential. This is essentially the same expression as those derived previously (*16*, *18*). Derivation of the equivalent equation for a stationary spherical electrode yields the standard spherical correction term for potentiostatic processes (*20*).

A "totally irreversible" process (see Appendix II) results in an equation containing τ.

$$\Delta i = nFAD_r^{1/2}C_r^{\circ}(\lambda_o - \lambda)\exp(\lambda_o^2\tau) \times \operatorname{erfc}(\lambda_o\tau^{1/2})\exp(\lambda^2 t)\operatorname{erfc}(\lambda t^{1/2}) \quad (2)$$

(16) G. C. Barker and A. W. Gardner, *At. Energy Res. Estab. Harwell*, C/R 2297 (1958).
(17) G. C. Barker, R. L. Faircloth, and A. W. Gardner, *ibid.*, C/R 1786.
(18) E. P. Parry and R. A. Osteryoung, ANAL. CHEM., 37, 1634 (1965).
(19) A. A. M. Brinkman and J. M. Los, *J. Electroanal. Chem.*, 7, 171 (1964).
(20) W. H. Reinmuth, *J. Amer. Chem. Soc.*, 79, 6358 (1957).

Table I. Concentration of Cd(II) *vs.* Peak Height

Concentration (M)	Peak height (μA)
4×10^{-5}	57.
4×10^{-6}	7.4
4×10^{-7}	0.92
4×10^{-8}	0.31

This equation becomes identical to that given by Barker (*16*) if ΔE is small and the $\lambda_0^2\tau$ terms are combined with $C_r°$. The dependence of τ shows that for long experiments—*i.e.*, the effective value of τ is large—sensitivity to irreversible reactions is decreased. Barker presents the same argument (*16*). Note that the concentration gradient again does not appear in the expression. However, higher than first-order terms would appear if included in the derivation. Their inclusion would, however, make the mathematics unduly complex.

Therefore, it is important when doing analysis by derivative pulse polarography to try to have the sought after species in a form which displays reasonable electrochemical reversibility at times of the order of the pulse width. A significant corollary to this behavior of irreversible systems is a decrease in the sensitivity to oxygen so that it will cause less interference than in, say, normal (integral mode) pulse polarography.

Signal Averaging. The theory of cross correlation is well developed (*7*, *21*). The signal is multiplied by a function synchronized with the signal. The signal is assumed to be periodic and its product with the cross correlation function is summed over the number of periods or cycles run to obtain a single output value. Several such summations may be seen simultaneously or seriatim to provide an ensemble average.

In this work the cross correlation function is a periodic binary sampling function synchronized with the beginning of each pulse. In effect, the result is ensemble averaging. It is reasonable to expect that for most random noise distributions encountered in practice, the signal-to-noise ratio will increase as the square root of the averaging cycles.

Digital Least Squares Smoothing. The method of smoothing employed for this paper is that given by Savitsky and Golay (*22*). The reader is referred to their paper and references for further details.

RESULTS AND DISCUSSION

Pulse polarograms were run on cadmium nitrate in potassium nitrate supporting electrolyte with the computerized pulse polarography system. The concentrations of cadmium ranged from $4 \times 10^{-5}M$ to $4 \times 10^{-8}M$ while the corresponding KNO_3 concentrations were $0.5M$ to $0.5mM$. Peak height as a function of concentration is given in Table I. There is an apparent increase of sensitivity at lower concentrations. While the dilutions were made with distilled water, thus lowering the ionic strength, resultant double layer effects or migration effects would be expected to be minor. The more likely cause of the loss of linearity is an instrumental one produced by increasing solution and current measuring resistances. With increasing uncompensated resistance, the potentiostat does not control until

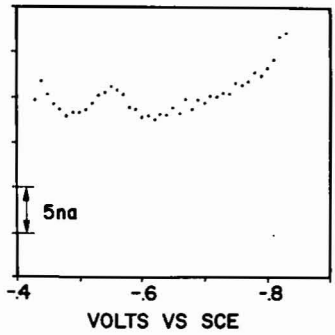

Figure 3. Derivative pulse polarogram of $4 \times 10^{-8}M$ Cd^{2+}, $5 \times 10^{-4}M$ KNO_3

20-cycle average without smoothing. A = 0.0414 cm². Pulse height = 50 mV. Pulse width = 20 msec. Delay = 200 msec

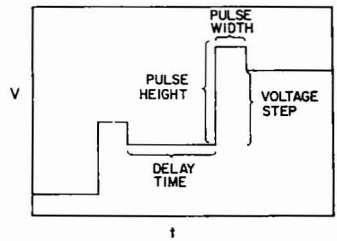

Figure 4. Voltage wave form for derivative mode pulse polarography

several milliseconds after the pulse is applied. The peak heights are readily reproducible at all except the lowest concentration where extreme care must be taken to eliminate oxygen. Figure 3 shows the response of the system to the lowest concentration studied, $4 \times 10^{-8}M$ Cd^{2+} in $0.5 \times 10^{-3}M$ KNO_3. A readily measurable peak is apparent. At higher concentrations, a large, well-formed peak is observed. With proper precautions, the detection limit for computerized pulse polarography of cadmium should be substantially less than $10^{-8}M$. This is better than has been previously reported for pulse polarography.

The reproducibility of the system described in this paper is demonstrated by a series of replicate runs. Data were output on the teletype. The largest value was taken as the peak, while the minimum value preceding the peak was taken as the base line. Four runs at $4 \times 10^{-6}M$ Cd^{2+} had a standard deviation of 1.5% while ten at $4 \times 10^{-7}M$ Cd^{2+} had a standard deviation of 10%. The drop area was reproducible to only about 1% accounting for most of the error in the first series. Since the background in the second series had a magnitude of roughly one-half of the peak and was not necessarily additive, it is likely that this is the predominant source of error. A longer pulse width than the 20 milliseconds employed plus better electronic circuitry should be sufficient to reduce the error considerably. Better oxygen scrubbing techniques are also indicated.

(21) D. J. Fisher, *Chem. Instrum.*, **2**, 1 (1969).
(22) A. Savitsky and M. J. E. Golay, ANAL. CHEM., **36**, 1627 (1964).

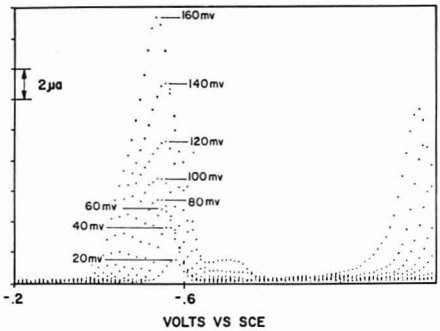

Figure 5. Derivative pulse polarograms of $4 \times 10^{-4}M$ Cd^{2+}, $0.5M$ KNO_3

5-cycle average without smoothing. $A = 0.0414$ cm². Pulse height = 20, 40, 60, 80, 100, 120, 140, 160 mV. Pulse width = 20 msec. Delay = 200 msec

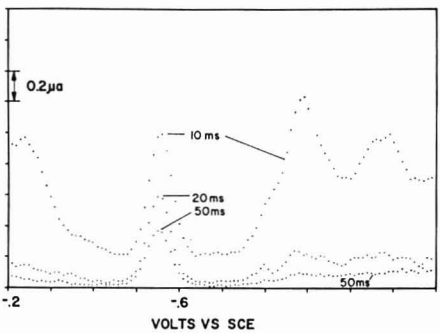

Figure 6. Derivative pulse polarogram of $4 \times 10^{-4}M$ Cd^{2+} $0.05M$ KNO_3

5-cycle average without smoothing. $A = 0.0414$ cm². Pulse height = 50 mV. Pulse width, delay = 10, 100 msec; 20, 200 msec; 50, 500 msec

Effort directed toward optimization of experimental parameters has been reported (*3*, *18*). Because there are new factors present in the hanging drop method and because of the importance of optimization to achieving maximum sensitivity, certain of these parameters have been investigated here. The parameters associated with the voltage wave form are shown in Figure 4. Calculations were made on the theoretical response for variations of pulse height. There can be no general optimal value since one individual may be concerned with peak separation, while another may desire only a maximum height to half-width ratio. The effect of pulse height on separation has already been discussed elsewhere (*3*). The result is that smaller pulse heights provide greater separation at the expense of sensitivity.

Since large pulse height will result in the peak approaching a maximum height while continually broadening and small pulses cause continually diminishing peak height but a constant, minimum peak width, it would seem that some intermediate pulse height should be optimal. An arbitrary

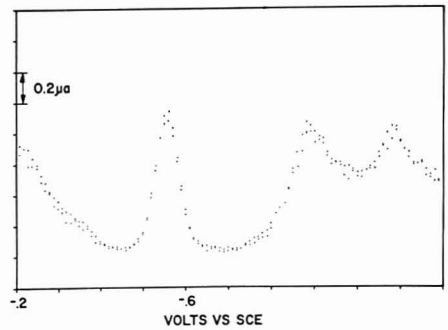

Figure 7. Derivative pulse polarogram of $4 \times 10^{-4}M$ Cd^{2+}, $0.05M$ KNO_3

5-cycle average without smoothing. $A = 0.0414$ cm². Pulse height = 50 mV. Pulse width = 10 msec. Delay = 100, 200 msec

measure of the optimal value is the ratio of peak height to the half-peak width. Hand calculations show that this quantity is a maximum when $nF\Delta E/RT = 2.1$ or $\Delta E = 63$ mV for a two-electron process at 25 °C. However, equally significant is the fact that the range of pulse heights allowed if a 10% variation of the above ratio is permitted, is $180/n$ mV to $84/n$ mV at 25 °C. It is therefore quite likely that the pulse height for any given experiment will be determined by other factors. This is especially true if two species undergoing reductions requiring different numbers of electrons are being studied simultaneously or if peak separation is a problem.

The actual results of variation of pulse height are shown in Figure 5. The 60-mV curve appears to be the best one. The asymmetry observed at large pulse heights is likely due to insufficient delay times between pulses. At pulse heights of 100 mV and greater, the trailing edge of the peak moves cathodic. However, if there are no nearby interfering ions, then high sensitivity can be achieved by using relatively large pulse heights.

For maximum response, the pulse width should be a minimum, although if too short, double layer relaxation will make a significant contribution and limit the sensitivity. The effect of pulse widths of 10, 20, and 50 milliseconds is displayed in Figure 6. The delay time is ten times the pulse width in each case. The heights obey the $t^{-1/2}$ law predicted by theory to better than 5%. Other experiments show that if the pulse width is greater than 0.1 sec, positive deviations are observed. These deviations are readily explained by convection and spherical effects. Much more significant is the effect on the background. The extreme change in the background level observed in Figure 6 is due to instrumental limitations. Positive feedback should be capable of reducing this effect, thus allowing the instrument to achieve still greater sensitivity.

The delay time between pulses allows for the relaxation of the disturbance. If the delay is too short, then the signal becomes noisy and sensitivity is decreased. Long delays increase measurement time. Therefore the delay must be a compromise between these effects. For the 50-mV pulses used in most of the work, a delay of ten times the pulse width was found to be satisfactory. Figure 7 shows the effect of 100- and 200-msec delays when the pulse width is

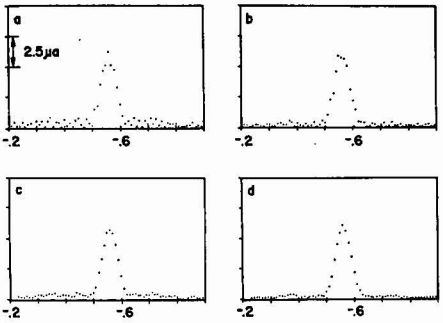

Figure 8. Derivative pulse polarograms of $4 \times 10^{-5}M$ Cd^{2+}, $0.5M$ KNO_3

Pulse height = 50 mV. Pulse width = 20 msec. Delay = 200 msec. (*a*) No smoothing, average × 1 (*b*) No smoothing, average × 9 (*c*) 9-pt smooth, average × 1 (*d*) 9-pt smooth, average × 9

10 msec. A slight sensitivity improvement is observed with the 200-msec. delay.

One of the primary advantages of a computerized experimental system is the acquisition and storage of data in digital form. These data can then be operated upon during or after the experiment to improve the quality of experimental results. In the present system, two means of operating on the data are employed. The data are averaged by taking several measurements at the same potential repetitively, and the data are smoothed by a least squares procedure after the experiment. Both of the operations are optional. The first has the effect of increasing the signal-to-noise ratio as the square root of the number of averaging cycles. There is no distortion created if the delay between pulses is sufficiently long to allow virtually complete relaxation of the disturbance created by the pulses. The second method improves the signal-to-noise ratio as the square root of the number of values over which each point is calculated. Distortion will be introduced if the order of the polynomial used to fit the data is too small to adequately represent the segment of the curve being fit. Test computations indicate that a nine-point quartic smooth will introduce no measurable distortion with data points spaced 10 mV apart. The two above methods affect the signal-to-noise ratio independently so that the addition of the nine point smoothing algorithm should have the same effect on the signal-to-noise ratio as multiplying the number of averaging cycles by nine. Figure 8 demonstrates the efficacy of these noise reduction techniques. In Figure 8*a* a raw curve is shown. Figure 8*b* shows the effect of averaging over nine cycles while, in Figure 8*c*, the nine-point smoothing routine is used. The two curves show roughly the same reduction in noise. Figure 8*d* is the result of applying both techniques. The effect of noise is virtually eliminated.

The experimental results indicate that through the use of an on-line computer a significant increase in the sensitivity of pulse polarography can be attained. Particularly important to this increase are the techniques of signal averaging and data smoothing and the ability to vary experimental parameters readily over a wide range.

The direct connection between the experiment and the computer with the experimentalist present gives a rapid turn-around capability which is highly beneficial in experiments of the type demonstrated. First, there is immediate knowledge of the success or failure of the experimental arrangement and parameters used. Second, quantitative results are available at the moment. No delays due to data conversion and processing are incurred. Third, there are advantages unrealized in this work such as removing the experimenter from the computer–experiment feedback loop by programming decision-making capabilities into the computer. This could even be done by computerized learning machine methodology.

A program listing or source tape may be had by writing to the authors.

ACKNOWLEDGMENT

Some of the programming ideas are due to George Lauer. The hardware interface was built by P. R. Mohilner and was based on a design for a similar interface by G. Lauer and R. A. Osteryoung. Helpful discussions with J. H. Christie are acknowledged.

APPENDIX I

Notation

n	= number of electrons transferred per mole of reactant
F	= Faraday
A	= electrode area
D_r	= diffusion coefficient of reactant
D_p	= diffusion coefficient of product
C_r and C_p	= concentrations
C_r° and C_p°	= concentrations at $t = 0$, $x = 0$
δ	$= D_p^{1/2}/D_r^{1/2}$
C_T	$= C_r^\circ + \delta C_p^\circ$
β	$= \exp(nF/RT\,\Delta E)$
ΔE	= pulse height
γ°	$= \exp[nF/RT(E_i - E^\circ)]$
E_i	= potential prior to application of pulse
E°	= formal standard potential of electrode reaction
$\lambda_\circ$	$= k_s D_r^{-1/2} \exp[-\alpha nF/RT(E_i - E^\circ)]$
λ	$= \lambda_\circ \exp(-\alpha nF/RT\Delta E)$
k_s	= formal standard heterogeneous rate constant
erfc (x)	= 1 − erf (x) where $\mathrm{erf}(x) = 2/\pi^{1/2}\int_0^x e^{-t^2}dt$
i	= current
i°	= current at $t = 0$
Q	$= k_s \exp[\alpha nF/RT(E_i - E^\circ)]\{D_r^{-1/2} + D_p^{-1/2} \exp[nF/RT(E_i - E^\circ)]\}$
μ	$= \lambda[1 + \delta^{-1} \exp[nF/RT(E - E^\circ)]]$

APPENDIX II

Derivation of Curve Shape for Derivative Mode Pulse Polarography at a Stationary Electrode

From Delahay (*23*),

$$i = nFAC_r^\circ\lambda_\circ D_r^{1/2} e^{Q^2\tau} \operatorname{erfc}(Q\tau^{1/2}) \qquad \text{(A1)}$$

From Fick's diffusion equation, after Laplace transformation and using semi-infinite linear diffusion,

$$\bar{C}_r = C_r^\circ/s + \bar{a} \exp[-x\sqrt{s/D_r}] \qquad \text{(A2)}$$

The new variable, $\bar{a}$, is an undetermined coefficient. Therefore,

$$(\bar{C}_r)_{x=0} = C_r^\circ + a \qquad \text{(A3)}$$

(23) P. Delahay, "New Instrumental Methods in Electrochemistry," Interscience, New York, N. Y., 1954, p 74.

and

$$(\partial \bar{C}_r/\partial x)_{x=0} = -\bar{a}\sqrt{s/D_r} \quad \text{(A4)}$$

However, using Equation A1,

$$(\partial \bar{C}_r/\partial x)_{x=0} = \frac{i}{nFAD_r} = \frac{C_r{}^0\lambda_0}{D_r{}^{1/2}}\frac{1}{s^{1/2}(s^{1/2}+Q)} \quad \text{(A5)}$$

Combining Equations A4 and A5 yields

$$\bar{a} = -\frac{C_r{}^0\lambda_0}{s(s^{1/2}+Q)} \quad \text{(A6)}$$

Substituting A6 into A3 and A4 and inverting the transform gives

$$C_r(0,\tau) = C_r{}^0 - C_r{}^0\lambda_0 Q^{-1}[1 - e^{Q^2\tau}\ \text{erfc}\ (Q\tau^{1/2})] \quad \text{(A7)}$$

and

$$\frac{\partial C_r(0,\tau)}{\partial x} = C_r{}^0\lambda_0 D_r{}^{-1/2}e^{Q^2\tau}\ \text{erfc}\ (Q\tau^{1/2}) \quad \text{(A8)}$$

Similarly,

$$C_p(0,\tau) = C_r{}^0\lambda_0\delta^{-1}Q^{-1}[1 - e^{Q^2\tau}\ \text{erfc}\ (Q\tau^{1/2})] \quad \text{(A9)}$$

and

$$\frac{\partial C_p(0,\tau)}{-\partial x} = -C_r{}^0\lambda_0\delta^{-1}D_p{}^{-1/2}e^{Q^2\tau}\ \text{erfc}\ (Q\tau^{1/2}) \quad \text{(A10)}$$

Now, assume that the concentration gradients are linear and can be represented by

$$C_r = c_0 + c_1 x \quad \text{(A11a)}$$

and

$$C_p = c_0' + c_1' x \quad \text{(A11b)}$$

Once again, solving Fick's equation in Laplace space yields

$$\bar{C}_r = \frac{1}{s}(c_0 + c_1 x) + \bar{b}\ \exp\left[-x\sqrt{s/D_r}\right] \quad \text{(A12)}$$

So that

$$\bar{C}_r(0,s) = c_0/s + \bar{b} \quad \text{(A13)}$$

and

$$\frac{\partial \bar{C}_r(0,s)}{-\partial x} = c_1/s - \bar{b}\sqrt{s/D_r} \quad \text{(A14)}$$

Similarly,

$$\bar{C}_p(0,s) = c_0' + \bar{b}' \quad \text{(A15)}$$

and

$$\frac{\partial \bar{C}_p(0,s)}{-\partial x} = c_1'/s - \bar{b}'\sqrt{s/D_p} \quad \text{(A16)}$$

Substituting into the absolute rate theory expression (*24*),

$$i = nFA\lambda D_r{}^{1/2}\left\{\bar{C}_r(0,s) - \bar{C}_p(0,s)\exp\left[\frac{nF}{RT}(E - E^0)\right]\right\} \quad \text{(A17)}$$

Note that

$$i = nFAD_r(\partial C_r/\partial x)_{x=0} \quad \text{(A18)}$$

Assume equal and opposite fluxes (*23*) and use Equations A14 and A16 with appropriate manipulation to give

$$\bar{b}' = c_1' D_p{}^{1/2}s^{-3/2} + c_1 D_r{}^{1/2}\delta^{-1}s^{-3/2} - \bar{b}\delta^{-1} \quad \text{(A19)}$$

(24) P. Delahay, "New Instrumental Methods in Electrochemistry," Interscience, New York, N. Y., 1954, p 34.

Substitute Equations A13, A15, and A19 into A17 and A14 into A18; equate currents to get

$$nFA\lambda D^{1/2}\left\{\frac{c_0}{s} + \bar{b} - \left[\frac{c_0'}{s} + \frac{c_1' D_p{}^{1/2}}{s^{3/2}} + \frac{c_1' D_r{}^{1/2}}{\delta s^{3/2}} - \frac{\bar{b}}{\delta}\right]\exp\left[\frac{nF}{RT}(E - E^0)\right]\right\} = nFAD_r(c_1/s - \bar{b}\sqrt{s/D_r}) \quad \text{(A20)}$$

Solve for $\bar{b}$ using (see Appendix I),

$$\bar{b} = \frac{c_1 D_r{}^{1/2}}{s(s^{1/2}+\mu)} - \frac{\lambda}{s(s^{1/2}+\mu)} \times \left\{c_0 - c_0'\exp\left[\frac{nF}{RT}(E - E^0)\right]\right\} + \frac{\lambda}{s^{3/2}(s^{1/2}+\mu)} \times \left(c_1' D_p{}^{1/2} + \frac{c_1 D_r{}^{1/2}}{\delta}\right)\exp\left[\frac{nF}{RT}(E - E^0)\right] \quad \text{(A21)}$$

Using Equations A18, A14, and A21 and inverting the transform

$$i = nFAD_r\left\{c_1 - c_1 e^{\mu^2 t}\ \text{erfc}\ (\mu t^{1/2}) + \frac{\lambda}{D_r{}^{1/2}}\left[c_0 - c_0'\exp\left(\frac{nF}{RT}(E - E^0)\right)\right]e^{\mu^2 t}\ \text{erfc}\ (\mu t^{1/2}) - \frac{\lambda}{\mu}\left(c_1'\delta + \frac{c_1}{\delta}\right)[1 - e^{\mu^2 t}\ \text{erfc}\ (\mu t^{1/2}]\exp\left[\frac{nF}{RT}(E - E^0)\right]\right\} \quad \text{(A22)}$$

Replacing c_0, c_0', c_1, and c_1' with the values given by Equations A7, A9, A8, and A10 and subtracting A1 gives

$$\Delta i = nFAD_r{}^{1/2}C_r{}^0\left\{\lambda\left[1 - \frac{\lambda_0}{Q}\left(1 + \delta^{-1}e^{\frac{nF}{RT}(E - E^0)}\right) \times (1 - e^{Q^2\tau}\ \text{erfc}\ (Q\tau^{1/2}))e^{\mu^2 t}\ \text{erfc}\ (\mu t^{1/2})\right] - \lambda_0 e^{Q^2\tau}\ \text{erfc}\ (Q\tau^{1/2})e^{\mu^2 t}\ \text{erfc}\ (\mu t^{1/2})\right\} \quad \text{(A23)}$$

Equation A23 is the general expression for a pulse applied at time τ after a step, using the approximation of linear concentration gradients. The limiting case of a totally irreversible reaction may be obtained from the following limits:

$$Q \to \lambda_0,\ \mu \to \lambda,\ \exp\left[\frac{nF}{RT}(E - E^0)\right] \to 0.$$

The result is

$$\Delta i = nFAD_r{}^{1/2}C_r{}^0(\lambda - \lambda_0)e^{\lambda_0^2\tau}\ \text{erfc}\ (\lambda_0\tau^{1/2})e^{\lambda^2 t}\ \text{erfc}\ (\lambda t^{1/2}) \quad \text{(A24)}$$

The limiting case of a totally reversible reaction can be obtained by taking $k_s \to \infty$. Then $\mu \to \infty$, $\lambda \to \infty$ and

$$\lambda e^{\mu^2 t}\ \text{erfc}\ (\mu t^{1/2}) \to \frac{\lambda}{\pi^{1/2}t^{1/2}\mu}$$

The result is

$$\Delta i = \frac{nFAC_r{}^0 D_p{}^{1/2}\gamma^0}{\pi^{1/2}t^{1/2}}\frac{1 - \beta}{(\gamma^0 + \delta)(\beta\gamma^0 + \delta)} \quad \text{(A25)}$$

In the above derivation, an electrochemical reduction has been assumed and the initial concentration of the product was zero. In the reversible case, the initial concentration of the product may be non-zero and the requirement of linearity of the concentration gradient may be relaxed.

Received for review August 13, 1970. Accepted December 21, 1970. This work was supported in part by NASA Grant Number NGR-06-002-088.

Rapid Analysis for Sub-Nanogram Amounts of Chromium in Blood and Plasma Using Electron Capture Gas Chromatography

Larry C. Hansen and William G. Scribner
Monsanto Research Corporation, Dayton, Ohio 45407

T. William Gilbert
Department of Chemistry, University of Cincinnati, Cincinnati, Ohio 45221

Robert E. Sievers
Aerospace Research Laboratories, Wright-Patterson Air Force Base, Ohio 45433

A rapid method for the quantitative determination of chromium in blood and plasma has been developed. A 0.050-ml sample is reacted in a sealed tube with a hexane solution containing 1,1,1-trifluoro-2,4-pentanedione. It is not necessary to digest or ash the sample in this direct reaction procedure. Components of the hexane extract are then separated using a gas–liquid chromatographic column, and chromium is detected as chromium trifluoroacetylacetonate using an electron capture detector with a tritium source. Chromium has been determined at the 50 ng/ml of blood or plasma level. The detector responds well to picogram amounts of chromium allowing determinations as low as 5 ng/ml without preconcentration or pretreatment of the blood or plasma. Live animal experiments have shown *in vivo* chromium can be chelated and extracted from blood and plasma using the recommended procedure. Time requirement per sample is about 1½ hours; however, analysis of four or more samples simultaneously decreases the average analysis time to less than 1 hour. Suggestions for the use of this method as a diagnostic tool are also made.

CHROMIUM IS ESSENTIAL to man for normal body functions and is important as a diagnostic tool. The occurrence and importance of chromium in the functioning of biological systems has been extensively reviewed by Mertz (*1*). In man, normal blood chromium levels are in the 20 to 50 nanograms per milliliter range. To better establish the relationships between chromium and body functions, such as glucose metabolism, a method to analyze for chromium at this level is needed. Evidence that chromium deficiency is a factor related to disturbances of glucose metabolism (*1*) points out the need for a method to analyze for chromium in blood plasma at levels down to 5 nanograms per milliliter. Because of these low chromium concentrations and the frequently limited sample size, a highly sensitive method for chromium detection is necessary for its determination.

Earlier studies have shown the extraordinary sensitivity with which fluorine-containing chelates such as chromium(III) trifluoroacetylacetonate can be detected by electron capture gas–liquid chromatography (*2*, *3*). The principal problem that remained was to develop a rapid and simple method for quantitative conversion of protein-bound chromium in blood to the trifluoroacetylacetonate.

1,1,1-Trifluoro-2,4-pentanedione [H(tfa)] has been used as the chelating agent by Savory *et al.* (*4*) for the determination of microgram quantities of chromium in serum; however, this method involved an acid digestion of the serum for 1 hour at 180 °C to destroy the otherwise interfering protein material. Taylor *et al.* (*5*) used H(tfa) for the determination of beryllium in various biological fluids in a rapid and simple reaction in a sealed tube between the biological sample and a benzene solution of the chelating agent. They reported that H(tfa) was effective as a chelating agent and resulted in quantitative $Be(tfa)_2$ formation in the presence of naturally-occurring complexing agents.

This report presents the optimum conditions for the rapid quantitative chelation, extraction, and electron capture GLC determination of chromium in blood and plasma using H(tfa) as a direct reaction chelating agent. 1,1,1,5,5,5-Hexafluoro-2,4-pentanedione [H(hfa)] and 1,1,1,2,2,3,3-heptafluoro-7,7-dimethyl-4,6-octanedione [H(fod)] were also evaluated for this purpose.

EXPERIMENTAL

Apparatus. A Hewlett-Packard Model 402 gas chromatograph with an electron capture detector utilizing a tritium source was used with the following column and conditions: column, 2 ft × 3/16 in. i.d. borosilicate glass tube packed with 5% Dow Corning LSX-3-0295 silicone gum on 60–80 mesh Gas Chrom P; column temperature, 132 °C; detector temperature, 190 °C; carrier gas, He; carrier flow rate, 20 ml/min; purge gas, 5% methane–95% argon; purge flow rate, 100 ml/min; pulse mode interval setting, 150. The following column under the same conditions (except where stated) was used for confirmation of the identity of the $Cr(tfa)_3$ peak: column, 4 ft × 3/16 in. i.d. borosilicate glass tube packed with 3.8% Union Carbide W-98 silicone gum on 80–100 mesh Anachrom ABS; column temperature, 133 °C.

Gamma counting of ^{51}Cr (0.325 Mev γ, $t_{1/2}$ = 27.8 d) used to establish optimum chelation and extraction conditions was performed in a well scintillation counter containing a sodium iodide crystal activated with thallium (Nuclear Measurements Corporation).

Reagents. H(tfa), H(hfa), and H(fod) (Pierce Chemical Company) solutions were prepared by dissolving freshly distilled material in Chromatoquality Hexane (Matheson, Coleman and Bell).

Cis-trans $Cr(tfa)_3$ was prepared by a method similar to that reported by Ross, Scribner, and Sievers (*6*) by mixing 100 mg of chromium powder, 1 ml of H(tfa), and 1 drop of concd HCl. The mixture was vigorously shaken and excess H(tfa) was removed later by adding 4.0 ml benzene and then extract-

(1) W. Mertz, *Physiol. Rev.*, **49**, 163 (1969).
(2) R. W. Moshier and R. E. Sievers, "Gas Chromatography of Metal Chelates," Pergamon Press, Oxford, 1965, and references therein.
(3) W. D. Ross and R. E. Sievers, ANAL. CHEM., **41**, 1109 (1969).
(4) J. Savory, P. Mushak, F. W. Sunderman, Jr., R. H. Estes, and N. O. Roszel, *ibid.*, **42**, 294 (1970).
(5) M. L. Taylor, E. L. Arnold, and R. E. Sievers, *Anal. Lett.*, **1**, 735 (1968).
(6) W. D. Ross, W. G. Scribner, and R. E. Sievers, Preprint of 8th International Symposium on Gas Chromatography, Ballsridge, Dublin, Ireland, Sept. 1970.

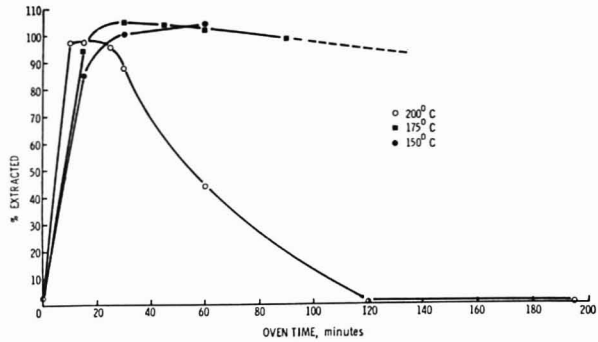

Figure 1. Per cent chromium extracted from blood with H(tfa) in hexane as a function of time

ing with 4.0 ml of 0.5*N* NaOH. The product was purified by fractional sublimation at 100–145 °C (0.05 mm). (Early condensing oily material was discarded.) If purification by recrystallization is attempted, care should be taken to avoid solvents that alter the natural trans to cis ratio (~4 to 1) in the final product, since both isomers are formed from chromium in blood. *Anal:* Calcd for $Cr(C_5H_4F_3O_2)_3$: C, 35.24; H, 2.37. Found: C, 34.86; H, 2.18. A stock $Cr(tfa)_3$ solution was prepared by dissolving 0.01005 gram of the pure material in 10 ml of Chromatoquality Hexane, resulting in a solution containing 1.02×10^{-4} gram Cr/ml. Standard solutions containing 1.53, 1.02, and 0.51×10^{-5} gram Cr/ml were prepared by appropriate dilutions with hexane.

A stock aqueous chromium solution was prepared by dissolving 0.1307 gram of pure chromium metal in 5 ml of hot HCl (concd). After boiling down to 1 ml, a dilution to 100 ml with distilled water resulted in a solution containing 1.304×10^{-3} gram Cr/ml. Standard solutions were prepared by appropriate dilutions immediately before use.

Whole blood samples were drawn from the donors with 10-cc disposable syringes with 1.5-inch (20 gauge) needles (TOMAC). Blood samples were placed in 10-cc Vacutainers (Becton, Dickinson and Co.) coated with sodium heparin. Plasma samples were obtained by centrifuging freshly drawn, heparinized whole blood and separating the top plasma layer from the cells. Blood and plasma samples were stored at 4 °C when analyses could not be performed immediately.

Recommended Procedure. The following procedure is recommended for the quantitative determination of chromium in blood or plasma. A glass reaction tube (4 in. × $^3/_{16}$ in. i.d.) is made by sealing the tapered end of a disposable pipet (Matheson Scientific) with an oxygen–methane torch. A 0.050-ml sample of the biological material is introduced into the glass tube followed by 0.50 ml of a hexane solution containing 0.005 ml of H(tfa). After introduction of the reaction mixture, the sealed end is immersed in an ice bath and the open end of the tube is then sealed at the constriction. The sealed tube is shaken for 15 seconds, wrapped in heavy duty aluminum foil, and placed on its side in a 175 °C oven for 30 minutes. After 5 minutes of cooling and 5 minutes of centrifuging, the reaction tube is opened and a 0.40-ml aliquot of the hexane phase is added to 0.50 ml of 1.0*N* NaOH in a 2-dram vial which is then sealed with a polyethylene-lined cap. After shaking for 5 minutes, the vial is centrifuged for 5 minutes. A sample of the hexane phase is placed in a 1-dram vial which is then tightly sealed. Five 1.0-μl injections of this hexane solution into the column are made alternately with five 1.0-μl injections of the appropriate standard $Cr(tfa)_3$ solution. Time savings can be effected with fewer injections with some sacrifice in precision. The average *trans*-$Cr(tfa)_3$ peak heights of the standard $Cr(tfa)_3$ solution are compared with those from the hexane solution from the reaction to calculate the concentration of chromium in the sample. The sample preparation time is about 60 minutes; the instrument time per injection is 12 minutes. If four or more simultaneous analyses are performed, the average time is less than 1 hour.

Optimization Experiments. The optimum conditions for the chelation and extraction of chromium from blood were determined by systematically varying the type of β-diketone, the chelating agent concentration, the reaction temperature, and the reaction time. H(tfa), H(hfa), and H(fod) were evaluated in concentrations from $4.1 \times 10^{-2}M$ to $8.7 \times 10^{-2}M$. Oven temperatures varied from 150 to 200 °C and reaction heating times from 0 to 195 minutes. The chelation and extraction was followed using radioactive ^{51}Cr which was incorporated into the blood sample by adding an aqueous chromium(III) chloride solution to an equal volume of blood. Therefore, the 0.050-ml blood sample actually consisted of 0.025 ml of blood and 0.025 ml of chromium(III) chloride solution in the chelation and extraction study. The blood solution contained 47 ng of Cr/ml and ~3.8 μCi of ^{51}Cr/ml (specific activity = 81.5 mCi/mg Cr). [Radiotracers were used only in these chelation and extraction studies and in the live animal experiments (to be discussed later) and are not necessary for the quantitative determination by the recommended procedure.] The reaction tube containing the blood-^{51}Cr solution was counted twice for 5 minutes in the scintillation counter, and the counts were averaged and corrected for background. After heating, cooling, and centrifuging, a 0.20-ml aliquot of the 0.50-ml hexane phase was placed in a 6-dram counting vial along with two 0.20-ml hexane rinses of the transfer pipet. The resulting 5-minute counts of the vial were averaged, corrected for background, multiplied by 250, and divided by the net average reaction tube 5-minute count to give the extraction efficiency (%*E*).

Quantitative gas chromatographic determinations were made on blood and plasma using the recommended procedure. Experiments were performed to determine whether known amounts of chromium could be accurately determined in the presence of potential interferences in blood and plasma. In these experiments, the blood and plasma samples were mixed with an equal volume of aqueous chromium(III) chloride (nonradioactive). The resulting blood solutions contained 104 ng and 52 ng of Cr/ml and the plasma solution contained 52 ng Cr/ml. Blanks consisting of 0.050-ml portions of blood or plasma solutions to which only equal volumes of distilled water had been added were also analyzed. The difference in the *trans*-$Cr(tfa)_3$ peak heights of the sample and the blank was then compared to the *trans*-$Cr(tfa)_3$ peak height of the standard solution to determine the amount of chromium added to the sample. Detector response was linear (peak height *vs.* amount Cr present) over the necessary range (1.5×10^{-11} to 5.1×10^{-12} g Cr), which allowed calculations by direct proportion.

Live animal experiments, used to show that *in vivo* chromium could be determined, were performed by injecting 0.5 ml of a saline (pH 8) Na_2CrO_4 solution into the tail vein of six laboratory rats. The 0.5 ml injected contained 100 μCi of ^{51}Cr and 15 μg of Cr. Blood samples were taken from the animals 1 and 3 hours after injection. Blood and plasma samples were then reacted as in the recommended procedure up to the point of extraction. The extraction efficiencies (%*E*) were determined by the radioactive counting of the samples and were calculated as previously described.

In an independent study of the determination of chromium in lunar rock samples, Ross and Wolf have established that the relative standard deviation of the gas chromatographic portion of the analysis is 2% (*7*).

RESULTS AND DISCUSSION

The systematic evaluation of H(tfa), H(fod), and H(hfa) as chelating agents for chromium in blood showed that with H(tfa) quantitative chelation and extraction were possible under certain conditions. Some of the results of the H(tfa) evaluation are shown graphically in Figure 1. The extraction efficiencies, which were calculated from the radioactive counting data, are plotted *vs.* reaction tube oven time. The H(tfa) concentration in the hexane used in these experiments was $8.7 \times 10^{-2}M$. As Figure 1 shows, the extraction efficiencies at 200, 175, and 150 °C peaked at 15, 30, and 60 minutes, respectively. Eleven additional experiments performed with $8.2 \times 10^{-2}M$ H(tfa) in hexane, 30 minutes heating time, and 175 °C oven temperature gave a mean extraction efficiency of 99.3% with a standard deviation of 2.0%.

H(fod and H(hfa) when reacted at the same times, temperatures, and concentrations as reported for H(tfa) showed similar %*E vs.* oven time curves, but the highest extraction efficiency for either agent never exceeded 50%. When H(hfa) was used, a white layer formed at the blood–hexane interface. This white solid was probably the dihydrate of H(hfa) reported by Schultz and Larsen (*8*) and its formation did not allow good mixing prior to heating. Also, the effective H(hfa) concentration was probably lowered enough to hinder quantitative chelation.

After a successful chelation and extraction reaction, it is expected that some excess H(tfa) will remain in the hexane layer. Also, knowing that the small amounts of chromium present are chelated and extracted, at least some iron would be expected to be chelated and extracted as $Fe(tfa)_3$ because of the large amounts of iron in red blood cells. In addition, various organic compounds freed from the blood might be extracted. Should interference occur in particular samples, other chromatographic columns could be used.

The electron capture detector is very sensitive to H(tfa), $Fe(tfa)_3$, and other volatile, hexane-soluble species with high electron affinities. The large excess of these materials may mask the $Cr(tfa)_3$ peaks, cause the detector to lose its sensitivity, or give a noisy, highly-sloped base line. Therefore, it is necessary to back-extract as much of the interfering material from the hexane phase as possible.

Ross and Sievers (*3*) reported that a backwash with 1.0*N* NaOH successfully removed excess H(tfa) and $Fe(tfa)_3$ with no loss of $Cr(tfa)_3$. Using gas chromatography, we have confirmed that a 5-minute back-extraction with 1.0*N* NaOH followed by centrifuging and layer separation successfully removed the excess H(tfa) from the hexane layer, and established (using radioactive ^{51}Cr) that 97% of the chromium remained in the hexane phase.

Table I. Results of Chromium Determinations in Blood (B) and Plasma (P)

Sample No.	Added Cr concn (ppm)[a]	Calculated amount of Cr injected GC, ng[b]	Amount of Cr determined by GC, ng	Recovery, %
B-1	0.104	0.0104	0.0104	100
B-2	0.104	0.0104	0.0086	83
B-3	0.104	0.0104	0.0091	87
B-4	0.104	0.0104	0.0096	92
B-5	0.104	0.0104	0.0097	94
				Mean 91%
B-6	0.052	0.0052	0.0047	90
B-7	0.052	0.0052	0.0044	84
B-8	0.052	0.0052	0.0045	86
B-9	0.052	0.0052	0.0046	88
B-10	0.052	0.0052	0.0048	92
				Mean 88%
P-1	0.052	0.0052	0.0046	88
P-2	0.052	0.0052	0.0050	96
P-3	0.052	0.0052	0.0047	90
				Mean 91%

[a] 0.050-ml sample of blood or plasma at this concn taken for analysis.
[b] 1.0 μl of 0.50-ml hexane phase injected.

It was considered important to establish beyond doubt that the peak thought to arise from chromium in blood was in fact *trans*-$Cr(tfa)_3$. Two blood samples, one containing 100 ng/ml of added chromium, were reacted at the recommended conditions. They were chromatographed on the two columns containing different liquid phases described in the experimental apparatus section. A standard $Cr(tfa)_3$ solution containing 1.64×10^{-8} g Cr/ml was also chromatographed on these columns. Both blood solutions showed clean peaks free of interferences at the same retention time as that of the *trans*-$Cr(tfa)_3$ peak in the standard solution. This was observed to be true on both columns. Also, the *trans*-$Cr(tfa)_3$ peak from the sample containing added chromium was significantly larger, on each column, as expected. The retention times of the *trans*-$Cr(tfa)_3$ peak and the impurity peaks were substantially different on the two liquid phases. These facts confirm that the peak in the blood extract is from *trans*-$Cr(tfa)_3$. Furthermore, the natural level of chromium in human blood can be easily measured.

The results of the determinations of chromium added to blood and plasma are shown in Table I. As these results show, 90% of chromium added to blood or plasma can be determined at normal concentrations using only a 0.050-ml sample.

Typical chromatograms of the standard and the hexane extracts from a plasma determination are shown in Figure 2. In *A* is shown the standard $Cr(tfa)_3$ dissolved in hexane. In *B*, a hexane extract from an unspiked plasma sample is illustrated showing the natural level of chromium in this plasma sample. Chromatogram *C* shows the analysis of the same sample as in *B*, except that chromium has been added. In all plasma chromatograms, the first peak is an unidentified electron-capturing species derived from the plasma.

(7) W. D. Ross and W. R. Wolf, private communication, W. D. Ross, Monsanto Research Corp., Dayton Laboratory, Dayton, Ohio 45429, and W. R. Wolf, Aerospace Research Laboratories, Wright-Patterson Air Force Base, Ohio 45433, November 1970.
(8) B. G. Schultz and E. M. Larsen, *J. Amer. Chem. Soc.*, 71, 3250 (1949).

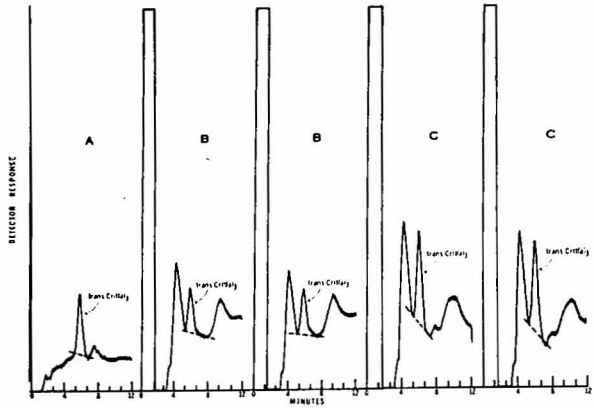

Figure 2. Chromatograms of *A*, 1.0-μl standard Cr(tfa)$_3$ solution containing 5.1 × 10^{-9} g Cr/ml; *B*, 1.0-μl hexane extract of plasma reaction with no added chromium; and *C*, 1.0-μl hexane extract of plasma reaction containing added chromium at the 0.052 ppm level

Column:	**2 ft 5% DC LSX-3-0295**
Column temp:	**132 °C**
Detector temp:	**190 °C**
He flow rate:	**20 ml/min**
CH_4-Ar flow rate:	**100 ml/min**
Range:	**10**
Attn:	**8**

Table II. Results of Chromium Extractions for *in vivo* Rat Experiments

Rat No.	Hours *in vivo*	Extraction efficiency, % Blood	Plasma
1	1	...	94.3
2	1	85.0	...
3	1	81.8	104.2
4	1	88.8	94.4
5	1	70.6	97.6
1	3	...	96.4
2	3	70.3	97.5
3	3	77.8	92.3
4	3	87.7	101.6
5	3	83.7	101.0
6	3	89.9	96.4
	Mean	81.7	97.6

A 0.5-μl injection of a standard Cr(tfa)$_3$ solution containing 6.5 × 10^{-9} g Cr/ml into the 2-ft LSX-3-0295 column (3.25 × 10^{-12} g Cr injected) resulted in a sharp *trans*-Cr(tfa)$_3$ peak of 175 mm height and a peak height to noise ratio of 14. Assuming this sensitivity, little interference, and a 0.050-ml blood or plasma sample, chromium could be determined at the 5 nanogram per ml of blood or plasma level with a 6.0-μl injection.

To demonstrate that *in vivo* chromium can be quantitatively extracted, live animal experiments were performed. The results of the chelation and extraction of *in vivo* chromium are presented in Table II. The blood samples removed after 1 hour from rats 2, 3, and 4 were reacted immediately. The remaining blood and plasma samples were reacted after overnight storage at −20 °C. Gray and Sterling (*9*) reported that chromate enters the red blood cells with over 90% efficiency, both *in vivo* and *in vitro*. Over 80% of the radioactive chromium in the fresh blood samples was extracted by H(tfa)–hexane; therefore, intercellular chromium can be determined. It is also noteworthy that the plasma extraction efficiency averaged 97%.

The combination of the *in vivo* and *in vitro* chelation and extraction results and the gas chromatographic results shows chromium can be determined rapidly and quantitatively at natural levels in blood and plasma using the recommended procedure. The advantages of this method include small sample size (0.050 ml), short reaction time (30 minutes), few and simple manipulations allowing batch analyses, and high sensitivity allowing determinations of natural levels without preconcentration.

Sterling and Gray (*10*) developed a method for the determination of circulating red cell volume using radioactive sodium chromate to tag the red blood cells. They reported chromate passes through the erythrocyte membrane and 80 to 90% of the chromate is firmly bound to the globin portion of the hemoglobin both *in vivo* and *in vitro*. Chromate is apparently reduced to chromium(III) after it enters the red blood cell.

Frank and Gray (*11*) also determined circulating plasma volume in man using radioactive chromium(III) chloride. They reported that 98% of the chromium(III) is rapidly bound by the plasma proteins both *in vivo* and *in vitro*. In both the red cell volume and the plasma volume measurements, a simple dilution technique is used. Radioactive chromium is also used for studying red cell survival time and in evaluating blood loss. All of these methods, which are simple and give

(9) S. J. Gray and K. Sterling, *J. Clin. Invest.*, 29, 1604 (1950).

(10) K. Sterling and S. J. Gray, *J. Clin. Invest.*, 29, 1614 (1950).
(11) H. Frank and S. J. Gray, *ibid.*, 32, 991 (1953).

precise results, have been invaluable diagnostic tools. However, the fact that radioactive materials are injected into the body makes these methods contraindicated for certain patients such as children and pregnant women. By use of nonradioactive chromium solutions and the new gas chromatographic method for the determination of chromium in blood and plasma, this diagnostic tool would be available to all patients. Procedures using radioactive chromium result in chromium increases of less than 1 ng/ml of blood. However, because of the relatively low toxicity of soluble chromium compounds (*1*), enough chromium can be used to give a 50 to 100 ng/ml of blood increase, which can easily be measured by the GC method. Also, this method could possibly be applied to other radioactive metals used for diagnosis so that radioactivity would not have to be injected or ingested by man.

ACKNOWLEDGMENT

The authors thank W. D. Ross, M. L. Taylor, and E. L. Arnold for their assistance and counsel.

RECEIVED for review August 24, 1970. Accepted December 7, 1970. Research was sponsored by the Aerospace Research Laboratories, Air Force Systems Command, United States Air Force, Contract No. F33615-69-C-1062. Research was performed at Monsanto Research Corporation, Dayton Laboratory, 1515 Nicholas Road, Dayton, Ohio 45407.

Rapid Scan Infrared Spectrometer for Operation with Support Coated Open Tubular or Packed Column Gas Chromatographs

R. A. Brown, J. M. Kelliher, and J. J. Heigl

Esso Research and Engineering Co., Linden, N. J.

C. W. Warren[1]

Instruments & Communications, Inc., Wilton, Conn.

An infrared spectrometer has been developed to record spectra of gas liquid chromatographic fractions from packed or support coated open tubular (SCOT) columns. The instrument employs a four filter Czerny-Turner monochromator with 90° phase null electronics. A Nernst source is chopped at 400 Hz in front of the sample and reference cells. Spectra are measured as sample flows through a windowless multiple internal reflectance cell of 1.0-ml volume. The cell is heated up to 250 °C. A helium cooled mercury doped germanium detector is used. Scan speeds of 5 to 20 seconds cover the 3700–750 cm^{-1} region. Conventional double beam transmittance and frequency data are presented on a linear wave number chart. Good quality spectra are obtained for as little as 20 μg of sample. Functional group bands are observed at the 3-μg level.

SINCE 1964, A NUMBER of infrared spectrometers have been modified or adapted to record spectra of gas chromatographic fractions (*1–3*). These instruments could be connected to packed column gas chromatographs and spectra observed of fractions "on the fly" or trapped in special sample cells. Moderate quality spectra were obtained at scan speeds of 5 to 40 seconds. Minimum sample requirements varied from 0.1–1.0 μl (100–1000 μg) depending upon the type of compound involved.

An advance in capability was achieved by Low and Freeman (*4*) who employed a multiple scan interference spectrometer to monitor effluents from a packed column gas chromatograph. This instrument can scan the 2500- to 250-cm^{-1} region in 1 second. Good sensitivity was attainable only when based on multiple scans (100–300 in number). More recently, Krakow (*5*) discussed the application of a grating spectrometer that continually produced spectra at the rate of one spectrum in 0.7 second. This particular instrument was limited in its spectral range of 3700 cm^{-1} to 1100 cm^{-1} due to the cryogenic detectors that were used. Wilks (*6*) and Gilby (*7*) used standard spectrophotometers equipped with micro cells to operate in the 25-μg range.

As Whetsel (*8*) notes, fractions from a gas chromatographic separation represent ideal samples for study by infrared. To more fully apply infrared to identification of chromatographic fractions, greater sensitivity is required. In an effort to achieve this as well as other improvements, a project was initiated to build a spectrometer that would be an effective analytical tool. Most of the original design goals were achieved. These are:

- Scan rate of five seconds to cover the spectral range, 3700 cm^{-1} to 650 cm^{-1}.
- Double beam operation.
- Handle sample sizes at the microgram level.
- Resolution sufficient to identify component(s) in a gas chromatographic fraction.

This paper describes the instrument and its applicability to packed column and support coated open tubular (SCOT) gas chromatography.

[1] Present address, American Cyanamid Co., Bound Brook, N. J.

(1) A. M. Bartz and H. D. Ruhl, ANAL. CHEM., **36**, 1892 (1964).
(2) P. A. Wilks, Jr., and R. A. Brown, *ibid.*, p, 1896.
(3) G. T. Keahl, Pittsburgh Conference on Analytical Chemistry and Applied Spectroscopy, Pittsburgh, Pa., Feb. 25, 1966, Paper 209.
(4) M. J. D. Low and S. K. Freeman, ANAL. CHEM., **39**, 194 (1967).
(5) Burton Krakow, ANAL. CHEM., **41**, 815 (1969).
(6) P. A. Wilks, Pittsburgh Conference on Analytical Chemistry and Applied Spectroscopy, Cleveland, Ohio, March 8, 1968.
(7) A. C. Gilby, Pittsburgh Conference on Analytical Chemistry and Applied Spectroscopy, Cleveland, Ohio, March 1970.
(8) Kermit Whetsel, *Chem. Eng. News*, **46**, (6), 82 (Feb. 5, 1968).

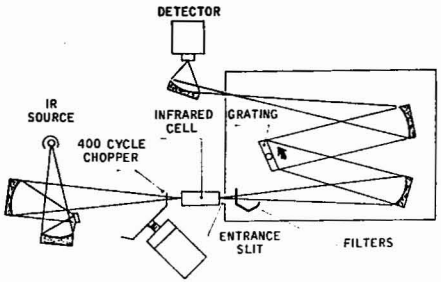

Figure 1. IR-GC spectrometer optical system layout

Reference and sample beams are chopped 90° out of phase, separated in the vertical plane and both beams are recombined by the detector

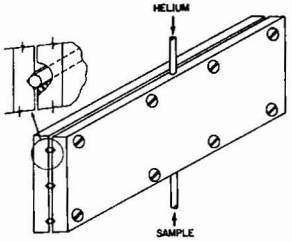

Figure 3. IR–GC spectrometer gas cell

EXPERIMENTAL

The Spectrometer. The phase null spectrophotometer (*9*) was selected for our application. In our initial assessment, it was felt that this system offered the best promise in meeting our design criteria set forth above. The phase null system achieves double beam operation by electronically ratioing the two beams. Fast response time is thus attained.

The overall spectrometer and associated components, shown in Figure 1, include a Nernst glower source which is focused by a three-mirror arrangement onto the entrance of the parallel plate sample cell. The beam is chopped directly before the sample cell. After passing through the monochromator's entrance slit, the beam passes through one of four filters which are automatically positioned in a timed sequence. The grating monochromator follows the Czerny–Turner design, with its single grating and two parabolic mirrors for beam focusing. From the exit slit, the beam is focused on the surface of the cryogenic detector which is refrigerated with liquid helium. As described in an earlier presentation (*10*), a two-grating system was originally constructed. Later this was replaced with a single grating. This eliminated discontinuities in the recorded spectrum at the point of grating change. Scan time was also reduced. These advantages were achieved with an insignificant loss in resolution.

(9) C. W. Warren, U. S. Patent 3,414,729 (1968).
(10) C. W. Warren, J. J. Heigl, R. A. Brown, and J. M. Kelliher, Pittsburgh Conference on Analytical Chemistry and Applied Spectroscopy, Cleveland, Ohio, March 8, 1968, Paper 217.

Phase Null Amplifier. In the phase null technique, shown in block diagram in Figure 2, the reference and sample beams are chopped 90° out of phase by a common rotating shutter and, after traversing the sample cell and monochromator, are recombined at the detector. The chopping frequency employed is 400 Hz per second. Synthesized reference and sample signals are synchronously produced by the chopping motor drive through a generator. The synthesized signals thus generated have the same relative phase separation as the optical signals produced by the detector. As shown in Figure 2, both sets of signals are treated electronically through amplification and comparison, before the combined signals are rectified, filtered, and recorded. A complete description of the phase null principle is included in Reference *9*.

The phase null method offers excellent response time characteristics and good photometric accuracy in regions of both high and low transmission. This permits scale expansion to be applied without drastically degrading signal-to-noise ratio. It is common practice in these laboratories to utilize this technique up to and beyond a 10-fold expansion factor.

Infrared Cell. The infrared cell consists of two optically flat, polished plates assembled as shown in Figure 3. Rods placed in V-grooves along the length of the plates divide the unit into separate sample and reference cells. The volume of each is 1 cubic centimeter as defined by the dimensions 10 cm × 0.1 cm × 1 cm. Sample or helium gas flows into the respective cells through the small tubes at the top and bottom. Outflow of gas occurs at both ends since no windows are used. Temperatures (up to a maximum of 250 °C) are maintained constant by a thermostatically controlled block in which the cell rests.

Some investigations were made of a special multi-reflective cell to optimize the path length to sample volume ratio.

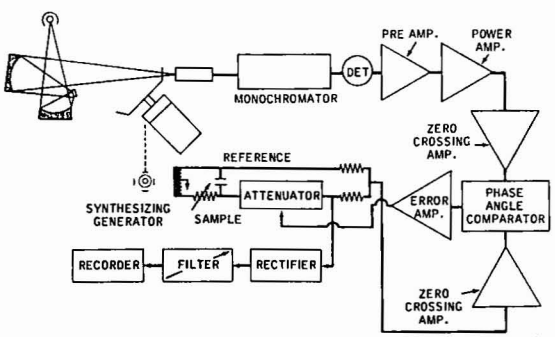

Figure 2. Phase null–block diagram

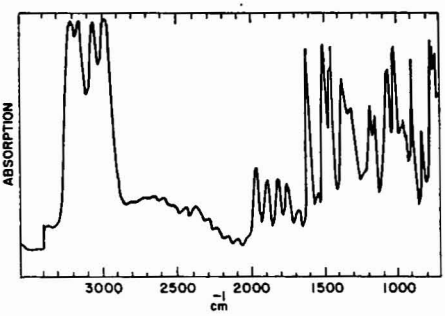

Figure 4. Spectrum of polystyrene (20-sec scan)

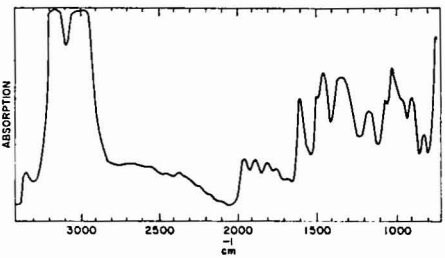

Figure 5. Spectrum of polystyrene (5-sec scan)

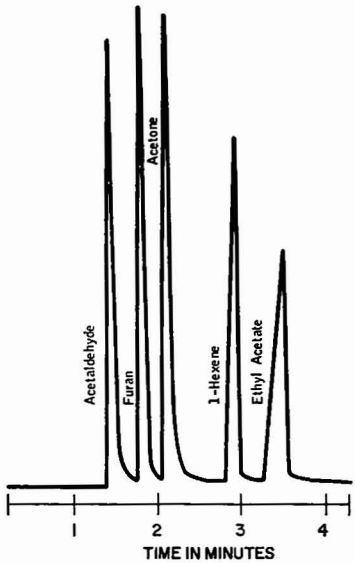

Figure 6. Chromatogram of five-component blend

Perkin-Elmer Model 226
50 ft × 0.02 inch i.d. column–Squalane coated
Flow rate 4 ml/min of helium
Column Temperature −40°C
Sample size, 3.0 μl
Sample splitter used
Attenuation X256

This cell has been described elsewhere (*11*). It consists of a gold cylinder with highly polished reflective surfaces with dual chambers for sample and reference gases. Provision is made to heat the entire assembly to prevent condensation of the higher boiling constituents. Gas inlet tubes are provided at the ends of the cylinder. The gas effluxes through the optical entrance and exit slits. The data, which are preliminary in nature, show that multiple reflection operation is attained. Under the experimental conditions employed, approximately 20 reflective paths were achieved. This is somewhat short of the expected path numbers calculated from theoretical considerations. An additional publication is planned to describe these experimental results.

Monochromator. The monochromator utilizes a Bausch and Lomb replica grating, 2540 lines per inch and blazed at 1790 cm^{-1}. It is used in the first order. The wavelength cam was constructed in accordance with a computer-derived design to produce a recorded output which is linear in frequency. Based on a comparison of spectra with precise measurements by Erley and Blake (*12*), accuracy of the wavelength scale is estimated to be within 0–20 cm^{-1} in the 1000 to 1500 cm^{-1} region. An error of 100 cm^{-1} may occur in the 3000 cm^{-1} region. While some improvement in wavelength scale accuracy is desired, this is not a serious limitation in gas chromatographic applications.

Slit construction is based on well established designs; the entrance slit is fixed and only the exit slit varied as the wavelength interval is scanned. High pass interference filters effectively prevent radiation of undesired orders from reaching the detector. These filters, four in number, are inserted sequentially at 2.4, 3.5, 6.4, and 9.0 microns. A rapidly operating solenoid-actuated rotary stepper is employed for filter insertion. A small recognizable signal may occur at filter change intervals.

Detector. The detector, which is refrigerated by liquid helium, is an impurity-activated type (*13*) manufactured by Texas Instruments, Inc. The germanium-mercury detector selected had been developed for the 700 cm^{-1}–1250 cm^{-1} region. No degradation in response is experienced at fast chopping frequencies. The order(s) of magnitude greater for D^* of this detector as compared with a thermocouple provides a significantly improved signal-to-noise ratio. Low noise spectra are observed as shown in Figures 4–10. Initially, some problems were encountered with loss of liquid helium but these were shortly overcome after storage and transfer facilities were improved.

The detector employed initially and with some success was a Golay unit (*14*) with its acoustic chamber filled with helium in order to decrease response time. The only problem encountered was the presence of occasional spurious signals attributable to microphonism of the detector. This problem was overcome by incorporating a pneumatic ballasting

(11) M. J. E. Golay, "Sixth International Symposium on Gas Chromatography and Associated Techniques, Rome, Italy, Sept. 20–23, 1966," A. B. Littlewood, Ed., Institute of Petroleum, London, 1967, p 333.
(12) D. S. Erley and B. H. Blake, "Infrared Spectra of Gases and Vapors," Vol. II—Grating Spectra, Dow Chemical Company, Midland, Mich., March 1965.
(13) Henry Levinstein, "Applied Optics and Optical Engineering," Vol. 2, R. Kingslake, Ed., Academic Press, New York, N. Y., p 311.
(14) H. A. Zahl and M. J. E. Golay, *Rev. Sci. Instrum.* **17**, 511 (1946).

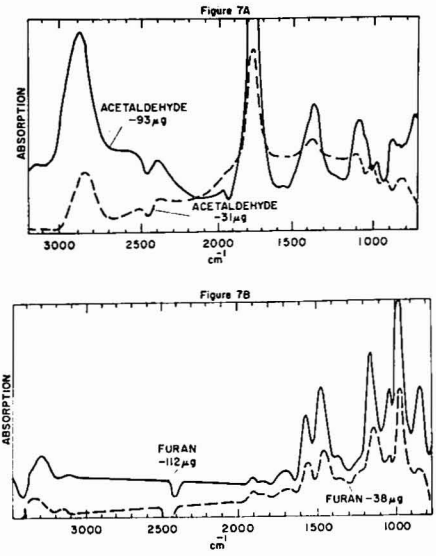

Figure 7. *A.* **Spectra of acetaldehyde**
B. **Spectra of furan**

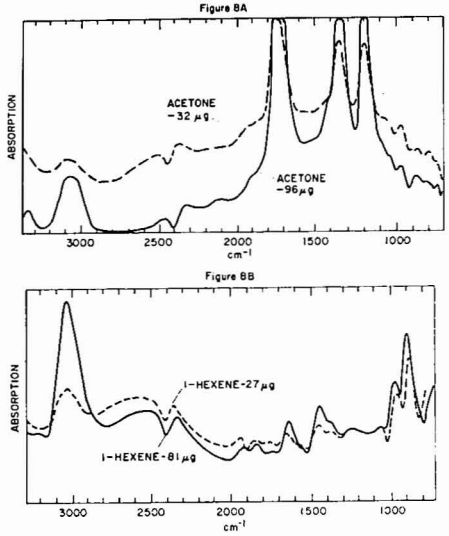

Figure 8. *A.* **Spectra of acetone**
B. **Spectra of 1-hexene**

feature. This feature was not available until after our investigations were concluded.

Polystyrene Spectra. The quality of the spectral data is indicated by the polystyrene spectra in Figures 4 and 5. These spectra were measured at scan speeds of 20 and 5 seconds, respectively. It will be noted that the 20-second scan gives a well resolved spectrum of grating quality. By comparison, the 5-second scan spectrum is inferior in resolution and also shows slightly lowered band intensities. In practice, the 5-second scan would usually be used in SCOT column work and a slower scan up to 20 seconds might be employed with packed column separations.

Operation of the Spectrometer/Chromatograph. SCOT COLUMNS. In our work a Perkin-Elmer Model No. 226 chromatograph was used in SCOT column work. This was fitted with a Gow-Mac microthermal conductivity detector. The connection between chromatograph and spectrometer consisted of a short, heated tubing of 0.02-inch i.d. To measure the infrared spectrum of a GC peak, it is desirable to know at what time the infrared cell contains most of the GC peak. By trial and error, it was found that this occurs at approximately 3 seconds after the GC peak reached its maximum height. Accordingly, each peak scan by IR would be started after this 3-second interval.

The volume of the infrared sample cell (1 ml) fits it to handle SCOT column fractions in an ideal manner. Typical SCOT column conditions provide a separation which approaches capillary column in efficiency. Mixtures are resolved as fairly narrow peaks that are 5 to 30 seconds in width. A 15-second peak width may be considered as about average. Thus, at a typical carrier gas flow rate of 4 ml per second, most of an average peak can be collected in the 1-ml gas cell $\left(\frac{15 \text{ sec}}{60 \text{ sec}} \times 4 \text{ ml} = 1 \text{ ml}\right)$.

A 50-foot squalane column of 0.02-inch inside diameter provided fractions for the infrared. One to three microliter samples were injected to the chromatograph and the 100:1 splitter was used. The 100:1 splitter allows 1/100 of the injected sample to enter the analytical column when that column has a diameter of 0.01-inch. A much larger proportion of a sample enters a 0.02-inch column such as employed in this work. Measurements of peak areas observed with and without the splitter indicated that approximately

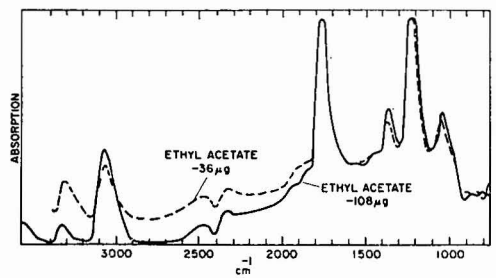

Figure 9. Spectra of ethyl acetate

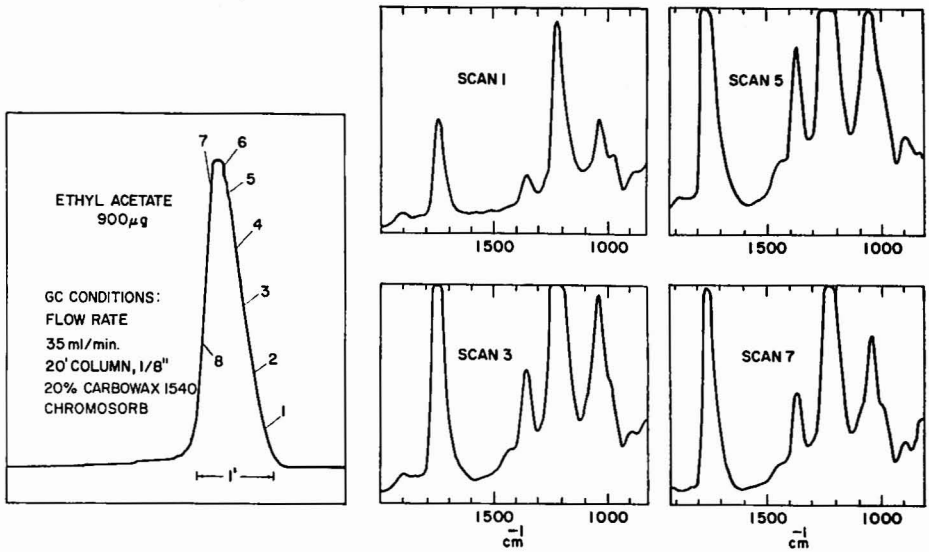

Figure 10. Infrared spectra of ethyl acetate as GC fraction

one fifth of a sample enters the column. This fractional value was used in calculating the amount of sample observed in the infrared spectrometer.

PACKED COLUMNS. A Perkin-Elmer Model F-11 chromatograph was connected to the spectrometer for packed column experiments. This connection was the same as that used for tieing in the Model 226 chromatograph. Experiments with the packed column were carried out as described for the SCOT column.

RESULTS AND DISCUSSION

Spectra of SCOT Column Fractions. The chromatogram in Figure 6 shows the mixture that was used to evaluate the spectrometer. It consists of a five-component blend containing twenty liquid volume per cent each of acetaldehyde, furan, acetone, 1-hexene, and ethyl acetate. Spectra were measured for 1 and 3 μl of injected sample. This gave levels of 30 and 90 μg for each component to be measured. Spectra are discussed in the order of elution from the chromatograph.

ACETALDEHYDE. Two spectra are shown in Figure 7*A*. It will be noted that 93 μg of sample resulted in 0% transmission for the carbonyl band at 1780 cm^{-1} and near 0% in the 2900 cm^{-1} carbon–hydrogen region. A number of other bands are also observed. Most of these bands can be seen for the smaller sample of 31 μg. The 1780 cm^{-1} band is quite intense and it is apparent that this band would be measurable for a substantially smaller amount of material.

FURAN. Spectra in Figure 7*B* show furan for 38 and 114 μg of sample. The weak carbon–hydrogen band at ~3250 cm^{-1} agrees with Erley and Blake (*10*) whose spectrum No. 50 indicates it to be a weak absorber. Numerous other bands are observed with the most intense one at 980 cm^{-1}. It can be estimated that this band would be observed at a level of 10 μg.

ACETONE. Spectra for 32 and 96 μg of acetone are shown in Figure 8*A*. This spectrum shows three intense bands at 1750 cm^{-1}, 1330 cm^{-1}, and 1200 cm^{-1}. The two latter bands would probably be apparent for 10 μg of acetone, whereas the carbonyl band at 1750 cm^{-1} would be noticeable for considerably less than 10 μg.

1-HEXENE. Figure 8*B* demonstrates the measurement of an olefin which is a weak absorber. The characteristic double bond band at 900 cm^{-1} is observed for 27 μg of sample and it would appear that a fairly intense band would occur for 15 μg of the compound.

ETHYLACETATE. As shown in Figure 9, ethylacetate is readily observed at 36 and 108 μg. Even at 36 μg, the carbonyl band at 1770 cm^{-1} as well as the ester band at 1210 cm^{-1} are very intense. It is apparent that the bands would be observed at a level of 3 μg.

Spectra of Packed Columns. Principal effort has been placed upon the role of SCOT column gas chromatography because the superior resolution offered by this technique provides an optimum capability for the infrared spectrometer to perform as an identification tool. The spectrometer also works well with a packed column chromatograph, however. In packed column chromatography peaks are relatively wide and there is ample time to obtain one or several spectra if desired. More material is also available than in SCOT column work. The manner in which the spectrometer functions is illustrated in Figure 10. One microliter of ethyl acetate was charged to a chromatograph having a 20-foot, 0.125-inch o.d. column packed with 20% K 1540 on chromosorb. As the peak eluted, eight successive five-second scans were taken. Alternately numbered scans are shown in Figure 10 as they were measured. It will be noted that intense spectra were recorded. Scan 8 is not shown but its spectrum was weak, indicating that sample was quickly swept from the cell as the end of the peak was reached.

CONCLUSION

The infrared spectrometer described herein can provide good quality spectra of gas chromatographic fractions at levels of 20 micrograms or more. Frequently, observable bands occur at the microgram level. Variable scan speeds of 5 to 20 seconds and the small sample cell allow the spectrometer to be used with either SCOT or packed columns.

ACKNOWLEDGMENT

H. D. Raymond contributed significantly to the mechanical design and construction. H. C. Tsien and J. A. Wilson also assisted on various phases of the project. Laboratory measurements were carried out by T. H. Sara.

RECEIVED for review September 8, 1970. Accepted December 18, 1970.

Simple and Inexpensive Electronic Conductivity Manometer for Monitoring Pressure Changes

Application to Pressuremetric Titrations of Iodate and Ammonium Ions

D. J. Curran and S. J. Swarin

Department of Chemistry, University of Massachusetts, Amherst, Mass. 01002

A novel pressure transducer system based on the electronic monitoring of the electrolyte level in a manometer with linear conductance circuitry has been developed. The instrument has a multirange capability and a high level dc output. It is simple in design and construction and can be built with readily available electronic units. Its response to the quantity of gas generated in a closed system is linear to within 2–4 parts per thousand. It has been applied to the pressuremetric titrations of iodate with hydrazine sulfate and ammonium ion with electrogenerated hypobromite. Accuracies and precisions of a few parts per thousand have been obtained, down to the concentration level where only 12 μmoles of gas are evolved.

IN RECENT YEARS there has been renewed interest in the applications of pressure measurements in chemistry. This undoubtedly is due to the availability of accurate, sensitive, and precise modern pressure transducer systems (*1*). Typical applications of these instruments include: monitoring gas evolution or absorption in reaction kinetics (*2–4*), end point detection in pressuremetric titrations (*5*, *6*), and monitoring analytical hydrogenations (*7–9*). Simple, inexpensive transducer systems are commercially available, but they lack multirange capability. Systems possessing the latter feature are also commercially available, but at a considerable increase in complexity and cost.

The manometer has always been a common instrument for pressure measurements because of its simplicity in principle and construction, and its low cost. However, manometry requires numerous readings and constant operator attention. As part of our studies of applications of pressure transducers in chemical analysis, we have developed a simple and inexpensive pressure transducer system, based on a U-tube manometer, which is sensitive, precise, and compact. This instrument has a multirange capability and a high level dc output suitable for recording. It appears to be suitable for use in all of the applications cited previously. Modular construction has been utilized to take maximum advantage of the economy and versatility of commercially available electronic units. We have demonstrated the applicability of this instrument as an end-point detection device in pressuremetric titrations of 14.33- and 1.433-mg samples of iodate with hydrazine sulfate and 4.737- and 0.4737-mg samples of ammonium ion with electrogenerated hypobromite. In the first case nitrogen is generated according to:

$$IO_3^- + 5I^- + 6H^+ \rightarrow 3I_2 + 3H_2O \quad (1)$$

$$2I_2 + N_2H_4 \cdot H_2SO_4 \rightarrow N_2 \uparrow + SO_4^{2-} + 6H^+ + 4I^- \quad (2)$$

And in the second case:

$$Br^- + 2OH^- \rightarrow BrO^- + H_2O + 2e^- \quad (3)$$

$$2NH_4^+ + 3\,BrO^- \rightarrow N_2 \uparrow + 3\,Br^- + 2H^+ + 3H_2O \quad (4)$$

PRINCIPLE OF OPERATION

In 1926, I. B. Smith (*10*) described a liquid-level detector based on the conductivity bridge principle. By placing two pairs of identical platinum electrodes in the arms of a U-tube manometer containing an electrolyte, and placing the resistance between each pair of electrodes in a Wheatstone bridge circuit, it was found that the difference in the height of the liquid in the two arms could be determined. Smith's work was based on the conductivity equation:

$$L = \frac{1}{R} = \frac{L_s A}{d} \quad (5)$$

where L is the conductance, R is the resistance, L_s is the specific conductance, A is the area of each electrode, and d is the distance between the electrodes. Since, for rectangular electrodes, the area is the product of length (l) and width (w), Equation 5 becomes:

$$L = \frac{1}{R} = \frac{L_s \cdot l \cdot w}{d} \quad (6)$$

(1) D. J. Curran, *J. Chem. Educ.*, **41**, A465 (1969).
(2) L. R. Mahoney, ANAL. CHEM., **36**, 2516 (1964).
(3) T. G. Traylor and C. A. Russel, *J. Amer. Chem. Soc.*, **87**, 3698 (1965).
(4) W. K. Rohwedder, *J. Catal.*, **10**, 47 (1968).
(5) D. J. Curran and J. L. Driscoll, ANAL. CHEM., **38**, 1746 (1966).
(6) D. J. Curran and J. E. Curley, *ibid.*, **42**, 373 (1970).
(7) A. Reuter, *Z. Anal. Chem.*, **231**, 356 (1967).
(8) D. J. Curran and J. L. Driscoll, ANAL. CHEM., **42**, 1414 (1970).
(9) D. J. Curran and J. E. Curley, *ibid.*, **43**, 118 (1971).
(10) I. B. Smith, *J. Opt. Soc. Amer.*, **12**, 655 (1926).

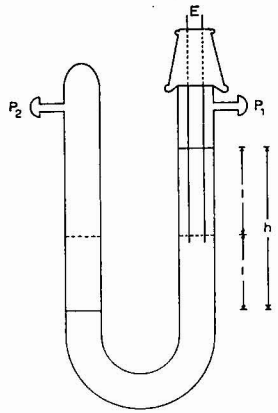

Figure 1. Electrolyte-filled manometer

---- Initial level of manometer fluid
—— Final level of manometer fluid
E Conductivity electrodes

Thus, the resistance is inversely related to the length of the electrodes immersed. Although Smith gave no data on the measurement of pressure with his special monometer, it is obvious that this is possible since the pressure difference between the arms of a manometer is given by:

$$P_2 - P_1 = \Delta P = \rho g h \tag{7}$$

where ρ is the density of the manometer liquid, g is the acceleration due to gravity, and h is the height difference between the two arms of the manometer. Figure 1 shows the relationship between h and l for the case where only one pair of electrodes is used. Since the electrode assembly occupies some volume, l is greater than l'. However, if the horizontal cross-sectional area of the electrode assembly is constant in the vertical plane, then the volume of electrolyte displaced by the assembly must be proportional to the depth of immersion of the assembly, and hence $h = kl$. For the case in which the volume displacement of the electrodes is negligible, $l = l'$ and $k = 2$. In either case, Equations 6 and 7 can be combined to yield:

$$L = \frac{1}{R} = K_1 \Delta P \tag{8}$$

where K_1 is a constant combining L_s, w, d, ρ, g, and k. Thus, the conductance is linearly related to pressure changes in the manometer.

In 1963 C. F. Morrison (*11*) reported the first linear conductance circuit using operational amplifiers. This circuit was based on the simple inverter amplifier where:

$$e_{out} = - e_{in} \frac{R_f}{R_{in}} \tag{9}$$

Here e_{out} is the output voltage, e_{in} is the input voltage, R_f is the feedback resistance, and R_{in} is the input resistance. If e_{in} and R_f are constant and R_{in} is the resistance of the conductivity cell, then

$$e_{out} = - K_2 \frac{1}{R_{in}} = - K_2 L_{in} \tag{10}$$

where K_2 is a constant and L_{in} is the conductance. A modification of this circuit utilizes a differential design so that any initial conductance can be nulled (*12, 13*).

We report the construction of suitable linear conductance circuitry using operational amplifiers and its application to liquid-level detection in a manometer, in order to obtain a pressure transducer system with linear output. The circuit, shown schematically in Figure 2, consists of an alternating current source (sine wave oscillator), an impedance isolator (voltage follower), and a signal conditioner (linear conductance monitor with null offset). Amplifier 2 is an amplitude stabilized Twin-Tee Sine Wave Generator (*14*) which produces a very pure sine wave when $R/2$ is properly adjusted. In this application, a 500-Hz 18-volt peak-to-peak sine wave is produced. This signal is then attenuated to 1-volt peak-to-peak and impedance isolated from the signal conditioning circuitry

(11) C. F. Morrison, ANAL. CHEM., 35, 1820 (1963).
(12) G. W. Ewing and T. H. Brayden, Jr., *ibid.*, 35, 1826 (1963).
(13) T. R. Mueller, R. W. Stelzner, D. J. Fisher, and H. C. Jones, *ibid.*, 37, 13 (1965).
(14) Tektronix, Inc., Beaverton, Ore., "Operational Amplifiers and Their Applications", p 6-2 (1965).

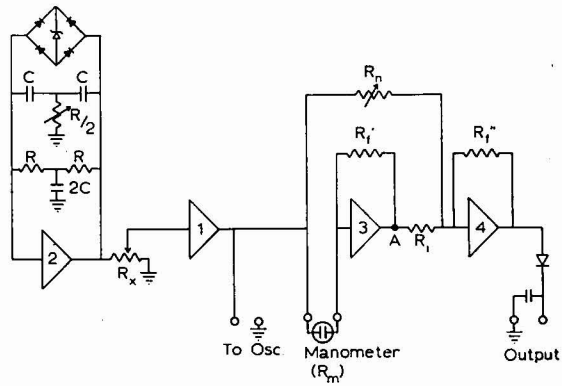

Figure 2. Schematic diagram of pressure transducer system

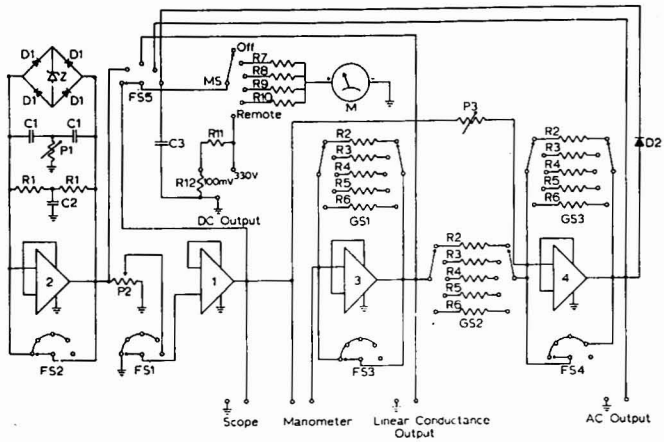

Figure 3. Circuit diagram of pressure transducer system

Starting at ground, the Heath EUW-19A amplifiers have pins numbered clockwise as 4, 5, 1, 2, and 3. They are, respectively: ground, noninverting input, inverting input, balance supply, and output

by a voltage follower (Amplifier 1). Tuning of the wave shape and amplitude is accomplished through oscilloscope connections placed after the follower. Alternatively, the potentiometers $R/2$ and R_z could be replaced by fixed value resistors. This would improve the reproducibility and ease of tuning and adjusting the alternating current source, but would decrease the overall flexibility of the instrument.

From Amplifier 1, the sine wave is applied as the excitation signal for the manometer electrodes (cell resistance = R_m) and for the null adjust potentiometer, R_n. Amplifiers 3 and 4 perform the function of a null offset linear conductance monitor. Considering first the pathway through the manometer, the signal developed at point A is given by:

$$e_{out_4} = -e_{in}\left(\frac{R_f'}{R_m}\right) \tag{11}$$

Now considering this signal as an input to Amplifier 4, along with the signal developed through R_n, we obtain:

$$e_{out_4} = -\left[\left(-e_{in}\frac{R_f'}{R_m}\right)\left(\frac{R_f''}{R_f}\right) + (e_{in})\left(\frac{R_f''}{R_n}\right)\right] \tag{12}$$

If $R_f' = R_f'' = R_f = R$

$$e_{out_4} = e_{in}R\left[\left(\frac{1}{R_m}\right) - \left(\frac{1}{R_n}\right)\right] = e_{in}R(L_m - L_n) \tag{13}$$

Following this amplification, the output signal of Amplifier 4 is rectified and filtered so that a high level dc output is produced. Thus, the output of the instrument is proportional to the conductance across the manometer electrodes, L_m, according to:

$$e_{out_{dc}} = e_{in}RK(L_m - L_n) \tag{14}$$

where K is a constant to take into account the ac to dc conversion. Since from Equation 8, the conductance is directly related to the pressure change sensed by the manometer, the output voltage is directly related to this pressure change. The potentiometer R_n, whose conductance is L_n, can be used to offset any initial conductance across the manometer electrodes so that the initial output is zero, provided there is no phase shift in the manometer and the phase shift through Amplifier 3 is exactly 180°. To improve this null adjusting capability, a variable capacitor may be added in parallel to R_n in order to null any initial capacitance of the conductivity cell.

Table I. Components for Figure 3

D1	IN4002 Texas Instruments
D2	IN 538 Texas Instruments
Z	9.0 Volt, 1-watt Zener diode
C1	0.0022 μF, 10%, paper
C2	0.0047 μF, 10%, paper
C3	0.22 μF, 10%, paper
R1	154 KΩ All are ½ watt, 1%, carbon film
R2	100Ω
R3	1 KΩ
R4	10KΩ
R5	100KΩ
R6	1 MegΩ
R7	20KΩ
R8	100KΩ
R9	200KΩ
R10	300KΩ
R11	992KΩ
R12	3.9 KΩ
P1	100KΩ, 0.5% linear, 10-turn wire wound potentiometer
P2	20KΩ, 0.5% linear, 10-turn wire wound potentiometer
P3	250KΩ, 10%, 2 watt carbon potentiometer
FS	Function Switch, ceramic rotary, 5P5T
GS	Gain Switch, ceramic rotary, 6P5T
MS	Meter Switch, ceramic rotary, SP6T
M	0–50 μA meter, Lafayette Radio No. 99-R-5042

EXPERIMENTAL

Apparatus. The complete circuit diagram of the pressure transducer system is given in Figure 3; and the components are listed in Table I. The Heath EUW-19A Operational Amplifier System (Heath Co., Benton Harbor, Mich.) was used. The components necessary to use these amplifiers in the circuit described were wired in a blank chassis (Heath

Model EUW-19A-1) which is made to plug directly onto the operational amplifier system.

The manometer used was a U-tube type constructed of 15-mm i.d. borosilicate glass. Connections to the reference and working pressure cells were made through ⅋ 12/5 ball joints as shown in Figure 1. The electrode assembly was fitted to the low pressure arm of the manometer by means of a ⅌ 29/42 inner member joint.

The electrode assembly consisted of two 5 × 100 × 0.076 mm sheets of platinum foil (E. H. Sargent and Co., Chicago) which were each cemented to a 9 × 190 × 2 mm section of glass plate using epoxy (2-Ton Epoxy, Devcon Co., Danvers, Mass.). The electrodes were mounted facing each other and spaced 5 mm apart by cementing glass tubing between the glass plates. Platinum lead wires were spot welded to the tops of the electrodes. This assembly was cemented into a ⅌ 29/42 outer member joint for connection into the manometer. The electrical leads passed through the epoxy seal at the top of the ⅌ 29/42 outer member joint.

Pressure signals for testing the linearity and reproducibility of the transducer were supplied in two ways: a Sargent Model C Automatic Constant Rate Buret with plunger driven assemblies of 50-, 10-, and 2.5-ml capacities; and a hydrogen-nitrogen coulometer designed according to the recommendations of Page and Lingane (*15*) and operated with a Sargent Model IV Constant Current Source. The recorder, constant temperature bath, submersible magnetic stirring motor, micrometer burets, potentiometer, and Ampot used in this study have all been previously described (*6*, *8*).

Pressuremetric titrations were conducted in all-glass reactors similar to those previously described by this laboratory. For volumetric titrations, the reactor described by Curran and Driscoll (*8*) was used. However, one of the microburets had a short glass stem so it would not withdraw solution when it was used to compensate the volume compression due to titrant addition. For titrations in which the titrant was generated electrochemically, the modified H-cell described by Curran and Curley (*6*) was used with a 12- and 25-cm² platinum anode and cathode, respectively.

Reagents and Solutions. All chemicals were reagent grade except as noted. Potassium iodate was primary standard grade. Hydrazine sulfate was Eastman White Label No. 575. Triton X-100 was obtained from Analabs, Inc. Laboratory distilled water which was redistilled from alkaline permanganate was used for all solutions.

Manometer fluid was $0.50 \times 10^{-3}M$ in potassium chloride and 0.03 wt % in Triton X-100. It was prepared by appropriate dilution of a stock 0.100*M* potassium chloride solution. The surfactant was added to ensure smooth, frictionless flow. It had no noticeable effect on the conductivity.

Stock potassium iodate solution, $8.192 \times 10^{-3}M$, was prepared by dissolving 0.8765 gram of the dried material in a 500-ml volumetric flask. A 10-fold dilution of this stock solution was taken as $8.192 \times 10^{-4}M$. Hydrazine sulfate solutions, approximately 1.0 and 0.10*M*, were prepared as described previously (*5*). The phosphate buffer was prepared by making a solution 0.5*M* in potassium monohydrogen phosphate, then adding sufficient potassium dihydrogen phosphate to bring the solution pH to 7.2 as determined with a Corning Model 7 pH meter. The starch indicator solution was prepared according to the procedure of Koltoff and Belcher (*16*).

Stock ammonium sulfate solution, $2.642 \times 10^{-2}M$ in ammonium ion, was prepared by dissolving 0.8729 gram of the dried material in a 500-ml volumetric flask. A 10-fold dilution of this stock solution was taken as $2.642 \times 10^{-3}M$. Hypobromite was generated from an anolyte solution containing 10.0 grams of sodium tetraborate decahydrate and 200 grams of sodium bromide in 500 ml of redistilled water. The pH of this solution was adjusted to 8.6 ± 0.1 (Corning Model 7 pH meter) by adding solid sodium hydroxide. In order not to evolve a gas at the cathode in the pressuremetric work, a solution which was 1.0*M* in ferric chloride hexahydrate dissolved in 2.0*N* sulfuric acid was used as the cathodic depolarizer.

Check Methods. To determine the accuracy of the pressuremetric end-point technique, check analyses were performed using the same samples, titrants, and buffers as used in the pressuremetric procedure, but using a different end-point detection method.

A. HYDRAZINE–IODATE. To a 25-ml Erlenmeyer flask were added 10.00-ml of stock potassium iodate solution, 0.5 gram of potassium iodide, 6 drops of 18*N* sulfuric acid, and 10.0 ml of phosphate buffer. Hydrazine sulfate titrant was added from a microburet, with starch indicator added only near the end point.

B. HYPOBROMITE–AMMONIUM. To a 30-ml beaker, fitted with a rubber stopper containing two platinum wire indicating electrodes, the generating electrode, and the frit-isolated cathode, were added 10.00-ml of stock ammonium sulfate solution and 10.0-ml of anolyte. Hypobromite was generated coulometrically; and the end point was determined amperometrically according to the procedure of Christian, Knoblock, and Purdy (*17*). Blanks were determined in a similar manner using 10.00-ml of redistilled water instead of the ammonium sulfate sample.

Procedure for Pressuremetric End-Point Detection. A. HYDRAZINE–IODATE. Ten milliliters of stock potassium iodate solution, 0.5 gram of potassium iodide, 6 drops of 18*N* sulfuric acid, and 30.0 ml of phosphate buffer were added to the pressuremetric titration vessel. The two microburets, one containing hydrazine sulfate titrant and the other empty save for a plug of water to ensure pressure tightness, were fitted into their appropriate positions with all joints well sealed with Dow Corning High Vacuum Grease. The reference vessel, similar in appearance to the reactor vessel except holding no microburets, was prepared by filling with the appropriate volume of water. The two cells were mounted on a ring stand; and the submersible magnetic stirring motor was placed in position under the titration vessel. The manometer, which had been filled to the bottom of the electrodes with the manometer fluid, was then connected to the cells and the ball and socket joints secured with clamps. The cells, stirring motor, and manometer were then immersed in the constant temperature bath until only the open stopcocks, the upper sections of the microburets, and the electrical leads to the manometer electrodes were above water. Electrical connection to the manometer electrodes was then made, and the amplifiers of the pressure transducer system were balanced. The function switch was then turned to the "on" position, and the frequency and amplitude of the alternating current source were adjusted. The titration vessel stopcock was then closed and stirring was begun. After a few minutes a steady pressure base line was attained, indicating equilibrium. Generally, four increments of titrant were added both before and after the end point. After the addition of each increment of titrant, the volume compression due to this addition was compensated by withdrawing the plunger of the second microburet. The output voltage was continuously monitored using the strip chart recorder. When a steady recorder trace indicated that equilibrium had been reached for a given increment, the output voltage was accurately measured with the potentiometer. End points were obtained from the inverted L-shaped titration curves which result when the transducer output in volts is plotted *vs.* microliters of titrant added.

B. HYPOBROMITE–AMMONIUM. Ten milliliters of stock ammonium sulfate solution and 10.0 ml of anolyte were added

(15) J. A. Page and J. J. Lingane, *Anal. Chim. Acta.*, 16, 175 (1957).
(16) I. M. Koltoff and R. Belcher, "Volumetric Analysis," 1st ed., Interscience, New York, 1957, Vol. III, p 208.
(17) G. D. Christian, E. C. Knoblock, and W. C. Purdy, ANAL CHEM., 35, 2217 (1963).

Table II. Linearity and Reproducibility of Pressure Transducer System

Pressure range (mm Hg, gauge)		No. of detn	Plunger source		H_2–N_2 coulometer		
Apparent[a]	Actual[b]		Reproducibility of slope, %	S_{yx}, %	Reproducibility of slope, %	S_{yx}, %	μmoles gas
144	6.30	9	0.41	0.22	0.29	0.31	280
88	3.84	9	0.26	0.30	0.41	0.24	171
44	1.92	9	0.48	0.26	0.36	0.29	85.5
14.4	0.630	8	0.51	0.25	0.28	0.35	28.0
7.2	0.315	8	...	...	0.25	0.27	14.0

[a] Determined from moles of gas evolved and assuming constant volume.
[b] Determined from the height difference between the two arms of the manometer.

Table III. Titration Results with Pressuremetric End Point Detection

Sample	Titrant	Taken, mg[a]	Found, mg	No. of detn	Rel std dev, %	Rel accuracy,[a] %
IO_3^-	$N_2H_4 \cdot H_2SO_4$	14.33 ± 0.02	14.32	8	0.1	−0.1
		1.433 ± 0.002	1.429	6	0.2	−0.3
NH_4^+	BrO^-	4.737 ± 0.007	4.742	7	0.1	+0.1
		0.4737 ± 0.0011	0.4746	6	0.5	+0.2

[a] Based on check method.

to the anode compartment of the titration vessel. To prevent the solution from flowing into the cathode compartment, sufficient catholyte was added so the liquid level of the catholyte was higher than that of the anolyte. All joints were well greased, and the electrodes were fitted into their positions. The procedure from this point was identical to the previous system, except that no compensation was required since the titrant was generated coulometrically.

RESULTS AND DISCUSSION

Table II summarizes the results obtained in testing the linearity and reproducibility of the pressure transducer system. These data were obtained over a one-month period using both the automatic plunger driven pressure source and the hydrogen-nitrogen coulometer. Dynamic conditions prevailed; that is, the pressure was varied and the output signal was recorded on a strip chart recorder. A least squares computer program (Wang Calculator) was used to obtain the statistical analysis. S_{yx} is the standard error of estimate of y on x defined by:

$$S_{yx} = \sqrt{\frac{\Sigma y^2 - a_0 \Sigma y - a_1 \Sigma xy}{N}} \qquad (15)$$

where x and y are the coordinates, a_0 and a_1 are the intercept and slope, respectively, of the regression line, and N is the number of points. Thus S_{yx} is a measure of the scatter about the regression line, and has properties analogous to those of the standard deviation. If lines parallel to the regression line are constructed at vertical distances of 1, 2, and 3 S_{yx}, then these lines will contain 68, 95, and 99.7% of the points, respectively. The linearity and reproducibility of the transducer system output is thus within 3 to 5 parts per thousand on all scales.

In order to achieve continuous recording of pressure signals, the "free manometer" technique of Goldstein was used (*18*). In this technique the manometer fluid is not levelled during a reaction, and both pressure and volume are allowed to vary. As a consequence, the volume capacity of the manometer is substantially increased while sensitivity is usually reduced. Thus it becomes possible to measure a total gas change much larger than that by standard manometry; but small quantities of gas cannot normally be detected. However, a linear function between the voltage output and the moles of gas evolved (or absorbed) is maintained (See Appendix). By electronically monitoring the liquid level in the manometer, small quantities of gas can be detected and measured. Experimental confirmation of the linear function between output voltage and moles of gas evolved is given in Table II; and the last column of this table shows the quantities of gas measured. It should also be noted that since the volume of the system is allowed to increase, the pressure inside the system is considerably less that expected. Thus the apparent pressure range given in column 1 of Table II is the pressure increase expected if the given number of micromoles of gas is evolved in a closed system with no volume change. The second column of this table gives the actual pressure increase in the reactor as determined from the height difference between the arms of the manometer.

Full scale output of the transducer system is 33.0 volts dc on the 144 and 14.4 mm Hg scales. The voltage-pressure relationship on these scales is thus 0.229 and 2.29 volts/mm Hg, respectively. On the more sensitive scale, the smallest significant voltage signals that could be distinguished was 5 mV, based on the practical consideration that the mechanical vibration of the water bath stirring motor imparted a ripple to the surface of the manometer fluid causing an uncertainty in voltage readings on this scale of ±2 mV. Thus the pressure sensitivity of this instrument is 2.2×10^{-3} mm Hg, which corresponds to the evolution of 4.2 nanomoles of gas.

Table III summarizes the results of volumetric and coulometric titrations utilizing the pressuremetric end-point technique. The theoretical basis of this technique has been presented previously (*5*, *6*). Briefly, it involves monitoring the pressure change in a closed system due to the evolution (or absorption) of a gas by the reaction of analytical interest. The precision and accuracy of the pressuremetric technique using this transducer system is a few parts per thousand. Titration curves for the titration of 4.737- and 0.4737-mg samples of ammonium ion with electrogenerated hyprobromite are shown in Figure 4 as an example of the method. In contrast to the work of Curran and Curley (*6*), a cathodic depolarizer which did not evolve a gas was used ($Fe^{3+} + e^- \rightarrow Fe^{2+}$). This led to less uncertainty in the intersection of the

(18) A. Goldstein, *Proc. Amer. Acad. Arts Sci.*, 77, 237 (1949).

Table IV. Least Squares Analysis of Titration Curves

Hydrazine: Iodate Titration	Before end point		After end point	
	Slope (V/μl)	S_{yx}, mV	Slope, V/μl	S_{yx}, mV
1	0.1624	19.5[a]	−0.0001	3.3[a]
2	0.1599	2.1	0.0002	4.7
3	0.1601	29.2	0.0001	7.8
4	0.1576	12.2	0.0000	7.6
Hypobromite: Ammonium				
1	0.0189[b]	17.8[c]	0.0001	12.2[c]
2	0.0190	28.5	0.0002	10.5
3	0.0186	28.5	0.0001	9.7

[a] Total output ≅ 18.1 volts.
[b] Slopes for coulometric titrations in V/μeq.
[c] Total output ≅ 14.3 volts.

two titration curve segments and improved accuracy and precision.

Normally, four increments of titrant are added both before and after the end point. However, to permit a least squares analysis of the titration curves obtained with this transducer system, some titrations were performed with the addition of eight increments of titrant both before and after the end point. Table IV shows the results of this analysis. Of particular interest is the stability after the end point where a gas is no longer evolved. These lines are virtually horizontal; and the S_{yx} ranges from 3 to 12 mV out of approximately 18 volts total output.

At high transducer sensitivities, fluctuations in ambient pressure and temperature had an effect on the stability of the signals measured. Particularly bothersome were gross pressure fluctuations produced by opening and closing the laboratory door. A reference volume was attached to the manometer; and pressure signals in these titrations were recorded *vs.* this closed reference rather than *vs.* ambient conditions. Since the volumetric displacement of the manometer was limited by the fixed reference volume, the resulting output signals were lower. However, it was found that if the reference volume is large enough (approximately 50–100 cm³), the linear function between voltage output and moles of gas evolved is maintained.

CONCLUSIONS

In this paper we have presented a simple and inexpensive pressure transducer system for use in chemical analysis. Although the pressures measured must be corrected for the volume of manometer fluid displaced, the instrument does produce a high level dc output which is a linear function of the moles of gas evolved or absorbed in a closed reactor system. Therefore it is suitable for use in reaction kinetics, analytical hydrogenations, and pressuremetric titrations. If information is desired on the total number of μmoles of gas evolved, a simple calibration with a hydrogen-nitrogen coulometer is required. We have demonstrated the applicability of this instrument as an end-point detection device in pressuremetric titrations of milligram samples of iodate and ammonium ion. Excellent precision and accuracy is obtained, even at the concentration level where only 12 μmoles of gas are evolved.

It has been observed by Smith (*10*) and confirmed in this laboratory that the conductivity electrode technique is capable of detecting a change of 30 μinches in the liquid level in the manometer. Thus the construction of a suitable capillary manometer of dimensions outlined in the Appendix should increase the sensitivity of the instrument to 6×10^{-5} mm Hg. However, even without modification this instrument fills the need for a multirange, dc output pressure transducer system which is simple in principle and construction and low in cost.

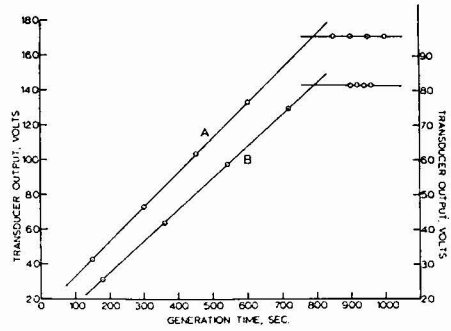

Figure 4. Pressuremetric titration curves of ammonium ion with electrogenerated hypobromite

A. 10.00 ml of 2.642 × 10^{-3} *M* NH_4^+
Left ordinate
Generation time × 0.1 = μequiv

B. 10.00 ml of 2.642 × 10^{-3} *M* NH_4^+
Right ordinate
Generation time × 0.01 = μequiv

ACKNOWLEDGMENT

S.J.S. is grateful to L. B. Jaycox for meaningful discussions on the electronic circuitry.

APPENDIX

Recording of the liquid level in a manometer is facilitated if the fluid is not levelled during a reaction. Furthermore, the errors introduced by the levelling procedure are avoided. Goldstein has called this procedure the "free manometer" technique (*18*), and he has derived the appropriate equations for a Warburg apparatus in which both pressure and volume are allowed to vary. The following derivation is more general, applying to all manometric readings. However, for simplicity it is assumed that the solution and gas phases are ideal and that the manometer fluid is saturated with the gas of interest.

Initially,

$$P_i V_i = n_i RT \tag{1}$$

where the subscript i refers to initial conditions and the symbols have their usual significance. If a gas is generated or absorbed,

$$P_f V_f = n_f RT \tag{2}$$

where the subscript f refers to final conditions and $n_f = n_i \pm \Delta n$. In the case where a gas is evolved in a closed reactor to which a fluid manometer is attached, the pressure in the system increases by an amount dependent on ρ, the density of the manometer fluid; g, the acceleration due to gravity; and h, the total height difference between the two arms of the manometer (Figure 1). Thus,

$$P_f = P_i + \rho g h \tag{3}$$

However, the volume of the closed system also increases by an amount dependent on πr^2, the cross-sectional area of the manometer and l', the length of the column of water displaced. Thus,

$$V_f = V_i + \pi r^2 l' \quad (4)$$

It has been previously shown that $h = kl$, so $h = k'l'$ and substituting in Equation 2

$$(P_i + \rho g h)\left(V_i + \frac{\pi r^2 h}{k'}\right) = (n_i + \Delta n)RT \quad (5)$$

$$\frac{h}{k'}[P_i \pi r^2 + k' V_i \rho g + \rho g \pi r^2 h] = \Delta n RT \quad (6)$$

Substituting the following constants: $\rho = 1.00$ g/cm³, $g = 980$ cm/sec², $\pi = 3.14$, and $P_i = 1.01 \times 10^6$ dynes/cm² (760 mm Hg)

$$h/k' \times 10^3[3171\, r^2 + 0.980\, k' V_i + 3.080\, r^2 h] = \Delta n RT \quad (7)$$

The relationship between h and Δn will be linear if the third term in the brackets is negligible compared with the sum of the other two. For the manometer system used in this work, $r = 0.75$ cm, $V_i = 50$ cm³, and $k' = 2.22$

$$h/2.22 \times 10^3[1784 + 109 + 1.73\, h] = \Delta n RT \quad (8)$$

and the third term is less than 0.9% of the sum of the other two if h is less than 10 cm. Thus this term can be dropped and the height difference between the two arms of the manometer is linearly related to the moles of gas evolved.

From Equation 4 it is seen that if r is small enough, the volume change caused by the movement of manometer fluid is negligible. Then $V_f = V_i$ and the pressure change measured in the manometer is a true differential pressure, *i.e.* it does not have to be corrected for the volume change. A simple calculation shows that if V_i is approximately 50 cm³, r would have to be 0.10 cm or less. But the placement of conductivity electrodes in a manometer of this size would be quite difficult. However, a suitable compromise between V_i, r, and sensitivity should be possible.

RECEIVED for review September 8, 1970. Accepted December 1, 1970. Thanks are due to the Analytical Chemistry Division of the American Chemical Society for the Anacon Summer Fellowship awarded to S.J.S.

Near Optimum Computer Searching of Information Files Using Hash Coding

Peter C. Jurs

Department of Chemistry, The Pennsylvania State University, University Park, Pa. 16802

The technique of hash coding has been applied to searching information files similar to those used in spectrometry laboratories. A discussion of several searching strategies, including the optimum one, is presented, and it is shown that hash coding yields nearly optimum matching algorithms for which search times are independent of file size. Two algorithms using hash coding have been implemented; the results of experiments with these algorithms are presented. The first algorithm matches blocks of unknown 16-bit spectra to a file of known spectra at the rate of approximately 20,000 spectra per second, independent of the number of unknown spectra being matched. The second system employs a double hashing procedure to search a data file of 20,000 spectra for one unknown at a time and verify its presence or absence in 40 milliseconds, on the average.

EXPERIMENTAL SITUATIONS routinely arise in which it is necessary to match an unknown spectrum to a file of known spectra. Several investigations which deal with the problem of computer searching of infrared spectrometry files have been reported. Anderson and Covert (*1*) reported a system using an IBM 7080 computer with magnetic tape input which could search 167 spectra per second. Erley (*2*) packed the words within the computer's memory and used logical operations to make the necessary comparisons. His system was developed with an IBM 1130 using a disk input, and it could process 1000 spectra per second. Lytle (*3*) used an inverted file of IR spectra and developed a system which could search 1000 spectra per second using a 500 card per minute card reader for input. This inverted file system suffers from the disadvantages that new spectra cannot be added to the file as conveniently as with the other systems and that only one search can be performed at a time. It can, however, find near matches relatively easily. Lytle and Brazie (*4*) have more recently reported a system which uses compressed IR spectra to obtain search rates of 333 spectra per second with 45-bit spectra on a small laboratory computer. They also use statistical data compression to develop a system on a XDS Sigma 5 computer using disk input which can process 18000 16-bit spectra per second. These 16-bit spectra do not contain all the information present in the original spectra, however.

A major drawback of most searching systems is that the search time is proportional to the number of members in the file being searched. This paper discusses a method, both in theoretical and experimental terms, for which this limitation is not present. A nearly optimal searching strategy can be developed by using hash coding to drastically reduce the time necessary to search files of data, such as IR spectra.

The problem of exactly matching an unknown query word to one of the members of a dictionary of words arises repeatedly in information handling applications. The problem of retrieving infrared spectra from a file of standard spectra is only one example of such an application. The terminology "word" for the query is used because the information, whether it is an actual English word or a number or a spectrum, is

(1) D. H. Anderson and G. L. Covert, ANAL. CHEM., **39**, 1288 (1967).
(2) D. S. Erley, *ibid.*, **40**, 894 (1968).
(3) F. E. Lytle, *ibid.*, **42**, 355 (1970).
(4) F. E. Lytle and T. L. Brazie, ANAL. CHEM., 1532 (1970).

stored in binary form in the computer memory and can be considered as a unit.

Let the dictionary of standard data file contain 2^a members. Each member, and, therefore, any possible query word, can be thought of as a b-bit binary number. The general problem is to determine whether an unknown b-bit query is or is not a member of the data set. If a match is found, then several courses of action may be open; however, the basic problem consists in determining if the query word is a member of the data set. This problem has been termed the exact matching problem, and it can be broken down into five cases, depending on the memory size, M, of the computer being used (*5*).

I. Optimum Case. A binary number made up of b bits can assume 2^b possible values. Therefore, a memory which contains 2^b bits can store every possible b-bit number or spectrum w as a "1" in the appropriate position, the wth position. Then, given any query word w, it can be matched to the data set by merely checking to see if the wth bit in memory is turned on. This is the optimum case of the exact matching problem in that only one memory reference involving one bit is needed to verify the presence or absence of any query word in the data set.

II. Impossible Case. The number of bits of memory necessary to store the unordered data set is $M = (b - a)2^a$. Storage of the data set in this size memory is done by putting the words comprising the data set in numerical order and then computing their successive differences. Each spectrum would then require $(b - a)$ bits on the average, and the entire data set would require $(b - a)2^a$ bits. If $M < (b - a)2^a$, then the data set cannot be stored, and matching of query words to the data file is impossible. The data set must be broken down into subsets, forming a new problem.

III. Exhaustive Search. If the memory is large enough to store the unordered data set, that is, if $M = (b - a)2^a$, then exhaustive searching routines can be employed. These involve sequentially looking through the data file until either a match is found or the end of the file is reached without a match. On the average, such exhaustive searching routines require $M/2$ matches, or memory references, of b bits each per query word.

IV. Logarithmic Sort. If $M = b2^a$, then the data set can be stored in ordered (numerical) sequence. The search can proceed by investigating half of memory, then a quarter, then an eighth, etc. This algorithm requires at most a inspections of words, each requiring b bit-matches.

V. Hash Coding. If $M = (1 + f)b2^a$, then hash coding can be used (*5*, *6*). The excess memory available, f, determines the average number of memory references per query for matching. For the case of $f = 1$, *i.e.*, the memory is twice as large as the data set to be used, the number of memory references will be less than two, on the average. This is very close to optimum.

Hash coding is implemented in two steps. A filing algorithm is used to set up the data set in memory, and a retrieval alogrithm is used to perform the matches. Both algorithms have available for their use a hashing algorithm $H(w,j)$. It uses two input parameters—w, the b-bit word being filed or retrieved, and j, an integer. It produces one output parameter—an integer $k = H(w,j)$. The integer produced by the hashing algorithm is randomly distributed over the interval $1 \leq k \leq m$, where m is the number of words of memory being used for storage of the data set. Thus, the hashing algorithm randomly (but algorithmically) produces an integer, given the b-bit word being filed or retrieved and an integer j.

The filing algorithm utilizes the hashing function in the following manner: To file the w_ith word of the data set, the filing algorithm computes $H(w_i, 1)$. If the memory location with this address is empty, then w_i is put into it. If that memory location is occupied, then the procedure is repeated for $H(w,2)$, $H(w,3)$, . . . until an unoccupied memory cell is found, and w_i is filed there. This process is repeated for all the members of the data set. When the filing algorithm has filed all the members of the data set, then a fraction of the memory is filled and the remainder is empty.

To retrieve a query word w from the data set, the retrieval algorithm computes $H(w,1)$. If memory location H(w,1) contains w, a match has been found, and the algorithm terminates. If $H(w,1)$ is empty, then w is not in the data set, and the algorithm terminates. However, if $H(w,1)$ is occupied by some other word, then the procedure is repeated for $H(w,2)$, $H(w,3)$, . . . until either an empty memory cell is found or w itself is found. On the average the retrieval algorithm makes very few memory references, since only a fraction of the memory is filled. (The actual number of memory references obtained for a particular data set depends on the fraction of the memory which is filled and the method employed for resolving conflicts, but *not* on the file size.) Thus hash coding is very close to optimum with relatively little excess memory.

(If an additional 2^b bits of memory are available, then the search time can be lowered further by using bit-mapping of the main data set. This involves assigning an extra bit to each memory location and setting that bit to 1 only if that memory location is nonzero. Then, on the average, a query word can be retrieved with $4 + b \cdot 2^{a-b} \cong 4$ bit-references (*5*). Such bit mapping requires, of course, both hardware and software which allow treatment of single bits.)

The method of hash coding can be successfully applied to the problem of retrieval of spectrometry data, such as infrared spectra.

EXPERIMENTATION AND RESULTS

A filing algorithm and a retrieval algorithm for use with simulated spectra have been fully implemented and tested on the Pennsylvaina State University Computation Center IBM 360/67. The hashing function $H(w,j)$ used is based on an 360/Assembler language random number generation subroutine in the 360/67 library. It uses the multiplicative congruential method of random number generation which is widely employed; the method is discussed in detail in (*7*) and (*8*). Any random number generator could be used; this one has been chosen because of availability and speed. The remainder of the coding was done in FORTRAN IV. All programs are available to interested parties from the author.

A few modifications and extensions of the basic hashing procedure described above are necessary for application to retrieval of simulated IR spectra. These are discussed in the following paragraphs.

Digitized spectra can be non-unique for chemical reasons

(5) M. Minsky and S. Papert, "Perceptrons," MIT Press, Cambridge, Mass., 1969, p 219*ff*.
(6) I. Flores, "Data Structure and Management," Prentice-Hall, Inc., Englewood Cliffs, N. J., 1970, p 146*ff*.
(7) W. H. Payne, J. R. Rabung, and T. P. Bogyo, *Comm. ACM*, **12**, 85 (1969).
(8) P. A. W. Lewis, A. S. Goodman, and J. M. Miller, *IBM System J.*, **8**, 136 (1969).

Table I. Investigation of Hashing Procedure 1

Trial	Bits per spectrum	No. of blocks	Spectra per block	f	Matches	Input device	Time, sec	Average memory references
1	32	10	2000	0.50	68	tape/disk	2	3.0
2	16	10	2000	0.50	68	tape/disk	1	3.0
3	32	10	2000	0.50	16	tape/disk	2	3.0
4	16	10	2000	0.50	16	tape/disk	1	3.0

Table II. Investigation of Hashing Procedure 2

Trial	Bits per spectrum	No. of blocks	Spectra per block	f	Matches	Input device	Time per query, sec	Average memory references
1	16	40	500	1	64	disk	0.04	3.8
2	16	40	500	1	58	disk	0.04	3.6
3	16	40	500	1	24	disk	0.04	3.0

even though the coding schemes are capable of representing all the spectra uniquely. For example, Lytle and Brazie (*4*) have pointed out that Sadtler Laboratories' Spec Finder data files have some identical codes for different molecules. To handle this possibility, the retrieval algorithm must be altered in the following way. During retrieval, when a match is found, the search must continue until an empty memory cell is found. This assures the retrieval algorithm of finding all matches for w, not just the first one. This modification increases the average number of memory references per query word slightly. (The necessity of finding all matches for each query word would require modifications of the other matching algorithms discussed in the previous section as well.)

The general discussion of filing and retrieval algorithms using a hashing function above assumed that only the actual word which is a member of the data set would be filed in memory. Actually, any information could be put there. For a file of infrared spectra it might be desirable to file a registry number with the spectrum itself, for example. Alternatively, a list of pointers could be developed by the filing algorithm to link the memory cells of the filed data with data files outside the computer. Then the retrieval algorithm need only report matches in terms of memory locations in the filed data and the operator can use this number to find the matched spectrum (in a book, etc.).

The filing and retrieval algorithms discussed above have been extensively tested with simulated spectral data. For convenience the spectra used were 16- and 32-bit spectra; this is totally arbitrary and the utility of the method is unrelated to word size. Several data sets of 20,000 spectra were generated; these were handled in subsets of 2000 spectra or less in order to better simulate the method as it might be implemented on a small laboratory computer. The IBM 360/67 utilized is in a multiprogramming environment and therefore timing of the algorithms is not accurate. The times do, however, give an idea of the speed of the method.

The procedures were implemented corresponding to two typical laboratory situations. Procedure 1 treats query spectra in blocks of, say, 100. The individual data subsets are input and searched in a sequential manner; input time is the limiting factor for searching speed. The time required for a search is almost completely independent of the number of query words involved, since the operations carried out internally are so fast compared to the input speed. Additional spectra can be added to the data file by inserting them into the existent subsets or by starting a new subset.

Table I shows some results obtained using a specific implementation of procedure 1. The 20,000 16- and 32-bit spectra used were divided into ten equal subsets. Approximately 1% of the spectra appear in the data set twice, in accordance with the possibility of non-unique spectra in IR spectral data collections, as mentioned above. Each 2000 spectra were filed in a memory block of 3000 words, *i.e.*, $f = 0.5$. The query spectra consisted of 100 randomly chosen spectra with different sets used for trials 1 and 2 than for 3 and 4; the number of matches found is given in column 5. The time necessary to do the entire problem was approximately equal for either tape or disk input due to buffered input on the system used. An average of 3.0 memory references was required per query spectrum. In the form reported, this system could be used on a smaller laboratory computer since the memory requirements are not severe. Only 3000 memory locations are used for the data file subsets. Thus, procedure 1 allows searching of a large data file for a block of query spectra in a very reasonable amount of time—up to 20,000 spectra per second—depending on the length of the spectra.

In procedure 2, query spectra are looked up one at a time. A double hashing method is employed. The data set is divided into n subsets. To file the w_ith spectrum, the filing algorithm computes $H'(w) = i$, a randomly chosen number i ($1 \leq i \leq n$). Then the spectrum being filed is inserted into the i*th* subset by the usual hashing procedure. The retrieval algorithm also works in two stages. Thus, only one subset of the data set need be accessed from storage for either filing or retrieval of a query word. This substantially reduces the amount of input which must be done during retrieval. Of course, procedure 2 requires a random access input device such as a disk or drum. This method is substantially superior to the first one for very small numbers of query spectra since it drastically cuts input time, which is the limiting factor in the overall speed of the search. New spectra to be added to the data set are inserted into the correct subset, which changes the fraction of memory filled in that subset and, therefore, the average memory references per query. If a great many spectra are added to the data set, the filing algorithm must rework the data set disposition with a larger number of subsets and a revised preliminary hashing function $H'(w)$ with the new expanded range.

Table II shows some results obtained using the double hash coding procedure. The 20,000 16-bit spectra employed were divided into 40 subsets of 500 spectra each. Once again, approximately 1% of the spectra appear in the data set twice.

Each memory block is half full, *i.e.*, each 500 spectra are stored in 1000 locations. Three sets of 100 randomly chosen query spectra were selected and matched to the data set with the results shown. Line 1 shows that 64 matches were found for the first set of query spectra and that 3.8 memory references were required per spectrum. On the average, each query was answered in 40 milliseconds. Line 2 shows the results for a different set of query spectra, with 58 matches and 3.6 average memory references; line 3 gives the results for a third set of query spectra. Thus, it is seen that procedure 2 is very fast for matching a few query spectra at a time to a large data file. This algorithm has also been implemented in a form that could easily be used on a smaller laboratory computer.

Some of the variables chosen for the investigations reported in Tables I and II are arbitrary. The fraction of memory used, number of data blocks, and number of spectra per block can be chosen to maximize efficiency on any particular computer system. The values chosen here are typical in that they demonstrate the methods, but they should not be considered as optimum choices. The number of bits per spectrum used in laboratory situations depends on the data involved; the method of hash coding is not at all dependent on the word size of the data set or query words, so convenience has led to the use of 16- and 32-bit words in this work. To summarize: the method of hash coding makes extremely fast information retrieval algorithms for laboratory computers feasible and makes the length of time to perform a search independent of the size of the file searched.

RECEIVED for review October 22, 1970. Accepted December 14, 1970.

Teflon, A Noninert Chromatographic Support

John R. Conder

Chemical Engineering Department, University College of Swansea, U.K.

Sorption by Teflon as support has been studied with di-*n*-nonyl phthalate as stationary phase, the liquid loading being varied from 0 to 20%. A substantial support contribution to retention is observed for a variety of both polar and nonpolar solutes. On a 6% loaded column more than 10% of the retention of water and about 14% of that of *n*-hexane are attributed to adsorption by Teflon. Retention and tailing effects are distinguished with the aid of a two-site sorption model. The implications for chromatographic analysis and physical measurement are described. In particular, absence of tailing should not be taken as evidence of an inert support: adsorption may still affect retention.

"TEFLON" (Du Pont) (POLYTETRAFLUOROETHYLENE) differs from diatomaceous earth supports used for gas–liquid chromatography in giving a nearly symmetrical water peak and no tailing with alcohol or amine solutes (*1–3*). This fact makes Teflon supports very useful for separating highly polar materials, but is also commonly taken to imply that Teflon approaches the ideal of an inert, nonadsorbent support. An "inert" support is one which adds nothing to solute retention on the liquid stationary phase, and so can safely be used for thermodynamic studies on the liquid phase or for identifying peaks by their retention parameters.

If Teflon were inert to adsorption of polar solutes, it might be expected to be inert also to nonpolar solutes. This deduction, however, conflicts with recent observations of substantial support adsorption of hydrocarbons by coated Teflon. The stationary phases were di-*n*-propyl tetrachlorophthalate (*4*), polyethylene glycol 400 (*5*), and squalane (*6*). In each case, total retention was actually greater on Teflon than on firebrick. Since adsorption is observed with such widely differing types of liquid phase and also since the activity coefficients of hydrocarbons in at least two of these phases are less than 2, the extra retention cannot be attributed solely to Gibbs adsorption at the liquid–gas interface, but may be due to adsorption by the support. Confirmation is provided by Graham, who observed and measured the adsorption of paraffins on uncoated Teflon in a static system (*7*). Extrapolation of his data leads one to expect a contribution to hydrocarbon retention of around several per cent from adsorption on Teflon, depending on the nature and percentage loading of the liquid phase. This suggests that other solutes, such as amines and alcohols, may also be adsorbed by the support even when no tailing is observed.

The present study was therefore undertaken to investigate the adsorption by Teflon of different types of solute, including both polar and nonpolar types; and to see whether absence of tailing is a sufficient criterion for supposing support adsorption to be absent. The contribution of support adsorption to total retention was measured by isolating it from the contribution of bulk solution in the stationary phase. This was done by varying the liquid loading and analyzing the results by a method developed previously (*8*). Di-*n*-nonyl phthalate was selected as a representative stationary phase of moderate polarity as distinct from the highly polar and nonpolar phases of previous studies (*3*, *5*, *6*).

EXPERIMENTAL

Apparatus and Materials. The gas chromatograph was a Phase Separations Model LC-2 with katharometer detector. A mercury manometer was added to measure the line pressure before the injector and a soap-bubble flowmeter with a 50-ml volume was attached at the exit from the chromatograph. The recorder was a Servoscribe RE.511, and the carrier gas, hydrogen. Columns were constructed in stainless steel tubing of 0.25-inch o.d., all approximately 36 in. long and

(1) C. Landault and G. Guiochon, *J. Chromatogr.*, **9**, 133 (1962).
(2) D. M. Ottenstein, *J. Gas Chromatogr.*, **1**, 11 (1963).
(3) J. J. Kirkland, ANAL. CHEM., **35**, 2003 (1963).
(4) J. R. Conder, unpublished results, 1966.
(5) M. B. Evans, and J. F. Smith, *J. Chromatogr.*, **30**, 325 (1967).
(6) W. Jequier and J. Robin, *Chomatographia*, **1**, 297 (1968).
(7) D. P. Graham, *J. Phys. Chem.*, **69**, 4387 (1965).
(8) J. R. Conder, *J. Chromatogr.*, **39**, 273 (1969).

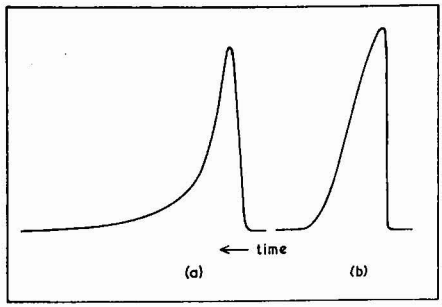

Figure 1. Two types of asymmetrical peak: (*a*) tailed peak; (*b*) skewed peak. Peaks are not to the same scale

Experimental conditions: (*a*) 0.1 μl water on 3-ft × 1/4-in. o.d. column of uncoated Teflon, 86 °C; (*b*) 15 μl acetone on 3-ft × 1/4-in. o.d. column of 12% DNP on Chromosorb G, about 75 °C

coiled, after packing, to a diameter of about 3 in. The packing was prepared by adding di-*n*-nonyl phthalate (DNP) (British Drug Houses Ltd., "for gas chromatography"), dissolved in acetone, to 30–60 mesh Teflon-6 (Te) (from Phase Separations Ltd.) so as to cover the support completely; the solvent was evaporated in a stream of nitrogen with gentle heating, the contents of the flask being swirled occasionally to promote an even distribution of DNP on Teflon. Packing of the column was facilitated by chilling the beaker containing the packing in an ice bath. The solutes were each of the highest grade of purity supplied by British Drug Houses Ltd.

Procedure. The oven temperature was 86 °C and the flow rate at the column outlet and at column temperature 51–52 ml/min. Liquid samples, 0.1 μl, were injected by syringe, and the retention time was obtained by measurement on the chart to the point of intersection of tangents constructed at the points of inflection on the peak sides. Usually the mean retention for 2 or 3 runs was obtained. The air peak retention was determined in a separate experiment for each column.

Calculation. It is assumed that the retention contributions are independent and that Gibbs adsorption at the liquid-gas interface is negligible. The net retention volume is then given (*8*) by:

$$V_N = K_L V_L + K_S A_S \qquad (1)$$

where K_L = molar partition coefficient for bulk solution
V_L = volume of liquid phase
K_S = molar distribution coefficient for support sorption
A_S = effective surface area for support sorption.

The most useful form (*8–10*) of this equation for plotting is

$$V_N/V_L = K_L + K_S A_S(1/V_L) \qquad (2)$$

which yields K_L as intercept and $K_S A_S$ as slope, provided V_N is measured at the same concentration (infinite dilution) on each column of different V_L. That effective infinite dilution was achieved throughout was shown by the skew ratios, η (= slope of trailing edge of peak ÷ slope of leading edge, at points of inflection). As indicated in Table I, values of η on DNP/Te were all in the linear chromatography region of 0.7–1.0 (*11*, *12*) except where slightly reduced by tailing which obscured the symmetry of the normal peak (see Discussion). Correction for concentration effects (*8*) was therefore unnecessary. The retention data for DNP/Te were first adjusted to a basis of exactly 16.00 grams support in each column and then plotted as (V_N/V_L) *vs.* $(1/V_L)$ (see data in Table II). The points were best represented by straight lines for each solute. K_L was obtained from the intercept and $K_S A_S$ from the slope. Precision was approximately: K_L ±2%, $K_S A_S$ ±15%. On uncoated Teflon V_L = 0 and so $K_S A_S$ was equal to the measured V_N.

The activity coefficients, γ^∞, of the solutes at infinite dilution in DNP were calculated from the equation:

$$\gamma^\infty = \frac{\rho_L RT}{M_L K_L p^\circ} \qquad (3)$$

where ρ_L is the density, and M_L the molecular weight (DNP = 418.6) of the stationary phase; R is the gas constant (= 6.236 × 10^4 ml mm Hg (°K mol)$^{-1}$); T, the column temperature; and p°, the vapor pressure of pure solute.

RESULTS

Values of K_L and $K_S A_S$ determined on DNP/Te columns having percentage loading in the range 2 to 20% are presented in Table I, together with $K_S A_S$ for a column containing uncoated Teflon. To provide some check on the measurements the activity coefficients were calculated from the K_L data and are shown in Table I. The activity coefficients are in broad agreement with literature values (*13–15*), though the latter are mostly of doubtful reliability owing to either use of diatomaceous earth supports with no correction for support adsorption of polar solutes, measurement of initial, insteady of peak, retention volumes (*15*), or use of a wrong value of M_L (*13*). Since low infinite dilution activity coefficients were observed for all but one of the solutes in an only moderately polar solvent, the possibility of significant adsorption at the gas-liquid interface is discounted (*16*, *17*) and has been neglected in Equation 1. Even for water, with γ^∞ = 9.7, any interfacial contribution to retention is expected to be less than the precision of the data.

Since A_S is not known with precision (*18*) and may vary with the solute if fine pores exist accessible only to small molecules, no attempt has been made to separate K_S from A_S. Values of $K_S A_S p^\circ$ have been calculated, to eliminate the effect of solute volatility on the adsorption coefficient and measure only the specific affinity of the solute for the surface by putting all solutes on the same basis of relative pressure. Graham (*7*) has shown that, for paraffins in a static system at temperatures of 0 to 25 °C, adsorption by Teflon is much faster than absorption, and absorption can be taken as completely negligible on the chromatographic time-scale. This can reasonably

(9) J. R. Conder, D. C. Locke, and J. H. Purnell, *J. Phys. Chem.* **73**, 700 (1969).
(10) D. F. Cadogan, J. R. Conder, D. C. Locke, and J. H. Purnell, ibid., p 708.
(11) J. R. Conder, "Progress in Gas Chromatography (Advances in Analytical Chemistry and Instrumentation, Vol. 6)," J. H. Purnell, Ed., Wiley, New York, N. Y., 1968, p 209.
(12) J. C. Giddings and H. Eyring, *J. Phys. Chem.*, **59**, 416 (1955).
(13) C. J. Hardy, *J. Chromatogr.*, **2**, 490 (1959).
(14) S. Evered and F. H. Pollard, *ibid.*, **4**, 451 (1960).
(15) D. E. Martire, "4th International Symposium on Gas Chromatography," L. Fowler, Ed., Academic Press, New York, 1963, p 33.
(16) D. E. Martire and L. Z. Pollara, "Advances in Chromatography," J. C. Giddings and R. Keller, Ed., Marcel Dekker, New York, N. Y., 1966, p 335.
(17) D. E. Martire, R. L. Pecsok, and J. H. Purnell, *Nature*, **203**, 1279 (1964).
(18) Differing values of A_S are given in Ref. 7 and in Leaflet FF-124 Chromosorb T (Teflon 6), Johns-Manville Inc., New York, N. Y.

Table I. Results for DNP/Te and Uncoated Te[a]

Solute	$p°$, mm Hg (86 °C)	DNP/Te columns K_L	γ^∞	K_SA_S, ml	$K_SA_Sp°$ × 10^{-3}	Uncoated Te K_SA_S, ml	$K_SA_Sp°$ × 10^{-3}	η at 6% loading	η on uncoated Te
n-Hexane	1270	37.7	1.03	6.9	8.8	5.3	6.7	0.8	0.6
n-Octane	217.8	...	...	...	...	30.0	6.5	...	0.5
Toluene	357.0	...	...	...	...	14.1	5.0	...	0.5
CCl_4	1011	88.8	0.55	8.3	8.4	6.2	6.3	0.7	0.4
n-Bu-NH_2	988.8	77.0	0.65	5.6	5.5	4.6	4.5	0.6	0.4
Acetone	1907	33.4	0.77	1.9	3.6	1.9	3.6	0.8	0.7
Ethanol	1023	28.6	1.68	1.4	1.4	0.7	0.7	0.8	0.7
Water	450.9	11.3	9.7	2.0	0.9	1.2	0.5	0.5	0.3
Air	...	...	...	...	...	...	...	0.6	0.7

[a] Mass of support in each column = 16.00 g. Corrected retention volume ($V_R°$) of air on uncoated Te column = 14.02 ml.

Table II. Retention Data at Varying Liquid Loadings for DNP/Te

Weight % loading of DNP	$1/V_L$ (ml^{-1})	V_N/V_L *n*-Hexane	CCl_4	*n*-$BuNH_2$	Acetone	Ethanol	Water
20.65	0.221	39.31	87.49	77.90	31.71	29.26	12.17
6.08	0.889	43.60	99.30	82.13	36.92	29.53	12.35
3.55	1.562	48.51	102.79	85.75	36.47	30.53	15.44
2.16	2.604	55.89	109.51	91.26	37.64	32.72	16.17

be assumed to be true for other solutes besides paraffins, and at the somewhat higher temperature of 86 °C, so that K_S and A_S, though defined so as to include possible absorption, are henceforth referred to as "adsorption" parameters.

DISCUSSION

Uncoated Teflon. An example of the peak shape observed with uncoated Teflon is shown in Figure 1*a*. All the solutes gave asymmetrical peaks, but the asymmetry consisted of tailing rather than skewing. The distinction between skewed and tailed peaks is shown in Figure 1. A skewed peak usually arises from concentration overloading sufficient to reveal nonlinearity of the distribution isotherm (*11*) and is characterized by having, first, one side virtually vertical and, second, a skew ratio, η, outside the range 0.7 to 1.0. A tailed peak, on the other hand, effectively consists of two parts: a "normal" peak with two sloping sides for which η lies in the range 0.7 to 1.0, together with a tail on the trailing side. If the tail is large, the symmetry of the normal peak will be obscured and η brought down toward 0.1, as shown by some of the η values in Table I. Tailing is not due to concentration overloading, and can occur even at very low concentrations, *i.e.*, in the presence of a linear isotherm.

The various possible kinetic mechanisms responsible for tailing have been taken into account in a model developed by Giddings (*19*) in which sorption occurs on two types of site. Fast exchange (sorption and desorption) takes place on normal sites and produces a Gaussian band profile. On this is superimposed a tail produced by sorption on slow-exchanging sites. The effects of sorption on retention and on tailing are thus distinct insofar as they arise from two different kinds of sorption site.

The effective adsorption coefficients, $K_SA_Sp°$, on uncoated Teflon given in Table I show no significant trends other than a rough correlation with size of the solute molecule. The fast exchange mechanism, to which the values of $K_SA_Sp°$ relate, may thus involve only dispersion forces and not such solute-specific interactions as dipolar interactions or hydrogen-bonding which would be expected to lead to higher values of $K_SA_Sp°$ for butylamine and ethanol.

(19) J. C. Giddings, ANAL. CHEM., 35, 1999 (1963).

When tailing occurs on Teflon, possible sites for slow-exchange include pores with several times the normal diffusion distance, high-energy adsorption sites, and absorption in the bulk support. Thus Kirkland (*3*) states that Teflon-6 contains a significant number of minute pores which contribute to its relatively high surface area. The actual size of the pores is not stated, but since no pores are visible in photomicrographs obtained by Sperati and Starkweather (*20*) at a magnification of 2 × 10^4, the pores must be less than 100 Å in diameter. High-energy adsorption sites could arise either from gegen-ions acquired during agglomeration of Teflon from an emulsion (*21*) or from carboxyl groups which terminate the polymer chains (*20*). Absorption, while unlikely, for reasons already given, to contribute to fast exchange, provides a further possible slow exchange mechanism.

The area of the tail relative to that of the normal peak paralleled the variation of $K_SA_Sp°$, except for water. Thus the first five solutes ($K_SA_Sp° > 4.5$) in Table I and water gave large tails, acetone ($K_SA_Sp° = 3.6$) gave a smaller tail, while the ethanol ($K_SA_Sp° = 0.7$) tail was no larger than the air tail caused by the small dead volume in the system. This behavior shows that the slow-exchange mechanism, whether due to micropores, adsorption, or absorption sites, resembles fast-exchange in having little selectivity for organic solutes. The anomalously large water tail also gives no clue as to the nature of the slow-exchange mechanism; it could be explained by assuming that high-energy adsorption sites have a specific interaction with water, that the surface contains very narrow micropores accessible only to water, or that absorption is easiest for small molecules.

DNP/Teflon. With the coated support, a third retention mechanism, bulk solution in DNP, is added to those of sorption on the two types of support site. Fast exchange can now occur both on the support surface and in solution, and so two terms appear in Equation 1 for retention of the normal peak. An indication of the importance of Teflon adsorption even with the coated support is given by extrapolating the data in Table II using Equation 2. This shows that adsorption on

(20) C. A. Sperati and H. W. Starkweather, Jr., *Fortschr. Hochpolym. Forsch.*, *Bd.* 2, S.465-495 (1961).

(21) R. S. Lehrle, Department of Chemistry, University of Birmingham, private communication, 1970.

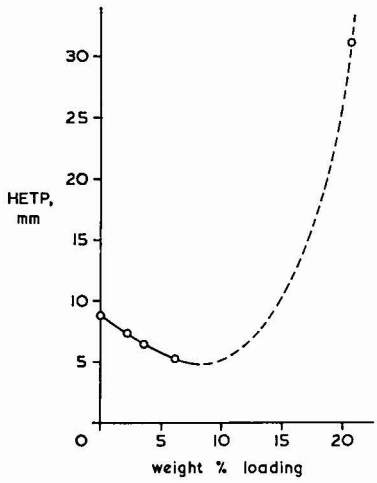

Figure 2. Variation of plate height (HETP) with weight percentage loading of DNP on Teflon for ethanol solute at 86 °C

fast-exchanging support sites contributes more to retention than does solution, at liquid loading below 0.3 to 1%, and is never negligible even at higher loadings. On a 6% loaded column, 14% of the retention of hexane is due to support adsorption.

Values of $K_S A_S p°$ for DNP/Te in Table I are similar in both magnitude and trend to those for the uncoated support. DNP apparently does not suppress Teflon surface activity in the way that polar phases, such as polyethylene glycol, suppress the surface activity of diatomaceous earth supports. It is possible that DNP is distributed as droplets, leaving most of the surface uncovered. Although several $K_S A_S p°$ values are higher for DNP/Te than for uncoated Te, the differences are within the limits of experimental error quoted earlier and do not point to a measurable gas–liquid interfacial adsorption.

As liquid loading increases, tailing decreases for all solutes. At high liquid loadings, whereas the fast-exchanging sites on Teflon still contribute substantially to retention, the presence of slow-exchanging sites is no longer revealed by tailing. On the 6% loaded column, only two solutes still showed significant tailing: butylamine was slightly, and water still quite strongly, tailed. Reduced tail size reveals the symmetry of the normal peaks and is responsible for the higher values of η seen in Table I compared with those on uncoated Teflon. These observations are as expected. Slow-exchanging sites become both less important as liquid-phase retention increases and also less distinct from fast-exchanging sites as mass transfer through the liquid takes longer with consequent band broadening.

The effect of liquid loading on band broadening is shown in a plate height (HETP) plot in Figure 2. The HETP was measured with ethanol, the solute showing least tailing, and at a fixed interstitial gas velocity, $\bar{u}$, of about 11 cm/sec. A notable feature of the plot is the rapid increase in HETP above about 10% loading, presumably due to growing dominance of the C_l term in the van Deemter equation (*22*, *23*). The large plate height of 30 mm at 20 weight % loading is much larger than observed on Firebrick at this loading and suggests that the effective liquid film thickness is larger on Teflon. Since the surface area of Teflon [variously quoted as 7–8 (*18*) and 11.7 (*7*) m^2/g] is about twice that of Firebrick, DNP must be very unevenly distributed on Teflon. This is consistent with Graham's finding (*7*) that only liquids, such as ethane and *n*-butane, with a lower surface tension than that of Teflon ($\approx$18 dyne/cm) spread freely on the surface; *n*-octane, with a higher surface tension, does not spread freely. DNP also has a higher surface tension and so its adsorption is localized. The liquid is probably distributed as droplets, as already suggested. Such a distribution would give a large C_l term because C_l is proportional to the square of the thickness of the largest liquid units (*24*). At high liquid loadings when, on this view, the droplets are large, sorption and desorption times of the normal peak are large. The distinction between fast- and slow-exchanging sites would then be reduced and tails appear relatively less extended.

CONCLUSIONS

Although Teflon gives symmetrical or only slightly tailed peaks when coated with sufficient stationary phase, it is apparently not inert as sometimes supposed. Absence of tailing does not necessarily indicate absence of a support contribution to retention, because sorption-induced tailing and peak retention arise in general from two different types of sorption site. Adsorption by Teflon appears to contribute substantially to retention of variety of both polar and nonpolar solutes at DNP loadings up to 20%. Thus, Teflon does not fulfill its promised role as ideal support for gas chromatographic studies of solutions, since the solution contribution to retention can be accurately determined only by varying the liquid loading. For nonpolar solutes this support seems, in fact, to be more adsorptive than diatomaceous earths.

In analytical work, Teflon is valuable for oxygenated solutes such as acetone and ethanol which tail more strongly than hydrocarbons on diatomaceous earths, but less strongly than these solutes on Teflon. Minimum plate height is attained at DNP liquid loadings of 5–10% depending on the interstitial gas velocity, $\bar{u}$. Higher percentage loadings give very poor column efficiency.

ACKNOWLEDGMENT

I wish to thank R. P. Taylor and A. B. W. Rehmtulla who carried out the experimental work.

RECEIVED for review July 31, 1970. Accepted November 5, 1970.

(22) J. H. Purnell, "Gas Chromatography," Wiley, New York, N. Y., 1962, Equation (8.18).
(23) A. B. Littlewood, "Gas Chromatography," Academic Press, New York, N. Y., 1962, Equation (5.68).
(24) J. C. Giddings, *J. Phys. Chem.*, **68**, 184 (1964).

Molecular and Unit Sheet Weights of Asphalt Fractions Separated by Gel Permeation Chromatography

Graeme A. Haley

School of Highway Engineering, University of New South Wales, Box 1, Kensington 2033, N.S.W. Australia

An unblown Kuwait asphalt and an asphaltene sample separated from an air blown Kuwait asphalt were fractionated by gel permeation chromatography. Molecular weight measurements, using a membrane and a vapor pressure osmometer in four solvents, toluene, chloroform, methylene chloride, and a dioxane–chloroform mixture showed the different abilities of each solvent to break up intermolecular association. In the less powerful solvents toluene and chloroform, incomplete asphaltene–asphaltene dissociation led to high molecular weights. Nuclear magnetic resonance 'unit sheet' weights were determined for fractions of both the asphalt and asphaltene. The asphalt fractions' molecular weights determined in the most powerful solvent, dioxane–chloroform, were consistent with their 'unit sheet' weights, for a value of the hydrogen to carbon ratio of the nonaromatic group of 1.92. The unit sheet weight of the asphaltene fractions was found to be about 1050 and substantially independent of molecular weight. This suggests that the asphaltene molecules consist of a number of unit sheets linked together rather than one large pericondensed aromatic ring system.

VAPOR PRESSURE OSMOMETRY (VPO), because of its use with a wide range of solvents and temperatures, together with its speed and small sample size, has become a convenient method for molecular weight determination of asphalt samples in recent years.

Benzene and chloroform have been the main solvents used for the determination of molecular weights by VPO although other solvents have also been tried. Girdler (*1*) found that for two unfractionated asphaltenes, trichloroethylene as a solvent gave a lower molecular weight than benzene. He believed that less association occurred in the more powerful solvent although some degree of association still remained. Dickie and Yen (*2*) in comparing tetrahydrofuran with benzene as VPO solvents for a number of asphaltene and resin samples stated that there appeared to be little difference between the molecular weight obtained for each of the samples. Neumann and Bellstedt (*3*), in determining the molecular weight of an unfractionated petroleum-ether asphaltene, tried a number of VPO solvents ranging in solvent power from carbon tetrachloride to pyridine at temperatures of 25 to 90 °C. They observed a distinct decrease in molecular weight with increasing temperature and increasing solvent power.

Molecular weight differences for different solvents should become more apparent when asphalt separation into more homogeneous fractions is carried out. Determination of the mean molecular weight by either VPO or membrane osmometry gives a number average and, for a material with a wide range of molecular sizes such as the whole asphalt the mean obtained is disproportionately influenced by the size of the lower molecular weight constituents. The molecular weight of a gel permeation chromatography (GPC) fractionated asphaltene has been determined by Altgelt (*4*). Toluene, benzene, chloroform, and xylene were used as VPO solvents for one fraction and the resultant molecular weights appeared quite similar. Aggregation or low solubility was indicated by convex concentration *vs.* molecular weight curves for some of the lower fractions. Altgelt proposed that the decrease in molecular weight was due to dissociation of low molecular weight contaminants from an asphaltene molecule rather than dissociation of an asphaltene–asphaltene aggregation.

Earlier measurements of asphalt molecular weights by VPO, as well as other methods, led Dickie and Yen (*2*) to propose that asphalt molecules can be built up by association of individual asphalt unit sheets. Dickson, Davis, and Wirkkala (*5*) attempted to obtain a comparison between the VPO molecular weight of a sample fractionated by GPC with its unit sheet weight, as determined from nuclear magnetic resonance (NMR) data by the method of Ramsey, McDonald, and Petersen (*6*). The molecular weight diverged from the unit sheet weight in the high molecular weight region. This divergence was attributed to association or polymerization of the asphalt units in solution.

Association may lead to larger molecular weights through the combination of unit cells held together by intermolecular forces. These intermolecular forces can be broken down by the use of more powerful solvents. Helm and Petersen (*7*) have compared the effect of methylene chloride and carbon tetrachloride, as solvents on the infra-red carbonyl absorption of an asphalt. The stronger absorption with the more powerful solvent, methylene chloride, indicated that some breakdown of intermolecular forces had occurred.

EXPERIMENTAL

Preparation of Sample. An asphaltene sample was obtained from an air blown Kuwait asphalt by the *n*-pentane precipitation method. The asphalt was diluted with 200 times its volume of *n*-pentane and, after refluxing, the asphaltene precipitate was recovered by filtration. The asphaltene sample and an unblown Kuwait asphalt were fractionated on a 2-cm id × 150-cm long column, packed with two pore size polystyrene gels prepared by the method described by Altgelt (*8*). The solvent system of a 90% benzene and a 10% methanol mixture was operated at a flow rate of 2 ml/min to give a fraction volume of 5.5 ml. A sample of 1 gram was used to give 25 asphaltene fractions and 35 asphalt fractions suitable for further analysis.

Molecular Weight Determinations. Molecular weights of GPC fractions were determined using four different solvents. Toluene was selected as a standardizing solvent and fractions which were thought to be above a molecular weight of 10,000

(1) R. B. Girdler, *Proc. Ass. Asphalt Paving Technol.*, **34**, 45 (1965).
(2) J. P. Dickie and T. F. Yen, ANAL. CHEM., **39**, 1849 (1967).
(3) H. J. Neumann and F. Bellstedt, *Erdoel Kohle*, **22**, 19 (1969).
(4) K. H. Altgelt, *Amer. Chem. Soc., Div. Petrol. Chem., Prepr.*, **13**(3), 37 (1968).
(5) F. E. Dickson, B. E. Davis, and R. A. Wirkkala, ANAL. CHEM., **41**, 1335 (1969).
(6) T. W. Ramsey, F. R. McDonald, and J. C. Petersen, *Ind. Eng. Chem., Prod. Res. Develop.*, **6**, 231 (1967).
(7) R. V. Helm and J. C. Petersen, ANAL. CHEM., **40**, 1100 (1968).
(8) K. H. Altgelt, *Makromol. Chem.*, **88**, 75 (1965).

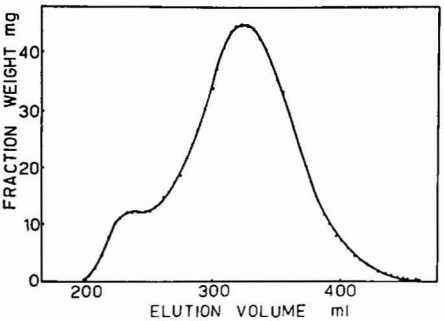

Figure 1. Weight distribution of fractions separated from the asphalt by GPC

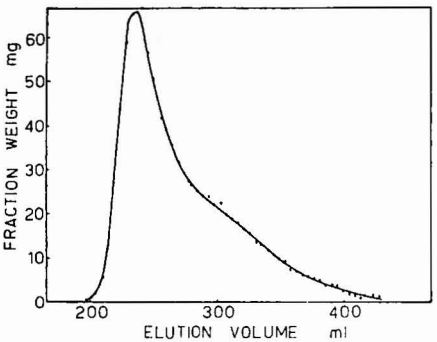

Figure 2. Weight distribution of fractions separated from the asphaltenes by GPC

were run on a 501 Mechrolab Membrane Osmometer at 37 °C. Four concentrations in the range 0.1–10 g/l. for each fraction were tested and readings were repeated until constant pressures were obtained. Samples below 10,000 were run at 37 °C on a 301A Mechrolab Thermoelectric Vapor Pressure Osmometer.

The other three solvents used were chloroform, methylene chloride, and a 50:50 v/v dioxane–chloroform mixture. The molecular weights of fractions dissolved in these solvents were all determined by VPO since the solvents were too volatile for membrane osmometry measurements on the high molecular weight fractions. Chloroform was used to allow a comparison to be made with the results of previous experiments while methylene chloride and the dioxane–chloroform mixture were used to examine the effect of more powerful solvents on the fraction molecular weight. Dioxane–chloroform rather than an acetone mixture was decided upon because of its higher boiling point although both have similar solvent–polymer interaction energies. Minimum sample size was 10 mg with a series of four concentrations for each fraction. Resistance readings were taken for all solvents after 2 min, except for the dioxane–chloroform mixture where a 5-min reading time was needed. All solvents were calibrated with benzil.

NMR Spectra. The NMR spectra were obtained using a Varian HA 60 spectrometer operating at 60 MHz with tetramethylsilane as an internal standard. All GPC fractions examined were dissolved in carbon tetrachloride and dried

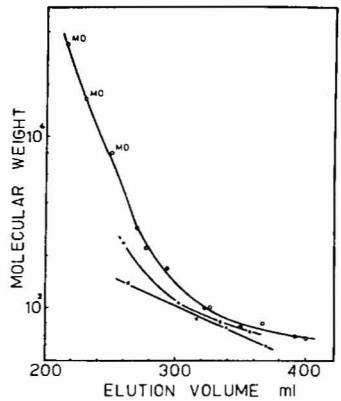

Figure 3. Molecular weights of selected fractions from the asphalt in different solvents

O **toluene**
● **chloroform**
+ **methylene chloride**
× **dioxane–chloroform**
M.O. membrane osmometer result

under vacuum to remove any absorbed benzene. Spectra and five integrals were recorded at a sweep width of 500 Hz and a scan speed of 500 sec. No proton signals were found in the 750–500 Hz range. Solutions of GPC fractions in the NMR solvent of deuterated chloroform were approximately 10% by weight and integrations were from high to low field.

RESULTS AND DISCUSSION

Molecular Weight Calculations. The membrane osmometry readings were plotted and extrapolated on an osmotic pressure-concentration *vs.* concentration graph.

The method of plotting vapor pressure osmometry readings on a resistance/concentration *vs.* concentration graph, although suitable for most fractions, was found to be unsatisfactory for some toluene and some chloroform solvent fractions. A method of calculation from the shortened McMillan and Mayer (*9*) virial expansion equation was used for these fractions. The equation is:

$$R = a_o + a_1 c + a_2 c^2 \quad (1)$$

and

$$a_1 = K/M \quad (2)$$

where

c = sample concentration (grams/cm³)
R = sample resistance at concentration c (ohms)
a_o, a_1 and a_2 = virial coefficients
K = solvent calibration factor
M = molecular weight.

The graphical method assumption that a_o is zero, is eliminated using the above equation. Difficulties with the graphical method were also experienced by Adicoff and Murbach (*10*) and Altgelt (*4*). It was found that for all frac-

(9) W. G. McMillan and J. E. Mayer, *J. Chem. Phys.*, **13**, 276 (1945).
(10) A. Adicoff and W. J. Murbach, ANAL. CHEM., **39**, 302 (1967).

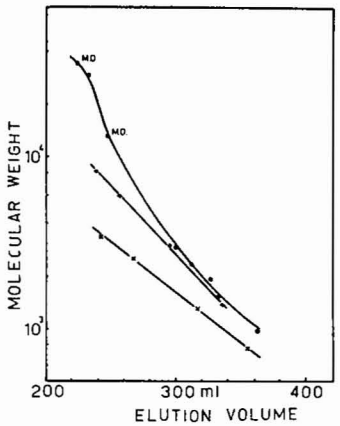

Figure 4. Molecular weights of selected fractions from the asphaltenes in different solvents

- O toluene
- ● chloroform
- \+ methylene chloride
- × dioxane–chloroform
- M.O. membrane osmometer result

tions examined a_2 was between +0.002 and −0.005. Chloroform gave a slightly positive a_2 while all other solvents had zero or negative a_2.

Effect of Solvent on Molecular Weight. The GPC chromatograms for the asphalt and the asphaltene samples are shown in Figure 1 and Figure 2. The extent to which intermolecular bonding can be broken up by the use of more powerful solvents is illustrated by Figure 3 and Figure 4. These curves can also be used to calibrate the chromatograms with respect to molecular weight. Fractions dissolved in toluene and chloroform give molecular weight results for calibration of chromatograms similar to those obtained by Altgelt (*8*, *11*), Dickson *et al.* (*5*), Snyder (*12*), and Bynum *et al.* (*13*). The results for the membrane osmometer appear interchangeable in the high molecular weight region with those of the vapor pressure osmometer. The molecular weights of the dioxane–chloroform fractions show a definite difference from those in other solvents, although the methylene chloride fractions were also slightly lower in molecular weight than those in toluene and chloroform.

The amount of aggregation in the dioxane–chloroform solvent can be judged from the concentration effect on resistance in Figure 5. The plots to determine the molecular weights for the dioxane–chloroform fractions do not have concave slopes in the low molecular weight range, although they do have a slightly negative slope. This slope tends to disappear as molecular weight increases with less dependence of molecular weight on concentration.

Altgelt (*4*) has plotted apparent molecular weight against concentration, which gives a concave slope if dissociation occurs. He suggested that the decrease in apparent molecular

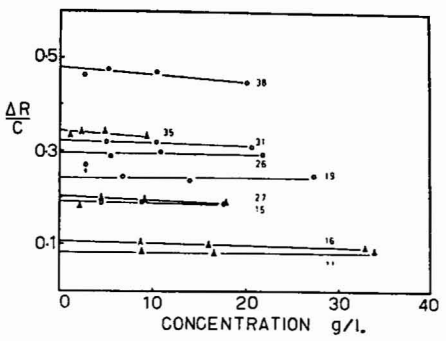

Figure 5. Effect of asphalt fraction concentration in VPO method for measuring molecular weight

O asphalt Δ asphaltenes

Table I. Aromatic Hydrogen to Carbon Ratios for a Pericondensed System

No. of rings	C_p	C_i	C_{ar}	H_{ar}/C_{ar}
1	6	0	6	1.00
2	8	2	10	0.80
3	10	4	14	0.71
4	10	6	16	0.62
5	12	8	20	0.60
6	12	10	22	0.54
7	12	12	24	0.50
9	14	16	30	0.47
17	18	32	50	0.36
22	20	42	62	0.32

weight, with a decrease in concentration, was caused by dissociation of low molecular weight contaminants from asphaltenes rather than asphaltene–asphaltene dissociation. From Figure 4 and Figure 5, there appears to be incomplete asphaltene–asphaltene dissociation with less powerful solvents. A contaminant–asphaltene aggregation, if not broken up by the GPC solvent of benzene–methanol, with the contaminants separated into the lower GPC fractions, is unlikely to be broken up in the less powerful VPO solvent of benzene, where the concentration is higher than the maximum GPC fraction concentration.

NMR Calculations. The Ramsey (*6*) assignments of proton bands in the NMR spectra of asphalts were used to determine the parameters of Brown and Ladner (*14*). These were the aromaticity, f_a, the degree of substitution, σ, and the aromatic hydrogen to carbon ratio, H_{ar}/C_{ar}, of the hypothetical unsubstituted aromatic material. These parameters depend on the assumptions that more than three rings are pericondensed and that no aromatic rings are joined by single bonds.

The theoretical aromatic hydrogen to carbon ratios for a number of hexagonal pericondensed structures are given in Table I. An equation can be obtained by a regression analysis of these data to relate the internal condensed carbon C_i to the peripheral carbon C_p. This equation is:

$$6C_i - C_p^2 + 8C_p - B = 0 \qquad (3)$$

(11) K. H. Altgelt, *J. Appl. Polym. Sci.*, **9**, 3389 (1965).
(12) L. R. Snyder, ANAL. CHEM., **41**, 1223 (1969).
(13) D. Bynum, R. N. Traxler, H. L. Parker, and J. S. Ham, *J. Inst. Petrol.*, **56**, 147 (1970).
(14) J. K. Brown and W. R. Ladner, *Fuel*, **39**, 87 (1960).

Table II. NMR Proton Ratios for Asphalt and Asphaltene Fractions

Fraction No.	H_α/H	H_β/H	H_γ/H	H_A/H
Asphalt	16.3	60.0	19.2	4.5
10/11	17.2	58.5	20.0	4.3
20	11.6	65.2	19.7	3.5
24	14.1	66.3	17.8	1.8
29	12.5	61.7	22.8	3.0
39/40	17.6	55.0	20.8	6.6
Asphaltene	21.6	50.0	20.4	8.0
8	19.8	50.4	22.7	7.1
12	19.5	52.2	21.1	6.2
14	19.7	54.3	20.0	6.0
18	20.8	49.7	21.6	7.9
24	20.8	51.9	21.0	6.3
32/33	23.6	45.9	20.7	9.8

Table III. Structural Parameters for Asphalt Fractions

Fraction No.	Elution volume, ml	C_N, %	C/H
10/11	243.5	24.1	0.826
20	288.8	15.0	0.670
24	307.7	15.9	0.643
29	326.2	14.9	0.636
39/40	378.5	21.0	0.707
Asphalt	...	15.5	0.649

where B is a variable which changes slightly, depending on the values of C_i and C_p. For the pericondensed model being considered, if C_{ar} is the aromatic carbon and H_{ar} is the aromatic hydrogen then:

$$C_{ar} = C_i + C_p \tag{4}$$

and

$$H_{ar} = C_p \tag{5}$$

Substituting Equations 4 and 5 in Equation 3 gives

$$C_{ar} = \frac{H^2_{ar}}{6} - \frac{H_{ar}}{3} + \frac{B}{6} \tag{6}$$

Results were calculated using a value of 12 for B, since this value gives an exact fit for one and two rings and a close if not exact fit for the other ring systems. The variation produced by having a number of C_i values for the same C_p is taken into account by allowing fractional values of C_p.

Rearranging Equation 6 and dividing both sides by C_{ar} gives

$$\frac{H_{ar}}{C_{ar}} = \frac{1 + \sqrt{6C_{ar} - 11}}{C_{ar}} \tag{7}$$

The value of the parameter H_{ar}/C_{ar} is known and its substitution in Equation 7 gives the amount of aromatic carbon. The total carbon, C_T, can be obtained by using the aromaticity parameter.

$$C_T = C_{ar}/f_a \tag{8}$$

The unit sheet weight, USW, is now given by:

$$\text{USW} = \frac{C_T \times 12 \times 100}{C_T\%} \tag{9}$$

where $C_T\%$ is the per cent carbon from elemental analysis.

A computer program can calculate the unit sheet weight using the above series of equations from the NMR proton ratios and the relative amounts of carbon, hydrogen, and other elements.

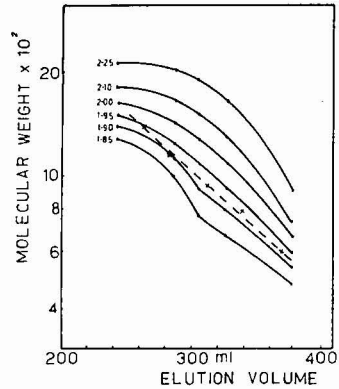

Figure 6. Best X ratio for coincidence of unit sheet weight with molecular weight for the asphalt fractions

× VPO molecular weights - - - - -
● NMR unit sheet weights ——

Asphalt Structure. The proton ratios in Table II for the asphalt GPC fractions show some interesting points. H_α/H, hydrogen alpha to aromatic rings, and H_A/H, aromatic hydrogen, both produce a minimum near the center of the molecular weight range while H_β/H, beta hydrogen and further removed methylene hydrogen, goes to a maximum. The methyl hydrogen gamma or further removed from an aromatic ring, H_γ/H, appears to remain constant. The highest molecular weight fraction is very similar to the lowest molecular weight fraction and it is only the difference carbon to hydrogen ratios, given in Table III, which causes a difference in unit sheet weight. The carbon to hydrogen ratio also goes to a minimum together with the naphthenic carbon, C_N, calculated by Williams' method (*15*), near the center of the molecular weight range. It appears from the variation of the different functions with molecular weight that the more paraffinic fractions occur in the central molecular weight range while the lower and higher molecular weight fractions contain the more naphthenic and aromatic structures.

A comparison between the asphalt molecular weight and its unit sheet weight is shown in Figure 6. Brown and Ladner (*14*) in studying a number of coals used a value of $x = y = 2.0$, where x and y are the respective hydrogen to carbon ratios for the alpha carbon groupings and the indirectly or unattached carbon groupings. They found that for this value of x and y, plots of NMR parameters against carbon content gave a linear correlation. Ramsey (*6*) and Dickson (*5*) adopted $x = y = 2.0$ for their asphalt NMR experiments. The value of $x = 1.92$ in Figure 6 gives a much better correlation between the unit sheet weight and the dioxane–chloroform molecular weight. All the molecular weights lie between $x = 1.89$ and 1.95 to give the desired link of molecular weight with unit sheet weight as sought by Dickson (*5*).

The development of a condensed naphthenic structure is needed to support a value of x and y lower than 2. Since the

(15) R. B. Williams, *Amer. Sci. Testing Mater.*, STP 224 (1957).

Table IV. Comparison of NMR Unit Sheet Weights with Interpolated VPO Molecular Weights for Asphaltene Fractions

Fraction No.	Elution volume	C_N %	C/H	Unit sheet weight[a]	Molecular weight
8	228.3	32.1	0.860	1000	4200
12	247.5	35.7	0.882	1350	3260
14	257.5	28.6	0.845	1080	2850
18	276.3	29.6	0.850	870	2220
24	303.9	32.8	0.856	1050	1540
32/33	342.3	28.0	0.896	780	910
Asphaltene	...	28.4	0.861	880	2900

[a] $x = y = 1.92$.

aromatic carbon appears to form a condensed ring structure, it is highly likely that the naphthenic carbon is also present in this form. The condensation of the naphthenic carbon will produce internal branching with a simultaneous lowering of the value of x and y. An artificial change in x and y will also be produced by the number average molecular weight comparison with the weight average unit sheet weight. This effect would be rather small, however, with fractionated samples.

Asphaltene Structure. The asphaltene fractions are all very similar in hydrogen distribution, and there appears to be no indication of increasing or decreasing proton ratios as was the case with the asphalt. The calculated factors, naphthenic carbon, carbon to hydrogen ratio, and the unit sheet weight, given in Table IV, are all similar for the different fractions. The unit sheet weights are contained within the range 1050 ± 300 for $x = y = 1.92$ whereas the molecular weights increase up to 4200. The most important differences between the asphaltene and asphalt results are shown in comparing their unit sheet and molecular weights. Since the asphaltene unit sheet weight does not change with molecular weight, then it is unlikely that the asphaltenes are formed by an extension of the asphalt pericondensed ring system.

The formation of asphaltenes through the polymerization of a number of unit sheet weights is in agreement with conclusions presented by Yen, Erdman, and Pollack (*16*), from X-ray data on asphaltenes and also with those of Ferris, Black, and Clelland (*17*). Ferris found, from X-ray diffraction techniques on a solvent fractionated asphaltene, that the unit sheets were all approximately the same dimensions and postulated a sixteen-ring structure of condensed aromatic sheets linked by saturated bridges. The sixteen-ring system with an aromaticity of 0.45–0.50 would give a unit sheet weight which would agree quite well with the results presented for the GPC fractionated asphaltene.

Further work to examine more closely the changes occurring during air blowing are at present being undertaken and this is expected to give a clearer picture of asphaltene formation.

ACKNOWLEDGMENT

The author thanks Professor D.F. Orchard, Dr. E. J. Dickinson, and Mr. N. W. West for their helpful criticisms and assistance.

RECEIVED for review September 21, 1970. Accepted November 16, 1970. Work supported by an Australian Road Research Board Fellowship.

(16) T. F. Yen, J. G. Erdman, and S. S. Pollack, ANAL. CHEM., **33**, 1587 (1961).
(17) S. W. Ferris, E. P. Black, and J. B. Clelland, *Ind. Eng. Chem., Prod. Res. Develop.*, **6**, 127 (1967).

Application of Photoelectron Spectrometry to Pesticide Analysis. II

Photoelectron Spectra of Hydroxy-, and Halo-Alkanes and Halohydrins*

A. D. Baker, D. Betteridge,[1] N. R. Kemp, and R. E. Kirby[2]
Department of Chemistry, University College of Swansea, Singleton Park, Swansea, Glam., U. K.

The photoelectron spectra of ethylene fluoro-, chloro-, bromo- and iodohydrin have been obtained and are discussed in relation to the photoelectron spectra of alkanes, halo alkanes and alcohols, which have also been measured. There is an interaction between the nonbonding orbitals in dihalo alkanes, ethylene chlorohydrin and ethylene bromohydrin. The extent of interaction depends on the degree of separation of the interacting orbitals and their relative energies. The spectra of the individual compounds are sufficiently different to allow qualitative identification. The analytical significance of the results is briefly discussed and correlation diagrams for 29 compounds are presented.

ETHYLENE OXIDE AND PROPYLENE OXIDE are widely used as fumigants, but they can react with chloride and bromide in cereals to give toxic chlorohydrins or bromohydrins. This has led to the development of methods for the determination of these toxic residues, most of which are based upon gas–liquid chromatography (*1–5*). Halohydrins are relatively simple molecules containing both an oxygen and a halogen atom and are thus well suited for examination by photoelectron spectrometry (PES) in its present form. This technique, which measures the binding energies of electrons in molecules,

* Part I, "Application of Photoelectron Spectrometry to Pesticide Analysis; Photoelectron Spectra of Five-Membered Heterocycles and Related Molecules" appeared in ANAL. CHEM., **42**, 1064 (1970).

[1] To whom communications concerning this paper should be addressed.

[2] On sabbatical leave from Queens College of the City University of New York, Flushing, N.Y. 11367.

(1) S. G. Heuser and K. A. Scudamore, *Chem. Ind. (London)*, **1967**, 1557.
(2) *Ibid.*, p 1054.
(3) S. Ben-Yehoshua and P. Krinsky, *J. Gas Chromatogr.*, **6**, 351 (1968).
(4) E. P. Ragelis, B. S. Fisher, and B. A. Klimeck, *J. Ass. Offic. Agr. Chem.* **51**, 709 (1968).
(5) F. Wesley, B. Rourke, and O. Derbyshire, *J. Food Sci.*, **30**, 1037 (1965).

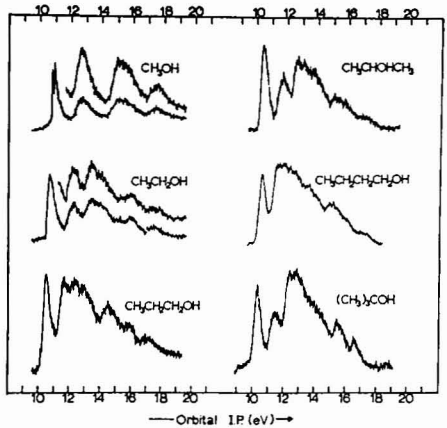

Figure 1. Photoelectron spectra of some aliphatic alcohols, excited by irradiation with 584-Å photons

and its applicability to analytical chemistry has been discussed elsewhere (*6–8*).

Preliminary investigations revealed common features in the photoelectron spectra of the halohydrins. Relatively sharp peaks due to the ejection of "lone-pair" electrons from the halogen and oxygen p-orbitals were present in all the spectra. (Photoelectron spectra indicate that all electrons in molecules are to some extent bonding electrons so that strictly speaking there are no "lone-pair" electrons. However, the term has been widely employed and will be used in its usual sense here and subsequently.) The relative positions of these peaks within the spectra showed marked dependence upon the nature of the halogen atom, and indicated that interactions between the halogen and oxygen p-orbitals were important. The study was therefore extended to include alcohols and mono- and di-haloalkanes, in order to see whether any general trends or correlations could be established.

The spectra of the compounds studied are individually characteristic and simplified methods of interpretation serve to correlate spectral and molecular structural features.

EXPERIMENTAL

The compounds studied were obtained commercially and purified as necessary. Purities were checked by infrared spectrometry and mass spectrometry.

Photoelectron spectra were obtained on a Perkin-Elmer PS.15 Photoelectron Spectrometer, modified as described in Part I (*8*).

RESULTS AND DISCUSSION

Photoelectron Spectra of Alcohols. Since alcohols can be regarded as alkyl substituted water molecules, their photoelectron spectra might be expected to contain some of the characteristic features of the spectra of water and the corresponding alkane, *viz.*, a sharp intense peak ascribable to a

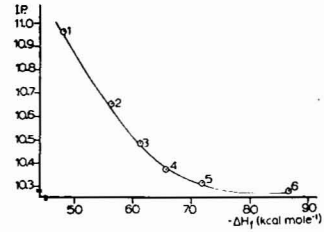

Figure 2. Graph showing variations in first ionization potentials and heats of formation of some aliphatic alcohols, ROH

R = (1) CH_3, (2) C_2H_5, (3) n-C_3H_7, (4) n-C_4H_9, (5) n-C_5H_{11}, (6) n-C_6H_{13}

2p lone pair of electrons on the oxygen (*9*), and a series of broader bands of moderate to low intensity which are characteristic of alkanes (*10*, *11*). The ionization potentials of the lone pair electrons would be expected to be lower in alcohols than in water because of the inductive effect associated with alkyl groups.

Further broad bands would be expected in the photoelectron spectra of alcohols owing to the ejection of electrons from orbitals principally responsible for O–H and C–O bonding. These *a priori* predictions do account for the overall forms of the spectra obtained (Figure 1), but refinements are needed to explain some of the observed features. Whereas the first band of the water spectrum, corresponding to the oxygen lone pair, is very sharp, the corresponding bands in the spectra of alcohols are appreciably broadened, indicating that the equivalent orbitals have more bonding character. In this context, Dewar and Worley (*12*) have calculated that only 75% of the highest occupied orbital in methanol is composed of an oxygen 2p atomic orbital, and also that this percentage decreases rapidly with increasing size of the alkyl group.

The high resolution photoelectron spectra of methanol and higher alcohols to some extent substantiate these calculations: the bands are much broader than would be expected for nonbonding electrons, and, in the case of methanol, there is fine structure showing appreciable population of high vibrational levels. The vibrational structure can be ascribed to the excitation of C–O stretching and C–H deformation modes.

Although the "oxygen lone pair" ionization potentials of higher alcohols have more or less a constant value, ionization potentials of the deeper orbitals decrease slowly. However, even for the highest alcohol examined in the present study (*n*-octanol) the "oxygen lone pair" band is still the lowest ionization energy band in the photoelectron spectrum.

The first vertical ionization potentials of the *n*-alcohols decrease rapidly from 10.95 to 10.37 eV on ascending the series from methanol to *n*-butanol, but then assume a nearly constant value of 10.3 eV. The ionization potential of a molecule is a measure of the difference between the heat of formation of the molecule and its molecular ion. The successive decreases

(6) D. Betteridge and A. D. Baker, ANAL. CHEM., 42 (1), 43A (1970).
(7) A. D. Baker, *Accounts Chem. Res.*, 3, 17 (1970).
(8) A. D. Baker, D. Betteridge, N. R. Kemp and R. E. Kirby, ANAL. CHEM., 42, 1064 (1970).
(9) C. R. Brundle and D. W. Turner, *Proc. Roy. Soc. (London), Ser. A*, 307, 27 (1968).
(10) A. D. Baker, C. Baker, C. R. Brundle, and D. W. Turner, *Int. J. Mass Spectrom. Ion Phys.*, 1, 285 (1968).
(11) A. D. Baker, D. Betteridge, N. R. Kemp, and R. E. Kirby, *J. Mol. Struct.*, in press.
(12) M. J. S. Dewar and S. D. Worley, *J. Chem. Phys.*, 50, 654 (1969).

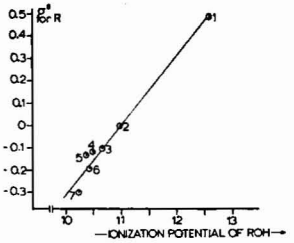

Figure 3. Plot of first ionization potentials of alcohols, ROH *vs.* Taft σ^* values for R

R = (1) H, (2) CH_3, (3) C_2H_5, (4) n-C_3H_7, (5) n-C_4H_9, (6) i-C_3H_7, (7) t-C_4H_9

in ionization potential up to *n*-butanol indicate therefore that for small alkyl groups, the molecular ion is stabilized to a greater extent than is the molecule by the introduction of a methylene group. Above *n*-butanol there would seem to be no difference between the stabilizing effects on molecule and ion. Figure 2 shows graphically the changes in first ionization potentials and heats of formation (*13*) of the alcohols studied.

A correlation between the ionization potentials of alcohols and Taft σ^* constants (*14*) for the alkyl substituents might be expected. Figure 3 shows the σ^* constants for –H, $-CH_3$, $-C_2H_5$, $-n$ - C_3H_7, $-n$ - C_4H_9, –iso-C_3H_7, and $-tert$-C_4H_9 plotted against the lowest ionization potentials of water and the appropriate alcohols. The line of best fit, with 95% confidence limits is given by IP = (10.81 ∓ 0.13) + (3.17 ∓ 1.11) (σ^* + 0.049). It is clear from the Equation and Figure 3 that although there is a linear relationship, there are some anomalies. Thus the ionization potential of 2-propanol falls between that of *n*-propanol and *n*-butanol, although the σ^* value for –iso-C_3H_7 is appreciably lower than that of either $-n$ - C_3H_7 or $-n$ - C_4H_9. The implication is that the electronic effects responsible for the differences between the ionization potentials are not wholly reflected by the σ^* values, although it appears that the latter could be useful for crude estimations of ionization potentials. These observations are in concord with the comments of Wiberg on the inductive effect exerted by *tert*-butyl (*15*).

There is some question as to whether the second highest occupied level in alcohols relates to a C–O or to some other type of orbital. Comparison of the spectra of methanol, 2-propanol, and *tert*-butanol (Figure 1) clearly suggests that in these compounds it is predominantly C–O, since the strongly electron-releasing branched alkyl groups produce the expected changes in the second ionization potentials. In the straight chain alcohols, however, the ionization potentials of electrons in C–H and C–C bonding orbitals appear to be lowered sufficiently to be comparable with those of electrons in the C–O σ-bonding orbitals. Thus, whereas the spectra of 2-propanol and *tert*-butanol both contain distinct "C–O" bands, the spectra of the straight chain isomers of these compounds show the "C–O" band to be swamped under the alkyl bands.

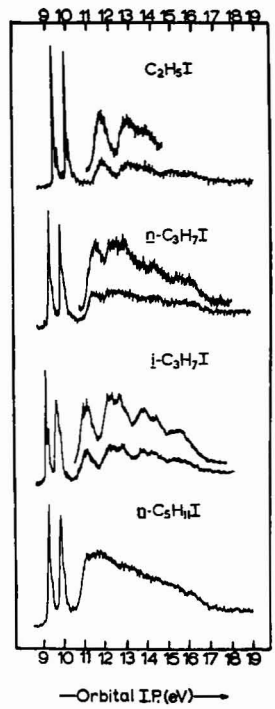

Figure 4. Photoelectron spectra of some aliphatic iodo compounds, excited by irradiation with 584-Å photons

Photoelectron Spectra of Halo-alkanes (Figure 4). The photoelectron spectra of some simple haloalkanes have been discussed previously (*16*). The most characteristic features of the spectra are the sharp "halogen lone pair" bands, spin-orbit split in some cases. The "halogen lone pair" ionization potentials of methyl halides correspond very closely to those of the phenyl halides, indicating a parity in the overall electron releasing natures of the methyl and phenyl groups. In both methyl and phenyl halides, the halogen lone pair ionization potentials plotted against the Pauling electronegativity of the halogen atom give a straight line (*17*).

In the present study we examined a series of iodoalkanes to investigate the variations in spin orbit coupling and in ionization potentials as the size of the molecule increased. We also examined some disubstituted chloroalkanes to further investigate the extent of 1:2, 1:3, and 1:4 interactions.

There appears to be very little decrease in the spin-orbit splitting (ΔSI) of the iodine lone pair peaks as the alkyl halide

(13) S. W. Benson, R. E. Cruickshank, D. M. Golden, G. R. Haugen, H. R. O'Neal, A. S. Rodgers, R. Shaw, and R. Walsh, *Chem. Rev.*, 69, 279 (1969).
(14) R. W. Taft in "Steric Effects in Organic Chemistry," M. S. Newman, Ed., Wiley, New York, N.Y., 1956, p 619.
(15) K. B. Wiberg, "Physical Organic Chemistry," Wiley, New York, N.Y., 1964, pp 128–129.
(16) D. W. Turner, A. D. Baker, C. Baker, and C. R. Brundle, "High Resolution Photoelectron Spectroscopy," Wiley, London, 1970.
(17) A. D. Baker, D. Betteridge, N. R. Kemp, and R. E. Kirby, *Int. J. Mass Spectrom. Ion Phys.*, 4, 90 (1970).

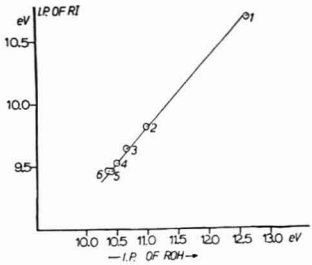

Figure 5. Graph showing the first ionization potentials of alcohols, ROH, plotted against the first ionization potentials of alkyl iodides

R = (1) H, (2) CH_3, (3) C_2H_5, (4) n-C_3H_7, (5) i-C_3H_7, (6) n-C_5H_{11}

series is ascended from methyl iodide ($\Delta SI = 0.61$ eV) to butyl iodide ($\Delta SI \simeq 0.55$ eV). The bands do become broader, however, and the fine structure less clearly defined (especially in the higher ionization band) as the series is ascended.

As with the alcohols, an approximate correlation exists between the lone pair ionization potentials of the alkyl iodides, and the Taft σ^* values of the alkyl groups. The mean ionization potential of the two peaks split by spin-orbit coupling is given, with 95% confidence limits by

$$IP = (9.79 \mp 0.04) + (1.80_8 \mp 0.18_4)(\sigma^* + 0.01_0) \quad (1)$$

The marked improvement in fit is mainly the result of having n-pentyl iodide and not *tert*-butyl iodide. The inclusion of –H as an alkyl radical is rather dubious, but excluding the point due to HI does not significantly affect the equation relating $\hat{IP}$ with σ^*.

The IP/σ^* relationship for alkyl iodides suffers from the same sort of anomalies as the corresponding relationship for alcohols. However, that the overall effects of the alkyl groups vary in a predictable way from series to series is indicated by Figure 5, which shows that the oxygen lone pair ionization potentials of alcohols plotted against the iodine lone pair ionization potentials of alkyl iodides is linear, and of the form

$$IP_I = (9.79 \mp 0.06) + (0.533 \mp 0.072)(IP_{OH} - 10.90) \quad (2)$$

Photoelectron Spectra of Dichloroalkanes. The photoelectron spectra of 1,2-dichloropropane, 1,3-dichloropropane, and 1,4-dichlorobutane (Figure 6) show important differences, especially in the 10.5–12.5 eV range. The classical picture of nonbonding electrons of chlorine being localized as lone pairs in the 3p orbitals and the argument that the intensity of a peak is roughly proportional to the number of filled equivalent orbitals from which ionization is taking place would lead one to expect that the spectra of the dichloropropanes would be similar to that of propylchloride but with the single "halogen lone-pair" peak being relatively twice as intense. It might be argued that the slightly different inductive effects operating on the carbon atoms in the 1 and 2 positions in 1,2-dichloropropane would give rise to two chlorine peaks or lead to a broadening of the single peak. Such an argument would not be applicable to 1,3-dichloropropane or 1,4-dichlorobutane and does not account for the number of peaks which are observed. It is therefore necessary to question the premise that the nonbonding lone pair electrons do not interact.

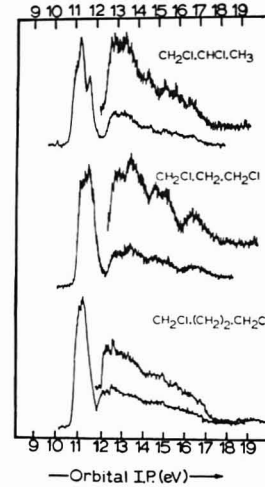

Figure 6. Photoelectron spectra of 1,2- and 1,3-dichloropropane and 1,4-dichlorobutane, excited by irradiation with 584-Å photons

A simplified molecular orbital approach is to treat the nonbonding orbitals as if they were atomic orbitals localized on two atoms within the molecule. The degree of separation of the orbitals and their symmetry with respect to each other is determined by the geometry of the molecule. If any two of the localized orbitals are close enough, have the same symmetry and comparable energy, they can interact to give two molecular orbitals, one of lower energy than the energy of the least energetic of the two atomic orbitals and one of higher energy than the energy of the highest orbital. If the atomic orbitals are identical, the energies of the two molecular orbitals will be symmetrically above and below the energy of the atomic orbitals. The molecular orbital of lower energy is formally a bonding orbital and the one of higher energy is an anti-bonding orbital. Since only interaction between filled orbitals is being considered, two electrons occupy both the bonding and the anti-bonding orbital so the net effect is nonbonding.

However, ionization would be from two nonequivalent orbitals and this should be reflected in the photoelectron spectrum. If the orbitals were too far apart to interact, or were of disparate energy, or of different symmetry, there would be no interaction and the orbitals would be looked on as nonbonding localized atomic orbitals. Thus, in a compound with two atoms with two p orbitals each, two of which could interact and two otherwise equivalent ones which couldn't, one would expect to see three peaks on the intensity ratio 1:2:1. The argument is not dissimilar to that used to explain π-bonding in ethylene at the introductory level or that used to explain the photoelectron spectra of compounds with halogen atoms adjacent to π-systems (*6*). It is a simplified picture insofar as it ignores completely interactions with any other orbitals of the same symmetry, and similar energy. A test of its validity is provided by dichloroalkanes.

Electrons associated with ionization energies in the 10.5–12.5 eV range come from orbitals derived principally from Cl

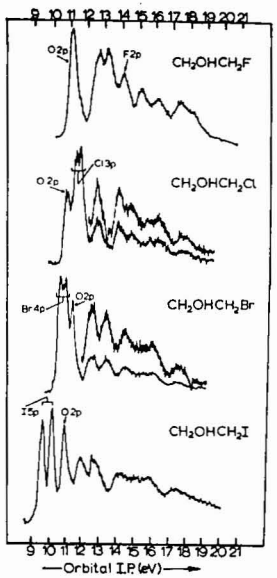

Figure 7. Photoelectron spectra of ethylene halohydrins, excited by ir-radiation with 584-Å photons

atomic 3p orbitals. Each of the chlorines has two sets of occupied lone pair orbitals, and if the sets of orbitals were so arranged that they had the same symmetry, straightforward interaction could produce four molecular orbitals having different energies. Four "chlorine" bands could therefore appear in the photoelectron spectrum. The greatest Cl–Cl interaction would be expected *a priori* to occur in the 1,2-isomer, and this is reflected in the photoelectron spectrum of this compound. Two of the resulting "chlorine molecular orbitals" seem to be degenerate in energy, and correspond to the most intense peak in the spectrum, centered at 11.26 eV. The other two Cl orbitals, corresponding to the shoulder at ~11.1 eV, and the peak at ~11.75 eV, however, differ appreciably in energy, indicating a large interaction.

Although much smaller, the Cl–Cl interaction in 1,3-dichloropropane is still considerable, and is still apparent in 1,4-dichlorobutane. In the spectra of these compounds, there are no single sharp chlorine peaks: rather broader bands containing two poorly resolved maxima are present. The half-width of the "chlorine" band for 1,3-dichloropropane is *ca.* 0.9 eV, and for 1,2-dichloropropane is *ca.* 0.65 eV. These results perhaps indicate that in these compounds there is an interaction which results in the formation of a pair of doubly degenerate orbital levels.

Photoelectron Spectra of Halohydrins (Figure 7). These molecules form an interesting series, since the nature of the highest occupied orbital may be either predominantly halogen lone pair or predominantly oxygen lone pair. The possibility of some sort of interaction involving one of the halogen lone pair orbitals and the oxygen 2p lone pair orbital also exists. In such a case, the degeneracy of the p_τ and p_ν type orbitals of the halogen could be lifted. The spectra confirm in fact

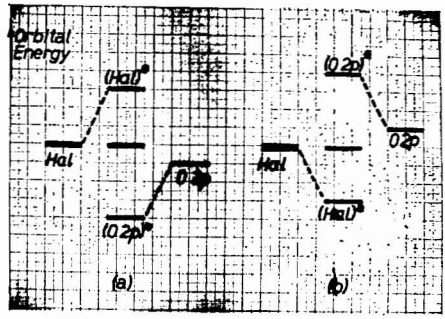

Figure 8. Interation of "oxygen lone pair" and "halogen lone pair" orbitals

(*a*) halogen lone pair ionization potential < oxygen lone pair ionization potential
(*b*) halogen lone pair ionization potential > oxygen lone pair ionization potential (see text)

that interactions of this sort may take place and thus provide the first experimental evidence for this type of phenomenon.

A number of different factors can, in fact, determine the relative positions of the oxygen and halogen peaks, and it is necessary to allow for these to account for the spectra. These factors can be considered to fall into three main categories.

Polarization or Inductive Effects. An ethylene halohydrin differs from a haloethane in containing the grouping $-CH_2CH_2OH$ in place of $-CH_2CH_3$ and from ethanol in containing the grouping $-CH_2CH_2Hal$ in place of $-CH_2CH_3$. The inductive effect of the electronegative oxygen atom in $-CH_2CH_2OH$ would be expected to reduce the electron density in the vicinity of the halogen atom, leading to higher halogen lone pair ionization potentials for halohydrins than haloethanes. Similarly, the oxygen 2p lone-pair ionization potentials would be expected to be greater in the halohydrins than in ethanol. Further, on the basis of inductive effects alone, the ionization potentials of the oxygen lone pairs of the halohydrins would be expected to increase in the order iodohydrin, bromohydrin, chlorohydrin, fluorohydrin.

Interaction of the Oxygen and Halogen Lone Pair Orbitals. The simplified molecular orbital theory of explaining the interaction between nonbonding electrons in dihaloalkanes predicts that there should be a similar interaction between nonbonding oxygen and halogen p orbitals. But as there is only one oxygen lone pair p orbital, for reasons of symmetry, only one of the two halogen lone pair orbitals can participate in such an interaction. To a first approximation the "mixing in" of a C–H contribution can be ignored, and the primary interaction can be considered as a direct one between an oxygen 2 p and a halogen p orbital to give energies above and below those of the interacting lone pair orbitals (Figure 7). The new orbitals are described as (halogen)* and (oxygen 2p)* in Figure 8. The largest interaction would be expected when the energies of the oxygen 2p orbital and the halogen p orbitals are closest. The ionization potential of an electron in the (halogen)* orbital could be either greater than, or lower than, the corresponding ionization potential for the unaffected halogen orbital, depending on the relative magnitudes of the energies of the interacting oxygen and halogen orbitals (Figure 7). Both orbitals would be fully occupied.

Spin-Orbit Effects. A further complication could arise

Table I. Ionization Potentials (eV) for the 20 Compounds Studied[a]

Compounds	1st Band		Bands								
	AI	VI	2nd	3rd	4th	5th	6th	7th	8th	9th	10th
Methanol	10.85	10.96	12.72	15.15	15.55	17.50					
Ethanol	10.65		12.20	13.31	13.82	15.85	17.35				
n-Propanol	10.48		11.73	12.34	13.04	14.60	16.00	17.14			
2-Propanol	10.42		11.71	12.68	13.08	13.75	15.14	15.80	17.20		
n-Butanol	10.37		11.48	11.95	12.25	12.55	13.55	15.10			
tert-Butanol	10.23		11.48	12.35	12.78	15.42	16.50				
Ethyl iodide	9.37		9.93	11.68	12.90	13.80	15.00	15.90			
n-Propyl iodide	9.27		9.84	11.46	12.25	12.80	14.25	15.30	15.95		
i-Propyl iodide	9.19		9.74	11.18	12.35	12.80	13.95	14.50	15.40		
n-Pentyl iodide	9.21		9.77	11.06	11.60	13.00	14.50	16.10			
2-Fluoroethanol	11.05		12.65	13.09	14.00	15.00	16.00	17.35	18.08		
2-Chloroethanol	10.90		11.45	11.71	12.62	13.90	14.62	15.78	16.18	17.60	
2-Bromoethanol	10.63		10.91	11.29	12.50	13.32	14.48	16.09	17.50		
2-Iodoethanol	9.62		10.18	10.87	11.85	12.65	14.00	15.78	17.34		
Epifluorohydrin	10.74		11.80	13.17	14.22	15.10	16.32	17.05			
Epichlorohydrin	10.64		11.33	11.52	13.78	15.04	15.45	16.47	17.40	19.65	
Epibromohydrin	10.46		10.70	10.99	11.50	13.34	13.72	14.65	15.15	16.20	17.20
1,2-Dichloropropane	10.73	11.06	11.29	11.73	12.93	13.45	14.57	15.30	15.86	16.55	
1,3-Dichloropropane	10.93		11.16	11.36	11.55	12.72	13.41	14.60	15.07	16.35	
1,4-Dichlorobutane	11.03		11.18	12.24	12.90	14.90	15.60	16.20			

[a] AI and VI indicate adiabatic and vertical ionization potentials, respectively.

out of spin-orbit coupling. This could result in two peaks in the photoelectron spectrum for every "halogen" orbital. However, the spectra of ethyl halides would lead one to expect appreciable spin-orbit effects only in the case of ethylene iodohydrin.

Having considered the factors which might be expected to influence the photoelectron spectra of the halohydrins as a whole, we are now in a position to discuss the individual spectra. The first point of interest is that the spectrum of ethylene iodohydrin contains three sharp peaks characteristic of lone pairs. These peaks are centered at 9.62, 10.18, and 10.87 eV. The spin-orbit iodine 5p peaks in the ethyl iodide spectrum occur at 9.37 and 9.93 eV, and thus the iodohydrin 9.62 and 10.18 eV peaks can be assigned fairly certainly to spin-orbit split iodine 5p orbitals. This leaves the 10.87-eV peak to be attributed to the oxygen 2p lone pair. This implies that the oxygen lone pair ionization potential is a little higher than that of ethanol (10.65 eV) but this, and the increase in the ionization potentials of iodine compared with ethyl iodide, is consistent with the inductive effect discussed above. There would appear to be no significant "lone pair orbital interaction" in ethylene iodohydrin, otherwise each of the iodine peaks would have split into two components. Such an interaction would be unlikely because of the large difference in the energies of the iodine 5p and oxygen 2p orbitals.

The spectra of ethylene chlorohydrin and ethylene bromohydrin also contain three "lone pair" peaks. The peaks at 11.45 and 11.71 eV in the spectrum of ethylene chlorohydrin are in positions characteristic of chlorine 3p lone pairs and the peaks at 10.63 and 10.91 eV in the spectrum of ethylene bromohydrin are characteristic of bromine 4p lone pairs. Thus the peaks at 10.90 eV in the chlorohydrin, and 11.29 eV in the bromohydrin would seem to characterize the "oxygen 2p" electrons in these compounds. These results are not explicable on the basis of polarization effects alone, which would predict the oxygen 2p lone pair ionization potential to be larger for the chlorohydrin than the bromohydrin. It is necessary, therefore, to invoke interaction of the oxygen and halogen lone pairs in these compounds.

In the detailed discussion of the nature of this interaction, three atomic orbitals must be taken into account, the oxygen 2p, the halogen p, which interacts, and the halogen p, which cannot interact for reasons of symmetry. It is assumed that the latter orbital has the energy that would be expected for a nonbonding, noninteracting orbital. It will thus be in between the interacting orbitals, one of which will be shifted to higher and the other to lower energy (higher I.P.). The interaction will produce two molecular orbitals, but the character of each will be largely that of the interacting atomic orbital closest in energy to the resultant molecular orbital.

The relative energies of the orbitals in order of decreasing energy is bromine 4p, oxygen 2p, and chlorine 3p (first ionization energies of HF, HCl, HBr, HI, and H_2O, respectively, being 16.05, 12.74, 11.67, 10.38 (*18*), and 12.62). These values imply that the ionization potential characterizing the halogen lone pair orbital "modified" by interaction (see Figure 7) would exceed that of the uninfluenced halogen orbital in the case of ethylene chlorohydrin, but that the reverse would be true for the bromohydrin. Similarly the ionization potential characterizing the "oxygen lone pair" would be lowered by interaction with the chlorine orbitals, but be increased by interaction with the bromine orbitals.

Since interaction splits the chlorine peaks by 0.26 eV, and the bromine peaks by 0.28 eV, the ionization potentials the oxygen lone pair electrons would have had if interaction had not occurred can be calculated by assuming that the energies of the oxygen orbitals were affected to the same extent by interaction as the halogen orbitals. Then, the "inductive-effect only" oxygen 2p ionization potentials are 11.16 eV for the chlorohydrin, and 11.01 eV for the bromohydrin, which gives the theoretically expected order.

As the bromine peaks are also split in the spectrum of epibromohydrin, similar interactions can presumably take place in this type of compound. Ionization potentials for these and the other compounds studied are collected in Table I.

The first four peaks in the fluorohydrin spectrum at 11.05, 12.65, 13.09, and 14.00 eV can tentatively be attributed to ionization from orbitals consisting mainly of oxygen lone pair C–O, C–C, and fluorine lone pair, respectively, by anology

(18) H. J. Lempka, T. R. Passmore, and W. C. Price, *Proc. Roy. Soc. (London), Ser., A.*, **304**, 53 (1968).

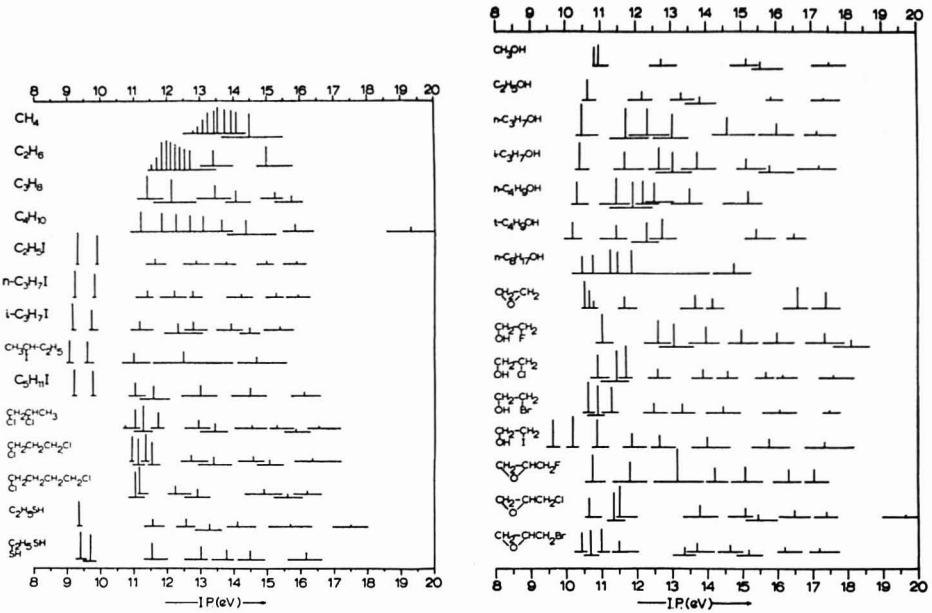

Figure 9. Correlation diagram of spectra of alkanes, haloalkanes, alcohols, and related compounds

Vertical lines indicate approximate peak intensity (strong, medium or weak). Horizontal lines are half-peak width. Overlapping horizontal lines indicate extrapolated half-peak widths for peaks only resolvable at 50–80% peak height

with other compounds. The oxygen lone pair and C–O ionization potentials would be increased by the inductive effect of fluorine, and the fluorine lone pair ionization potential would be expected in the region of 14–15 eV. As in other fluorine containing compounds, the lone pair peak is much less sharp than those of the other halogens. The energy difference between the oxygen and fluorine 2p orbitals is too great for interaction to be noticeable. The C–O and C–C orbitals will presumably have an appreciable C–H contribution.

Analytical Applicability. The conclusions reached in Part I about the analytical value of the method are confirmed by the results obtained in this study. The photoelectron spectra of the compounds examined are sufficiently different to form the basis of qualitative identification. This is emphasised in the stylized presentation of the spectra of the compounds discussed, and some related compounds, in the form of a correlation diagram (Figure 9). Again it is obviously best to obtain a compound in a pure state before running its spectrum, although some impurities with well defined spectra may be readily recognizable, *e.g.*, water, nitrogen, hydrogen, chloride, etc. To confirm this conclusion, the spectrum of a 1:1 (v/v) mixture of chlorohydrin and bromohydrin was obtained. As expected, most of the peaks overlapped, but a careful worker would readily deduce that there was an impurity in his spectrum of chlorohydrin or bromohydrin.

Again, the potential value of the method in structural analysis is shown. A full understanding of the extent and nature of interactions of nonbonding electrons could have far reaching implications in this connection.

RECEIVED for review July 6, 1970. Accepted October 5, 1970. We thank the Agricultural Research Council (U. K.) for providing the photoelectron spectrometer, and a research fellowship (to A.D.B.). We also thank the Science Research Council for the award of a research studentship (to N.R.K.).

Computerized Learning Machine Applied to Qualitative Analysis of Mixtures by Stationary Electrode Polarography

L. B. Sybrandt and S. P. Perone

Department of Chemistry, Purdue University, Lafayette, Ind. 47907

A computerized learning machine approach has been evaluated for qualitative analysis of mixtures by stationary electrode polarography. The limiting effects of concentration ratios, degree of peak overlap, and peak potential variation have been investigated. The results were evaluated not only from an overall statistical accuracy, but also the specific nature of errors made was investigated. This procedure allowed for the specification of optimum categorization criteria. Results indicate that resolution is limited by the precision of the experimental data and the concentration ratios. Ideally precise overlapping polarograms could be identifed with 2-mV peak separation over a 20-fold range of concentration ratios. For data obtained under ordinary experimental conditions, resolution was limited to peak separations of 35–40 mV for about a 10-fold range of concentration ratios. Peak identification could be performed reliably under conditions where peak overlap precluded visual resolution.

CHEMICAL MEASUREMENTS have often been plagued with the problem of overlapping signals from two or more species in a mixture. This overlap sometimes results in difficult qualitative analysis of the sample. Mass spectral analysis, ultracentrifuge schlieren pattern analysis, and kinetic analysis are examples where this problem may exist when one must deal with mixtures. These authors are particularly concerned with this problem in electroanalytical methods. The work presented here demonstrates the applicability of binary pattern classifiers to the qualitative analysis of mixtures by stationary electrode polarography.

Binary pattern classifiers have recently been used for molecular formula determinations from low resolution mass spectra (*1*, *2*). They have also been applied to the classification of infrared spectrometry data according to chemical class (*3*), and to the interpretation of combined mass spectra, infrared spectra, and melting and boiling points for the determination of certain chemical characteristics, such as double bond presence (*4*). Multicategory pattern classification by least squares has been used for molecular formula and molecular weight determination from mass spectra (*5*). In each of the above applications, the data patterns resulted from measurements on a pure chemical species. Wangen and Isenhour (*6*) have recently used a learning machine approach for semiquantitative analysis of mixed gamma-ray spectra. The work to be described here demonstrates a different learning machine approach to the qualitative analysis of mixtures. This approach included consideration of experimental deviations in real analytical data. Qualitative results were not evaluated solely on a statistical basis, but the nature of specific errors made was considered. Finally, attempts were made to optimize decision criteria by methods not previously reported.

The theory of learning machines can be found in texts by Nilsson (*7*) and Fu (*8*). The mathematical approach discussed below is essentially that of Jurs, Kowalski, Isenhour, and Reilley (*2*). A two-category patterns classifier can be defined by a discriminate function which is a scaler, single valued function of the pattern. If the patterns to be classified are assumed to be *linearly separable*, then the discriminate function takes the form

$$s = \sum_{i=1}^{d+1} w_i x_i \tag{1}$$

where x_i is the ith component of a pattern having d points, x_{d+1} equals one, w_i is the weight corresponding to the ith component, and s is the scaler result. The category in which a given pattern is placed is determined by the sign of s. The convention used here is

$$\begin{aligned} s > 0 &\text{ species present} \\ s < 0 &\text{ species absent.} \end{aligned} \tag{2}$$

The set of weights, $w_1, w_2, \ldots, w_{d+1}$, represents a $(d + 1)$-dimensional weight vector. This weight vector is determined by an error-correction procedure. The vector is initiallized arbitrarily to all ones. A set of representative patterns, the training set, is presented sequentially to the classifier. When a pattern is incorrectly categorized according to Equations 2, the weights of Equation 1 are immediately adjusted in a manner to correct that error. The adjusted weight, w_i', is defined as

$$w_i' = w_i + cx_i \tag{3}$$

for $i = 1, 2, \ldots, d + 1$, where c is the correction increment. The correction increment is determined such that the new scaler will equal the original scaler in magnitude, but have the opposite sign. Thus, c, as derived by Jurs *et al.*, (*2*) is simply

$$c = \frac{-2s}{\sum_{i=1}^{d+1} x_i^2} \tag{4}$$

If the training set is linearly separable, this procedure will converge to a single weight vector which can correctly classify all the patterns. Training is terminated when the vector is perfectly trained, or when a preset number of iterations through the training set is reached. The above training procedure is repeated for each desired component of the mixture. Thus, there is a weight vector corresponding to each species to be identified.

(1) P. C. Jurs, B. R. Kowalski, and T. L. Isenhour, ANAL. CHEM., **41**, 21 (1969).
(2) P. C. Jurs, B. R. Kowalski, T. L. Isenhour, and C. N. Reilley, *ibid.*, p 690.
(3) B. R. Kowalski, P. C. Jurs, T. L. Isenhour, and C. N. Reilley, *ibid.*, p 1945.
(4) P. C. Jurs, B. R. Kowalski, T. L. Isenhour, and C. N. Reilley, *ibid.*, p 1949.
(5) B. R. Kowalski, P. C. Jurs, T. L. Isenhour, and C. N. Reilley, *ibid.*, p 695.
(6) L. E. Wangen and T. L. Isenhour, *ibid.*, **42**, 737 (1970).
(7) N. J. Nilsson, "Learning Machines," McGraw-Hill Book Co., New York, N. Y., 1965.
(8) K. S. Fu, "Sequential Methods in Pattern Recognition and Machine Learning," Academic Press, New York, N. Y., 1968.

A large number of patterns are usually required to train the weight vectors. For many analytical techniques, it is impractical to make measurements on actual mixtures to obtain this large training set. It is therefore necessary to have a means by which synthetic mixtures can be generated. For stationary electrode polarography (SEP), the current contributed by each species is usually additive over the whole curve in a mixture. This relationship is valid for mixtures of Cd(II), In(III), and Sb(III) (*9*). Here, a set of standard curves for single-component solutions was obtained experimentally at one concentration. These standards were multiplied by random numbers to represent concentration variations and then summed to generate synthetic mixtures for training.

EXPERIMENTAL

Digitized stationary electrode polarograms were obtained for single-component solutions of Cd(II), In(III), and Sb(III), each at $5 \times 10^{-5}M$ in $1.0M$ HCl. The computer-controlled dual-cell apparatus is described elsewhere (*9*). The potential sweep was from -0.100 V to -0.800 V *vs.* SCE. A sweep rate of 1.00 V/sec was used. Data were digitized at 2-mV intervals. Data were obtained under conditions approximating as closely as possible those under which routine electroanalytical data would be obtained. That is, procedures were careful, but not rigorous. Cell temperatures were ambient; instrument recalibration was not carried out before each run; solutions were not deaerated between each run; etc.

All chemicals used were reagent grade. The distilled water was further purified by passage through a mixed bed cation–anion exchange resin. Three separate presumably identical solutions were prepared for each species. Each sample solution was placed in the cell, deaerated with high purity nitrogen, and 4 runs were obtained, with an ensemble average of 8 voltage scans per run. The averaged data for each sample were punched on paper tape for later use. These 36 polarograms are termed the standard curves.

All learning machine experiments to be discussed were performed on a Hewlett-Packard 2116A 16-bit digital computer with an 8K-word core memory. Peripheral devices included an ASR/35 teletype, high speed paper tape punch, high speed photoreader, Calcomp plotter, and a Hewlett-Packard Model 2020 magnetic tape unit. The external, rapid-access magnetic tape storage device was required because of the limited core memory size, since a large amount of data must be processed to train the weight vectors. All programs were written in Hewlett-Packard FORTRAN or BASIC. (These programs are available from the authors upon request.)

LEARNING MACHINE PROCEDURE

Three separate programs were used to implement the pattern classifier. The first program constructed synthetic mixtures from the standard SEP curves. The standard curves were loaded into core memory *via* the high speed photoreader. A set of random numbers, previously generated on paper tape, was then loaded *via* the reader in groups of three, each corresponding to a component in the synthetic mixture. The mixture was calculated and stored on magnetic tape, followed by the random numbers representing the concentrations in that mixture. Additional synthetic mixtures were generated with subsequent groups of random numbers until the desired number of mixtures was obtained for the training set, usually 200. A training program was then used to calculate weight vectors for qualitative analysis using the training set data stored on magnetic tape. These vectors were trained sequentially because of core limitations. Each trained weight vector was punched on paper tape before proceeding with the next vector. A third program utilized the trained weight vectors for recognition and prediction. For this work, *recognition* will designate the qualitative analysis of mixtures generated by the same standard curves as used in training, and *prediction* will refer to the qualitative analysis of synthetic mixtures which are generated from other standard curves.

Table I. Distribution of Random Numbers Representing Concentrations for the Generation of 200 SEP Patterns of Cd(II), In(III), and Sb(III) in the 0.1 to 2.0 Concentration Range

	Training set			Prediction set		
Concentration	Cd	In	Sb	Cd	In	Sb
0.000–0.000	31	33	31	36	27	32
0.100–0.199	10	8	8	10	11	9
0.200–0.299	8	10	13	8	5	15
0.300–0.399	11	10	5	8	3	5
0.400–0.499	12	18	19	11	11	11
0.400–1.599	102	80	98	97	110	95
1.600–1.699	2	8	11	4	12	9
1.700–1.799	4	12	9	8	6	4
1.800–1.899	9	13	10	10	9	12
1.900–2.000	11	8	6	8	6	8

RESULTS AND DISCUSSION

The random numbers used to calculate concentrations were varied from 0 to 2.0, with all numbers less than 0.1 set to 0. Since the standard polarograms were obtained at $5 \times 10^{-5}M$, this represents a concentration range of $5 \times 10^{-6}M$ to $1 \times 10^{-4}M$. A zero concentration is an important consideration for training, so the random number generator was further biased to provide an additional 10% probability of this occurrence. Thus, the total probability of a zero concentration for a given component is about 15%. The random number distributions for the training and prediction sets of 200 synthetic mixtures each are shown in Table I. Weight vectors trained on this concentration range are applicable to any other 20-fold range, provided a conversion factor is applied to the sufficiently precise data. For the sake of simplicity, concentrations will be referred to by the random numbers used to generate the synthetic mixtures.

Peak locations for the 36 standard polarograms are shown in Table II. Because of the manner in which these curves were obtained, the peak locations varied considerably more between samples than between runs of a sample. Maximum peak height variations were about 3, 4, and 5%, respectively, for Cd(II), In(III), and Sb(III). A mixture of Cd(II), In(III), and Sb(III) results in a polarogram with a well-resolved Sb(III) peak, and considerable overlap of the Cd(II) and In(III) signals. A typical stationary electrode polarogram for an approximately equimolar mixture of Cd(II), In(III), and Sb(III) is shown in Figure 1. This figure demonstrates the reasons for selecting this particular system for study here. The well-separated Sb peak provides a relatively uncomplicated identification problem, whereas the In–Cd peaks overlap so strongly as to create a very challenging analysis problem.

Weight vectors can be perfectly trained at the 0.1–2.0 concentration range if the data fluctuation is kept to a minimum. A set of 100 mixtures randomly generated from a single run for each component was correctly dichotomized

(9) W. F. Gutknecht and S. P. Perone, ANAL. CHEM., 42, 906 (1970).

Table II. Peak Locations of Standard SEP Curves of Cd(II), In(III), and Sb(III) *vs.* SCE

Sample No.	Species	Run No. 1	No. 2	No. 3	No. 4	Relative location[a]
1	Cd	−628 mV	−628	−628	−626	H
2	Cd	−622	−620	−620	−620	L
3	Cd	−624	−624	−624	−624	M
1	In	−588	−588	−588	−588	H
2	In	−582	−582	−580	−580	M
3	In	−580	−580	−580	−580	L
1	Sb	−154	−154	−154	−154	L
2	Sb	−156	−160	−160	−160	H
3	Sb	−156	−156	−156	−156	M

[a] H = High, M = Middle, L = Low.

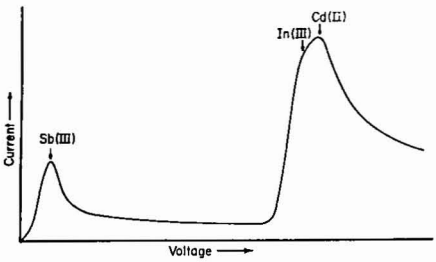

Figure 1. Stationary electrode polarogram of Sb(III), In(III), and Cd(II) in 1.0*M* HCl

after 12 iterations for Sb(III), and 5 iterations each for Cd(II) and In(III). Perfect training also resulted with training sets comprised of all 4 runs of a given sample for each component. In these cases, the training sets consisted of 200 mixtures, 50 mixtures each of runs No. 1–4. Training was no more difficult than when a single run of each species was used, even though these sets incorporated the data fluctuation between runs. In all training situations above, recognition was perfect when the same data and different random numbers were used to generate the synthetic mixtures. However, prediction was often very poor using data other than those used in training. For example, percentage error in prediction was 15.0% for Cd, 5.0% for In, and 3.5% for Sb when trained on all 4 runs of a given sample. More critically, however, Cd(II), In(III), and Sb(III) were incorrectly classified in 100, 30, and 22%, respectively, of the mixtures where these species were absent, ($C = 0$).

Independent Effects of Peak Overlap and Uncertainty in Peak Location. A combination of peak overlap and data fluctuation adversely affects training, but either condition alone does not. A single Sb(III) run was artificially shifted 1 data point cathodic and called a new species, *X*. As a mixture, this represents two identically shaped peaks separated by only 2 mV. The concentrations of Sb(III) and *X* were randomly varied as before. It was possible to qualitatively identify either component in 100 binary mixtures after 4 iterations per weight vector. Conversely, the peak location of Sb in an Sb, In, Cd mixture has been allowed to vary as much as 8 mV, using 8 different runs in the training set. The Sb weight vector trained to perfection for mixtures in the 0.1–2.0 concentration range, regardless of the training difficulty observed for Cd(II) and In(III).

Generation of a Representative Training Set. The training set should contain patterns which are representative of the patterns which might occur in a prediction set. For the electrochemical data considered here, variations in peak locations must be represented in the training set. If signal variations are primarily instrumental in nature, a peak shift of a given magnitude and direction for one species will correspond to an equivalent shift for all other species in that mixture. By generating synthetic mixtures with constant relative peak locations, training is simplified since overlapping peaks will be no closer for a given mixture than would be observed experimentally.

Table III. Results of Training Weight Vectors to Qualitatively Determine Cd(II), In(III), and Sb(III) in the 0.1–2.0 Concentration Range. Training Set = 200 Patterns

	Species	Iteration	Error corrections
	Cd	25	4
	In	25	5
	Sb	9	0
Training set:	Cd	Samples No. 1, 2, Runs 1–4.	
	In	Samples No. 1, 3, Runs 1–4.	
	Sb	Samples No. 1, 2, Runs 1–4.	

To achieve a more representative training set from the polarograms shown in Table II, the samples representing maximum (High) and minimum (Low) peak locations were chosen. However, consistent with the preceding discussion, each mixture was generated with either all high or all low curves for each component, using the random numbers of Table I. All runs of these samples were included in the training set. The results of training three weight vectors to qualitatively determine Cd(II), In(III), and Sb(III) in ternary mixtures are shown in Table III. The right-most column represents the number of weight vector corrections necessary during the iteration designated. Only the Sb weight vector trained perfectly.

A different weight vector was obtained after each error correction. These vectors differed in their ability to perform qualitative analysis. The four Cd and five In weight vectors obtained in the training process summarized by Table III are identified by the letters A thru E. Table IV depicts the different recognition abilities of these vectors. Analysis is based on the sign of *s*, as expressed in Equations 2. The Cd weight vectors, C and D, and the In weight vectors, *A*, *B*, and *C*, incorrectly classified a large percentage of mixtures where these species were *absent* ($C = 0$), and are not very useful for qualitative analysis. However, the Cd weight vectors, *A* and *B*, and In weight vectors, *D* and *E*, usually determine the absence of a component, and have a high probability of identifying the component when it is present. It is significant that the errors occur only at the lower limits of concentration, and only when the interfering peak is

Table IV. Recognition Ability of Weight Vectors Obtained after Each Error Correction of Table III for Cd, In, and Sb

Weight vector symbol	Total errors	Error, %	C = 0 errors/ total C = 0	C > 0 errors: Concn range	C > 0 errors: Min/max Cd:In ratio
			a. Cd		
A	7	3.5	0/31	0.12–0.44	0.10/0.22
B	5	2.5	0/31	0.12–0.27	0.10/0.17
C	19	9.5	19/31	...	...
D	12	6.0	12/31	...	...
			b. In		
A	24	12.0	24/33	...	...
B	10	5.0	10/33	...	...
C	7	3.5	7/33	...	...
D	5	2.5	2/33	0.15–0.26	6.18/9.22
E	5	2.5	0/33	0.15–0.26	4.66/9.24
			c. Sb		
...	0	0	0/31	...	...

Table V. Prediction Ability of Best Weight Vectors of Table IV

Total errors	Error, %	C = 0 errors/ total C = 0	C > 0 errors: Concn range	C > 0 errors: Min/max Cd:In ratio
		a. Cd-weight vector *B*		
8	4.0	0/36	0.10–0.31	0.06/0.25
		b. In-weight vector *D*		
1	0.5	0/27	0.13–0.13	9.85/9.85
		In-weight vector *E*		
4	2.0	0/27	0.11–0.18	2.99/9.85
		c. Sb–Perfectly trained weight vector		
0	0	0/32	...	...

present at a 5:1 or larger concentration ratio. The Cd weight vector *B* correctly classified 4 mixtures which had Cd:In ratios between 0.10 and 0.16. In was correctly identified by In weight vector *D* in 5 mixtures with Cd:In ratios between 6.6 and 13.6. The Sb weight vector correctly classified all mixtures in the training set.

The prediction ability of these weight vectors is shown in Table V. This prediction set was formed from Cd sample No. 3, In sample No. 2, and Sb sample No. 3, runs No. 1–4, using the concentration distribution shown in Table I. These samples have peaks at different locations than those used in training. The Cd weight vector *B* could not identify Cd in 8 of the 14 patterns which had Cd:In ratios of 0.25 or smaller. The In weight vector *D* erred once, on a mixture with a 9.85 Cd:In ratio. The Sb weight vector correctly predicted all 200 patterns.

Comparison of Recognition and Prediction Capability Using Fixed Set of Concentration Ratios. The results presented in Tables IV and V depend significantly on the number of difficult mixtures which must be classified, and this will vary for different random number sets. A valid comparison of the recognition and prediction ability for various weight vectors can be made if the same set of concentrations, all known, is used for both cases. Here, training sets and prediction sets would be generated from different groups of standard curves, but identical sets of concentration ratios would be used. To achieve this end, a set of known mixtures was generated which have concentration ratios of varying degrees of difficulty. The complete set of mixtures is shown in Table VI for the 0.1–2.0 concentration range. This set was used for further work reported here.

A recognition set of curves was generated from the compositions of Table VI and the same standard curves used in training the weight vectors evaluated in Tables III and IV. The best weight vectors in Table IV were then used to classify this recognition set. The results showed that Cd can be correctly identified at a 1:10 or 1:4 Cd:In ratio, depending on the sample tested. Likewise, In presence was recognized at a 4:1 or 10:1 Cd:In ratio. All mixtures in which Cd or In were absent were correctly categorized. Sb classification errors involved only zero or 0.1 concentration levels and the per cent error was 1.1% averaged over all samples.

The prediction ability of the weight vectors was evaluated using the set of compositions given in Table VI and the standard curves used for Table V. The results were comparable to those for the recognition set. Cd could be identified correctly at a 1:4 Cd:In ratio, and In was identified correctly at a Cd:In ratio of 7:1 or 5:1, depending on the particular standard curve used to synthesize the mixture. No errors in classifying Sb were observed.

Effects of Modifying Criterion for Classification. The weight vectors of Table IV which were considered acceptable classifiers were those giving the fewest C = 0 classification errors, based on the sign of s as shown in Equations 2. Only two of the four possible Cd weight vectors were acceptable on this basis. However, the remaining weight vectors may become better classifiers if the decision is based on an s value greater or less than some positive number, s', rather than the sign of s alone. The number s' is set slightly larger than the largest value of s which occurs when a weight vector makes C = 0 classification errors in the training set. The two-category classification is then

Table VI. Concentrations of Cd, In, and Sb for Mixtures[a] Used to Test Weight Vectors

Mix No.	Species	Concn	Mix No.	Concn	Mix No.	Concn	Mix No.	Concn	Mix No.	Concn	Mix No.	Concn
1	Cd	0.0	18	0.4	35	1.0	52	1.0	69	2.0	86	1.0
	In	0.0		1.0		0.5		0.5		2.0		1.0
	Sb	0.0		1.0		0.5		1.0		0.2		0.8
2	Cd	2.0	19	0.5	36	2.0	53	1.0	70	2.0	87	1.0
	In	2.0		1.0		0.0		0.6		2.0		1.0
	Sb	2.0		1.0		2.0		1.0		0.3		0.9
3	Cd	0.0	20	0.6	37	2.0	54	1.0	71	2.0	88	1.0
	In	2.0		1.0		0.1		0.7		2.0		1.0
	Sb	2.0		1.0		2.0		1.0		0.4		1.0
4	Cd	0.1	21	0.7	38	2.0	55	1.0	72	2.0	89	0.5
	In	2.0		1.0		0.2		0.8		2.0		0.5
	Sb	2.0		1.0		2.0		1.0		0.5		0.0
5	Cd	0.2	22	0.8	39	2.0	56	1.0	73	2.0	90	0.4
	In	2.0		1.0		0.3		0.9		2.0		0.4
	Sb	2.0		1.0		2.0		1.0		0.6		0.0
6	Cd	0.3	23	0.9	40	2.0	57	1.0	74	2.0	91	0.3
	In	2.0		1.0		0.4		1.0		2.0		0.3
	Sb	2.0		1.0		2.0		1.0		0.7		0.0
7	Cd	0.4	24	1.0	41	2.0	58	0.5	75	2.0	92	0.2
	In	2.0		1.0		0.5		0.0		2.0		0.2
	Sb	2.0		1.0		2.0		0.5		0.8		0.0
8	Cd	0.5	25	0.0	42	2.0	59	0.4	76	2.0	93	0.1
	In	2.0		0.5		0.6		0.0		2.0		0.1
	Sb	2.0		0.5		2.0		0.4		0.9		0.0
9	Cd	0.6	26	0.0	43	2.0	60	0.3	77	2.0	94	0.0
	In	2.0		0.4		0.7		0.0		2.0		2.0
	Sb	2.0		0.4		2.0		0.3		1.0		0.0
10	Cd	0.7	27	0.0	44	2.0	61	0.2	78	1.0	95	0.0
	In	2.0		0.3		0.8		0.0		1.0		1.0
	Sb	2.0		0.3		2.0		0.2		0.0		0.0
11	Cd	0.8	28	0.0	45	2.0	62	0.1	79	1.0	96	1.0
	In	2.0		0.2		0.9		0.0		1.0		1.0
	Sb	2.0		0.2		2.0		0.1		0.1		2.0
12	Cd	0.9	29	0.0	46	2.0	63	2.0	80	1.0	97	0.5
	In	2.0		0.1		1.0		0.0		1.0		0.5
	Sb	2.0		0.1		2.0		0.0		0.2		1.0
13	Cn	1.0	30	0.0	47	1.0	64	1.0	81	1.0		
	In	2.0		0.0		0.0		0.0		1.0		
	Sb	2.0		2.0		1.0		0.0		0.3		
14	Cd	0.0	31	0.0	48	1.0	65	1.0	82	1.0		
	In	1.0		2.0		0.1		2.0		1.0		
	Sb	1.0		0.0		1.0		1.0		0.4		
15	Cd	0.1	32	0.0	49	1.0	66	0.5	83	1.0		
	In	1.0		1.0		0.2		1.0		1.0		
	Sb	1.0		0.0		1.0		0.5		0.5		
16	Cd	0.2	33	0.0	50	1.0	67	2.0	84	1.0		
	In	1.0		0.0		0.3		2.0		1.0		
	Sb	1.0		1.0		1.0		0.0		0.6		
17	Cd	0.3	34	2.0	51	1.0	68	2.0	85	1.0		
	In	1.0		1.0		0.4		2.0		1.0		
	Sb	1.0		1.0		1.0		0.1		0.7		

[a] Mix 24 = Mix 57 = Mix 88; Mix 31 = Mix 94; Mix 32 = Mix 95.

$$s - s' > 0 \text{ species present}$$
$$s - s' < 0 \text{ species absent} \qquad (5)$$

Tables VII and VIII describe the ability of the weight vectors to classify the mixtures of Table VI using data of the training set and prediction set, respectively. Classification is based on the scheme shown in Equations 5. Qualitative analysis of the training set data is not so good as that based on Equations 2, and the weight vectors of Table V. The Cd weight vectors incorrectly classify C = 0 conditions where In is present at a 2.0 concentration. They also erred on mixtures 62 and 93, where In is not present or present in a minimal amount. Two of the In weight vectors gave similar results.

Classification of the prediction set, Table VIII, gave better results than in Table VII. Moreover, the results were better than when using Equations 2 and the weight vectors of Table V. The Cd weight vectors again missed mixtures 62 and 93, but could classify correctly for Cd:In ratios of about 1:7 or larger. The In weight vectors B and C incorrectly categorized only 2 or 3 mixtures in the 10:1 to 20:1 Cd:In ratio range. No incorrect C = 0 decisions were made.

By classifying patterns according to Equations 5, one can

Table VII. Ability of Weight Vectors to Qualitatively Classify the Mixtures of Table VI Using the Data of the Training Set. Decisions Based on Equations 5

Mixtures Incorrectly Classified			
Set 1[a]	Set 2	Set 3	Set 4
a. Cd—weight vector C, $s' = 4200$			
3	3	4–5	3
31	62	15	15
62	93	62	62
93–94		93	93
Cd—weight vector D, $s' = 3680$			
3	3	4–5	4
31	31	15	15
62	62	62	62
94	94	93	93
b. In—weight vector A, $s' = 5476$			
29	29	29	29
37–38	37–38	93	36
48–49	48–49		93
93	93		
In—weight vector B, $s' = 3910$			
29	29	None	36
37–39	37–39		63
48–49	48–49		
93	93		
In—weight vector C, $s' = 3622$			
37–39	37–39	None	63
48–49	48–49		
93	93		

[a] Sets 1 and 2 corresponded to standard curves from Runs 1 and 2 of Cd, In, Sb Samples 1 (Table II). Sets 3 and 4 correspond to standard curves from Runs 1 and 2 from Cd and Sb Samples 2 and In Sample 3 (Table II).

Table VIII. Ability of Weight Vectors to Qualitatively Classify the Mixtures of Table VI Using Data of the Prediction Set. Decisions Based on Equations 5

Mixtures Incorrectly Classified			
Set 1[a]	Set 2	Set 3	Set 4
a. Cd—weight vector C, $s' = 4200$			
4–5	4	4	4
15	15	15	15
62	62	62	62
93	93	93	93
Cd—weight vector D, $s' = 3680$			
4–5	4	4	4
15	15	15	15
62	62	62	62
93	93	93	93
b. In—weight vector A, $s' = 5476$			
29	29	29	29
37–38	37	37	37
48	48	48	48
93	93	93	93
In—weight vector B, $s' = 3910$			
37–38	37	37	37
48	48	48	48
In—weight vector C, $s' = 3622$			
37–38	37	37	37
48	48	48	48

[a] Sets 1 to 4 correspond to standard curves from Runs 1 to 4 of Cd and Sb Samples 3 and In Sample 2 (Table II).

Table IX. Qualitative Classification Ability of Cd Weight Vectors Based on Equations 5. s' Chosen to Give Only One C = 0 Error in Training Set

Mixtures Incorrectly Classified			
a. Training set data[a]			
Set 1	Set 2	Set 3	Set 4
Cd—weight vector C, $s' = 1724$			
3	3	4	4
14	14		
31–32	31–32		
94–95	94–95		
Cd—weight vector D, $s' = 1594$			
3	3	4	4
14	14	15	
31–32	31–32		
94–95	94–95		
b. Prediction set data[b]			
Set 1	Set 2	Set 3	Set 4
Cd—weight vector C, $s' = 1724$			
4	4	None	None
15	Cd—weight vector D, $s' = 1594$		
4–5	4	None	4
15			

[a] Sets 1 thru 4 correspond to those for Table VII.
[b] Sets 1 thru 4 correspond to those for Table VIII.

choose the type of results obtained by an appropriate choice of s'. A large s' will classify C = 0 conditions correctly, while incorrectly classifying smaller peak ratios. A smaller s' will classify larger peak ratios correctly, but miss more C = 0 conditions. Thus, a compromise might be considered. Table IX shows the results of lowering s' from 4200 to 1724 for the Cd weight vector C, and from 3680 and 1594 for the Cd weight vector D. Both of these lower s' values were selected to allow only one C = 0 error on the randomly generated training set. Table IX refers to mixtures generated with the concentrations listed in Table VI. Comparing Table IX, part *a*, with Table VII, part *a*, it is observed that mixtures 62 and 93 are now correctly classified at the 0.1 concentration level for sets No. 1 and No. 2, whereas mixtures 14 and 32 are now incorrect. Overall, there are a considerable number of C = 0 errors for sets No. 1 and No. 2. However, sets No. 3 and No. 4 are classified very well by using the compromise s', as Cd weight vector C only missed the 1:20 Cd:In ratio. The prediction data, Table IX, part *b*, shows a marked improvement in qualitative analysis by using the compromise s' as opposed to the maximum s' (Table VIII) or minimum ($s' = 0$). Cd can be identified at about 1:10 Cd:In ratios in the prediction set. Cd weight vector C correctly classified all mixtures of Table VI for sets No. 3 and No. 4 of the prediction set.

In summary, inspection of specific errors made shows that two samples resulted in good qualitative analysis. These were one of the two used in training and the sample used for prediction. Cd indentification was successful at about 1:10 Cd:In ratios. No C = 0 errors were made on these samples. In classification was correct at 10:1 Cd:In ratios, again with no C = 0 errors. Sb can be classified perfectly for these two samples. Sample No. 1 (sets No. 1 and No. 2, part *a*, Table IX) was more difficult to classify for all three species. Cd was considered present in mixtures where In was present at 1.0 or 2.0 concentration levels. In could only be detected at 5:1 Cd:In ratios or smaller. Sb was classified

Table X. Recognition Ability of Weight Vectors Obtained after Training Errors for Cd, *X*3, and Sb Mixtures. Decision Based on Equations 2. Not all Weight Vectors Listed

Weight vector symbol	Total errors	Error, %	C = 0 errors/ total C = 0	C > 0 errors: Concn range	C > 0 errors: Min/max Cd:*X*3 ratio
			a. Cd		
A	9	4.5	1/31	0.10–0.45	0.10/0.22[a]
B	9	4.5	0/31	0.10–0.45	0.10/0.22
C	5	2.5	1/31	0.12–0.25	0.10/0.14
D	7	3.5	0/31	0.12–0.45	0.10/0.22
			b. *X*3		
A	32	16.0	0/33	0.11–1.30	1.10/13.6
B	14	7.0	3/33[b]	0.11–0.50	3.14/12.2
C	11	5.5	0/33	0.11–0.50	3.50/12.2
D	16	8.0	2/33	0.11–0.50	1.10/12.2
E	16	8.0	0/33	0.11–0.50	1.10/12.2
			c. Sb		
...	0	0	0/31	...	...

[a] One *X*3 concentration was 0.
[b] All missed when [Cd] = 0 and [Sb] > 1.2.

as absent in 20:20:1 Cd:In:Sb mixture, and incorrectly identified when Cd was present at a 1.0 or 2.0 concentration and In was also absent.

Effect of Increased Peak Overlap. The effect of increased peak overlap on training was investigated. Weight vectors were trained to qualitatively determine Cd(II), *X*3, and Sb(III), where the species *X*3 represents In(III) data moved 10 mV (5 data points) cathodic toward the Cd peak. The training set was otherwise identical to that of Table III. After 25 iterations, there remained 12 errors for the Cd weight vector and 13 errors for the *X*3 weight vector. The Sb weight vector was perfectly trained in 7 iterations. Table X describes the recognition ability of certain Cd and *X*3 weight vectors obtained after error corrections during the training. Comparing those results with those of Table IX, it is observed that Cd can be identified nearly as well when the peaks are separated by 30 mV as it can when the peaks are at their normal separation of 40 mV. However, when the Cd:*X*3 ratio is greater than about 3.5:1, *X*3 is incorrectly classified in the best case. This does not compare favorably to the minimum 4.7:1 Cd:In ratio at normal peak separation.

CONCLUSIONS

The work described here obviously represents only the first steps toward providing computerized interpretation of electroanalytical data by pattern recognition. The unique problems afforded by normal fluctuation of electroanalytical data and severe peak overlap have been considered. Consideration of the specific nature of classification errors made has allowed the optimization of categorization criteria. Qualitative analysis of severely overlapped peaks by the learning machine approach is about as good as second-derivative measurements in stationary electrode polarography (*9*). Both methods are successful to about 10:1 peak ratios for a separation of around 40 mV. However, it is encouraging to note that as one allows no experimental deviation in reduction peaks, the qualitative resolution afforded by the pattern recognition approach here was 2 mV. Further investigation of this fact seems worthwhile, as does the extension to other electroanalytical techniques, such as second-derivative SEP. In addition, the quantitative evaluation of electroanalytical data by learning machine methods should be investigated.

ACKNOWLEDGMENT

The authors thank W. F. Gutknecht for the electrochemical data used in this study.

RECEIVED for review August 24, 1970. Accepted November 13, 1970. L. B. Sybrandt received Fellowships granted by Hercules, Inc., and the Analytical Division of the American Chemical Society. This work also supported by the National Science Foundation, Grant No. GP-21111.

Determination of Hydrogen Sulfide, Sulfur Dioxide, Carbonyl Sulfide, Carbon Disulfide, and Carbon Dioxide in a Gas Mixture

Arthur Schwartz

Development Center, Chemical Construction Corporation (CHEMICO), New Brunswick, N. J. 08903

The objective of the work undertaken was to determine hydrogen sulfide in the presence of other sulfur gases which usually interfered. A cupric sulfate solution quantitatively removes hydrogen sulfide as a cupric sulfide precipitate, while another cupric sulfate solution in the presence of chloride ions oxidizes sulfur dioxide to sulfur trioxide. These gases are then determined by applying simultaneous equations to reactions involving the increase of acid and the loss of copper. Carbonyl sulfide and carbon dioxide, which are acidic gases, and carbon disulfide, which is not soluble in water solutions, are not absorbed in the aqueous acidic copper solutions. Simultaneous equations are applied to results obtained by an iodination and by a bromination to determine these sulfur gases, while a standard acid–base analysis determines carbon dioxide. An accuracy of better than 3% and a precision of 0.5% is possible for the determination of hydrogen sulfide and sulfur dioxide.

THIS WORK was originally begun after studying anomalous results obtained by a standard procedure for the determination of hydrogen sulfide in the presence of sulfur dioxide using aqueous ammoniacal cadmium chloride solutions as the absorbent (*1*). Although carbonyl sulfide is not very soluble in aqueous solutions, and carbon disulfide even less so, sufficient quantities remain in the high concentration of ammonia and react with cadmium chloride to precipitate as cadmium sulfide, thus falsely indicating a high concentration of hydrogen sulfide.

Although a method has been described for the determination of these gases by gas chromatography, (*2*), water interferes with the determination of H_2S. In addition, in order to separate COS from SO_2, the required flowrate and temperature were such that it took more than an hour before the CS_2 peak was observed, making it impractical to take samples from several points within a short period of time.

EXPERIMENTAL

Scope. The normal amount of copper sulfate recommended in the procedure, 50 ml of 0.5*N*, should oxidize a maximum of 50 cc of sulfur dioxide at standard temperature and pressure within a reasonably short time of gas–liquid contact. Either the volume of inert gas taken must be adjusted to contain this maximum of sulfur dioxide, or the volume of 0.5*N* copper sulfate must be increased for larger amounts of SO_2.

The capacity of copper sulfate for hydrogen sulfide removal is greater than that for sulfur dioxide—about 100 cc per 50 ml of 0.5*N* $CuSO_4$. The amount of copper sulfate and/or the volume of inert gases taken must be adjusted accordingly for any combination of these two gases.

Apparatus used consisted of a wet-test meter or water displacement gas-measuring apparatus (similar to Reich test apparatus); a nitrogen cylinder; 12.5-cm Whatman No. 541 filter paper; 24-cm Whatman No. 2 filter paper; a 80 mm long stem funnel; a 150-mm powder funnel; 3 Fleming gas purifier jars with tapered internal inlets, each 150 mm high; a 500-ml plastic storage bottle with rubber stopper through which a glass tube is inserted for making dropwise additions of 40% NaOH; and a 2-inch length of Kel-F tubing for making connection to a hot sample line.

Reagents. 0.5*N* COPPER SULFATE. Weigh 250 g of reagent grade, fine crystal cupric sulfate·5 H_2O (mol wt 249.686) into a clean, dry, tared 3-liter beaker; add 1600 ml of water while stirring the mixture. Quantitatively transfer the clear solution to a 2-liter volumetric flask and add distilled water to the mark. After thoroughly mixing the solution, filter it through a 24-cm Whatman No. 2 filter paper supported by a large powder funnel resting on a 2-liter Erlenmeyer flask. Stopper the flask and label it: "0.5*N* Copper Sulfate for SO_2 Reduction."

To obtain 25% sodium chloride, 25% potassium bromide, 25% potassium iodide, and 25% barium chloride, dissolve 250 g of each salt, respectively, in water, and dilute each to 1 liter in a graduate.

2.5% SODIUM CHLORIDE. Fifty ml of 25% sodium chloride plus 450 ml of distilled water was stored in a plastic wash bottle.

40% SODIUM HYDROXIDE. Use standard aqueous solution on a weight to weight basis.

0.05*N* HYDROCHLORIC ACID. Dilute 100 ml of 0.5*N* hydrochloric acid to 1 liter with water.

ACID INDICATOR "A" was prepared by using 0.1 gram 4-(4-dimethylamino-1-napthylazo)-3-methoxybenzenesulfonic acid (E.K. No. 1954) in 100 ml of water. Add 0.1*N* sodium hydroxide dropwise, until a solution results. (A small amount of precipitate is acceptable.) Store in a brown bottle.

BROMATE INDICATOR "B." One-tenth gram of 4-(*p*-ethoxyphenylazo)-*m*-phenylene-diamine monohydrochloride (E.K. No. 5314) in 100 ml of water. Store in a brown bottle.

CARBONATE INDICATOR "C." Dissolve 0.06 gram of bromcresol green and 0.04 gram of methyl red in 100 ml of ethanol. Store in a brown bottle.

ALCOHOLIC POTASSIUM HYDROXIDE SOLUTION. Weigh 100 grams of potassium hydroxide pellets into a dry 1-liter beaker. Add 950 ml of absolute ethanol. Stir the mixture by magnetic agitation, using a large Teflon-coated spin bar. Occasionally a glass rod may be required to stir KOH pellets that have accumulated near the walls of the beaker. When the bulk of the pellets is in solution (potassium carbonate remains as a residue), filter the mixture through a piece of glass wool in a large, plastic powder funnel supported by a 1-liter Erlenmeyer flask. Add 50 ml of distilled water directly to the flask, and stir the solution. Stopper the flask loosely with a rubber stopper; when the solution has cooled, stopper the flask tightly and store it in a refrigerator when not in use.

Procedure. A. SAMPLING. Three Fleming gas purifier jars were filled as follows: Jar 1—as indicated in Table I; Jar 2–25 ml of 0.5*N* copper sulfate, 40 ml of 25% sodium chloride; Jar 3–75 ml of alcoholic potassium hydroxide. They were connected in order, directly to the sample source

(1) V. J. Altieri, "Gas Analysis and Testing of Gaseous Materials," The American Gas Association, Inc., 420 Lexington Avenue, New York, N. Y., 1945, p 346.

(2) H. M. McNair and E. J. Bonelli, "Basic Gas Chromatography," *Varian Aerograph*, Varian Associates, Palo Alto, Calif., March 1969, p 64.

Table I. Composition of First Jar

Estimated % H_2S	0.5*N* $CuSO_4$	25% NaCl	H_2O
<0.5	25 ml	25 ml	15 ml
0.5 to 10	25	10	30
>10	50	10	0

Table II. Volume of Inert Gas Sample

Estimated concentration[a]		Optimum volume, inerts (uncorrected),
% H_2S	% SO_2	cc
5	<5	800
10	5	400
20	10	200
30	15	150
...	20	100

[a] For a mixture of the two gases, add half the estimated % H_2S to the estimated % SO_2 and use this figure as "total SO_2."

via a 2-inch length of Kel-F tubing, or separated from the source by a 14-inch length of glass tubing if the source was over 800 °C. The volume of gas taken was monitored by a wet-test meter attached to Jar No. 3. The flowrate was adjusted to 25 to 40 cc per minute, and the volume of nonreactive or inert gas was taken as indicated in Table II. The temperature of the gas, the water-vapor pressure at that temperature, and the barometric pressure were recorded, and the jars purged with nitrogen for 1 to 2 minutes.

The contents of Jar No. 1 were filtered through a Whatman No. 541 filter, into a 500-ml volumetric flask, and the jar and residue were rinsed by a 2.5% sodium chloride solution. The solution of Jar No. 2 was added directly to the flask unless it was cloudy, in which case it was filtered also. The combined filtrate was then diluted to 500 ml with distilled water.

The contents of Jar No. 3 were diluted with distilled water and made up to 200 ml in a volumetric flask.

B. Analysis. Five drops of Indicator A were added to a 50-ml aliquot from the 500-ml volumetric flask, and the aliquot was titrated with 0.1*N* sodium hydroxide to a pale yellow color (disappearance of pink, or pH 4.2). If the end point had been passed accidentally, 1 ml of 0.1*N* sulfuric acid was added, after which the titration was continued with 0.1*N* sodium hydroxide. The volumes of acid and base were recorded.

After 10 ml of concentrated hydrochloric acid and 5 drops of Indicator B were added, 0.02*N* potassium bromate was added until one drop caused the solution to turn from purple to green. The solution was then neutralized with 40% sodium hydroxide until one drop of caustic caused a cloudy mixture, after which 0.5*N* hydrochloric acid was added until one drop cleared the mixture. After cooling the solution in a running water bath for 5 minutes, 25 ml of 25% potassium iodide was added; after 1 minute, 100 ml of distilled water was added and the mixture titrated with 0.1*N* sodium thiosulfate to a starch end point, and the volume of thiosulfate used was recorded.

To a 50-ml aliquot from the 200-ml flask, 20 ml of 25% potassium bromide, 25.0 ml of 0.1*N* potassium bromate, and 20 ml of concentrated hydrochloric acid were added. After a few seconds, 15 ml of 25% potassium iodide was added, the solution was titrated with 0.1*N* sodium thiosulfate to a starch end point, and the volume of thiosulfate used was recorded for this "Bromination" titration.

To another 50-ml aliquot from the 200-ml volumetric flask, 20 ml of 25% potassium iodide, 25.0 ml of 0.1*N* potassium bromate, and 20 ml of concentrated hydrochloric acid were added. After 30 seconds, the mixture was titrated with 0.1*N* sodium thiosulfate to a starch end point, and the volume of thiosulfate used was recorded for this "Iodination" titration.

To a 10-ml aliquot from the 200-ml flask, 40 ml of a 25% barium chloride solution, 50 ml of distilled water, and 3 drops of phenolphthalein indicator were added. Half-normal hydrochloric acid was added to a 1-drop clear point followed by the addition of 0.1*N* sodium hydroxide to a pink end point. The mixture was then carefully adjusted with 0.05*N* hydrochloric acid to a clear end point, and the buret re-zeroed. After 10 drops of Indicator "C" was added, 0.05*N* hydrochloric acid was added until the mixture was colorless, and the volume of acid used was recorded.

Three blanks were determined on 75 ml of alcoholic potassium hydroxide in a 200-ml volumetric flask in the same manner just described.

Standardization. 0.5*N* Copper Sulfate. The same technique was used to standardize the copper sulfate solution as was used in the analysis, except that Fleming jars were omitted, Indicator "A" was not added, and titration with 0.1*N* sodium hydroxide was not done. Sodium thiosulfate was used as the standard.

Calculations. The calculations were based on the reactions described under Results and Discussion; the volume of a mole of sulfur dioxide at standard temperature and pressure was taken as 21.9 liters, and the molar volumes of the other gases as 22.4 liters.

RESULTS AND DISCUSSION

Theory. The following reactions are pertinent to the analyses to be described:

$$Cu^{2+} + H_2S \rightarrow CuS\downarrow + 2H^+ \quad (1)$$

$$Cu^{2+} + {}^1/_2\,SO_2 + Cl^- + H_2O \rightarrow CuCl\ (\text{complex}) + {}^1/_2\,SO_4^{2-} + 2H^+ \quad (2)$$

$$Cu^{2+} + 2I^- \rightarrow {}^1/_2\,I_2 + CuI\downarrow \quad (3)$$

$${}^1/_6\,BrO_3^- + Cu^+ + H^+ \rightarrow {}^1/_6\,Br^- + Cu^{2+} + {}^1/_2\,H_2O \quad (4)$$

$${}^1/_6\,BrO_3^- + {}^1/_3\,COS + {}^7/_6\,H_2O \xrightarrow{Br^-+H^+} {}^1/_3\,CO_2 + {}^1/_3\,SO_4^{2-} + {}^1/_{12}\,Br_2 + {}^7/_3\,H^+ \quad (5)$$

$${}^1/_6\,BrO_3^- + {}^1/_{12}\,CS_2 + {}^1/_3\,H_2O \xrightarrow{Br^-+H^+} {}^1/_{12}\,CO_2 + {}^1/_6\,SO_4^{2-} + {}^1/_{12}\,Br_2 + {}^2/_3\,H^+ \quad (6)$$

$${}^1/_6\,BrO_3^- + 2\,COS + 9.5\,H_2O \xrightarrow{I^-+H^+} 2\,CO_2 + 2\,SO_4^{2-} + {}^1/_2\,Br_2 + 19\,H^+ \quad (7)$$

$${}^1/_6\,BrO_3^- + CS_2 + {}^3/_2\,H_2O \xrightarrow{I^-+H^+} CO_2 + 2\,S + {}^1/_6\,Br^- + 3\,H^+ \quad (8)$$

$${}^1/_6\,BrO_3^- + {}^5/_6\,Br^- + H^+ \rightarrow {}^1/_2\,Br_2 + {}^1/_2\,H_2O \quad (9)$$

$${}^1/_2\,Br_2 + I^- \rightarrow {}^1/_2\,I_2 + Br^- \quad (10)$$

Cupric sulfide is one of the most insoluble of metallic sulfides, being exceeded in insolubility only by the sulfides of silver and mercury. As seen in Reaction 1, one mole of cupric ions is required per mole of hydrogen sulfide, yielding one mole of cupric sulfide precipitate and two equivalents of acid.

In Reaction 2, one mole of cupric ions is required for each half mole of sulfur dioxide. Chloride ions are required to complex the resulting cuprous ions to inhibit them from reoxidizing to cupric ions (*3*). Two equivalents of acid are produced for each half mole of sulfur dioxide.

When iodide ions are added to a mixture of cupric sulfate and cuprous chloride, only the cupric ions will react as seen in Reaction 3. One mole of cupric ions yields one equivalent of iodine and one mole of cuprous iodide—a white precipitate.

(3) Therald Moeller, "Inorg. Chemistry," John Wiley & Sons, Inc., New York, N. Y., 1952, p 826.

In order to determine the hydrogen sulfide content, it is necessary to determine the total copper left after the cupric sulfide has been filtered off. Since iodide ions do not react with cuprous ions, it is necessary to oxidize cuprous to cupric ions as shown in Reaction 4. By subtracting the hydrogen sulfide content from the total acid produced, the sulfur dioxide content is determined.

One sixth mole of bromate ions will react with $^1/_3$ mole of carbonyl sulfide and with $^1/_{12}$ mole of carbon disulfide as seen in Reaction 5 and 6, respectively; however, as seen in Reaction 7, the same amount of bromate reacts with 2 moles of carbonyl sulfide, while in Reaction 8, with one mole of carbon disulfide. In Reactions 5, 6, and 7, the sulfur is oxidized to sulfate, while in Reaction 8, the sulfur is reduced to elemental sulfur.

Excess bromate is then determined as shown in Reaction 9 and 10, followed by a thiosulfate titration for the iodine produced.

The following reactions may clarify the formulas used to calculate cc of COS and of CS_2:

$$^1/_3\,COS + {}^1/_{12}\,CS_2 = \text{Bromination titration} = Br_2 \quad (11)$$

$$2\,COS + CS_2 = \text{Iodination titration} = I_2 \quad (12)$$

$$\frac{(12\,I_2 - Br_2)}{3} \times 22.4 = \text{cc } COS \quad (13)$$

$$\frac{(Br_2 - 6\,I_2)}{12} \times 22.4 = \text{cc } CS_2 \quad (14)$$

The concentration and quantity of copper sulfate and sodium chloride outlined in Table I was changed when a larger gas sample was desired, or when the concentration of SO_2 or H_2S fell outside the range indicated in the Table.

Chloride ions were not required for H_2S but were very essential for SO_2; therefore, with high concentrations of H_2S and low concentrations of SO_2, the salt was reduced as seen in Table I. Indeed, in the presence of chloride, too much H_2S, and therefore too much CuS, caused errors (high H_2S, low SO_2):

$$H_2S + CuCl_2 \rightarrow CuS + 2\,HCl \quad (15)$$

$$CuS + CuCl_2 \rightarrow Cu_2Cl_2 + S \quad (16)$$

These errors are shown in Table III.

Mixtures of H_2S and SO_2 for the experiments shown in Table III were not made up in one tank in order to prevent any reaction between the two gases; however, it was felt that the stepwise addition of H_2S, followed by SO_2 would not be significantly different analytically from passing a mixture of the two gases from a single sample point through the copper sulfate solution. The results shown in Table III are averages of two experiments each, with a maximum deviation of ± 0.03% from the averages.

After washing the precipitate carefully, it was found that occasionally solids passed through the filter paper. This was solved by washing the precipitate with a 2.5% sodium chloride solution which effectively removed all the H^+, Cu^+, and Cu^{2+} ions, but prevented any elemental sulfur present from peptizing, flowing through the filter paper, and causing errors as indicated by the following formulas:

$$S + 2\,HI \rightleftarrows H_2S + I_2 \quad (17)$$

$$H_2S + Cu^{2+} \rightarrow CuS\downarrow + 2\,H^+ \quad (18)$$

$$Cu^{2+} + 2\,I^- \rightarrow CuI\downarrow + {}^1/_2\,I_2 \quad (19)$$

Table III. Effect of Sodium Chloride on H_2S and SO_2

Known concentration[a]		Observed Concentration With No NaCl		4% NaCl		10% NaCl	
$\%H_2S$	$\%SO_2$	$\%H_2S$	$\%SO_2$	$\%H_2S$	$\%SO_2$	$\%H_2S$	$\%SO_2$
14.0	4.0	14.0	3.7	14.1	3.9	14.5	3.6
3.3	13.7	3.3	13.3	3.3	13.6	3.2	13.7
14.0	...	14.0	0	14.2	Negative	14.6	Negative
...	13.7	0	12.9	0	13.4	0	13.6
...	4.0	0	3.8	0	3.9	0	4.0
3.3	...	3.3	0	3.3	0	3.5	Negative

[a] Two mixtures of SO_2 in nitrogen and two of H_2S in nitrogen were made up and analyzed with standard acidic iodine solution. Known volumes of the H_2S, then the SO_2 gas mixtures were passed through copper sulfate solutions similar in composition to those in Table I.

Although the forward reaction of Equation 17 is slight, it is accelerated by the formation of the precipitate in Reaction 18. Each mole of the H_2S normally yields $^1/_2$ mole of iodine and consumes one mole of Cu^{2+} as shown in Equations 18 and 19; when sulfur is present, each mole of H_2S is equivalent to one mole of iodine.

The acid indicator ("A") chosen has two fortunate qualities: the color changes from lavender to colorless at pH 4.2—the precise pH of the blank copper sulfate solution (the yellow or green color seen at the end point is that of the copper solution which is masked by the indicator until pH 4.2 is reached); and the indicator is destroyed by bromine, thus permitting the reversible bromate indicator ("B") to function without interference (the acid indicator may also be used as a bromate indicator, but since it is not reversible, it was difficult to approach the true end point without over-titrating). As indicated in the analysis instructions, a titration to pH 4.2 may be done in lieu of a titration with Indicator "A."

The choice of the bromate indicator ("B") was made because of its reversibility and because of its warning indication of the end-point approach (*4*). A low pH is necessary for the bromate to oxidize cuprous ions; however, the optimum pH range for the reaction between I^- and Cu^{2+} ions was found to be 3.0 to 4.5 (*5*). A 40% solution NaOH was chosen to raise the pH because the total volume must not be too great if complete reaction between I^- and Cu^{2+} is to take place. A 50% NaOH solution was also used, but it was found to be too viscous for dropwise addition. The first drop of excess caustic caused the pH to rise to 4.8; when 0.5*N* HCl was added to just clear the solution, the pH ranged between 4.0 and 4.5, thus obviating the need for an indicator or a pH meter. Although the bromate titration is an accurate one for the determination of cuprous ions (an indication of SO_2 concentration), the method was found unreliable unless air was excluded; the addition of a large excess of sodium chloride to the filtrate (*6*) permitted a bromate titration in the presence of air, and the result coincided with that obtained by the iodine titration.

Reactions 5 through 8 under "Theory" are simplified (to aid in understanding the stoichiometry of the reactants actually used) for calculation purposes. Acidified bromate and

(4) I. M. Kolthoff and E. B. Sandell, "Textbook of Quantitative Inorganic Analysis," 3rd ed., The Macmillan Co., New York, N. Y., 1952, p 588.
(5) *Ibid.*, pp 600–601.
(6) "The Encyclopedia of the Chemical Elements," Clifford A. Hampel, Ed., Reinhold Book Corp., New York, N. Y., 1968, p 168.

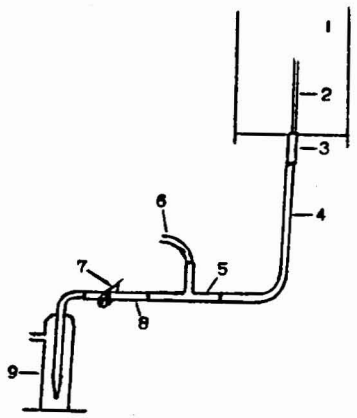

Figure 1. Connection to sample point of high temperature SO_2 reduction reactor

1. Reactor
2. Sample point
3. Kel-F Elastomer
4. 1-foot Glass tubing
5. Glass T
6. By-pass vent
7. Control clamp
8. Rubber tubing
9. First absorption jar

halogen salt actually react with the corresponding xanthates which result from the reaction between the two sulfur gases and alcoholic potassium hydroxide (*7*):

$$S{=}C{=}O + KOH + C_2H_5OH \rightarrow H_2O + S{=}C(OC_2H_5)(OK) \quad (20)$$

$$S{=}C{=}S + KOH + C_2H_5OH \rightarrow H_2O + S{=}C(OC_2H_5)(SK) \quad (21)$$

Both salts are yellow, and stable; however, when each was acidified and iodinated, elemental sulfur appeared from the latter but not from the former xanthate. The free xanthic acids which are unstable, release COS and CS_2 which react with iodine as indicated in Reactions 7 and 8.

The solution in the 3 gas purifier jars were purged with nitrogen to sweep any remaining COS from the copper sulfate solutions, although COS has very limited solubility in such acidic solutions of high salt content.

One-sixth molar potassium bromate was chosen as a reference standard throughout this paper, as this is equivalent to 0.1*N* sodium thiosulfate on which most of the analyses depend, and with which bromate and copper sulfate solutions were standardized.

(7) K. E. Perepelkin and Ya. Z. Sorokin, *Zavod. Lab.*, **23**, 1414–17 (1957).

Carbon dioxide, as well as carbon disulfide and carbon oxysulfide, is absorbed by the alcoholic potassium hydroxide solution. Barium carbonate is insoluble on the alkaline side, but soluble on the acid side; therefore, when 0.1*N* NaOH was added to bring the pH up slightly, there was a tendency for $BaCO_3$ to precipitate because of local over-alkalinity. As the bulk of the solution was still slightly on the acid side, the pink phenolphthalein color faded as the $BaCO_3$ dissolved: thus the reason for deliberately over-titrating slightly with caustic before obtaining the first end point with 0.05*N* HCl.

The mixed indicator (*8*), "C," has two fortunate characteristics: the color change is sharp, and the pH at which the color change takes place yields an answer that is within 0.5% of the true concentration of CO_2 (sulfide ions do not interfere).

Normally, CO_2 is determined by Orsat apparatus. The gas sample must pass through acidic iodine scrubber before being absorbed in the aqueous KOH solution of the Orsat—otherwise the SO_2 and H_2S gases, which are also acid gases, would be analyzed as CO_2 according to accepted theory. However, this was precisely what happened with COS which was not completely scrubbed out by iodine; the resulting high CO_2 analysis was another reason for this investigation.

Normally, analyses of SO_2 and H_2S mixtures were taken with the first absorption jar as close to the sample point as possible in order to prevent reaction between the cooled gases and water-vapor which would distort the analyses. In one experiment, where only H_2S was present and the temperature was over 800 °C, part of the gas was oxidized by the copper sulfate solution as evidenced by the production of too much acid and too little copper sulfide. Upon passing the gas through a 5-foot cooling coil, the reaction was quantitative.

When mixtures of the two gases were analyzed, there was little difference between results obtained when the first absorption jar was close to the source and those obtained when the jar was at a small distance—unless the temperature was high. As a matter of fact, SO_2 results obtained by the gas chromatograph substantially agreed with those obtained by the copper sulfate procedure, where the SO_2 analysis depended on a correct H_2S analysis; yet, the gas in the hypodermic syringe had ample time to cool and for water vapor to condense before the injection was made.

As regards the fundamental reaction $SO_2 + 2\,H_2S = 2\,H_2O + 3\,S$, this is slow and incomplete and takes place only in very concentrated media, as shown in the Kipp apparatus. If an anhydrous medium could be used which would prevent the formation of acids, the process might work (*9*).

The sulfur that sometimes appeared on the walls of the glassware and tubing before the first absorption jar evidently was not due to the above reaction after the gases left the sample point, but was due to this reaction while hot and with the aid of a reduction catalyst. Indeed, the above reaction is used extensively in industry; there are many examples in the literature that indicate requirements of high temperature and a catalyst for any reasonable yield of sulfur (*10*, *11*).

Despite the foregoing, a compromise was made on the basis of some contrary evidence in actual results and in the literature (*12*, *13*). By experiment, it was found that with an exit

(8) I. M. Kolthoff and E. B. Sandell, "Textbook of Quantitative Inorganic Analysis," 3rd ed., The MacMillan Co., New York, N. Y., 1952, p 432.
(9) Ch. Chorower, *Am. Fis. Quim.*, **38**, 105-48 (1942).
(10) *Ibid.*, **51**, 11, 675 *f.* (1957).
(11) *Ibid.*, **64**, 4653 *b.* 1966.
(12) H. D. Axelrod, J. H. Cary, J. E. Bonelli, and J. P. Lodge, Jr., ANAL CHEM., **41**, 1856 (1969).
(13) J. R. Birk, C. M. Larsen, and R. G. Wilbourn, *ibid.*, **42**, 273 (1970).

Table IV. Analyses by Different Analytical Techniques

Gas	Run No.	Gas chromatography[a]	Orsat[b]	$CuSO_4$ and alcoholic KOH bubblers
% H_2S	1	0.98		1.06
	2	2.98		2.91
	3	3.84		3.74
	4	1.24		1.27
% SO_2	1	3.39		3.42
	2	2.98		2.91
	3	3.84		3.74
	4	6.04		5.92
% COS	1	2.05		1.95
	2	2.09		2.03
	3	0.85		0.87
	4	1.67		1.70
% CS_2	1	1.19		1.20
	2	1.05		1.01
	3	1.91		1.85
	4	2.10		2.14
% CO_2	1	5.9	6.4	6.1
	2	5.3	6.0	5.5
	3	6.0	6.0	6.0
	4	3.6	3.7	3.4

[a] Conditions used with Perkin Elmer 154-D Chromatograph were column temp, 92 °C; flow at 10 psig, 50 cc/min; sample volume, 1 ml; column, 6-ft Porapak Q which was conditioned with 5% SO_2 gas before each analysis. Retention times were H_2S, 1.95 min; COS, 3.00 min; SO_2, 4.20 min; and CS_2, 70.00 min. Peak height was used for calculating the gas concentration. Calibration was done with a standard gas mixture. Magnesium perchlorate was used to scrub water from the gas to prevent reaction between H_2S and SO_2.

[b] A solution of acidic iodine was used to scrub H_2S and SO_2 from the gas.

temperature of 1000 °C, the optimum distance between the first absorption jar and the sample point was about 18 inches. The connection was made with a one-foot piece of 1/4-inch glass tubing with a small piece of Kel-F tubing at one end and a piece of rubber tubing at the other. A glass "T" with a rubber tubing vent was used between the rubber and the glass tubing as a bypass (see Figure 1). The elemental sulfur that had already formed in the reactor was seen to condense on the walls of the glass tubing well before the rubber connection; however, the temperature was still cool enough to inhibit reaction between H_2S and Cu^{2+} ions, yet hot enough to keep water in the gaseous state, thus preventing possible catalytic action of water on H_2S and SO_2.

CONCLUSIONS

Table IV indicates good correlation between results obtained by the copper sulfate–alcoholic potassium hydroxide method and those obtained by other methods. Only one result was recorded for each Run Number, since all were results of actual production runs, and time did not permit duplicate analyses.

The lengthy discussion on choice of conditions attempts to deal with high temperatures and/or high concentrations of H_2S when encountered in some SO_2 reduction units.

ACKNOWLEDGMENT

The author thanks John D. O'Brien for his encouragement to pursue this work and for his work in checking results with the gas chromatograph. The author appreciates the helpful discussions with A. Warshaw concerning the progress of this work.

RECEIVED August 13, 1970. Accepted November 20, 1970.

Simultaneous Determination of Two Electroactive Species by Alternating Current Polarography

A. M. Bond and J. H. Canterford[1]

Department of Inorganic Chemistry, University of Melbourne, Parkville, Victoria 3052, Australia

It has been established that alternating current polarography may be used for simultaneous analytical determination of two reversibly reduced electroactive species provided there is no overlap of the two ac waves. Where overlap occurs, despite the fact that two distinct peaks may be resolved, the analytical use of the peak heights is not recommended. Where overlap occurs, complete separation of the two waves by selective complexation is a much simpler, more accurate, and reliable analytical approach than trying to compute true peak heights from the summation.

IN PRINCIPLE, alternating current (ac) polarography should be extremely useful for the simultaneous determination of several electroactive species in the same solution from the one scan. It is obviously markedly superior to dc polarography because a common base line exists for all electroactive species. Figure 1*a* shows an ac polarogram of a solution containing cadmium(II) and lead(II) while Figure 1*b* gives the corresponding dc polarogram. Comparison of these two Figures clearly illustrates the common base line with ac polarography, whereas for dc polarography, determination of the more negatively reduced cadmium(II) requires the assignment of a new base line which is dependent upon the previous reduction process. Obviously this would lead to a lowered precision for determination of cadmium(II) by dc polarography.

If the reduction potentials of the two depolarizers are close together and the waves overlap, the problem of sorting out the two waves from dc polarography makes the analytical determination of the two species virtually impossible. The equivalent ac polarogram for such a system may well show two distinguishable peaks and it may appear that concentrations of both species may be accurately determined. Certainly it has been shown that in many cases where the dc wave is unresolvable in either the qualitative or quantitative sense that ac polarography can provide two distinct peaks. Figure 2 shows a comparison of the ac and dc polarograms

[1] Present address, Division of Mineral Chemistry, CSIRO, P. O. Box 124, Port Melbourne, Victoria 3207, Australia.

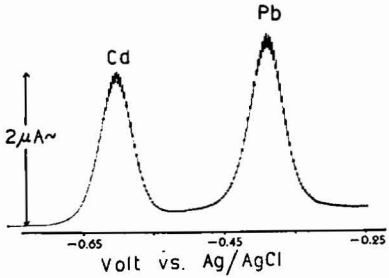

Figure 1*a*. Ac polarogram of $8 \times 10^{-4}M$ Cd(II) and $8 \times 10^{-4}M$ Pb(II) in $1M$ NaCl

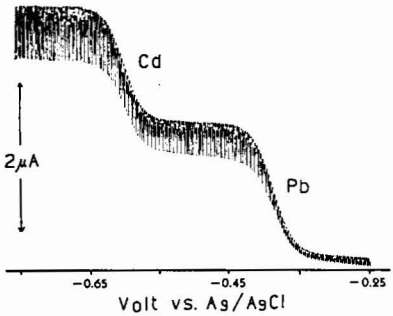

Figure 1*b*. Dc polarogram of same solution as in 1*a*

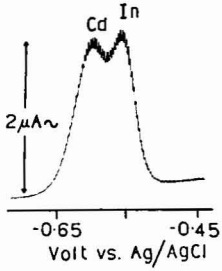

Figure 2*a*. Ac polarogram of $8 \times 10^{-4}M$ Cd(II) and $4 \times 10^{-4}M$ In(III) in $1M$ NaCl

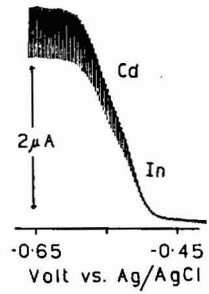

Figure 2*b*. Dc polarogram of same solution as in 2*a*

of a solution containing cadmium(II) and indium(III). The half-wave potentials differ by only 40 mV in $1M$ NaCl and the mixture is unresolvable by dc polarography. However, two peaks appear on the ac polarogram and at least qualitatively it is possible to distinguish both species. It is also possible to measure peak heights for both species. However, very little quantitative information appears in the literature to show whether this peak height gives the correct concentration of either or both species. Examination of what little quantitative information is available in the literature on the various forms of ac polarography (*1–3*) would indicate that the correct concentrations would often not be obtained simply from the peak heights of incompletely resolved ac waves and it is surprising that implications that they are readily usable in routine analysis are so widespread (*2–5*). The problem with the figures given by the early enthusiastic workers in the field (*2, 3*), which are of the same type as Figure 2, is that they represent the situation for only a small number of selected concentration ratios and are not typical of the entire range of ratios liable to be encountered in routine analysis. Unfortunately the early work has been reported in reviews without any critical comment (*4, 5*). They are also reproduced extensively in advertising material.

We have therefore set out to investigate experimentally if overlapping ac polarograms can or should in fact be used to quantitatively determine the concentration of either or both species giving rise to the overlapping waves.

The systems chosen for the present study were cadmium(II), indium(III), lead(II), and thallium(I) with $1M$ NaCl as the supporting electrolyte. These particular systems were chosen for several reasons as follows:

(a) They are reversibly reduced, or nearly so, at the dropping mercury electrode (DME) in the ac sense as well as in the dc sense. Thus the shapes of the waves can be mathematically represented by relatively simple equations. Furthermore, the peak heights of such systems should be independent of the rate of the electrode reaction and complications due to the first (more positive) reduction process altering the kinetics of the second reduction reaction are minimized (*6*).

(b) The dc potential range over which a reversible ac electrode process occurs is inversely proportional to the number of electrons, n, involved in the charge transfer. The systems chosen provide examples where n equals 1, 2, and 3, for which different effects would be expected, with regard to overlapping waves.

(c) The summit potentials, E_s, of these four systems in $1M$ NaCl are such that various differences in E_s ranging from virtual overlap to complete separation can be achieved by appropriate choice of two of them in combination.

(d) The products of the electrode processes are amalgams and complications due to soluble products are minimized (*6*).

EXPERIMENTAL

Reagents. All chemicals used were of reagent grade quality. Cadmium(II), lead(II), and thallium(I) solutions were prepared from the respective nitrates, while indium(III) sulfate in $10^{-3}M$ HCl was used for the indium(III) solutions. The supporting electrolyte in all cases was $1M$ NaCl.

Apparatus. Polarograms were recorded with a Metrohm Polarecord E 261. Ac polarography was carried out using the Metrohm ac Modulator E 393 with an applied ac voltage of 10 mV, rms at 50 Hz. To minimize cell impedance, the modulated ac voltage was applied through an auxiliary tungsten electrode. Maximum damping was applied and the

(1) J. Devay, T. Garai, L. Meszaros, and B. Palagyi-Fenyes, Hungarian Scientific Instruments, 1968, No 15, 1.
(2) B. Breyer, F. Gutmann, and S. Hacobian, *Aus. J. Sci. Res., Ser. A*, 3, 558 (1950).
(3) *Ibid.*, p 567.
(4) B. Breyer and H. H. Bauer, "Alternating Current Polarography and Tensammetry," Interscience, New York/London, 1963, pp 14, 128–135.
(5) H. Schmidt and M. von Stackelberg (trans. by R. E. W. Madison) "Modern Polarographic Methods," Academic Press, New York/London, 1963, pp 48–49.
(6) A. M. Bond and J. H. Canterford, in preparation.

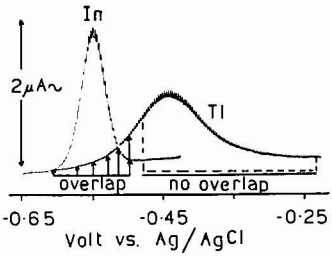

Figure 3a. Ac polarograms of 8 × $10^{-5}M$ Tl(I) and 4 × $10^{-5}M$ In(III)

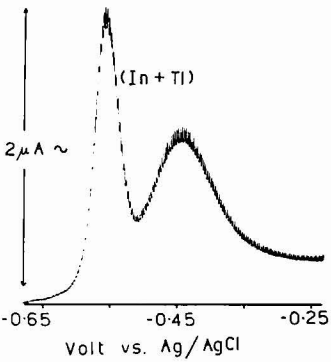

Figure 3b. Ac polarogram of 8 × $10^{-5}M$ Tl(I) and 4 × 10^{-5} In(III) when both are present in the one solution

slowest scan rate of dc potential (1 volt/12 min) was used in accordance with previous work (*7*). The waves were recorded using the maximum sensitivity possible for each wave individually to obtain the highest precision possible.

All solutions were degassed with argon and thermostated at (25.0 ± 0.1)°C. All potentials were measured relative to Ag/AgCl.

RESULTS AND DISCUSSION

Cadmium(II) and Lead(II). In 1*M* NaCl the two electrode processes

$$M(II) + 2e \rightleftharpoons M(amalgam)\ (M = Cd,Pb) \qquad (1)$$

have E_s values *vs.* Ag/AgCl of −0.601 V [Cd(II)] and −0.398 V [Pb(II)], that is, a separation of about 200 mV. No overlap of the two waves was observed over the various concentration ratios used, namely 10:1 to 1:10, and the peak heights of both waves were exactly the same when recorded with both species present in the one solution, or individually in separate solutions. This indicates that the preceding reduction of lead(II) does not interfere in any way with the subsequent reduction of cadmium(II) and that where no overlapping waves occur with reversible electrode processes, simultaneous determination of two species in the one solution is possible.

(7) A. M. Bond and J. H. Canterford, submitted to ANAL. CHEM.

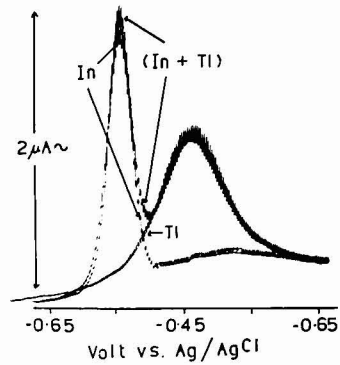

Figure 4. Diagram to show that observed ac wave in Figure 3b is the addition of the two ac waves in Figure 3a

It is, of course, possible for the product of the preceding (more positive) electrode process to interfere with the second electrode process (*b*), and this would invalidate the simultaneous determination but for a different reason.

Indium(III) and Thallium(I). The E_s values *vs.* Ag/AgCl for the reactions

$$In(III) + 3e \rightleftharpoons In(amalgam) \qquad (2)$$

and

$$Tl(I) + e \rightleftharpoons Tl(amalgam) \qquad (3)$$

in 1*M* NaCl were found to be −0.557 V and −0.450 V, respectively, that is, a separation of approximately 100 mV. The thallium(I) wave is extremely broad relative to the indium(III) wave being a one-electron reduction and overlap of the two waves occurs. Figure 3 shows a typical polarogram of this system. Figure 4 shows that the observed polarogram is in fact the addition of the two individual waves.

To determine the concentrations of the two species the true peak height, $i_d\sim$, which is the alternating current corresponding to E_s, is used. As the two waves are superimposed, they can overlap without causing interference to the analytically used $i_d\sim$ value at potential E_s if the following two conditions hold: (a) Overlap of the more positive wave, in this case thallium(I), must not extend to the E_s value of the more negative wave, in this case indium(III). (*b*) Overlap of the more negative wave [indium(III)] must not extend to the E_s value of the more positive wave [thallium(I)].

For the indium(III)–thallium(I) system, thallium(I) exhibits a broad wave relative to that of indium(III) as the number of electrons involved in charge transfer is in the ratio 1:3. With an E_s separation of about 100 mV, thallium (I) nearly always overlaps beyond the E_s value of indium(III) and alters the true $i_d\sim$ value of indium(III) (see Figure 3). However, the relatively narrow indium(III) wave does not overlap the thallium(I) wave at its E_s value unless the concentration of indium(III) is substantially greater than that of thallium(I).

Table I gives the theoretical and experimental concentrations for a series of indium(III) and thallium(I) solutions, where the experimental concentrations are those obtained from normal calibration curves. It can be seen from this

Table I. Comparison of Theoretical and Experimental Concentrations of Indium(III)–Thallium(I) Mixtures

Indium(III)			Thallium(I)		
Theor M	Exptl M	$-E_s$ (volt vs. Ag/AgCl)	Theor M	Exptl M	$-E_s$ (volt vs. Ag/AgCl)
2.00×10^{-5}	2.61×10^{-5}	0.558	8.00×10^{-5}	8.01×10^{-5}	0.448
2.00×10^{-5}	2.71×10^{-5}	0.562	2.00×10^{-4}	2.00×10^{-4}	0.452
2.00×10^{-5}	3.06×10^{-5}	0.573	4.00×10^{-4}	4.03×10^{-4}	0.453
4.00×10^{-5}	4.06×10^{-5}	0.560	4.00×10^{-5}	3.98×10^{-5}	0.446
4.00×10^{-5}	4.13×10^{-5}	0.561	8.00×10^{-5}	8.00×10^{-5}	0.451
4.00×10^{-5}	4.25×10^{-5}	0.568	2.00×10^{-4}	2.03×10^{-4}	0.452
4.00×10^{-5}	4.51×10^{-5}	0.577	4.00×10^{-4}	4.01×10^{-4}	0.450
1.00×10^{-4}	1.00×10^{-4}	0.563	4.00×10^{-5}	3.98×10^{-5}	0.450
1.00×10^{-4}	1.00×10^{-4}	0.562	8.00×10^{-5}	7.99×10^{-5}	0.452
1.00×10^{-4}	1.01×10^{-4}	0.561	2.00×10^{-4}	1.97×10^{-4}	0.451
1.00×10^{-4}	1.09×10^{-4}	0.578	4.00×10^{-4}	4.00×10^{-4}	0.449
2.00×10^{-4}	2.00×10^{-4}	0.560	4.00×10^{-5}	4.02×10^{-5}	0.446
2.00×10^{-4}	2.00×10^{-4}	0.563	8.00×10^{-5}	7.97×10^{-5}	0.454
2.00×10^{-4}	2.00×10^{-4}	0.564	2.00×10^{-4}	2.01×10^{-4}	0.453

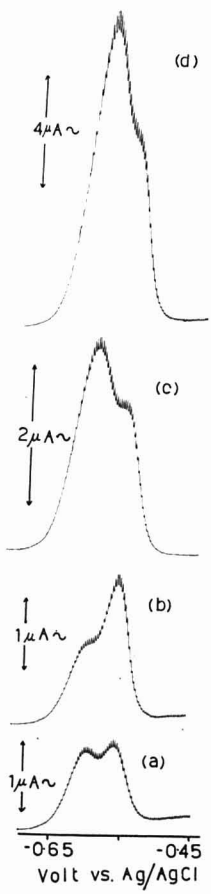

Figure 5. Observed ac polarograms of various mixtures of indium(III) and cadmium(II)

a. $2 \times 10^{-5}M$ In(III) + $4 \times 10^{-5}M$ Cd(II)
b. $4 \times 10^{-5}M$ In(III) + $4 \times 10^{-5}M$ Cd(II)
c. $4 \times 10^{-5}M$ In(III) + $2 \times 10^{-4}M$ Cd(II)
d. $1 \times 10^{-4}M$ In(III) + $4 \times 10^{-4}M$ Cd(II)

table that thallium(I) can be determined in the presence of indium(III) under all concentration conditions examined. However, indium(III) can only be determined accurately when the concentration of indium(III) is equal to, or greater than that of thallium(I).

It is interesting to note that where interference of indium (III) by the presence of excess thallium(I) occurs, subtraction of the thallium(I) wave from the apparent indium(III) wave gave the correct indium(III) concentration as expected from Figure 4. Subtraction could be achieved either with the aid of the calibration curve prepared in the absence of indium (III), or by assuming that the thallium(I) wave is symmetrical on both sides of E_s and knowing the more positive side to the thallium(I) wave is not affected by indium(III) overlap. This latter type of correction is reasonably convenient where one of the two systems does not suffer from overlap at the E_s potential.

Cadmium(II) and Indium(III). The cadmium(II) and indium(III) electrode reactions

$$\mathrm{Cd(II)} + 2e \rightleftarrows \mathrm{Cd(amalgam)} \quad (4)$$

and

$$\mathrm{In(III)} + 3e \rightleftarrows \mathrm{In(amalgam)} \quad (5)$$

in $1M$ NaCl have E_s values relative to Ag/AgCl of -0.601 V and -0.557 V, respectively. That is, there is a very small difference of only about 40 mV in the two E_s values. Figure 5 shows ac polarograms of various concentration ratios of cadmium(II) and indium(III). It can be seen that sometimes two peaks are resolvable; however, usually one of the species appears as a shoulder and an $i_d\sim$ value for this species cannot be evaluated.

Table II gives the theoretical and calculated concentrations for various ratios of cadmium(II) and indium(III). It can be seen from Table II that simultaneous analytical determination of cadmium(II) and indium(III) in the same solution in $1M$ NaCl is not possible. However, one species may be determined if that particular species dominates the polarogram and the other is only discernible as a small shoulder or causes the polarogram to tail-off.

It is interesting to note that almost the correct E_s value can occur even though there is gross interference and the observation of the correct E_s value is not a suitable criterion for the

Table II. Comparison of Theoretical and Experimental Concentrations of Cadmium(II)-Indium(III) Mixtures

Cadmium(II)			Indium(III)			
Theor M	Exptl M	$-E_s$ (volt vs. Ag/AgCl)	Theor M	Exptl M	$-E_s$ (volt vs. Ag/AgCl)	Comments
4.00×10^{-5}	4.09×10^{-5}	0.598	2.00×10^{-5}	2.28×10^{-5}	0.560	Two distinct peaks
4.00×10^{-5}	...	...	4.00×10^{-5}	3.95×10^{-5}	0.558	Cd(II) as shoulder
4.00×10^{-5}	...	...	1.00×10^{-4}	1.00×10^{-4}	0.554	Cd(II) as weak shoulder
4.00×10^{-5}	...	...	2.00×10^{-4}	2.01×10^{-4}	0.560	Cd(II) as very weak shoulder
8.00×10^{-5}	7.98×10^{-5}	0.600	2.00×10^{-5}	...	...	In(III) as shoulder
8.00×10^{-5}	8.30×10^{-5}	0.604	4.00×10^{-5}	4.01×10^{-5}	0.557	Two distinct peaks
8.00×10^{-5}	...	...	1.00×10^{-4}	0.98×10^{-4}	0.558	Cd(II) as shoulder
8.00×10^{-5}	...	...	2.00×10^{-4}	2.10×10^{-4}	0.564	Cd(II) as weak shoulder
2.00×10^{-4}	2.00×10^{-4}	0.603	2.00×10^{-5}	...	...	In(III) as very weak shoulder
2.00×10^{-4}	2.01×10^{-4}	0.602	4.00×10^{-5}	...	...	In(III) as shoulder
2.00×10^{-4}	2.10×10^{-4}	0.604	1.00×10^{-4}	1.05×10^{-4}	0.563	Two distinct peaks
2.00×10^{-4}	...	...	2.00×10^{-4}	2.12×10^{-4}	0.565	Cd(II) as shoulder
4.00×10^{-4}	4.00×10^{-4}	0.606	2.00×10^{-5}	...	...	Cd(II) wave tails off on more positive side
4.00×10^{-4}	4.01×10^{-4}	0.605	4.00×10^{-5}	...	...	In(III) as shoulder
4.00×10^{-4}	4.03×10^{-4}	0.605	1.00×10^{-4}	1.23×10^{-4}	0.565	Two distinct peaks

lack of interference. It was also noted that interference of indium(III) by cadmium(II) is more marked than that of cadmium(II) by indium(III). This is because the indium(III) wave (three-electron reduction) is significantly narrower in the dc potential range it occupies than the cadmium(II) wave (two-electron reduction).

CONCLUSIONS

From the present study, it is obvious that ac polarographic analysis where two or more ac waves overlap is liable to gross error if the observed peak height is used for the determination. Despite the fact that the correct or almost correct peak potential is recorded for one or both waves, the correct peak height and, therefore, correct concentration is not necessarily observed. In some instances it may be possible to determine one (or both) of the two electroactive species from the overlapping waves if the overlap of the two waves is not significant at one (or both) summit potentials. However, in general it is not practical to use an overlapping ac wave for analytical purposes as it is fraught with danger. Separation by selective complexation as used in dc polarography when overlapping dc waves occur is considered a much better technique for simultaneous determination of two species when overlap of ac waves is observed.

The present study has been restricted to overlapping reversible ac processes involving amalgam formation for simplicity. The presence of a nonreversibly reduced species, whose theoretical wave shape and height are complicated functions and dependent upon the kinetics of the reaction, would provide an even more complex situation. Complete resolution of all waves would then be even more strongly advised.

It should be stressed that the fact that ac polarography is more discriminating than dc polarography should not be taken to imply that the determination of species with overlapping ac waves allows their simple quantitative determination. Overlapping ac waves allow only qualitative determination of the species present in most cases and simple quantitative analysis still cannot generally be achieved. As each of the two reversible ac waves may be mathematically described fairly readily (*8*), then obviously the equation to the composite ac wave could also be obtained. Consequently, it should be theoretically possible to directly calculate the concentration of both species with the aid of a small computer by mathematically reconstructing the two individual waves from the observed composite wave.

Alternatively, a series of various concentration ratios of the two species could be recorded and the unknown composite wave measured by reference to the calibration solutions again with the aid of a computer. This type of analytical computational approach described by Perone and coworkers (*9–11*) for stationary electrodes would be theoretically feasible for ac polarography. However, such approaches are only applicable to situations in which the electrochemistry of the species causing the overlapping wave is particularly well known and extremely well characterized and controlled to rigorously standardized conditions.

In most practical cases handled in the laboratory, the ac waves are not completely reversible and many subtleties exist in their mathematical description. Computational analysis or separation in most cases could be a lengthy and probably difficult procedure. Choice of a different electrolyte to provide two completely resolved ac waves would usually be a much simpler and must be a more accurate method for determination of two species than resolution of the composite wave by computational procedures. This latter fact alone makes chemical separation of the two waves an ideal approach, other considerations aside, and it seems hard to recommend mathematical separation except in exceptional circumstances.

Finally, it should be noted that although this paper refers to simultaneous determination of both species from an overlapping wave, determination of only one of the species is a more common problem in routine analysis. Cadmium for instance may be determined by a standard method on hundreds of samples. Other species besides cadmium in the sample may not be known. Occasionally an ac wave is observed in which the presence of an overlapping wave is encountered. From this work, it has been shown that determination of cadmium in this sample should not be considered completely quantitative until resolution of the ac wave has been examined closely or the determination repeated in a different electrolyte.

RECEIVED for review September 11, 1970. Accepted November 16, 1970.

(8) D. E. Smith in "Electroanalytical Chemistry," A. J. Bard, Ed., Marcel Dekker, New York, N. Y. 1966, Chap. 1.

(9) W. F. Gutnecht and S. P. Perone, ANAL. CHEM., 42, 906 (1970).
(10) S. P. Perone, D. O. Jones, and W. F. Gutnecht, *ibid.*, 41, 1154 (1969).
(11) S. P. Perone and T. R. Mueller, *ibid.*, 37, 2 (1965).

A Laboratory-Based Computer System

Marvin Shapiro and Arthur Schultz
National Institutes of Health, Bethesda, Md.

A computer system for the acquisition of data from analytical instruments used in biomedical research was designed and is now operating in a laboratory environment. Six remotely located instruments have been interfaced to the computer, and data can be collected simultaneously from them while other programs are running in a background mode. Features of the system include a remote operator's console for communication between the computer system and the laboratory and additions to the manufacturer-supplied software to allow rapid interrupt processing.

WHILE A NUMBER of real-time computer systems have been implemented recently in support of laboratory research, no standard approach has been developed. Each laboratory instrument presents its unique problems when interfaced with a computer, and in an environment where a number of instruments are present, various approaches to the design of a computer-instrument system can be taken (*1*, *2*). We are reporting here on a system which was designed to meet some of the computational needs of a group of scientists working at the National Institutes of Health on research in molecular and physical biology.

The desirability of such a system first became apparent three years ago when a number of scientists working in one building at NIH were making plans to request purchase of instruments or accessories which incorporated data acquisition hardware and digital recording devices. Data analysis was to be accomplished in the NIH central computer facility. With the high density of instrumentation in this building, the aggregate cost of this approach, if widely used, would have approached the cost of one centrally located computer-based data acquisition system. In many ways, this group of scientists located together presented an ideal opportunity for experimenting with such facilities at NIH because of the diversity of physical instrumentation and problems they were working on. The implementation of a computer system presented a more flexible approach than using any of the highly specialized devices which could have been purchased, and, in addition, provided sufficient capability to permit considerable data manipulation, signal averaging, and more complicated data reduction.

Over the past three years a computer system was designed and made operational. It is a time-shared system which acquires data simultaneously from a number of different types of analytical instruments while running one or more analysis programs in a background mode. The instruments currently connected are spectrophotometers, a spectropolarimeter, a Raman spectrometer, an analytical ultracentrifuge, and a computer of average transients (CAT). All of these instruments are located at distances ranging from 50 to 200 feet from the computer, which is centrally located in the building.

Two applications in the building utilize small dedicated computers that will be connected to the building computer to take advantage of its peripheral devices, principally mass storage. In one application a 16-bit computer with 4K core and high-speed (150 KHz) analog-to-digital conversion is used to capture transient signals. The other application is a commercially available X-ray diffraction system that both controls the diffractometer and acquires data.

With these research needs in mind, a system was designed around commercially available hardware and software components. A medium size real-time computer (Honeywell DDP-516) with 24,576 words of 16-bit, 0.96 μsec cycle time memory (later expanded to 32,768 words) was purchased, with the following peripheral equipment: two ASR teletypes, line printer (300 lpm), high-speed paper tape equipment, card reader (200 cpm), 10-inch, 10-mil step incremental plotter, nine-track magnetic tape, and 1.8 million word moving head disk. In addition, a digital I/O multiplexer for handling up to 576 bits, a 35 KHz, 12-bit A/D converter, sample-and-hold amplifier, and multiplexer, and three digital-to-analog converters were purchased. A standard foreground-background monitor, oriented around disk operation, was provided with the system. A diagram of the system components as currently configured is shown in Figure 1.

The principal additions which our own staff made to the system included: (a) Hardware: (1) a remote operator's console (ROC) for communication between the laboratory and computer was designed and built, (2) a data acquisition and display subsystem (DADS) for conditioning signals, for use in checkout, and for displaying system status, was designed and built, and (3) instrument interfacing and a data transmission system was designed and completed; (b) Software: (1) system interrupt response was greatly improved by specially written programs for data collection, and (2) a series of programs was written and incorporated into the operating system to provide interactive communication with remote operating consoles located in the laboratories. A staff of three programmers and two electronics engineers (with part-time help from an electronics technician for fabrication) worked for a total of eight man-years to bring the system to an operational status. Once the system was operational, staffing to support further additions and improvements was reduced to two programmers and one engineer.

The system was considered operational when it could support data acquisition and the scientist's use of the remote operator's console. However, until application programs were written to support the analysis of the data collected, the system attracted few users. General programs for data manipulation, plotting, and mathematical analysis of data have been written and work is continuing to provide specialized computations for specific instruments.

Essentially no knowledge of computers is required for the scientists to accomplish data acquisition, file management, and the initiation of programs from the laboratory. A short demonstration of less than an hour, plus a copy of the ROC user's manual, is all that is needed. Use of the system's FORTRAN capabilities, however, now requires that each user operate the computer himself, and, in addition, requires that he have some minimum knowledge about the system, including how the disk program storage is laid

(1) *IBM J. Res. Develop.*, **13**, No. 1 (1969).
(2) Proceedings IBM Scientific Computing Symposium on Computers in Chemistry, Thomas J. Watson Research Center, Yorktown Heights, N. Y., August 1969.

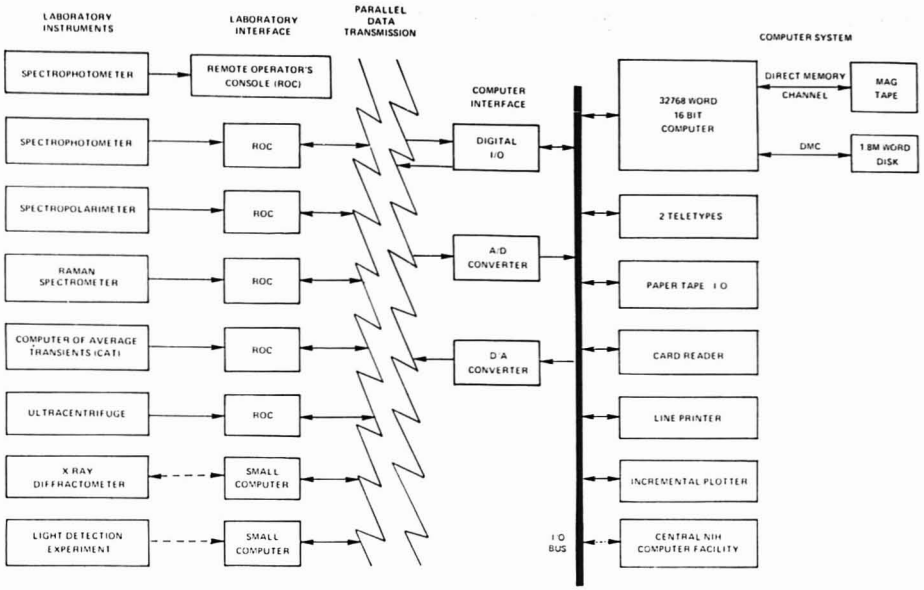

Figure 1. Diagram of the laboratory-based computer system

Dashed lines represent connections which have not yet been made

out. It generally takes a number of hours of hands-on use for a FORTRAN user to be able to use the computer without difficulty.

Generally, the system has been reliable for data collection. Each instrument was checked individually with specialized programs and with hardware tests for data transmission accuracy before being incorporated into the system. A number of software difficulties have been encountered in the form of system failures while running in a multi-programming environment. While most of these problems have been identified and corrected, it is expected that all such errors will be eliminated only after the system has seen heavy use for a long period of time.

The system has been operational for less than a year with a small, but gradually increasing, number of users. With this amount of experience in mind, this paper is directed toward explaining how a working system was designed and how it is used, as opposed to discussing long range effects on scientific research.

COMMUNICATION WITH THE LABORATORY

In designing a system for the acquisition of data it was clear that each instrument, although possessing similarities to another instrument, would require a unique interface. At the same time, the console that was adopted for entry of control information for each instrument could readily be standardized. The technique adopted combined within the same package a standard system for the entry of control parameters and sufficient space for the construction of an instrument interface. The package containing these elements is called the Remote Operator's Console (ROC), and one such console is associated with each instrument.

Each Remote Operator's Console (ROC) is composed of a Status/Control panel, a parameter entry panel, an X-Y storage scope, the instrument interface, and an intercom to the computer room. Figure 2 illustrates the functions that are implemented within a ROC. In addition to the indicator SYSTEM-UP, there are four button switches—SIGN ON, RUN, HALT, and SIGN OFF—on the Status/Control panel. In order to assure the operator that the switch action has been received by the computer and recognized by the operating system, each switch (except SIGN OFF) is backlighted, and is turned on by a signal generated by the computer. The correct operation of SIGN OFF is observed by the extinction of SIGN ON.

A parameter entry panel is also a part of the ROC and is the means of entering the specific information that will be used to condition the operating system for the particular data acquisition and/or processing task desired. A decade thumbwheel switch of six digits is used for parameter entry. The switch is divided into two sections, a two-digit control number and a four-digit parameter number. Two buttons, ENTER and CANCEL, are also a part of the parameter entry panel.

In order to provide the operator of an instrument with comprehensive information concerning the results of data acquisition and processing without requiring that he visit the computer room, a storage oscilloscope is included in the ROC. (In one case, two instruments located in the same room share a scope.) The Tektronix Type 601 Storage Display unit has been used for this application. To write a dot requires an analog signal on the vertical and horizontal axis to position the beam and, after the beam is positioned, a store signal to unblank the beam on the z axis. Alpha-

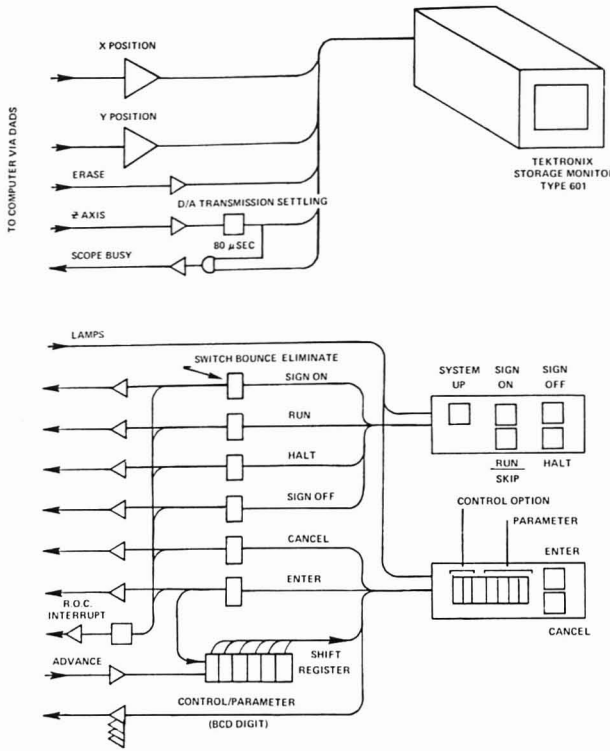

Figure 2. Simplified schematic of the interface to a remote operator's console

On the top, the storage display scope and below, the console buttons and thumbwheel digits

numerics and graphics are produced by the proper sequence of dots generated under software control. The scope can be erased either locally or under program control. Generation of beam position is by means of two digital-to-analog converters (DACs) located in the computer. Writing on a scope continues until either a message or plot is complete. Two DACs are used for the entire system. The output of the DACs is fed continuously to all connected scopes, but only the particular scope which is to write receives the signal to unblank its beam. The procedure for using a remote console is described later.

Interconnection between each remote console and the computer is by parallel transmission of signals, analog and digital, over twisted-pair shielded cables. This is a relatively simple approach from an engineering standpoint and also of low cost when all instruments are located in one building. Also, this technique does not require multiplexing/demultiplexing hardware and individual analog-to-digital converters at each instrument site. The cost of transmitting one digital signal is approximately $22.00, of which $9.00 is the cost of 300 feet of cable. In a situation where installation of cables is not easy or where large distances result in very large cable costs, this approach might not be practical.

All ROC cabling terminates within the computer room at the Data Acquisition and Display Subsystem (DADS). DADS is the focal point for both analog and digital data transmission and in addition contains timing logic and presents a visual display of the current system status.

A very useful feature of the DADS, for system checkout allows a local ROC, mounted in the DADS, to be substituted for any specific remote console. Thus, all the buttons, lights, and the scope on a standard ROC are built into the DADS unit. Other functions available on the DADS include an analog input channel for test data, one dedicated priority interrupt, and an intercom to the instrument areas. Since high current devices (including two elevators) operate within the building, the electrical environment between the ROC consoles and the DADS unit is relatively noisy. A differential signal was used for all signals (except lighting indicators) passed between DADS and the ROC to achieve maximum noise rejection. Analog signals are routed through individual low capacitance cable while digital signals are in multiconductor cables. Digital integrated circuit line drivers and receivers were chosen for this application.

Coupling of the digital signals from each ROC, via DADS, to the computer occurs at the Process Interface Control

(PIC). PIC functions as a digital input/output multiplexer which routes signals from the DDP-516 I/O bus to addressable external locations. The 576 bits in the PIC are divided into 48 addressable groups of 12 bits each. Each of the 48 locations may function as either an input or output. To meet the requirements for our system, two types of digital inputs, digital outputs, and two digital-to-analog converters were purchased as part of the PIC. Digital inputs with storage are used to record the occurrence of ROC button pushes, since the button may be released before the system responds. Digital inputs without storage are used for reading in instrument abscissa values (wavelength, wavenumber, etc.) and thumbwheel digit information. Digital outputs are used to turn on lights on the remote console and to synchronize some digital functions.

INSTRUMENT INTERFACES

The existing outputs of the instruments were modified by us to obtain signals for input to the computer rather than our attempting to modify the internal design of the instrument. Thus, data collection by the computer does not alter instrument performance.

Each remote console contains the electronic circuits to convert (or adapt) data from the form which exists within the particular instrument to a voltage signal suitable for transmission to the computer room. All the instruments involved have a stand-alone capability prior to any connection to the computer. The basic requirement for most instruments is to derive a sampling signal at some fundamental unit of the instrument (such as wavelength or wavenumber) and use this signal to direct sampling of the dependent variable. A dedicated external interrupt is used for this type of sampling. In some cases the dependent variable is sampled as a function of time. For sampling using a time base, a special real-time clock is used, and a rate is derived from its basic interval of 0.25 millisecond.

In most ROC instrument interfaces, both analog and digital signals are transmitted between the ROC and the computer room. When the value of the independent variable is known absolutely (*e.g.*, via a shaft encoder), the selection of starting and stopping values for the data to be sampled can be specified in terms of this variable. The desired starting value is entered as a parameter; then during the instrument run, sampling begins automatically when this value is reached.

Cary 60 Interface. A block diagram of the Cary 60 spectropolarimeter interface is shown in Figure 3, and the functional aspects of this interface are presented below.

Wavelength range on the Cary 60 is from 1850–6000 Å. Scanning of wavelengths occurs in a linear manner at scan speeds between 0.2–30 Å second and is continuously variable. A shaft encoder was attached to the wavelength readout to give a direct wavelength reading in Ångstroms. Encoder readout is 4 digits of 8421 BCD, where 2 bits of gray code (0–3), repeated 50 times per turn (∴ 200 counts/revolution), are logically combined to create the low order bit of the units digit. As with all the shaft encoders, each increment of the units digit is used to create an interrupt which in this case directs the computer to sample the optical rotation. A linear slidewire, attached in parallel to the servo mechanism slidewire to acquire optical rotation, produces a voltage of approximately −7.5 to +7.5 volts over the 10-inch chart presentation. Three controls on the Cary 60 are available to allow scaling of the independent variable on the chart record. This scaling changes the interpretation of the voltage received

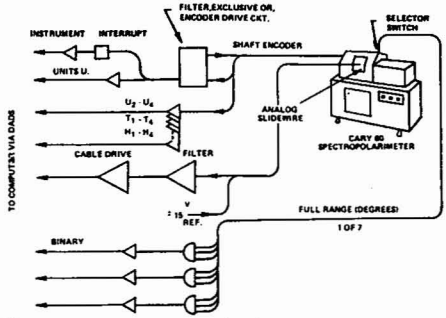

Figure 3. Simplified schematic of the computer interface to the Cary 60 spectropolarimeter

by the computer. Two of the control settings, zero offset and zero suppression, are entered through the parameter entry unit in the ROC. An addition was made to the third control, full-scale, to allow the computer to read its setting.

Cary 14 Interface. The Cary 14 spectrophotometer is a double beam optical instrument capable of operating between 2000 and 26,000 Å, thereby covering the ultraviolet, visible, and near infrared regions. The encoder is coupled directly to the Cary 14 such that its output reads directly in Å units. The electrical output of the encoder is presented in BCD and has a range of 0–39,999. The least significant bit (LSB) of the encoder units digit is delayed to allow discrimination against pulses of less than several hundred microseconds to reject noise. After passing through the delays, either edge of the LSB that is present is used to generate an interrupt. A potentiometer attached to the absorbance recorder produces a proportional voltage which is transmitted to the computer.

IR-7 Interface. The Beckman IR-7 produces a spectrum by varying the frequency in a linear manner over a part or all of the wavenumbers between 650 and 4000. A shaft encoder is attached to the wavenumber drive and a strip encoder to the absorbance recorder chart drive to acquire data. To define wavenumber, a shaft encoder of 100 counts per revolution is attached to the IR-7 wavenumber readout with gears establishing the ratio of one-tenth encoder revolution per wavenumber. Each revolution of the encoder generates a cyclic gray code of eight bits. Logical circuits within the ROC were designed to detect the encoder crossing 99-00 count up, and 00-99 count down. Since the encoder repeats every 10 wavenumbers, a counter external to the encoder is required to determine the scan position of the IR-7 relative to a starting point. In order to limit the initialization procedure, the counter has the capability of counting both up and down; therefore, once the ROC is turned on and the counter is initialized, the position of the encoder is known absolutely until power is turned off. An eight-bit parity circuit coupled to the encoder readout will produce an output for each shaft increment. This parity circuit output is used to develop the IR-7 instrument interrupt.

Much of the analysis done of the IR-7 depends on temperature. The sample area may be chilled or heated by circulation of fluids from devices external to the IR-7. Measurement of sample temperature is by means of a thermistor attached to a telethermometer. An analog signal available as an output and normally used to drive a chart recorder

Table I. System Software Priority Levels

Software priority level	Program function
8	Write data onto disk
7	Respond to console button push
6	Program initiated from remote console
5	Write remote scope
1–4	FORTRAN, assembly language programs

has been coupled to the ROC where it is buffered, amplified, and subsequently transmitted to the computer.

Cary 81 Interface. The Raman effect measured by the Cary 81 spectrometer uses a laser as the exciting source. Currently, the instrument is being modified to accept laser light from one of two sources. One source is a He–Ne gas laser with the major output of 50 milliwatts at 6328 Å (red). A second, more powerful Argon laser has for its most intense line 1.5 watts, at 5145 Å (green). A maximum of 4000 wavenumbers may be scanned beginning, approximately, with the laser excitation source. The Cary 81 has two mechanical wavenumber indicators, both of which are linear in wavenumber. One indicator denotes the current absolute wavenumber of the instrument optical system, the other is the displacement in wavenumbers from the excitation source, Δ cm^{-1}. A shaft encoder capable of defining 100,000 positions, 1000 per turn, 100 turns full-range, has been coupled to the instrument wavenumber drive mechanism. Gears added between the instrument drive and the encoder establish the ratio of 25 encoder counts per wavenumber. Therefore, the encoder range 0–100,000 corresponds to the instrument range 0–4000 Δ cm^{-1}.

It is necessary to adjust the relative wavenumber indicator for each change in the laser source that is used. An electric clutch under control of a toggle switch has been placed between the wavenumber drive on the instrument and the encoder gear drive to facilitate manual setting of the encoder to zero when the excitation source is changed. An analog representation of the Raman lines is acquired from a potentiometer attached to the instrument chart recorder.

Computer of Average Transients Interface. In this particular application, data are being accumulated in a Computer of Average Transients (CAT) used with a Varian HR-220 NMR spectrometer. After sufficient iterative scans have been accumulated in the CAT, the data are transferred from the CAT memory to the DDP-516 for analysis. A binary output of both memory address (10 bits) and memory contents (17 bits) is available from the CAT. An instrument interrupt is developed from each edge of the least significant address bit. Readout of the CAT memory to the computer requires enabling the instrument interrupt by the normal sign-on procedure, then placing the CAT in the readout mode at a rate selected by controls on the instrument.

Although the CAT is being used in this application with the HR-220, it has a general utility and is used in other applications. The interface deals only with the CAT in its readout mode and, therefore, may be applied in the other applications (disregarding problems of physical locations).

Analytical Ultracentrifuge Interface. Analysis of samples on the ultracentrifuge varies considerably from the instruments previously discussed. Multiple samples may be present in the rotor so it is necessary to have a positive identification of which sample is producing the analog data signal. Cell identification is continuously available to the computer as a 3-bit binary number derived by sensing the centrifuge scanner. Rotor velocity is derived by counting a pulse signal, used internally for speed control, which is proportional to rotor velocity. This signal is counted in the interface for one second, then the total count is made available to the computer for the succeeding second. The counter is enabled by the computer and will continue to cycle every 2 seconds until disabled by the computer. Optical bench position is sensed via a potentiometer that has been attached to the bench drive mechanism. The optical density data signal resulting from the scan of the cell as a function of bench position is also transmitted to the computer as an analog signal. It has been acquired from the scanner electronics, a standard part of the instrument.

THE SOFTWARE SYSTEM

The software monitor, called OLERT (On-Line Executive for Real-Time), is a state-of-the-art system which provides scheduling, input-output, and FORTRAN capabilities. Up to eight software levels of priority are allowed for the running of programs (the highest level being eight). For our purposes this means that the foreground data acquisition programs will run at the highest priority level, the programs supporting data collection will run at lower levels, and the background FORTRAN and assembly language programs will run at the lowest levels. The use of the eight software levels is shown in Table I.

Any number of FORTRAN or assembly language programs can be running at levels 1–4, the only limit being the amount of memory available and the availability of I/O equipment. These programs are initiated from the computer console. The OLERT monitor does not (at this time) allow for program swapping so that no new program can be initiated until memory space is available. However, programs can be segmented. These segments reside on the disk and are requested and loaded as needed.

In order to make the input of laboratory data as fast as possible, the data are collected at a hardware interrupt level which has a higher priority than the eight software levels. Also, all interrupts are inhibited during the input of a laboratory data point. Software levels five, seven, and eight contain the programs which support data acquisition. Auxiliary tasks, such as emptying a data buffer to disk or identifying a console interrupt and responding to it, are scheduled for levels eight and seven, respectively. The actual driving of the scopes is done at levels five. All programs initiated from remote consoles are run at level six. One such program displays file ID information and plots data on remote scopes.

One major area of modification which was made to the monitor involves the method of responding to interrupts. Hardware interrupts can be initiated from one of the following six sources: (1) peripheral equipment (teletypes, card reader, paper tape reader/punch, printer, magnetic tape, or disk); (2) internal events (power failure, memory violation, etc.); (3) real-time clock; (4) another computer; (5) the independent variable associated with each instrument (wavelength, time, etc.); and (6) remote console buttons.

The OLERT monitor handles the internal interrupts and contains the driving programs to handle the peripheral equipment and real-time clock, on an interrupt basis. Drivers to process external interrupts from experiment runs [types (5) and (6) above] could have been written, following the procedure used for peripherals, and incorporated into the system; however, this was not done. A rough breakdown

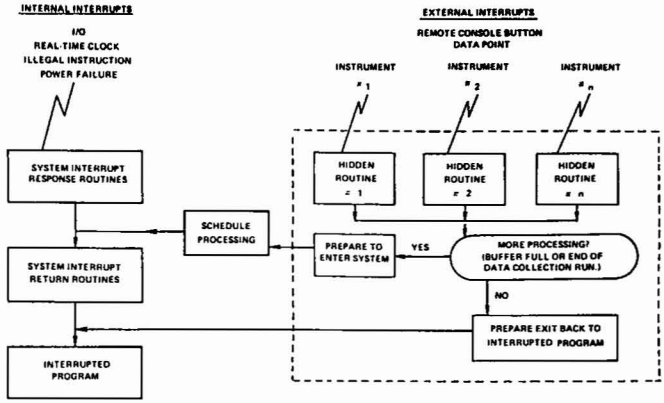

Figure 4. Diagram of software interrupt processing

Programs enclosed in dashes are not under system control

of the time required for executing an analog-to-digital conversion, using a standard system driving program, is the following: 150 μsec (approximately 150 machine cycles) to recognize the interrupt, 300 μsec to execute the A/D conversion and store the value, and 50 μsec to return to the interrupted program. (Actual A/D conversion time is only 35 μsec but the monitor requires that the conversion be scheduled, which results in a large software overhead.) This total time of approximately 500 μsec would limit the overall system data acquisition rate to about 2 KHz.

To allow overall sampling rates considerably above 2 KHz within the system, the executive program was modified to give faster response to data acquisition requests (*3*). This was done by incorporating into the system an interrupt program, for each instrument, which does not run under system control. That is, once it has gained control from the system through the initiation of a hardware interrupt, the special routine (called a "Hidden Routine," since it is hidden from the system) performs the necessary input (normally A/D conversion and input) and returns to the system in the same way a standard interrupt does. Since this hidden routine needs to save and restore only a very few registers, as opposed to the large number saved by the interrupt program provided by the system, and, in general, has much less overhead than that associated with general system interrupt response, it is possible to reduce the response and return time from 500 μsec to less than 100 μsec. Thus, using the Hidden Routine approach, an overall system data collection rate of about 10 KHz can be attained. Actual A/D conversion of data can be initiated as little as 13 μsec from the time of the interrupt as opposed to about 200 μsec using a standard A/D driver.

A hidden routine normally exits back to the system after each point is collected, but when a data buffer is filled the hidden routine branches to another path to first switch buffers and write the last buffer onto the disk before returning to the system. A diagram of the relation between hidden routines and system interrupt processing is shown in Figure 4.

A typical foreground-background use of the system with two FORTRAN programs requiring, say, 1536 and 5120 words of storage, and running simultaneously with data acquisition, might find memory allocated as follows:

Location 0-12797 (25 sectors of 512 words each) OLERT operating system
12800–13311 (3 sectors) FORTRAN program one
16374–21493 (10 sectors) Data Acquisition and ROC communication monitor
21494–26613 (10 sectors) FORTRAN program two

The OLERT and Data Acquisition Systems are permanently resident in the locations indicated, while FORTRAN or other programs are loaded into the remaining available memory as directed by the user.

APPLICATION PROGRAMS

Some basic programs have been written for general use in analyzing the data collected. In general, small scale calculations are done on the local machine and computations requiring a large amount of memory or time will be done on the NIH central computer system located in another building.

One of the programs for processing data gathered from an instrument performs linear operations on spectra, catenates spectra, and does smoothing. The results can be saved and/or printed. The user specifies the name(s) of the file(s) to be manipulated, the option desired, and the name for the resulting file. As with all application programs, this one can be initiated and run while data are being collected.

Other programs are available for further, more complex analyses of data. Once a spectrum has been normalized and a base-line spectrum subtracted, curve fitting calculations can be performed with another program which does a least

(3) J. Buzen, IEEE Computer Group Conference, Minneapolis, Minn., June 1969.

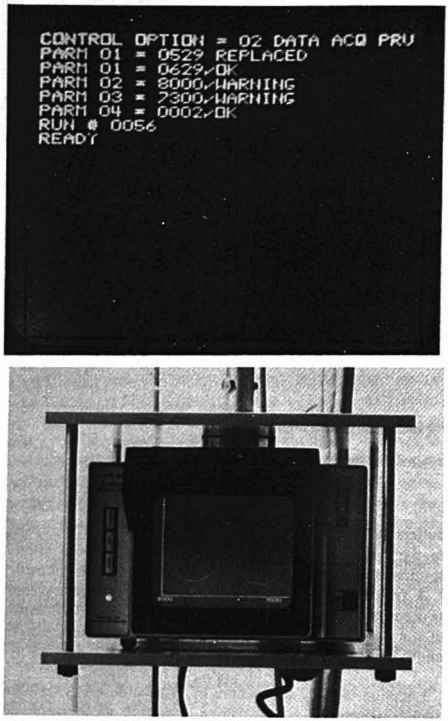

Figure 5. ROC displays during a data acquisition run

At the top, during parameter entry; at the bottom, at the completion of a run

square fit of specified spectra to another spectrum to determine its components.

Raw data or files resulting from the programs just described can be output using a set of general plotting routines which provides scaling and labeling.

There is a continuing effort in the development of applications programs and programs that support data collection. These programs range in complexity from the computation of standard formulas to, in the case of the ultracentrifuge, the detection of subtle patterns in the data. With the ultracentrifuge, some simple pattern recognition will be done in real-time to reduce the volume of data, while more complex analysis will be done after the data are collected.

USE OF THE REMOTE OPERATOR'S CONSOLE

A standard procedure is used for operating the remote consoles. Before beginning operation, the user must check that the SYSTEM UP light is on, which indicates that the console supporting software is operational. SYSTEM UP extinguishes unless refreshed at least once per second by the operating system. If the SYSTEM UP delay is not refreshed prior to timing out, it is assumed that the operating system is no longer in a reliable condition and the laboratory interrupts are disabled in the DADS (hardware). The remaining buttons on the console, SIGN ON, SIGN OFF, HALT, and RUN, are used, respectively, to initiate console use, to terminate console use, to stop data acquisition before the normal end of run, and to initiate data acquisition.

Table II. Control Options Which Can Be Initiated from a Remote Operator's Console

Control option	Function
01	Data Acquisition Run with standard parameters
02	Data Acquisition Run with previous parameters
03	Restart run after Halt
21	Delete a data file
31	Display ID information from file
32	Display data from file
33–39	Initiate specified program

The parameter entry panel is used for entering (or canceling) control option and parameter information. The function of each run is specified by the two digit control option number entered. Currently the system allows the options shown in Table II.

The dialogue is begun by the user pressing SIGN ON. The system responds by asking (on the scope) for the scientist's user number. Each file of data collected is stored on the disk in an area reserved for the user number specified. Following entry of the user number, the system asks for the two digit control option. After the control option is entered, parameter values are requested, the number and meaning of each depending on the control option and laboratory instrument being used. Normally, for a data acquisition run (option 01, 02, or 03), the parameters consist of a file identification number, beginning and end values and sampling increment for the independent variable (wavelength, etc.), and instrument settings. For a data run, the user initializes the instrument properly, presses RUN on the console and starts the instrument scan. Values are collected from the beginning abscissa value specified, using the specified increment, until the final value is reached or HALT is pressed. When a buffer of 25 points is collected, it is displayed on the scope and stored on the disk. The dialogue from a typical data acquisition run, with four parameters, is shown in Figure 5. The figure shows also the display of data at the completion of a run. At the end of a run a new control option can be entered or use of the console can be terminated by pressing SIGN OFF.

The system software tests that parameter values are within an allowed range by comparing them with a table of values prepared for each instrument. If a possible error is detected in information entered from the remote console, a message is displayed on the scope and the CANCEL light is turned on. The message given is only a warning and can be ignored.

FURTHER WORK

Improvements to the present version of the system are being made to make it more responsive to the needs of the scientists and new work is being planned in a number of areas. The connections to other computers (the dotted lines in Figure 1) are now being developed. Communication with them will be controlled by background programs running simultaneously with data acquisition.

The system has the capacity for handling a number of additional instruments using complete parallel I/O techniques. The tables containing information for each instrument are at present permanently core-resident so that the main limita-

tion to adding more instruments is the amount of available memory. In terms of hardware data acquisition capabilities, a total of ten instruments in the slow-to-medium speed range (say, less than 500 points/sec each) could easily be accommodated. When (and if) the number of instruments interfaced to the computer increases to the point where their table information begins to saturate memory, one acceptable solution (and one easy to implement) would be to restrict the number of data collection runs that can be made simultaneously. This number will depend on the characteristics (rates, amount of processing, etc.) of the particular instruments being run.

Instrument control via the computer presents another area for further development of the system. Monitoring and control of a single variable, such as temperature, could be done relatively simply with the present hardware but there is no immediate need for such control with the instruments now interfaced. The development of such control loops will depend on the particular instruments which will be connected in the future.

One complex area to be analyzed involves obtaining better system performance through modification of the instruments. In many instruments the mechanism for producing a chart record restricts the speed of scanning and, in addition, is a limiting part of the control network. Increased speed and greater signal resolution, if obtained, could lead to the need for analog to digital conversion at the instrument.

Presently, only instruments located within the building can be connected to the computer because of the parallel transmission of signals. It is conceivable that a simple telemetering system could be designed and implemented that would allow the multiplexing of digital control and data signals over a low capacity telephone line or dedicated transmission cable. This would allow expansion of the system beyond the confines of the present location.

ACKNOWLEDGMENT

We acknowledge the contributions of a number of coworkers to the design and implementation of the system—in particular the contributions of William Holsinger, who designed the DADS unit; Jay Vinton, who wrote the software system for utilizing the remote consoles; Jeff Buzen, who wrote the programs for improving interrupt response time; and Mrs. Marie Chang and Dr. Richard Simon who provided much of the system and application software.

RECEIVED for review September 23, 1970. Accepted December 15, 1970.

Digital Methods of Photopeak Integration in Activation Analysis

Philip A. Baedecker

Department of Chemistry and Institute of Geophysics and Planetary Physics, University of California, Los Angeles, Calif. 90024

A study of the precision attainable by several methods of gamma-ray photopeak integration has been carried out. The "total peak area" method, the methods proposed by Covell, Sterlinski, and Quittner, and some modifications of these methods have been considered. A modification by Wasson of the total peak area method is considered to be the most advantageous because of its simplicity and the relatively high precision obtained. A computer routine for the analysis of spectral data from nondestructive activation analysis experiments employing a Ge(Li) detector–spectrometer system is described. The routine processes the spectral data, applies appropriate corrections for decay, and provides a readout in concentration units.

THE PRECISION OBTAINABLE in an activation analysis experiment is to a large degree dependent on the precision with which the analyst can determine radionuclide abundance from counting data, most often obtained from gamma-ray spectrometry. Several methods of photopeak integration have been proposed and evaluated in the literature. Some of these treat the digital data directly (*1–6*), while others fit the data to a function and integrate that function to determine peak area (*7–9*). In developing computer programs for reducing activation analysis data, I have evaluated several digital methods for photopeak integration.

Methods of Analysis. Seven methods of peak area estimation have been examined in the present study. These methods are illustrated diagrammatically in Figure 1 [with the exception of method (g) described below], and are summarized by the following equations:

(a) Total Peak Area method (TPA):

$$A = \sum_{i=l}^{i=r} a_i - (a_l + a_r) \times (r - l + 1)/2$$

where

a_i = number of counts accumulated in channel i
l = channel number at left hand limit of photopeak
r = channel number at right hand limit of photopeak

(b) A modification by Wasson of the TPA method (*10*):

$$A = \sum_{i=-n}^{i=+n} a_i - \left(n + \frac{1}{2}\right)(b_n + b_{-n})$$

where

n = the number of channels on the left and right from channel zero (the centermost channel)
b_n = the background in channel n as determined from a straight line drawn between channels l and r (the left and right hand limits of the peak)

(1) D. F. Covell, ANAL. CHEM., **31**, 1785–90 (1959).
(2) S. Sterlinski, *ibid.*, **40**, 1995–8 (1968).
(3) *Ibid.*, **42**, 151–5 (1970).
(4) P. Quittner, *ibid.*, **41**, 1504–6 (1969).
(5) H. P. Yule, *ibid.*, **40**, 1480–6 (1968).
(6) P. Quittner, *Nucl. Instrum. Methods*, **76**, 115–24 (1969).
(7) R. G. Helmer, R. L. Heath, M. Putnam, and D. H. Gipson, *ibid.*, **57**, 46–57 (1967).
(8) J. T. Routti and S. G. Prussin, *ibid.*, **72**, 125–42 (1969).
(9) L. Varnell and J. Trischuk, *ibid.*, **76**, 109–14 (1969).
(10) J. T. Wasson, private communication,

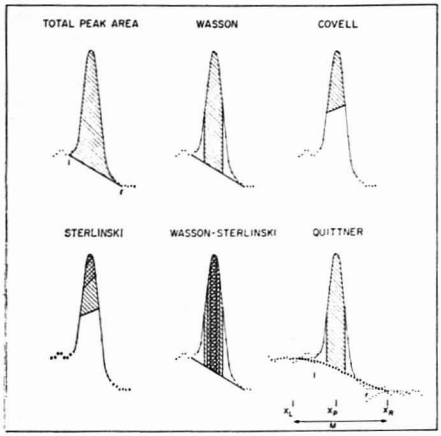

Figure 1. Six of the seven methods of photopeak integration employed in this study

(c) Covell's method (*1*):

$$A = \sum_{i=-n}^{i=+n} a_i - \left(n + \frac{1}{2}\right)(a_n + a_{-n})$$

(d) Sterlinski's method (*2, 3*):

$$A = na_o + \sum_{j=1}^{n} \left(n - 2j + \frac{1}{2}\right)(a_{-j} + a_j)$$

(e) A combination of the Wasson and Sterlinski methods:

$$A = na_o + \sum_{j=1}^{n} (n - j + 1)(a_{-j} + a_j) - \sum_{j=1}^{n} \left(j + \frac{1}{2}\right)(b_{-j} + b_j)$$

(f) Quittner's method:

$$A = \sum_{i=-n}^{i=+n} (a_i - C_i)$$

where

C_i = the background in channel i as determined from the following expression provided by Quittner (*4, 6*)

$$C_i = p_l + q_l(X_p + i - X_L) + \left[\frac{3(p_r - p_l)}{M^2} - \frac{(q_r + 2q_l)}{M}\right](X_p + i - X_L)^2 + \left[\frac{2(p_l - p_r)}{M^3} + \frac{(q_r + q_l)}{M^2}\right](X_p + i - X_L)^3$$

where

$2k + 1$ channels are fitted to a quadratic on each side of the photopeak
X_L and X_R are the center channels in the left and right quadratics, respectively ($X_L = l - k$, $X_R = r + k$)
X_p is the centermost channel
p_l and p_r are the values of the quadratics at X_L and X_R
q_l and q_r are the slopes of the quadratics at X_L and X_R
$M = X_R - X_L$

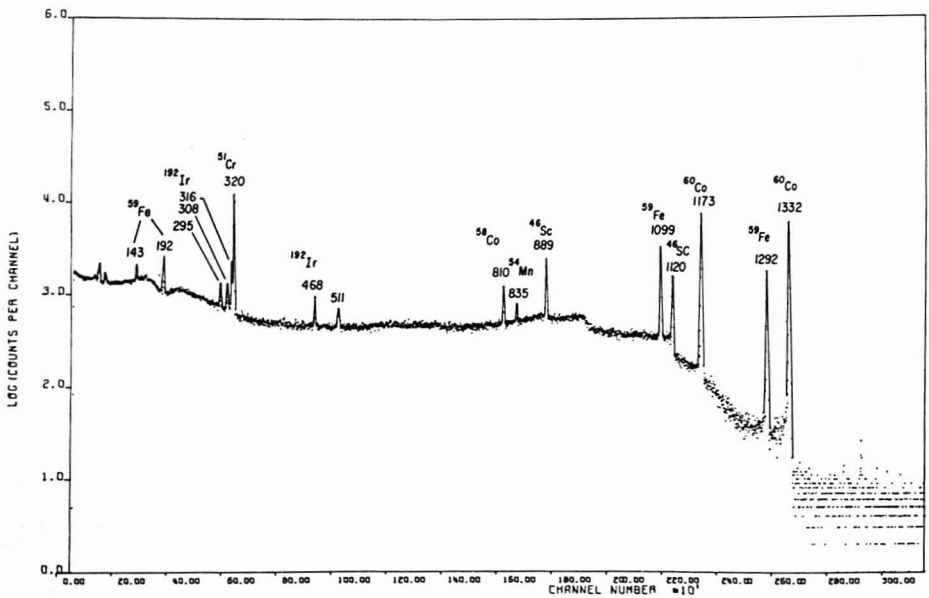

Figure 2. Gamma-ray spectrum of the Allende chondrite, two weeks following irradiation

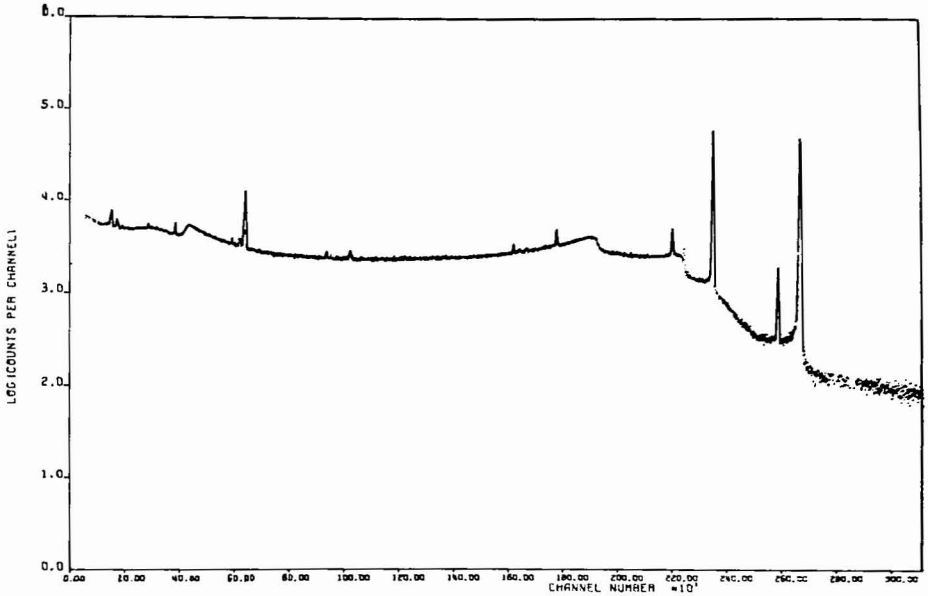

Figure 3. Gamma-ray spectrum of the Allende chondrite plus a ^{60}Co source

^{60}Co activity is 8.3 times the activity measured in the spectrum in Figure 2

(g) A combination of the Sterlinski and Quittner methods:

$$A = na_0 + \sum_{j=1}^{n} (n - j + 1)(a_{-j} + a_j) - \sum_{j=1}^{n} \left(j + \frac{1}{2}\right)(C_{-j} + C_j)$$

Methods a, c, d, and f have been previously described and evaluated (*1–6*). The TPA method of integration (a) achieves the greatest total number of counts for a given peak. Wasson has modified this method (b) to allow for the fact that while the channels in the wings of the photopeak add considerably to the error of a peak integration, they add little to the net number of counts (*10*). Covell's method (c) has the theoretical advantage over the total peak area method that only those channels which have the smallest relative standard deviation are used in the analysis, and uncertainties with regard to choosing the best base line are removed. Sterlinski's method (d) is based on the observation that the calculated relative standard deviation (based on counting statistics) for the calculated intensity of a photopeak will be smaller by giving increasingly greater weight to those channels which have increasingly greater total accumulated counts. However, both Covell and Sterlinski have failed to consider the fact that the calculated variances using their techniques are increased by virtue of the fact that the summation is carried out using a relatively high base line, rather than one drawn across the limits of the photopeak. For example, using Covell's method the variance on the area can be calculated as

$$V_{(c)} = \sum_{i=-(n-1)}^{i=(n-1)} a_i + \left(n - \frac{1}{2}\right)^2 (a_n + a_{-n})$$

whereas in Wasson's method

$$V_{(b)} = \sum_{i=-(n-1)}^{i=(n-1)} a_i + (a_n + a_{-n}) + \left(n + \frac{1}{2}\right)^2 (b_n + b_{-n})$$

and if

$$a_n \gg b_n,\ V_{(c)} > V_{(b)}$$

Quittner's approach employs a nonlinear base-line subtraction technique. Several channels (Quittner recommends using between 15 and 23 channels) are taken on each side of the peak, to the left and right of the peak limits, and the data points fitted to second-order polynomials using the methods described by Savitzky and Golay (*11*). The calculated values and slopes of the polynomials at the center channels are used to define a cubic equation which describes the base line under the peak. Quittner points out that his technique gives greater precision than Covell's method. However, this would be expected, since the base line is lower. Whether or not Quittner's technique would provide greater precision than methods (a) or (b) is not immediately apparent. If the modified version of Sterlinski's technique provides greater precision than Wasson's method (as would be expected from purely statistical considerations), the combination of Sterlinski's and Quittner's approaches should provide greater precision than either method alone.

(11) A. Savitzky, and M. J. E. Golay, ANAL. CHEM., **36**, 1627–39 (1964).

Table I. Relative Standard Deviations for Integrations of 12 Counts of Nine Photopeaks by Seven Methods of Photopeak Integration

Peak	Method (*)	Full peak (a)	Wasson (b)	Covell (c)	Sterlinski (d)	Wasson–Sterlinski (e)	Quittner (f)	Quittner–Sterlinski (g)
308	(2312)	5.48	4.51	6.65	6.11	4.39	45.06	43.21
468	(2039)	5.88	5.04	5.53	6.32	4.82	5.12	4.92
810	(3316)	3.80	2.39	4.14	5.15	1.77	3.08	2.51
889	(8007)	2.49	1.62	3.73	3.80	1.72	1.57	1.74
1099	(12746)	1.65	1.35	3.49	3.86	1.49	1.42	1.53
1120	(5813)	2.18	1.67	3.06	3.77	1.60	1.16	1.27
1173	(32700)	0.73	0.71	2.39	3.80	0.77	0.69	0.76
1292	(8051)	1.47	0.93	2.82	3.77	0.82	0.99	0.87
1332	(28391)	0.85	0.74	1.92	2.12	0.81	0.73	0.81

* Peak area as measured by Wasson's method.

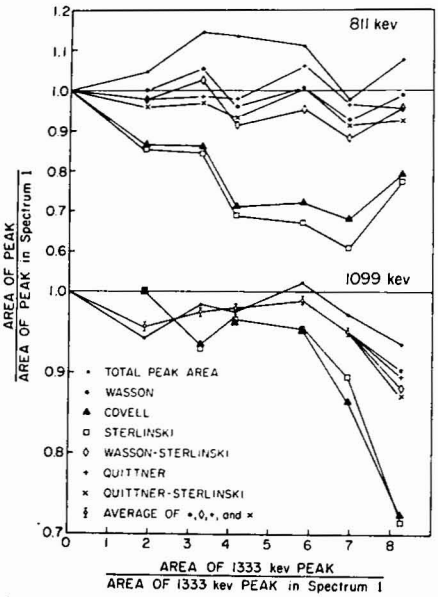

Figure 4. Variation in measured photopeak intensity for the 811-KeV and 1099-KeV photopeaks, for the seven methods studied, with increasing ^{60}Co activity

Data points are the measured areas relative to the intensities of the photopeaks in the irradiated chondrite counted alone

EXPERIMENTAL

An 0.5-g sample of a chondritic meteorite (Allende) was irradiated for 3 hours at a flux of 2×10^{12} n/cm^2/sec in the UCLA reactor. After the sample was allowed to decay for 2 weeks, it was counted 12 times in succession, using a Ge(Li) detector which has a resolution of 2.4 KeV for the 1333 KeV photopeak of ^{60}Co, and an efficiency of 6.4% relative to a 3-inch × 3-inch NaI(Tl) detector at 25 cm. The detector was coupled to a 4096 channel analyzer, and the resulting spectra read out onto punched paper tape for computer processing. A typical spectrum is shown in Figure 2. The principle activities are ^{46}Sc, ^{51}Cr, ^{59}Fe, ^{58}Co, ^{60}Co, and ^{192}Ir. The meteorite sample was also counted seven times with increasing amounts of ^{60}Co.

A computer program was written to process the spectral data by any one of the several methods listed above. The program could first smooth the spectral data by the method of Savitzky and Golay (*11*, *12*), or the smoothing routine could be bypassed. The program then determined the first derivative at each channel, and used the first derivatives to locate photopeaks and determine the peak limits (*5*, *13*). Compton edges were eliminated from consideration by finding the maximum value of the first derivative on the left side of each peak and the minimum value on the right, and requiring that the absolute values be the same within ±50%. As each photopeak in the spectrum was located and the peak limits determined, its area was estimated by one of the methods previously described.

For methods (b) through (g), n (the number of channels on each side of the centermost channel used in the summation) was set equal to 3. In Quittner's method, k (the number of channels to the left and right of the boundary channels X_L and X_R fitted to a quadratic) was set equal to 7. In methods (a), (b), and (e), the number of counts in the background channels l and r was taken to be the average of the counts accumulated in three channels on each side of the photopeak $(l, l-1, l-2)$ and $(r, r-1, r-2)$. In each case the spectra were smoothed before processing.

RESULTS AND DISCUSSION

In order to measure the precision of each method of analysis, the standard deviation for each photopeak appearing in the spectrum of the irradiated meteorite was calculated from the 12 successive counts of the meteorite sample. The results are summarized in Table I. As anticipated from the considerations above based on counting statistics, for each photopeak (with the exception of the 309 KeV peak of ^{192}Ir) the methods proposed by Covell and Sterlinski showed poorer precision than the other five methods. The total peak area method gave consistently poorer results than methods (b), (e), (f), and (g), which indicates that including the channels in the lower part of the photopeak in the peak area estimation may lead to a loss of precision. The large per cent standard deviations observed for Quittner's method and the Sterlinski–Quittner method for the 309-KeV photopeak were due to the fact that the right quadratic was fitted to a portion of the 317 KeV ^{192}Ir photopeak. As Quittner points out, his method is useful only when the photopeaks are separated by greater than about 20 channels. For all other photopeaks the precisions obtained using methods (b), (e), (f), and (g) were comparable although on the average, the Wasson–Sterlinski method was slightly better.

(12) H. P. Yule, *Nucl. Instrum. Methods*, **54**, 61–5 (1967).
(13) H. P. Yule, ANAL. CHEM., **38**, 103–5 (1966).

Table II. Relative Standard Deviations for Integrations of Seven Photopeaks by Seven Methods of Photopeak Integration, Based on Seven Counts, with Each Count Having Increasing Activities of ^{60}Co

Peak	Method	Full peak (a)	Wasson (b)	Covell (c)	Sterlinski (d)	Wasson–Sterlinski (e)	Quittner (f)	Quittner–Sterlinski (g)
308	[a]	23.90	20.62	41.11	56.97	13.19	32.59	30.94
468	[b]	6.23	4.02	8.09	10.0	4.21	5.65	5.17
810		6.12	4.18	14.01	17.16	5.18	3.58	3.65
889		6.44	4.51	6.08	7.02	4.48	4.90	4.88
1099		2.82	3.32	10.72	10.78	4.19	3.67	4.52
1120		8.39	8.46	9.79	10.50	8.63	9.75	9.75
1292		2.19	3.05	8.33	9.28	3.64	2.98	3.53

[a] Determined from four spectra.
[b] Determined from five spectra.

Table III. Observed Standard Deviations of Integrations of 12 Counts of Nine Photopeaks by the Wasson Method Compared with That Expected from Counting Statistics

	Photopeak, KeV	308	468	810	889	1099	1120	1173	1292	1332
Rel std dev, %	Obsd	4.51	5.04	2.39	1.62	1.35	1.67	0.71	0.93	0.74
	Calcd	6.92	5.95	4.11	2.01	1.20	2.05	0.59	1.19	0.60

Since the relatively poor precision observed for Covell's method, and the modification of Covell's method proposed by Sterlinski, is caused by choosing relatively high base lines, the precision obtainable using either technique could be increased by carrying out the integration over a greater number of channels. Yule (*5*) has shown that Covell's method can provide comparable precision to the TPA method if similar boundary channels are chosen. Selecting integration limits which are too narrow or too broad will result in a loss of precision. The effect of using wider boundaries on Sterlinski's method was investigated by allowing n in Equation (d) above to range from 3 to 14. When the integration was carried out well past the wings of the photopeak, the precision was found to be comparable to that obtained by methods (b), (e), (f), and (g), although on the average the precision was less than that of the Wasson–Sterlinski method. Increasing the number of channels used in the integrations by the Wasson or Wasson–Sterlinski techniques did not systematically affect the observed precision.

One would expect that any benefit to be derived from Quittner's technique would be most apparent where the background varies under the photopeak. This situation arises most markedly in our spectra for the 1120-KeV photopeak of ^{46}Sc (which was plotted in Figure 1), which sits on the Compton edge of the 1333-KeV peak of ^{60}Co. It can be seen from Table I that for this photopeak Quittner's method does, in fact, show the lowest relative standard deviation on the various methods of photopeak estimation.

In order to check the performance of the various methods when the shape of the spectrum was changing, the meteorite sample was counted seven times with increasing amounts of ^{60}Co. During this part of the experiment, the deadtime of the analyzer increased from 5 to 20% and the integrated area of the 1333-KeV photopeak of ^{60}Co increased by a factor of 8.3. The last spectrum is shown in Figure 3. The seven spectra were treated in the same way as the 12 spectra accumulated in the first part of the experiment, and the results are summarized in Table II. The computer routine employed in reducing the data failed to locate the 308-KeV photopeak in three of the spectra, and the 468-KeV peak in two of the seven spectra. Again, the methods proposed by Covell and Sterlinski (where n was set equal to 3) yielded consistently poorer results than the other methods. The precision obtained using the remaining five methods was comparable. In general, Wasson's method showed the best precision, although for the higher energy photopeaks at 1099, 1121, and 1293 KeV, the observed relative standard deviations were lowest for the total peak area method. This may be partly due to a loss of resolution at higher deadtimes. The width of the 1099-KeV photopeak of ^{59}Fe increased from 2.3 KeV in the first spectrum to 2.5 KeV in the last.

It is of interest to see how the quantity (peak area/peak area in spectrum 1) varies for the various methods as one increases the activity due to ^{60}Co. Figure 4 shows a plot of this quantity plotted against (area of 1333 peak of ^{60}Co/area of 1333 peak in spectrum 1) for the photopeaks at 811 KeV and 1099 KeV which were the least and most intense photopeaks in the spectrum other than those from ^{60}Co and ^{192}Ir. For the 1099 KeV photopeak, the points for methods (b), (e), (f), and (g) virtually overlap in all spectra except the last, and in these cases, average values for the four methods are plotted, the bars showing the range of values observed. The same behavior was observed in similar plots for the 889, 1121, and 1292 KeV photopeaks (not shown). In general, the quantity (peak area/peak area in spectrum 1) decreases for all methods with increasing activity due to ^{60}Co. (This decrease is more pronounced for the 889, 1121, and 1292 KeV photopeaks than for those plotted in Figure 4.) In all cases the decrease is more rapid for Covell's and Sterlinski's methods than for the other techniques studied. For the last three spectra in the series (with the highest amounts of ^{60}Co), the decrease is least for the TPA method. Therefore, in activation analysis experiments where there are large differences in deadtime between sample and flux monitor, and where changes in resolution may be a problem, the TPA method appears to be the best choice. This observation has previously been made by Yule (*5*).

The fact that the more complex methods proposed by Sterlinski and Quittner did not provide significantly greater precision than the more simple methods leads us to generally favor the Wasson technique for peak area estimation. In general, the observed relative standard deviations for the various photopeaks based on the 12 repeated counts of the meteorite sample, and integrated by the Wasson method, are close to the standard deviations expected based on counting statistics alone, as shown in Table III.

The Wasson method described above is used routinely in

our laboratory in a computer routine (SPECTRA) for processing activation analysis data. (The TPA method is included as an option in the program.) The spectral data are recorded on punched paper tape, along with spectra of appropriate gamma-ray standards. After searching out a photopeak, as described above, the centroid of the peak is determined using the method of Savitzky and Golay (*11*), and the energy of the photopeak determined using the energy calibration provided by the analysis of the gamma-ray standards. Thus, the energy and intensity of the photopeaks in each spectrum are determined. The energies of the photopeaks to be used in the activation analysis experiments are read in on cards, along with the half-lives of the corresponding radionuclides and the concentration of the element in the flux monitor. A second set of data cards lists the sample or flux monitor weight, time of day that the count of the sample was started, live time duration, and, when appropriate, clock time duration, for each spectrum on the tape. The program first analyzes the flux monitor spectra and calculates the "specific counting rates" for each photopeak. The program makes corrections for decay, and, for the case where very short-lived isotopes are being measured, for the variations in deadtime of the analyzer. When the flux monitor spectra have been processed, the sample spectra are processed and the concentration of each element in each sample is calculated.

ACKNOWLEDGMENT

The author wishes to thank Dr. John T. Wasson for helpful discussions during the course of this work.

RECEIVED for review August 10, 1970. Accepted December 21, 1970. This work was supported by the National Aeronautics and Space Administration under contract NAS 9-8096.

Potentiometric Studies with an Ion Permselective Membrane

Sudarshan Lal and Gary D. Christian

Department of Chemistry, University of Kentucky, Lexington, Ky. 40506

A dithizone-containing membrane is described which shows varying degrees of permselectivity to a large number of cations and anions, including mono-, di-, and trivalent ions. It has been used successfully for the potentiometric monitoring of precipitation, chelometric, redox, acid-base, and nonaqueous titrations. Relative selectivities of the membrane toward different ions are used to interpret different shapes of titration curves. Effects of sample concentration, organic solvents, and extraneous salts on the shapes of titration curves are reported. The effect of the membrane plasticizer on permselectivity to different ions and on titration curves has been studied. The membrane is stable for several months, except when used in purely nonaqueous solvents.

A GOOD DEAL OF INTEREST has developed during the past decade in the prospective use of ion selective electrodes for monitoring various ions. Several membranes that have been used as ion sensing devices have recently been summarized by Rechnitz (*1*). A number of membranes have been used successfully for potentiometric titrations; some exhibit Nernstian response but others do not. Some recently described membranes include ion exchange membranes (*2–6*) used for certain acid–base and precipitation titrations, and the barium arsenate impregnated parchment paper membrane of Liteanu *et al.* (*7*) used for limited acid–base titrations. Reviews of ion exchange membrane electrodes have been presented by Gregor (*8*), Spiegler (*9*), and Lakshminarayanaiah (*10*).

Bloch, Kedem, Vofsi, and coworkers (*11–16*) have described membranes in which permeability is made possible by specific solvation or complexation of a particular permeant by the membrane matrix. These are the so-called solvent membranes. They have been used for separation of iron(III) from aluminum(III) in high concentrations of hydrochloric acid(II) and for the separation of uranyl nitrate from a mixture containing iron and aluminum (*12*). In the former case, the active membrane contains an alkyl-phosphoric ester such as tributyl phosphate, which selectively "extracts" the uranyl nitrate. The ester also serves as a plasticizer for the polymeric polyvinyl chloride matrix. These membrane separations have been likened to solvent extraction systems, hence the name "solvent membrane." Recent evidence (*17*) has indicated that the mechanism of transport involves distribution of the metal ion at the aqueous solution–membrane interface and the rate (kinetics) of complex formation in the membrane.

Solvent membranes have recently received attention as possible active ion selective membranes in electrodes. Bloch, Shatkay, and Saroff (*18*) described a calcium selective electrode in which the membrane consisted of polyvinyl chloride, tributyl phosphate as plasticizer, and thenoyltrifluoroacetone as the selective chelating agent. The electrode showed high selectivity for calcium in the presence of sodium, magnesium,

(1) G. A. Rechnitz, *Chem. Eng. News*, **43** (25), 146 (1967).
(2) F. P. Ijssling and E. van Dalen, *Anal. Chim. Acta*, **36**, 166 (1966).
(3) *Ibid.*, **40**, 421 (1968).
(4) *Ibid.*, **43**, 77 (1968).
(5) J. S. Parson, ANAL. CHEM., **30**, 1262 (1958).
(6) S. K. Sinha, *J. Indian Chem. Soc.*, **32**, 36 (1955).
(7) C. Liteanu, M. Mioscu, and I. Popescu, *Rev. Roum. Chim.*, **13**, 569 (1968).
(8) H. P. Gregor, *Ann. Rev. Phys. Chem.*, **8**, 463 (1957).
(9) K. S. Spiegler, "Ion Exchange Technology," F. C. Nachod and J. Schubert, Ed., Academic Press, New York, N. Y., 1956, pp 118–181.
(10) N. A. Lakshminarayanaiah, *Chem. Rev.*, **65**, 491 (1965).
(11) R. Bloch, O. Kedem, and D. Vofsi, *Nature*, **199**, 802 (1963).
(12) R. Bloch, A. Finkelstein, O. Kedem, and D. Vofsi, *Ind. Eng. Chem., Process Des. Develop.*, **6**, 231 (1967).
(13) R. Bloch, A. Katchalsky, O. Kedem, and D. Vofsi, U. S. Patent **3,450,630**, June 1969.
(14) *Ibid.*, **3,450,631**.
(15) R. Bloch, A. Katchalsky, O. Kedem, and D. Vofsi, Brit. Patent **1,049,041** (1966).
(16) Yeda Research and Development Co., Ltd., *ibid.*, **1,090,096** (1967).
(17) D. Vofsi, O. Kedem, R. Bloch, and S. Marian, *J. Inorg. Nucl. Chem.*, **31**, 2631 (1969).
(18) R. Bloch, A. Shatkay, and H. A. Saroff, *Biophys. J.*, **7**, 865 (1967).

and barium, as confirmed by Stucky, Johnson, and Sutula (*19*).

The present communication describes a plastic membrane impregnated with dithizone which has been found to be permselective toward a large variety of ions, including mono-, di-, and trivalent cations or anions. Because of this permselectivity, the electrode has been successfully employed for potentiometric precipitation titrations, acid–base titrations, redox titrations, complexometric titrations, and nonaqueous titrations. The effects of extraneous salts, organic solvents, and membrane composition are reported.

EXPERIMENTAL

All chemicals employed in this investigation were of reagent grade and their solutions were prepared with deionized distilled water by standard analytical procedures. The solutions were stirred during titration by means of a Teflon-coated (DuPont) magnetic bar, and the measurements of potentials were made with a Keithley 610-B Electrometer. All cables were shielded and the cell assembly was placed in a copper gauze cage in order to ensure stable reading and adequate grounding. The potential differences were measured *vs.* the SCE (Beckman sleeve type) and solutions were connected through a saturated NH_4NO_3–agar salt bridge with the cell:

SCE| $10^{-3}M$ $Pb(NO_3)_2$| Membrane|

Sample solution	Satd NH_4NO_3 Agar Bridge	SCE (sleeve type)

The membrane was prepared as follows: (Available from Miles Laboratories, Inc., Ames Company Division, Elkhart, Ind., as Membrane #10980.) Dithizone, 40 mg, were dissolved in 6 ml of the plasticizer, dipentylphthalate (DPP). 5% polyvinyl chloride, 40 ml, in cyclohexanone (wt/vol) were added to this and mixed thoroughly. The mixture was cast on a clean glass plate (8-inch × 8-inch) and was allowed to dry in the dark in a draftless area. The dried membrane was cut circularly for mounting in a Teflon probe. The diameter of the exposed membrane was 8 mm.

The probe was filled with $10^{-3}M$ lead nitrate solution. The electrode was stored in the open for 48 hours for preconditioning of the membrane. During this time the membrane turned red, because of formation of the lead dithizone chelate. The formation of the lead chelate stabilizes the dithizone against oxidation. It may also be involved in an ion exchange mechanism for determining the potential. A saturated calomel electrode was used as the internal reference electrode by dipping in the $10^{-3}M$ lead ion solution.

The potential readings on the stirred solutions were recorded after an interval of 1–2 minutes.

Other plasticizers investigated were diphenylphthalate, di-*n*-octylphthalate (DOP), and di-(2-ethylhexyl)isophthalate (DEI). Except when noted, all studies were made using the DPP membrane.

RESULTS AND DISCUSSION

Relative Selectivities of Electrode toward Various Cations and Anions. The relative millivolt readings of the membrane in $10^{-1}M$ and $10^{-2}M$ solutions of several cations and anions are summarized in Table I. Solutions of the cations were all prepared from the nitrates unless otherwise specified, while solutions of the anions were prepared from the potassium salts. Cations cause the potential to increase with increased concentration while anions cause the potential to decrease. From the titration curves described below, the relative changes in the potential upon a tenfold increase in concentration appear to give a fairly good indication of the permselectivity of the membrane toward the various ions. In some cases, however, and in principle, it depends to some extent on their relative initial readings at a given concentration. A negative change in potential for a cation upon increased concentration indicates that the membrane is more permselective toward nitrate ion than for the cation. The reverse is true for anions, *i.e.*, a positive change in potential means the membrane is more selective toward potassium ion than to the anion.

Table I. Dipentylphthalate Membrane Response to Various Cations and Anions

	Potential, mV		
Cations	$10^{-1}M$	$10^{-2}M$	ΔE, mV
Ag^+	195.0	244.5	49.5
Tl^+	84	115	31
H^+	−13	16	29
Cs^+[a]	39	34	−5
K^+	24	10	−14
Rb^+[a]	66	36	−30
Na^+	36	2	−34
Cu^{2+}	−26	3	29
Ni^{2+}	−38	−33	5
Pb^{2+}	63	67	4
Ca^{2+}	1.5	−6.5	−8.0
Zn^{2+}	−29	−41	−12
Mg^{2+}	−19.5	−33.0	−13.5
Ba^{2+}	42	22.5	−19.5
Sr^{2+}	46.5	15.0	−31.5
La^{3+}	69	63	−6
Al^{3+}	50	42	−8
Anions			
MnO_4^-	97	22	−75
SCN^-	3.9	−15.2	−19.1
NO_3^-	24	10	−14
Cl^-	37	26	−11
I^-	−18	−25.5	−7.5
Br^-	7.5	1.2	−6.3
F^-	17	13	−4
OH^-	−105	−93	12
SO_4^{2-}	13	4	−9
$Cr_2O_7^{2-}$	90	85	−5
$C_2O_4^{2-}$	−47	−33	14

[a] Chloride salt.

It should be pointed out that the measured potentials, as seen from Table I, do not appear to be Nernstian in nature. The potentials are actually bi-ionic potentials; bi-ionic is defined here to mean that the electrode responds to both cations and anions simultaneously. Hence, it is difficult to determine whether the electrode response to a particular ion is Nernstian. The change in potential upon change in a given ion concentration will depend on the counter ion of the salt used. In view of the limited understanding of bi-ionic potentials, a quantitative interpretation of the measured potentials and, consequently, of permselectivities is not possible. This is the reason the primary use of the membrane is restricted to measurements of potential changes (potentiometric titrations) as opposed to direct potentiometric measurements.

Direct comparisons of relative permselectivities toward ions of different valences cannot be made because of the change in the cation:anion ratio with changing valences. Also, monovalent ions should in principle show twice the

(19) G. L. Stucky, D. H. Johnson, and C. L. Sutula, 157th National Meeting of the American Chemical Society, April 13–18, 1969, Minneapolis, Minn.

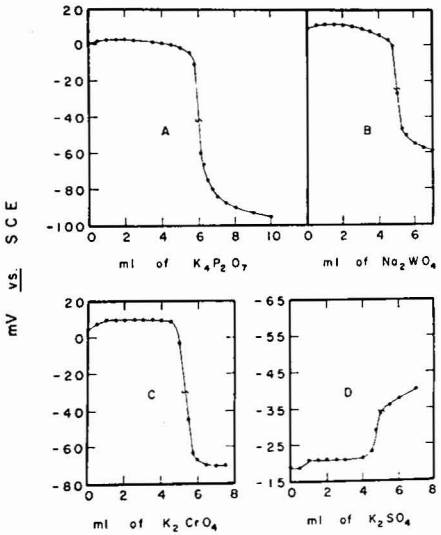

Figure 1. Titration of 50 ml of 0.01*M* $Pb(NO_3)_2$

A. With $K_4P_2O_7$
B. With Na_2WO_4
C. With K_2CrO_4
D. With K_2SO_4

response that divalent ions show, etc. Based upon the potential changes, the membrane has the following approximate order of permselectivity toward monovalent cations: $Ag^+ \gg Tl^+ = H^+ \gg Ca^+ > K^+ > Rb^+ > Na^+$. The permselectivity toward divalent cations is: $Cu^{2+} \gg Ni^{2+} = Pb^{2+} > Ca^{2+} > Zn^{2+} \simeq Mg^{2+} > Ba^{2+} > Sr^{2+}$. Al^{3+} and La^{3+} show about equal response. Monovalent anions show the order: $MnO_4^- \gg SCN^- > NO_3^- > Cl^- > I^- \simeq Br^- > F^- > OH^-$. Divalent anions show the order: $SO_4^{2-} > Cr_2O_7^{2-} > CrO_4^{2-}$.

Precipitation Titrations. TITRATIONS OF LEAD ION. The titration curves for the titration of lead with a number of precipitating agents are shown in Figure 1. The equivalence points are indicated on the titration curves. A well defined S-shaped curve was obtained for the titration of lead with pyrophosphate, tungstate, chromate, sulfate, oxalate, and ferrocyanide. It is likely that larger potential breaks can be obtained by adding an organic solvent, as has been reported for the potentiometric titration of lead with sulfate (*20*). The potassium or sodium salts of the precipitating agents were used and the electrode responses to these ions were sufficiently small compared to lead ion that they had little effect on the shape of the titration curve. The magnitude of the potential break at the end point was, in general, a function of a combination of the solubility of the lead salt and the response of the electrode to the precipitating anion beyond the end point. The more insoluble the precipitate and the greater the electrode response to the anion, the larger should be the break. In several cases, the potential increased slightly at the beginning of the titration and then decreased.

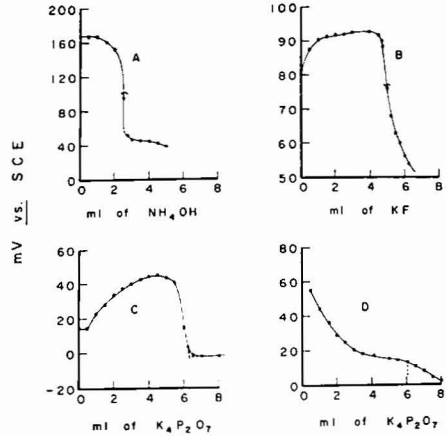

Figure 2.

A. Titration of 50 ml of 0.01*M* $Al_2(SO_4)_3$ with NH_3
B. Titration of 50 ml of 0.01*M* $La(NO_3)_3$ with KF
C. Titration of 50 ml of 0.01*M* $Zn(NO_3)_2$ with $K_4P_2O_7$
D. Titration of 50 ml of 0.01*M* $Mg(NO_3)_2$ with $K_4P_2O_7$

In titrations with iodide, an initial large drop in potential was recorded followed by a gradual decrease until the end point. Titrations with potassium iodate were not successful.

TITRATIONS WITH SILVER ION. Since the membrane displays a high degree of selectivity toward silver ion, titrations utilizing silver were performed with several reagents. A large potential break was obtained for the titration of silver with iodide ion and vice versa.

A mixture of $10^{-2}M$ KCl and KI was titrated with a standard solution of $AgNO_3$. The titration curve exhibited two inflection points at the stoichiometric values. The first break corresponded to iodide and the second one to the chloride. However, no separate inflection point could be achieved with a mixture of iodide, bromide, and chloride. Martin (*21*) reported that total halide can be determined accurately, but individual halide determinations are generally in error because of mixed halide precipitation and adsorption of halides onto the precipitates.

Titrations of mixtures of silver and lead with KCl or KI were attempted. A large potential break was obtained corresponding to the silver end point. Even though the lead chloride or iodide could be seen to precipitate beyond the silver end point, no second break for the lead end point and no distortion of the silver end point occurred. This was due to the fact that the membrane is very much more responsive for silver than for lead and even the small concentration of free silver ions beyond the end point, combined with the relatively high solubility of lead chloride and iodide, was sufficient to suppress the lead end point break. A mixture of iodate and chloride was titrated with a standard silver nitrate solution. Two inflection points were obtained with the first corresponding to the chloride end point.

Titration of silver with thiocyanate exhibited a large potential break. Silver was titrated with thioacetamide as follows. A buffer solution of pH 5 was prepared by mixing

(20) J. W. Ross and M. S. Frant, ANAL. CHEM., **41**, 967 (1969).

(21) H. J. Martin, ANAL. CHEM., **30**, 233 (1958).

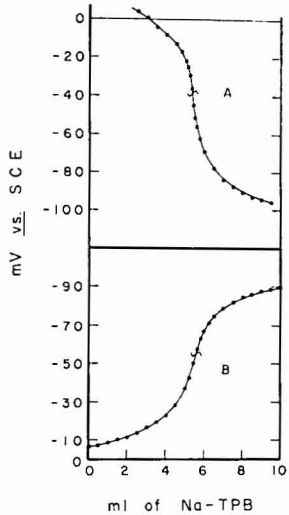

Figure 3.

A. Titration of 25 ml of 0.01*M* RbCl with NaTPB
B. Titration of 25 ml of 0.01*M* KCl with NaTPB

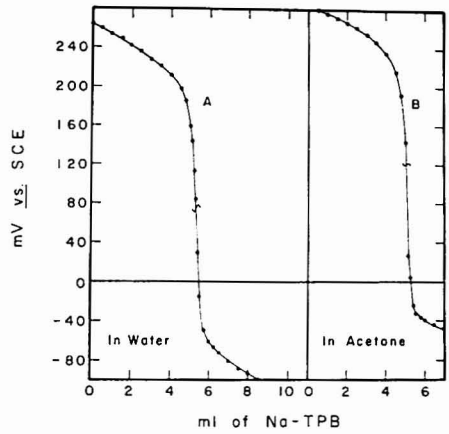

Figure 4.

A. Titration of 25 ml of 0.01*M* $AgNO_3$ in water with NaTPB in water
B. Titration of 25 ml of 0.01*M* $AgNO_3$ in 50% acetone with NaTPB in 50% water

0.1*M* potassium acid phthalate and 0.05*M* trisodium phosphate solutions in the ratio of 50 to 24 parts by volume and 0.5 gram of powdered thymol per liter was added as a bactericide. A 0.2*N* stock solution of thioacetamide was prepared in the above buffer solution. The thioacetamide was standardized potentiometrically with $AgNO_3$–EDTA (*22*). Twenty-five milliliters of the 0.01*N* $AgNO_3$ solution were titrated with 0.1*N* thioacetamide solution. An inflection point was obtained at the stoichiometric value.

Titration of Magnesium and Zinc with Pyrophosphate. Fifty milliliters each of $10^{-2}M$ solutions of magnesium nitrate and zinc nitrate were titrated against 0.04*M* potassium pyrophosphate. The characteristic curves for these titrations are shown in Figure 2, C and D. The titration curve for zinc is unusual. However, the end point can be determined by extrapolation (dashed lines). The titration plot for magnesium also is not so well defined. This is indicative that the electrode is not very sensitive for these cations. The theoretical titer value for both titrations was 6.25 ml. The volume at the intersection for zinc was 6.30 ml and for magnesium 6.10 ml.

Titration of Trivalent Cations. A standard solution of aluminum sulfate was titrated with 0.58*M* ammonia. A sharp break occurred at the equivalence point (Figure 2*A*). A standard lanthanum solution was prepared as described by Fritz *et al.* (*23*), and was titrated with 0.3*M* KF solution. A nonsymmetrical titration curve was obtained (Figure 2*B*).

Titrations with Sodium Tetraphenyl Boron. Sodium tetraphenyl boron (TPB) has proved to be a versatile reagent for the quantitative determination of K^+, Rb^+, Cs^+, NH_4^+, and other metals. The potentiometric determination of potassium with TPB has been described by Geyer and Frank (*24*). Recently, Rechnitz *et al.* (*25*) employed a cation-sensitive glass electrode for the determination of alkali metals. But they used Ca-TPB as the precipitating reagent because the glass electrode was too responsive to sodium ions. In the present case, the membrane responded well to the changes in concentration of K^+, Rb^+, Cs^+, and NH_4^+ ions and yielded potentiometric curves with sufficiently sharp inflection points when Na-TPB was used as the titrant. The Na-TPB solution was standardized against a standard solution of silver nitrate in slightly acidic medium (diluted acetic acid), potentiometrically using a silver wire as the indicator electrode.

Stock solutions of the univalent ions were prepared by weight from reagent grade salts and more dilute solutions were prepared by diluting aliquots of these solutions to appropriate volumes. The pH of the solution for the titrations was adjusted to 3.2 by addition of dilute acetic acid. Twenty-five milliliters of $10^{-2}M$ KCl were titrated with 0.045*M* solutions of Na-TPB. A symmetrical S-shaped curve was obtained (Figure 3*B*). Similarly, titrations of solutions of Rb, (Figure 3*A*) Cs, NH_4^+ Hg(I), Tl(I), and Ag (Figure 4) were successfully conducted.

The results indicate that the titrations can be performed with good accuracy. The titrations can be accomplished in nonaqueous medium. This was shown by titrating silver with Na-TPB in 50% acetone solution (Figure 4*B*). Attempts were also made to titrate mixtures of Rb and K, K and Cs, and Tl and Ag. The resulting titration curves gave only a

(22) C. L. Wilson and D. W. Wilson, "Comprehensive Analytical Chemistry," Vol. IIA, Elsevier Publishing Co., New York, N. Y., 1960, p 130.
(23) J. S. Fritz, F. T. Oliver, and D. J. Pietrzyk, Anal. Chem., **30**, 1111 (1958).
(24) B. Geyer and H. Frank, *Z. Anal. Chem.*, **179**, 99 (1961).
(25) G. A. Rechnitz, S. A. Katz, and S. B. Zamochnick, Anal. Chem., **35**, 1322 (1963).

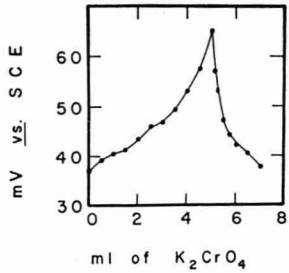

Figure 5. Titration of 50 ml of 0.01*M* $BaCl_2$ with K_2CrO_4

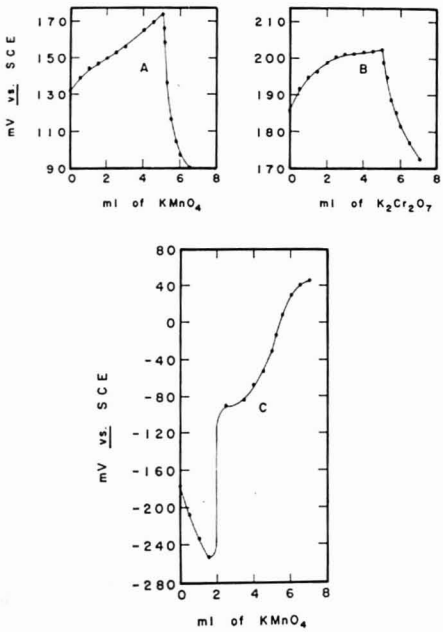

Figure 6.

A. Titration of 50 ml of 0.01*M* $FeSO_4 \cdot (NH_4)_2SO_4$ *vs.* $KMnO_4$
B. Titration of 50 ml of 0.01*M* $FeSO_4 \cdot (NH_4)_2SO_4$ *vs.* $K_2Cr_2O_7$
C. Titration of 50 ml of 0.01*M* KI with $KMnO_4$

single inflection point corresponding to the total of the mixture of the cations used. The failure to obtain separate inflection points corresponding to the individual cations is probably due to coprecipitation, as there is not a wide difference in the solubility of the respective tetraphenyl borates. The superiority of the electrode lies in the fact that titrations can be performed in acid medium and with the sodium salt of TPB.

Titration of Other Cations. Titration of the alkaline earth metals Sr, Ca, and Ba, as well as Tl(I), were attempted with some common precipitating agents. Ill defined titration curves were obtained for the titration of strontium or calcium with potassium sulfate. A small, but ill defined break was obtained for barium. Barium titrated with chromate gave a "first derivative" type peak at the end point (Figure 5). The increase in potential before the end point was probably due to the response to potassium ion as it replaced the relatively nonpermselective barium ion, while the decrease in potential beyond the end point was due to the response of the electrode to the chromate anion. Thallium, titrated with KI or K_2CrO_4, exhibited small S-shaped breaks of 10 mV or less.

Table II. Comparison of DPP Membrane Response to Different Oxidation States of Iron, Manganese, and Chromium

Salt	Potential, mV	Change in Potential, mV
$10^{-3}M$ $FeSO_4$	63	
$10^{-2}M$ $FeSO_4$	66	+3
$10^{-3}M$ $Fe_2(SO_4)_3$	114	
$10^{-2}M$ $Fe_2(SO_4)_3$	126	+12
$10^{-3}M$ $MnSO_4$	39	
$10^{-2}M$ $MnSO_4$	38	−1
$10^{-3}M$ $KMnO_4$	97	
$10^{-2}M$ $KMnO_4$	22	−75
$10^{-3}M$ $Cr(NO_3)_3$	86	
$10^{-2}M$ $Cr(NO_3)_3$	22	−20
$10^{-3}M$ $K_2Cr_2O_7$	90	
$10^{-2}M$ $K_2Cr_2O_7$	85	−5

Redox Titrations. Curves for the titration of Mohr's salt in the presence of dilute sulfuric acid with $KMnO_4$ and $K_2Cr_2O_7$ are shown in Figure 6. In these titrations, several ions to which the membrane responds, are present in the solution throughout the titration. In the titration with $KMnO_4$, for example, Fe^{2+}, NH_4^+, SO_4^{2-}, and H^+ are initially present and the iron is converted to Fe^{3+} as K^+ and Mn^{2+} (from MnO_4^-) ions are added. Beyond the end point, K^+ and excess MnO_4^- are added. The concentration of the NH_4^+, SO_4^{2-}, and H^+ ions remain fairly constant throughout the titration, while the others change. Table II lists the potential readings of 10^{-3} and $10^{-2}M$ solutions of salts of the different oxidation states of iron, manganese, and chromium employed in these titrations. Only approximate comparisons can be made because of the dependence of the concentration of the counter ion on the valence of the element in question. It is apparent from the change in potentials, however, that the membrane responds more to Fe(III) than to Fe(II). Note that a small potential change does not necessarily mean the electrode is unresponsive to a cation but rather than this response is not significantly greater than that due to the anion, which results in an opposing change in potential. The absolute potential change in going from Fe(II) to Fe(III) is larger than +12 mV since the SO_4^{2-}/Fe ratio in the latter case is increased (the increased anion concentration opposes the positive potential change). Note also that for a Nernstian electrode (which this is not) the potential changes for Fe(II) and Fe(III) would be +30 and +20 mV, respectively. So the larger Fe(III) potential change is quite significant. This is supported also by the fact that the initial potential reading for Fe(III) is 51 mV more positive than for Fe(II).

The response to Mn(II) is very small or negligible as compared to MnO_4^-. The membrane response to the permanganate anion is very large. From these data, the titration curve in Figure 6*A* can be predicted. Throughout

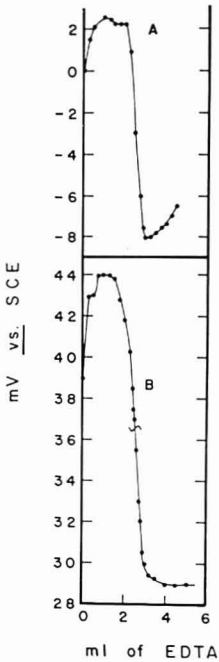

Figure 7. Titration of 25 ml of 0.01*M* $Cu(NO_3)_2$ with EDTA

A. **pH 3**
B. **pH 5**

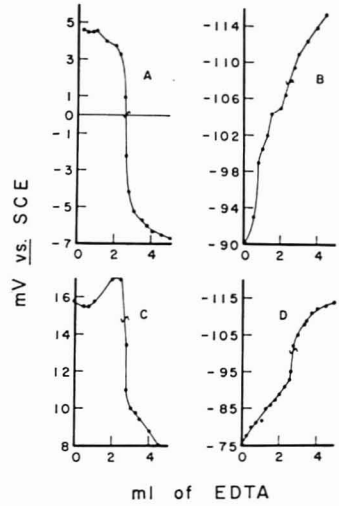

Figure 8.

A. **Titration of 25 ml of 0.01*M* $Ni(NO_3)_2$ with EDTA, pH 5**
B. **Titration of 25 ml of 0.01*M* $Ni(NO_3)_2$ with EDTA, pH 10**
C. **Titration of 25 ml of 0.01*M* $Hg(NO_3)_2$ with EDTA, pH 5**
D. **Titration of 25 ml of 0.01*M* $Hg(NO_3)_2$ with EDTA, pH 10**

the titration up to the end point, the relatively nonpermselective ion, Fe(II), is being replaced by the permselective ion, Fe(III), plus nonpermselective Mn(II), causing the potential to increase. Beyond the end point, the highly permselective anion, MnO_4^-, is added causing a large decrease in the potential. Similar arguments apply to Figure 6*B*, except that the membrane shows apparently no or very little response to Cr(III) and a small response to $Cr_2O_7^{2-}$. Hence the end point is less sharp than the titration with permanganate. The equivalence point of both these titrations occurred at the maximum in the titration curve.

An unusual titration curve, Figure 6*C*, was obtained for the titration of acidified potassium iodide with potassium permanganate. The potential initially decreased and then increased and gave an S-shaped break at the equivalence point, as I^- was replaced by Mn(II) and I_2 or I_3^-. A possible explanation of this might be that soluble I_3^- decreased the potential while the I_2 was nonpermselective. At the beginning of the titration, there was sufficient I^- to form I_3^- with the I_2 produced, but as the titration progressed, less I_3^- was formed with that originally formed being removed.

Iodometric titration of potassium dichromate or potassium iodate gave only gradual increases in the potential throughout the titration. The high background of iodide ion rendered these titrations useless. Titration of arsenic(III) with iodine was successful, however, in spite of the fact that iodide ion was added along with the iodine. A nonsymmetrical S-shaped curve was obtained. The iodide ion added probably accounts for the nonsymmetrical shape.

Complexometric Titrations. The applicability of the membrane for potentiometric titrations with EDTA was examined. Cu(II), Ni(II), Pb(II), and Ag(I) were titrated. A standard EDTA solution was prepared by titration of a standard zinc solution prepared from zinc metal.

Copper nitrate ($10^{-2}M$) was prepared in acetate buffer solutions of pH 3 and 5 and was titrated with 0.1*M* EDTA. The end point was simultaneously noted by 1-(2-pyridylazo)-2-naphthol (PAN). In general, EDTA titrations were successful only for those metals to which the membrane exhibited a high permselectivity and which formed stable EDTA chelates. The membrane is quite permselective to copper and a small but sharp break was obtained at the equivalence point (Figure 7). At pH 10 (ammoniacal buffer), however, no break could be obtained. Similar results were found for nickel. A sharp break was found at pH 5 but at pH 10 the potential decreased throughout the titration (Figure 8,*A* and *B*). Figures 8,*C* and *D* illustrate the curves for the titration of mercury(II). The membrane would be expected to have good permselectivity to mercury as for silver. Successful titrations were carried out at pH 10 as well as at pH 5. Attempts were made to study the complexometric titrations of silver and lead at various pH values. Titrations for these metal ions were not successful. In the case of silver, no significant change in potential readings could be noticed with subsequent addition of EDTA. This is due to the fact that silver does not form a sufficiently stable EDTA complex

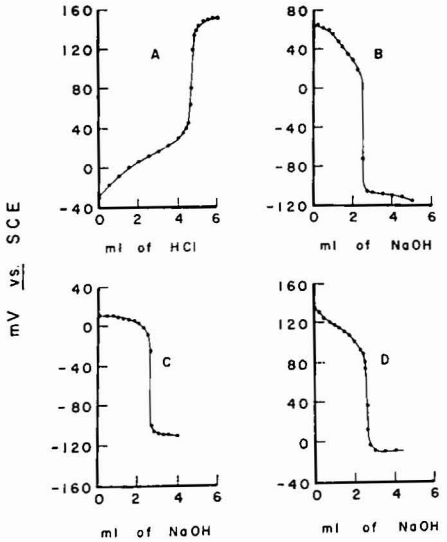

Figure 9.

A. Titration of 50 ml of 0.01*M* NH_3 with HCl
B. Titration of 50 ml of 0.01*M* $H_2C_2O_4$ with NaOH
C. Titration of 50 ml of 0.01*M* HCl with NaOH
D. Titration of 50 ml of 0.01*M* $HC_2H_3O_2$ with NaOH

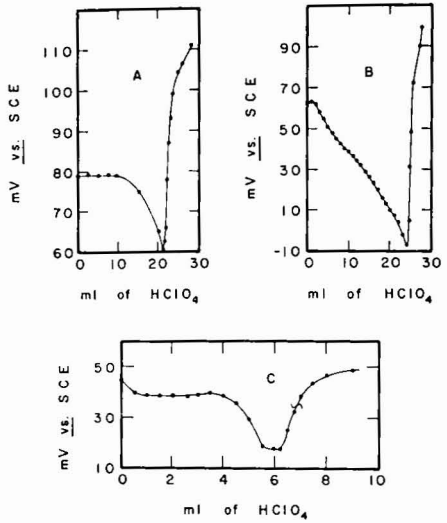

Figure 10.

A. Titration of KHP in 25 ml of glacial acetic acid with 0.1*M* $HClO_4$ in glacial acetic acid
B. Titration of KHP in 25 ml of glacial acetic acid with 0.1*M* $HClO_4$ in dioxane
C. Titration of pyridine in 25 ml of glacial acetic acid with 0.1*M* $HClO_4$ in glacial acetic acid

(*26*). For lead at pH 10 (in the presence of about 2 grams of potassium hydrogen tartrate), no S-shaped curve could be obtained. Similarly, titrations of alkaline earth metals were unsuccessful, probably because of the relatively low permselectivity to these ions.

The small changes in potential were likely superimposed by changes in the liquid junction potential. The fact that the potential remained nearly constant (1.5 mV range) when no complexation occurred (silver titration) suggests that these changes should be quite small. The solutions were also 0.01*M* or less.

Acid-Base Titrations. Titrations of strong acid *vs.* strong base, weak acid *vs.* strong base, and weak base *vs.* strong acid were carried out. The potential break was compared with visual indicator end points. The titration curves are summarized in Figure 9. Sharp breaks of approximately the same magnitude were obtained for all the titrations. The magnitude of the break is apparently determined by the electrode's response to hydrogen and hydroxyl ions as well as to the other ions in solution. The response due to hydroxyl ions is small, however (see Table I). Oxalic acid gave a single potential break corresponding to the titration of both hydrogens. Boric acid titrated with NaOH exhibited a gradual decrease in the potential throughout the titration with a change in the slope at the equivalence point.

Nonaqueous Titrations. The membrane was found to respond to several nonaqueous acid–base titrations. Twenty-five milliliters of 0.1*M* potassium acid phthalate (KHP) was titrated in glacial acetic acid with approximately 0.1*N* perchloric acid in acetic acid. The end point was marked visually by adding methyl violet indicator in chlorobenzene. The potential decreased and then increased markedly at the equivalence point, as shown in Figure 10*A*. The titration could be performed in reverse. A similar but even sharper, titration curve was obtained for the titration of KHP in glacial acetic acid with perchloric acid dissolved in dioxane (Figure 10*B*). The titration could not be performed in the reverse, however, because in the presence of dioxane solvent, the membrane becomes unstable and a high resistance develops.

Nitrogen containing organic bases were titrated in glacial acetic acid. With aniline, the potential increased gradually throughout the titration with a small levelling occurring at the methyl violet end point. This was of no analytical use, however. The titration of pyridine gave a curve qualitatively similar to KHP, but the minimum in the potential occurred before the end point, and an S-shaped inflection point marked the equivalence point (Figure 10*C*).

Attempts were also made to conduct some titrations in other organic solvents. Titration of 0.1*M* benzoic acid in a benzene–methanol mixture (3:1) with sodium methoxide in benzene–methanol was performed. The potential increased linearly with the addition of benzoic acid until at the end point a slight inflection point was noticed. The determination was of little analytical value, however. Titrations of aniline or pyridine in acetonitrile with perchloric acid in dioxane failed. Similarly, titrations of phenol in dimethyl formamide and of phenol in ethylenediamine with sodium methoxide were not successful. The membrane became swollen and turned cherry red in ethylenediamine, but at the end of the

(26) C. L. Wilson and D. W. Wilson, "Comprehensive Analytical Chemistry," Vol. IB, Elsevier Publishing Co., 1960, New York, N. Y., p 359.

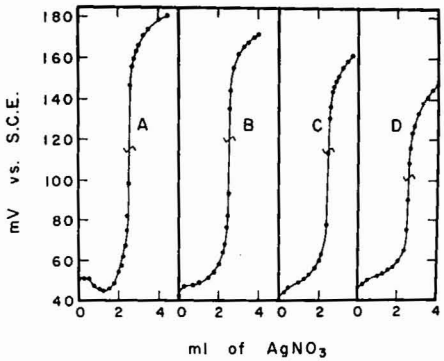

Figure 11. Titrations of 25 ml of 0.01*M* KCl with $AgNO_3$ in the presence of varying concentrations of KNO_3

A. **0.0*M* KNO_3**
B. **0.1*M* KNO_3**
C. **1.0*M* KNO_3**

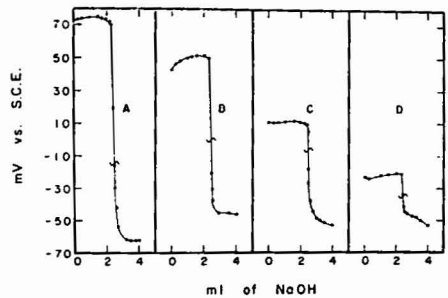

Figure 12. Titrations of 25 ml of 0.01*M* HNO_3 with NaOH in the presence of varying concentrations of KNO_3

A. **0.0*M* KNO_3**
B. **0.01*M* KNO_3**
C. **0.1*M* KNO_3**
D. **1.0*M* KNO_3**

titrations it became colorless and brittle. It was found that the membrane electrode could be used to study only a few solvent systems and was most suitable in glacial acetic acid medium.

Membrane Stability. All the titrations reported here, except for the nonaqueous acid–base titrations, were performed using a single membrane. The electrode was stored in the air between uses, and it was used for a period of several months. Formation of the red lead–dithizone chelate in the membrane undoubtedly protects against oxidation of the dithizone.

When precipitation titrations in 50% acetone were conducted, the membrane could still be used to indicate titrations in aqueous solutions (Ag^+ *vs.* I^-), although the potential response and magnitute of the end-point break was somewhat decreased. This study was done after all aqueous studies were complete.

When used in pure nonaqueous solvents, the membrane had to be changed frequently. The red lead–dithizone chelate in the membrane could be seen to leach out, although this did not seem to affect the membrane response during the titration. The membrane often became swollen and brittle after use in nonaqueous solvents.

Effects of Extraneous Salts. Because the electrode responds to many ions, studies were conducted to determine the effect of some of the most frequently encountered electrolyte ions and of ions with different valence.

PRECIPITATION TITRATIONS. Potentiometric titrations of KCl were conducted with a standard solution of $AgNO_3$ in the presence of the extraneous electrolytes KNO_3, $Mg(NO_3)_2$, and $Al(NO_3)_3$ at varying concentrations. Typical titration curves in the presence of KNO_3 are depicted in Figure 11. Curve I denotes the titration of $10^{-3}M$ KCl alone. The lower portion of the distorted S-shaped curve in the beginning shows a trough which was modified at higher concentrations of KNO_3. In addition, the limiting potential value was decreased. The net result was a decreased potential span at the end point. There was practically no change in titer values.

Thus, the extraneous electrolyte affects the accuracy of the determination in the sense that less sharp inflection points are encountered. The decrease in the voltage span is due both to the increased ionic strength which causes a decrease in the activity of the ions being measured and the competitive response of the membrane to the extraneous electrolyte ions. It is difficult to assign the effects of each because the membrane response to most ions is non-Nerstian. The decrease in the potential span is steep with initial increases in ionic strength and then it falls exponentially.

In the presence of magnesium nitrate, the foot of the wave became more regular and occurred at less positive potentials, but the upper portion of the curves tended to be more drawn out. The entire curve was shifted to more negative potentials. In the presence of 1*M* magnesium nitrate, the titer value was higher by 1.9%, possibly because of impurities.

Similar behavior was also noticed in the presence of aluminum nitrate and the results were about 1.5% higher than the normal value. At 1.0*M* aluminum nitrate, the titration curve was very much distorted with the upper and lower portions drawn out, but this effect was not observed in 0.01*M* and 0.1*M* aluminum nitrate.

Titrations of KCl with $AgNO_3$ in the presence of varying amounts of nitric acid were also attempted. The lower and upper parts of the curves first became drawn out (0.01*M* HNO_3) and then the potential span was decreased (0.1*M* and 1*M* HNO_3). However, a sharp end point was still obtained. The experiments above show that the membrane responds efficiently toward the ions K^+, Rb^+, Cs^+, Pb^{2+}, Ag^+, Ca^{2+}, Al^{3+}, and La^{3+} when titrated with reagents which stoichiometrically form precipitates with them. Titrations of these ions in the presence of mineral acids were successful.

ACID-BASE TITRATIONS. Titrations of HNO_3 *vs.* NaOH were carried out in presence of varying concentration of KNO_3 and the typical curves are shown in Figure 12. The voltage span of the titration curves was greatly decreased with increasing concentrations of KNO_3.

Effect of Organic Solvents. Precipitation titrations in 50% acetone were shown above to be successful. Acid–base titrations were performed in presence of 20, 40, and 60% (vol/vol) of ethanol or acetone. The characteristic curves for ethanol solutions are given in Figure 13. The membrane still exhibited a sharp end point and the potential readings were sufficiently stable in presence of these organic solvents. The end points obtained with the electrode were compared with visual end points using phenolphthalein and all agreed

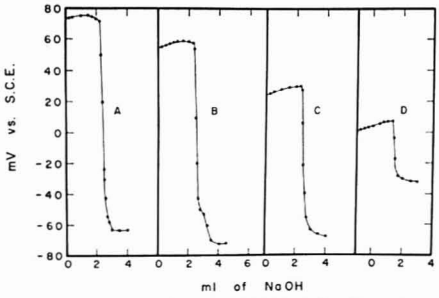

Figure 13. Titrations of 25 ml of 0.01*M* HNO_3 with NaOH in the presence of varying concentrations of ethanol (vol/vol)

A. 0% ethanol
B. 20% ethanol
C. 40% ethanol
D. 60% ethanol

Table III. Di(2-Ethylhexyl)Isophthalate Membrane Response to Various Cations and Anions

Cations	Potential, mV $10^{-3}M$	Potential, mV $10^{-2}M$	ΔE, mV
Ag^+	152	198	46
Tl^+	−31	3	34
K^+	−26	−16	10
Rb^+[a]	−42	−33	9
Cs^+[a]	−35	−33	2
H^+	161	130	−11
Na^+	−21	−33	−12
Zn^{2+}	−32	9	41
Mn^{2+}[b]	−57	−36	21
Ni^{2+}	−53	−33	20
Pb^{2+}	32	51	19
Mg^{2+}	−77	−68	9
Ca^{2+}	−67	−57	10
Sr^{2+}	80	−75	5
Cu^{2+}	108	105	−3
Al^{3+}[b]	−36	−18	18
Cr^{3+}[b]	−4	12	16
La^{3+}	−73	−69	4
Anions			
SCN^-	−30	−35	−5
I^-	−43	−33	10
NO_3^-	−26	−16	10
Br^-	−36	−26	20
Cl^-	−51	−26	25
Ac^-	−72	−46	26
OH^-	−86	−36	50
SO_4^{2-}	−34	−22	12
CrO_4^{2-}	−57	−40	17
$C_2O_4^{2-}$	−51	−32	19
CO_3^{2-}	−77	−35	42

[a] Chloride salt.
[b] Sulfate salt.

within 0.01 to 0.06 ml; there existed a little lag between the potentiometric end point and the visual end point, the former being higher than the latter. At higher ethanol concentrations, the curves were less symmetrical, and less reliable results may be expected.

Similar behavior was found for acetone solutions.

Studies with Other Membrane Plasticizers. It was apparent from early work that the nature of the plasticizer had an effect on the membrane permselectivity, particularly with regard to the alkali metals and other monovalent ions. Hence, studies were made to determine the effect of membrane composition on titration curves. The results show that the DPP membrane generally gives the most well defined and sharp titration curves. The diphenylphthalate membrane behaved as a dried plastic and displayed nonpermselectivity to common ions. Hence, further studies with this membrane were abandoned.

Table IV. Di-*n*-Octylphthalate Membrane Response to Various Cations and Anions

Cations	Potential, mV $10^{-3}M$	Potential, mV $10^{-2}M$	ΔE, mV
Ag^+	76	93	27
Rb^+[a]	17	21	4
Tl^+	35	32	−3
Cs^+[a]	33	28	−5
K^+	17	12	−5
Na^+	15	9	−6
H^+	80	57	−23
Mn^{2+}	−3	14	17
Zn^{2+}	18	20	2
Sr^{2+}	10	8	−2
Ni^{2+}	19	13	−6
Mg^{2+}	25	23	−8
Pb^{2+}	37	28	−9
Ca^{2+}	30	16	−27
Cu^{2+}	66	39	−27
Al^{3+}[b]	36	44	8
La^{3+}[b]	15	5	−10
Cr^{3+}[b]	45	28	−17
Anions			
SCN^-	10	−40	−50
I^-	−19	−43	−24
Br^-	15	7	−8
Ac^-	−10	−18	−8
NO_3^-	17	12	−5
Cl^-	30	26	−4
OH^-	−99	−29	70
$C_2O_4^{2-}$	18	−5	−23
CO_3^{2-}	30	22	−8
CrO_4^{2-}	−34	−39	−5
SO_4^{2-}	23	33	10

[a] Chloride salt.
[b] Sulfate salt.

Relative Permselectivity of Membranes toward Various Cations and Anions. The relative millivolt readings of the membranes in $10^{-3}M$ and $10^{-2}M$ solutions of several cations and anions are summarized in Tables III and IV. Solutions of cations were all prepared from the nitrates unless otherwise specified, while solutions of the anions were prepared from the potassium salts. Based upon the relative potential changes, the following approximate order of permselectivity toward various cations and anions is obtained from the data in Tables III and IV.

DEI Membrane. monovalent cations:

$$Ag^+ \gg Tl^+ > K^+ > Rb^+ > Cs^+ > H^+ > Na^+$$

divalent cations:

$$Zn^{2+} > Mn^{2+} > Ni^{2+} > Pb^{2+} > Ca^{2+} > Mg^{2+} > Sr^{2+} > Cu^{2+}$$

trivalent cations:

$$Al^{3+} > Cr^{3+} > La^{3+}$$

monovalent anions:

$$SCN^- > I^- = NO_3^- > Br^- > Cl^- > Ac^- > OH^-$$

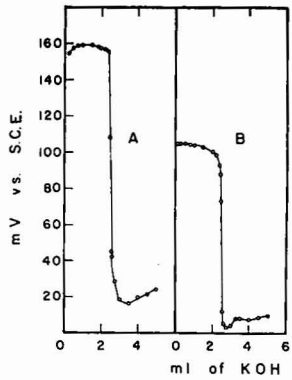

Figure 14. Titration of 25 ml of 0.01*M* HNO_3 *vs.* KOH with different membranes

A. **DEI membrane**
B. **DOP membrane**

divalent anions:

$$SO_4^{2-} > CrO_4^{2-} > C_2O_4^{2-} > CO_3^{2-}$$

DOP Membrane. monovalent cations:

$$Ag^+ \gg Rb^+ > Tl^+ > Cs^+ = K^+ > Na^+ > H^+$$

divalent cations:

$$Mn^{2+} > Zn^{2+} > Sr^{2+} > Ni^{2+} > Mg^{2+} > Pb^{2+} > Ca^{2+} > Cu^{2+}$$

trivalent cations:

$$Al^{3+} > La^{3+} > Cr^{3+}$$

monovalent anions:

$$SCN^- > I^- > Br^- > Ac^- > NO_3^- > Cl^- > OH^-$$

divalent anions:

$$C_2O_4^{2-} > CO_3^{2-} > CrO_4^{2-} > SO_4^{2-}$$

As evident from these comparisons, the relative response of the membranes varies greatly with the nature of the plasticizer and this fact can be utilized for enhancing the selectivity of one ion over another. With different plasticizers, the membranes differ in chemical composition with their mode of inner structure resulting in varying porosity and permeability. It is immaterial whether the static equilibrium is established at the plastic–solution interface with a chemical potential difference ($\mu_{\text{plastic}} - \mu_{\text{solution}}$) which consequently develops the electrical potential or the steady state potential is reached due to different mobilities of various ions through the matrix, and the magnitude of potential gives a fairly good idea of the selectivity of a membrane toward a particular ion. A few general inferences are drawn:

(i) All membranes show high response to silver ions.
(ii) These membranes seem to be less responsive to hydrogen ions than the DPP membrane in comparison to alkali metal ions.
(iii) The DOP membrane is not very responsive to lead ions.
(iv) The membranes show good response toward manganese and zinc ions and least toward copper(II) ions.

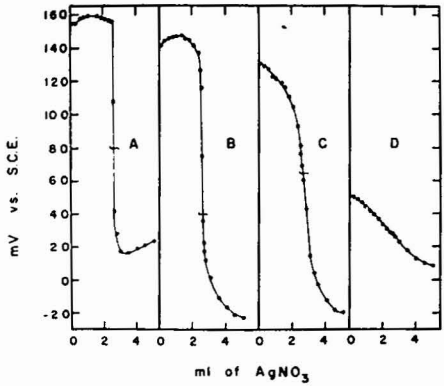

Figure 15. Titration of 25 ml HNO_3 *vs.* KOH with the DEI membrane

A. **0.01*M* HNO_3**
B. **0.001*M* HNO_3**
C. **0.0001*M* HNO_3**
D. **0.00001*M* HNO_3**

(v) Among the monovalent anions, thiocyanate and iodide are the most responsive, whereas OH^- ions are the least.
(vi) These membranes monitor aluminum ions.

In order to explore the relative effectiveness of these membranes, several potentiometric titrations were performed.

ACID-BASE TITRATIONS. Titrations of strong acid *vs.* strong base (HNO_3 *vs.* KOH), monobasic weak acid *vs.* strong base (CH_3COOH *vs.* KOH), dibasic weak acid *vs.* strong base (oxalic acid *vs.* KOH), weak acid *vs.* weak base (CH_3COOH *vs.* NH_4OH), and strong acid *vs.* weak base (HNO_3 *vs.* NH_4OH) were carried out. The potential break was compared with visual indicator end points. Typical titration curves are shown for the first case in Figure 14. It is evident from the inspection of the titration curves that titrations with the DEI membrane show the sharpest inflection points with a maximum voltage span for a titration. In strong acid–strong base titrations, the curves were fairly symmetrical but tended to rise beyond the end points. Titration plots for weak acids–strong bases or weak bases–weak acids did not show a levelled plateau in the beginning of titrations, but instead displayed a drawn out character with the potential decreasing rapidly from the beginning of the titration; but the same rise in potential beyond the end point occurred. Oxalic acid gave a large potential break corresponding to the titration of both hydrogens.

Titrations with these membranes were done at different concentrations of acid and bases. The behavior for the DEI membrane is shown in Figure 15. Typically, the potential beyond the end point decreased and the curve became more drawn out as the concentration was decreased. Only strong acid–base titrations were attempted and these could be performed in the concentration range $10^{-1}M$ to $10^{-4}M$. Similar changes in the titration curves using the DOP membrane were found.

TITRATIONS WITH SILVER ION. An analogous behavior is met with in precipitation titrations. The DEI membrane, displaying the highest selectivity for silver ions, exhibited a

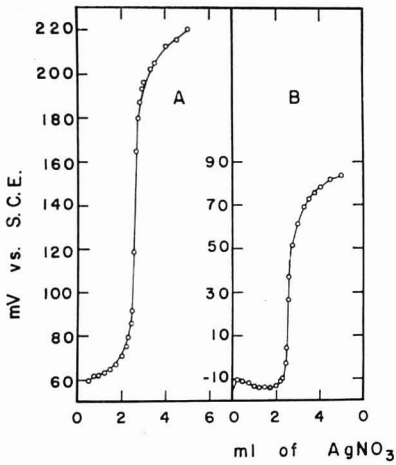

Figure 16. Titration of 25 ml of 0.01*M* KCl *vs.* $AgNO_3$ with different membranes

A. **DEI membrane**
B. **DOP membrane**

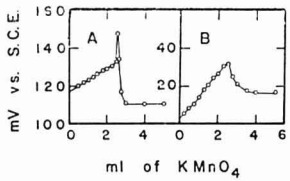

Figure 17. Titration of 25 ml of Mohr's salt (0.01*N*) *vs.* $KMnO_4$ with different membranes

A. **DEI**
B. **DOP**

symmetrical S-shaped curve with a large voltage span. The DOP membrane resulted in a less symmetrical and less sharp end point (see Figure 16). Titrations at varying concentrations of KCl, $10^{-1}M$ to $10^{-4}M$, were conducted. The curves became more drawn out with dilution and less accurate results were obtained. Titrations at $10^{-4}M$ KCl were not highly accurate, particularly with the DOP membrane.

TITRATION OF LEAD WITH SODIUM OXALATE. Fifteen milliliters of $10^{-2}M$ lead nitrate was titrated with 0.1*M* sodium oxalate. Titration curves with the DEI membrane were symmetrical and sharp whereas for the DOP membrane the curve was ill-defined with no sharp inflection point. The ill-definition and distortion of the titration curve is explicable from the response value of the membrane toward lead ion.

REDOX TITRATIONS. Twenty-five milliliters of Mohr's salt ($10^{-2}N$) plus 10 ml of 2*N* H_2SO_4 was titrated with 0.1*N* $KMnO_4$ solution. At the end point, a maximum was obtained with both membranes, being less sharp for the DOP membrane (Figure 17). Measurements of the membrane responses to Fe(II), Fe(III), MnO_4^- and Mn^{2+} revealed that

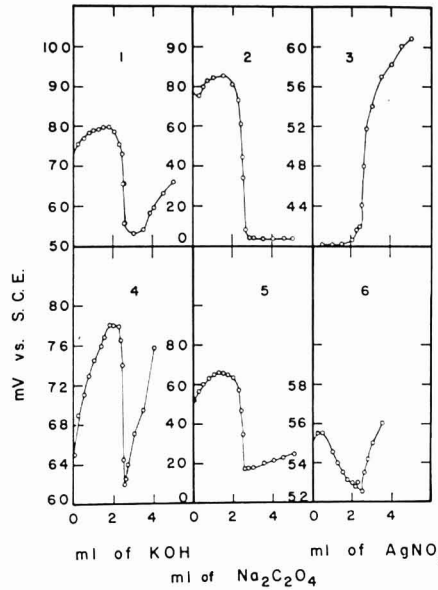

Figure 18. Titrations with DPP and DEI membranes containing no dithizone

A. **DEI membrane**
1. **25 ml of 0.01*M* HNO_3 *vs.* KOH**
2. **25 ml of 0.01*M* $Pb(NO_3)_2$ *vs.* sodium oxalate**
3. **25 ml of 0.01*M* KCl *vs.* $AgNO_3$**

B. **DPP membrane**
4. **25 ml of 0.01*M* HNO_3 *vs.* KOH**
5. **25 ml of 0.01*M* $Pb(NO_3)_2$ *vs.* sodium oxalate**
6. **25 ml of 0.01*M* KCl *vs.* $AgNO_3$**

the curves could be explained in a manner similar to the DPP membrane.

EDTA TITRATIONS. Titrations of standard solutions of Pb(II), Ni(II), and Ca(II) at pH 4.6 and 9.8 were attempted. Irregular, distorted curves with no distinct equivalence point were obtained for these cations. The DEI membrane did not exhibit any measurable potential changes in titrations of Ni(II) at either pH value. The membranes are unsuitable for chelometric titrations.

The absolute response of the membranes may vary somewhat from one preparation to another. Hence, the relative selectivities and shapes of titration curves may differ slightly with each preparation. In all cases the relative selectivity to different ions is in proportion to the relative potential change with changing concentrations of the ions.

Role of the Chelating Agent, Dithizone. In order to investigate the role of dithizone in governing the permselectivity, two membranes with DPP and DEI plasticizers were cast with the usual ingredients but in the absence of dithizone. Both of the membranes were colorless, translucent and stable. Their relative response to H^+, Ag^+, Na^+, K^+, Pb^{2+}, Ca^{2+} cations is given in Table V.

Both the membranes showed an almost equal response toward silver ions but the relative response did increase in the presence of dithizone (*cf.* Tables I and II, DPP = Δ50 mV

DEI = Δ46 mV). The DPP membrane was still highly permselective to hydrogen ions. Response toward lead ion by both the membranes was still appreciable. However, in the absence of dithizone, the membranes showed more permselectivity to K^+, Na^+, and Ca^{2+}.

Acid–base and precipitation titrations were attempted with membranes without dithizone and the results are shown in Figure 18. In the titration of HNO_3 *vs.* KOH, the DPP membrane registered a sharp minimum at the end point. The DEI membrane yielded a less sharp break. The potential span of the titrations was considerably increased when dithizone was present in the membrane matrix.

These results clearly demonstrate that dithizone contributes in some way to increase the response to several ions and the response ultimately governs the general morphology of the curves. The membrane with dithizone when preconditioned by immersing in dilute $Pb(NO_3)_2$ solution, becomes cherry red. Probably, the lead–dithizone chelate formed in the network of the plastic controls the mobility of various ions and helps in attainment of an equilibrated diffusion potential at the membrane–solution interface.

In summary, the described DPP membrane is useful for monitoring potential changes in cases where the absolute magnitude of the potential is unimportant, as in potentiometric titrations. It functions well in all types of titrations, regardless of the nature or valence of the ion and to a limited extent in pure nonaqueous solvents. Because of the bi-ionic nature of the membrane potential, its use in direct potentiometric measurements will probably be restricted to situations in which calibration curves can be prepared under strictly defined conditions. The fact that it responds to nearly all ions may make it valuable for measuring ions for which electrodes are not available, under well defined conditions. Kinetic measurements involving changes in ion concentrations or valence might provide an example.

Varying the composition of the membrane changes its relative response to different ions and it is apparent that both the plasticizer and the chelating agent play important roles in this regard. The DDP membrane results in the best defined titration curves.

Table V. Response to Various Cations of DPP and DEI Membranes without Dithizone

	DPP membrane potential, mV			DEI membrane potential, mV		
Cation	$10^{-3}M$	$10^{-2}M$	ΔmV	$10^{-3}M$	$10^{-2}M$	ΔmV
Ag^+	23	59	36	64	102	38
H^+	144	261	117	105	144	39
Na^+	22	21	−1	57	67	10
K^+	30	73	43	62	78	16
Pb^{2+}	43	79	36	120	140	20
Ca^{2+}	12	20	8	58	75	17

ACKNOWLEDGMENT

Gary L. Stucky provided valuable discussion.

RECEIVED for review December 22, 1969. Accepted December 18, 1970. A post doctoral research fellowship to S. L. from Miles Laboratories, Inc., Ames Company Division, is gratefully acknowledged.

Use of Syringaldazine in a Photometric Method for Estimating "Free" Chlorine in Water

Robert Bauer and Chauncey O. Rupe

Ames Company, Division of Miles Laboratories, Inc., Elkhart, Ind. 46514

A colorimetric method for estimating "free" chlorine (hypochlorous acid, hypochlorite ion) in water has been developed using syringaldazine buffered at pH 7 as the chromophoric agent. The reagent is sensitive to hypochlorite but is insensitive to bound chlorine such as chloramines, thus making it an important reagent for free chlorine in the presence of chloramines. Syringaldazine reacts with chlorine on a mole for mole basis. Under these conditions, the molar absorptivity (ϵ) for the reaction is about 65,000 at $\lambda = 530$ nm. The developing color does not follow strictly Beer's law, but in dilute solutions of syringaldazine and chlorine, the standard curve (absorbance *vs.* chlorine concentration) is a straight line deviating only slightly from the origin.

DIFFERENCES in the bactericidal properties of "free" (hypochlorous acid or hypochlorite ion) and "bound" chlorine has focused attention on the need for a test for free chlorine in water. Nicolson (*1*) has studied nine different methods seeking an ideal colorimetric method. Several of these methods were found to adequately measure free chlorine if certain precautions were taken. But only the *o*-tolidine test has been widely accepted as a convenient field test, even though it is known to react with various chloramines (*2*). With most natural water, this presents a minor problem; but in water containing ammonia and other contaminants, the *o*-tolidine test may indicate adequate chlorination where little or no unbound chlorine exists.

The wide use of chlorine in bleaches and disinfectants has further increased the need for new chlorine tests, especially those tests which measure free chlorine.

In searching for a convenient test for free chlorine, several compounds which produce colored oxidation products were studied. Since Bradley (*3*) and Gretton (*4*) have demonstrated the usefulness of syringaldazine and vanillinazine in the estimation of hydrogen peroxide, it was decided to investigate

(1) N. J. Nicolson, *Analyst*, **90**, 187–198 (1965).

(2) "Chlorine, Its Manufacture, Properties, and Uses," J. S. Sconce, Ed., Reinhold, New York, N. Y., 1962, pp 461–482.

(3) Wm. Bradley, Diagnostic Composition, U. S. Patent 3,233,974 (1966).

(4) N. B. C. Gretton and J. T. Rees, Test Composition and Device for Detecting Glucose, U. S. Patent 3,290,228 (1966).

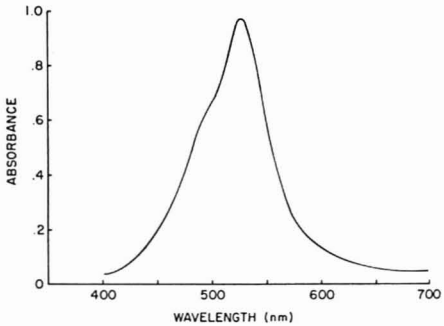

Figure 1. Absorption spectrum of color produced by the syringaldazine–chlorine reaction in 0.025*M* phosphate buffer, pH 7

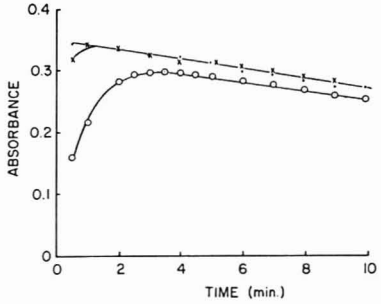

Figure 2. Rate of fading of color produced by the syringaldazine–chlorine reaction in 0.025*M* phosphate buffer

⊙—⊙ pH 6
×—× pH 6.5
●—● pH 7

these compounds as to their use in determining chlorine in water. A crude spot plate check of the two reagents showed syringaldazine in phosphate buffer pH 3–8, to be quite sensitive to chlorine, while vanillinazine under the same conditions was rather insensitive even to chlorine concentrations as high as 5 ppm. Because of the low sensitivity of vanillinazine for chlorine, it was dropped from further study.

EXPERIMENTAL

Reagents. PHOSPHATE BUFFERS. A stock solution of 0.1*M* disodium phosphate (analytical grade) was prepared from which aliquots were taken and adjusted to the desired pH (3–9) with either hydrochloric acid or sodium hydroxide as needed.

SYRINGALDAZINE SYNTHESIS. Syringaldazine was prepared as follows: Syringaldehyde (Aldrich) in the amount of 3.6 grams (0.02 mole) was dissolved in 50 ml of methanol. Two hundred milliliters of 0.1*N* sodium hydroxide were added with stirring. A pale yellow solution developed. Hydrazine dihydrochloride 1.05 gram (0.01 mole) dissolved in 50 ml of distilled water was added with stirring. Within 5 minutes, yellow crystals began to appear. Gentle stirring was continued at room temperature for another 2 hours.

The solution was then filtered by suction, and the precipitate washed on the filter with a small amount of distilled water.

The precipitate was redissolved in 400 ml of hot ethanol and filtered. Upon cooling to room temperature, needle-like yellow crystals began to form. After 2 hours at room temperature, the solution was filtered. The precipitate was air-dried to remove the ethanol, and then placed in a vacuum oven at 50° overnight.

The total yield of syringaldazine was 2.8 grams, 61% theoretical. Corrected melting point was found to be 210–211 °C.

STOCK SYRINGALDAZINE SOLUTION. A 0.1% solution of syringaldazine was prepared by dissolving, with the aid of heat, 100 mg in reagent alcohol containing 90% ethanol, 5% methanol, and 5% isopropanol and diluting to a total volume of 100 ml with the same reagent alcohol. At room temperature, this is close to a saturated solution. A 0.01% solution of the reagent was prepared by diluting this solution 1:10 with reagent alcohol.

CHLORINE STANDARD. Chlorine standards containing 0–2 ppm expressed as chlorine (Cl_2) were prepared from either stock sodium hypochlorite solution or chlorine water, whose chlorine concentration was established by the thiosulfate method.

The diluent was chlorine-free distilled water previously treated with chlorine and ultraviolet irradiation according to Nicolson (*1*) to remove any preexisting chlorine demand. The standards were prepared just before use because of the instability of the more dilute chlorine solutions.

Procedure. SPECTROPHOTOMETRIC STUDIES. The color response of syringaldazine with chlorine was studied spectrophotometrically in phosphate buffer at pH 3, 5, 6, 7, 8, and 9. In each setup, 1 ml of phosphate buffer was placed in each of three small flasks, which had been repeatedly washed with distilled water to remove any trace of detergents or material that might react with chlorine. To one was added 10 ml of chlorine water containing 1 ppm chlorine and 1 ml of 0.01% syringaldazine; to the second flask, 10 ml of chlorine free water and 1 ml of syringaldazine; and to the third, 10 ml of water. Approximately 1 minute was given for color development, and the spectrum was run using the solution in the third flask in the reference cell. At all pH levels, an intense violet color was produced. Both color development and stability were pH dependent. At pH 3, the color developed quickly and faded rapidly to an almost colorless solution. As the pH was increased from 3 to 6, both color development and fading became slower. At pH 7, the color developed rapidly but fading remained slow. At pH 8, the color developed rapidly and fading also was rapid. At pH 9, the color was less intense and quickly faded to a bright yellow solution. The spectrum obtained at pH 7 is shown in Figure 1.

The violet color produced had an absorption maximum at λ = 530 nm. Changes in pH did not influence the position of the absorption peak but did affect its height. These changes possibly were related to color development and fade rate.

The rate of color development and fading was studied more carefully over a pH range of 6–7 where the best color response occurred. Syringaldazine, 0.005%, was prepared by placing 2.5 ml of 0.1% alcohol stock solution in a 50-ml volumetric flask, with 25 ml of 0.05*M* phosphate buffer of the desired pH, and diluting to volume with reagent alcohol. One milliliter was added to 10 ml of water containing 0.5 ppm chlorine. A reagent blank was used as the reference solution. Each solution was read at λ = 530 nm at 30- and 60-second and at 1-minute intervals for a total of 10 minutes.

The results are shown in Figure 2. At pH 6, three minutes were required for maximum color development. At pH 6.5, 60 seconds were required and 30 seconds at pH 7. The rate of fading was about the same for all three test solutions. Fading appeared to set in almost immediately and to proceed

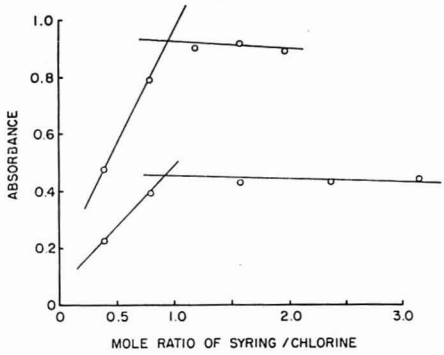

Figure 3. Effect of increased mole ratio of syringaldazine to chlorine (Cl_2) upon color intensity

Lower curve: Chlorine held constant at $0.705 \times 10^{-5}M$
Upper curve: Chlorine held constant at $1.41 \times 10^{-5}M$

at a slow but constant rate. By buffering at pH 7, advantage can be taken of the rapid color development and the slow fade rate.

Between pH 6 and 7, the syringaldazine reagent changed from pale yellow to an intense yellow solution having an absorption peak at 410 nm. This peak was completely absent at pH 6. The color change could be reversed by lowering the pH. This was taken to mean a change in the ionization of syringaldazine had taken place, possibly involving the protonation of the azine group in the molecule.

STOICHIOMETRY OF THE CHLORINE-SYRINGALDAZINE REACTION. Syringaldazine reagents were prepared in phosphate buffer from the stock solution as described above. Concentrations ranged from 2.75×10^{-5} to $27.5 \times 10^{-5}M$. Each solution was checked with chlorine (Cl_2) concentrations of 0.5 ppm ($0.705 \times 10^{-5}M$) and 1 ppm ($1.41 \times 10^{-5}M$). One milliliter of the reagent was placed in a small Erlenmeyer flask and 10 ml of chlorine water were added. After 1 minute, the absorbance was read in the spectrophotometer at $\lambda = 530$ nm against its appropriate reagent blank. These results are presented in Figure 3 with the mole ratio of syringaldazine to chlorine plotted against absorbance.

On each curve, the break occurred at a molar ratio of approximately 1, indicating a definite stoichiometric relationship in the reaction between chlorine and syringaldazine. The intensity of the color resulting from the reaction was quite strong, having a molar absorptivity (ϵ) of approximately 65,000 where the reactants were present in equal molar amounts.

DETERMINATION OF FREE CHLORINE IN WATER. A working chromogenic reagent containing 0.008% (22×10^{-5}) molar syringaldazine was prepared as follows: Eight ml of 0.1% syringaldazine in reagent alcohol were placed in a 100-ml volumetric flask containing 15–20 ml of alcohol; 50 ml of $0.05M$ phosphate buffer (pH 7) were added, and the total volume was brought to 100 ml with alcohol. A clear yellow solution resulted. This reagent contained enough syringaldazine in 1 ml to react with the chlorine in 10 ml of water containing 1 ppm chlorine. The working solution was prepared fresh each day to ensure maximum color development.

One milliliter of the reagent was placed in a series of small Erlenmeyer flasks to which was added 10 ml of water containing 0, 0.1, 0.2, 0.4, 0.6, 0.8, and 1.0 ppm chlorine. One minute was allowed for color development. Each solution was read in a spectrophotometer at $\lambda = 530$ nm using the chlorine free sample as the blank. The resulting standard curve is shown in Figure 4.

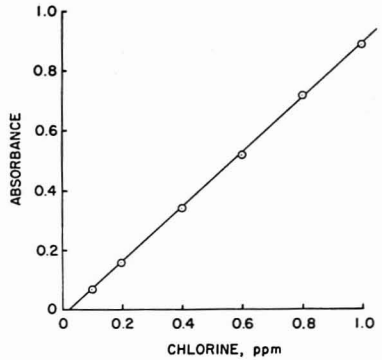

Figure 4. Standard curve for the chlorine–syringaldazine reaction

1 ml syringaldazine, 0.008% in $0.025M$ phosphate buffer, pH 7; 10 ml chlorine water. $\lambda = 530$ nm

Table I. Comparison of the Syringaldazine Method of Estimating Chlorine in Water with the *o*-Tolidine (OT) and the *o*-Tolidine–Arsenite (O-TA) Methods

Water sample No.	Chlorine content, ppm		
	O-T	O-TA	Syring.
1	1.12	0.98	1.01
2	0.45	0.395	0.40
3	0.97	0.72	0.87
4	0.94	0.78	0.87
5	1.02	0.98	1.06
6	1.12	0.91	0.95
7	0.99	...	0.91
8	0.85	0.70	0.73

The method used in preparing the standard curve was compared with the spectrophotometric procedures of the *o*-tolidine and *o*-tolidine–arsenite methods. The comparisons were made on laboratory tap water. The *o*-tolidine and the *o*-tolidine–arsenite methods were carried out at room temperature according to "Standard Methods for the Examination of Water and Wastewater" (5). The results are shown in Table I.

The *o*-tolidine–arsenite method measures free or unbound chlorine, while *o*-tolidine measures total chlorine (5). The differences between these values were quite small, indicating the amount of bound chlorine in the tap water was also small. Most of the syringaldazine test values fell between the two *o*-tolidine test values, thus showing good agreement with the *o*-tolidine test.

In order to determine whether the syringaldazine test was measuring total or free chlorine, samples of distilled water were prepared containing 1 ppm chlorine and varying amounts of ammonium sulfate added to bind portions of the chlorine as chloramines.

All samples were analyzed for free chlorine by the syringaldazine, *o*-tolidine–arsenite, and amperometric titration methods. They were also analyzed for total chlorine by the

(5) "Standard Methods for the Examination of Water and Wastewater, 12th Ed.," Amer. Public Health Assoc., Inc., 1790 Broadway, New York, N. Y. 10019, 1965, pp 93–102.

Table II. Estimation of Chlorine in the Presence of Ammonia by the Syringaldazine, *o*-Tolidine–Arsenite, *o*-Tolidine, and Free and Total Amperometric Methods (ppm)

NH_3 added as $(NH_4)_2SO_4$	Syring-aldazine	O-TA, free	Ampero, free	O-T, total	Ampero, total
0.00	1.03	1.03	1.03	1.03	
0.05	0.70	0.91	0.63	1.03	0.97
0.10	0.41	0.73	0.35	1.00	0.95
0.20	0.15	0.66	0.11	1.00	0.99
0.50	0.00	0.15	0.01	0.94	1.00

Table III. Estimation of Chlorine in Tap (T) and Swimming Pool (SP) Waters by the Syringaldazine and Amperometric Methods

Sample	Syring-aldazine, ppm	Ampero, free, ppm	Ampero, total, ppm
1 (T)	0.00	0.00	0.00
2 (T)	1.12	1.12	1.32
3 (T)	0.30	0.26	0.38
4 (SP)	0.20	0.24	1.12
5 (SP)	2.48	2.50	3.52
6 (SP)	0.03	0.04	0.76
7 (SP)	1.14	0.96[a]	1.25

[a] End point erratic.

Table IV. Reproducibility of the Syringaldazine Test

Sample No.	O-T test	O-TA test	Syring. test
1	1.02	0.98	1.056 ± 0.011 (10)[a]
2	0.45	0.395	0.399 ± 0.013 (11)
3	0.16	0.07	0.055 ± 0.011 (10)

[a] Number of trials with syringaldazine test.

o-tolidine and amperometric methods. The results are given in Table II.

The syringaldazine values agreed well with those obtained with the amperometric titration method for free chlorine. Values by the *o*-tolidine–arsenite procedure were slightly higher. This might be expected since these samples were run at room temperature rather than at 1 °C. In general, the data indicate that the syringaldazine method is responding to free chlorine and not to chloramines.

The syringaldazine method was compared with the amperometric titration method, free and total, using chlorinated tap and swimming pool waters. These results are summarized in Table III. Samples 1 through 3 represent three different sources of tap water; samples 4 through 7 were swimming pool water samples.

Results obtained with the syringaldazine method agreed well with those for free chlorine by amperometric titration, except for Sample 7.

The titration of this sample for the free chlorine gave an atypical end point, which may account for the observed discrepancy. This was not encountered in any of the other titrations.

In several samples of tap water from the same source, a substance other than chlorine was found which gave a trace reaction with syringaldazine. The presence of such a component was first suspected when the values obtained with the syringaldazine method fell between those obtained with the *o*-tolidine and the *o*-tolidine–arsenite methods. This suspicion was substantiated in a sample of tap water rendered free of chlorine by heat and ultraviolet irradiation. On this sample, syringaldazine gave a reading of 0.05 ppm expressed as chlorine, and the *o*-tolidine test read 0.0. In all samples encountered, the apparent quantity was small, 0.05 ppm or less.

The agent responsible for the trace reaction with syringaldazine was not identified. The addition of Fe(II), Mn(II), Cu(II), Ca(II), and Mg(II) up to 10 ppm produced no color response. Fe(III) at 1 ppm gave no color, but in a concentration of 10 ppm an absorbance reading equivalent to 0.01 ppm chlorine was obtained. It is unlikely that Fe(III) was the causative agent, since the water sample contained less than 3 ppm iron.

The reproducibility of the syringaldazine test was checked in tap water samples containing 1, 0.4, and 0.05 ppm free chlorine. The results are given in Table IV.

At all three chlorine levels, the new method showed a high degree of reproducibility.

DISCUSSION

The oxidation of syringaldazine by chlorine appears to be on a mole to mole basis (Figure 3), possibly involving a shift of two electrons similar to the oxidation of hydroquinone to quinone. The reaction may be represented as follows:

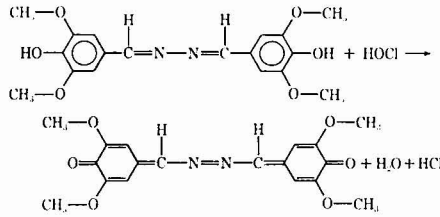

The reaction produces an intense color having a narrow absorption maximum at 530 nm, with a small shoulder at approximately 495 nm. The position and shape of the absorption curve is not altered by change of pH (3 to 9) nor by diluting the colored component.

The amount of color produced depends upon the concentration of both syringaldazine and chlorine. By keeping the concentration of syringaldazine low ($10^{-5}M$), and the chlorine concentration 1 ppm or less, the amount of color produced can be made chlorine dependent; although it does deviate slightly from Beer's law. The deviation is so slight that good quantitation can be made by using either a standard curve or a chlorine standard.

Syringaldazine does not react with chloramines which are found as common contaminants in swimming pool water. The importance of this lies in the difference in the bactericidal properties of free and bound chlorine. Free chlorine in concentrations of 0.5–1 ppm has been shown to be an effective bactericidal agent, whereas chloramines are rather ineffective (*6*).

Situations can and do arise where adequate chlorination is indicated by the *o*-tolidine procedures, but little or no germicidal activity is present. The *o*-tolidine–arsenite procedure, in addition to being cumbersome, may indicate free chlorine levels in excess of those actually present unless the entire reaction is run at or near 1 °C (*5*).

In cases where little or no bound chlorine exists, the *o*-tolidine and syringaldazine methods are in close agreement (Table I); but as the amount of chloramines increases, the discrepancy between the two tests becomes greater (Table II). In this particular case (Table II), *o*-tolidine is reacting with

(6) C. T. Butterfield, *Pub. Health Rep.*, 63, 934–940 (1948).

both free and bound chlorine and syringaldazine with only the free, as indicated by the amperometric procedure.

In some waters, where a large percentage of the chlorine exists in the bound form, it is quite possible more free chlorine may be indicated by the *o*-tolidine–arsenite test than is actually present. The effect of bound chlorine upon the free chlorine values can be minimized by chilling the water before adding the *o*-tolidine and arsenite reagents (*2*). For reasons of convenience, this restriction is rarely used in practice. Either the test is run at room temperature or no attempt is made at estimating the free chlorine content.

With the syringaldazine procedure, free chlorine can be measured easily without interference from chloramines (Tables II and III). The necessity of using a blocking agent, such as arsenite or controlled temperatures, is eliminated.

The reagent itself should be prepared fresh each day from a stock alcohol solution of 0.1% syringaldazine. Buffered solutions left standing at room temperature for 24 hours or more showed a gradual decrease in color production. This does not represent a major problem, since the working reagent can be prepared quickly from stock solutions of syringaldazine and phosphate buffer.

RECEIVED for review September 14, 1970. Accepted December 21, 1970.

Intrinsic End-Point Errors in Precipitation Titrations with Ion Selective Electrodes

Peter W. Carr

Department of Chemistry, University of Georgia, Athens, Ga. 30601

Investigations on the effect of ionic interferences in potentiometric precipitation titrations with ion selective electrodes are reported. When the inflection point of the titration curve is used to locate the end point, serious errors (>1%) can result which are often outside the range of the ultimate analytical precision (0.1%) achievable in such analyses. Results are presented in terms of β, a dimensionless variable related to the solubility product and the initial analyte concentration, and b, a parameter related to the concentration and selectivity ratio of interfering ions. In general, errors result from finite selectivity ratios and from the intrinsic absence of symmetry in the titration curve. The errors are negligible only in the limit of very sparingly soluble materials or in the absence of any interfering ions.

THE PAST SEVERAL YEARS have witnessed a renaissance of potentiometry as an analytical tool (*1–3*). Most of this is due to the development of both anion and cation selective electrodes which measure the activity rather than the concentration of the species of interest. For thermodynamic and kinetic studies, activity is of principal importance (*4*). Analytical measurements, however, are mainly concerned with determining the concentration of analyte. Concentration can be measured from a calibration curve, a plot of cell potential *vs.* the decadic logarithm of concentration, from the measured activity and knowledge of activity coefficients, by precision null point potentiometry (*5, 6*), or by titration. Titration to the inflection point of the potential–volume curve will generally be more precise and accurate than any of the above direct measurement techniques. This method minimizes errors due to variations in activity coefficients, liquid junction potentials, and spurious interferences which change the activity of the analyte. The cost of this increased accuracy and precision is a decrease in the speed and convenience of measurement.

It is widely recognized that ion selective electrodes are not perfectly selective (*7, 8*) and that in actual practice the absolute accuracy of direct potentiometric measurements with such electrodes depends critically upon the presence of potential determining foreign ions. It is generally considered that the presence of these interfering ions in a potentiometric titration ultimately limits the magnitude of the "end point break" and, concomitantly, the precision of measurement. The fact that such interferences can seriously influence the position of the inflection point of a titration curve and thus its analytical accuracy has not yet been widely appreciated (*9*). As will be shown, such errors often amount to several per cent, well outside the range of the precision (±0.1–0.2%) routinely obtainable by potentiometric titration.

Although there has been some discussion (*10, 11*) as to evaluation of the extent of electrode selectivity, there seems to be fairly general agreement that if the liquid junction and reference electrode potentials are constant, then the potential of a cell containing an ion selective electrode is well represented as follows:

$$E = \text{const} + \frac{RT}{z_X F} \ln (\gamma_X C_X + B) \qquad (1)$$

In this equation (*12*), species X is the ion of interest (gen-

(1) G. A. Rechnitz, *Accounts Chem. Res.*, **3**, 69 (1970).
(2) "Ion Selective Electrodes," R. A. Durst, Ed., National Bureau of Standards, Special Publication 314 (1969).
(3) "Glass Electrodes for Hydrogen and Other Cations: Principles and Practices," G. Eisenman, Ed., Marcel Dekker, New York, N. Y., 1967.
(4) E. A. Guggenheim, *J. Phys. Chem.*, **34**, 1758 (1930).
(5) H. V. Malmstadt and J. D. Winefordner, *Anal. Chim. Acta*, **20**, 283 (1959).
(6) R. A. Durst, ANAL. CHEM., **40**, 931 (1968).
(7) J. W. Ross, Jr., "Solid State and Liquid Membrane Ion Selective Electrodes," in Ion Selective Electrodes, R. A. Durst, Ed., National Bureau of Standards, Special Publication 314 (1969).
(8) G. A. Rechnitz, *Chem. Eng. News*, **43** (25), 146 (1967).
(9) M. Whitfield and J. V. Leyendekkers, *Anal. Chim. Acta*, **45**, 383 (1969).
(10) M. S. Frant, ANAL. CHEM., **40**, 457 (1968).
(11) A. Shatkay, *ibid.*, p 458.
(12) G. A. Rechnitz, "Analytical Studies on Ion Selective Membrane Electrodes," in Ion Selective Electrodes, R. A. Durst, Ed., National Bureau of Standards, Special Publication 314 (1969).

Table I. Analytical Error[a,b] In Precipitation Titrations with Ion Selective Electrodes Sensitive to the Analyte

b^d	0.1			3.16×10^{-3}			10^{-3}			3.16×10^{-4}			10^{-4}			0		
β^c	$\nu = 1$	$\nu = 2$	$\nu = 1/2$	$\nu = 1$	$\nu = 2$	$\nu = 1/2$	$\nu = 1$	$\nu = 2$	$\nu = 1/2$	$\nu = 1$	$\nu = 2$	$\nu = 1/2$	$\nu = 1$	$\nu = 2$	$\nu = 1/2$	$\nu = 1$	$\nu = 2$	$\nu = 1/2$
10^{-1}	13.21	61.74	−15.54	8.18	57.51	−21.03	1.88	56.00	−23.88	0.62	55.50	−25.04	0.20	55.35	−25.45	0.06	55.28	−25.59	0	55.26	−25.65
10^{-2}	8.64	31.34	−7.34	4.18	27.79	−2.81	1.69	26.37	−4.21	0.60	25.88	−4.99	0.20	25.72	−5.34	0.06	25.67	−5.46	0	25.65	−5.53
10^{-3}	4.86	16.54	0.72	2.73	13.84	0.03	1.32	12.60	−0.47	0.53	12.14	−0.82	0.19	11.98	−1.03	0.06	11.93	−1.13	0	11.91	−1.19
10^{-4}	2.49	9.00	0.46	1.54	7.16	0.22	0.86	6.17	0.05	0.42	5.75	−0.07	0.17	5.60	−0.15	0.06	5.55	−0.21	0	5.53	−0.26
10^{-5}	1.21	4.99	0.21	0.79	3.85	0.12	0.48	3.13	0.06	0.27	2.78	0.02	0.13	2.64	−0.07	0.05	2.59	−0.03	0	2.57	−0.06
10^{-6}	0.57	2.79	0.09	0.38	2.12	0.05	0.25	1.65	0.03	0.15	1.38	0.02	0.09	1.26	0.07	0.04	1.21		0	1.19	
10^{-7}	0.27	1.57		0.18	1.18		0.12	0.90		0.08	0.72		0.05	0.62		0.03	0.57		0	0.55	
10^{-8}	0.13	0.88		0.09	0.66		0.06	0.50			0.38			0.31		0.02	0.28		0	0.26	
10^{-9}	0.06	0.50			0.37		0.03	0.28			0.21			0.16		0.01	0.14		0	0.12	
10^{-10}		0.28			0.21			0.16			0.12			0.09			0.07		0	0.06	
10^{-11}		0.14			0.12			0.09			0.07			0.05							
10^{-12}		0.07			0.07			0.05													

[a] A blank value indicates that the absolute error is less than 0.05%. A positive error indicates that the inflection point precedes the equivalence point.
[b] The data were computed assuming that dilution is negligible; $r = 0$.
[c] $\beta = \frac{z(K_{sp})^{1/m})}{(C^\circ_A)^{\nu+1}}$.
[d] $b = B/\gamma_A \cdot C^\circ_A$.

erally that ion which the electrode has been designed to measure); z_X, γ_X, and C_X are this ion's charge, activity coefficient, and concentration, respectively. The term B represents the cumulative interference due to all other ions present in the test solution and may be written as:

$$B = K_I(\gamma ICI)^{zI/zX} \tag{2}$$

The variable, K_I, is generally termed a selectivity ratio which would be zero for all species if the electrode were perfectly selective for X. At present there are no electrodes, including glass electrodes for pH measurement, which are perfectly selective.

In order to compute the effect of a finite selectivity ratio on the inflection point of titration curves, we have adapted a mathematical procedure developed by Meites and Goldman (*13*, *14*) for evaluating the effect of dilution on acid–base and precipitation titration curves. The basic method is to represent, in terms of the relevant derivatives of concentration, the inflection point condition, *i.e.*, the point where the second derivative of potential with respect to the added volume of titrant or a related variable such as the fraction titrated becomes zero. In the present context:

$$\frac{d^2E}{df^2} = \frac{RT}{z_XF}\frac{d^2 \ln (\gamma_X C_X + B)}{df^2} = 0 \tag{3}$$

The fraction titrated, f, is generally defined as the ratio v/v^*, v being the volume of titrant added, and v^* the volume of titrant required to reach the equivalence point. Equation 3 is equivalent to:

$$(\gamma_X C_X + B)\frac{d^2\gamma_X C_X}{df^2} = \left[\frac{d\gamma_X C_X}{df}\right]^2 \tag{4}$$

When this condition is imposed on the relevant chemical equilibrium, the resultant equations allow computation of the fraction titrated at the end point (f_{ep}) from which the titration error (ϕ) defined implicitly below can be determined.

$$\% \text{ error} \equiv 100\phi = 100(1 - f_{ep}) \tag{5}$$

The presence of the term B in Equation 4 results in major differences between the inflection point and the equivalence point.

Consider a generalized precipitation reaction between two species, A, the analyte, and T, the titrant.

$$nA + mT \leftrightharpoons A_nT_m(\downarrow) \tag{6}$$

The chemical reaction can be represented by an equation for the concentration of either A or T in terms of the fraction titrated, which results from considering the formal solubility product, related mass balances, and dilution factors.

$$C_A{}^{\nu+1} - \alpha C^\circ_A C_A{}^\nu - \nu K_{SP}{}^{1/m} = 0 \tag{7}$$

and

$$\nu C_T(\alpha C^\circ_A + \nu C_T)^\nu - \nu K_{SP}{}^{1/m} = 0 \tag{8}$$

where C°_A is the initial concentration of analyte, C°_T is the concentration of titrant, ν is a stoichiometry coefficient defined as the ratio, n/m, and α and K_{sp} are given below:

$$K_{sp} = C_A{}^n C_T{}^m \tag{9}$$

$$\alpha = \frac{\nu(1 - f)}{\nu + rf} \tag{10}$$

(13) L. Meites and J. A. Goldman, *Anal. Chim. Acta*, **29**, 472 (1963).
(14) *Ibid.*, **30**, 18 (1964).

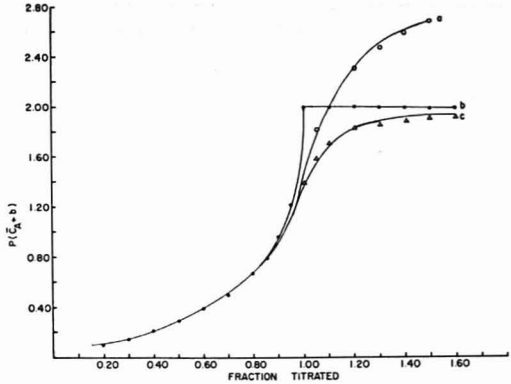

Figure 1. Computed titration curves—plot of $-\log_{10}(C_A + b)$ *vs.* the fraction titrated for the reaction

$A + T \rightleftharpoons AT(\downarrow)$
Curve *a*. $\beta = 10^{-3}, b = 0$
Curve *b*. $\beta = 0, b = 10^{-2}$
Curve *c*. $\beta = 10^{-3}, b = 10^{-2}$

Where r is the ratio (C°_A/C°_T). When dilution is negligible, as in titrations with extremely concentrated reagents or coulometric titrations, r is zero.

From this stage, it is important to note that Equation 4 results only when certain restrictions are imposed. We will assume that activity coefficients, junction potentials, and the cumulative interference effect, B, are invariant as the titration proceeds even though the volume of the system may change. This is an unrealistic assumption since B must vary as titrant is added. As will be shown later, this is not a serious problem. The above restrictions allow the reformulation of Equations 1 and 4 as:

$$E = \text{const}' + \frac{RT}{z_X F} \ln (\bar{C}_X + b) \tag{11}$$

$$(\bar{C}_X + b)\frac{d^2\bar{C}_X}{df^2} = \left[\frac{d\bar{C}_X}{df}\right]^2 \tag{12}$$

where $\bar{C}_X$ is the normalized variable C_X/C°_A and:

$$b = \frac{B}{\gamma_X C^\circ_A} \tag{13}$$

Equations 7, 8, and 9 can also be put in dimensionless form by dividing by $(C^\circ_A)^{r+1}$ resulting in:

$$\bar{C}_A{}^r(\bar{C}_A - \alpha) - \beta = 0 \tag{14}$$

$$\nu\bar{C}_T(\nu\bar{C}_T + \alpha)^2 - \beta = 0 \tag{15}$$

$$\beta \equiv \frac{\nu K_{sp}{}^{1/m}}{(C^\circ_A)^{r+1}} \tag{16}$$

Two categories of measurement can be discerned—those in which species A is sensed by the electrode, *i.e.*, $X = A$ and those in which the titrant is sensed, $X = T$. The first case will be described in detail. The second constitutes a straightforward extension.

Calculation of the Analytical Error. If the inflection point conditions as stated by Equation 4 with $X = A$ are imposed on the second derivative of Equation 14, the following expression results:

$$\left(\frac{d\alpha}{df}\right)^2 \{\bar{C}_A{}^2(1 - \nu^2) - \bar{C}_A[(\nu + 1)\cdot b - \alpha\nu] + \alpha b\nu(\nu + 1)\}^2 = [(\nu + 1)\bar{C}_A - \nu\alpha]^2(\bar{C}_A + b)\frac{d^2\alpha}{df^2} \tag{17}$$

The derivatives present above are easily computed from the definition of α. When Equations 14 and 17 are solved simultaneously, one obtains for a given value of ν and r algebraic equations for α in terms of the parameters b and β. Since in general the equation for the end-point error, ϕ, is of third and higher order, the detailed results of this calculation for the most common cases, *i.e.*, $\nu = 1$, $1/2$, and 2 are presented in Table I.

In order to illustrate the effect of the term b on the titration curve and on the position of the inflection point, the data of Figures 1 and 2 were computed. Three cases are discussed—first, $\beta = 10^{-3}$ and $b = 0$; second, $\beta = 10^{-3}$ and $b = 0.01$; and last, $\beta = 0$ with $b = 0.01$. As indicated by

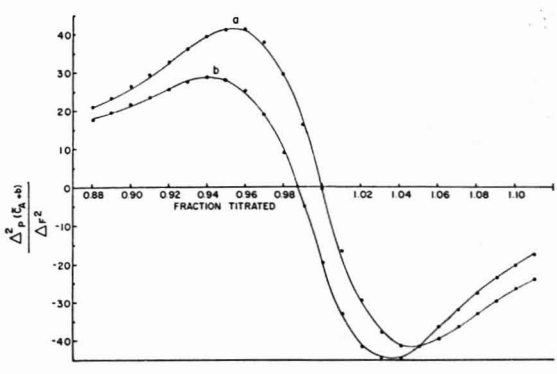

Figure 2. Computed second derivative titration curves—plot of $-\Delta^2 \log_{10}(C_A + b)/\Delta f^2$ *vs.* the fraction titrated for the reaction:

$A + T \rightleftharpoons AT(\downarrow)$
Curve *a*. $\beta = 10^{-3}, b = 0$
Curve *b*. $\beta = 10^{-3}, b = 10^{-2}$

Table II. Analytical Error in Precipitation Titrations with Ion Selective Electrodes Sensitive to the Titrant

b	0.1		3.16×10^{-2}		10^{-2}		3.16×10^{-3}		10^{-3}		0	
β	$\nu = 1/2$	$\nu = 2$	$\nu = 1/2$	$\nu = 2$	$\nu = 1/2$	$\nu = 2$	$\nu = 1/2$	$\nu = 2$	$\nu = 1/2$	$\nu = 2$	$\nu = 1/2$	$\nu = 2$
10^{-1}	−28.85	17.41	−26.77	35.09	−26.02	46.23	−25.77	51.85	−25.69	54.10	−25.65	55.26
10^{-2}	−7.78	0.79	−6.48	11.17	−5.87	18.34	−5.64	22.57	−5.56	24.54	−5.53	25.65
10^{-3}	−2.36	−3.83	−1.81	2.15	−1.47	6.45	−1.30	9.31	−1.23	10.87	−1.19	11.90
10^{-4}	−0.74	−4.21	−0.56	−0.75	−0.43	1.74	−0.34	3.51	−0.29	4.62	−0.26	5.53
10^{-5}	−0.23	−3.39	−0.17	−1.36	−0.13	0.08	−0.10	1.12	−0.08	1.83	−0.06	2.57
10^{-6}	−0.07	−2.44	−0.06	−1.22	−0.04	−0.38	−0.03	0.22	−0.02	0.65	−0.01	1.19
10^{-7}		−1.66		−0.92		−0.42		−0.08		0.17		0.55
10^{-8}		−1.09		−0.64		−0.34		−0.14		0.01		0.25
10^{-9}		−0.71		−0.43		−0.24		−0.12		−0.04		0.13
10^{-10}		−0.46		−0.28		−0.17		−0.09		−0.04		0.10
10^{-11}		−0.29		−0.18		−0.11		−0.06		−0.04		0.10
10^{-12}		−0.18		−0.16		−0.07		−0.04		−0.03		0.09

curve *b* of Figure 1, the potential changes very rapidly when $\beta = 0$ as long as $f < 1.00$; at the equivalence point, all of species *A* is consumed by the titrant and the potential of the electrode is determined solely by the term *B* (see Equation 1). The condition of total insolubility and invariance of *B* forces a discontinuity on the titration curve, causing a point of inflection to occur at the equivalence point and obviating any determinate errors. When $b = 0$ but β is finite (see curve *a*, Figure 1), the potential continues to rise after the equivalence point since there are no interfering ions determining the electrode potential. In this case, of course, the titration curve in the absence of dilution is symmetrical about the equivalence point (see Figure 2, curve *b*) and there is no end-point error. When both β and b are finite, an end-point error occurs. This is illustrated most clearly in Figure 2, curve *b*. The data presented here were obtained by computing the titration curve in fraction-titrated increments of 0.005 units. The second derivative was obtained using a central difference approximation. In this case interpolation indicates an end-point error of 1.65%. If the computation is repeated with $\Delta f = 0.001$ unit, an error of 1.38% is obtained, which is in excellent agreement with the *a priori* approach discussed later.

If the term *b* is set equal to zero in Equation 17, the equations of Meites and Goldman result. More importantly, if dilution is neglected by setting $r = 0$ in all equations, then the second derivative of α with respect to f vanishes and Equation 17 simplifies to:

$$\phi = \frac{(\nu^2 - 1)\cdot\bar{C}_A{}^2 + \nu(\nu + 1)b\bar{C}_A}{\nu^2\bar{c}_A + \nu(\nu + 1)b} \qquad (18)$$

The data presented in Table I were computed by solving Equations 14 and 18, simultaneously. The resulting equation was solved numerically using Horner's scheme and the Newton–Raphson technique for polynomials.

Table II presents the results for the analogous situation in which the titrant species is sensed by the electrode. The general inflection point condition when $X = T$ and $r = 0$, can be written as:

$$\phi = \nu(\nu + 1)\bar{c}_T\left[\frac{(\nu - 1)\bar{C}_T - b}{\bar{c}_T + b(\nu + 1)}\right] \qquad (19)$$

It is important to note that Equations 18 and 19 hold only at the inflection point. This condition superimposed on Equation 15 was used to generate the data of Table II. The results for $\nu = 1$ are not presented since the errors in this case are identical in magnitude but of opposite sign to the case where $X = A$ and $\nu = 1$.

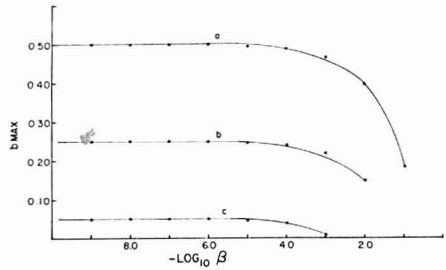

Figure 3. Plot of the maximum value of *b* *vs.* $\log_{10}\beta$ which will permit a titration of the indicated precision in accord with Equation 22

Curve *a*. Precision = 2.30%
Curve *b*. Precision = 1.15%
Curve *c*. Precision = 0.23%

In order to assess whether these errors are outside the range of normal precisions, one can calculate the end-point precision from the "sharpness" index, η, which has been described extensively by Butler (*15*).

$$\eta \equiv \left|\frac{dpX}{df}\right|_{f=1} = 0.4343\left|\frac{z_X F}{RT}\frac{dE}{df}\right|_{f=1} \qquad (20)$$

For the case where $\nu = 1$ and dilution is negligible, η is given by

$$\eta = \frac{1}{2}\frac{0.4343}{b + \sqrt{\beta}} \qquad (21)$$

The per cent uncertainty in locating the equivalence point is given approximately by Equations 20 and 21 as follows:

$$\%\Delta f = 100\frac{\Delta pX}{\eta} = 460.6\Delta pX\cdot(b + \sqrt{\beta}) \qquad (22)$$

This equation realistically predicts that as β and b become larger, the precision decreases. A reasonable estimate of the uncertainty in pX is ±0.01. At 25 °C, this corresponds to an error of ±0.6 mV($z_X = 1$) in the end-point potential. Equation 21 was used to compute the maximum value of b such that the titration can be performed with a precision of 2.30, 1.30, or 0.23% at a given value of β. Figure 3 illustrates

(15) J. N. Butler, "Ionic Equilibrium, A Mathematical Approach," Addison-Wesley, Reading, 1964.

Table III. Effect of Dilution on the Analytical Error[a]

β	0.10	3.16×10^{-2}	10^{-2}	3.16×10^{-3}	10^{-3}	3.16×10^{-4}	0
10^{-2}	28.29[b]	20.58	17.64	16.61	16.28	16.17	16.12
10^{-3}	8.92	5.12	3.06	2.12	1.77	1.66	1.60
10^{-4}	4.11	2.39	1.29	0.64	0.34	0.22	0.16
10^{-5}	1.97	1.22	0.72	0.38	0.17	0.07	0.02
10^{-6}	0.94	0.60	0.38	0.22	0.12	0.05	
10^{-7}	0.44	0.29	0.19	0.12	0.07	0.04	
10^{-8}	0.21	0.14	0.10	0.06	0.04	0.02	
10^{-9}	0.10	0.06	0.04	0.03	0.02		
10^{-10}	0.04	0.03	0.02	0.01			

[a] All data was computed assuming that the electrode is sensitive to the analyte, that $\nu = 1$ and that $r = 1$.
[b] Values below or to the right of the double line may be obtained by summing the error due to dilution and the error due to imperfect selectivity.

these results. A cursory examination of the data of Tables I and II and Figure 3 indicates that the errors caused by finite values of β are outside the precision of measurement. Equation 22 demonstrates that the interference ratio has a very deleterious effect on the precision of analysis, *e.g.*, when $\beta = 10^{-6}$ and $b = 0$, a precision of 0.005% would result, *i.e.*, if volumetric errors are negligible; however, when $\beta = 10^{-6}$ and $b = 0.1$, the precision can not be better than about 0.5%.

Effect of Dilution on the Titration Curve. In any practical titration, with the exception of coulometric titrations, the volume of the system will change perceptively because of the addition of titrant. This increase can be minimized by using a titrant concentration, C°_T, which is much larger than the analyte concentration, C°_A. This must be recommended in titrations with ion selective electrodes, particularly under circumstances where the interference ratio is finite. This is mandated by the fact that dilution effects always act to decrease the magnitude of the potential break, *i.e.*, decrease η, and second often increase the discrepancy between the inflection point and equivalence point, at least when $\nu = 1$. The data presented in Table III were computed from Equation 17, using $\nu = r = 1$. It should be emphasized that this treatment is not exact, since we assumed earlier in the derivation of Equation 17 that the term b was independent of the fraction titrated. This is not precisely true, since as the volume changes, the concentration of species contributing to b will vary; however, the approach does allow an approximate computation of the effect of dilution on the analytical accuracy.

RESULTS AND DISCUSSION

A comparison of the data of Tables I and II and Figure 3 indicates that the errors caused by finite selectivity ratios are well outside the range of the computed end-point uncertainty. The magnitude of these errors is not surprising. Even though the selectivity term may be small with respect to C°_A, in the vicinity of the equivalence point b may be larger than $\bar{C}_A$ and, therefore, be the predominant term in Equation 11 which defines the inflection point.

In order to discuss the data of Tables I and II, we will refer to a symmetry error, *i.e.*, the end-point error, when $b = 0$ and a selectivity error, *i.e.*, the difference between the symmetry error and the computed error, when b is finite. The two principal variables which must be considered are ν and whether the electrode is sensitive to species A or T.

When $\nu = 1$ the system is quite simple. There is no symmetry error and the selectivity errors are equal in magnitude but opposite in sign; the inflection point precedes the equivalence point when $X = A$ and follows the equivalence point when $X = T$. At a given value of b, the error decreases monotonically as β decreases, the error being zero when the solubility is vanishingly small. Similarly at a given value of β, the error decreases monotonically to zero as b approaches zero.

Whenever $\nu \neq 1$, the error in the absence of any interfering materials is not zero but depends strongly on the parameter β. One can show from the work of Meites and Goldman (*14*) that the error in the absence of dilution will be given by

$$\phi = (\nu^2 - 1)\left(\frac{\beta}{\nu^{2\nu}}\right)^{1/\nu+1} \tag{23}$$

Equation 23 indicates that the symmetry error will be positive when $\nu > 1$ and negative when $\nu < 1$. It should be obvious that when ν is other than unity, the magnitude of the symmetry error generally requires that the precipitate be rather insoluble (small K_{sp}) or that the titration be carried out at high concentration (large C°_A), since either circumstance tends to decrease β and, therefore, the symmetry error.

The selectivity error is positive when species A is measured and negative when T is measured. As witnessed by the data of Tables I and II, only under those circumstances where the two errors, *i.e.*, selectivity and symmetry, reinforce one another will the overall error be a monotonically decreasing function of β. This occurs when $X = A$ and $\nu > 1$ or when $X = T$ and $\nu < 1$. Under these circumstances the sign of the error is invariant and the error decreases uniformly toward zero as β approaches zero. Under the alternate set of circumstances, *i.e.*, $X = T$ and $\nu > 1$ or $X = A$ and $\nu < 1$, the error does not decrease monotonically as β decreases and the sign of the error is not invariant, although in the limit as β approaches zero, the error goes to zero. This results because the two errors are of opposite sign and either one or the other will predominate for a given value of β and b.

It is quite interesting to note that in those cases where the sign of ϕ oscillates, the error becomes negligibly small at larger values of β than in those cases where the sign is invariant. This, somewhat surprisingly, suggests that the order of reagent addition may improve the accuracy of the titration. For example, consider the following titration process:

$$2A + T \leftrightharpoons A_2T \tag{24}$$

Under these circumstances $\nu = 2$, $m = 1$, and β is defined below.

$$\beta_1 = 2K_{sp}/C^{\circ}{}_A{}^3 \tag{25}$$

Now interchange the titrant and reagent species, keep all else constant, *i.e.*, use the same electrode, electrolyte, initial concentration, etc. The reaction becomes:

$$A + 2T \leftrightharpoons AT_2 \tag{26}$$

with $\nu = 1/2$, $m = 2$, and β is redefined as:

$$\beta_2 = \frac{{}^1/_2 K_{sp}{}^{1/2}}{(C^\circ_A)^{3/2}} \tag{27}$$

This may be summarized as:

$$\beta_2 = \frac{(C^\circ_A)^{3/2}}{4K_{sp}{}^{1/2}} \cdot \beta_1 \tag{28}$$

With reference to Tables I and II, it is clear that whenever $\beta_2 < \beta_1$, the analytical error must be decreased by an interchange of the analyte and titrant species. This situation will result whenever:

$$(C^\circ_A)^2 \leq 16K_{sp} \tag{29}$$

If $\beta_2 > \beta_1$ the error may or may not decrease depending upon the specified values of b, β_1, and β_2. Of course, when Equation 29 is realized, β_1 and β_2 would be so large that the titration is impractical. Indeed as has been pointed out (*14*), an inflection point may not occur when C°_A is extremely low.

It should be noted that the magnitude of the end-point error depends strongly on the reaction stoichiometry and upon the initial concentration of analyte, since both β and b are as indicated by Equations 13 and 16 related to C°_A. Generally, the error increases as the analyte becomes more dilute, since this increases both β and b. The solubility product, K_{sp}, has been formulated rather unusually (see Equation 3), and for the titration of a divalent cation with a divalent anion has a value equal to the square root of the more conventionally defined solubility product. All else being equal, errors in such titrations will be much larger than in a similar titration involving univalent species.

The magnitude of the errors computed here is such as to be a serious limitation in the use of ion selective electrodes as inflection point indicators in titrations involving only moderately insoluble salts. Every attempt should be made to assess the presence of ions whose selectivity coefficients are large and to minimize their concentration or replace them with ions which interfere less significantly. In general, it appears that the addition of an electrolyte for masking interferences and maintaining ionic strength and or junction potentials must, in terms of these errors, be viewed with suspicion.

It is instructive to compare these data for precipitation titrations to Whitfield and Leyendekker's (*9*) results on the effect of ion selectivity ratios on the complexometric titration of calcium and magnesium. They computed a number of theoretical titration curves, *i.e.*, plots of electrode potential *vs.* f, and examined the influence of finite interference ratios on these curves. They found that the inflection point coincided with the equivalence point whenever a large end-point break (2–3 pX units) occurred. It is difficult to contrast our work with theirs since the reactions studied are fundamentally different and the range of equilibrium constants investigated was quite narrow (10^{10}–10^{12}). Second, a comparison of Figures 1 and 2 of this work indicates that conventional titration curves are not particularly sensitive to this effect, although second derivative titration curves are very sensitive. It may be that the cases studied by these workers represent the limit of large equilibrium constants where any deviations are negligibly small.

A number of alternative approaches to the problem of finite interference ratios are possible. A first approach is titration to a predetermined equivalence point potential. In this case, one must minimize errors due to changes in activity coefficients, junction potential, and spurious materials which can alter the activity of the analyte. A second approach is the method of Gran (*16*, *17*) plots, where the analyte concentration is computed from the measured electrode potential and plotted against the volume of titrant added. A linear titration curve results, whose extrapolated branches intersect to yield an end point free of these errors. As b becomes larger, the precision of such a technique would be seriously impaired.

Table III presents a compilation of analytical errors for $\nu = 1$ titration with $r = 1$, *i.e.*, equal titrant and initial analyte concentrations. These data were computed using Equations 14 and 17 and approximately correcting for the effect of dilution on the term b in Equation 17 by assuming that the effective value of b around the inflection point was exactly one half its initial value. The last column of Table II, which is in agreement with the equation of Meites and Goldman (*13*), indicates that even when the interference ratio is zero, considerable end-point errors will occur. This results because the titration curve becomes quite asymmetrical about the inflection point due to the distortions caused by dilution. Those values of the titration error in Table II which fall below or to the right of the double line can be obtained by merely adding the dilution error (Table III, $b = 0$) to the selectivity error (Table I, $\nu = 1$). In all cases the two values differ by no more than 0.3% in their absolute value. In the light of the data, one can assume that in the limit of either a small b or β, the two errors are virtually independent and are, therefore, additive. When both β and b are large, the coupling of the two effects is stronger and the computed error is larger than the simple sum of the two independent errors.

CONCLUSIONS

Titrations with ion selective electrodes are not free of errors related to the selectivity ratio. Finite concentrations of interfering ions can affect both the analytical accuracy and precision when the titration end point is taken as the inflection point of the potential–volume curve. In general, the determinate errors are often well outside the range of the achievable precision whenever the precipitate has a finite solubility. End-point errors are largest when the reaction is not symmetrical ($\nu \neq 1$). Such reactions require extremely small solubility products in order to avoid both symmetry and selectivity errors.

Within the range of practical titrations, the error is negligible as long as $\beta \leq 10^{-9}$ or $b < 3 \times 10^{-4}$. The magnitude of the errors and the effect of b on the analytical precision suggest that such titrations should be carried out with minimal supporting electrolyte concentration and at the greatest possible concentrations of both analyte and titrant.

Work is in progress in these laboratories to assess the effect of selectivity errors on complex formation titrations and to develop experimental alternatives to the method of end-point location.

ACKNOWLEDGMENT

The author thanks Leon N. Klatt of this department for many interesting and fruitful discussions in connection with this work. Funds for computer time provided by the University of Georgia Computer Center are gratefully acknowledged.

RECEIVED for review October 26, 1970. Accepted December 14, 1970.

(16) G. Gran, *Acta Chem. Scand.*, **4**, 559 (1950).
(17) T. Anfalt, D. Dryssen, and D. Jagner, *Anal. Chim. Acta*, **43**, 487 (1968).

Determination of the Formation Constants of Iron(III) and Vanadium(V) with β-Isopropyltropolone Using the Extraction Method

Oscar Menis,[1] B. E. McClellan,[2] and David S. Bright

Analytical Chemistry Division, National Bureau of Standards, Washington, D. C. 20234

Equilibrium constants of ferric and vanadyl ions for the formation of the chelate with β-isopropyltropolone (HIPT) were determined by the extraction method. The values for these constants were derived by graphic and least squares computer calculations. The constants for the vanadyl system are reported for the first time. It is postulated that an adduct $VO_2IPT \cdot HIPT$ is formed and its formation constant, log $\beta_N = K_1 K'$, was determined as 13.8 and 13.6 ± 0.8 by graphic and least squares calculations, respectively. The partition constant, K_{DC}, was 2.45 and 2.6 ± 0.4, respectively. The values for $Fe(IPT)_2$ complex were for log β_N, 37.7 and 37.8 ± 0.1, respectively, while the log K_{DC} was 2 and 2.0 ± 0.1, respectively. It was also possible to calculate the overall stepwise constants, log $\beta_1 = 13.0 \pm 0.2$ and log $K_2K_3 = 24.8 \pm 0.1$ by the least squares method. The other experimental parameters which were studied were the effect of solvent and ionic strength.

THE OCCURRENCE of adduct formation in numerous metal chelate systems is now widely recognized and its subsequent enhancement of the solvent extraction of various metal ions is frequently utilized for their more effective separation. Freiser has recently discussed these types of reactions (*1*). In common with many other organic ligand systems, β-isopropyltropolone (HIPT) forms adduct complexes. This ligand, as has been pointed out by Dyrssen (*2*), has a considerably larger distribution constant in chloroform/water than thenoyltrifluoroacetone (TTA) and does not undergo any hydration equilibria such as encountered with TTA. Finally, unlike TTA, HIPT does not decompose rapidly in alkaline media. Since it has become more readily available recently, it should find greater use over the better known TTA system.

Dyrssen (*3*) has studied the extraction characteristics of large numbers of metals with HIPT and Dutt *et al.* (*4*) have reviewed some of the analytical applications of this reagent. Of the elements reported, Dyrssen (*3*) as well as Dutt and Singh (*5*), have also determined the stability constant of Fe^{3+}–HIPT complex using spectrophotometric methods. No data were reported on the equilibrium constants for the VO_2^+ chelate.

Menis and Iyer (*6*) have studied the extraction of VO_2^+ with HIPT as a means of spectrophotometric determination of vanadium in steel samples. This led to our study to establish the several equilibrium constants of adduct complex VO_2-IPT·HIPT and to derive new values for the $Fe(IPT)_2$ complex from extraction data. These were calculated by both graphic and least squares methods. The latter calculations with the aid of fast computers can facilitate reporting these constants and also provide estimates of errors.

EXPERIMENTAL

Apparatus. All extractions were performed in 60-ml separatory funnels having polytetrafluoroethylene stopcocks and stoppers. The samples were agitated on a mechanical shaker. Radioactivity measurements were made with a modular counting system connected to a 2-in. × 2-in. NaI (Tl) well-type scintillation detector. Measurements of pH were made with an expanded scale pH meter. Spectral measurements were made with either a half-meter quartz prism spectrophotometer or a recording double beam spectrophotometer provided with a quartz prism-grating arrangement.

Materials. A stock solution of $10^{-2}M$ Fe^{3+} in $10^{-2}M$ $HClO_4$ was prepared by dissolving high purity iron wire in perchloric acid and adding ^{59}Fe radiotracer solution. A stock solution of $10^{-2}M$ VO_2^+ in $10^{-2}M$ $HClO_4$ was prepared by dissolving ammonium vanadate in perchloric acid and adding ^{48}V radiotracer. In tests to pH 3, with tracers, no effect on the VO_2^+ stability was observed.

The β-isopropyltropolone (HIPT) was obtained from Columbia Organic Chemicals Co., Columbia, S. C. It was recrystallized from 96% ethanol and dried under vacuum prior to use. Solutions of HIPT were prepared by weighing the carefully purified and dried reagent. All other reagents were of Reagent Grade quality.

Procedure. DISTRIBUTION STUDIES. All extractions were performed using equal volumes (10 ml) of aqueous and organic phases at 25 ± 1 °C. Radioactive isotopes ^{48}V and ^{59}Fe were used to determine the distribution ratio. Distribution studies were performed on both VO_2^+ and Fe^{3+} at various HIPT concentrations and at various acidities. The formation constants, as well as overall extraction constants log K^* and the partition constant log K_{DC} were determined at ionic strength, $\mu = 1$, from the distribution data by both the graphic and least squares methods. The effect of several solvents was also studied.

An examination was made of the effect of ionic strength on equilibrium extraction of Fe^{3+} with HIPT dissolved in $CHCl_3$. The $[H^+]$ was 0.1, $[Fe^{3+}]$ was $1 \times 10^{-3}M$, and the shaking time was 16 hours. The distribution ratio was independent of $[ClO_4^-]$ between 0.1 and $4M$. Most measurements were made using an ionic strength of unity for the aqueous phase.

An equilibration time in excess of 16 hours was always used. This was more than sufficient for equilibrium to be attained. $Fe(HIPT)_3$ extraction was complete in about 6 hours (*7*), and VO_2 IPT·HIPT extracted within 1 hour.

In the experiment to determine the partition constant K_{DR} of the reagent, 10 ml of $0.01M$ HIPT was equilibrated for 30 minutes with 10 ml of $1M$ $HClO_4$. Following equilibration, the absorbance of both phases was read at 345 nm and compared with previously prepared calibration curves to obtain the concentration of HIPT in the two phases.

[1] To whom inquiries should be addressed.

[2] Present address, Department of Chemistry, Murray State University, Murray, Ky. 42071.

(1) H. Freiser, *Critical Rev. Anal. Chem.*, **1**, 47 (1970).
(2) D. Dyrssen, *Acta Chem. Scand.*, **15**, 1614 (1961).
(3) D. Dyrssen, *Trans. Roy. Inst. Technol., Stockholm*, No. **188**, 1962.
(4) Y. Dutt, R. P. Singh, and M. Katyal, *Talanta*, **16**, 1369 (1969).
(5) R. P. Singh and Y. Dutt, *Indian J. Chem.*, **4**, 214 (1966).
(6) O. Menis and C. S. P. Iyer, National Bureau of Standards, Washington, D. C., unpublished results, 1969.
(7) B. E. McClellan and O. Menis, ANAL. CHEM., **43**, 436 (1971).

Table Ia. Definitions of Constants

IRON

Distribution of reagent

$$HIPT \overset{K_{DR}}{\rightleftharpoons} HIPT_o \qquad K_{DR} = \frac{[HIPT]_o}{[HIPT]}$$

Dissociation of acid

$$HIPT \overset{K_a}{\rightleftharpoons} H^+ + IPT^- \qquad K_a = \frac{[H]\,[IPT]}{[HIPT]}$$

Formation of chelate

$$Fe^{3+} + IPT^- \overset{K_1}{\rightleftharpoons} Fe(IPT)^{2+} \qquad \beta_1 = K_1 = \frac{[Fe\,IPT]}{[Fe]\,[IPT]}$$

$$Fe(IPT)^{2+} + IPT \overset{K_2}{\rightleftharpoons} Fe(IPT)_2^{+1} \qquad \beta_2 = K_1K_2 = \frac{[Fe(IPT)_2]}{[Fe]\,[IPT]^2}$$

$$Fe(IPT)_2^{1+} + IPT \overset{K_3}{\rightleftharpoons} Fe(IPT)_3 \qquad \beta_3 = K_1K_2K_3 = \frac{[Fe(IPT)_3]}{[Fe]\,[IPT]^3}$$

Distribution of chelate

$$Fe(IPT)_3 \overset{K_{DC}}{\rightleftharpoons} Fe(IPT)_{3o} \qquad K_{DC} = \frac{[Fe(IPT)_3]_o}{[Fe(IPT)_3]}$$

Distribution ratio

$$D = \frac{|M|_o}{|M|} = \frac{\text{Total concentration of M in organic phase}}{\text{Total concentration of M in aqueous phase}}$$

$$K^* = K_{DC}\beta_3\frac{K_a^3}{K_{DR}^3}; \quad \text{or } \beta_3 = \frac{K^*\,K_{DR}^3}{K_{DC}K_a^3}; \text{ or}$$

$$\log \beta_3 = \log K^* + 3 \log K_{DR} - \log K_{DC} - 3 \log K_a$$

Table Ib. Definition of Constants

VANADIUM

Distribution of reagent

$$HIPT \overset{K_{DR}}{\rightleftharpoons} HIPT_o \qquad K_{DR} = \frac{[HIPT]_o}{[HIPT]}$$

Dissociation of acid

$$HIPT \overset{K_a}{\rightleftharpoons} H^+ + IPT^- \qquad K_a = \frac{[H]\,[IPT]}{[HIPT]}$$

Formation of chelate

$$VO_2^+ + IPT^- \overset{K_1}{\rightleftharpoons} VO_2IPT \qquad K_1 = \frac{[VO_2(IPT)]}{[VO_2]\,[IPT]}$$

Formation of adducted species

$$VO_2IPT + HIPT \overset{K'}{\rightleftharpoons} VO_2IPT\cdot(HIPT) \qquad K' = \frac{[VO_2(IPT)\cdot HIPT]}{[VO_2(IPT)]\,[HIPT]}$$

Distribution of chelate

$$VO_2IPT \overset{DC}{\rightleftharpoons} VO_2IPT_o \qquad K_{DC} = \frac{[VO_2(IPT)]_o}{[VO_2(IPT)]}$$

Distribution of adducted species

$$VO_2IPT(HIPT) \overset{K'_{DC}}{\rightleftharpoons} VO_2IPT(HIPT)_o \qquad K'_{DC} = \frac{[VO_2(IPT)\cdot HIPT]_o}{[VO_2(IPT)\cdot HIPT]}$$

Distribution ratio

$$D = \frac{|M|_o}{|M|} = \frac{\text{Total concentration of M in organic phase}}{\text{Total concentration of M in aqueous phase}}$$

$$K^* = K'_{DC}K'K_1\frac{K_a}{K_{DR}^2}$$

The value of the pK_a was determined spectrophotometrically at $\mu = 1$. HIPT has two absorption maxima in the UV region at 322 and 340 nm, while the IPT^- exhibits maxima at 330 and 390 nm. Since the absorption of the HIPT species is negligible at 390 nm, it is a simple matter to determine the relative concentrations of IPT^- and HIPT at any pH. The absorbance of the IPT^- was measured at pH values of 7.02 and 7.56 and the concentration of IPT^- determined from a previously prepared calibration curve of IPT^- in 1*M* NaOH. The concentration of HIPT was obtained by difference and the pK_a value calculated from $K_a = [H]\,[IPT]/[HIPT]$.

RESULTS AND DISCUSSION

The value for log K_{DR}, the distribution constant for HIPT in $CHCl_3$ for 1*M* $HClO_4$ was found to be 2.45 ± 0.05. Dyrssen (*3*) reported a value of log K_{DR} of 3.37 for $CHCl_3$ from 0.1*M* ClO_4^- solutions.

The average pK_a value determined at $\mu = 1$ was 7.5 with a standard error of the mean of ±0.2 based on four replicates determined at two pH values. Dyrssen (*3*) reported at $\mu = 0.1$, a pK_a of 7.04. Our value compared well with that of Hseu (*8*) when his values at various ionic strengths were extrapolated to $\mu = 1$. Hseu's extrapolated value was 7.4 (*8*). Based on Hseu's data, Dyrssen's lower value can be attributed to the lower ionic strength.

Iron(III) extracts in 1.0×10^{-2} *M* HIPT in $CHCl_3$ over a range from 10^{-6} to 5*M* acid. In the higher acid region (1–5*M*), however, the extraction occurs very slowly. Above pH 6, hydrolysis of Fe^{III} becomes a factor and decreases the distribution ratio. Benzene and cyclohexane are also excellent solvents for this extraction, both yielding, within the experimental error, quantitative extraction in acid (0.1–1*M*) solutions.

Vanadyl extracted essentially quantitatively with 1.0×10^{-2}*M* HIPT in $CHCl_3$ over a range from 10^{-3} to 6*M* acid. Benzene is also a suitable solvent. However, in the extraction with cyclohexane, an insoluble blue-violet chelate was observed.

Equilibrium Constants for the Fe^{3+}–HIPT System. Graphic Method. The distribution ratio, *D*, is defined as

$$D = \frac{|Fe|_o}{|Fe|}$$

where $|Fe|$ represents the total concentration of iron in the particular phase and subscript *o* designates the organic phase. Assuming that only mononuclear species are present and no hydrolysis occurs and that the extracted complex is $Fe(IPT)_3$, *D* is expressed as:

$$D = \frac{[Fe(IPT)_3]_o}{[Fe^{3+}] + [Fe(IPT)^{2+}] + [Fe(IPT)_2^{+}] + [Fe(IPT)_3]} \qquad (1)$$

After substituting for all the species in terms of (IPT) and the equilibrium constant defined in Table I and cancelling $[Fe^{3+}]$, and omitting charges for simplification, then one obtains:

$$D = \frac{K_{DC}\beta_3[IPT]^3}{1 + \beta_1[IPT] + \beta_2[IPT]^2 + \beta_3[IPT]^3} \qquad (1a)$$

In the region of $[IPT^-]$ where the metal is most important, *D* can be closely approximated by

$$D = \frac{K_{DC}\,\beta_3[IPT]^3}{1} \qquad (1b)$$

since $[Fe(IPT)_i]$ and thus $\beta_i\,[IPT]^i$ are negligible in the denominator, where $i = 1, 2, 3$. Also $[HIPT]_{o\,initial} = [HIPT]_o$ as the reagent was supplied in sufficient excess to make this true. Using the definitions of the constants above

$$[IPT^-] = \frac{K_a}{[H]}[HIPT] = \frac{K_a}{[H]}\frac{[HIPT]_o}{K_{DR}} \qquad (1c)$$

Substituting this equation into 1b we express *D* in terms of $[HIPT]_o$

$$D = K_{DC}\,\beta_3\frac{K_a^3}{K_{DR}^3}\frac{[HIPT]_o^3}{[H]^{3-}} = K^*\frac{[HIPT]_o^3}{[H^+]^{3-}} \qquad (1d)$$

or $\log D = \log K^* + 3 \log [HIPT]_o$ when $[H] = 1$ where K^* is the overall extraction constant which includes all the con-

(8) T. M. Hseu, *J. Chinese Chem. Soc.*, (*Taipei*), **6**, 38 (1959).

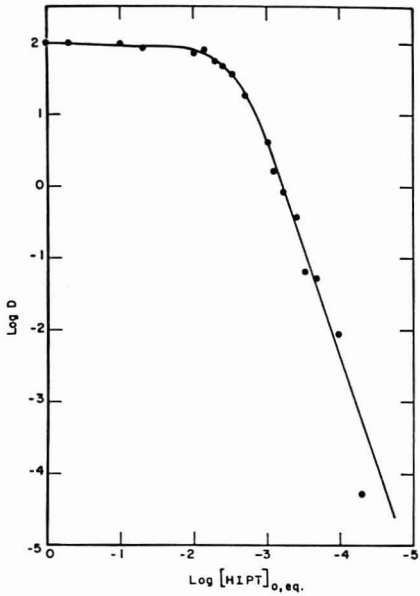

Figure 1. Plot of log D vs. log [HIPT]$_o$
$[H^+] = 1.0$, $[Fe^{3+}] = 1.0 \times 10^{-5}$, $\mu = 1$
Slope = 3.0
Extrapolated intercept = 10

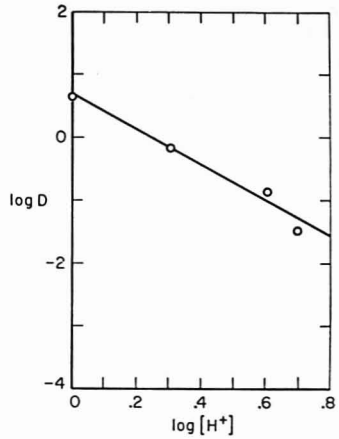

Figure 2. Plot of log D vs. log [H$^+$] for Fe(III)
$Fe^{3+}] = 1.0 \times 10^{-5}$, $[HIPT]_o = 1.0 \times 10^{-3}$
Slope = 2.7
Log D intercept = 1.0

stants of Equation 1d. A slope of 3, shown in Figure 1 represents the number of ligands which combine with the metal ion and thus supports our assumptions in Equations 1 through 1d. The intercept of the curve, gives a log K^* value of 10, which agrees with Dyrssen's value (*3*). The horizontal portion of the curve yields a value for log K_{DC} of 2.0. Solving Equation 1d for β_2 (see Table I*a*) and substituting in the D values at $[HIPT]_o = 1$ gives a value for log β_3 of 37.7. This is somewhat higher than Dyrssen's of 31.63 at $\mu = 0.1$ (*3*). With the exception of [H$^+$], activity equilibrium concentrations were used in all the calculations. It is realized that the activities are somewhat different from concentrations, however, a constant ionic strength of one was used throughout the study.

Log D vs. log [H] is plotted in Figure 2. From Equation 1d, the slope should be 3.0; the actual value was 2.7. The error probably is due to the scatter in the data and the variation of ionic strength from 1 to 10. The intercept is log K^* + 3 log $[HIPT]_o \sim 1.0$, thus log $K^* = 10$, in agreement with an extrapolation of the slope 3 portion of Figure 1. These results together with the values obtained by the subsequently described least squares method are summarized in Table II.

Least Squares Method (Iron). When Equation 1a is inverted, as in Equation 2, it becomes suitable for least squares fitting by a method analogous to Rydberg's (*9*).

$$\frac{1}{D} = \frac{1}{K_{DC}\beta_2}\frac{1}{[IPT]^2} + \frac{\beta_1}{K_{DC}\beta_2}\frac{1}{[IPT]^2} + \frac{\beta_2}{K_{DC}\beta_2}\frac{1}{[IPT]} + \frac{1}{K_{DC}} \quad (2)$$

A computer program called OMNITAB available at NBS provides a program for least squares curve fitting (*10*). OMNITAB was tested on the thorium–acetylacetone data of Rydberg (*11*), with agreement to 1% of the coefficients and their standard deviations (*9*). Similarly, for Equation 2, the function D was fitted to the vectors: $[IPT]^{4-}$, $[IPT]^{2-}$, $[IPT]^{-1}$ and 1.0 by the method of least squares giving values of the coefficients

(9) J. Rydberg, *Acta Chem. Scand.*, **15**, 1723 (1961).
(10) OMNITAB, "A Computer Program for Statistical and Numerical Analysis," U. S. Dept. of Commerce, NBS Handbook 101, p 112 (1966).
(11) J. Rydberg, *Acta Chem. Scand.*, **4**, 1603 (1950).

Table II. Equilibrium Constants for Extraction of Fe^{3+} and VO_2^+ with HIPT

Chelate	Method	Log K^*	Log K_1	Log K_2K_3	Log K_{DC}	Log β_N
$Fe(IPT)_3$	Graphic	10	...	...	2.0	37.7
	Least squares	9.9 ± 0.4[a]	13.0 ± 0.2	24.77 ± 0.1	1.97 ± 0.1	37.8 ± 0.1
$VO_2(IPT)\cdot HIPT$	Graphic	4.2	...	...	2.45[b]	13.8
	Least squares	3.8 ± 0.1	...	...	2.6 ± 0.4	13.6 ± 0.8[c]

[a] The uncertainties indicated are estimated standard errors.
[b] log K'_{DC}.
[c] $\beta_N = K_1K'$.

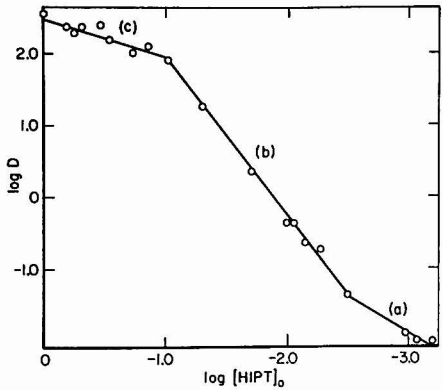

Figure 3. Plot of log D *vs.* log [HIPT]$_o$ for VO_2^+

$[H^+] = 1.0$, $[VO_2^+] = 1.0 \times 10^{-4}$, $\mu = 1$
Region *a* slope = 1.0
Region *b* slope = 2.15
Log D intercept = 4.2

$$\frac{1}{K_{DC}}\,\frac{1}{\beta_3}\,\frac{1}{K_{DC}}\,\frac{\beta_1}{\beta_3}\,\frac{1}{K_{DC}}\,\frac{\beta_2}{\beta_3}\,\frac{1}{K_{DC}}$$

The third coefficient had a large enough relative standard deviation indicating that the data could not be used to resolve β_2/β_3. Omitting the third parameter, OMNITAB was used again to fit $1/D$ to $[IPT]^{3-}$, $[IPT]^{2-}$ and 1.0. Thus only β_3, β_1, and K_{DC} could be resolved, but not separately the step constants K_2 and K_1. The remaining coefficients did not change appreciably, verifying that the third parameter was not significant.

Weighting methods were used which were analogous to those described by Rydberg (*12*, *13*). Thus:

$$D = \frac{|\mathrm{Fe}|_o}{|\mathrm{Fe}|} = \frac{I_o}{I_w}$$

where I = number of counts.

The error in D was considered to be solely due to the tracer counting error of I_o and I_w. Because the least squares fit program minimizes the square of the difference between $1/D$ obtained from the data and $(1/D)_{calcd}$ calculated from Equation 2, $1/D$ values are weighted inversely to the square of their expected "spread" or standard deviation, *i.e.*

$$w = \frac{1}{\sigma^2_{1/D}}$$

Using the propagation of error formulas, and knowing the standard deviation of the organic and water phase σ_o and σ_w from the number of counts in sample and background, then:

$$w = \frac{D^2}{\frac{\sigma_o^2}{I_o^2} + \frac{\sigma_w^2}{I_w^2}}$$

The weighting factors covered a range of about 8 orders of magnitude. This arises from the fact that the values of $1/D$ varied over a similarly large range.

(12) J. Rydberg and J. C. Sullivan, *Acta Chem. Scand.*, 13, 2057 (1959).
(13) J. Rydberg, *ibid.*, 14, 157 (1960).

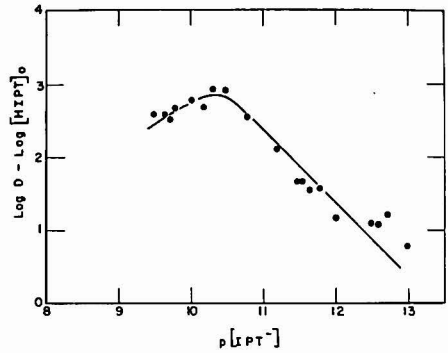

Figure 4. Plot of log D $-$log [HIPT]$_o$ *vs.* p[IPT$^-$] for VO_2^+

$[H^+] = 1.0$, $[VO_2^+] = 1.0 \times 10^{-4}$, $\mu = 1$
Slope = 1

Equilibrium Constants for VO^{2+}–HIPT System. Graphic Method. Figure 3 shows a plot of log D *vs.* log [HIPT]$_o$ for VO_2^+ complex.

The distribution ratio, D, omitting signs is defined as:

$$D = \frac{|\mathrm{M}|_o}{|\mathrm{M}|} = \frac{[VO_2(IPT)]_o + [VO_2(IPT\cdot HIPT)]_o}{[VO_2^+] + [VO_2(IPT)] + [VO_2(IPT)\cdot HIPT]} \tag{3}$$

[H] = 1 throughout the experiment, therefore

$$[IPT^-] = \frac{K_a}{K_{DR}}\,[HIPT]_o$$

Solving Equation 3 for D in terms of [HIPT]$_o$, using the defined constants, and cancelling $[VO_2^+]$ gives:

$$D = \frac{K_{DC}K_1\frac{K_a}{K_{DR}}[HIPT]_o + K'_{DC}K'K_1\frac{K_a}{K^2_{DR}}[HIPT]_o^2}{1 + K_1\frac{K_a}{K_{DR}}[HIPT]_o + K'K_1\frac{K_a}{K^2_{DR}}[HIPT]_o^2} \tag{4}$$

The linear portions of Figure 3 may be associated with Equations 3 and 4 as follows:

REGION *a*. Lowest range of [HIPT]: The simple complex is the extracted species. The uncomplexed metal predominates in the aqueous phase.

$$D = K_{DC}K_1\frac{K_a}{K_{DR}}[HIPT]_o \qquad \text{Theoretical slope} = 1 \tag{5}$$

REGION *b*. Intermediate range of [HIPT]: The adduct complex is extracted, but the uncomplexed metal is still predominant in the aqueous phase.

$$D = \frac{[VO_2(IPT)\cdot HIPT]_o}{[VO_2^+]} = \frac{K'_{DC}K'K_1\frac{K_a}{K^2_{DR}}[HIPT]_o^2}{1} \tag{6}$$

Theoretical slope = 2

REGION *c*. Highest range of [HIPT]. The adducted complex is extracted, and is also the predominant species in the aqueous phase.

$$D = \frac{[VO_2(IPT)\cdot HIPT]_o}{[VO_2(IPT)\cdot HIPT]} =$$

$$\frac{K'_{DC}K'K_1\dfrac{K_a}{K^2_{DR}}[HIPT]_o^2}{K'K_1\dfrac{K_a}{K^2_{DR}}[HIPT]_o^2} = K'_{DC} \quad (7)$$

Theoretical slope = 0

Thus the value for D expresses merely the partition constant of the adduct between the two phases.

According to the distribution Equation 5 (region *a*), of Figure 3, should show a slope of unity if VO_2IPT is formed and VO_2^+ predominates in the aqueous phase. The graphical data allow this interpretation. The region *c*, with a reduced slope, has an intercept of 2.45, from which log K'_{DC} can be estimated assuming the adduct predominates in both phases. The extrapolated intercept of region *b*, gives the value for log K^* of 4.2. These equations describing this system are analogous to those given by Chou, Fernando, and Freiser (*14*, *15*) for the Zn(II)–8-quinolinol reaction in which the extracted species is an adduct $Zn(OX)_2\cdot HOX$.

As discussed in their work, a plot of log D − log $[HIPT]_o$ *vs.* log $[IPT^-]$ should reach a constant maximum value at high log [IPT] values if VO_2 (IPT) predominates in the aqueous phase. If the adduct species, VO_2 (IPT)·xHIPT, predominates in the aqueous phase, this plot does not give constant values. Figure 4 shows that a constant value was not obtained; therefore, an adduct species predominates in the aqueous phase. The slope in Figure 3 (region *b*) is 2, indicating one chelated IPT and one adducted HIPT. Figure 4 shows a plot with a slope of unity and along with Figure 3 the extracted species is indicated to be $VO_2IPT\cdot(HIPT)$.

Least Squares Method. In Equation 3, the first term of the numerator corresponds to the extraction of the chelate without the adduct. Because of this extra term, the equation is not linear using ordinary linear least squares. It can be changed to the form

$$\frac{1}{D} = a\frac{[HIPT]_o}{D} + b\frac{1}{[HIPT]_o} + c + d[HIPT]_o \quad (8)$$

However, this mixing of the dependent and independent variable was found unsuitable for least squares fitting. In part, this was due to the scatter in values for D, giving artificial scatter in the first term of Equation 8.

If only the adducted species is assumed to be important in the organic phase, then Equation 4 becomes, by first inverting, then omitting the first term in the denominator, and rearranging:

$$\frac{1}{D} = \frac{K^2_{DR}}{K'_{DC}K_1K'K_a(HIPT)_o^2}\frac{1}{} + \frac{K_{DR}}{K'_{DC}K'}\frac{1}{[HIPT]_o} + \frac{1}{K'_{DC}} \quad (9)$$

which is now suitable for least squares fitting. The four lowest points of the graph of log D *vs.* log $[HIPT]_o$ were omitted (Figure 3), as they have a slope of 1 and thus were in the region of very low [HIPT] where the chelate without the adduct was in fact the extracted species. The remaining points fitted to $\frac{1}{[HIPT]^2}, \frac{1}{[HIPT]}, 1.0$, gave numerical values for the respective coefficients $\frac{K^2_{DR}}{K'_{DC}K_1K'K_a}, \frac{K_{DR}}{K'_{DC}K'}, \frac{1}{K'_{DC}}$. The second coefficient, however, had a high standard deviation of 80% and was analogous to the third coefficient for the iron complex.

The overall extraction constant, K^*, can be evaluated by altering Equations 3 and 4. First, for values of [HIPT] in the region where K^* is calculated (Figure 3, region *b*, extrapolation to the intercept), one can omit the first term of the numerator because VO_2 IPT is negligible compared to the adduct species $VO_2IPT\cdot HIPT$. Second, the two terms in the denominator can be omitted because $[VO_2^+]$ is the predominant species in the aqueous phase. We then have the following:

$$D = \frac{K'_{DC}K'K_1\dfrac{K_a}{K^2_{DR}}[HA]^2}{1} = K^*[HA]^2 \quad (10)$$

It is evident as shown in Table II that the standard deviation associated with the least squares value for K_{DC} is larger than the graphical data would indicate, *i.e.* the region *c* of Figure 3 of log D *vs.* HIPT at log [HIPT] = 0. This stems from the mathematical relationship in a linear fit where scatter of points anywhere on the line will affect the standard deviation of the intercept. This was noted when points at lower [HIPT] concentration, which normally in the graphic method have no relationship to the K_{DC} value, were omitted and yielded different estimates of the standard deviation of the intercept. However, as in the case of the $Fe(IPT)_3$ chelate, least squares methods serve a very useful purpose of obtaining information on the stepwise (K) constants and provide an estimate of the precision of the data.

RECEIVED for review June 5, 1970. Accepted November 23, 1970.

(14) F. Chou, Q. Fernando, and H. Freiser, ANAL. CHEM., 37, 361 (1965).
(15) F. Chou and H. Freiser, *ibid.*, 40, 34 (1968).

Correction

Determination of Unsaturation by Analytical Hydrogenation and Null Point Pressuremetry

In this article by D. J. Curran and J. L. Driscoll [ANAL. CHEM., 42, 1414 (1970)] reference is made, on page 1415, to an instrument manufactured by RGI, Vineland, N.J. The name of this company has been changed to Roger Gilmont Instruments, Inc., and is now located at 161 Great Neck Rd., Great Neck, N.Y. 11021.

NOTES

Kinetics and Mechanism of Extraction of Iron(III) with β-Isopropyltropolone

B. E. McClellan[1] and Oscar Menis[2]

Analytical Chemistry Division, National Bureau of Standards, Washington, D. C. 20234

HONAKER AND FREISER (*1*) and McClellan and Freiser (*2*) pointed out that, in favorable cases, solvent extraction can be used to study the rates of quite rapid chelation reactions. Many workers (*3–5*) have studied the extraction characteristics of metal ions with β-isopropyltropolone (HIPT). Dyrssen (*3*) indicated that the extraction of Fe(III) with HIPT occurs very slowly from acid solution, and postulated that some step in the formation of the extractable complex, $Fe(IPT)_3$, is slow. The purpose of this study was to apply the extraction technique for studying the kinetics of reaction to the Fe(III)–HIPT system. It was hoped that an analysis of the kinetic data would lead to the elucidation of the mechanism and rate-determining step in the extraction process. Iyer and Menis (*6*) found VO_2^+ extraction to reach equilibrium relatively rapidly (less than 1 hour from 0.01 *M* HIPT) compared to the slow (1 to 4 days) equilibrium for Fe^{3+} reported by Dyrssen. Both of these metal ions extract quantitatively from strong acid solutions (1*M*). Hopefully, a detailed study of the kinetics of extraction of the system would lead to a method for the separation of Fe(III) and VO_2^+ based on the large difference in the extraction rates.

EXPERIMENTAL

Apparatus. All extractions were performed in 60-ml separatory funnels having polytetrafluoroethylene stopcocks and stoppers. The samples were agitated on a mechanical shaker. Radioactivity measurements were made with a modular counting system connected to a 2-in. × 2-in. NaI (Tl) well-type scintillation detector. Measurement of pH was done with an expanded scale pH meter.

Reagents. The radioactive isotopes ^{59}Fe and ^{48}V were obtained from International Chemical and Nuclear Company. The β-isopropyltropolone (HIPT) was obtained from Columbia Organic Chemicals Co., Columbia, S. C. It was recrystallized from 95% ethanol and dried under vacuum prior to use. Triple distilled water was used throughout the study. All other reagents were of Reagent Grade quality.

Procedure. All extractions were performed using equal volumes (10 ml) of aqueous and organic phases at room temperature (21 ± 1 °C). In the experiments to determine the reaction order in HIPT, the initial Fe(III) was 1.0×10^{-3} *M*, the $[H^+]$ was 1 *M*, and the ionic strength was unity. The iron solutions contained enough activity as ^{59}Fe to give an initial count rate of at least 10,000 counts/minute for a 5-ml aliquot. The iron stock solution was prepared by dissolving pure iron metal in $HClO_4$, and the $[H^+]$ was varied using $HClO_4$. The ionic strength (μ) was usually unity, but in experiments in which μ was varied $NaClO_4$ was used. The HIPT dissolved in $CHCl_3$ varied from 3.0×10^{-3} to 2.0×10^{-2} *M*. The samples were agitated for time intervals ranging from 2 minutes to 2 hours. Following agitation, the solutions were allowed to stand until complete phase separation had occurred (about 5 minutes). The phases were then physically separated and 5-ml aliquots were taken for gamma counting in disposable counting vials. The log of the ratio of the initial aqueous phase count rate, C_i, to the aqueous phase count rate, C_{aq}, at time, t_1, (log C_i/C_{aq}) is equal to log $[Fe^{III}]_{t=0}/[Fe^{III}]_t$. This was plotted *vs.* time and the slopes were measured.

A similar procedure was used to determine the effect of $[H^+]$ on the reaction rate. The Fe(III) was again 1.0×10^{-3}. The [HIPT] in $CHCl_3$ was held constant at 1.0×10^{-2} *M*. In the $[H^+]$ range of 0.1 to 1 *M*, the μ was constant at 1, while in the range of 2 to 5 *M* $[H^+]$, μ was 5.

The $[H^+]$ was 1, the Fe(III) was 1.0×10^{-3}, and the [HIPT] was 1.0×10^{-2} in the study of the effect of ionic strength on the extraction rate. The μ was varied from 1 to 5 with $NaClO_4$, and the shaking times varied from 2 to 20 minutes.

RESULTS AND DISCUSSION

The reaction order with respect to metal ion was determined from plots of log $[Fe^{III}]_{t=0}/[Fe^{III}]_t$ *vs.* time. These plots yielded straight lines, indicative of a first-order reaction with respect to metal ion in all cases. An example of such a plot is shown in Figure 1. The deviation from zero intercept reflects the statistical error of counting of the ratio of activities in two phases. The change in the values of the slopes of these lines at various reagent concentrations was used to obtain the reaction order with respect to reagent. The kinetic data for the extraction of iron with HIPT are shown in Table I. As shown in Figure 2, a slope of 1.1 was obtained indicating a first-order reaction in HIPT. A similar study of the effect of $[H^+]$ on the rate of reaction showed the rate to be independent of $[H^+]$, at constant ionic strength, between 0.1 and 5 *M* H^+. Since the pK_a for the reaction

$$HIPT \overset{K_a}{\rightleftharpoons} H^+ + IPT^-$$

is 7.5 at $\mu = 1$, at high H^+ only the HIPT will exist. Therefore, no dependence on H^+ in the high acid range would be expected. However, at lower $[H^+]$ one would expect a negative first-order dependence on $[H^+]$ as was observed for the zinc-dithizone system by McClellan and Freiser (*2*). In sup-

[1] Present address, Department of Chemistry, Murray State University, Murray, Ky. 42071.

[2] To whom inquiries should be addressed.

(1) C. B. Honaker and Henry Freiser, *J. Phys. Chem.*, **66**, 127 (1962).
(2) B. E. McClellan and Henry Freiser, ANAL. CHEM., **36**, 2262 (1964).
(3) David Dyrssen, *Trans. Roy. Inst. Technol., Stockholm, No.* **188**, 1962.
(4) R. P. Singh and Yat Dutt, *Indian J. Chem.*, **4**, 214 (1966).
(5) Kuan Pan and T. M. Hseu, *J. Chinese Chem. Soc.*, **2**, 23 (1955).
(6) C. S. P. Iyer and Oscar Menis, National Bureau of Standards, Washington, D. C., unpublished data, 1970.

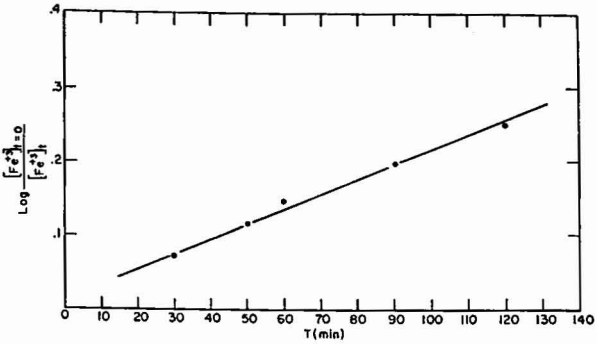

Figure 1. Plot of log $[Fe^{III}]_{t=0}/[Fe^{III}]_t$ *vs.* time

$[HIPT] = 3.0 \times 10^{-3}$, $[H^+] = 1.0$, $[Fe^{III}] = 1.0 \times 10^{-3}$
Slope = 0.0020

Table I. Kinetic Data for Extraction of Iron with β-Isopropyltropolone

$[HIPT]_o$	$[H^+]$	Slope[a]	k'[b]
3.0×10^{-3}	1.0	0.0020	1.54
5.0×10^{-3}	1.0	0.0038	1.75
7.0×10^{-3}	1.0	0.0061	2.01
1.0×10^{-2}	1.0	0.0063	1.45
2.0×10^{-2}	1.0	0.0163	1.88
			$\bar{k}' = 1.73$
			$\sigma = 0.23$

[a] Slope of a plot of log $\frac{[Fe^{III}]_{t=0}}{[Fe^{III}]_t}$ *vs.* time.

[b] $k' = 2.303 \times \text{slope} \times \frac{[H^+]}{[HIPT]_o}$.

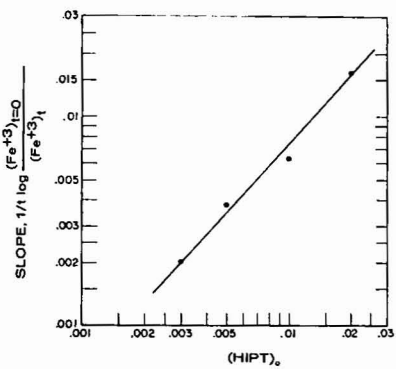

Figure 2. Plot of log (slope) *vs.* log $[HIPT]_o$ for Fe(III)–HIPT

$[H^+] = 1.0$, $[Fe^{III}] = 1.0 \times 10^{-3}$
Slope = 1.1

port of this, one experiment at a pH of 4 and [HIPT] of 5.0×10^{-3} showed very rapid extraction. The extraction was complete in about 10 minutes. However one can also postulate the existence under those conditions of a mixed hydroxy $FeOH(IPT)_2$ complex. Also, an experiment to determine the effect of H^+ on the distribution ratio showed much slower extraction at higher $[H^+]$. The extraction was essentially

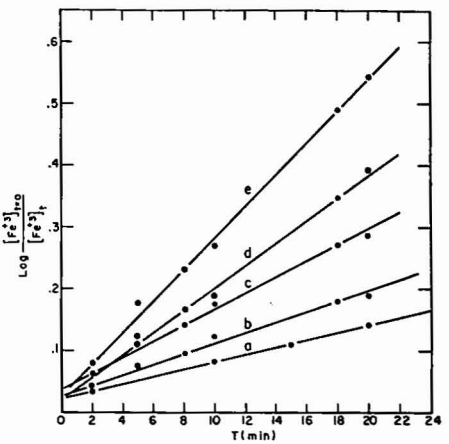

Figure 3. Plot of log $[Fe^{III}]_{t=0}/Fe^{III}]_t$ *vs.* time at various ionic strengths

$[H^+] = 1.0$, $[Fe^{III}] = 1.0 \times 10^{-3}$, $[HIPT]_o = 1.0 \times 10^{-2}$
a. $\mu = 1$, slope = 0.0058
b. $\mu = 2$, slope = 0.0086
c. $\mu = 3$, slope = 0.0105
d. $\mu = 4$, slope = 0.0182
e. $\mu = 5$, slope = 0.0256

complete in 30 minutes at pH = 2, while at least 6 hours were required to attain equilibrium from 1*M* $HClO_4$ using 1.0×10^{-2} HIPT in $CHCl_3$.

It was observed that the reaction rate was effected by ionic strength as changed by the addition of $NaClO_4$. Figure 3 shows plots of log $[Fe^{III}]_{t=0}/[Fe^{III}]_t$ *vs.* time at various ionic strengths ranging from 1 to 5. Figure 4 shows a plot of log (slope) *vs.* log ($NaClO_4$). A slope of 1.1 was obtained indicating a possible first-order dependence on $NaClO_4$. Although the rate was dependent on the $NaClO_4$, the equilibrium distribution ratio was found to be independent of the $NaClO_4$ concentration in the range of 0.1 to 4*M* acidity. Since perchlorate forms ion pair complexes in iron chelate systems, the observed rate effect may be due to this process. However, this phase of study was not pursued further.

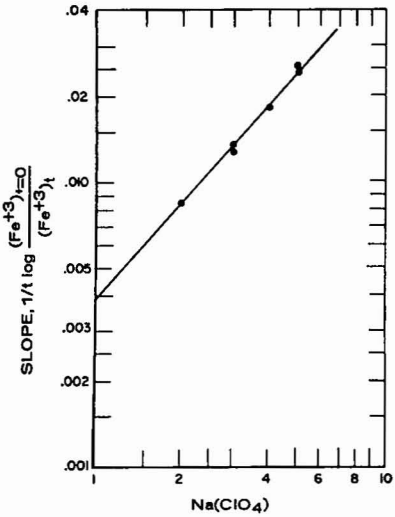

Figure 4. Plot of log (slope) *vs.* log [$NaClO_4$]
$[H^+]$ = 1, $[Fe^{III}]$ = 1.0 × 10^{-3}, $[HIPT]_o$ = 1.0 × 10^{+2}
Slope = 1.1

The steps involved in the reaction for the extraction of iron with HIPT are as follows:

$$HIPT \overset{K_{Dr}}{\rightleftharpoons} HIPT_{(o)} \quad (1)$$

$$HIPT \overset{K_a}{\rightleftharpoons} H^+ + IPT^- \quad (2)$$

$$Fe^{3+} + IPT^- \overset{K_1}{\rightleftharpoons} Fe(IPT)^{2+} \text{ (at low } [H^+]) \quad (3a)$$

$$Fe^{3+} + HIPT \overset{K_1}{\rightleftharpoons} Fe(IPT)^{2+} + H^+ \text{ (at high } [H^+]) \quad (3b)$$

$$Fe(IPT)^{2+} + IPT^- \overset{K_2}{\rightleftharpoons} Fe(IPT)_2^+ \quad (4)$$

$$Fe(IPT)_2^+ + IPT^- \overset{K_3}{\rightleftharpoons} Fe(IPT)_3 \quad (5)$$

$$Fe(IPT)_3 \overset{K_{DC}}{\rightleftharpoons} Fe(IPT)_{3\,(o)} \quad (6)$$

These reactions are analogous to those for the zinc–dithizone system which was studied by Honaker and Freiser (*1*) and by McClellan and Freiser (*2*). These workers reported the addition of the first ligand to be the rate-determining step in the extraction of zinc with dithizone. Similarly, in the iron–IPT system, the reaction order in IPT was unity indicating that the addition of the first ligand is the rate-determining step. The rate expression is

$$-\frac{d[Fe^{III}]}{dt} = k[Fe^{III}][IPT^-] \quad (7)$$

Substitution from Equations 1 and 2 above yields the expression

$$-\frac{d[Fe^{III}]}{dt} = k'\frac{[Fe^{III}][HIPT]_o}{[H^+]} \quad (8)$$

or

$$-\frac{d[Fe^{III}]}{dt} = k\frac{K_a}{K_{Dr}} \times \frac{[Fe^{III}][HIPT]_o}{[H^+]} \quad (9)$$

Hence, dividing the value of k' by K_a/K_{Dr} yields the rate constant, k, for the reaction. The value for K_a at μ = 1 is 3.16 × 10^{-8} and the value for K_{Dr} is 2.83 × 10^3 at μ = 1 (*7*). The value for k is then 1.5 × 10^{10} M^{-1} minute^{-1}. This value is somewhat higher than the k values reported for the metal–dithizonates by McClellan and Freiser (*2*).

The addition of ethanol to the aqueous phase was found to greatly increase the rate of extraction for Fe(III). This may reflect the change of K_{Dr} in mixed solvent media, whereas as much as 2 to 6 hours may be required to reach equilibrium in the case of the extraction of Fe(III) from strongly acid (1*M*) solutions with 0.01*M* HIPT, equilibrium is reached in 30 minutes in the presence of ethanol under the same conditions. On the other hand, although no detailed kinetic study was made on the VO_2^+ system in the absence of ethanol, its extraction was found to be complete in 5 minutes from a 1*M* H^+ with 0.1*M* HIPT in $CHCl_3$. Therefore, the separation of VO_2^+ from Fe(III) should be possible, based on the wide difference in the extraction rates with HIPT dissolved in $CHCl_3$ and free from alcohol.

RECEIVED for review June 5, 1970. Accepted November 9, 1970.

(7) Oscar Menis, B. E. McClellan, and D. S. Bright, ANAL. CHEM., 43, 431 (1971).

Determination of Nitrogen and Hydrogen at Parts-per-Million Levels in Milligram Steel Samples

G. L. Hargrove, R. C. Shepard, and Harry Farrar IV

Atomics International, A Division of North American Rockwell Corporation, Canoga Park, Calif. 91304

RECENT EXPERIMENTS indicate that nitrogen, through its relatively high (n,α) cross section, is a major contributor of helium in stainless steel irradiated in fast neutron spectra (*1*). The helium in turn severely limits the ductility of austenitic stainless steels at elevated temperatures (*2*, *3*), and in the presence of a high fast neutron flux, helium atoms can serve as nuclei for void formation. There is also evidence that hydrogen, which is formed in fast neutron fluxes by (n,p) reactions with many elements, also contributes to void formation (*4*). Because of the resulting dimensional instabilities, void formation has become a critical problem in the development of liquid-metal fast-breeder reactors (*5*). High specific radioactivity of irradiated steels makes it desirable in the study of these effects, therefore, to measure small amounts of hydrogen, helium, and nitrogen in specimens no larger than 10 milligrams. A high sensitivity gas mass spectrometer system (*6*) is being used to measure helium concentrations down to 10^{-6} wt ppm, and the technique reported here is designed to complement this capability by measuring very low levels of nitrogen and hydrogen.

Inert gas fusion methods have been used for years in the determination of hydrogen, nitrogen, and oxygen in metals (*7*). Holt and Goodspeed (*8*) adapted an inert gas fusion method for the determination of oxygen developed by Smiley (*9*) to the analysis of hydrogen and nitrogen in milligram size samples. However, their technique, which uses capillary manometers and a helium carrier gas, has detection limits for a 1-mg sample of ~200 wt ppm and ~10 wt ppm for nitrogen and hydrogen, respectively, set primarily by the operational blank. These detection limits are an order of magnitude too high for the application described above.

If care is given to the preliminary outgassing of the sampling system involved, stable isotope dilution techniques (*10*) and spark source mass spectrometry (*11*) can yield the required sensitivities. These latter methods were considered, but a simpler steady-state approach seemed quicker and more convenient. Therefore, the inert gas fusion methods men-

(1) W. N. McElroy, H. Farrar IV, and C. H. Knox, *Trans. Amer. Nucl. Soc.*, **13**, 314 (1970).
(2) D. Kramer, H. R. Brager, C. G. Rhodes, and A. G. Pard, *J. Nucl. Mater.*, **25**, 121 (1968).
(3) D. R. Harries, *J. Brit. Nucl. Energy Soc.*, **5**, 74 (1966).
(4) D. Kramer, "Void Formation in Stainless Steel by Proton Irradiation," submitted for the 1970 AEC Report on Fundamental Nuclear Energy Research.
(5) C. Cawthorne and E. J. Fulton, *Nature*, **216**, 575 (1967).
(6) H. Farrar IV and C. H. Knox, *Trans. Amer. Nucl. Soc.*, **11**, 503 (1968).
(7) W. E. Dallmann and V. A. Fassel, ANAL. CHEM., **39**, 133R (1967).
(8) B. D. Holt and H. T. Goodspeed, *ibid.*, **35**, 1510 (1963).
(9) W. G. Smiley, *ibid.*, **27**, 1098 (1955).
(10) C. R. Masson, *Metallurg. Rev.*, **117**, 147 (1967).
(11) G. Vidal, P. Galmard, and P. Lanusse, ANAL. CHEM., **42**, 98 (1970).

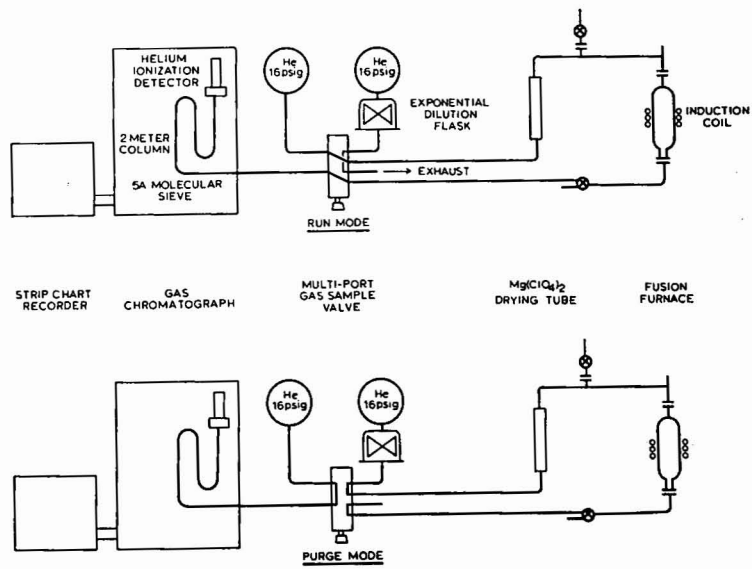

Figure 1. Micro-inert gas fusion system

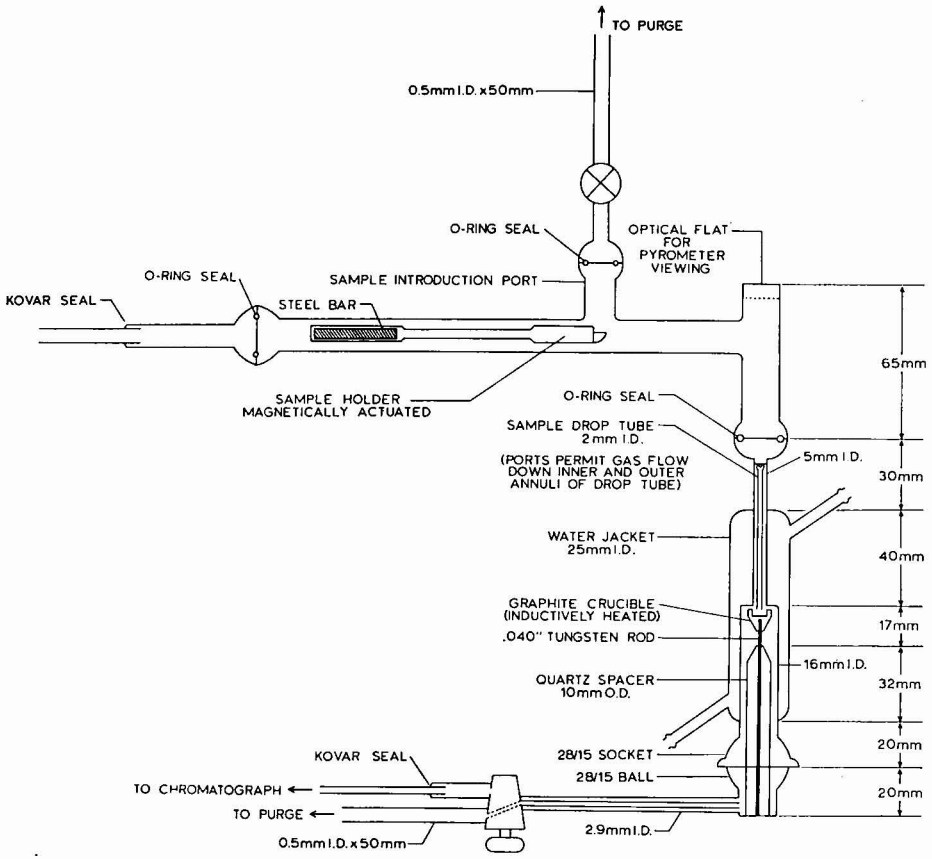

Figure 2. Fusion furnace detail

tioned earlier (*8*, *9*) were optimized and coupled with a high sensitivity gas chromatograph to yield a micro-inert gas fusion technique with more than the required sensitivity. Using this technique, an analysis for both hydrogen and nitrogen can be completed in 90 minutes.

PRINCIPLE OF OPERATION

The manometers used earlier (*8*, *9*) to measure the gases evolved during the fusion of the sample are replaced by a gas chromatograph with a helium ionization detector which has a limiting sensitivity for hydrogen and nitrogen of between 10^{-11} and 10^{-12} gram.

The operational blank has been eliminated by development of a new fusion furnace design and mode of operation. The fact that the nitrides and hydrides involved decompose quickly during sample fusion allows the fusion furnace, at temperature, to be made an integral part of the chromatographic system. With ultra pure helium as the carrier gas, the standing current of the detector is sufficiently low to allow measurement of very low levels of chromatographically separated hydrogen and nitrogen. In this way, impurities from the carrier gas and from system degassing do not contribute to the operational blank as in the earlier trap-out methods (*8*, *9*), but instead they produce a steady-state detector current on top of which the desired elements are determined.

EXPERIMENTAL

Apparatus. The gas chromatograph, a Model 1532-2B (Varian Aerograph, Walnut Creek, Calif.), was equipped with a helium ionization detector (HID) whose output was fed to a Sargent Model DSR Strip Chart Recorder (E. H. Sargent Corp., Anaheim, Calif.) operated at 5 cm/min chart speed. The chromatographic column consisted of a 2.0 meter long, 6.35-mm o.d. Type 316 stainless steel tube packed with 50/60 mesh molecular sieve 5A (Perco Supplies, San Gabriel, Calif.). The induction unit used with the fusion furnace was a LECO Model 537, 4.5 kW, 1-mHz generator (Laboratory Equipment Corp., St. Joseph, Mich.) with a 60-mm o.d. induction coil made from 4.75-mm o.d. copper tubing. A schematic diagram of the micro-inert gas fusion system is shown in Figure 1. More details of the micro-fusion furnace, which was constructed of quartz, are shown in Figure 2. The furnace

Table I. HID Calibration Data

Detector voltage	Element	Calibration Factor, gm/cm³ (Attenuation ×1)	Applicable range, grams
200 VDC	Hydrogen	$1.15\ (\pm 0.11)^a \times 10^{-9}$	$10^{-9}-10^{-6}$
	Nitrogen	$1.35\ (\pm 0.06) \times 10^{-8}$	$10^{-8}-10^{-5}$
375 VDC	Hydrogen	$6.71\ (\pm 0.47) \times 10^{-11}$	$10^{-11}-10^{-8}$
	Nitrogen	$8.76\ (\pm 0.44) \times 10^{-10}$	$10^{-10}-10^{-7}$

[a] Standard deviation, σ, of calibration factor determined at five points in applicable range.

and crucible designs represent compromises which provide positive sample delivery to the crucible and minimum dilution of the gases evolved during sample fusion.

The furnace must be periodically cleaned to remove residues which condense on the walls of the furnace. The build-up of these residues over a period of time results in an increased noise level. The furnace is cleaned by rapidly dipping it in concentrated HF, rinsing in distilled water, and drying at 150 °C for 4 hours.

Procedure. Samples to be analyzed are cut to a size (0.3–10 mg) which will negotiate the quartz sample drop-tube (2 mm id) and are degreased in analytical reagent grade carbon tetrachloride. After drying in air for 20 minutes (in a place appropriate for radioactive specimens, if necessary), they are weighed and stored in a screw-top glass vial.

Before an analysis, the gas fusion system is put in the purge mode shown in Figure 1. The chromatographic column is activated for 30 minutes at 300 °C with the 99.9999% pure helium carrier gas (Dye Oxygen Co., Gardena, Calif.). Meanwhile the sample introduction port cover is removed and the sample is placed with tweezers into the cup of the sample holder which is positioned as shown in Figure 2. After the port cover is replaced and held with two clips, the stopcock in the port cover and the 3-way stopcock at the base of the furnace are opened and the system is purged for 15 minutes at a rate of ~1000 ml/min. Following this, the port cover stopcock is closed, the 3-way stopcock at the furnace base is turned to allow helium to flow as far as the multi-port gas sample valve (Varian Aerograph). After 5 minutes, the fusion crucible is brought to temperature (1800 °C measured by optical pyrometer) by adjusting the induction coil current to 120 mA. The chromatograph is cooled to ambient temperature (~10 minutes) and the multi-port gas sample valve is switched to the run mode shown in Figure 1. The chromatograph is operated with inlet and outlet pressures of 16 psig and 0 psig, respectively, and with a helium carrier-gas flow-rate of 250 ml/minute.

When the HID base line stabilizes (5–7 minutes), the sample holder is moved along the tube and rotated with the aid of magnets, dropping the sample from the cup into the hot crucible (ATJ Graphite). All gases evolved during sample fusion pass to the chromatograph and the hydrogen and nitrogen peaks elute from the chromatographic column in 0.5 and 3.0 minutes, respectively. The peak areas of the HID response are measured with the aid of a planimeter (Lietz, Inc., Los Angeles, Calif.).

The system is calibrated by the use of an exponential dilution flask (*12*) (Varian Aerograph) and a calibrated sample loop. C.P. grade calibration gases (Matheson Co., East Rutherford, N. J.) are added to the exponential dilution flask with either 0.25- or 5.0-ml "pressure lok" syringes (Precision Sampling Corp., Baton Rouge, La.) during which time the calibrated sample loop is substituted at the multiport gas sample valve in place of the fusion furnace. Because of the nonlinearity of the HID, calibration factors must be obtained at several detector voltages in order to cover a wide range of hydrogen and nitrogen concentrations.

(12) J. E. Lovelock, ANAL. CHEM., **33**, 162 (1961).

Table III. Concentration Data on Consecutive Specimens

Sample	Mass, mg	Hydrogen concn, wt ppm	Nitrogen concn, wt ppm
1	5.02	1.25	337
2	7.21	1.21	306
3	11.10	1.11	270
4	5.40	1.08	320
Mean		1.16	308
Std dev		±0.08	±28

RESULTS

Calibration data obtained at two detector voltages are shown in Table I. The limiting sensitivities, which correspond to twice the base-line noise level for a 1-mg sample, are 0.02 wt ppm for hydrogen and 0.3 wt ppm for nitrogen. A summary of 11 analyses performed on two NBS standards is given in Table II.

To test the effect of the residue of earlier samples left in the crucible, four specimens of 0.23-mm thick Type 316 stainless steel foil of unknown hydrogen and nitrogen content were analyzed by dropping them successively into the crucible. The data shown in Table III indicate no significant bias in the later results due to the presence of earlier specimens and also show the level of reproducibility that can be expected from this technique. This limited amount of data suggests therefore that the number of samples of steel that can be analyzed without changing the crucible is limited only by the capacity of the crucible, which in this case was about 30 mg.

Using this micro-inert gas fusion technique, the nitrogen content was determined (*13*) at four positions along a Type 304 stainless steel safety rod guide thimble irradiated in the Experimental Breeder Reactor-II (EBR-II) for four years to a peak total neutron fluence of 8.8×10^{22} n/cm². The results reveal a 35% depletion of nitrogen at the lower axial positions of the guide thimble with respect to the pre-irradiation concentration, and show a steady increase in nitrogen to pre-irradiation levels at the higher positions. The fact that these concentrations followed a temperature gradient along the thimble has important implications (*13*). If nitrogen moves about in a reactor core, its relatively high (n,α) cross section for fast neutrons gives it the potential to create the same sort of neutron capture and helium production

(13) N. D. Dudey, S. D. Harkness, and H. Farrar IV, *Nucl. Appl.*, **9**, 700 (1970).

Table II. Analyses of Hydrogen and Nitrogen in NBS Standards

Standard	Element	Specimen mass range, mg	NBS value, wt ppm	Micro-inert-gas fusion results, wt. ppm: Values	Mean value	1 σ std dev
352	Hydrogen	0.2–0.7	32	39, 32, 29, 29, 34, 28	32	4
101e	Nitrogen	0.4–8.0	390	356, 370, 388, 430, 476	404	50

problems in fast reactors that boron creates in thermal reactors.

CONCLUSIONS

Micro-inert gas fusion chromatography has been shown to be a very sensitive, accurate, and relatively precise technique for the determination of hydrogen and nitrogen in small samples. The technique has been used in this laboratory to determine hydrogen and nitrogen contents ranging from 1 to 1000 wt ppm. At present the technique is limited to samples where chemical decomposition is not required for the release of nitrogen or hydrogen, and therefore cannot be applied to the determination of nitrogen in, for example, Ti, Ta, and W. Work is now in progress, however, to extend the technique to the determination of nitrogen in other materials including those which form refractory nitrides.

ACKNOWLEDGMENT

The assistance of C. H. Knox is gratefully acknowledged.

RECEIVED for review July 10, 1970. Accepted November 4, 1970. This work was supported in part by the U. S. Atomic Energy Commission.

Novel Method of Determining Weak Bases in Small Amounts

Elio Scarano, Marco Mascini,[1] and Giovanni Gay

Institute of Analytical Chemistry, Faculty of Pharmacy, University of Genoa, Italy

CRITCHFIELD AND JOHNSON (*1*, *2*) have found that concentrated (up to saturation or 8*M*) aqueous solutions of strong acid–strong base salts (NaCl, NaI, LiCl, $CaCl_2$) can be conveniently used as media for visual and potentiometric titrations of bases with pK_b as high as 11–12. This is due to the enhanced potentiometric break at the equivalence point. The high protonation of weak bases is explained in terms of low activity of water and high hydrogen ion activity.

Hisashi Kubota and Costanzo (*3*) have carried out potentiometric titrations of hydrolyzable cations in 10*M* LiCl. Rosenthal and Dwyer (*4*) have studied acid-base equilibria in concentrated salt solutions, particularly 4 and 8*M* LiCl. These authors also agree in the enhancement of the hydrogen ion activity in these media.

Moreover dilute hydrogen chloride and concentrated lithium chloride solutions have high values of the hydrogen chloride gaseous pressure, which are much higher than that of hydrogen chloride aqueous solutions at the same hydrogen chloride concentration (*5*). So an aqueous 0.1*M* HCl solution can be boiled for 1 hour without appreciable loss of hydrogen chloride if the evaporated water is continuously replaced (*6*), while a solution $\sim 5 \times 10^{-3} M$ of hydrogen chloride in 13*M* LiCl loses 1% (or 50%) of hydrogen chloride if a nitrogen volume 6 (or 420) times that of the solution is forced to pass through it (*5*).

In this paper a simple and inexpensive method is described for weak base (pK_b up to 10) determinations in the μmole range. The method is based on the high hydrogen ion activity and the high hydrogen chloride pressure of dilute hydrogen chloride–concentrated lithium chloride solutions. A nitrogen flow forced through the hydrogen chloride–lithium chloride solution strips the hydrogen chloride which is collected and determined. Two hours of stripping are sufficient to collect practically all the hydrogen chloride. The base is dissolved in a known amount of hydrogen chloride and introduced into the lithium chloride saturated solution. Only the excess of hydrogen chloride is stripped, thus allowing the base determination.

EXPERIMENTAL

C. Erba reagent grade LiCl (with 0.03%, as Li_2CO_3, declared alkalinity) was used as purchased or in the form purified by crystallization.

The acid-base substances [with pK_a at 25 °C (*7*)] were: Merck (according to Sörensen) glycine (2.35); Merck reagent grade succinic acid (4.21); Merck reagent grade aniline (4.60); Merck *p*-toluidine (5.09); Aldrich Chemical picolinic acid (5.32); Merck sodium-5-5′-diethylbarbiturate, for buffer (7.98).

The apparatus shown in Figure 1 consisted of two 15-ml glass tubes, with ground glass sockets; a glass bridge with caps for the tubes and holes for burets; two microburets (1 ml, 0.01-ml division) with the closure on the tip (*8*).

Experiments were carried out in a thermostatic bath at 25 °C.

Saturated lithium chloride solution 13 grams (about 10 ml) and 1.2 grams of lithium chloride were weighed in the *A* tube; 2 ml of water and 0.1 ml of $10^{-4} M$ methyl red solution were poured into tube *B*. The tubes were tightly joined together with the glass bridge. A buret filled with a standard hydrogen chloride solution was inserted in tube *A*; a buret with 0.01 or 0.02*M* NaOH in tube *B*. A stream of nitrogen (120 ± 5 ml/min) was then passed through the solutions into the tubes. The hydrogen chloride solution was poured into tube *A*. The stripped hydrogen chloride passed into tube *B* where it was titrated at regular intervals of time with the sodium hydroxide solution. Preliminary investigation proved that hydrogen chloride did not escape from tube *B*.

RESULTS AND DISCUSSION

The influence of lithium chloride purity is shown in Figure 2. The presence of a base in the commercial product was

[1] Present address, Institute of Analytical Chemistry, University, of Rome, Italy.

(1) F. E. Critchfield and J. B. Johnson, ANAL. CHEM., 30, 1247 (1958).
(2) *Ibid.*, 31, 570 (1959).
(3) H. Kubota and D. A. Costanzo, *ibid.*, 36, 2454 (1964).
(4) D. Rosenthal and J. S. Dwyer, *ibid.*, 35, 161 (1963).
(5) D. Glietenberg and M. von Stackelberg, *Ber. Bunsenges. Phys. Chem.*, 72, 565 (1968).
(6) H. A. Laitinen, "Chemical Analysis," McGraw-Hill, New York, N. Y., 1960, p 85.
(7) V. E. Bower and R. G. Bates, "Handbook of Analytical Chemistry," L. Meites, Ed., 1st ed., McGraw-Hill, New York, N. Y., 1963, pp 1–20.
(8) E. Scarano and M. Forina, *J. Chem. Educ.*, 47, 482 (1970).

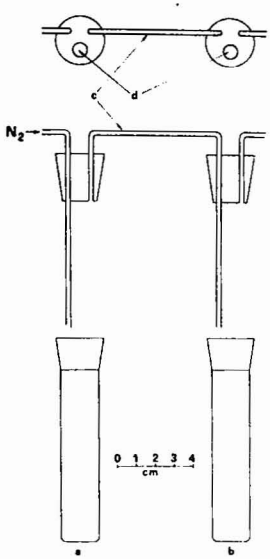

Figure 1. Apparatus

(*a*) A tube (stripping cell); (*b*) B tube (analysis cell); (*c*) glass bridge; (*d*) holes for burets

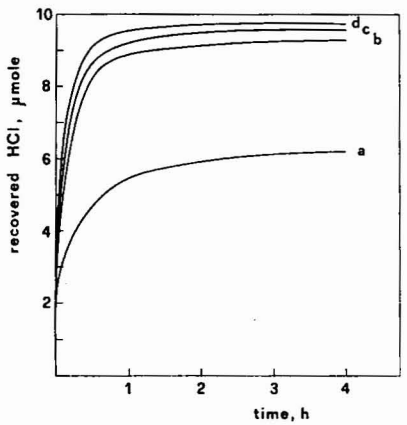

Figure 2. Influence of lithium chloride purity

Saturated solutions prepared with: (*a*) commercial product; (*b*) monocrystallized lithium chloride; (*c*) bicrystallized lithium chloride; (*d*) tricrystallized lithium chloride; 10 µmole hydrogen chloride added for each experiment

confirmed. However, the declared alkalinity was higher than that found. The amount of base found depended on the stock of lithium chloride used. The recovery of hydrogen chloride was not complete even after 4 hours with tricrystallized lithium chloride. This should be due to the residual alkalinity and to the very low hydrogen chloride stripping rate at low values of hydrogen chloride concentration.

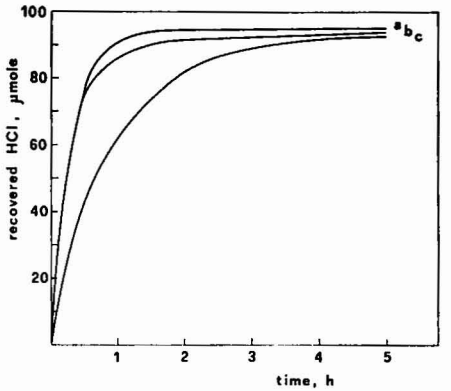

Figure 3. Influence of lithium chloride concentration

(*a*) 19.75*m* (saturated solution); (*b*) 19*m*; (*c*) 18*m*. Solutions prepared with commercial product. 100 µmole hydrogen chloride added for each experiment

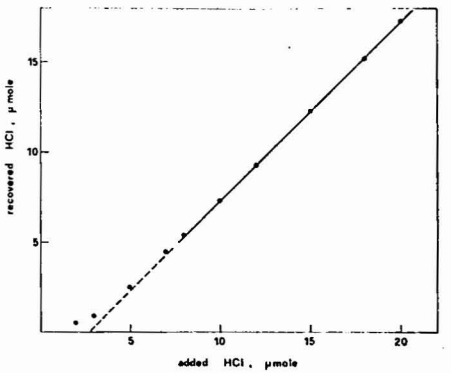

Figure 4. Recovery of hydrogen chloride after 2-hour stripping

Lithium chloride saturated solutions prepared with commercial product

The hydrogen chloride volatility was strongly dependent on the lithium chloride concentration and diminished with it (Figure 3).

The curve in Figure 4 shows the relation between the micromole of hydrogen chloride recovered after a 2-hour stripping and the added micromole of hydrogen chloride in the lithium chloride saturated solution. The curve becomes a straight line between 6 and 20 µmole of recovered hydrogen chloride, with a slope of 1 ± 0.005. The intercept depended on the lithium chloride stock solution used and its basic impurity. Points above the straight line, at low hydrogen chloride micromole values, can be explained in terms of competition between the two following equilibria:

$$Cl^- + H^+ = HCl\ (g) \qquad (1)$$

$$CO_3^{2-} + 2H^+ = H_2O + CO_2\ (g) \qquad (2)$$

where g refers to the gaseous phase.

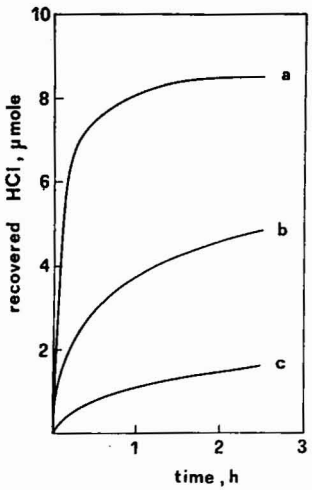

Figure 5. Behavior of weak acids

(a) **HCl;** *(b)* **glycine hydrochloride;** *(c)* **succinic acid. Lithium chloride saturated solutions prepared with commercial product. 10 μmole of acid for each experiment**

When the added hydrogen chloride was in strong excess, CO_3^{2-} was rapidly and completely eliminated as CO_2, which was not absorbed and detected in tube *B*. When instead the hydrogen chloride quantity was inferior to the base present, the faster Reaction 1 prevailed and some hydrogen chloride was stripped. However, these points can also be explained with the presence of a nonvolatile partially-protonated weak base ($pK_b > 10$) in the lithium chloride (see below).

The effects of nonvolatile acids of different strengths when added in tube *A*, as hydrogen chloride substitutes, are shown in Figure 5. Medium strength acids were able to donate protons to chloride ions, thus allowing hydrogen chloride to be stripped by the nitrogen stream. When an acid of lower strength was used, the rate of hydrogen chloride stripping decreased. The weaker acids, with $pK_a \gtrsim 4$, such as aniline hydrochloride, *p*-toluidine hydrochloride, picolinic acid, 5,5′-diethylbarbituric acid and boric acid, did not give any hydrogen chloride production.

Table I. Determination of Sodium-5,5′-Diethylbarbiturate[a]

Experiment	Recovered hydrogen chloride, μmole	
	Blank	Sample
1	8.10	7.00
2	8.00	7.00
3	8.00	6.90
4	7.95	7.05
	Av 8.01	Av 6.99
Base given	1.01 μmole.	
Base found	1.02 μmole.	

[a] Blank solution: $10^{-3}M$ HCl. Sample solution: $10^{-3}M$ HCl and $1.01 \times 10^{-3}M$ $C_8H_{11}O_3N_2Na$. Eight experiments were carried out; four with the blank solution and four with the sample solution; 1 ml of solution was used for each experiment. Saturated lithium chloride solution prepared with commercial product.

The above results permitted simple determination in the micromole range of bases with pK_b up to 10. Each base was dissolved in a known amount of hydrogen chloride and the excess of hydrogen chloride (6–20 μmole) was recovered. A blank was carried out with the same amount of hydrogen chloride under the same experimental conditions. The base quantity was given by the difference between the two recovered quantities of hydrogen chloride.

The base could be determined as accurately as the measurements of the volumes of the hydrogen chloride and sodium hydroxide standard solutions. For example, the results relative to the minimum determined quantity of a base are reported in Table I.

The very small required quantities of bases reduced problems caused by the low solubility of bases in the concentrated lithium chloride solutions (*4*). An advantage was offered by the solubility power of the hydrogen chloride solution. The method appears unsuitable for volatile acids and bases. However, it should be useful for base determinations in the presence of colored materials. By improving the hydrogen chloride stripping process and by using a more sensitive and reliable method for stripped hydrogen chloride determination, the amount of base to be analyzed may be reduced and precision may be increased.

Principles underlying this work have been developed for studies of solvent systems (*9*).

RECEIVED for review August 18, 1970. Accepted October 26, 1970.

(9) E. Scarano, G. Gay, and M. Forina, ANAL. CHEM., 43, 206 (1971).

Improved Method for Determination of Chlorinated Hydrocarbon Pesticide Residues in Whole Blood

S. J. Henderson, J. G. DeBoer, and H. M. Stahr

Chemistry Laboratory, Veterinary Diagnostic Laboratory, Iowa State University, Ames, Iowa 50010

THE AUTHORS' laboratory has frequent need for the analysis of pesticides in whole blood.

Existing methods involving saponification (*1*), direct extraction (*2–5*), and chemical reaction (*4*) have yielded undesirable results in our laboratory. Many are designed for the analysis of serum. The most-used method (Dale *et al.*) is neither reproducible nor accurate as Bonderman (*6*) has shown. In addition, the original workers who developed the method did so as a screening procedure.

Our purpose required a method which was both accurate and precise to allow veterinary research to be done on chlorinated pesticide transport and deposition, as well as a diagnostic test for toxicological specimens.

Curry (*7*) used sulfuric acid to clean up tobacco and smoke with a partition into hexane to allow analysis of the sample by gas–liquid chromatography (GLC). Kirk *et al.* (*5*) used an acetone–ether extraction. Sulfuric acid carryover in our attempts with hexane–ether and the hazard of large scale evaporations of ether necessary to concentrate samples for analysis in the latter method motivated the chemistry laboratory staff to do the following work.

EXPERIMENTAL

Reagents. Pesticide grade solvents were used throughout. Sulfuric acid was Mallinckrodt analytical reagent grade.

Stock solutions of several pesticides were prepared by weight from standards obtained from the Pesticides Research Laboratory, Perrine, Fla. Mixed standards in acetone were prepared such that if 100 μl of standard was added to 2 ml of freshly drawn heparinized blood, the levels would be 50 parts per billion of γ-BHC, heptachlor, and aldrin, respectively, 250 ppb of *o,p'*-DDE and dieldrin, and 400 ppb of *o,p'*-DDD and *o,p'*-DDT.

A second standard solution, prepared using the same amount of standard per milliliter of blood, gave levels of pesticides of 75 ppb of γ-BHC, 150 ppb of aldrin, 300 ppb of *p,p'*-DDE and heptachlor epoxide, and 750 ppb of *p,p'*-DDT and *o,p'*-DDT. Standard II was also used to spike bloods at a lower level of 15 ppb of γ-BHC, 30 ppb of aldrin, 60 ppb of heptachlor epoxide and *p,p'*-DDE, and 150 ppb of *p,p'*-DDT and *o,p'*-DDT.

Analytical Procedure. A 2-ml aliquot of the spiked blood was pipetted into a 30-ml glass-stoppered centrifuge tube. A 1.5-ml aliquot of 60% sulfuric acid (w/w) was added to the blood, and the solution was mixed briefly using a vortex mixer. A second 1.5-ml aliquot of 60% H_2SO_4 was added with mixing; and finally 2 ml of 60% H_2SO_4 was added (5 ml of acid total), and the solution was again mixed. After cooling for several minutes, 3 ml of acetone:hexane (1:9) was added to the sample and acid. The resulting solution was mixed for 1 minute using the vortex mixer. After centrifuging at 2000 rpm to separate the layers, the upper solvent phase was carefully removed using a disposable pipet and placed in a 10-ml graduated concentrator tube (Kontes). The extraction was repeated twice with 3 ml of the acetone:hexane solvent, combining extracts. The combined extracts were evaporated with a gentle stream of dry nitrogen to less than 5 ml, brought to 5 ml with hexane and 20 mg of SilicAR CC-4 (Mallinckrodt) was added to the pesticide extract. The tube was inverted several times to mix and centrifuged before analysis by gas chromatography.

Toxicological samples are processed by the same procedure and brought to a final concentration to obtain quantifiable peaks by GLC analysis.

Instrumental. The gas chromatograph was a Micro Tek MT 220 with a tritium foil electron capture detector. The column oven was operated isothermally at 200 °C and the detector at 205 °C. The inlet port was held at 235 °C, and the injections were made off column.

Two columns (*8*) were used, each connected to the same EC detector by a duo-transfer line (stainless steel). Work was done on a 1.5% OV 17/1.95% QF1 two-phase column and cross-checked on a 4% SE 30/6% QF1 two-phase column. All phases were loaded on Chromasorb W, DMCS HP 100/120 and packed in $^1/_4$ in. o.d. × 6-ft borosilicate glass columns. Columns were conditioned at 235 °C and silicated (Silyl-8, Pierce Chemical Co.) at 200 °C before operation.

High purity dry nitrogen (Linde) was passed over activated molecular sieves before being used as the carrier gas. Carrier gas flow rate was set at 80 cc/min for a chromatogram about 12 to 15 minutes in length.

RESULTS AND DISCUSSION

Recoveries in excess of 90% were observed for all the pesticides in the fortified samples with the exception for the lower levels of γ-BHC and aldrin where the recovery levels were about 88% (Table I). The extraction was relatively rapid; a series of 12 samples could be easily extracted in a two and one-half hour period. No difference in efficiency was noted for human, equine, bovine, or ovine blood. Heparin, EDTA and sodium citrate were each used as anticoagulants in the course of this work, and no difference was noted in the recovery of pesticides.

Acetone was selected as the solvent for those pesticides used for spiking the blood in these studies. Because of the miscibility of acetone with blood, it was felt that more intimate contact between the pesticides and the blood would be achieved than if the more traditional solvents and methods were used. The levels of pesticides were prepared to match prepared GLC standards as well as the levels most commonly observed in this laboratory. Further consideration was given to the volume of acetone added to the blood to prevent pro-

(1) J. G. Reynolds, *Bol. Of. Sanit. Panamer.*, 527 (1957).
(2) A. Richardson, J. Robinson, B. Bush, and J. M. Davies, *Arch. Environ. Health*, **14**, 703 (1967).
(3) W. E. Dale, A. Curley, and C. Cueto Jr., *Life Sci.*, **5**, 47 (1966).
(4) V. W. Kadis and O. J. Jonasson, *Can. J. Pub. Health*, **56**, 433 (1965).
(5) P. L. Kirk, N. C. Jain, and C. R. Fontan, *Proc. Can. Soc. Forensic Sci.*, **4**, 155 (1965).
(6) D. P. Bonderman, U. Y. Choi, H. L. Hetzler, and L. R. Long, *J. Ass. Offic. Anal. Chem.*, **52**, 1063 (1969).
(7) Zorra, Curry, Philip Morris Research Center, Richmond, Va., private communication, 1970.
(8) J. F. Thompsen, A. R. Walker, and R. F. Moseman, *J. Ass. Offic. Anal. Chem.*, **52**, 1263–1277 (1969).

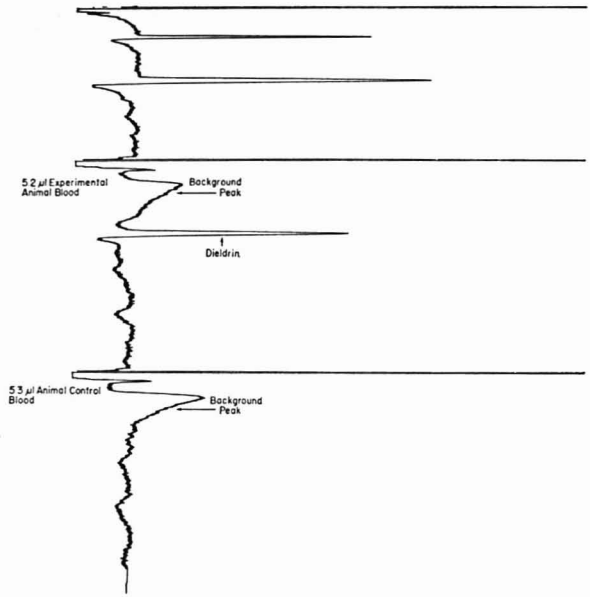

Figure 1. Chromatogram of blood extracts

Table I. Recovery Results under Optimum Conditions

Pesticide	Level added, ppb	Average, ppb	Recovered, %	Std dev, %
γ-BHC	15	13	88	
	50	47	94	2.9
	75	71	94	4.9
Aldrin	30	27	89	
	50	48	95	2.6
	150	131	90	5.2
Heptachlor	50	48	96	2.1
Dieldrin	250	226	90	3.1
o,p'-DDD	400	386	96	2.8
o,p'-DDE	250	239	96	2.9
o,p'-DDT	150	137	91	
	400	383	96	
	750	744	91	6.8
p,p'-DDE	60	57	95	
	300	273	93	5.5
p,p'-DDT	150	158	105	
	750	694	96	7.4
Heptachlor epoxide	60	56	94	
	300	284	93	5.1

Table II. Effect of Silica Gel on Quantitation of GLC Peaks[a]

Level of silica gel, mg	Level of dieldrin, ppm
0	0.338
20	0.346
35	0.319
50	0.323

[a] Data taken from blood of live experimental animal.

tein precipitation and dilution of the blood. A large quantity of blood was spiked at one time to eliminate errors in measurement from one sample to another.

The optimum conditions for the extractions procedure were determined using different concentrations of acetone: hexane and various concentrations of sulfuric acid. After comparing 2, 5, 9, and 10% acetone in hexane using three extractions of 3 or 5 ml each with recoveries ranging from 50% or less to >95%, three 3-ml extractions with 10% acetone: hexane were selected. This appeared to give better recoveries than any of the other systems examined.

An acid concentration of 70% sulfuric acid was used initially (7). Although recoveries were good using 70% sulfuric acid, several preliminary studies were completed to determine the most effective concentration. An error in diluting the acid during one experiment suggested that there was severe breakdown of dieldrin due to contact with the acid during extraction if the concentration of acid was greater than 75% (w/w). Lower concentrations of acid were used to see if yields could be improved. The optimum concentration of acid, based on per cent recovery of pesticides, appeared to be 60 to 65%. Below 60% H_2SO_4, a permanent emulsion formed.

Chromatograms of the blood extracts indicated that something other than pesticides was being extracted. A broad hump appeared in each chromatogram (Figure 1) and made quantitation of the peaks extremely inaccurate. The components of this material have not been determined. However, it has been discovered that the addition of 20 mg of SilicAR CC-4 (Mallinckrodt) to the extract after evaporation to volume will completely eliminate the problem (Table II). Sorption of the pesticides occurred when more silica gel was added.

Table III. Effect of Method of Evaporation on Recovery Efficiency[a]

Pesticide	Block, % recovery	N_2, % recovery
γ-BHC	70	99
Heptachlor	72	100
Aldrin	70	99
o,p'-DDE	70	97
Dieldrin	70	95
o,p'-DDD	73	93
o,p'-DDT	78	97

[a] Data cited are from the evaporation of solvent spiked with the same amount of pesticides used in the blood.

Several other factors have been shown to be important to the extraction. Decomposition of the pesticides, especially dieldrin, occurred when they were allowed to be in contact with the blood-acid mixture for an excessive length of time. Three to four hours did not appear to be critical, but if all three extractions were not completed and the solution was left overnight, recoveries were considerably lower.

Recovery data indicated that evaporation using a heating block (Kontes) resulted in erratic loss of pesticides (Table III). Subsequently, all evaporation has been carried out by blowing a very gentle stream of clean, dry nitrogen over the surface of the solvent at room temperature.

Because of the easy availability to this laboratory of blood from sheep containing dieldrin *in vivo*, a large pooled sample of this blood was obtained. Repetitive analyses of this blood were made. The level of dieldrin was shown to be 0.32 ppm with a standard deviation of 3.0% with two operators (twelve samples were analyzed). Freezing the blood did not affect the recovery of pesticides.

SUMMARY

A rapid and accurate method for the analysis of pesticides in blood has been developed. Recoveries have been shown to be >90% with a relative standard deviation of ±3%. Twelve samples can easily be extracted in two and one-half hours. Comparison of this method with other methods indicates this to be an improvement in accuracy, precision, and time for analysis.

ACKNOWLEDGMENT

The authors thank W. B. Buck, G. A. Van Gelder, and J. J. O'Toole for helpful discussions and for providing research samples for this work.

Received for review March 11, 1970. Accepted November 23, 1970. This work was supported in part by the Iowa Community Pesticides Study, Public Health Service Subcontract No. PH 86-66-NEG-26, William B. Buck, Principal Investigator.

Quantitative Cation Exchange Separation of Zirconium and Hafnium in Formic Acid Media

Mohsin Qureshi and Khadim Husain

Chemistry Department, Aligarh Muslim University, Aligarh, India

Separation of zirconium from hafnium has become very important in recent years because of the increasing use of zirconium metal as construction material in nuclear reactors, where even a slight impurity of hafnium plays a dominant role in retarding the nuclear chain reaction to a considerable extent. Many workers have reported the separation of these two elements by ion-exchange chromatography using different media—particularly hydrofluoric acid, hydrochloric acid, sulfuric acid and citric acid (*1–7*). However, no effort has been made to separate these elements by ion exchange in formic acid media. The present communication briefly describes the adsorption behavior of these two elements in dilute as well as concentrated formic acid solutions and quantitative separation of zirconium from hafnium in varying ratio.

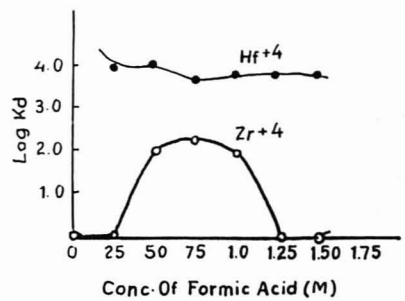

Figure 1. Log Kd *vs.* concentration of formic acid (dilute)

EXPERIMENTAL

Dowex 50 W-X8 (20–50 mesh) in hydrogen form was used for distribution studies and column operations. Cationic solutions of zirconium and hafnium of appropriate concentration were prepared using zirconium oxychloride "pro analysi" grade and hafnium oxide (99.5% supplied

(1) K. Street, Jr., and G. T. Seaborg, *J. Amer. Chem. Soc.*, **70,** 4268 (1948).
(2) K. A. Kraus and G. E. Moore, *ibid.*, **71,** 3263 (1949).
(3) E. H. Huffman and R. C. Lilly, *ibid.*, p 4147.
(4) B. A. J. Lister, *J. Chem. Soc.*, **1951,** 3123.
(5) Joseph T. Benedict, Walter C. Schumb, and C. D. Coryell, *J. Amer. Chem. Soc.*, **76,** 2036 (1954).
(6) F. W. E. Strelow and C. J. C. Bothma, Anal. Chem., **39,** 595 (1967).
(7) C. L. Luke, *Anal. Chim. Acta*, **41,** 453–8 (1968).

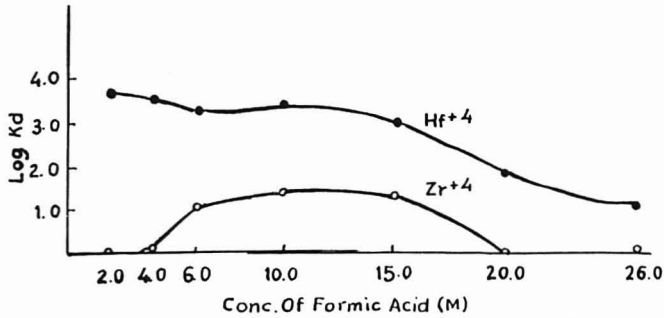

Figure 2. Log Kd *vs.* concentration of formic acid (concentrated)

by National Bureau of Standards, U.S.A.). Distribution coefficients were determined in dilute as well as concentrated formic acid solution by batch process and the estimation of the cations before and after equilibration was made chelometrically using xylenol orange as indicator after destroying formic acid. The results thus obtained are plotted as log Kd *vs.* concentration of formic acid (See Figures 1 and 2).

For separation of zirconium from hafnium, a column of 0.28-cm internal diameter made of borosilicate glass with a plug of glass wool to support 1.0-gram resin heads was used. After thoroughly washing the column, the resin was washed with 3.0*M* HCl and, subsequently, with demineralized water. The column was then saturated with 1.0*M* formic acid. The mixture of zirconium and hafnium in 1.0*M* formic acid was loaded on the column and an elution curve was plotted by collecting several fractions of effluent and titrating with 0.01*M* EDTA solution (See Figure 3). Then mixtures containing varying amounts of hafnium were tried. Zirconium was eluted with 1.0*M* formic acid. About 100–120 ml of the effluent was collected at a flow rate of 5.0 ml/min. and the amount of zirconium was determined. Then the column was washed with water. Hafnium was eluted with 4.0*M* nitric acid at a flow rate of 1.0 ml/min, and the total effluent collected was 100–150 ml. Excess of nitric acid was removed

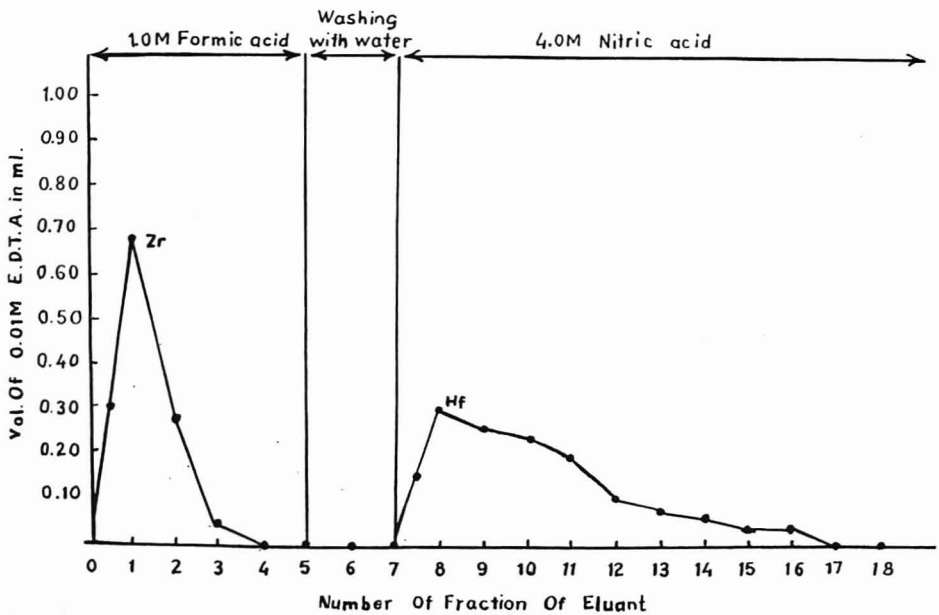

Figure 3. Separation of zirconium and hafnium over Dowex 50 W-X8 column in 1.0*M* formic acid

(I) Amount of Zr = 0.5 ml ≡ 1.0 ml 0.01*M* EDTA
(II) Amount of Hf = 0.5 ml ≡ 1.32 ml 0.01*M* EDTA
(III) One fraction = 5.0 ml of eluant

Table I. Quantitative Separation of Zirconium from Hafnium

Amount of Zr and Hf taken in the mixture, mg		Zr found, mg	Hf found, mg	Zr error	Hf error
Zr	Hf				
0.91	2.32	0.91	2.34	0.0	+0.02
1.82	4.64	1.82	4.60	0.0	−0.04
3.64	2.32	3.60	2.32	−0.04	0.00
0.91	0.464	0.93	0.464	+0.02	0.00
1.82	0.93	1.81	0.92	−0.01	−0.01
1.82	1.39	1.78	1.43	−0.04	+0.04
1.82	2.78	1.82	2.70	0.0	+0.02
1.82	3.75	1.81	3.70	−0.01	−0.05
1.82	0.24	1.83	0.26	+0.01	+0.02
1.82	2.43	1.81	2.43	−0.01	0.00

by evaporation and hafnium content was determined chelometrically. It was ascertained by loading the column with halfnium solution and eluting with formic acid that hafnium was completely retained in the column. The results are given in Table I.

DISCUSSION AND RESULTS

It is clear from the results that formic acid offers an exceedingly favorable separation factor for the separation of these two elements. We have demonstrated the importance of the method by choosing the less favorable concentration of formic acid—*i.e.*, 1.0*M*. At this concentration, the separation factor is about 40 and the separation is easily achieved. In more favorable cases, the separation factor is still greater—*i.e.* >100 and better separations should be possible.

The plot of log Kd *vs.* concentration of formic acid given in Figure 1 is very interesting. It appears that hafnium forms a positively charged stable complex with formic acid at concentrations from 0.25–1.75*M* and, therefore, in these concentrations the Kd values are very high and almost constant. However, in case of Zr it appears that two complexes are formed with formic acid in this range. First a positively charged complex is formed at 0.75*M*, and there is an increase in Kd value up to 1.0*M*. When the concentration of formic acid is increased further, an uncharged complex is formed and, hence, the Kd value falls abruptly. The reactions involved may tentatively be postulated as follows:

$$ZrO^{2+} + HCOOH \rightarrow ZrO(HCOO)^{+} + H^{+} \quad (1)$$

$$ZrO(HCOO)^{+} + HCOOH \rightarrow ZrO(HCOO)_2 + H^{+} \quad (2)$$

When the concentration of formic acid is increased further, Hf shows a decrease in the Kd value after 10.0*M* formic acid. At this concentration, there is probably a formation of uncharged Hf complex—*i.e.*, $HfO(HCOO)_2$. The bimodal behavior shown by zirconium in 4.0*M*–20.0*M* formic acid is probably due to adsorption and not to ion exchange.

ACKNOWLEDGMENT

The authors are thankful to Dr. S.M.F. Rahman for providing research facilities.

RECEIVED for review July 6, 1970. Accepted October 8, 1970. One of us (K. H.) extends his heartfelt gratefulness to C.S.I.R. India, New Delhi, for providing financial assistance.

Plutonium Determination in Soil by Leaching and Ion-Exchange Separation

Norton Y. Chu

Health and Safety Laboratory, U. S. Atomic Energy Commission, New York, N. Y. 10014

DURING MAY 1969 a fire occurred at the Dow Chemical Company's Rocky Flats, Colo., facility where plutonium components for nuclear weapons are fabricated. After the accident, many soil samples were taken in the immediate and outlying vicinity of the facility to determine the extent of the radioactive contamination. This report describes the methods used at the Health and Safety Laboratory (HASL) to determine the levels of plutonium in 100 gram samples of soil.

Over a number of years plutonium analyses (*1–8*) have been performed on different biological and environmental samples for monitoring purposes. These samples include air, food, water, excreta, fused rock, and soil. Several authors have used anion exchange systems to isolate plutonium from complex matrices (*9–11*). The ion-exchange separation scheme used here was suggested by the investigations of Kressin and Waterbury (*10*). Plutonium has been measured in 1–10 grams of soil and while this is adequate when the plutonium concentrations are sufficiently high, such small sample sizes may prevent plutonium detection when the levels are low. Except for deBortoli (*6*), the analysis for plutonium has not been made routinely on 100 grams of soil although plutonium and other actinides have been measured on kilograms of fused rock (*5*). For the analysis of the Colorado soils, it seemed desirable to analyze a minimum 100-gram

(1) Health and Safety Laboratory Manual of Standard Procedures, J. H. Harley, Ed., U. S. At. Energy Comm. **NYO-4700**, Rev. 1970.
(2) H. Levine and A. Lamanna, *Health Phys.*, **11**, 117–125 (1965).
(3) P. J. Magno, P. E. Kauffman, and B. Schleien, *ibid.*, **13**, 1325–1330 (1967).
(4) E. E. Campbell and W. D. Moss, *ibid.*, **11**, 737–742 (1965).
(5) K. Wolfsberg, W. R. Daniels, G. P. Ford, and E. T. Hitchcock, *Nucl. Appl.*, **3**, 375–377 (1967).
(6) M. C. deBortoli, ANAL. CHEM., **39**, 375–377 (1967).
(7) K. C. Pillai, R. C. Smith, and T. R. Folsom, *Nature*, **203**, 568–571 (1964).
(8) E. L. Geiger, *Health Phys.*, **1**, 405–408 (1959).
(9) D. B. James, *Los Alamos Scientific Laboratory Rep.*, **TID-4500**, January 1967.
(10) I. K. Kressin and G. R. Waterbury, ANAL. CHEM., **34**, 1598–1601 (1962).
(11) R. F. Buchanan, J. P. Farris, K. A. Orlandini, and T. P. Hughes, *U. S. At. Energy Rep.*, **TID-7560**, 1958, p 179.

sample since a wide range of plutonium concentrations was expected.

Briefly, the method consists of leaching soil with a mixture of nitric and hydrochloric acids in the presence of ^{236}Pu tracer. After leaching, plutonium in the leachate is converted to $Pu^{(IV)}$ with sodium nitrite and absorbed from 8*N* nitric acid onto Dowex 1-X4 ion exchange resin. The major constituents of the sample pass through the resin. Plutonium is removed from the exchanger with a mixture of dilute nitric and hydrofluoric acids and finally electroplated on a platinum disk from slightly acid ammonium chloride solution which is sufficient to prevent hydrolysis. The plated disk is counted on an alpha spectrometer. Identification of the plutonium isotopes in the sample is made by comparison of the sample spectrum with an electrodeposited standard source. The results obtained by leaching were found to be in good agreement with plutonium measurements of reference soils analyzed at HASL by complete solution of the sample.

EXPERIMENTAL

Reagents and Apparatus. All reagents used in the chemical method are of analytical grade; standardized plutonium-236 tracer solution—about 10 dpm/gram; 0.4*N* HNO_3–0.01*N* HF solution; 0.1% methyl red indicator solution; 5% sodium nitrite solution, freshly prepared; analytical grade Dowex 1-X4 (100–200 mesh) resin, Bio-Rad type AG; Platinum disks, 17.6-mm diameter × 0.005 in., one side mirror finished; Nickel disks, 17.6-mm diameter; electrolytic cell; electrolytic analyzer; and large and small ion-exchange colums.

Resin Preparation. About 15 ml of Bio-Rad AG 1-X4 (100–200 mesh) resin are used for each sample and are prepared as needed by conversion from chloride to the nitrate form with 1:1 nitric acid. Prolonged storage of the resin in high nitric acid concentrations will promote degradation.

Column I Preparation. The column is made from borosilicate glass. The outside diameter is 17 mm with a reservoir at the top of the column (35-mm diameter and 75 mm long) and a glass stopcock at the lower end. The overall length of the column is 315 mm. Fill the column to the reservoir with 1:1 nitric acid and position a plug of glass wool at the base. Transfer 5 ml of resin to the column with 1:1 nitric acid.

Column II Preparation. The column is made from borosilicate glass. Dimensions are the same except that the outside diameter is 11 mm. Prepare column II in the same way as column I, except add 2 ml of resin.

Electrodeposition Apparatus. The electrodeposition of plutonium is carried out in a cell (*1*) based on numerous other designs. It consists of an elongated 22-mm cap which holds a 1-oz polyethylene bottle with the bottom removed. The cap has space for an 18-mm diameter platinum plating disk and a nickel backing disk and may be screwed firmly into the polyethylene bottle forming a leak-tight plating cell. A threaded brass bushing is molded into the cap and allows electrical contact to be made with the platinum disk cathode by clip leads. The cell may be supported in the ice-water bath with a clamp stand; our cell is supported on a Lucite pedestal which makes it easier to center the anode stirrer. The anode is a $^1/_{16}$-in. platinum–iridium rod 4 inches long with a half inch diameter platinum disk riveted at one end. The disk has a number of $^1/_8$-in. holes cut into it to lighten the stirrer. It is connected through a variable speed (50 to 500 rpm) stirrer to the positive outlet of the electroanalyzer.

A Power Designs transistorized power supply (Model 2015R) furnishes a constant current ranging from 0–1.5 amperes and a constant voltage ranging from 0–20 volts. It is connected in parallel with an "Elaviscript 3" chart recorder which plots voltage *vs.* time at constant current during electrodeposition.

Sample Preparation. Complete details of the sampling procedure for the Colorado soils are given by Krey and Hardy (*12*) and are similar to those used for soil sampling at the Health and Safety Laboratory (*1*). The air-dried weight of the samples collected averaged about 20 kilograms. Associated rock and vegetation from the sample were separately crushed, ground, and blended, then combined with the soil and the whole blended again. The sample was quartered and about a kilogram of the material taken at random. The kilogram sample was further pulverized and blended so that 100-gram aliquots could be taken for analysis.

Chemical Method. Weigh 100 grams of the prepared soil sample into a 1-liter beaker and add a known amount (~3 dpm) of plutonium-236 tracer. Add slowly 300 ml of nitric acid. Foaming may be prevented by adding a few drops of *n*-octyl alcohol. After the reaction has subsided, add 100 ml of hydrochloric acid. Allow the mixture to react at room temperature for an hour; then boil for an hour while stirring. Cool to room temperature. Decant the liquid into another 1-liter beaker and reserve. Repeat the nitric–hydrochloric acid leach for another hour with stirring and boiling, and cool to room temperature. Decant, combine the liquid with the reserved solution and evaporate to about 200 ml. If siliceous material is present, dilute with an equal volume of water and filter, then wash the residue with dilute nitric acid. Reserve the filtrate. Transfer the filter and residue to a platinum crucible and ignite. Cool, add hydrofluoric and nitric acids, and evaporate to dryness. Add nitric acid and evaporate again to dryness. Dissolve the residue in nitric acid and combine with the reserved filtrate. Adjust the solution to 8*N* in nitric acid.

Ion-Exchange Procedure. Heat the 8*N* nitric acid sample solution to 90 °C and add 2 ml of freshly prepared 5% sodium nitrite solution. Cool in an ice-water bath to room temperature. Add 5 ml of the conditioned ion-exchange resin to the sample and stir for 5 minutes. Transfer the sample and the resin to column I. Allow the solution to flow through the resin bed at full flow until the liquid level reaches the top of the resin. Discard the effluent. Elute plutonium with 150 ml of 0.4*N* HNO_3–0.01*N* HF. Discard the resin. Evaporate the solution to dryness and convert the residue to nitrate by twice adding 5 ml of nitric acid and evaporating to dryness. Dissolve the residue with 15 ml of 1:1 nitric acid and heat to 90 °C. Add 0.25 ml of 5% sodium nitrite and cool to room temperature in an ice-water bath. Add 2 ml of the conditioned resin to the solution and stir for 5 minutes. Transfer the sample and resin with 1:1 nitric acid to column II and allow the solution to flow through the resin bed at full flow until the liquid level reaches the top of the resin. Wash the resin with 15 ml of 12*N* hydrochloric acid, three 10-ml portions of 1:1 nitric acid and discard the effluent and washings. Elute plutonium with 100 ml of 0.4*N* HNO_3–0.01*N* HF. Discard the resin. Evaporate the solution to dryness and convert the residue to chloride by adding 1 ml of hydrochloric acid twice and evaporating to dryness after each addition.

Electroplating Procedure. The electroplating is largely based on the procedure described by Mitchell (*13*). Add 1 ml of hydrochloric acid to the dried plutonium residue and heat gently. Transfer the solution with a transfer pipet to the electrolytic cell. Wash the beaker and pipet with two 1-ml portions of water and combine the sample in the cell. Add 1 drop of methyl red indicator and adjust the pH to just basic with ammonium hydroxide. Make the solution just acid with 1:5 hydrochloric acid and add 2 drops in excess. Dilute to 5 ml with water. Electroplate at a current of 1.2 amperes for 1 hour. Quench the electrolyte with 1 ml of ammonium hydroxide at the end of the electroplating period. Dismantle the cell and rinse the platinum disk with water then

(12) P. W. Krey and E. P. Hardy, Jr., *U. S. At. Energy Rep.*, HASL-235, Aug. 1970.
(13) R. F. Mitchell, ANAL. CHEM., 32, 326–328 (1960).

Table I. Plutonium Recovery from Soil Leached with Nitric–Hydrochloric Acids and Separated by Ion Exchange

Analysis No.	dpm ^{238}Pu Added	dpm ^{238}Pu Found	Chemical yield, %
1	1.84	1.43	77.8
2	1.86	1.46	78.5
3	1.94	1.64	84.5
4	1.95	1.63	83.6
5	2.12	1.71	80.7
6	2.13	1.97	92.5
7	2.13	1.96	92.0
8	2.18	1.94	89.0
9	2.19	1.82	83.1
10	2.55	2.10	82.4

Table II. Comparison of Plutonium Analysis in Soil by Nitric–Hydrochloric Acid Leach and Sodium Carbonate Fusion Methods

Sample number	Method	dpm/100 g $^{239, 240}Pu$	dpm/100 g ^{238}Pu	Chemical yield, %
1A	Leach	308 ± 11	5.9 ± 0.2	53
1B	Fusion	318 ± 12	6.6 ± 0.3	59
2A	Leach	1629 ± 87	32 ± 2	56
2B	Fusion	1607 ± 82	35 ± 2	66
3A	Leach	6.0 ± 0.2	0.19 ± 0.01	58
3B	Fusion	8.0 ± 0.3	0.13 ± 0.01	61

ethanol. Flame the disk to red heat over a burner to convert plutonium to the oxide. Assay the disk on the alpha spectrometer and resolve the plutonium isotopes.

Standardization. An electrodeposited standard source containing ^{236}Pu, ^{241}Am, and ^{244}Cm is measured in the alpha spectrometer system. The spectrum supplies a calibration curve of alpha energy *vs.* channel number as well as the detection efficiency of the system. Measurement of individual electrodeposited standard sources of ^{236}Pu, ^{241}Am, and ^{244}Cm shows that the detection efficiency is independent of alpha energy over the energy range of interest.

DISCUSSION AND RESULTS

An effort was made to shorten existing separation and collection procedures for removing plutonium from complex matrices. Classical methods used to remove minute quantities of plutonium from the bulk of the sample, such as phosphate collection, solvent extraction, or rare earth fluoride scavenging, could be omitted for an experimental soil sample. Plutonium was removed from the leachate of the soil by ion exchange. A resin bed with a height less than 5 cm for column I operation where the sample volume averaged about 300 ml tended to lose plutonium because of the amount of wash solution necessary to remove extraneous ions. The final purification step of plutonium on column II required a minimum 5 cm in height resin bed to satisfactorily retain plutonium. The ion-exchange column sizes used in this work were available in this laboratory and used as a matter of convenience.

The experimental samples shown in Table I were collected in an area of New York where the soil type is a fine silt loam. Also, Table I gives the amounts of plutonium-236 tracer recovered from two ion-exchange passes of the soil leachate from ten 100-gram aliquots of the experimental samples. The recovery of plutonium-236 tracer ranged from 78 to 93%.

Duplicate 100-gram aliquots of three soil types were selected from samples taken from various locations in the Colorado area. The samples, 0–20 cm, from this area were generally sandy loam and mixed with rock and vegetation as described previously. One aliquot was analyzed by the nitric–hydrochloric acid leach method and the other by complete solution of the soil using sodium carbonate fusion. The plutonium-239 + 240 and plutonium-238 values obtained by the two methods are shown in Table II. The overall chemical yield of the plutonium-236 tracer ranged from 53 to 66%. We believed in this early work the reason these chemical yields were lower than those of our experimental soil samples was probably because of mineral variations. Since that time further analyses have shown that the chemical yields obtained at HASL by the leach method have improved and range between 78–86%. It is shown from the measurements in Table II that good agreement was obtained between

Table III. Interlaboratory Comparison Analysis of Plutonium in Soil[a]

Sample location	Laboratory	Method	dpm/100 g $^{239, 240}Pu$	dpm/100 g ^{238}Pu
Colorado 1	A	HNO_3–HCl leach	400 ± 4	7.2 ± 0.2
	HASL	HNO_3–HCl leach	308 ± 11	5.9 ± 0.2
	HASL	Na_2CO_3 fusion	318 ± 12	6.6 ± 0.3
Colorado 2	A	HNO_3–HCl leach	1600 ± 33	31.8 ± 1.3
	HASL	HNO_3–HCl leach	1629 ± 87	31.8 ± 2.0
	HASL	Na_2CO_3 fusion	1607 ± 82	37.3 ± 1.6
Colorado 3	A	HNO_3–HCl leach	10.2 ± 0.2	0.20 ± 0.03
	HASL	HNO_3–HCl leach	6.0 ± 0.2	0.20 ± 0.01
	HASL	Na_2CO_3 fusion	8.0 ± 0.3	0.13 ± 0.01
Illinois 1	B	HNO_3–HCl leach	0.74 ± 0.25	...
	HASL	NA_2CO_3 leach	0.51 ± 0.03	...
New York 1	A	HNO_3–HCl leach	1.7 ± 0.1	0.04 ± 0.01
	HASL	NA_2CO_3 fusion	1.7 ± 0.1	0.41 ± 0.02
New York 2	B	HNO_3–HCl leach	0.41 ± 0.07	0.27 ± 0.21
	B	HF dissolution	0.35 ± 0.15	0.09 ± 0.18
	B	HF dissolution	0.49 ± 0.07	0.04 ± 0.04
	HASL	Na_2CO_3 fusion	0.41 ± 0.02	0.03 ± 0.02
New York 3	B	HNO_3–HCl leach	4.82 ± 0.23	0.03 ± 0.03
	B	HF dissolution	4.58 ± 0.25	0.20 ± 0.10
	B	HF dissolution	4.49 ± 0.24	0.14 ± 0.09
	HASL	HNO_3–HCl leach	4.13 ± 0.17	0.32 ± 0.02

[a] Error term for all measurements is a single Poisson error due to counting.

the shorter leaching method and the more lengthy sodium carbonate fusion dissolution method.

Since a large number of sample analyses were necessary to evaluate the extent of plutonium radioactivity in the Colorado area, commercial laboratories were asked to assist in this work. They were requested to analyze the soils by the nitric-hydrochloric acid leach and to compare this method with their internal methods. The results of the intercomparison are shown in Table III. The error term shown for all measurements is a single Poisson error due to counting. Measurements from Laboratory A for the Colorado soils in two out of three cases show higher plutonium-239 + 240 results than the measurements at HASL. A systematic error was not found for this difference. The sample collected in Illinois is a glacial silt "black" soil and this type has been used in this laboratory as a reference soil. The New York soils, 1, 2, and 3, also silt loam, were collected at a different site than the experimental sample; soil 1 was collected in 1967 from 0–20 centimeters and soils 2 and 3 were collected in 1969 at 5–20 and 0–5 centimeters, respectively. Except for New York sample 3 which was 50 grams, all soils in Table III were analyzed using 100 grams. From the plutonium 239 + 240 results shown, the leaching method is comparable to other methods for the determination of plutonium in soil containing fresh and aged fallout. Also, from these results, it was concluded that either of the methods tested would be adequate for plutonium soil analysis although the nitric-hydrochloric acid leach method required one third the analysis time as compared to the method of complete solution by sodium carbonate fusion.

A more detailed interpretation of the results obtained from Colorado soils as well as the extent of plutonium contamination found in the Rocky Flats area has been made by Krey and Hardy (*12*).

RECEIVED for review September 1, 1970. Accepted November 10, 1970.

Isothermal Gas Chromatographic Separation of Carbon Dioxide, Carbon Oxysulfide, Hydrogen Sulfide, Carbon Disulfide, and Sulfur Dioxide

Willis L. Thornsberry, Jr.

Research and Development Laboratory, Freeport Sulphur Company, Belle Chasse, La. 70037

THERE HAS BEEN a persistent need for a simple and rapid method for analyzing mixtures of CO_2, H_2S, SO_2, COS, and CS_2. The importance of such a method has been greatly magnified by the increased emphasis placed on monitoring the concentration of these components in waste gas streams. Although the procedure described here is not applicable to concentrations below the 50-ppm concentration range, it is useful for the monitoring of gases emitted from sulfuric acid plants, Claus recovery units, and for various other process control and laboratory applications. Recent papers by Stevens *et al.* (*1*, *2*) describe a gas chromatographic system for the analysis of some sulfur gases in the concentration range extending below 1 ppm using a 34-ft Teflon (Du Pont) column containing 40–60 mesh Teflon packing coated with polyphenyl ether and phosphoric acid. A sulfur selective flame photoluminescent detector was used in this study.

In the past ten years, a number of papers have been published which are concerned with the development of gas chromatographic columns for the separation and analysis of sulfur gases.

Several of these papers were discussed in a previous communication from this laboratory (*3*). Since that time other methods have been published. Brinkmann (*4*) discussed the development of a column for the separation of these five gases; however, the method is hampered by a tailing SO_2 peak and the fact that no base-line separation is obtained either between CO_2 and the inert gases, or between H_2S and COS. The development of porous polymer beads has provided what is probably the best and most trouble-free method for separating these gases when carbon disulfide is not present (*5*, *6*). A 6-ft × 1/4-in. aluminum column of Porapak Q-S was tested in this laboratory and CO_2, COS, H_2S, and SO_2 were eluted within 6 minutes; however, a CS_2 peak was not observed until about 40 minutes after sample injection. The column temperature was 98 °C and the helium carrier gas flow rate was 55 cc/min.

An earlier communication from this laboratory outlined an analytical procedure for the simultaneous, isothermal separation and analysis of CO_2, COS, H_2S, SO_2, and CS_2 using a silica gel column (*3*). Since that time, numerous columns have been prepared from this same batch of silica gel. All of these columns have been used successfully both in the laboratory and (with the addition of a precut column to remove moisture) in process instruments for continuous analysis. However, attempts to reproduce these results with silica gel from other sources and even with different lots obtained from the same source have failed.

Various methods of treating these silica gels have been tried, including silanizing; acid washing, using conditions ranging from simple washing to refluxing with concentrated hydrochloric acid for 2 to 3 hours; and conditioning the

(1) R. K. Stevens *et al.*, *Environ. Sci. Technol.*, **3**, 652 (1969).
(2) R. K. Stevens and A. E. O'Keeffe, ANAL. CHEM., **42**, (2), 143A (1970).
(3) C. T. Hodges and R. F. Matson, *ibid.*, **37**, 1065 (1965).
(4) H. Brinkmann, *Chem. Tech. (Leipzig)*, **17**, 168 (1965).
(5) E. L. Obermiller and G. O. Charlier, *J. Gas Chromatogr.*, **6**, 446, (1968).
(6) E. L. Obermiller and G. O. Charlier, *J. Chromatogr. Sci.*, **1**, 580 (1969).

Table I. Operating Characteristics of Column[a]

Component	Concentration (Volume, %)	Retention time R	"Q" factor, Q	Separation factor S	Resolution, R	Width, W	No. of theoretical plates, N
Air	balance	0.12	...	...	...	...	...
CO_2	3.00	0.66	3.47	0.82	2.84	0.19	192
COS	1.11	1.22	3.30	0.46	1.52	0.37	174
H_2S	4.30	1.85	4.12	0.34	1.40	0.45	272
CS_2	1.52	4.40	3.52	0.58	2.04	1.25	198
SO_2	4.10	6.85	3.70	0.36	1.33	1.85	219

[a] Operating conditions: Deactigel 60/80 mesh. Lot No. 795/10B acid washed 2 ft × 1/4 in. Al. Col. at 122 °C with a He flow rate of 55 cc/min. Using a 5-cc syringe sample.

column in a stream of the sulfur gases. None of these procedures produced an acceptable column. Tailing peaks, especially the SO_2 peak, were always a problem. Variations among different batches of silica gel are not unusual and this problem has often been reported (*3*, *7*).

This work relates to the use of a treated silica gel, "Deactigel," supplied by Applied Science Laboratories, State College, Pa. Although significant batch to batch variations were observed with Deactigel, a simple acid wash treatment consistently produced a column material which gave very good separation.

EXPERIMENTAL

An F and M model 720 dual-column, programmed-temperature chromatograph equipped with a Gow Mac W-2 thermal conductivity detector and a 1-mV Honeywell recorder was used for this work. Helium carrier gas was used throughout all tests. Gas mixtures for calibration were obtained from Matheson Corporation and other test mixtures were prepared in the laboratory.

Acid washing of the Deactigel was done by placing 10 grams of the Deactigel in a Buchner funnel with a medium porosity glass frit bottom and washing with 30 ml of concentrated hydrochloric acid, 90 ml of distilled water, and 90 ml of acetone in that order at a rate of 5 cc/min. The Deactigel was then air dried. The columns were prepared and conditioned overnight in the gas chromatograph oven at 200 °C with a helium flow of 55 cc/min through the column. This column has been used for the analysis of these gases in the concentration ranges of 0.01 to 20% by volume. A 5-cc sample, both syringe sample and a gas sampling loop, was used throughout this work.

RESULTS AND DISCUSSION

The chromatogram in Figure 1 shows the separation obtained using a 2-foot × 1/4 inch column of acid washed Deactigel at a temperature of 122 °C and a carrier gas flow rate of 55 cc/min. These conditions were found to produce the best separation.

The data presented in Table I constitute a detailed analysis of the chromatogram including a tabulation of the column description, operating conditions and retention times, and peak widths obtained for each component on each column. In addition, a number of parameters normally used to express the efficiency of gas chromatographic columns are tabulated. These include the Q value, separation factor, resolution, and the number of theoretical plates. These various terms, as used in this paper, are defined as follows:

Q Value: Q = retention time/peak width

Separation Factor: $S = \dfrac{t_A - t_B}{t_B}$

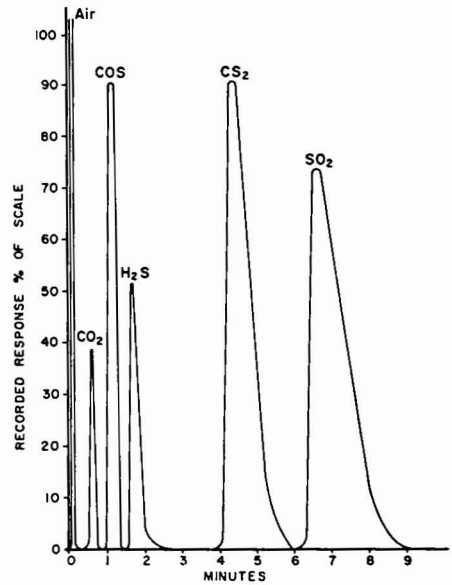

Figure 1. Separation of sulfur gases on a two-foot column of acid washed Deactigel

where

t_A = retention time of the preceding peak
t_B = retention time of peak for which separation factor is being calculated

Resolution: $R = (Q)(S)$

Number of theoretical plates: $N = 16(Q)^2$

If water vapor is present, it may be desirable to make special provisions to handle this. Possible solutions have been previously discussed (*3*). However, water does not interfere with the analysis and unless an unusually high water concentration is present or a large number of consecutive samples are being taken, as in a process instrument, this will present little or no problem.

Aluminum, glass, or stainless steel tubing may be used to prepare these columns.

Received for review August 14, 1970. Accepted November 12, 1970.

(7) H. Hall, Anal. Chem., 34, 61 (1962).

Optimization of Experimental Conditions for Spectrofluorimetric Determination of Europium, Samarium, and Terbium as Their Hexafluoroacetylacetone–Trioctylphosphine Oxide Complexes

R. P. Fisher and J. D. Winefordner

Department of Chemistry, University of Florida, Gainesville, Fla. 32601

THE USE OF β-DIKETONE chelating agents in the spectrofluorimetric determination of trace amounts of rare earth ions has been described (*1*, *2*), and the basis of the enhancement of the fluorescence by synergic agents has been discussed elsewhere (*3*). Fluorescence analysis of the rare earths in solution by this method is potentially quite useful because the intense, line-like spectra obtained are characteristic of the metal ions themselves and are relatively independent of interferences. The purpose of this study was to investigate the effect of pH on the fluorescence of the hexafluoroacetylacetone/tri-*n*-octylphosphine oxide complexes of the rare earths with the ultimate aim of optimizing experimental conditions so as to provide a useful analytical method.

EXPERIMENTAL

The oxides of cerium, praseodymium, neodymium, samarium, lanthanum, europium, gadolinium, terbium, dysprosium, holmium, erbium, thulium, ytterbium, and lutetium (Rare Earth Division, American Potash and Chemical Corp., West Chicago, Ill.) were obtained in purities of 99.9% or better, except for Dy and Ho which were of 99% minimum purity. Hexafluoroacetylacetone (HFA) was J. T. Baker practical grade: initial experiments were performed with HFA purified according to the extraction method of Rydberg (*4*, *5*); this later proved unnecessary, and the practical grade HFA was thenceforth used without further purification. Tri-*n*-octylphosphine oxide (TOPO) was practical grade (obtained from Pfaltz and Bauer, Inc., Flushing, N. Y.). Several grades of methylcyclohexane were tried, but it was found that Eastman practical grade could be used without further purification. Stock solutions of the rare earth ions were prepared by dissolving the rare earth oxide in concentrated HCl or HNO_3 and diluting with sodium hydroxide solution to obtain 500 ml of 0.01*M* rare earth ion at approximately pH 5. Serial dilutions of the stock solutions were made with acetic acid/sodium acetate buffer solutions at the pH of interest in the given experiment.

Fluorescence spectra and analytical curve data were taken using an Aminco-Bowman spectrofluorometer (American Instrument Co., Inc., Silver Spring, Md.) equipped with a high pressure xenon arc source (powered by a Harrison 6268A DC Power Supply, Hewlett-Packard, Orlando, Fla.), an Aminco Ellipsoidal Condensing System, and an R136 (red sensitive) multiplier phototube. Phototube power and readout was provided by an Aminco Photomultiplier Microphotometer, and spectra were recorded on an Aminco X-Y recorder. pH measurements were made with a combination pH electrode (Model 4858 L60, A. H. Thomas Co., Philadelphia, Pa.) and a pH meter (Model LS, E. H. Sargent and Co., Chicago, Ill.)

The procedure for the preparation of the chelates was as follows: to a 15-ml glass-stoppered centrifuge tube were added 3 ml of rare-earth ion solution, 3 ml of $6 \times 10^{-4}M$ HFA in methylcyclohexane, and 3 ml of 0.01*M* TOPO in methylcyclohexane. The tube was stoppered and shaken for approximately 15 seconds, the layers were allowed to stratify (about 1 minute), and approximately 3 ml of the upper layer was poured into a 1 cm × 1 cm quartz cell.

Apparent fluorescence excitation and emission spectra were obtained at room temperature, and optimum excitation and emission wavelengths were selected from these spectra. In the preparation of the analytical curves, all fluorescence intensity readings were referred to a standard chelate solution whose fluorescence intensity was measured often, so as to compensate for long-term source variation. All intensity readings were corrected for a blank, prepared by extracting 3 ml of the acetate buffer used in the given experiment with 6 ml of the HFA/TOPO solution.

OPTIMUM EXPERIMENTAL CONDITIONS

As expected, only europium, samarium, and terbium yielded analytically useful fluorescent chelates. [Note that Stanley *et al.* (*6*) have suggested that by using an instrument utilizing a monochromator and transducer capable of providing resolution and detection in the near infrared, one should be able to determine the majority of the rare earth ions by the β-diketone fluorescence method.]

Several factors should be noted concerning the extraction method used in the present study:

Preparation of a solid sample for analysis did not involve the evaporation of quantities of concentrated acids.

The reagents could be used as obtained commercially; no further purification was necessary.

Multiple extractions, although they would undoubtedly increase the efficiency of the method, were not necessary to obtain linear analytical curves and low limits of detection. The extraction time was not critical; apparently equilibrium is attained quite rapidly.

Only one stock solution of chelating/synergic agent was necessary to cover the entire concentration range of the method.

A pH of 3 was found to be most suitable for analytical measurements of the three rare earths. It is to be expected that there would be a pH which would yield optimum extraction of the rare earth ions by HFA; at low pH values, hydronium ion competition with the metal ion for an enolate ion should reduce extraction efficiency, while at high pH, the metal ion should form hydrated hydroxides rather than chelate complexes. An experiment in which fluorescence intensity of a europium chelate was measured as a function of initial (pre-extraction) europium solution pH showed results in agreement with those of Shigematsu *et al.* (*2*)—namely, that optimum extraction

(1) R. Belcher, R. Perry, and W. I. Stephen, *Analyst*, **94**, 26 (1969).
(2) T. Shigematsu, M. Matsui, and R. Wake, *Anal. Chim. Acta*, **46**, 101 (1969).
(3) F. Halvorsen, J. S. Brinen, and J. R. Leto, *J. Chem. Phys.*, **41**, 157 (1964).
(4) J. Rydberg, *Sv. Kem. Tidskr.*, **62**, 179 (1950).
(5) J. Stary, "The Solvent Extraction of Metal Chelates," The Macmillan Company, New York, N. Y., 1964, p 51.
(6) E. Stanley, B. Kinneberg, and L. Varga, ANAL. CHEM., **38**, 1362 (1966).

Table I. Analytical Determination of Samarium, Europium, and Terbium[a]

Ion	λ_{ex},[b] nm	λ_{em},[c] nm	Range of analytical curve linearity, moles rare earth ion/liter in solution to be extracted
Samarium	350	565	1×10^{-4} to 5×10^{-7}
Europium	360	615	1×10^{-4} to 1×10^{-9}
Terbium	350	550	1×10^{-4} to 1×10^{-7}

[a] All analytical curves were prepared using the extraction method described in text; [HFA] = $6 \times 10^{-4}M$, [TOPO] = $0.01M$, pH = 3 (acetate buffer).
[b] Approximate wavelength of excitation.
[c] Approximate wavelength of observation of emission, chosen to facilitate the analysis of mixtures of the three ions.

occurs near pH 6. However, analytical curves obtained from europium solutions at pH 6 (other conditions same as described above) showed anomalous "humps," limiting the useful range of the method to a lower limit of about $10^{-7}M$ europium. When, however, the pH was reduced to 3, the analytical curve was useful to europium ion concentrations of 10^{-9} moles per liter. A pH of 3 was also found to be useful for samarium and terbium.

In Table I, the results obtained for the three rare earths which exhibited appreciable fluorescence by this method are given. The lower limits represent the lowest concentrations for which reproducible results could be obtained, consistent with the remainder of the analytical curve. Note that for all three rare earths, concentrations one to three orders of magnitude below the lower limits listed could be detected above the blank, but the intensity values were not consistent or reproducible. The precision and selectivity of measurement were similar to those found by Belcher *et al.* (*1*) and Shigematsu *et al.* (*2*). No recovery data will be given here; however, students in an undergraduate instrumental analysis course (during three different terms) have obtained essentially complete recovery of europium (with no apparent difficulties) in synthetic solutions with this extraction–measurement procedure.

RECEIVED for review August 12, 1970. Accepted November 16, 1970. Research was carried out as a part of a study on the phosphorimetric analysis of drugs in blood and urine, supported by a U. S. Public Health Service Grant (GM-11373-07).

Kinetic Study of the Beckmann Rearrangement of 6α-Methyl-17α-Acetoxyprogesterone-3-Oxime by Cathode Ray Polarography

Arvin P. Shroff and Charles J. Shaw

Analytical Research Group, Division of Organic Chemistry, Ortho Research Foundation, Raritan, N.J. 08869

THE BECKMANN REARRANGEMENT has offered the organic chemist a convenient method by which to introduce a nitrogen into the steroid ring system. These heterocyclic steroids have been prepared using a variety of solvents and such catalysts as tosyl chloride (*1–6*), thionyl chloride (*7, 8*), phosphorus pentachloride (*1, 2*), *p*-acetylaminobenzenesulfonyl chloride (*4*), and *p*-aminobenzenesulfonyl chloride (*9, 10*). The yield of the lactam obtained by these methods has been variable because it is believed (*11, 12*) that only the syn isomer participates in the rearrangement of the α,β-unsaturated ketoxime. The kinetics of this transformation as followed by cathode ray polarography is the subject of this paper.

Previous methods of analysis in the study of rates of rearrangement of cyclic and acyclic ketoximes, involved refractive index (*13*), gravimetric analysis (*14, 15*), colorimetric assay (*16*) and ultraviolet methods (*17, 18*). All of these methods, though appropriate for the particular problems, lack sensitivity or specificity or both.

A literature survey indicated that only a few electrochemical reduction studies have been made with C=N in contrast to C=O compounds which have received a substantial amount of attention from the polarographers. They have indicated (*19, 20*) that amines are the products of reduction in protic solvents such as ethanol.

The present investigation was undertaken to evaluate the applicability of cathode ray polarography in studying the kinetic transformation of 6α-methyl-17α-acetoxyprogesterone 3-oxime (MAPO) to its corresponding lactam (Scheme 1). It would offer sensitivity with concurrent selectivity when used with the appropriate supporting electrolyte. The data

(1) S. Hara, *Pharm. Bull (Japan)*, **3**, 209 (1955).
(2) S. Hara, *Yakugaku Zasshi*, **78**, 1027 (1958).
(3) *Ibid*, p 1030.
(4) S. Kaufmann, *J. Amer. Chem. Soc.*, **73**, 1779 (1951).
(5) R. H. Mazur, *ibid.*, **81**, 1454 (1959).
(6) K. Tsuda and R. Hayatsu, *ibid.*, **78**, 4107 (1956).
(7) B. M. Regan and F. N. Hayes, *ibid.*, p 639.
(8) C. W. Shoppee and J. C. Sly, *J. Chem. Soc.*, **1958**, 3458.
(9) H. Heusser, J. Wohlfahrt, M. Muller, and R. Anliker, *Helv. Chim. Acta.*, **38**, 1399 (1955).
(10) R. Anliker, M. Muller, J. Wohlfahrt, and H. Heusser, *ibid.*, p 1404.
(11) C. W. Shoppee, M. I. Akthar, and R. E. Lack, *J. Chem. Soc.*, **1962**, 1050.
(12) C. W. Shoppee, R. E. Lack, R. N. Mirrington, and L. R. Smith, *ibid.*, **1965**, 5868.
(13) D. M. Dimitrijevic and O. K. Stejanovic, *Glas. Hem. Drust., Beograd*, **28**, 353 (1963); *C.A.*, **63**, 2868(1965).
(14) D. E. Pearson, J. F. Baxter, and J. C. Martin, *J. Org. Chem.*, **17**, 1511 (1952).
(15) D. E. Pearson and J. D. Bruton, *ibid.*, **19**, 957 (1954).
(16) P. T. Scott, D. E. Pearson, and L. J. Bircher, *ibid.*, p 1815.
(17) P. T. McNulty and D. E. Pearson, *J. Amer. Chem. Soc.*, **81** 612 (1959).
(18) N. G. Zarakhani, V. V. Budylina, and M. I. Vinnik, *Zh. Fiz. Khim.*, **39**, 1561 (1965).
(19) H. Lund, *Acta, Chim. Scand.*, **13**, 249 (1959).
(20) P. Zuman and O. Exner, *Collect. Czech. Chem. Commun.*, **30**, 1832 (1965).

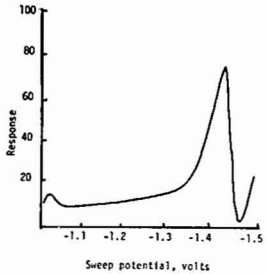

Figure 1. Typical polarogram of 0.02*M* MAPO in 40% ethanolic Michaelis phosphate buffer and 0.1*M* tetraethylammonium chloride

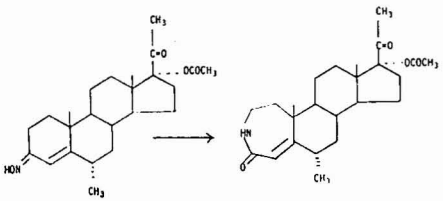

Scheme 1

obtained would enhance our knowledge of the stereochemical features necessary for the Beckmann rearrangement and the mechanism of electrochemical reduction of steroidal oximes. The synthesis and yield of the compounds in Scheme 1 were recently reported (*21*).

EXPERIMENTAL

Apparatus. All the analytical work was done with a Davis Differential Cathode Ray Polarotrace, Model 1660A manufactured by Southern Instruments Ltd., Camberley, England. Cells and electrodes, supplied with the instrument and a mercury pool anode were used in all measurements. The cells were thermostated at 25 ± 0.1 °C. A 50-millisecond time constant for R.C. derivative was used throughout the experiment. The time cycle for dislodging mercury drops was 5 seconds and the sweep period was 2 seconds during which a voltage change of 0.5 volt was applied. Routine but scrupulous cleaning procedures for all equipment were carried out to exclude the introduction of reducible and surface active impurities.

Material. All reagents employed in this investigation were reagent grade and were obtained commercially. The steroids, 6α-methyl-17α-acetoxy progesterone, 6α-methyl-17α-acetoxy progesterone 3-oxime (MAPO) and the lactam were supplied by our Division of Organic Chemistry. Commercial absolute ethanol was distilled over sodium ethoxide and diethyl phthalate (*22*) to remove reducible impurities. A polarographic grade of tetraethylammonium iodide was used as the supporting electrolyte. Buffers were prepared as per Michaelis and Walpole (*23*).

Kinetic Experiment. A 50-ml round bottom flask containing a solution of 2 grams of MAPO in 30 ml of dioxane was

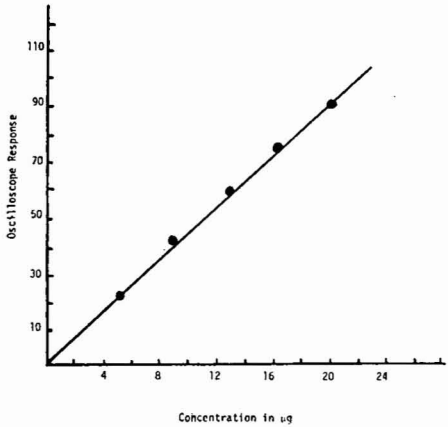

Figure 2. Plot of peak current *vs.* concentration

placed in a constant temperature bath (Blue M Electric Co.) at 30 ± 0.1 °C. After 0.5 hr, a 5-ml portion of thionyl chloride, also kept at 30 ± 0.1 °C was added to the mixture. A 50-µl sample was withdrawn at 5-minute intervals (when the reaction was carried out at 15 °C the samples were withdrawn at 10-minute intervals) and placed into a 25-ml volumetric flask containing 1 ml of 0.1*M* tetraethylammonium iodide. Each solution was diluted to volume with 40% ethanolic Michaelis phosphate buffer (pH 8.4) and a representative sample transferred to an electrolysis cell (kept at 25 ± 0.1 °C) and deoxygenated with nitrogen for 15 minutes. The polarograms were viewed immediately on the oscilloscope and the peak height and sensitivity dial reading recorded.

DISCUSSION

The solubility of steroids in water is too low for electrochemical study. A preliminary investigation of solvent effects and solubility lead to the selection of 40% ethanol 60% water (v/v) as the most suitable medium. Polarographic examination of the oxime, its corresponding ketone, and the lactam was carried out at various pH's using a variety of supporting electrolytes. In our hands tetraethylammonium iodide gave satisfactory results with the reduction of the ketone and oxime. A two-step reduction of the oxime, equivalent to 4*e*, took place in 40% ethanolic Walpole acetate buffer (pH 3.6–5.6) and Michaelis phosphate buffer (pH 5.3–8.4). The mechanism of reduction (Scheme 2) appears to be similar to the one proposed by Lund (*19*). At a pH of 8.4, the two peaks coalesced (Figure 1) with a peak potential (E_p) of −1.41

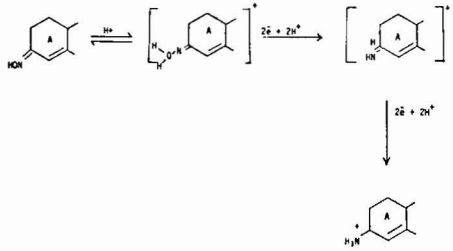

Scheme 2

(21) A. P. Shroff, *J. Med. Chem.*, 13, 748 (1970).
(22) L. F. Fieser, "Experiments in Organic Chemistry," 3rd ed., D. C. Heath & Co., Boston, Mass., 1955, p 286.
(23) M. Brezina and P. Zuman, "Polarography in Medicine, Biochemistry and Pharmacy," Interscience, London, 1958, p 731.

Table I. Effect of Temperature on Rate Constant[a]

Expt No.	k at 15 °C	k at 30 °C
1	2.10	8.98
2	1.90	8.98
3	1.98	7.85
4	2.23	8.60
Mean	2.05	8.60
Std dev	0.14	0.53
Std error	0.07	0.26
$t_{1/2}$	33.8 min	8.1 min

[a] k = moles/liter/min × 10^3.

Table II. Effect of Varying Amounts of $SOCl_2$ and Oxime on Rate Constant

$SOCl_2$, ml[a]	k	Oxime, g[b]	k[c]
1	8.27	1.0	7.58
3	9.69	1.5	8.98
4	8.43	2.0	8.98
5	8.00	2.5	7.81
Mean	8.85		8.34
Std dev	0.64		0.75
Std error	0.32		0.37

[a] 2.0 g of oxime was used for each experiment.
[b] 5.0 ml of $SOCl_2$ was used for each experiment.
[c] k = moles/liter/min × 10^3.

Table III. Comparison of Per Cent Syn Isomer Found by Polarography and Nonaqueous Titrimetry

No.	Polarography	Nonaqueous Titrimetry
1	28.0	27.1
2	27.0	29.2
3	30.0	30.8
4	25.6	28.2
5	29.5	29.6
Mean	28.0	30.0
Std dev	1.80	1.40
Std error	0.81	0.63

volts. This E_p is shifted by −0.18 volt in the kinetic experiment. The ketone under the same conditions exhibited an E_p of −1.73 volts. The lactam, however, could not be reduced under these conditions but in 40% ethanolic 0.1N lithium bromide and 0.1N tetraethylammonium perchlorate it underwent smooth reduction at E_p of −1.57 volts.

We chose the one-step reduction of the oxime at pH 8.4 for our kinetic measurements. A calibration curve employing first derivative polarograms is shown in Figure 2. The kinetic experiment was conducted at 15 and 30 °C because of the exothermic nature of the reaction. The oxime concentrations were calculated from the equation

$$i = kc$$

where i is the peak height, c is the concentration of the oxime in moles per liter, and k is a constant determined experimentally.

The Beckmann rearrangement (Scheme 1) follows the first order rate law at both 15 and 30 °C. A plot of the log of oxime concentration *vs.* time is depicted in Figure 3. The linear equation is

$$\log C_{syn} = \log[C_{syn}]_0 - Kt/2.303$$

where C_{syn} is concentration of oxime remaining in solution, $[C_{syn}]_0$ is initial concentration of the oxime solution, k = rate constant, and t = time in minutes.

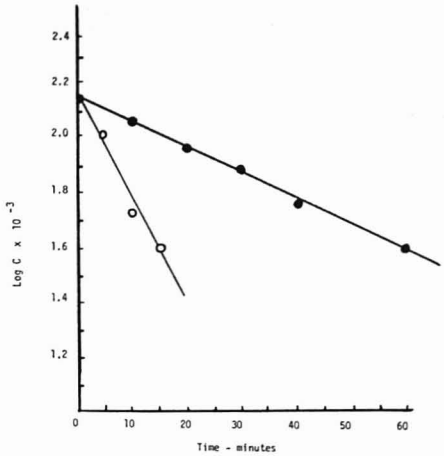

Figure 3. Plot of the logarithm of MAPO concentration vs. time at two different temperatures

● 15 °C
○ 30 °C

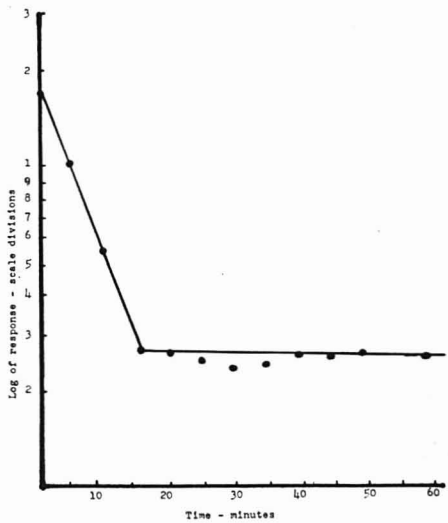

Figure 4. Plot of the log of response *vs.* time for a 30 °C experiment

The rate constants, tabulated in Table I, may be calculated from the linear equation or from the slope of the line which is equal to $-k/2.303$. The rate of rearrangement is quadrupled by changing the temperature from 15 to 30 °C.

The first order rate kinetics was further confirmed by varying the concentration of the oxime at a fixed concentration of thionyl chloride and vice versa. The data tabulated in Table II indicate that the rearrangement was independent of the concentration of thionyl chloride, provided it was in excess.

The stereochemical feature necessary for the rearrangement was investigated for the 30 °C reaction. A plot of the log of response *vs.* time is represented in Figure 4. A sharp drop in current is observed for the first 15 minutes followed by constant diffusion current. This is attributed to the fact that α,β-unsaturated ketoxime exists in two isomeric forms, syn and anti (Scheme 3) and that only the syn participates in the rearrangement. The calculation of the isomers was carried out as follows and compared with nonaqueous titrimetric method (Table III)

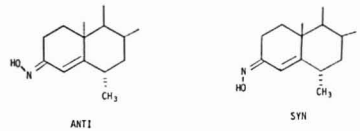

Scheme 3

$$\frac{\log C_o - \log C_t}{\log C_o} \times 100 = \%\ \text{syn isomer}$$

where C_o = concentration at time 0 and C_t represents concentration at the end of 16 minutes (or point of inflection). The values in Table III show a good correlation and suggest that only the syn isomer participates in the rearrangement. The values also indicate that anti isomer does not isomerize to the syn form or vice versa in solution. Further, they strongly suggest that polarography can be a potential technique for the determination of syn and anti isomers of similar compounds. The advantage of this technique over the nonaqueous titrimetric method is obvious when one considers that in the latter method a preliminary separation by preparative thin-layer chromatography is essential before the titration can be performed with 0.1*N* perchloric acid.

ACKNOWLEDGMENT

The authors are indebted to Dr. Irving Scheer for his encouragement and to Mr. Richard E. Huettemann for assistance in performing the nonaqueous titrations.

RECEIVED for review July 6, 1970. Accepted November 5, 1970.

Spectrophotometric Determination of Cobalt with Benzil Mono-(2-Pyridyl)Hydrazone

Ronald T. Pflaum and E. Scott Tucker III[1]

Department of Chemistry, University of Iowa, Iowa City, Iowa

MONO-(2-AZAARYL)HYDRAZONES ACT as nonselective ligands toward transition metal ions. Benzil mono-(2-pyridyl)hydrazone reacts with cobalt(II) ion to form the bis-[benzil mono(2-pyridyl)hydrazone] cobalt(III) complex. In a 60% ethanol–water solvent system, this colored chelate cation exhibits a wavelength of maximum absorption at 535 nm with a molar absorptivity of 27,400. Solutions of the complex conform to Beer's law over the concentration range studied, 6.1×10^{-5}–6.1×10^{-6}*M*. In a neutral to slightly basic ethanolic solution, color development is complete in 30 minutes in the presence of a 25-fold excess of reagent. The color intensity of the cobalt complex is unchanged by the addition of strong acid. Other transition metal complexes are decomposed upon treatment with acid. A method is proposed for the determination of cobalt in selected samples.

The spectrophotometric methods most frequently employed for the determination of cobalt utilize the nitroso–naphthol reagents. These form intensely colored tris chelates with the cobalt(III) ion in weakly acidic or neutral solutions. The reagents are not selective but react readily with other transition metal ions. However, only the water soluble cobalt complex of nitroso-R salt and the insoluble 1-nitroso-2-naphthol and 2-nitroso-1-naphthol cobalt species are stable in highly acidic solution (*1*).

Methods utilizing the above colored complexes suffer from interferences due to the presence of other metal complexes and to excess reagent in the measured systems. Interferences due to metals may be eliminated by a preliminary separation (*1–3*) and by decomposition of the metal complexes with hydrochloric acid (*1*, *3–5*). The interference of excess reagent may be circumvented by measurement at a secondary absorption maximum of the cobalt complex (where absorption of the reagent is negligible) and by removal of reagent with strong base (*1*, *3–5*). Multiple washing steps, in which acidic and basic washes of the nonaqueous medium containing the cobalt complex are carried out, are required in order to completely eliminate interferences.

The use of benzil mono-(2-pyridyl)hydrazone as a reagent for the spectrophotometric determination of cobalt offers advantages over the nitroso naphthol reagents. Prior removal of diverse metal ions and extraction of the cobalt species are not requisite in the hydrazone method. In addition, direct measurement without separation precludes the necessity of multiple washing steps.

EXPERIMENTAL

Apparatus. All absorption measurements were made with a Cary Model 14 recording spectrophotometer at room temperature in 10- and 20-mm matched silica cells. All pH

[1] Present address, Organic Division, Research Department, Monsanto Company, St. Louis, Mo.

(1) E. B. Sandell, "Colorimetric Determination of Trace Metals," 3rd ed., Interscience, New York, N. Y., 1959, pp 420–422.

(2) E. Cogan, ANAL. CHEM., **32**, 973 (1960).
(3) R. C. Rooney, *Metallurgia*, **62**, 175 (1960).
(4) L. J. Clark, ANAL. CHEM., **30**, 1153 (1958).
(5) M. Needleman, *ibid.* **38**, 915 (1966).

measurements were made with a Corning Model 12 pH meter equipped with a standard glass-calomel electrode.

Reagents. Benzil mono-(2-pyridyl)hydrazone, BMPH, was prepared by the general method of Chiswell, Lions, and Tomlinson (*6*). Stoichiometric amounts of the reactants, 2-hydrazinopyridine (Aldrich Chemical Co.) and benzil (0.1 mole), were dissolved in a minimum amount of ethanol (500 ml) containing several drops of glacial acetic acid and the reaction mixture heated under reflux for 30 minutes. Upon cooling in an ice bath, the monohydrazone crystallized out of solution. The yield was 60–70% after one recrystallization from ethanol (mp 140–141 °C).

A 1% (w/w) reagent solution was prepared by dissolving 7.8 grams of the reagent in 1 liter of ethanol with the aid of moderate heating.

A standard cobalt solution was prepared by the dissolution of approximately 18 grams of hydrated cobalt perchlorate in 1 liter of distilled water. The cobalt content was standardized by electrodeposition and all subsequent cobalt solutions were prepared by dilution.

All other reagents used were of reagent grade quality.

Recommended Procedure. Pipet a suitable aliquot of the sample solution into a 25-ml volumetric flask. Add 15 ml of the 1% reagent solution and make the solution neutral to slightly basic with 1*M* sodium hydroxide. After allowing the color to develop for 30 minutes, add 6 ml of 8*M* HCl and dilute to volume with water.

Measure the absorbance of the sample solution *vs.* an ethanol blank at 535 nm. Calculate the amount of cobalt present from a previously prepared calibration curve.

RESULTS AND DISCUSSION

Benzil mono-(2-pyridyl)hydrazone is a light yellow stable crystalline solid insoluble in water and dilute acid. The ligand is very soluble in common organic solvents. Solutions of BMPH in ethanol were stable for a period of 6 months.

The reagent acts as a nonselective organic ligand toward most of the transition metal ions. Of the metal complexes formed, only the bis[benzil mono-(2-pyridyl)hydrazone]cobalt(III) complex is kinetically inert toward dissociation by hydrogen ion. This unique feature of the cobalt complex permits its determination in the presence of the other transition metal ions.

In solutions of 30–80% ethanol–water, BMPH reacts with the cobalt(II) ion to form a highly colored complex having an absorption maximum at 535 nm. Mole ratio and continuous variations studies showed that the absorbing species is the bis hydrazone complex. Complexation was shown to involve deprotonation of the ligand and oxidation of Co(II) to the Co(III) ion. It was demonstrated that dissolved molecular oxygen is the active oxidant in the system.

Complex formation is a relatively slow process due to the necessary transformations in both the ligand and the metal ion. The rate of complex formation increases with increasing ligand concentration and pH. Maximum color is observed after 30 minutes for a 60% ETOH–H_2O solution containing a 25:1 ratio of ligand to metal ion. The apparent pH of the system is approximately 7.5. Maximum color is developed in less than 10 minutes in a similar mixed solvent of pH 12 containing a 5:1 ratio of reactants.

Once formed, the chelate complex of cobalt(III) is chemically inert toward hydrogen ion. No dissociation of the complex is apparent over a hydrogen ion concentration of $2M - 1 \times 10^{-3}M$. In strongly acidic solution, the absorbance of a solution remained unchanged for a period of 12 hours. In acidic solution, the complex exhibits a wavelength of maximum absorption of 535 nm and a molar absorptivity of 27,400. Beer's law is obeyed over a cobalt ion concentration of 6.1×10^{-5}–$6.1 \times 10^{-6}M$.

Table I. Determination of Cobalt in Selected Metal Samples

Sample	Cobalt, % Present	Cobalt, % Found
NBS-126 B (High Nickel Steel) (35.99% Ni)	0.032	0.031[a] 0.033[b]
NBS-153 A (Co–Mo–W Steel) (8.85% Mo–1.76% W)	8.46	8.49[b]
NBS-157 A (Cu–Ni–Zn alloy) (58.60% Cu–11.82% Ni–29.06% Zn)	0.020	0.018[b]

[a] Measurement after ion exchange separation.
[b] Measurement without prior separation.

The effects of diverse ions on the cobalt–BMPH system were determined. Diverse metal ions can interfere in two ways: by the formation of colored complexes with overlapping absorption bands, or by consuming reagent before it can react with the cobalt present, thereby preventing complete formation of the cobalt complex. The first mode of interference is eliminated by the addition of acid which dissociates the labile metal complexes, but not the inert cobalt complex. Thus, transition metal ions, although forming highly colored complexes with the reagent, do not offer a serious source of interference. The second type of interference can be prevented, for the most part, by increasing the amount of ligand present in the solution.

The method for cobalt was found to be relatively interference free. Common anions do not interfere. However, citrate and tartrate ions cannot be tolerated in concentrations greater than 20 ppm. The alkali and alkaline earth metal ions likewise do not offer interference to the formation and measurement of the cobalt complex. The group III metals (with the exception of aluminum), Cd^{2+}, Hg^{2+}, and Pb^{2+} in 200-ppm concentration do not interfere. Chrominum, molybdenum, tungsten, and uranium in the same concentrations offer interferences by precipitation or complexation.

Results of Determinations on Selected Samples. The results of the determination of cobalt in selected samples are presented in Table I. These results demonstrate that cobalt in the presence of transition metal ions can be determined with good accuracy. Each measured value represents the average obtained on 5 separate aliquots of sample. For the samples analyzed, the direct determination of cobalt without the benefit of a separation proved to be as accurate as the method involving a separation. The BMPH method, in which the high stability of the cobalt complex precludes the necessity of a separation step, thus offers a distinct advantage over existing methods. In addition, the high molar absorptivity of the complex permits the accurate determination of trace concentrations of cobalt to 0.3 μg/ml.

RECEIVED for review June 29, 1970. Accepted November 5, 1970. The authors are grateful for the Traineeship provided E. S. Tucker by the National Aeronautics and Space Administration.

(6) B. Chiswell, F. Lions, and M. L. Tomlinson, *Inorg. Chem.*, **3**, 492 (1964).

Analysis of Polyethylene Terephthalate Prepolymer by Trimethylsilylation and Gas Chromatography

E. R. Atkinson, Jr., and S. I. Calouche

Analytical and Chemical Section, Firestone Synthetic Fibers Company, Box 450, Hopewell, Va. 23860

THE PRODUCTION of polyethylene terephthalate (PET) from terephthalic acid (TA) and ethylene glycol (EG) involves basically a two-step process. The first step consists of reacting TA with EG (esterification) in the presence of a catalyst to form a prepolymeric mixture which then undergoes polycondensation to the desired product (step two).

The esterification product prepared in the first step contains bis-(2-hydroxyethyl)terephthalate (BHET), ethylene glycol (EG), diethylene glycol (DEG) (*1*), terephthalic acid (TA), mono-(2-hydroxyethyl)terephthalate (MHET), and higher molecular weight oligomeric polyesters.

An analytical technique was required for determining compounds such as the above when present together in a complex mixture. Gas liquid chromatography (GLC) best fills this need. Methods for the determination of carboxylic acids (*2–4*), ethylene and diethylene glycol (*5–12*), and polyhydric alcohols (*13*), have been reported. There is no report, however, demonstrating the use of this technique for the determination of either mono- or bis-(2-hydroxyethyl)terephthalate.

This paper proposes a qualitative and quantitative procedure for the determination of MHET and BHET as well as EG, DEG, and TA in polyester prepolymers by conversion to their TMS derivatives followed by GLC. The sample to be analyzed is dissolved in pyridine and treated with bis-(trimethylsilyl)trifluoroacetamide (BSTFA). The resulting solution is chromatographed and the TMS derivatives separated and determined using the technique of internal standardization.

EXPERIMENTAL

Chromatographic Equipment. All chromatograms were obtained using a Hewlett-Packard 5750 gas chromatograph equipped with a linear temperature programmer and dual flame ionization detectors.

Operating Conditions. The flame ionization detector and injection port temperatures were 280 and 270 °C, respectively. Helium was used as the carrier gas at a flow rate of 50 ml/min measured at room temperature at the column exit. The column temperature was held at 80 °C for 3 minutes after sample injection and then programmed to 265 °C at 15°/min. A coiled stainless steel column (6 ft, 0.125-in. o.d., 0.085-in. i.d.) packed with 3% OV-101 on 80–100 mesh Chromosorb W was used. The development of the chromatogram takes less than 20 minutes under these conditions.

A piece of aluminum foil was placed between the septum and injection port to reduce peak interferences from degradation of the silicone surface by the pyridine/BSTFA reaction mixture. As a precaution, unpacked glass inserts were used in all cases to minimize interaction of the sample with the injection port.

Chemicals and Reagents. Bis-(trimethylsilyl)trifluoroacetamide (BSTFA) was obtained from Regis Chemical Company. Spectro-quality pyridine from Mallinckrodt Chemical Company was used as the solvent. Ethylene glycol, diethylene glycol, terephthalic acid, and bibenzyl standards were all obtained in high purity from Fisher Chemical Company. Bis-(2-hydroxyethyl)terephthalate was prepared by the transesterification of dimethyl terephthalate with ethylene glycol (mp 110 °C). Mono-(2-hydroxyethyl)terephthalate was obtained by partial saponification of the BHET (mp 180 °C).

The column packing, 3% OV-101 on 80–100 mesh Chromosorb W, was obtained from Pierce Chemical Company.

Procedure. An internal standard solution of bibenzyl, 2.00 mg/ml, was prepared. Approximately 20 mg of sample, weighed to 0.1 mg accuracy, were placed in a small screw cap septum vial, and 0.50 ml of internal standard solution and approximately 0.50 ml of bis-(trimethylsilyl)trifluoroacetamide were added. The screw cap septum was then replaced and the sample heated in an oven at 80 °C for 10 minutes. Two microliters of the reaction mixture were then injected and a chromatogram was obtained, utilizing the previously stated conditions.

Quantitation. Peak areas were measured using a Hewlett-Packard Model 3370A electronic integrator. The relative weight responses for each compound to internal standard were determined from known solutions by measuring the slope of the curves obtained when the weight ratios for each compound were plotted *vs.* their respective area ratios. The per cent of the unknown compound present in a sample is then expressed by the following relationship:

$$\% \text{ Unknown} = \frac{F \times A_r \times W_{I_s}}{W_s} \times 100,$$

where F is the correction factor (1/relative weight response) for the compound of interest (see Table I), A_r is the area ratio of the unknown peak to that of the internal standard, and W_{I_s} and W_s are the weights of the internal standard and sample, respectively.

Results. Conditions necessary for quantitative conversion to the TMS derivatives were arrived at by noting the variations in the relative peak heights when the reaction conditions were selectively varied. A 1:1 mixture of pyridine and bis-(trimethylsilyl)trifluoroacetamide was used in all cases to ensure the presence of excess reagent. It was found that quantitative conversion was achieved for all of the compounds when the solutions were heated at 80 °C for 3 minutes. Without heating, approximately 75% conversion was achieved.

(1) S. G. Hovenkamp and J. P. Munting, *J. Polym. Sci., Part A-1*, **8**, 679 (1970).
(2) M. Schnitzer and J. G. Desjardins, *J. Gas Chromatogr.*, **2**, 270 (1964).
(3) J. F. Klebe, H. Finkbeiner, and D. M. White, *J. Amer. Chem. Soc.*, **88**, 3390 (1966).
(4) M. L. Kaufman, S. Friedman, and I. Wender, ANAL. CHEM., **39**, 1011 (1967).
(5) J. R. Lindsay Smith and D. J. Waddington, *J. Chromatogr.*, **36**, 145 (1968).
(6) D. F. Wisniewski and G. C. Stalker, *Petrol. Refiner*, **40**, 117 (1961).
(7) T, Nakagawa, H. Inoue, and K. Kuriyama, ANAL. CHEM., **33**, 1524 (1961).
(8) L. Ginsburg, *ibid.*, **31**, 1822 (1959).
(9) S. Spencer and H. G. Nadeau, *ibid.*, **33**, 1626 (1961).
(10) M. K. Withers, *J. Gas Chromatogr.*, **6**, 242 (1968).
(11) B. Smith and O. Carlasson, *Acta. Chem. Scand.*, **17**, 455 (1963).
(12) G. G. Esposito, ANAL. CHEM., **40**, 1902 (1968).
(13) G. G. Esposito and M. H. Swann, *ibid.*, **41**, 1118 (1969).

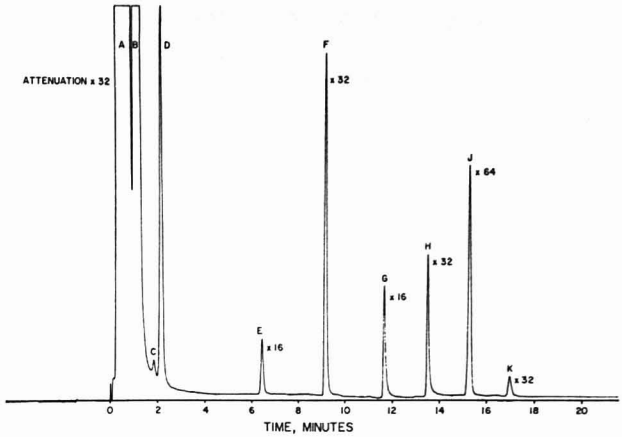

Figure 1. Typical chromatogram of PET prepolymer sample

A. **Pyridine and mono-(trimethylsilyl)trifluoroacetamide**
B. **Bis-(trimethylsilyl)trifluoroacetamide**
C. **Reagent impurity**
D. **Ethylene glycol (TMSD)[a]**
E. **Diethylene glycol (TMSD)**
F. **Bibenzyl (internal standard)**
G. **Terephthalic acid (TMSD)**
H. **Mono-(2-hydroxyethyl)terephthalate (TMSD)**
J. **Bis-(2-hydroxyethyl)terephthalate (TMSD)**
K. **Unknown**

[a] **Trimethylsilyl derivative.**

Table I. Retention Times of TMS Derivatives Relative to That of Bibenzyl

Compound	Relative[a] retention time	Correction factors
Ethylene glycol (TMSD)	0.28	0.65
Diethylene glycol (TMSD)	0.73	0.91
Bibenzyl	1.00	
Terephthalic acid (TMSD)	1.25	1.00
Mono-(2-hydroxyethyl)terephthalate (TMSD)	1.45	1.55
Bis-(2-hydroxyethyl)terephthalate (TMSD)	1.63	1.44

[a] Values relative to bibenzyl. RT = 9.4 min.

Table II. Precision for Analysis of Polyester Prepolymer

	N	$\bar{X}$, %	σ	σ rel., %
Ethylene glycol	10	4.9	±0.2	4.1
Diethylene glycol	10	0.2	0.01	5.1
Terephthalic acid	10	1.0	0.08	8.2
Mono-(2-hydroxyethyl)terephthalate	10	3.9	0.3	7.7
Bis-(2-hydroxyethyl)terephthalate	10	14.6	0.5	3.4

The quantitative aspects of the above reactions were also studied by obtaining the infrared spectra of each compound in pyridine before and after the addition of the TMS reagent. In each case, the –OH stretching bands observed for the pyridine solutions disappeared after the TMS reagent was added and the samples were heated for 3 minutes. In order to ensure quantitative conversion, a ten-minute heating time was selected for use in the procedure.

A series of solutions containing from 0.50 mg/ml to 2.00 mg/ml of ethylene glycol, diethylene glycol, terephthalic acid, and both mono- and bis-(2-hydroxyethyl)terephthalate in pyridine were prepared and known amounts of internal standard were added to each. The solutions were treated with the TMS reagent as discussed above, chromatographed, and calibration curves constructed for each compound. A typical chromatogram is shown in Figure 1. The peaks were identified from the retention data obtained with the known solutions above.

Table II shows the overall precision of the method for the analysis of a prepolymer sample. For each compound, the accuracy was established using known samples and was found to be within the precision of the method.

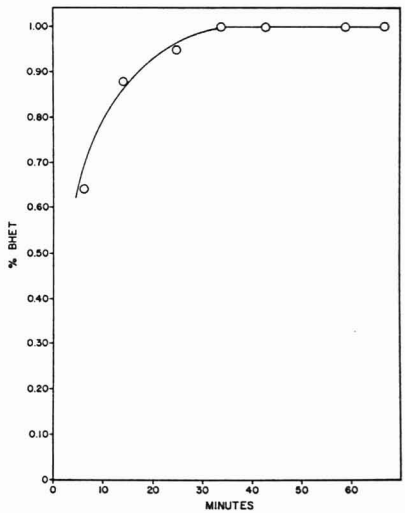

Figure 2. Per cent BHET *vs.* heating time for highly polymerized prepolymer sample

DISCUSSION

Both *N,O*-bis-(trimethylsilyl)acetamide (BSA) and BSTFA were initially used as silylating agents. Quantitative conversion to the TMS derivatives was observed for each. However, chromatographic interferences from reagent and reagent impurities with the determination of ethylene glycol were encountered when using BSA. Consequently BSTFA was selected for use in the procedure.

The correction factors used in the quantitations were checked periodically for a month, during which time they re-

mained essentially constant. To ensure accuracy, however, response factors were checked weekly and, where necessary, the sample weights for unknown samples were adjusted so that the area ratios for each compound were within those used for calibration.

As was mentioned previously, the samples analyzed contained high molecular weight oligomeric polyester compounds and, consequently, exhibited various degrees of solubility in the reaction mixture. The samples normally dissolve completely upon heating. When cooled, the reaction mixture becomes cloudy, apparently because of the precipitation of the high molecular weight compounds. This does not, however, appear to affect the results.

In some instances the samples were highly polymerized and total solution was not possible. For such cases, longer heating times were required to extract the compounds of interest from the crystal lattice of the polymeric material. The time necessary for this varied with the particular sample and was established by plotting the per cent compound *vs.* heating time (see Figure 2). Results obtained from samples of this type may or may not be accurate because of the uncertainty of effectively removing all the compounds from the insoluble materials.

ACKNOWLEDGMENT

The authors thank B. D. Stabley and E. J. Corrigan for their helpful discussions, and C. H. Wilson and R. G. Cozart for their excellent technical assistance.

RECEIVED August 19, 1970. Accepted November 10, 1970.

Gas–Liquid Chromatography of Some Irritants at Various Concentrations

Samuel Sass, Timothy L. Fisher, Michael J. Jascot, and John Herban

Chemical Research Laboratory, Research Laboratories, Edgewood Arsenal, Edgewood Arsenal, Md. 21010

THIS REPORT DESCRIBES the application of gas–liquid chromatography (GLC) to the detection and quantitative analysis of irritant compounds, some of which have been used by military and law enforcement agencies. The compounds used as examples in this work were α-bromobenzylnitrile (brombenzylcyanide, CA), *o*-chlorobenzalmalononitrile (CS), and α-chloroacetophenone (CN). A previous report published by these laboratories employed thin-layer chromatography for the detection of these compounds (*1*). The GLC procedures discussed here further increase the possibilities for absolute identification of these as well as similar compounds while also allowing their quantitative analysis from the milligram through the nanogram range. Also included here are methods for the assay of individual irritant samples and for the detection of some characteristic impurities that could represent hydrolysis or other residues of these irritant compounds. The procedures are applicable to the estimation of irritants as concentrated and dilute solutions and when sampled directly as vapor or aerosol.

EXPERIMENTAL

Equipment and Materials. The studies described here were performed on F&M Scientific Corp. (now a division of Hewlett-Packard) Model No. 810 gas chromatograph equipped with thermal conductivity (TC), flame ionization (FI), or electron capture (EC) detector; and a 1-mV Minneapolis-Honeywell recorder with a disc integrator. Injections were performed using Hamilton syringes. The column coatings and supports were obtained from Applied Science Laboratories, State College, Pa. All solvents used were of CP grade except for the spectro-quality hexane used in determinations employing the electron capture detector. The 1,10-dibromodecane (used as the internal standard) was obtained through Eastman Organic Chemicals, Rochester, N. Y.

Irritant Standards. CA was purified by fractional freezing followed by several recrystallizations from ethyl alcohol and washing with cold petroleum ether. The resultant CA produced near theoretical results by elemental analysis and showed no detectable impurity by thin-layer chromatography (*1*) and only the product peak by GLC. The purity was better than 99.5% and the melting point, 25 °C. CS, originally of 96.5 purity (mp 93–95 °C), was recrystallized from cyclohexane as a white solid melting at 96 °C, with a single GLC peak and no detectable impurity by TLC (*1*), and with a determined purity of 99.5%. CN, as recrystallized material, was of better than 98% purity based on melting point (54.5 °C), elemental analysis, ketone determination, GLC peak, and TLC detection.

PROCEDURES

SEMIMICRO TO MACRODETERMINATION (MILLIGRAM QUANTITIES). Relative-thermal conductivity-response factor (RTCF) determinations were made for each irritant *vs.* the internal standard (1,10-dibromodecane). Separate benzene solutions containing 50 mg/ml of the individual irritants were prepared along with a 50 mg/ml solution of 1,10-dibromodecane. Under identical conditions, each solution was injected in 5-μl increments from 5- to 50-μl volumes. The respective slopes of the irritant concentration *vs.* response curves were normalized with respect to that of the 1,10-dibromodecane. Similar solutions containing each irritant in combination with the internal standard were prepared and analyzed. The resultant normalized slopes were identical to those obtained with the separate solutions. Assigning the value of 1.000 to 1,10-dibromodecane resulted in RTCF values of 1.030 for CA, 1.176 for CN, and 1.111 for CS.

To determine purity, a weighed sample of irritant (CA, CN, or CS) and a similar weight of internal standard (1,10-dibromodecane) were placed in a 10-ml volumetric flask and made up to volume with benzene to yield an agent concentration of about 50 mg/ml. Aliquots of sample were injected directly onto a 5.5-ft × $^1/_4$-in. o.d. borosilicate glass column packed with 10% QF-1 on 60/80 mesh Gas-Chrom Q. A helium carrier gas-flow of 90 ml/min was used with temperature-programming from 65–200 °C at 6 °C/min.

MICRODETERMINATION (MICROGRAMS). To detect irritants (CA, CN, and CS) in microgram quantities, the chromato-

(1) W. D. Ludemann, M. H. Stutz, and S. Sass, ANAL. CHEM., 41, 679 (1969).

graph was fitted with its dual hydrogen-flame ionization detector and employed the identical column and conditions as described previously for the macrodetermination. The hydrogen and air-flow rates were 50 ml and 250 ml/min, respectively.

A weighed sample of irritant of known purity (as determined *via* internal standard using TC detection) was dissolved in solvent (benzene, chloroform, or ether) and made up to volume prior to constructing a calibration curve. Using this curve, the irritant peak areas from the unknown samples were measured and extrapolated to the abscissa to determine the agent content.

TRACE DETERMINATION (NANOGRAMS). The gas chromatograph was fitted with a tritium-source electron capture detector. The identical QF-1 packed column (under isothermal temperatures and with a carrier gas mixture comprised of 90% argon and 10% methane) was used for the detection and estimation of nanogram quantities of the irritants. The carrier gas flow rate was maintained at 85 ml/min while the detector was purged with a flow of 10 ml/min of the identical gas mixture.

Samples and standards were prepared in spectro grade hexane with calibration performed in the range of 5 to 50 ng of irritant. The isothermal column temperature was 150 °C for CS and 130 °C for CA and CN.

RESULTS AND DISCUSSION

Semimicro to Macrodetermination. The elution data obtained for CA using the GLC system with thermal conductivity detection showed elution times of 15 min (153 °C) for CA, 12 min (137 °C) for benzylcyanide, and 20 min (185 °C) for 1,10-dibromodecane. A standard deviation of 1.0% was calculated on the basis of 16 separate samples involving more than 50 individual sample injections. The maximum range found for a given sample was ±2.2%. As no other absolute quantitative method was available for comparison purposes, these values reflected only the precision of the GLC system. However, confirmation of accuracy was obtained through the analysis of synthetic CA samples containing weighed amounts of added known impurities of CA including benzylcyanide, α-bromobenzylimidobromide, α,α′-dibromobenzylcyanide and a combination of all of these.

For determining CN purity, the system gave a standard deviation of 1.0% on the basis of repetitive analysis. Weighed mixtures of 1,10-dibromodecane, CN, and acetophenone were dissolved in benzene or chloroform and aliquots of these were analyzed by GLC. A range of 50 to 99.5% CN purity was simulated in this test. Under conditions of the prescribed procedure, CN eluted at 14.5 min at 149 °C while acetophenone eluted in 9 min at 119 °C.

The determination of CS purity using this method showed a standard deviation for accuracy and precision of 1%, based on both the inherent system and on comparison with a macrovolumetric method (*2*). For this study, a batch of CS (96.5%), recrystallized product (99.9% from cyclohexane), and mixtures with impurities were used. Since prepared mixtures of CS with *o*-chlorobenzaldehyde and malononitrile could, on solution, produce some additional CS, the effect of analysis on one or the other of these two intermediates was simulated. Tested mixtures represented CS in purities from 50 to 99.9%. With this procedure CS elutes in 22 min at 193 °C, malononitrile in 7 min at 101 °C, and *o*-chlorobenzaldehyde in 7.5 min at 110 °C.

(2) S. Sass *et al.*, CWLR 2396, "Analytical Methods for CS. Part II. Volumetric Determination of CS Purity" (1960), Edgewood Arsenal, Md. internal publication.

Table I. Accuracy of Assay Method for CA and CN Using Weighed Mixtures of Components

Sample No.	Component	Weight, %	Average irritant found, %	Difference, %
1	CA	87.8	87.2	−0.6
	Benzylcyanide	10.4		
	Others[a]	1.8		
2	CA	79.7	79.7	0.0
	α-Bromobenzylimidobromide[b]	19.0		
	Others[a]	1.3		
3	CA	87.8	86.6	−1.2
	α,α-Dibromobenzylcyanide	10.7		
	Others[a]	1.5		
4	CA	71.2	70.6	−0.6
	Benzylcyanide	8.0		
	α-Bromobenzylimidobromide[b]	11.3		
	α,α-Dibromobenzylcyanide	8.5		
	Others[a]	1.0		
5	CN	45.6	44.4	−0.7
	Acetophenone	54.4		
6	CN	59.4	60.5	+1.1
	Acetophenone	40.6		
7	CN	74.9	75.3	+0.4
	Acetophenone	25.1		
8	CN	86.2	87.1	+0.9
	Acetophenone	13.8		
9	CN	94.2	93.5	−0.7
	Acetophenone	5.8		
10	CN	99.5	99.1	−0.4

[a] "Others" refers to unidentified contaminants found in the samples of CA and components used.
[b] Bromobenzylimidobromide did not dissolve in significant quantity.

Chemical assay methods previously established for the quality control of CA and CN had entailed, essentially, elemental analysis and physical methods such as melting point determination. The application of GLC to the assay of these irritants and also to CS increased the specificity of analysis while allowing the identification and estimation of elutable impurities. Data obtained on prepared synthetic mixtures of the separate irritants with characteristic impurities are summarized in Tables I and II.

Microdetermination. The results obtained *via* flame ionization detection proved this system was most useful for analyzing irritants in solution concentrations in excess of 50 μg/ml. The minimum quantity of irritant detectable was 2 μg while the overall accuracy was ±2.0% at the 10- to 200-μg level for all the irritants. The elution data were identical to those reported with the semimicro to macrodetermination.

Trace Determination. Results obtained *via* the electron capture detector indicated that solutions containing CA in quantities as low as 0.2 μg/ml could be analyzed. A measure of the precision of this system was calculated on the basis of replicate 12.5-μl injections at the 7 μg/ml concentration level. The standard deviation thus derived was 2.0%. As with most methods, the accuracy of the method declined as the lower limit of detection was approached. For example, replicate CA vapor concentration determinations in the 30–35 mg/m³ range showed a deviation of approximately 1.4 mg/m³; while in the 5–10 mg/m³ range, the deviation was of the order of 1 mg/m³. The minimum amount of CA detectable using this method was about 4 ng (or 4×10^{-9} g). The retention time of CA was 6.5 min with a column temperature of 130 °C.

Table II. Accuracy of Assay Method for CS Using Known Mixtures of Components and Comparison with Macro-Volumetric Method

Sample	Component mixture	Component weight, %	CS found		Difference of GLC from Weighed Mixture, %[b]
			GLC, %	Macro-Volumetric Method, %[a]	
CS, recrystallized	CS	99.9	99.5	99.9	−0.4
CS, production lot	CS	96.5	95.9	96.5	−0.6
1	CS	54.9	85.3[c]	...	...
	Malononitrile	23.7			
	o-Chlorobenzaldehyde	21.4			
2	CS	88.5	89.4	89.4	+0.9
	Malononitrile	11.5			
3	CS	63.7	64.0	62.8	+0.3
	Malononitrile	36.3			
4	CS	76.0	76.8	75.5	+0.8
	o-Chlorobenzaldehyde	24.0			
5	CS	49.9	48.9	50.5	−1.0
	o-Chlorobenzaldehyde	50.1			

[a] The standard deviation of the macro-volumetic method (*2*) is 0.7%.
[b] For CS with no additive, the purity value is assumed that of the macro-volumetric method.
[c] The total calculated quantity of CS present, if other components reacted 100% to form additional CS, is 86.3%.

For CN, a standard deviation of 2% at the 90-ng level was derived, based on injections of 7 μl of a 12.5 μg/ml CN solution. Replicate CN vapor determinations in the 5 to 10-mg/m³ range resulted in a deviation of 0.5 mg/m³. The minimum amount of CN detectable using this method was about 0.2 ng (or 2×10^{-10} g) and the retention time was 6.0 min at a column temperature of 130 °C.

For CS, the system also indicated a standard deviation of 2% at the 80-ng level from injections of 8 μl of 10 μg/ml CS solution. Replicated CS vapor determinations in the 5 to 10-mg/m³ range resulted in a deviation of 0.4 mg/m³. The minimum amount detectable, using this method, was about 0.1 ng. The retention time for CS (column temperature = 150 °C) was 12 min.

Minimum vapor concentrations detectable for each of the agents, using this procedure, are: CA, 0.4 mg/m³; CN, 0.02 mg/m³; and CS, 0.01 mg/m³. These values were determined with 10-ml vapor samples. It was demonstrated that cloth, soil, water, or other media could be "sniffed" for these compounds *via* syringe or other gas sampling apparatus, providing the vapor concentration was above these detection thresholds. Most of the problem in vapor sampling appeared to be due to heterogeneity of sample resulting from irritant condensation on the walls of the gas-tight syringe. This could be precluded by using a heated syringe. Measurements of CA and CN vapor, using GLC, were actually used in determining the volatilities of these compounds at various temperatures (*3*). (In an associated study, it was found possible to analyze both solution and vapor samples of ethyl bromoacetate using the basic EC procedure given for the other irritants. As little as 0.1 ng of the compound could be detected as a small peak eluting at 4.8 min, using an isothermal column temperature of 60 °C.)

The systems for "macro" to trace analysis of CA, CN, and CS were designed to fit the most difficult of the three compounds, namely CA. The compound was known to pyrolize readily in the presence of metals to form stilbene types and a variety of other products. To preclude metal-catalyzed decomposition, all-glass systems were used wherever possible. Diluted solutions of the compound showed less of this effect. Samples injected *via* syringe (containing a metal needle) were retained in the syringe for only a minimum of time. With electron-capture, reducing the detector temperature from 220 to 160 °C increased the maximum sensitivity time from a week to greater than two months. When sluggishness was noted, periodic flushing of the column and/or detector with methanol restored the sharpness of peaks and also detector sensitivity. CN and CS showed far less thermolability in the presence of metals.

A number of column coatings were tested for satisfactory elution of CA. These included SE-30 (methylsilicone gum rubber), DC-200 silicone oil, and QF-1 (trifluoropropyl–methyl silicone fluid). None of these coatings eluted dibromobenzylcyanide or the bromobenzylimidobromide present in CA samples. Benzylcyanide, however, was eluted in all cases just prior to the CA peak. QF-1 was selected as the coating giving the cleanest separation and peaks.

Direct calibration with CA was discarded as CA of near 100% purity would be difficult to keep on hand for long periods of time.

The internal standard procedure of calibration required high purity CA only during the initial relative-thermal conductivity-response factor (RTCF) determinations. 1,10-Dibromodecane was chosen as the internal standard for several reasons: it eluted close to CA but in an area free of peaks characteristic of CA impurities; it was a stable compound available in high purity or readily purified; and it also was a halogenated compound and did not react with constituents of the CA samples.

Unlike CA, CN and CS were compatible with metal columns, injection port vaporization, and with Apiezon-N and DC-LSX-3-0295 (trifluoropropyl-vinyl-methyl silicone gum polymer) coatings. However, since a more universally applicable procedure was desired, the method developed for CA, including the internal standard, was applied to the other irritants.

(3) J. J. Martin, S. Sass, *et al.*, EATR 4086, "Soil Stability of CA and CN. Analytical Methods for Trace Quantities of the Agents" (1967), Edgewood Arsenal, Md., internal publication.

Received for review August 26, 1970. Accepted November 10, 1970.

Suppression of Interferences by Sodium Sulfate in Trace Chromium Analyses by Atomic Absorption Spectrometry

J. A. Hurlbut and C. D. Chriswell

Department of Chemistry, Metropolitan State College, Denver, Colo. 80204

CHROMIUM ANALYSES are frequently performed by atomic absorption spectrometry, and a large number of elements are known to interfere with these analyses. The principal reported interferences are Ni, Ag, Co, Fe, Mn, Al, W, and Ti (*1–4*). In some cases these interferences can be overcome by duplicating the sample matrix in calibration samples (*4*), by using the method of standard additions (*4*), by using an oxidizing, air–acetylene flame (*4, 5*), by using a nitrous oxide–acetylene flame (*4, 5*), or by using an interference suppressor such as NH_4Cl (*4, 6, 7*), $SrCl_2$ (*3*), $LaCl_3$ (*8*), $K_2S_2O_8$ (*2*), or $K_2S_2O_7$ (*9*). The use of these chemical suppression agents appears to be the most common method of overcoming interferences; however, these suppression agents do not work on all interferences, and reports of their usage are limited and scattered throughout the literature. The presence of 1 to 2% NH_4Cl is known to reduce the depressant effect of Fe on the absorption of Cr at 3579 Å (*6, 7*), and more recently, both $K_2S_2O_7$ (*9*) and 1% $K_2S_2O_8$ (*2*) were found to suppress the interferences caused by Al, Fe, and Ti. The addition of $LaCl_3$ (*8*) was found to overcome interfering phosphate and Al, and $SrCl_2$ (*3, 6*) has been used to mask the interferences caused by low concentrations of various substances.

Work in this laboratory has led to the use of a new wide range interference suppressor and absorption enhancer for Cr analyses. This new suppressing agent is Na_2SO_4, and the purpose of this study is to report and to demonstrate the effectiveness of Na_2SO_4 in trace Cr analyses. The effectiveness of 1% Na_2SO_4 against relatively large amounts of many interfering substances will be compared to that of other suppressing agents.

EXPERIMENTAL

Apparatus and Instrumental Parameters. A Perkin-Elmer Model 303 atomic absorption spectrophotometer equipped with a Cr hollow cathode lamp and a single slot burner utilizing an air–acetylene flame was used to obtain the experimental data. The air–acetylene ratio was set at 7.5:10, and the fuel flow was then adjusted for maximum absorption using a standard containing only 10.0 ppm Cr for all runs except for those runs noted in the discussion. The air–fuel ratio was in terms of arbitrary flow units which were governed by the standard regulator supplied with the instrument. A wavelength of 3579 Å was used. No attempt was made to minimize interferences by instrument adjustment, and new calibration curves were prepared for every separate run in order to help minimize experimental deviations.

Table I. Recovery[a] of 10.0 ppm of Cr from Mixtures Containing Acids and Bases, Both in the Presence of and in the Absence of Either 1% NH_4Cl or 1% Na_2SO_4

Contaminant present	Cr recovered, ppm: With no masking agent added[b]	With 1% NH_4Cl added[c]	With 1% Na_2SO_4 added[d]
0.10*M* HNO_3	10.2	10.1	10.2
1.0*M* HNO_3	10.2	9.9	10.0
0.10*M* HCl	10.3	10.1	10.1
1.0*M* HCl	10.1	10.1	9.4
0.10*M* H_2SO_4	8.3	10.0	10.2
1.0*M* H_2SO_4	8.4	8.6	9.2
0.10*M* H_3PO_4	9.8	9.3	9.8
1.0*M* H_3PO_4	7.9	7.7	7.6
0.10*M* $HClO_4$	10.3	10.1	9.9
1.0*M* $HClO_4$	10.2	8.7	9.5
0.10*M* NH_4OH	9.6	10.1	10.0
1.0*M* NH_4OH	9.0	10.3	10.2
0.10*M* NaOH	10.4	9.8	10.1
1.0*M* NaOH	9.9	9.4	8.3

[a] Any deviation from 10.0 ppm of Cr by more than ±0.3 ppm was considered to be due to interferences, and all values are based on at least three determinations.

[b] Values obtained from a calibration curve made by utilizing standard solutions containing only $K_2Cr_2O_7$.

[c] Values obtained from a calibration curve made by utilizing standard solutions containing $K_2Cr_2O_7$ and 1% NH_4Cl.

[d] Values obtained from a calibration curve made by utilizing standard solutions containing $K_2Cr_2O_7$ and 1% Na_2SO_4.

Reagents. A stock solution containing 100 ppm of Cr was made from a standard stock solution containing 1.414 g of dry primary standard $K_2Cr_2O_7$ in 500 ml of water. Dilute standard solutions were freshly made before use and were used for preparing the calibration curves and for preparing the test solutions. These test solutions always contained either no suppressing agent or 1% (w/v) of a suppressing agent. The suppressing agents, Na_2SO_4, Na_2SO_3, K_2SO_4, $K_2S_2O_8$, and NH_4Cl, were reagent grade chemicals. The compounds used for preparing the stock, interference solutions are given in the footnotes to Table II, and stock solutions containing 10000 ppm of each interference were prepared.

RESULTS AND DISCUSSION

The presence of small amounts of Na_2SO_4 in a Cr sample was found to enhance the absorption at 3579 Å. For example, when an air–acetylene ratio of about 7.5:10 was used, the presence of 100 to 20000 ppm of Na_2SO_4 increased the absorption signal at least 10%. When an air–acetylene ratio of about 7.5:14 was used in the presence of Na_2SO_4, then the signal was enhanced at least 100%, but the noise level was also increased; so, this rich mixture was not used. Ammonium chloride, $K_2S_2O_8$, K_2SO_4, and Na_2SO_3 also enhanced the absorption. Because of this interference it was necessary to prepare several calibration curves as given in the footnotes to the tables. These absorption–concentration curves passed through the origin and were linear up to 13 ppm of Cr. Cali-

(1) M. A. Biancifiori, C. Bordonali, and G. Besazza, *Chim. Ind. (Milan)*, **50**, 423 (1968).
(2) B. B. Elrod and J. B. Ezell, *At. Absorption Newslett.*, **8**, 40 (1969).
(3) P. J. Belling, *Effluent Water Treat. J.*, **9**, 314 (1969).
(4) "Analytical Methods for Atomic Absorption Spectrophotometry," Perkin-Elmer Corp., Norwalk, Conn., 1968, pp 1–24, Cr 1–Cr 6.
(5) Walter Slavin, "Atomic Absorption Spectroscopy," Interscience Publishers, New York, N. Y., 1968, p 97.
(6) W. J. Price and P. A. Cooke, *Spectrovision*, **18**, 2 (1967).
(7) Lucien Barnes, Jr., ANAL. CHEM., **38**, 1083 (1966).
(8) A. M. Tenny, *Instrum. News*, **18**, 14 (1967).
(9) Y. Endo, T. Hata, and Y. Nakahara, *Bunseki Kagaku*, **18**, 833 (1969).

Table II. Recovery[a] of 10.0 ppm of Cr from Mixtures Containing 1000 ppm Contaminant Both in the Presence of and in the Absence of Either 1% NH_4Cl or 1% Na_2SO_4

Contaminant present at 1000 ppm[b]	Cr recovered, ppm: With no masking agent added[c]	With 1% NH_4Cl added[d]	With 1% Na_2SO_4 added[e]
Na	10.0	10.0	10.0
K	10.0	10.0	10.1
Mg	8.9	8.3	6.5
Ca	9.9	9.8	9.3[f]
Ba	7.9[f]	7.6[f]	10.0[f,g]
Ti	6.3[h]	7.1[h]	9.8[h]
Mo	8.9	10.0	10.0
W	10.6	10.0	10.1
Mn	7.2	10.0	9.9
Fe	2.8[i]	10.2[i]	10.1[i]
Co	3	9.1	10.0
Ni	3.7	9.0	9.7
Cu	8.9	10.1	10.0
Ag	5.9[f]	10.0[f]	9.9[f]
Zn	9.8	10.0	10.0
Cd	11.1	10.5	10.1
Hg	9.5[i]	9.4[i]	10.1[i]
Al	9.1[i]	9.1[i]	9.9[i]
Si	10.2	8.6[f]	10.2
Pb	10.1[f]	9.8[f]	9.8[f,k]
Bi	10.7[f]	10.0[f]	10.0[f]
Ce	10.8[i]	10.4[i]	10.0[i]

[a] Any deviation from 10.0 ppm Cr by more than ±0.3 ppm was considered to be due to interferences, and all values are based on at least three determinations.

[b] All added contaminants were present as the nitrate salts except for the following. Titanium tetrachloride was the source of Ti; $(NH_4)_6Mo_7O_{24}\cdot 4H_2O$ was the source for Mo; $Na_2WO_4\cdot 2H_2O$ was the source of W; and $Na_2SiO_3\cdot 5H_2O$ was the source for Si. Mercury, Mn, Fe, and Ce were in the +2, +2, +3, and +3 oxidation states, respectively.

[c] Values obtained from a calibration curve made by utilizing standard solutions containing only $K_2Cr_2O_7$.

[d] Values obtained from a calibration curve made by utilizing standard solutions containing $K_2Cr_2O_7$ and 1% NH_4Cl.

[e] Values obtained from a calibration curve made by utilizing standard solutions containing $K_2Cr_2O_7$ and 1% Na_2SO_4.

[f] The solution was 1.0*M* in HNO_3.

[g] Barium sulfate precipitated.

[h] The solution was 0.10*M* in HCl.

[i] The solution was 0.10*M* in HNO_3.

[j] The solution was 1.0*M* in NH_4OH.

[k] Lead sulfate precipitated.

bration curves made from Cr(III) appeared to be identical to those made from Cr(VI).

Since many Cr analyses are performed in the presence of acids or in some cases in the presence of bases, it was desirable to first determine the effects of acids and bases upon the Cr absorption. Table I summarizes this data. Of the seven compounds tested at a concentration of 1.0*M*, three of them, H_3PO_4, H_2SO_4, and NH_4OH, were found to interfere with the absorption by Cr. The presence of 1% Na_2SO_4 corrected this interference in the case of NH_4OH, but the solutions which contained 1% Na_2SO_4 and which were 1.0*M* in either HCl, $HClO_4$, H_3PO_4, H_2SO_4, or NaOH gave low absorption values. Solutions which contained 1% NH_4Cl and which were 1.0*M* in either $HClO_4$, H_3PO_4, H_2SO_4 or NaOH also suffered from interferences; however, solutions which contained either 1% NH_4Cl or 1% Na_2SO_4 and which were 0.10*M* in either HNO_3, HCl, H_2SO_4, $HClO_4$, NH_4OH or NaOH gave satisfactory absorption values.

Table II summarizes the effects of 1000 ppm of various contaminants upon the absorption by 10.0 ppm of Cr. Changes in the instrument settings, such as a change in the air–acetylene ratio, caused changes in the degree of interference in some cases. For example, Al was an absorption depressant when an air–acetylene ratio of about 7.5:10 was used, but it was an absorption enhancer when an air–acetylene ratio of about 7.5:14 was used. Also, slightly different results were sometimes obtained when the chloride form of the contaminant was used in place of the nitrate form; so, only the nitrate salts were used.

Table III. Recovery[a] of 10.0 ppm of Cr from Mixtures Containing 1000 ppm Each of Mo, Mn, Fe, Co, Ni, Cu, Al, and Cd Both in the Presence of and in the Absence of Masking Agents

Masking agent present[b]	Cr recovered, ppm[c,d]
None	6.3
1% Na_2SO_4	10.0
1% Na_2SO_3	9.3
1% K_2SO_4	8.2
1% $K_2S_2O_8$	7.7
1% NH_4Cl	7.1

[a] Any deviation from 10.0 ppm Cr by more than ±0.3 ppm was considered to be due to interferences, and all values are based on at least three determinations.

[b] The solutions were 0.10*M* in HNO_3.

[c] Values obtained from calibration curves made by utilizing standard solutions containing $K_2Cr_2O_7$ and 1% of the indicated masking agent.

[d] These solutions had to be analyzed shortly after preparation because of the slow formation of a precipitate.

Of the twenty-two contaminants added at a concentration of 1000 ppm each, sixteen of them, Mg, Ba, Ti, Mo, W, Mn, Fe, Co, Ni, Cu, Ag, Cd, Hg, Al, Bi, and Ce, interfered with the absorption by Cr. When the same contaminants were in the presence of 1% NH_4Cl, nine of them, Mg, Ba, Ti, Co, Ni, Cd, Hg, Al, and Ce, still interfered; and, in addition, Si now interfered. One per cent NH_4Cl effectively suppressed the interferences caused by 1000 ppm of Mo, W, Mn, Fe, Cu, Ag, and Bi. When the contaminants were in the presence of 1% Na_2SO_4, only Mg still interfered, and a 7% interference in the sample containing Ca appeared; however, this interference in the sample that contained 1000 ppm of Ca and 1% Na_2SO_4 disappeared when the Ca concentration was reduced to 500 ppm. One hundred ppm of Mg still caused at least a 20% depression in the absorption, both in the presence of and in the absence of the masking agents. One per cent Na_2SO_4 effectively suppressed the interferences caused by 1000 ppm each of Ba, Ti, Mo, W, Mn, Fe, Co, Ni, Cu, Ag, Cd, Hg, Al, Bi, and Ce.

Solutions which contained 10.0 ppm of Cr along with 1000 ppm each of eight species present in the same solution, which interfered with the Cr analyses, were analyzed both in the absence of and in the presence of various masking agents. Table III summarizes this data. This combination of contaminants produced a 37% depression in the absorption in the absence of a suppressing agent, a 29% depression in the presence of 1% NH_4Cl, a 23% depression in the presence of 1% $K_2S_2O_8$, and no depression in the presence of 1% Na_2SO_4. These results demonstrate that the addition of 1% Na_2SO_4 to samples to be analyzed for Cr will eliminate the effects caused by large amounts of known contaminants.

Ammonium chloride and $K_2S_2O_8$ are probably two of the more effective suppressing agents for Cr analyses, but they are not as effective as Na_2SO_4. The data in Table III also shows that Na_2SO_3 and K_2SO_4 are interference suppressors, but they too are not as effective as Na_2SO_4.

RECEIVED for review September 22, 1970. Accepted November 23, 1970.

Separation of Perrhenate, Molybdate, and Selenite Ions on Silica Gel

Alan M. Phipps[1]
Raytheon Co. MPT Division, Waltham, Mass.

THE INCREASED USE of alloys containing molybdenum and rhenium in the electronics and other industries over the past few years has magnified the need for a simple and rapid identification of rhenium in a variety of materials. Molybdenum interferes with virtually all methods for the qualitative or quantitative estimation of rhenium and a prior separation is therefore essential.

Several liquid–liquid extraction and anion exchange chromatographic procedures have been described [*e.g.*, (*1–6*)]. In general, these techniques are rather time-consuming, in some cases extremely so. The application of paper chromatography has not been particularly promising as a rapid technique. According to data reported by Ossicini (*7*), the separation of MoO_4^{2-} from ReO_4^- is possible in nitric acid using an anion exchange resin impregnated paper. Chang and Yang (*8*) reported a separation using paper impregnated with tributylphosphate. Separation on untreated paper after a nine-hour development with saturated aqueous sodium chloride was described by Duca *et al.* (*9*). The latter authors indicate that the solvent system butanol–HBr gives a poor separation although the data of Lederer and Bagliand (*10*) indicates that a separation is possible on Whatman No. 3MM paper using butanol–hydrochloric or perchloric acid mixtures.

We have found *vide infra* that a wide separation between rhenium and molybdenum is rapidly obtained on silica gel coated polyester sheets with methanolic solvents. Because a useful separation is not observed with this solvent on silica gel-coated glass plates, we have undertaken an investigation of the influence of solvent composition on the R_f values of the anions: ReO_4^-, SeO_3^{2-}, and MoO_4^{2-} on silica gel.

EXPERIMENTAL

Rhenium solutions were prepared from the spectrographically standardized metal obtained from Johnson Matthey Co. The other reagents used were analytical grade. Solutions of the oxyanions were prepared by dissolving the metals in a minimum amount of concentrated nitric acid and diluting to a volume giving a concentration of 1 mg/ml for rhenium and molybdenum and 2 mg/ml for selenium.

ACS Reagent grade solvents and acids were used. The influence of acid concentration on R_f was studied primarily with methanol solutions containing 10 grams of water per 100 ml. The acid concentration was varied by appropriate combination of water and concentrated acid, and in the case of hydrochloric acid, with anhydrous hydrogen chloride gas. Other solvent systems were employed as noted under results and discussion.

Ascending thin-layer chromatograms with 10.0 ± 0.5 cm solvent travel were obtained on "Chromagram" silica gel sheets (Eastman No. 6061; polyvinyl alcohol binder, no indicator), Whatman No. 1 chromatographic paper, and glass plates coated according to standard procedures with 250 mμ layers of silica gel G, silica gel H, and silica gel H containing 5% polyvinyl alcohol. These materials were allowed to equilibrate in air at approximately 70% relative humidity before being placed in 12-cm i.d. cylindrical tanks previously equilibrated with the developing solvent. In the interests of relative uniformity, the three ions were developed at the same time on a single sheet at each acid concentration used. After development, the spots, containing 0.001–0.002 mg of the metal, were identified by spraying with a 1:1 mixture (prepared fresh daily) of 10% aqueous KSCN and 10% $SnCl_2$ in 1*M* HCl. A red-orange spot is obtained for SeO_3^{2-}, red for MoO_4^{2-} and yellow for ReO_4^-. The SeO_3^{2-} is reduced to metalic selenium, the reactions of MoO_4^{2-} and ReO_4^- form the basis of standard colorimetric methods for these compounds (see Ref. *11*).

The partition column was prepared from water-washed 100–200 mesh desiccant silica gel (Davison No. 923) and rinsed exhaustively with the eluting solvent. Fractions of the eluent 1.0–4.0 ml, were diluted with methanol and the rhenium and molybdenum concentrations determined colorimetrically with a Beckman model B spectrophotometer using the methods described by Sandell (*11*).

RESULTS AND DISCUSSION

R_f values obtained for the perrhenate, molybdate, and selenite ions as a function of acid concentration in a solution of approximately constant methanol–water ratio are shown in Figures 1 and 2, respectively. A well-defined spot for selenium could not be obtained in the absence of acid. The R_f values of MoO_4^{2-} and ReO_4^- continue to decrease beyond the 4*M* HCl limit of Figure 1. Values in the vicinity of 0.3 were observed for all three anions at 5*M* HCl but the spots were of poor quality.

Maxima of the type exhibited by ReO_4^- and MoO_4^{2-} have been reported for ascending paper chromatography of several cations using a methanol–aqueous HCl developer (*12*, *13*).

The reason for the large difference in the R_f values of MoO_4^{2-} and ReO_4^- at low acid concentration is not immediately apparent. The cation exchange characteristics of silica gel would not be expected to influence the separation of these anions. R_f values in the range 0.7–0.8 for MoO_4^{2-} and ReO_4^- have been reported on cation exchange impregnated paper with aqueous HNO_3 (*7*). A partition mechanism is

[1] Present address to which correspondence should be sent, The Gillette Co., Toiletries Division, So. Boston, Mass. 02106

(1) S. Tribalat, *Anal. Chim. Acta.* **3**, 113 (1949).
(2) Y. A. Bakovskig, A. F. Iyevinsh, and E. A. Luksha, *Zh. Anal. Khim.*, **14**, 714 (1959).
(3) R. J. Meyer and C. L. Rulfs, ANAL. CHEM., **27**, 1387 (1955).
(4) H. Hamaguchi, K. Kawabuchi, and R. Kuroda *ibid.*, **36**, 1654 (1964).
(5) V. W. Meloche and A. F. Preuss, *ibid.*, **26**, 1911 (1954).
(6) J. Korkisch and F. Feik *Anal. Chim. Acta*, **37**, 364 (1967).
(7) L. Ossicini, *J. Chromatogr.*, **17**, 625 (1965).
(8) C. Chang and H. Yang, *Chem. Abstr.*, **63**, 7634d (1965).
(9) A. Duca, D. Stanescu, and M. Puscasu, *Rev. Roum. Chim.*, **11**, 839 (1966).
(10) M. Lederer and G. Bagliand, *Ric. Sci.*, **36**, 51 (1966).
(11) E. B. Sandell "Colorimetric Determination of Traces of Metals," 2nd ed., Interscience, New York, N. Y., 1950.
(12) T. Oncescu and D. Zugravescu *Rev. Roum. Chim.*, **9**, 131 (1964).
(13) T. Nascutiu, *ibid.*, p 273.

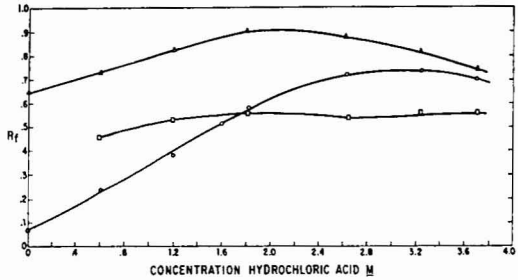

Figure 1. Dependence of R_f on concentration of HCl in methanol–water

△ ReO_4^-; □ SeO_3^{2-}; ○ MoO_4^{2-}

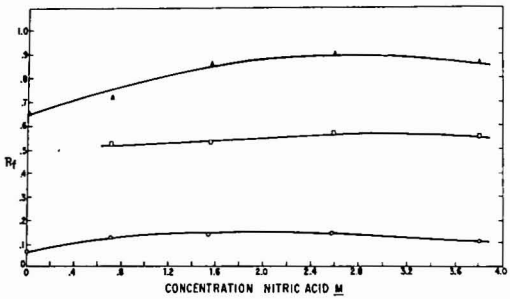

Figure 2. Dependence of R_f on concentration of HNO_3 in methanol–water

△ ReO_4^-; □ SeO_3^{2-}; ○ MoO_4^{2-}

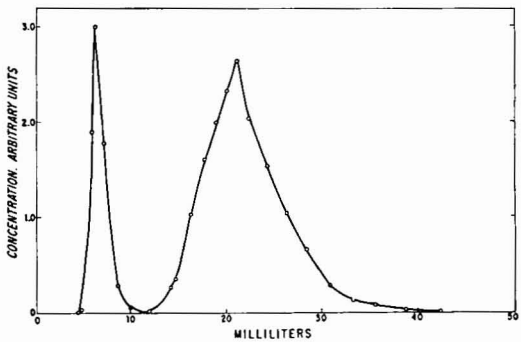

Figure 3. Elution of anions from a 100–200 mesh silica gel column with 1-butanol 0.6*M* in HCl and saturated with H_2O

5–10 ml ReO_4^-; 15–35 ml MoO_4^{2-}

suggested by the fact that very elongated spots showing little or no separation were observed for the entirely aqueous HCl and HNO_3 systems and for the anhydrous methanol–HCl system on oven dried sheets. In addition, development with a solution of 1-butanol 0.6*M* in HCl and saturated with water gives essentially the same separation as indicated in Figure 1. Use of the higher alcohols substantially increases the development time. A 10-cm solvent travel on the Chromagram sheet for an alcoholic solution 0.6*M* in HCl and containing 10 grams H_2O per 100 ml required 55 minutes with methanol, 135 min with ethanol, and 185 min with 1-butanol.

This wide separation of R_f values was observed only on the Chromagram sheets. Using the technique described above, glass plates coated with silica gel G, silica gel H, or silica gel H with 5% polyvinyl alcohol and Whatman No. 1 chromatographic paper gave R_f values for ReO_4^- and SeO_3^{2-} which were approximately the same as those shown in Figures 1 and 2. The R_f value for MoO_4^{2-} however, was only 0.1 unit or less lower than the R_f value for ReO_4^- in all cases. The binder and support contained in the "Chromagram" sheets are generally assumed to have no effect on the adsorbant. We have found that approximately the same R_f values are observed on these sheets as on coated glass plates for a variety of inorganic anions following handbook procedures, including the halides, chromate, arsenite, and several oxyanions of sulfur.

Use of Chromagram silica gel sheets developed with methanol 0.6*M* in HCl containing 10 grams of H_2O per 100 ml has been found useful for the rapid identification of rhenium in alloys containing molybdenum and/or tungsten. A development of 20–25 min on 4-inch strips is adequate. The

tungsten remains at the point of origin at all acid concentrations and is identified as a blue spot with the same $SnCl_2$–KSCN reagent.

We have applied this method to the routine identification of rhenium in molybdenum–rhenium alloys containing 20–50% Re, and tungsten–rhenium alloys containing 3% Re. Prepared mixtures indicate that all four elements discussed here are readily identifiable in one solution containing as little as 1% Re. An amount of sample sufficient to provide 0.001–0.002 mg per spot of each element is a convenient working range but a factor of ten less material is detectable.

In expanding the rhenium–molybdenum separation to milligram amounts, it was impossible to obtain a good separation with methanol–HCl or HNO_3 eluent on a reasonably short column. Using 1-butanol, 0.6*M* in HCl and saturated with water as eluent, a separation of 10 mg of rhenium from 10 mg of molybdenum was obtained on a 15 × 1 cm column at a flow rate of 0.4 ml cm^{-2} min^{-1} (Figure 3).

RECEIVED for review May 14, 1970. Accepted November 3, 1970.

Fluorometric Determination of Submicrogram Quantities of Zirconium

T. D. Filer

Health Services Laboratory, U.S. Atomic Energy Commission, Idaho Falls, Idaho

FLUOROMETRIC METHODS for the determination of zirconium have been developed using flavonol (*1*), morin (*2*), quercetin (*3*), datiscin (*4*), and calcein blue (*5*) as reagents. All methods show good sensitivity for the detection of submicrogram quantities of zirconium. All methods also consider interferences due to fluorescent complexes formed by the reagent and foreign ions. However, the flavonol procedure requires a time-consuming electrolysis in a Melaven cell to remove trace quantities of iron and other heavy metals which are serious negative interferences. Morin forms fluorescent complexes with aluminum, gallium, thorium, uranium, tin, and antimony in addition to zirconium. Therefore, zirconium must be determined by difference in the presence of these interferences by repeating the measurement after the addition of a masking agent for zirconium which does not affect the others.

The quercetin method requires an extraction with 2-thenoyltrifluoroacetone to avoid milligram quantities of common interferences such as iron, vanadium, and titanium. Microgram quantities of iron, molybdenum, titanium, and thorium are serious interferences in the datiscin procedure. The calcein blue method is more sensitive than any other zirconium procedure but suffers from a lack of selectivity and common elements such as silver, aluminum, bismuth, cadmium, copper, iron, molybdenum, manganese, nickel, lead, thorium, and arsenic interfere seriously. None of these procedures employs a pyrosulfate fusion as a method of sample decomposition and, therefore, cannot ensure that the highly refractory compounds of zirconium are converted to ionic forms suitable for complexation with the flavone.

The present method using 3,4′,7-trihydroxyflavone as the fluorometric reagent is no more sensitive to zirconium than the other compounds, but the fluorescence is measured in a sulfuric acid solution which permits use of pyrosulfate fusion as the method of sample dissolution. However, the greatest advantage of the present procedure is that many of the common elements associated with zirconium alloys and ores do not interfere in milligram quantities, thus making the direct determination of zirconium possible.

EXPERIMENTAL

Apparatus. The instrumentation used was a Beckman DU spectrophotometer with a fluorescence accessory modified as described (*6*). A combination of Corning Filters with color specification Nos. 0-51 and 7-51 having over 1% transmittance between 360 and 435 nm with a maximum of 40% was used for the primary. A combination of Corning Filters with color specification Nos. 3-2 and 5-56 having over 1% transmittance between 440 and 590 nm with a maximum transmittance of 59% was used for the secondary. A tungsten source was used in the present work, but a medium pressure mercury lamp can be used with the same filter combinations with similar results.

Reagents. STANDARD ZIRCONIUM SOLUTIONS, 1 mg/ml and 5 μg/ml. Fuse 1.3508 grams of high purity zirconium dioxide with 5 grams of anhydrous sodium sulfate and 3 ml of concentrated sulfuric acid in a 250-ml Erlenmeyer flask. Cool the melt, add 10 ml of concentrated sulfuric acid, 100 ml of water, and dissolve the melt with cooling. Dilute to 1 liter. Dilute 5.00 ml of the stock solution and 10 ml of concentrated sulfuric acid to 1 liter. The solutions contain 1 mg/ml and 5 μg/ml of zirconium, respectively.

SODIUM SULFATE IN SULFURIC ACID, 10%. Dissolve 10 grams of anhydrous sodium sulfate in 100 ml of concentrated sulfuric acid with heating as required. Cool and store in a glass-stoppered borosilicate glass bottle.

SULFURIC ACID SOLUTION, 0.5*M*. Dissolve 5.0 grams of sulfamic acid and 14.0 ml of concentrated sulfuric acid in enough water to make 500 ml of solution. Cool and store in a glass-stoppered borosilicate glass bottle.

3,4′,7-TRIHYDROXYFLAVONE SOLUTION, 6.75×10^{-2}%. The preparation of the flavone has been described (*7–9*).

(1) W. C. Alford, L. Shapiro, and C. E. White, ANAL. CHEM., 23, 1149 (1951).
(2) R. A. Geiger and E. B. Sandell, *Anal. Chim. Acta.*, 16, 346 (1957).
(3) D. M. Hercules, *Talanta*, 8, 485 (1961).
(4) A. P. Golovina, I. P. Alimarin, E. A. Bozhevol'nov, and L. B. Agasyan, *Zh. Anal. Khim.*, 17, 591 (1962).
(5) R. V. Hems, G. F. Kirkbright, and T. S. West, ANAL. CHEM., 42, 784 (1970).
(6) C. W. Sill and C. P. Willis, ANAL. CHEM., 31, 598 (1959).
(7) D. G. Roux and G. C. deBruyn, *Biochem. J.*, 87, 439 (1963).
(8) Katsuzo Yamaguchi, *Nippon Kagaka Zasshi*, 1963 148.
(9) Z. I. Jerzmanowska and M. Michalska, *Rocz. Chem.*, 35, 353 (1961).

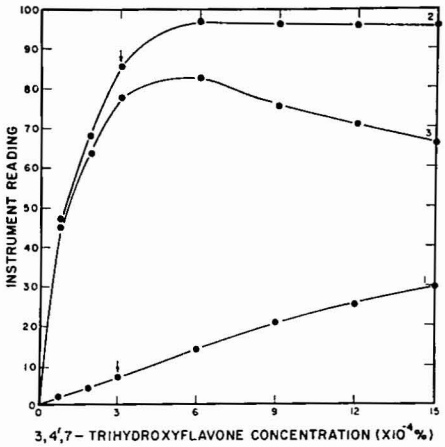

Figure 1. Effect of 3,4',7-trihydroxyflavone concentration

1. Blank
2. 5-μg Zr standard
3. 5-μg Zr standard corrected for blank

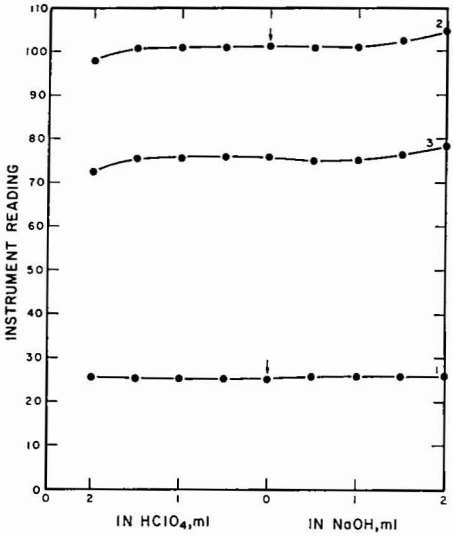

Figure 2. Effect of acidity

1. Blank
2. 5-μg Zr standard
3. 5-μg Zr standard corrected for blank

Transfer 6.75 mg to a 100-ml volumetric flask and dilute to volume with 95% ethanol.

Procedure. The procedure given below for preparation and measurement of the fluorescence is that used in the development of the procedure using pure zirconium solutions. It is also to be followed when zirconium has been separated and can be obtained in concentrated sulfuric acid free of interfering elements. However, many applications of this procedure can be made without separations, provided the sample size is chosen so that the heavy metal content does not exceed the permissible levels described below.

Place the zirconium standard or other zirconium solution into a 100-ml beaker. Add 2 drops of 72% perchloric acid, 1 ml of 10% sodium sulfate in sulfuric acid, and evaporate the solution carefully to dryness on an asbestos-covered hot plate. Heat until all the sulfuric acid including that condensed on the beaker walls has been volatilized and fuming has ceased.

Cool the sodium acid sulfate residue, add 2 ml of water, and 3 drops of 25% hydroxylammonium sulfate. Cover the beaker with a watch glass and boil the solution until the volume has been reduced to about 0.5 ml. Remove the cover glass and rinse with a few drops of water. Add 15.00 ml of the sulfuric acid solution and transfer the solution quantitatively to a 25-ml volumetric flask. Add 1.00 ml of 3,4',7-trihydroxyflavone solution, mix, and dilute to volume. Mix thoroughly and place in a constant-temperature bath at 25 °C for 20 minutes. Measure the fluorescence using the technique described previously (*6*, *10*). Permanent glass standards (*6*) can be used to reproduce the same instrumental sensitivity from day to day.

Place 1 ml of water for a blank and 1 ml of the 5-μg/ml standard zirconium solution in separate 100-ml beakers, add 1 drop of 72% perchloric acid and 1 ml of the sulfuric acid-sodium sulfate solution. Evaporate carefully to dryness on an asbestos-covered hot plate until evolution of sulfuric acid fumes has ceased, and treat as described above. Substract the blank from the standard and express the sensitivity as microgram zirconium per net scale division. Correct the samples for an appropriate blank carried through the entire procedure including separations, if any, and calculate their zirconium content from the sensitivity value obtained from the standard.

Sample Preparation. Because of the refractory nature of the compounds of zirconium and associated elements and the inability to dissolve them completely even in boiling concentrated acids, pyrosulfate fusion is always employed to ensure their complete dissolution and conversion to a soluble ionic form. A procedure for the decomposition of refractory silicates which involves a potassium fluoride fusion and a transposition to a mixed alkali pyrosulfate fusion has been described (*11*). In cases where silicates are known to be absent, the potassium fluoride fusion can be omitted and the sample treated initially with the appropriate mineral acid followed by pyrosulfate fusion. The solution obtained can be diluted to any desired volume and an appropriate aliquot taken for analysis and treated as described previously.

Many samples can be analyzed directly following dissolution, but others will require separation of zirconium from other elements. This will be true when only trace amounts of zirconium are present in a large excess of some interfering element. Zirconium can be extracted quantitatively from beryllium, aluminum, lanthanum, thorium, cobalt, nickel, manganese, lead, zinc, bismuth, gallium, scandium, indium, thallium, and yttrium by chloroform in the presence of 0.005*M* cupferron at pH values less than zero (*12*). Hindman (*13*) has also shown that zirconium can be extracted from large amounts of iron(II) by using the same system in the presence of ascorbic acid and potassium thiocyanate.

(10) C. W. Sill, C. P. Willis, and J. K. Flygare, Jr., ANAL. CHEM., 33, 1671 (1961).

(11) C. W. Sill, ANAL. CHEM., 33, 1684 (1961).

(12) Jiri Stary, "The Solvent Extraction of Metal Chelates," The Macmillan Co., New York, N.Y., 1964, pp 115–21.

(13) F. D. Hindman, Health Services Laboratory, U. S. Atomic Energy Comm., Idaho Falls, Idaho, work in progress, 1970.

RESULTS AND DISCUSSION

Effect of 3,4′,7-Trihydroxyflavone Concentration. The results obtained when various concentrations of 3,4′,7-trihydroxyflavone were used are given in Figure 1. Curve 2 shows that the intensity of fluorescence of 5 μg of zirconium increases with increasing flavone concentration to a maximum at about 6×10^{-4}%. If the highest precision is desired, the higher concentration of flavone should be used because the maximum fluorescence signal is produced at this level and the instrument can be operated in the range that has maximum stability. Also, at the higher concentration of flavone, small changes in concentration will not produce significant variations in fluorescence readings. However, the concentration of flavone can be adequately controlled so that it will not be a significant factor in precision even on the steeper portion of curve 2. On the other hand, the intensity of the zirconium fluorescence per unit blank fluorescence is greater at lower concentrations of the flavone. If the instrumental sensitivity can be increased so that the relatively weak fluorescence obtained at lower flavone concentrations can be spread over the full range of the instrument without significant loss of precision of measurement through instrument instability, smaller quantities of zirconium can be detected. The minimum detectable quantity of zirconium and the proper concentration of flavone to be used are dependent on the value of the blank, and the stability and sensitivity of the instrument. The arrows show that the recommended flavone concentration occurs at 3×10^{-4}%. Lower concentrations result in smaller blanks, but the instrumental instability at these levels causes a significant decrease in precision.

Effect of Acidity. The effect of changes in acidity on the fluorescence of the zirconium-3,4′,7-trihydroxyflavone complex was studied. The excellent efficiency and high buffering capacity of the system is shown in Figure 2. The arrows mark the points on the buffer curves that result under the recommended conditions.

Spectral Characteristics. Figure 3 shows the excitation and emission spectra for the reagent and its zirconium complex in 1*M* perchloric acid. The fluorescence of 3,4′,7-trihydroxyflavone exhibits its excitation maximum at 377 nm and a fluorescence emission maximum at 485 nm. The zirconium complex shows its excitation maximum at 417 nm and fluorescence emission maximum at 475 nm. All values are uncorrected for emission characteristics of the light source or the response of the detector.

Detection Limit and Precision. The detection limit and determination limit of this procedure were determined as defined by Currie (*14*). To determine these values and the precision obtained with larger quantities of zirconium, 10 blanks and ten 5-μg zirconium standards were analyzed under the recommended conditions, including the evaporation of zirconium solutions to dryness in the presence of sulfuric acid and the transfer from beaker to volumetric flask. The mean for the 5-μg zirconium standards was 95.8 scale division with a standard deviation of ± 0.5 scale division. The mean for the blanks was 25.1 scale divisions with a standard deviation of ± 0.2 scale division. The results indicate a detection limit of 0.05 μg of zirconium. The minimum quantity of zirconium that can be determined with a precision of 10% is 0.14 μg.

Linearity. The effect of zirconium concentration on the fluorescence was investigated at a 3,4′,7-trihydroxyflavone concentration of 2.50×10^{-7} mole per 25 ml to determine the linearity under analytical conditions. Nonlinearity is not detectable up to 10 μg of zirconium since it is not greater than the precision of the procedure—*i.e.*, about 1%. As the quantity of zirconium is increased beyond 10 μg, deviation from linearity becomes very pronounced.

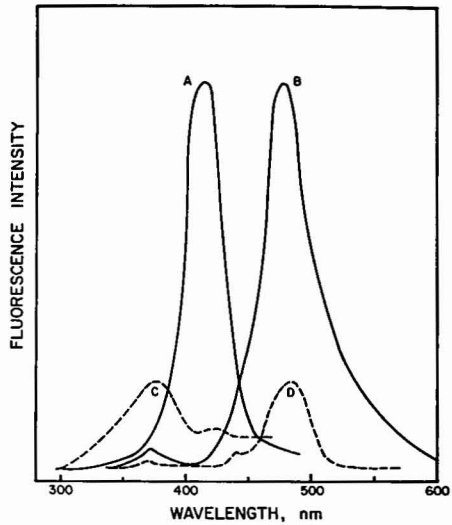

Figure 3. Excitation and emission spectra of reagent and zirconium complex in 1*M* perchloric acid

A. Zr + reagent. Excitation at 417 nm
B. Zr + reagent. Emission at 475 nm
C. Reagent alone. Excitation at 377 nm
D. Reagent alone. Emission at 485 nm

Effects of Other Substances. In anticipation of applying the present procedure to a wide variety of sample types without separations, a detailed investigation was made of the effect of many other substances on both blanks and 5-μg zirconium standards. The element or compound investigated was added before fuming with sulfuric and perchloric acids to determine its effect under the recommended conditions. No error could be detected on blanks and less than 1% on 5-μg zirconium standards in the presence of 5 mg of lithium, potassium, beryllium, cerium, magnesium, zinc, gadolinium, lutetium, and iron or 1 mg of mercury, arsenic, calcium, manganese, cadmium, platinum, rubidium, and cesium. Errors produced by other substances are shown in Table I.

HAFNIUM, ANTIMONY, AND TIN. Hafnium, antimony, and tin produce a fluorescence with the reagent of sensitivity such that not more than about 0.02 μg of any of these can be present without producing detectable error. Fluorescence due to hafnium in a sample will be reported as zirconium. Both antimony and tin can be removed easily as the bromides from sulfuric acid by volatilization with hydrogen bromide (*15*). This can best be accomplished by adding three 0.5-gram increments of solid sodium bromide to the fuming sulfuric acid solution and sweeping the bromides from the solution

(14) L. A. Currie, ANAL. CHEM., **40**, 586–93 (1968).

(15) J. E. Hoffman and G. E. F. Lundell, *J. Res. Nat. Bur. Stand.*, **22**, 22 (1939).

Table I. Effects of Other Substances

Element	Quantity, mg	Error, scale division[a] Blanks	5 μg Zr	Remarks
Hf	0.005	+40.0	>+10	Fluorescent; 0.125 μg/sc. div.
Sb	0.001	+8.6	+4.9	Fluorescent; 0.12 μg/sc. div.
Sn	0.001	+9.0	+10.2	Fluorescent; 0.11 μg/sc. div.
Al	1.0	+25.4	>+10	Fluorescent; 39 μg/sc. div.
Ga	0.01	+5.6	+3.3	Fluorescent; 1.8 μg/sc. div.
In	1.0	+2.2	+1.6	Fluorescent; 450 μg/sc. div.
Tl	1.0	+3.7	+2.0	Fluorescent; 270 μg/sc. div.
B	1.0	+1.8	+3.3	Fluorescent; 560 μg/sc. div.
Th	1.0	+1.9	0.0	Fluorescent; 530 μg/sc. div.
W	0.01	−2.2	−11.0	Yellow color when flavone is added
Mo	0.1	−1.1	−2.1	Yellow color when flavone is added
Nb	0.01	−12.1	−62.3	Yellow color when flavone is added
Ta	0.01	−0.3	−5.6	Yellow color when flavone is added
Bi	0.1	−4.1	−15.2	Yellow color when flavone is added
Ge	1.0	+8.9	−50.8	Yellow color when flavone is added
Co	1.0	0.0	−3.9	Faint pink color
Ni	1.0	−1.3	−0.5	Faint green color
Cu	1.0	−1.9	−2.0	Faint blue color
U	1.0	+3.9	−4.4	Faint yellow color
Cr	0.1	+3.0	−35.9	Very turbid because of anhydrous $Cr_2(SO_4)_3$
Si	1.0	+3.1	−2.1	Few flocs of dehydrated SiO_2 present
Ba	1.0	+2.1	−11.0	Turbid
Sr	1.0	+3.0	−3.7	Slight turbidity
Au	1.0	+32.5	−6.0	Elemental gold precipitates
Ag	1.0	+6.2	+3.6	
Ti	0.1	+0.7	−2.6	
Sc	1.0	+4.8	−8.2	Yellow color when flavone is added
La	1.0	−1.9	−0.1	
Y	1.0	0.0	−4.3	
V(+5)	1.0	0.0	−6.2	Bright yellow in concentrated H_2SO_4
Se	1.0	+1.2	−2.2	
P	1.0	+0.5	−81.4	Added as NaH_2PO_4 before fuming
F	1.0	+2.2	−0.8	Added before fuming

[a] Blank, 25.1 sc. div.; 5 μg Zr standard, 95.8 sc. div.; sensitivity, 0.0708 μg/sc. div. Differences larger than ±0.4 sc. div. on blanks or ±1.0 sc. div. on standards probably indicate significant effect of added substance.

by careful addition of 5 ml of concentrated hydrochloric acid.

ALUMINUM AND GALLIUM. Aluminum and gallium produce a fluorescence with the reagent of sensitivity such that not more than 100 μg of aluminum or 0.5 μg of gallium can be present without producing detectable error. Both interferences can be eliminated by an extraction with chloroform in the presence of cupferron as described previously. However, gallium is not abundant enough to cause much concern, and aluminum can be accommodated without loss of reliability by proper choice of sample size. For example, if the total sample taken for analysis is limited to 1 mg, zirconium can be determined in concentrations greater than 5×10^{-3}% without detectable interference from as much as 10% aluminum. Because the average soil or air dust sample would not be expected to have more than 10% aluminum, direct determination of zirconium on such samples is possible.

OTHER FLUORESCENT COMPLEXES. Indium, thallium, boron, and thorium show some interference at the 1-mg level due to their fluorescence with the reagent. Part of the fluorescence observed might be due to traces of zirconium.

CHROMIUM, NIOBIUM, AND TANTALUM. Chromium, niobium, and tantalum are particularly serious interferences because of their strong absorption of both the emitted zirconium–3,4′,7-trihydroxyflavone fluorescence and the exciting radiation, and because of the insolubility of anhydrous chromic sulfate, niobic acid, and tantalic acid. The presence of chromium can be detected quite sensitively by evaporating the solution to fumes of sulfuric acid in the presence of perchloric acid. A bright yellow color will develop with less than 0.1 mg of chromium, but will disappear quite rapidly because of thermal decomposition of the dichromate in the fuming sulfuric acid. Niobium and tantalum can also be detected quite sensitively by the appearance of a yellow color when the flavone is added. Chromium can be removed easily from sulfuric–perchloric acids by volatilization with hydrogen chloride gas as chromyl chloride. Niobium and tantalum, unfortunately, are not readily separated from zirconium, and the presence of trace amounts will interfere seriously with this procedure.

OTHER COLORED COMPLEXES. Tungsten, molybdenum, bismuth, germanium, and scandium form yellow complexes with the reagent. Bismuth and scandium interferences can be eliminated by the cupferron extraction. Tungsten and molybdenum are incompletely extracted by chloroform in the presence of cupferron and, therefore, are still serious interferences.

TITANIUM. Titanium produces very little interference at the 0.1-mg level. If more titanium is present, however, turbidity will be encountered because of its extreme hydrolytic tendencies. However, if the sample size is limited to 1 mg, zirconium can be determined in concentrations greater than 5×10^{-3}% without detectable interference from as much as 10% titanium.

FLUORIDE AND PHOSPHATE. The presence of fluoride or phosphate in the final solution used for fluorometric determination produces serious negative interference, 1 mg of either being sufficient to complex the zirconium and eliminate the fluorescence completely. Fortunately, the fluoride will be eliminated from the original sample by the pyrosulfate fusion. Pyrosulfate fusion should be carried out in platinum ware rather than in glass when fluoride is present to prevent dissolution of zirconium from glassware.

IRON. In the absence of sulfamic acid and hydroxylammonium sulfate, iron produces serious negative interference, 1 mg of iron being sufficient to eliminate the fluorescence completely. This is due to the strong absorption of both the emitted zirconium–3,4′,7-trihydroxyflavone fluorescence and the exciting radiation by the ferric ion. However, the reduction to ferrous sulfamate virtually eliminates this interference and 5 mg of iron can be tolerated without separation.

ACKNOWLEDGMENT

The author acknowledges the assistance of his associates during many helpful discussions. Special thanks are due to E. G. Paul for preparation of the flavone used in the present investigation.

RECEIVED for review July 31, 1970. Accepted November 4, 1970.

Liquid–Liquid Extraction of Rhenium(VII) with Mesityl Oxide

V. M. Shinde and S. M. Khopkar

Department of Chemistry, Indian Institute of Technology, Bombay-76, India

SOLVENT EXTRACTION STUDIES of transition elements with mesityl oxide showed that rhenium(VII) can be quantitatively extracted with 75% mesityl oxide–methyl isobutyl ketone from 1*M* hydrochloric acid containing 1*M* potassium chloride. Rhenium from the organic phase is stripped with dilute ammonia and is subsequently determined photometrically at 430 mμ as its thiocyanate complex (*1*).

Various extracting agents were used for the solvent extraction of rhenium. Among alcohols, butyl alcohol (*2*), amylalcohol (*3*), isopentyl alcohols (*4*) were used for its extraction and separation from few ions, while in ketones, ethyl methyl ketone (*5*) or methyl isobutyl ketone (*6*) were used. Pyridine (*7*) or quinoline (*8, 9*) were used for its extraction from alkaline solutions. The ion association complexes of rhenium with tetraphenyl arsonium chloride (*10*) or with tributyl ammonium salt (*11*) were extracted in chloroform or dichloromethane. Tributyl phosphate (*12, 13*) was used for its extraction from mineral acids. However, most of these methods suffered from several disadvantages. Thus, backstripping of rhenium from the organic phase was cumbersome and needed special reagents (*13*); it was essential to use high concentration of the extractant to effect quantitative extraction at lower acidity (*12*); the extractions were quantitative only if larger volumes of extractants were used and multiple extraction was needed (*3, 4*); at other times it was necessary to preequilibrate the extractant with alkali hydroxide before metal extraction was carried out (*7, 9*); and, finally, it was possible to accomplish good separation if temperature was critically controlled (*3, 4*).

The solvent extraction of rhenium(VII) with mesityl oxide eliminates all such limitations. It is possible to quantitatively extract rhenium at low acidity with 75% mesityl oxide in only 30 seconds, while rhenium from the organic phase can be stripped just by shaking with dilute ammonia (0.3*N* NH_4OH). It is necessary neither to use large volumes of organic phase nor employ multiple extractions. Thus, rhenium is quantitatively removed with only 10 ml of mesityl oxide in a single extraction. It is not necessary to preequilibrate mesityl oxide before actual extraction. Mesityl oxide is less volatile as compared to other extractants like ether; and it can be reused after distillation. The extraction can be carried out without any critical control of temperature. The method suggested by us is thus very rapid, extremely simple, reproducible, and affords clean cut separation of micrograms of rhenium in the presence of several cations as well as anions.

EXPERIMENTAL

Apparatus and Reagents. Type 3 KH 57 filter photometer was used.

The stock solution of rhenium(VII) was prepared by dissolving 0.1550 gram of potassium perrhenate (Spec. pure of Johnson Matthey and Co., London) in 1 liter of water containing 5 ml of 6*N* sulfuric acid. The solution was standardized gravimetrically by the Nitron method (*14*). It contained 100 μg of Re(VII) per ml. The test solutions [25 μg of the Re(VII) per ml] were prepared by fourfold dilution.

Mesityl oxide (B.D.H., bp 128.7 °C) was used after double distillation.

General Procedure. An aliquot of solution containing 25 μg of rhenium(VII) was mixed with hydrochloric acid and potassium chloride to a volume of 10 ml so that the concentration of acid and salting-out agent was 1*M*. It was then introduced into a separatory funnel and shaken for 30 seconds with 10 ml of 75% mesityl oxide in methyl isobutyl ketone. The two layers were allowed to settle and separate. The aqueous layer was removed first and then rhenium was removed from the organic layer by back extraction with 10 ml of 0.3*N* ammonium hydroxide and then with 10 ml of water. Rhenium(VII) from the aqueous phase was determined colorimetrically as its thiocyanate complex at 432 mμ (*1*).

RESULTS AND DISCUSSION

Effect of Acidity and Mesityl Oxide Concentration. The concentration of hydrochloric acid was varied from 0.125–1.0*M* and that of mesityl oxide from 19–100% (1.62–8.70*M*)

(1) E. B. Sandell, "Colorimetric Determination of Traces of Metals," 3rd ed., Interscience, New York, N. Y., 1959, p 758.
(2) H. Skiba and M. Wojtwosicz, *Chem. Anal.* (*Warsaw*), **10**, 183 (1965).
(3) V. Yatirajam and R. Prosad, *Z. Anal. Chem.*, **220**, 343 (1966).
(4) *Ibid.*, p 340.
(5) T. M. Cotton and A. A. Woolf, ANAL. CHEM., **36**, 248 (1964).
(6) V. Yatirajam, *Z. Anal. Chem.*, **219**, 128 (1966).
(7) D. T. Meshri and B. C. Haldar, *J. Sci. Ind. Res.*, **20B**, 551 (1961).
(8) U. B. Talwar and B. C. Haldar, *Ind. J. Chem.*, **3**, 452 (1965).
(9) S. J. Rimshaw and G. F. Malling, ANAL. CHEM., **33**, 751 (1961).
(10) S. Tribalat, I. Pamm, and M. L. Jungfleisch, *Anal. Chim. Acta.*, **6**, 142 (1952).
(11) M. Ziegler and H. Schroeder, *Z. Anal. Chem.*, **212**, 395 (1965).
(12) V. I. Plotnikov, L. I. Zelenskaya, and L. P. Ustova, *Sb. Inst., Tsvet. Metall.*, **112** (1965).
(13) N. Iordanov and S. Mareva, *C. R. Acad. Bulg. Sci.*, **19**, 913 (1966).
(14) W. W. Scott, "Standard Methods of Chemical Analysis," Vol. I, D. Van Nostrand, New York, N. Y., 1939.

Table I. Distribution Ratio as Function of Acidity

Rhenium(VII), 25 μg; 1*M* KCl, as salting-out agent

Mesityl oxide concn	HCl, *M*	Extraction, %	Distribution ratio, *D*
19% (1.62*M*)	0.12	57.14	1.33
	0.25	64.28	1.79
	0.50	76.78	3.30
	1.00	82.14	4.59
25% (2.17*M*)	0.12	71.42	2.49
	0.25	75.00	3.00
	0.50	83.92	5.21
	1.00	87.50	7.00
50% (4.35*M*)	0.12	75.00	3.00
	0.25	78.57	3.66
	0.50	87.50	7.00
	1.00	89.28	8.32
75% (6.52*M*)	0.12	76.78	3.30
	0.25	82.14	4.59
	0.50	91.07	10.19
	1.00	100.00	∞
100% (8.70*M*)	0.12	85.71	5.98
	0.25	87.50	7.00
	0.50	92.85	12.98
	1.00	100.00	∞

by dilution with methyl isobutyl ketone. The results in Table I show that the quantitative extraction of rhenium(VII) is possible with 75% mesityl oxide from solutions containing 1*M* HCl and 1*M* KCl as the salting-out agent. Various other solvents such as benzene, toluene, xylene, *n*-butanol, isobutyl acetate, cyclohexane, and chloroform were also tried as diluents. However, the extraction was incomplete in all these cases. Methyl isobutyl ketone was, therefore, preferred as the diluent. Previous workers (*6*) also preferred methyl isobutyl ketone as the suitable diluent.

Effect of Salting-Out Agent. Varying concentrations of chlorides of potassium, lithium, and magnesium were used as the salting-out agents. The results in Table II show that it is possible to extract rhenium quantitatively from 1*M* hydrochloric acid solution in the presence of either 1*M* KCl, 1*M* $MgCl_2$ or 10*M* LiCl as the salting-out agents. However, for the routine work 1*M* KCl was preferred as the salting-out agent. In all these studies, 75% mesityl oxide was used as an extractant.

Diverse Ions. A number of representative ions were tested for interference. The tolerance limit was set at the amount required to cause ±2% error in rhenium recovery. Thalium (I), lead(II), bismuth(III), rhodium(III), manganese(II), cobalt(II), nickel(II), thorium(IV), zirconium(IV), cerium(IV), beryllium(II), calcium, strontium, barium, zinc, tungstate, selenite, tellurite, oxalate, tartrate, thiocyanate, and EDTA are tolerated in large ratios (>1:40). Ions such as cadmium, osmium(VI), titanium(IV), malonate, citrate, fluoride, and bromide are tolerated in ratios >1:8; while copper(II), platinum(IV), palladium(II), ruthenium(III), chromium(III), uranium(VI), vanadate, and acetate are tolerated in ratio of <1:4. Only ions such as mercury, antimony, tin, iridium, iron, thiosulfate show strong interferences. The interferences of some ions can be eliminated by using masking agents like oxalic acid, EDTA, or potassium thiocyanate (*15*). From ten runs with 25 μg of rhenium(VII), using the general procedure, the average recovery was 98.5 ± 1.5% with a standard deviation of 1.8%. Each determination took a total of 30 minutes.

Table II. Effect of Salting-Out Agent

Rhenium(VII) = 25 μg; mesityl oxide = 75% in MIBK

Salting-out agent, *M*	Initial HCl, *M*	Extraction, %	Distribution ratio, *D*
KCl, 0.5	0.12	78.57	3.66
	0.25	82.14	4.59
	0.50	89.29	8.32
	1.00	92.85	12.98
	2.0–3.0	100.00	∞
1.0	0.12	83.92	5.21
	0.25	85.71	5.98
	0.50	92.85	12.98
	1.0–3.0	100.00	∞
LiCl, 4	0.25	57.14	1.33
	0.50	58.92	1.43
	1.00	64.28	1.79
	2.00	75.00	3.00
	3.00	89.28	8.32
6	0.25	64.28	1.79
	0.50	71.42	2.49
	1.00	78.57	3.66
	2.00	89.28	8.32
	3.00	92.85	12.98
8	0.25	85.71	5.98
	0.50	85.71	5.98
	1.00	89.28	8.32
	2.0–3.0	100.00	∞
10	0.25	89.28	8.32
	0.50	92.85	12.98
	1.0–3.0	100.00	∞
$MgCl_2$, 0.5	0.25	57.14	1.33
	0.50	58.92	1.43
	1.00	62.50	1.66
	2.00	85.71	5.98
	3.00	91.07	10.19
1.0	0.25	82.14	4.59
	0.50	85.71	5.98
	1.0–3.0	100.00	∞

RECEIVED for review June 6, 1969. Accepted November 9, 1970. Work supported from the financial grant of Council of Scientific and Industrial Research (India).

(15) A. K. De, S. M. Khopkar, and R. A. Chalmers, "Solvent Extraction of Metals," Van Nostrand, Reinhold, London, 1970, p 217.

Emission Spectrochemical Determination of Tantalum in Curium Oxide

R. H. Gaddy

Savannah River Laboratory, E. I. du Pont de Nemours & Company, Aiken, S. C. 29801

AN EMISSION SPECTROCHEMICAL method was developed for the determination of tantalum impurity in ^{244}Cm oxide. ^{244}Cm is being produced (*1*) for evaluation as a radioisotopic power source and is a precursor in the production of ^{252}Cf, a spontaneous fission neutron source. Tantalum impurity may be introduced into the curium product from tantalum equipment used in some processing operations.

Metallic impurities must be separated from the actinide elements before emission spectrographic analysis, because the relatively complicated spectra of the actinide elements and the associated background obscures the emission lines of many impurities. The carrier distillation method (*2*) has been used extensively for determining impurities more volatile than the matrix actinide oxide. However, this method is not suitable for the determination of tantalum in actinide materials because of the refractory nature of Ta_2O_5.

The analytical chemistry of tantalum has been reviewed (*3–8*), but the spectrographic analysis of tantalum in curium or curium compounds has not been reported. The amine extraction of microgram quantities of tantalum from plutonium and its subsequent spectrographic determination was reported by Ko (*9*). Vita (*10*) and Burnett *et al.* (*11*) reported the spectrographic determination of tantalum in uranium after extracting the *N*-benzoylphenyl-hydroxylamine complex into chloroform. Barton (*12*) determined tantalum spectrographically after separation from plutonium by precipitating plutonium trifluoride. Werning *et al.* (*13*) and Waterbury and Bricker (*14*) extracted tantalum into methylisobutyl ketone from HCl–HF mixtures and H_2SO_4–HF mixtures, respectively. This paper describes the potassium carbonate leaching of tantalum from curium oxide, the methylisobutyl ketone extraction of the tantalum, and its spectrographic determination.

EXPERIMENTAL

Apparatus. A Bausch & Lomb dual grating spectrograph was used with a National Spectrographic Laboratories Model 6487 source unit. Sample excitations were conducted in a stainless steel glove box designed to contain radioactive materials. The optical bench in the glove box was aligned with the spectrograph located outside. The emitted light left the glove box through a fused quartz window. An Applied Research Laboratories densitometer was used for visual comparison of spectra of samples and standards.

Reagents. 4-Methyl-2-pentanone (referred to as MIBK) was obtained from Eastman Organic Chemicals and was used without further treatment. Tantalum pentachloride was obtained from Alfa Inorganics, Inc., Beverly, Mass. All other chemicals were Baker Analyzed Reagent grade.

Preparation of Standards. A stock solution containing 1000 μg of Ta/ml was prepared by dissolving tantalum pentachloride in 6*N* HCl–0.5*N* HF. A series of standard solutions was prepared by diluting the stock solution to give tantalum concentrations with ratios of 10:5:2, ranging from 0.5 to 1000 μg of Ta/ml. The solutions were prepared and stored in polyethylene bottles.

Procedure. Ten milligrams of curium oxide is weighed on a torsion balance and transferred to a small platinum boat. Of the 50 mg of potassium carbonate used for the fusion, about 30 mg is mixed with the curium oxide sample. The remaining 20 mg is poured on top of the mixture. The boat with the sample mixture is heated at 920 °C for 15 min in a furnace with a mullite tube liner. Although a clear melt is not produced (perhaps because the sample is not completely dissolved), the tantalum oxide is converted completely to a soluble form. After cooling, the melt is leached with 2.0 ml of 6*N* HCl–0.5*N* HF. The curium precipitates as the insoluble trifluoride. Tantalum is extracted from the solution with 2.0 ml of MIBK by shaking on a vortex mixer for 5 minutes. (The MIBK is pre-equilibrated with 6*N* HCl–0.5*N* HF containing 25 mg of K_2CO_3/ml.) The tantalum is then stripped from the 2 ml of MIBK by shaking with 1.0 ml of 4% H_2O_2 for 5 min.

Fifty microliters of the H_2O_2 solution containing the tantalum is evaporated onto the face of a flat-top graphite electrode previously treated with paraffin-ether solution to prevent absorption of the solution into the electrode. Four electrodes are prepared for each sample or standard to provide for duplicate exposures. The prepared electrodes are used for both anode and cathode during excitation. Two or more standards are extracted and exposed in duplicate on each photographic plate with the samples. Spectrum Analysis No. 3 plates are used in the wavelength region 2460–3460 Å. The 2675.90 or 2685.11 Å tantalum lines of the samples and standards are compared visually to determine the concentration.

The instrument parameters for the analysis are as follows: current, A, 13.5 RF; Potential, V, 250; Capacitance, μf, 0.0025; Inductance, mH, 0; Analytical gap, mm, 2; Exposure time, sec, 30; and Slit width, μ, 20.

(1) H. J. Groh, R. T. Huntoon, C. S. Schlea, J. A. Smith, and F. H. Springer, *Nucl. Appl.*, **1**, 327 (1965).
(2) B. F. Scribner and H. R. Mullin, Report A-2907, National Bureau of Standards, Washington, D. C., 1945.
(3) J. W. Mellor, "A Comprehensive Treatise on Inorganic and Theoretical Chemistry," Vol. IX, Longmans, Green and Co., London, 1947.
(4) R. E. Kirk and D. F. Othmer, "Encyclopedia of Chemical Technology," Vol. 13, Interscience, New York, 1954.
(5) F. T. Sisco and E. Epremian, "Columbiam and Tantalum," John Wiley & Sons, Inc., New York, 1963.
(6) W. T. Elwell and D. F. Wood, *Anal. Chim. Acta*. **26**, 1 (1962).
(7) R. W. Moshier, "Analytical Chemistry of Niobium and Tantalum," Macmillan Co., New York, 1964.
(8) F. Cuttilla, "Annotated Bibliography of the Analytical Chemistry of Niobium and Tantalum, January 1935–June 1953," Geological Survey Bulletin 1029-A, United States Govt. Printing Office, Washington, D. C., 1957.
(9) R. Ko, ANAL. CHEM., **36**, 1290 (1964).
(10) O. A. Vita, USAEC Report GAT-524, Goodyear Atomic Corp., Portsmouth, Ohio, 1966.
(11) H. M. Burnett, J. V. Pena, C. J. Martell, and R. T. Phelps, USAEC Report LA-3985, Los Alamos Scientific Laboratory, Los Alamos, N. M., 1968.
(12) H. N. Barton, *Appl. Spectrosc.*, **19** (5), 159 (1965).
(13) J. R. Werning, K. B. Higbie, J. T. Grace, B. F. Speece, and H. L. Gilbert, *Ind. Eng. Chem.*, **46**, 644 (1954).
(14) G. R. Waterbury and C. E. Bricker, ANAL. CHEM., **29**, 1474 (1957).

Table I. Effect of K_2CO_3 on Tantalum Analysis

Tantalum, μg/ml	% Transmission of Tantalum Lines: No K_2CO_3	25 mg K_2CO_3/ml
500	1.5[a]	4.2[a]
250	3.0[a]	8.0[a]
100	6.7[b]	6.0[b]
50	10.5[b]	11.0[b]
25	26.5[b]	27.0[b]
10	35.5[b]	36.0[b]
5	22.5[c]	23.0[c]
2.5	32.5[c]	33.5[c]

[a] 2661.3 Å line.
[b] 2680.6 Å line.
[c] 2685.1 Å line.

Table II. Analysis of 10 mg of Curium Oxide Samples Spiked with Tantalum

Tantalum, μg: Present	Found
5	5
10	10
25	25
105	100

DISCUSSION

Curium oxide is usually prepared by the calcination of curium oxalate or hydroxide at a temperature of about 700 °C for several hours. Thus, any tantalum impurity in the curium oxide should be present as the pentoxide. Tantalum pentoxide is not readily soluble in common mineral acids but is soluble in concentrated hydrofluoric acid after heating at elevated temperatures for an extended period of time. Tantalum hydrolyzes slowly in concentrated acid solutions unless a complexing agent such as the fluoride ion or oxalate ion is present.

In the present method, the curium oxide sample is fused with K_2CO_3 to convert the tantalum to a form that dissolves rapidly and completely in 6*N* HCl–0.5*N* HF solution. However, the conditions for analysis must be adjusted to avoid loss of tantalum by precipitation of K_2TaF_7. The solubility of K_2TaF_7 is reported to be 7.5 g/l. in water at 20 °C (*7*); its solubility in 1% (~0.5*N*) HF is given as 8 g per 1000 g of solvent (*5*). The solubility of tantalum in the present system has not been reported.

The limit imposed on the analysis by the solubility of K_2TaF_7 was determined in the tests summarized in Table I. Standard solutions of tantalum in 6*N* HCl–0.5*N* HF and of tantalum with K_2CO_3 added to simulate solution compositions that would result from the fusion step were analyzed. The tantalum was extracted with MIBK from the above solutions and analyzed spectrographically. The presence of K_2CO_3 had no effect to about 100 μg of Ta/ml. This concentration corresponds to 2 wt % tantalum in a 10-mg sample of curium oxide. At higher concentrations, tantalum slowly precipitated from solution. Thus, the method is not reliable for tantalum concentrations greater than 200 μg in 10 mg of curium oxide.

The limit of detection of tantalum is approximately 1 μg of tantalum in 10 mg of curium oxide. This detection limit can be improved by adjusting the volume of peroxide strip solution or increasing the volume of strip solution evaporated on each electrode. Interferences in the method were not tested.

The spectrochemical method was evaluated by analyses of curium oxide samples spiked with known amounts of tantalum. As shown by the data in Table II, 100% recovery of the tantalum is obtained. This satisfactory performance has been verified by continuing use of the procedure in support of the production of large quantities of curium oxide.

RECEIVED for review August 14, 1970. Accepted November 20, 1970. The information contained in this article was developed during the course of work under Contract AT(07-2)-1 with the U. S. Atomic Energy Commission.

Novel Technique for Surface Analysis of Solid Metallic Specimens Using Selected Anodic Current–Voltage Characteristics

George Todd and G. A. Wild
Royal Armament Research and Development Establishment, Fort Halstead, England

ALTHOUGH CURRENT–VOLTAGE characteristics at the cathode are used extensively in the electrochemical analysis of solutions by polarography, little attention has been paid to the development of a technique for the analysis of solid specimens using anodic corrosion characteristics. If this could be done successfully, it could provide a method yielding information about the surface of a specimen—often with negligible damage to the specimen itself.

EXPERIMENTAL

Specimens. The technique to be described was originally suggested by observations made with a potentiostat in the course of etching specimens of Fe-Al-Mn alloys. These had been prepared for phase-diagram work, and the potentiostat was employed in an attempt to selectively etch out minor phases. The alloys used had been homogenized after casting by cold-rolling down to an approximate diameter of $^5/_8$ inch, soaking at 1200 °C, and quenching. After sectioning, specimens were mounted in epoxy resin and polished to provide irregular disk-like faces. Electrical contact was made by a screwed-rod penetrating the resin. Chemical analyses for aluminum and manganese were available for the castings and gave an approximate composition for the homogenized rod and for the specimens.

Apparatus. Anodic current–voltage characteristics of the specimens were measured with a Wenking Potentiostat, Type 6184TR using a saturated calomel electrode to monitor voltage changes at the anode or working electrode. A bath temperature of 21 °C was used, and the bath was stirred. The working principle of the potentiostat and the experimental arrangement used are shown in Figure 1.

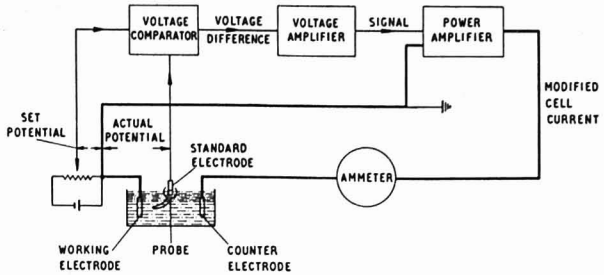

Figure 1. Working principle of the potentiostat

The actual potential between the working electrode and the standard electrode is compared with the set potential, and any difference referred as a signal to the power amplifier. The current through the cell is thereby modified so that the potential difference is nullified. The time constant is equal to 10 μsec

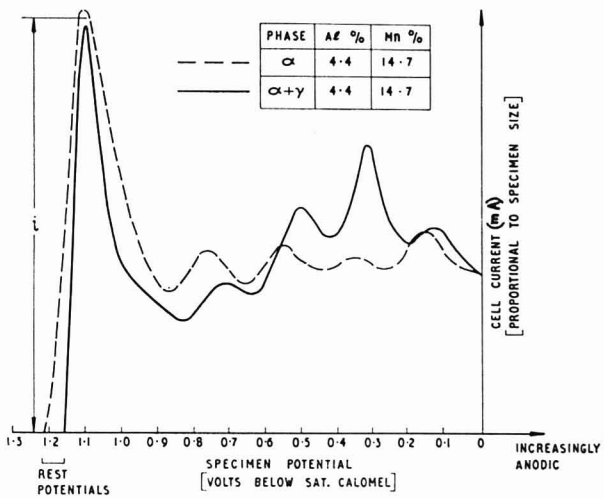

Figure 2. Initial range of the anodic current–voltage characteristic in 30% NaOH for two alloys of the same chemical composition but different phase constitution

Although other detail varies, the first current maximum (i) is essentially the same in each case in view of the fact that the specimens are not identical in area

Method and Results. Specimens were irregular disks of approximately $^5/_8$-inch diameter. No attempt was made to calculate the area in each case, and total anodic currents rather than current densities are quoted in any statement of results.

The potentiostat was originally set at the rest potential of the specimen in the chosen electrolyte so that no current flowed. The specimen was then progressively made more positive using a motor-driven control at a rate of 200 mV/min and changes in the corresponding corrosion current were measured.

This was done with a number of essentially single phased body-centred cubic (α) and face-centred cubic (γ) alloys, in a variety of electrolytes over an anodic range of about 1.2 V, but few corrosion differences were observed of sufficient magnitude to be useful in α/γ discrimination. Differences in the current–voltage characteristics with composition were much more striking, and certain corrosion maxima appeared to be independent of phase character.

Figure 2 shows the current–voltage scan carried out in 30% NaOH solution for two alloys of the same chemical composition but different phase constitution. Although the detail of the scans is apparently dependent upon phase composition, the initial current maximum (i) is approximately the same in both cases.

It was further discovered that if this phase-insensitive max-

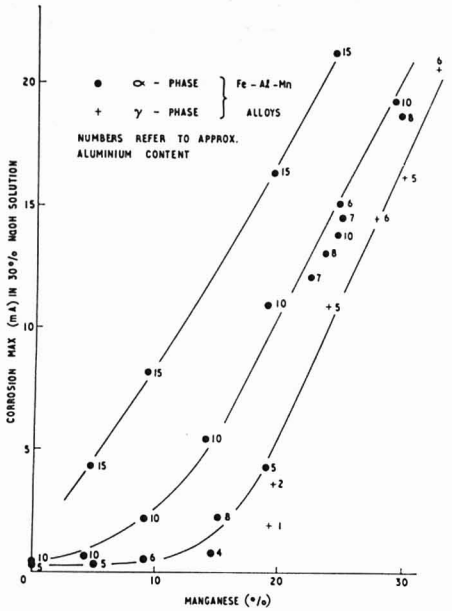

Figure 3. Plot of phase-insensitive corrosion maxima in 30% NaOH solution *vs.* manganese content for a number of alloys
Corresponding aluminum content for each specimen is recorded and the 5, 10, and 15% aluminum contours roughly drawn in

imum was selected and the current (i) plotted against the manganese content, a system of points lying on aluminum or iron contours was obtained. Such an array is illustrated in Figure 3. The potential at which peak current occurred varied slightly with composition but this factor was ignored. This array could be simplified and the points brought to a common locus by plotting current maximum against a linear function of the aluminum and manganese content. This was done initially by trial and error giving coefficients approximately to the first place of decimals, but a computer became available and a curve fitting program was eventually employed. The linear function was derived as equal to (0.863 Mn% + Al%) and a plot of the value of this function *vs.* current maxima together with the best curve is shown in Figure 4.

This plot enabled the value of a linear function of the Al and Mn content of an unknown alloy to be obtained from the corrosion current maximum but did not in itself enable an analysis of the alloy to be obtained. If, however, a second electrolyte could be found in which the electrochemical processes were different, a second such relationship would enable such an analysis to be carried out by the solution of the two equations obtained.

In the case of Fe-Al-Mn, such an electrolyte was found in 10% $(COOK)_2$ solution and the results are given in Figure 5. This shows the plot of the value of the function (Mn% − 4.536 Al%) *vs.* a phase-insensitive current maximum in this second electrolyte, the procedure being as before.

In principle it was now sufficient to solve the two equations:

$$0.863\ \mathrm{Mn} + \mathrm{Al} = a, \text{ corresponding with } i_1 \qquad (1)$$

$$\mathrm{Mn} - 4.536\ \mathrm{Al} = b, \text{ corresponding with } i_2 \qquad (2)$$

to obtain the composition of the surface of an unknown

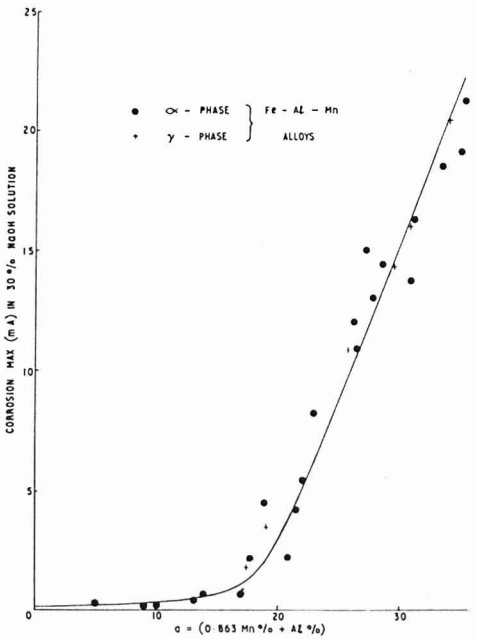

Figure 4. Plot of phase-insensitive corrosion maxima in 30% NaOH solution *vs.* a equal to a linear function of the manganese and aluminum content of the corresponding alloys

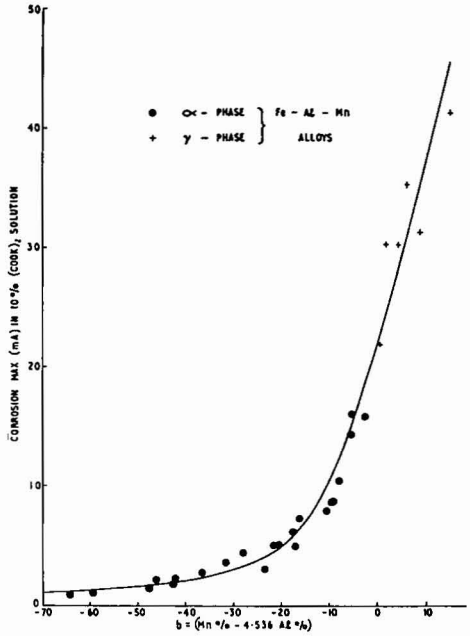

Figure 5. Plot of phase-insensitive corrosion maxima in 10% $(COOK)_2$ solution *vs.* *b* equal to a linear function of the manganese and aluminum content of the corresponding alloys

Table I. Comparison of Experimental and Derived Values of Composition and Corrosion Maxima for Iron–Aluminum–Manganese Alloys

Composition						Peak height			
Chemical		Calculated		Discrepancy		i_1(mA)		i_2(mA)	
Al%	Mn%	Al%	Mn%	ΔAl%	ΔMn%	Exptl	Calcd	Exptl	Calcd
0.8	19.4	1.5	19.9	0.7	0.5	1.7	1.1	41.0	45.3
2.3	19.6	3.1	20.5	0.8	0.9	3.4	2.0	31.0	35.0
5.1	0.0	6.4	−0.1	1.3	−0.1	0.2	0.2	2.8	3.8
4.8	5.0	4.8	1.9	−0.0	−3.1	0.2	0.3	4.7	5.8
5.5	9.0	5.1	9.0	−0.4	0.0	0.4	0.4	7.1	6.2
4.4	14.7	4.1	12.8	−0.3	−1.9	0.6	1.0	14.1	14.8
5.3	19.0	5.1	18.9	−0.2	−0.1	4.1	4.4	15.8	15.1
5.2	24.0	5.4	24.8	0.2	0.8	10.7	9.6	21.6	22.1
5.2	30.0	4.7	30.3	−0.5	0.3	15.9	16.2	35.0	30.8
6.0	24.8	6.9	26.8	0.9	2.0	14.9	11.5	15.6	18.3
5.7	27.8	5.0	28.4	−0.7	0.6	14.2	14.4	30.0	24.2
6.2	32.6	5.9	32.8	−0.3	0.2	20.3	20.5	30.0	27.9
7.0	22.5	7.8	23.2	0.8	0.7	11.9	10.2	8.4	10.7
7.5	23.7	8.1	23.7	0.6	−0.0	12.9	12.2	7.7	9.8
7.2	25.0	7.7	25.3	0.5	0.3	14.3	13.2	10.2	12.2
8.0	15.0	7.3	13.9	−0.7	−1.1	2.1	3.6	4.8	4.3
8.4	29.3	8.8	27.8	0.4	−1.5	18.4	19.6	8.5	11.1
10.1	0.0	7.9	−1.8	−2.2	−1.8	0.2	0.3	2.0	1.6
10.2	4.4	9.5	6.6	−0.7	2.2	0.6	0.5	2.1	1.8
10.0	9.1	9.4	11.5	−0.6	2.4	2.1	1.3	2.6	2.1
10.0	14.2	9.0	15.6	−1.0	1.4	5.3	5.0	3.4	2.6
10.3	19.0	9.2	20.4	−1.1	1.4	10.8	10.6	4.2	3.0
9.9	24.6	9.3	22.9	−0.6	−1.7	13.6	16.3	4.9	4.5
10.2	29.1	9.7	27.3	−0.5	−1.8	19.0	21.7	5.9	5.6
15.1	4.6	17.4	5.0	2.3	0.4	4.4	1.9	0.9	1.1
15.1	9.3	15.9	10.2	0.8	0.9	8.1	6.1	1.1	1.2
14.7	19.3	15.2	18.4	0.5	−0.9	16.2	16.6	1.4	1.5
14.7	24.3	14.7	23.4	−0.0	−0.9	21.1	22.2	1.7	1.7

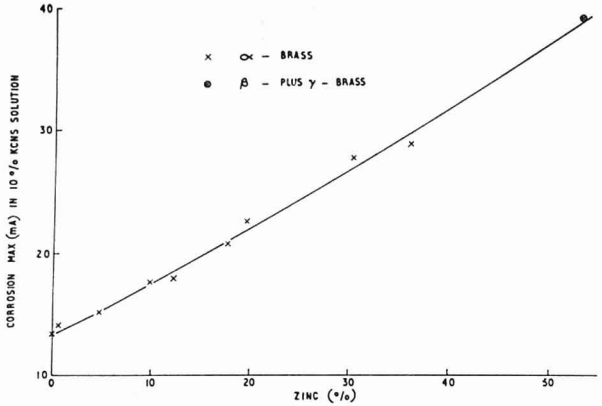

Figure 6. Plot of phase-insensitive corrosion maximum in 10% KCNS solution *vs.* zinc content for a number of brasses

For a binary alloy, this single plot is sufficient for analysis purposes

ternary alloy with current maxima i_1 and i_2 in NaOH solution and $(COOK)_2$ solution, respectively.

This was done for a series of Fe-Al-Mn alloys and the results are shown in Table I. The mean deviations of the calculated Mn and Al contents from the chemical values are 1.1% and 0.7%, respectively.

DISCUSSION

These results are encouraging when one considers the following:

1. Discrepancies may be partially real and indicative of differences between bulk analysis figures and those of the surface.
2. The chemical figures refer to the as-cast ingot and only approximate to the values for the homogenized bar.
3. Little attention was paid to controlling the temperature and concentration of the electrolyte.
4. Specimens were mounted in an epoxy resin and errors due to mounting material have been recognized (*1*).
5. Corrosion current is proportional to specimen area and the data were obtained from specimens of only approximately equal area. When a similar exercise was applied to accurately machined Cu/Zn specimens in 10% KCNS solution, a much more regular plot was obtained (Figure 6).

Errors discussed under 3, 4, and 5 can be reduced by the use of a cell now widely used for potentiostatic work. In this, the specimen area is reduced to a standard size by a screen of chemically inert material, and electrolyte, carefully regulated with respect to temperature and concentration, is recirculated from a reservoir.

If the accuracy of the technique can be improved in this way and results tested using, for example, X-ray fluorescence analysis, the method may provide a way of deriving useful information with respect to the surface composition of a variety of suitable metallic specimens.

(1) N. D. Greene, "Experimental Electrode Kinetics," Rensselaer Polytechnic Institute, Troy, N.Y. 12181, (1965).

RECEIVED for review July 24, 1970. Accepted November 23, 1970.

Boron–Polyethylene Irradiation Containers for High Energy Neutron Activation Analysis

W. A. Jester and K. N. Prasad

Department of Nuclear Engineering, The Pennsylvania State University, University Park, Pa. 16802

A NUCLEAR REACTOR is an excellent intense source of high energy neutrons, *i.e.*, uncollided fission neutrons. These neutrons can be used to induce (n,p), (n,α), (n,2n), and (n,n') reactions, especially in the lower weight elements. This capability is not usually employed in thermal reactor activation analysis because of interference from (n,γ) reactions. The traditional way of treating this problem is to surround the sample with cadmium, which is effectively black to thermal neutrons. However, this approach does not significantly remove resonance neutrons above the cadmium cut-off. Thus, elements such as manganese and cobalt can still become highly activated because of their high resonance cross sections. Also, if a pneumatic transfer system is employed for short half-life work, the sample carrier is usually a hydrocarbon material such as polyethylene which will moderate some of the high energy neutrons passing through the cadmium, adding to the (n,γ) interference. In this work, two types of boron–polyethylene irradiation containers were constructed and tested to evaluate their effects in reducing (n,γ) reactions. The boron-10 in the containers has a large 1/V neutron capture cross section which extends well into the resonance region and, therefore, is effective both in reducing the resonance flux reaching a sample and in absorbing any neutrons thermalized in the polyethylene. The boron also does not become significantly activated so that pneumatic sample carriers made of this composite material can be safely handled.

Fast Neutron Activation with Nuclear Reactors. The fissioning of the most common reactor fuel, uranium-235, results in a spectrum of neutrons with energies from below 0.1 MeV to about 20 MeV. The average energy of this fission spectrum is about 1.9 MeV and the most probable energy is about 0.65 MeV, with 66% of the neutrons having energies between 0.5 and 3 MeV. The number of neutrons falls off exponentially with energy above 3 MeV. The intensity of the fast flux component of most research reactors utilized for activation analysis is in the range of 10^{11} to 10^{14} neutrons/sec-cm^2. The intensity and energy of these neutrons are enough to induce usable (n,p), (n,α), (n,2n), and (n,n') reactions in many elements. Some of the more interesting threshold reactions are listed in Table I for isotopes that are analyzed more easily this way than with thermal neutron reactions.

The neutron flux spectrum contains two other components beside the fast neutron component (Figure 1) (*1*). These are the resonance or epithermal component which consists of neutrons that have been partially slowed down, and the thermal component which consists of neutrons that have slowed down completely and are in thermal equilibrium with the moderator.

The relative intensity of these three components varies with position in and around the reactor core, and with reactor types. It is primarily a function of the moderator. For the common light water research reactor, the thermal flux will be about a factor of three to five more intense than the fast flux. This difference in flux intensity combined with the fact that the (n,γ) thermal reactions have cross sections which are usually larger by two or more orders of magnitude, usually results in the masking of any threshold activation products. In addition, the threshold reaction often produces the same activation product as an (n,γ) reaction with a neighboring isotope. For example, phosphorus-32 is produced from both sulfur and phosphorus.

Table I. Threshold Reactions of Interest

Reaction	Half-life	Threshold, MeV	Cross-section, barns[a]
$^{14}N(n,2n)^{13}N$	10 min	10.6	...
$^{16}O(n,p)^{16}N$	7.1 sec	10.2	1.4×10^{-4}
$^{19}F(n,p)^{19}O$	29 sec	4.2	5×10^{-4}
$^{31}P(n,\alpha)^{28}Al$	2.3 min	2.0	1.4×10^{-3}
$^{32}S(n,p)^{32}P$	14 days	0.95	6.0×10^{-2}
$^{45}Sc(n,\alpha)^{42}K$	12 hr	0.61	5×10^{-3}
$^{56}Fe(n,p)^{56}Mn$	2.6 hr	2.9	8.7×10^{-4}
$^{203}Tl(n,p)^{203}Hg$	47 days	−0.30	2×10^{-6}
$^{204}Pb(n,n')^{204m}Pb$	68 min	2.2	...

[a] Approximate fission flux averaged cross sections.

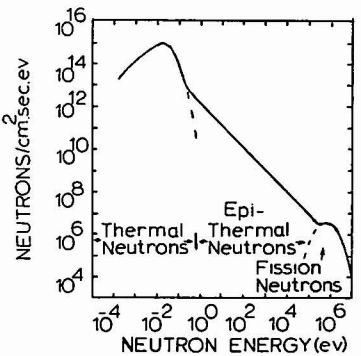

Figure 1. Reactor neutron energy distribution

Suppression of (n,γ) Reactions Using Neutron Shields. The common method of reducing the amount of (n,γ) reactions occurring in an irradiated sample is to surround the sample with a cadmium liner. The existence of a large resonance at 0.173 eV makes cadmium an effective neutron shield for thermal neutrons of energy below 0.5 eV (Figure 2). However, it is not effective in reducing the (n,γ) activation due to the epithermal neutrons. The (n,γ) cross sections of all the elements have 1/V tails which extend into the epithermal region. In addition, many of them have large resonances in this region. Examples of two such cross-sections are shown in Figure 2.

(1) F. F. Dyer, in "Guide to Activation Analysis," W. S. Lyon, Jr., Ed., D. Van Nostrand Company, Princeton, N. J., 1964, p 15.

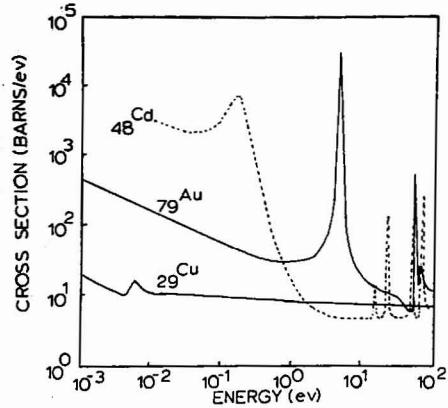

Figure 2. Neutron cross sections

Some researchers have used boron in combination with cadmium to obtain suppression in both the thermal and epithermal ranges (*2*). As shown in Figure 3, boron-10 in natural boron has a large 1/V cross section that extends from the thermal well into the resonance range (*3*).

Difficulties in Employing Neutron Shields. Cadmium metal in the form of thin sheets has found wide application as a thermal neutron shield. Most research reactors have cadmium-lined vertical tubes and pneumatic rabbit terminals for thermal neutron suppression. Boron unfortunately is not available in a form usable in a similar manner at such facilities.

Another problem that is encountered when conducting activation analysis involving short-lived radioisotopes is related to the hydrogenous containers used in pneumatic transfer systems. Inserting container materials such as polyethylene into a shielded irradiation terminal will cause thermalization of fast neutrons within the shielded region, considerably increasing the (n,γ) reactions.

Table II. Some Common (n,γ) Interference Reactions

Reaction	Half-life	Cross-section, barns*
$^{23}Na(n,\gamma)^{24}Na$	15 hr	5.3×10^{-1}
$^{27}Al(n,\gamma)^{28}Al$	2.3 min	2.3×10^{-1}
$^{31}P(n,\gamma)^{32}P$	14 days	1.9×10^{-1}
$^{37}Cl(n,\gamma)^{38}Cl$	37 min	4.3×10^{-1}
$^{40}Ar(n,\gamma)^{41}Ar$	1.8 hr	6.3×10^{-1}
$^{55}Mn(n,\gamma)^{56}Mn$	2.6 hr	1.3×10^{1}
$^{63}Cu(n,\gamma)^{64}Cu$	13 hr	4.5×10^{0}

* Approximate cross section at 0.025 eV.

The authors encountered these problems in two projects attempting to utilize threshold reactions for activation analysis using the Penn State TRIGA Reactor. One case involved the pulsed neutron activation analysis for oxygen (*4*) using the $^{16}O(n,p)^{16}N$ threshold reaction (Table I) to measure the oxygen content of minute amounts of rare earth oxides. In this case, the 6.13 and 7.12 MeV gamma rays of nitrogen-16 are well above those of almost all other activation products. The problem encountered was that even using the rabbit terminal with a 20-mil cadmium liner, enough (n,γ) activation products were produced to cause such an intense sample activity, that high analyzer dead time and considerable random summing of detector pulses up into the range of the nitrogen-16 peaks caused unacceptable errors in this analysis.

A second case involved the analysis for the protein in meat and leaves by determining the nitrogen content using the $^{14}N(n,2n)^{13}N$ threshold reaction (Table I). The 0.511 MeV annihilation photon was to be used for this analysis, but the amount of interference from the $^{55}Mn(n,\gamma)^{56}Mn$ reaction (Table II) made this technique unusable. ^{56}Mn has a high (n,γ) cross section in the thermal as well as resonance regions. Even using the cadmium lined rabbit terminal, a satisfactory analysis could not be obtained because of this interference.

Polyethylene–Boron Rabbits. In searching for a solution for the problems of resonance activation and thermalization of fast neutrons by the hydrogen in the rabbits, it was noted that polyethylene bricks containing boron were available on the market at a relatively low price. These bricks are sold as neutron shielding materials. It was decided to purchase

(2) D. C. Borg, R. E. Segel, P. Kienle, and L. Cambel, *Int. J. Appl. Radiat. Isotop.* **11**, 10 (1961).
(3) D. DeSoete, R. Gijbels, and J. Hoste, "Proceedings, International Conference, Modern Trends in Activation Analysis," Vol. II, National Bureau of Standards, Washington, D. C., 1968, pp 699–750.
(4) W. F. Naughton and W. A. Jester, *ibid.*, Vol. I, pp 490–494.

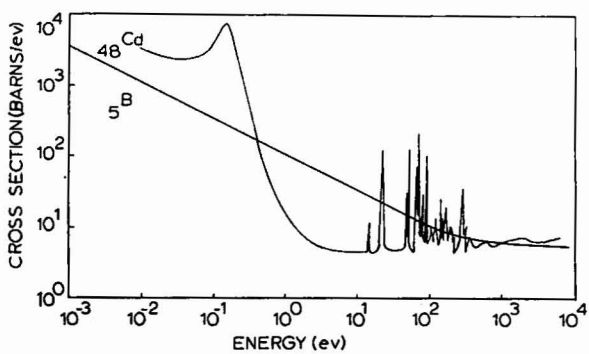

Figure 3. Neutron cross sections

Table III. Induced Activities (Relative) under Various Neutron Shielding Conditions

Reaction	Unshielded	Cd liner, Basis	5% B + Cd liner	30% B + Cd liner
	No Strong Resonances			
$^{27}Al(n,\gamma)^{28}Al$	...	1	0.44	0.12
$^{31}P(n,\gamma)^{32}P$	22	1	...	0.23
$^{63}Cu(n,\gamma)^{64}Cu$	27	1	0.49	0.28
	Strong Resonances			
$^{55}Mn(n,\gamma)^{56}Mn$	...	1	0.79	0.37
$^{59}Co(n,\gamma)^{60}Co$	33	1	0.74	0.34
$^{197}Au(n,\gamma)^{198}Au$	11	1	0.91	0.21
	Threshold Reactions			
$^{27}Al(n,\alpha)^{24}Na$	...	1	0.93	0.925
$^{32}S(n,p)^{32}P$	1.05	1	...	0.91

Table IV. Relative Induced Phosphorus-32 Activities for Equal Weights of Phosphorus and Sulfur under Three Different Shielding Conditions

Reaction	Unshielded	Cd liner	30% B + Cd liner
$^{31}P(n,\gamma)^{32}P$	16	0.71	0.17
$^{32}S(n,p)^{32}P$	1 (Basis)	0.93	0.88

two of these bricks to use in constructing rabbits, and then to test their utility for our needs. It was hoped that the boron would compensate for the neutron moderation in the polyethylene. One brick contained 5% boron powder. The second brick contained 30% boron in the form of boron carbide powder. Upon receipt of the bricks, it was found that the composite materials were too weak to machine the threads required in the rabbit design being employed. Thus, both bricks were irradiated in the Penn State cobalt-60 irradiation facility to a dose of 10^8 rads, cross-linking the polyethylene, and thereby improving the strength and machinability of both bricks.

Figure 4 shows the rabbit design employed. The design essentially encloses the sample in at least 1/4 inch of polyethylene–boron material in all directions. The 5% boron material did not pose any machining problems, but the material containing boron carbide was extremely difficult to machine because of the high rates of tool wear in both high speed steel and tungsten carbide tools. The high speed steel tools had to be reground for every 1 minute of cutting time. This tool wear also added contamination to the finished rabbit, which increased its activity upon neutron irradiation.

It was anticipated that the presence of the boron carbide on the surface of the rabbit would also cause erosion to the aluminum tubing of the rabbit system in addition to contaminating the rabbit with aluminum-28 activity. This potential problem was overcome by using a solution of polystyrene in benzene to periodically coat the wear points with a layer of polystyrene.

Testing of Polyethylene–Boron Rabbits. Table III shows the results of testing these two rabbits on eight neutron reactions, three with no strong resonances in the epithermal region, three with strong resonances in the epithermal region, and two threshold reactions. Four experimental conditions were employed. The unshielded condition employed a standard General Atomic polyethylene rabbit and in-core terminal not containing a cadmium liner. The second condition employed the standard General Atomic polyethylene rabbit along with a 20-mil cadmium lined in-core terminal. All the data were normalized to this condition, since each reaction was evaluated using this set-up. The third and fourth conditions employed the same cadmium lined terminal with, respectively, the 5% boron rabbit and the 30% boron rabbit.

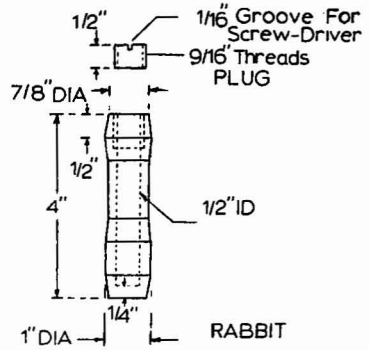

Figure 4. Schematic of polyethylene-boron rabbit

The results shown in Table III indicate a number of points which would be expected. The greatest reduction of activation occurred with those reactions which have essentially 1/V cross sections, where a reduction of two orders of magnitude was obtained between the unshielded and the 30% boron plus cadmium liner conditions. The reductions were somewhat less for the reactions involving the strong resonances, with the worst case being the reduction in the manganese-56 activity. This is probably due to the higher energy of the resonances of this reaction being in a region where the boron cross section has fallen off to a relatively low level. The resonance of cobalt-59 is also higher than that of gold-197 and this explains its higher degree of activation.

The two threshold reactions indicate the relatively small loss of fast neutrons in passing through the shielding materials and thus the small reduction in the amount of sample activation.

Phosphorus-Sulfur Measurements. An examination was made of the utility of the 30% boron rabbit plus the cadmium liner to reduce the interference from the (n,γ) reaction to a threshold reaction, where the activation products are the same.

Equal amounts of phosphorus and sulfur in the form $NH_4H_2PO_4$ and $(NH_4)_2SO_4$ were irradiated in three of the above-mentioned conditions. The relative amount of the phosphorus-32 produced in each case was normalized to the activity of the sulfur irradiated in the unshielded condition. Table IV shows that in the unshielded case, the activity of the ^{32}P from the phosphorus was about 16 times more than that from the sulfur. Using only the cadmium liner, the activity from the phosphorus was about 77% of that from the sulfur. Using the 30% boron rabbit plus the cadmium liner, the activity from the phosphorus was only 20% of that produced from the sulfur, a net improvement of about a factor of 80 over the unshielded case in the ability to measure sulfur in the presence of phosphorus.

This capability has been exploited for measuring the position of phosphorus and sulfur compounds separated on chromatographic strips. A 30% boron brick was cut in half and a slot machined to take the strip and flux monitors. The brick

did not require initial irradiation hardening since the two pieces were held together by aluminum wire. The chromatographic strips are placed in the polyethylene boron brick and inserted into a vertical irradiation tube containing a 20-mil cadmium liner. After irradiation, the strips are scanned for the location of the ^{32}P peaks from the $^{32}S(n,p)^{32}P$ reaction. The strips are then irradiated with no shielding to locate the ^{32}P peaks from the $^{31}P(n,\gamma)^{32}P$ reaction.

Irradiation Effects on Boron-Polyethylene Material. Irradiation containers constructed from the boron–polyethylene should be limited to relatively short irradiation periods because of two reasons. First, the boron-10 nuclear reaction, $^{10}B(n,\alpha)^{7}Li$, results in tremendous deposition of energy into the polyethylene matrix by the recoil energy of the alpha particle and the lithium-7 nucleus.

An experiment was conducted in which the above mentioned irradiation brick was exposed to a total thermal neutron dose of about 5×10^{16} nvt over a three-hour period. Some melting and fusing of the material occurred caused primarily by the heating effect of these recoiling activation products. In the other measurements involved in this work, irradiation doses did not exceed 3×10^{15} nvt each time over a 9-minute period. In these tests, no such heating effects were observed.

The second factor that limits the use of these irradiation containers is the deterioration of the polyethylene matrix with accumulative neutron doses in excess of about 10^{17} nvt. This deterioration results in a serious swelling and loss of tensile strength. Therefore, the authors have limited the use of this material to the construction of containers for short irradiation periods.

Suggested Methods for Improving This Technique. The first step in improving the manufacturing of these rabbits and other types of polyethylene–boron irradiation containers would be to obtain material made from boron instead of the boron carbide. In addition, if the boron is enriched with boron-10, the effectiveness of the containers as absorbing material would be improved without increasing the amount of this foreign material in the polyethylene.

Another approach which might help solve the problems of neutron moderation in irradiation containers and irradiation deterioration of the containers and also obtain larger epithermal neutron absorption capabilities might be to produce such containers from boron carbide or boron nitride. Modern sintering technology could be employed to produce such containers from these ceramic compounds.

RECEIVED for review March 16, 1970. Accepted November 20, 1970.

Determination of Iron by EDTA Titrimetry of the Thiocyanate Complex

Antonio de A. Figueiredo

Instituto de Tecnologia Alimentar, Rua Jardim Botanico, 1024, ZC-20, Rio de Janeiro, Brasil

THE THIOCYANATE IRON COMPLEX is not satisfactory for analytical purposes since the color is neither stable nor proportional to the concentration and may be influenced by various factors (*1–3*). These inconveniences and interferences can be eliminated if the $[Fe(SCN)n]^{(3-n)+}$ complex is extracted with an organic solvent, such as isoamyl alcohol. The complexometric titration with EDTA in acid medium (pH 2–3) is selective for iron since the majority of metal ions will not undergo complex formation at such low pH values (*4*).

The association of the two mentioned conditions—extraction of the iron(III)-thiocyanate complex with isoamyl alcohol, and EDTA titration in acid medium—enables a simple and accurate volumetric determination of iron. In the proposed method, water is added to the isoamyl alcohol solution of the iron(III)-thiocyanate complex and the conditions are adjusted to optimize the complexation of iron. The titration is performed directly, with both the aqueous and organic layers present in the titration flask. The end point—decoloration of the organic phase—is easily observed.

EXPERIMENTAL

Reagents. Reagent grade chemicals were used throughout: 25% (v/v) aqueous hydrochloric acid; concentrated nitric acid; isoamyl alcohol; 20% aqueous potassium thiocyanate; sodium acetate; and 0.01*M* EDTA solution (obtained by dilution of 0.1*M* stock solution standardized against zinc chloride).

Procedure. Three or four drops of concentrated nitric acid are added to about 20 ml of iron solution which is heated on the water bath for 30 minutes in order to ensure total oxidation of the iron. After cooling, the solution is transferred to a 125-ml separatory funnel; 10 ml of isoamyl alcohol and 5 ml of 20% potassium thiocyanate are added, upon which the characteristic red color of iron(III)-thiocyanate appears immediately (Equation 1).

$$Fe^{3+} + n SCN^- \rightarrow [Fe(SCN)n]^{(3-n)+} \quad (1)$$

The contents of the separatory funnel are well shaken for approximately 1 minute and afterward decanted. The almost colorless aqueous layer is transferred back to the same beaker in which the solution was heated; the colored organic layer is transferred to an Erlenmeyer flask for subsequent titration. The aqueous phase is re-extracted twice with isoamyl alcohol (1×10 ml, 1×5 ml). To the combined organic solutions, 25 ml of water and a small amount of sodium acetate (300–400 mg) are added. This results in a decoloration of both phases caused by the equilibrium (Equation 2).

$$[Fe(SCN)n]^{(3-n)+} + \text{Acetate} \rightleftarrows \text{Aceto complexes} + n SCN^- \quad (2)$$

Hydrochloric acid, 25% (v/v), is added carefully until the pH reaches a value between 2 and 3. The red color will reappear. The solution is heated on a water bath to 40–50 °C and titrated with 0.01*M* EDTA solution until the color dis-

(1) C. A. Peters, M. M. MacMaster, and C. L. French, IND. ENG. CHEM., ANAL. ED., **11**, 502 (1939).
(2) M. E. Kahane, *Bull. Chim. France*, **41**, 1403 (1927).
(3) H. W. Winsor, IND. ENG. CHEM., ANAL. ED., **9**, 453 (1937).
(4) G. Schwarzenbach, "Complexometric Titrations," 2nd ed., Methuen & Co. Ltd., London, 1960, p 77–78.

appears in both phases (Equation 3).

$$[Fe(SCN)n]^{(3-n)+} + Y^{4-} \rightarrow FeY^{-} + nSCN^{-} \quad (3)$$

For amounts of iron below 1 mg, a microburet should be used. When the end point approaches, the amyl alcohol layer will be slightly pink. (A few more drops of the titrant will promote complete decoloration.) From this point on, after each drop of titrant, the flask must be agitated vigorously and then allowed to stand for 20 to 30 seconds and the color of the amyl alcohol layer observed. The end point is reached when this is colorless. The result of the determination is calculated from the volume of EDTA consumed.

RESULTS AND DISCUSSION

Good results were obtained with amounts of iron in the range 50 to 1000 μg with almost the same precision. The values of several determinations are presented in Table I.

The interference due to the presence of phosphates, fluorides, and oxalates is eliminated by extraction with isoamyl alcohol (*5*). The small amounts of foreign ions such as Ag^{+}, Cu^{2+}, Co^{2+}, Zn^{2+}, etc., do not interfere as can be seen in Table II.

The method has been successfully used in the determination of iron in samples of coarse salt and calcinated bone meal used as supplements in cattle feeding. Thirty-nine ppm of iron could be determined in a sample of coarse salt. It was also used for the determination of iron in plants. In this case, the previous mineralization was made after Ward and Johnston (*6*).

(5) G. W. Monier-Williams, "Trace Elements in Food," Chapman & Hall, Ltd., London, 1949, pp 257–261.
(6) G. M. Ward and F. B. Johnston, "Chemical Methods of Plant Analysis," Canada Department of Agriculture; Publication 1064, Feb. 1960.

Table I. Precision of Method in Terms of Relative Standard Deviation

Iron taken, μg	No. of detn	Iron found, μg	Rel std dev
84.89	3	83.78	1.3
169.78	3	167.55	1.3
424.45	4	418.88	1.5

Table II. Levels of Interference from Various Cations

Iron taken, μg	Diverse ion added	μg	Iron found, μg	Difference, %
169.78	Co	16	173.13	1.9
169.78	Ni	25	167.55	1.3
169.78	Mn	44	167.55	1.3
169.78	Cu	36	167.55	1.3
169.78	Ag	80	167.55	1.3
169.78	Zn	41	167.55	1.3

The proposed method is probably suitable for determination of iron in foods, feeds, pharmaceuticals, and minerals.

ACKNOWLEDGMENT

The author wishes to express his indebtedness to Dr. David Goldstein, Laboratório da Produção Mineral, Rio de Janeiro, for his experienced help in preparing the final manuscript.

RECEIVED for review September 21, 1970. Accepted November 19, 1970.

Confirmation of the High Aromaticity of Anthracite by Broadline Carbon-13 Magnetic Resonance Spectrometry

H. L. Retcofsky and R. A. Friedel

U. S. Department of the Interior, Bureau of Mines, Pittsburgh Energy Research Center, 4800 Forbes Ave., Pittsburgh, Pa. 15213

ANTHRACITIC COALS are generally considered to be highly aromatic substances. The aromaticity of coal as well as of other carbonaceous materials is defined as the number of aromatic carbon atoms divided by the total number of carbon atoms and is designated f_a. Literature values of f_a for anthracites lie in the range 0.90 to 1.00 (*1*). A large variety of physicochemical techniques including measurements of sound velocity, heat of combustion, proton magnetic resonance, and graphical densimetric methods have been used to arrive at these values. Detailed discussions of these and other methods of estimating f_a for coals have appeared in several books (*1–4*). The main objections to each of these methods are that none of them yields a truly direct measure of f_a and that all f_a's calculated from the data obtained from the particular measurement involved require *a priori* assumptions about the structure of coal. The present investigation was undertaken to explore the use of broadline carbon-13 nuclear magnetic resonance (^{13}C NMR) spectrometry of solids in studies of coal structure. For this purpose, ^{13}C spectra of an anthracitic coal and the completely saturated hydrocarbon adamantane were obtained. ^{13}C NMR of solids, a relatively new technique, is potentially a method for the direct determination of aromaticities of coals and other organic materials of limited solubility.

(1) D. W. van Krevelen, "Coal," Elsevier, Amsterdam, 1961, p 447.
(2) H. Tschamler and E. DeRuiter, "Chemistry of Coal Utilization," Suppl. Vol., H. H. Lowry, Ed., Wiley, New York, 1963, p 35.
(3) W. Francis, "Coal," 2nd ed., Edward Arnold, London, 1961, p 720.
(4) H. Tschamler and E. DeRuiter, "Coal Science," R. F. Gould, Ed., Amer. Chem. Soc., Washington, D.C., 1966, p 332.

EXPERIMENTAL

NMR spectra were obtained using a Varian Associates Model DP-60 spectrometer operating at 15.085 MHz and equipped with a time-averaging computer and Fieldial scanning unit. Broadline detection of the dispersion mode was employed throughout, thus all spectra produced are first derivative curves. The modulation amplitude was 0.156 G

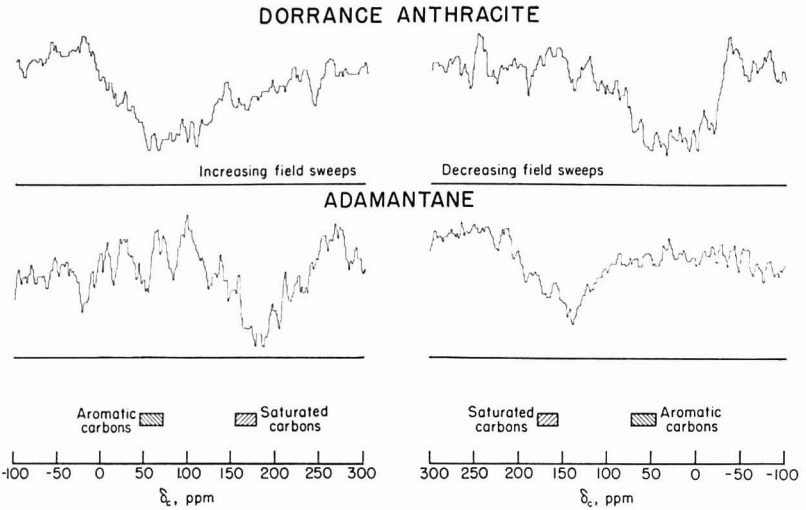

Figure 1. ^{13}C NMR spectra of Dorrance anthracite and solid adamantane

at a sweep frequency of 40 Hz. Chemical shifts are referred to neat carbon disulfide and are designated δ_c. In order to minimize errors due to sweep nonlinearities or peak asymmetries, all chemical shift and linewidth measurements are average values from two sets of time-averaged spectra: one obtained while scanning the magnetic field from low to high field, the other while scanning from high to low field.

RESULTS AND DISCUSSION

Broadline ^{13}C NMR spectra of Dorrance anthracite (moisture and ash-free analysis: 92.70% C, 2.53% H, 2.95% O, 0.98% N, 0.84% S) are reproduced in Figure 1 (upper traces). Spectra obtained during both increasing field sweeps (738 scans) and decreasing field sweeps (564 scans) are shown. The chemical shift δ_c was measured to be 53 ppm, however, errors of several ppm are probable. The spectral linewidth at one-half intensity ΔH is 1.5 G. Spectra of adamantane obtained during increasing field sweeps (277 scans) and decreasing field sweeps (571 scans) are also shown. For solid adamantane δ_c = 163 ppm and ΔH = 0.8 G. A chemical shift correlation chart indicating the general spectral region of absorption by aromatic and saturated carbon atoms in selected hydrocarbons appears near the bottom of the figure. The chart is based on published data for methyl- and ethylbenzenes (*5–7*), hydroaromatic hydrocarbons (*7*), and aromatic compounds containing one fused partially saturated 5-membered ring (*7*).

Chemical Shifts. The chemical shift of the anthracite sample (53 ppm) plus the fact that little if any absorption occurs in the spectral region attributed to resonances of saturated carbon atoms attest to the high aromaticity of anthracite. The purpose of obtaining spectra of solid adamantane was to extend the region of saturated carbon atom absorption shown in Figure 1 to include the effects of at least some proton dipolar line broadening. Although some overlap with the anthracite resonance is apparent, the amount is small. These results, though qualitative, leave little doubt that anthracitic coals are highly aromatic substances. The present work also suggests that measurements made with more sophisticated spectrometers operating at higher magnetic fields should eventually lead to quantitative determinations of the aromaticity of coals and other solid substances.

A second qualitative conclusion concerning the chemical structure of anthracite can be drawn if anthracite's elemental constitution is viewed in light of the ^{13}C NMR results. The high aromaticity of Dorrance anthracite together with its very low atomic H/C ratio (0.325) can be best explained by assuming the presence of large condensed polynuclear aromatic structures in the coal structure. The ordering of these structures in graphite-like layers may account for the anisotropy of both the magnetic susceptibility (*8*) and the electron spin resonance g value (*9*) found for this material.

Spectral Linewidths. A large portion of the linewidth in the ^{13}C NMR spectrum of solid adamantane is undoubtedly due to dipolar line broadening by protons in the molecule. Grant (*10*) has measured the chemical shifts of the two nonequivalent groups of carbon nuclei in adamantane in solution by high-resolution NMR and found them to differ by ~9 ppm. No spin-spin coupling constants were measured since proton decoupling was used. Assuming reasonable values of 130 Hz for $J_{^{13}C-H}$, the total spread of the high-resolution adamantane spectrum can be estimated to be ~330 Hz (~0.3 G) at 15.085 MHz. The observed linewidth in the solid is more than twice this amount. McCall and Douglas (*11*) have

(5) P. C. Lauterbur, *J. Amer. Chem. Soc.*, **83**, 1838 (1961).
(6) W. R. Woolfenden and D. M. Grant, *ibid.*, **88**, 1496 (1966).
(7) H. L. Retcofsky and R. A. Friedel, "Spectrometry of Fuels," R. A. Friedel, Ed., Plenum Press, New York, 1970, p 90.
(8) D. Bivins and S. Ergun, *Science*, **159**, 83 (1968).
(9) H. L. Retcofsky, G. P. Thompson, and R. A. Friedel, U. S. Bureau of Mines, Pittsburgh, Pa., unpublished work, 1969.
(10) D. M. Grant, Abstracts 6th Experimental NMR Conf., Pittsburgh, Pa., 1965.
(11) D. W. McCall and D. C. Douglas, *J. Chem. Phys.*, **33**, 777 (1960).

shown the importance of proton dipolar line broadening in the proton spectrum of solid adamantane and found that motional narrowing of the adamantane resonance first appears ~−130 °C. ^{13}C NMR measurements at low temperatures would be needed to assess the importance of proton dipolar line broadening on the carbon resonance in adamantane.

The linewidth in Dorrance anthracite is not easily explained. Possible contributors to the linewidth include proton dipolar interactions, unresolved carbon chemical shifts, chemical shift anisotropy, and line broadening by paramagnetic impurities (free radicals) which are known to be present in the anthracite (*12*). The paramagnetic contribution to the linewidth can be approximated using the Equation (*13*, *14*)

$$\Delta H = 3.8\gamma\hbar n$$

where γ is the magnetogyric ratio of the electron, $\hbar$ is the modified Planck constant, and n is the concentration of unpaired spins in the sample. The value of n for Dorrance anthracite has been reported previously (*12*). Substitution of this value (5.3×10^{19} g^{-1}) into the equation yields a theoretical linewidth about twice that observed experimentally at room temperature. It is unlikely that unresolved chemical shifts play an important part since these are known to cover only a small range in the case of polynuclear aromatics (*15–17*). It is possible, however, that chemical shift anisotropy in the solid may be important. Although it is not possible to estimate this effect, it should again be noted that anisotropies do exist in other magnetic properties of anthracites.

RECEIVED for review October 5, 1970. Accepted November 17, 1970. Reference to trade names is made for identification only and does not imply endorsement by the Bureau of Mines.

(12) H. L. Retcofsky, J. M. Stark, and R. A. Friedel, ANAL. CHEM., **40**, 1699 (1968).
(13) A. Abragam, "Principles of Nuclear Magnetism," Oxford Univ. Press, London, 1961, p 128.
(14) M. N. Alexander, *Phys. Rev.*, **172**, 331 (1968).
(15) T. D. Alger, D. M. Grant, and E. G. Paul, *J. Amer. Chem. Soc.*, **88**, 5397 (1966).
(16) H. L. Retcofsky, J. M. Hoffman, Jr., and R. A. Friedel, *J. Chem. Phys.*, **46**, 4545 (1967).
(17) R. J. Pugmire, D. M. Grant, M. J. Robins, and R. K. Robins, *J. Amer. Chem. Soc.*, **91**, 6381 (1969).

New Method for Separation of Americium from Curium and Associated Elements in the Zirconium Phosphate–Nitric Acid System

Fletcher L. Moore
Analytical Chemistry Division, Oak Ridge National Laboratory, Oak Ridge, Tenn.

TO ACHIEVE THE SEPARATION of americium from curium in an all-inorganic system is the subject of a continuing study at this laboratory. Current methods based on ion exchange resins or organic solvents suffer from resin degradation, excessive gassing, and solvent instability. Although several inorganic systems (*1–3*) exist for this separation, they either provide inadequate decontamination, require excessive manipulations, or they are too time-consuming for analytical and process applications.

At present the most widely-used method is based on the precipitation of Am(V) as the double carbonate (*1*). It is unsatisfactory because it requires multiple precipitations involving the use of concentrated potassium carbonate solutions. Various workers have found the subsequent removal of coprecipitated curium and large amounts of carbonate salts to be tedious and difficult. In addition, the carbonate precipitation method for americium cannot be used for the final removal of small amounts of americium from curium.

The cation exchanger, zirconium phosphate, was selected as a promising candidate for the separation of americium from curium because it is stable in oxidizing media, strong nitric acid, and elevated temperatures; moreover, it exhibits superior resistance to ionizing radiation over the organic ion exchangers and organic solvents.

The new method described here is based on the negligible sorbability of Am(V) on zirconium phosphate from dilute nitric acid solutions. Under the conditions used, Cm(III) and a number of other elements are strongly sorbed.

For analytical applications the isotope dilution technique in conjunction with alpha spectrometry is used for an accurate determination of ^{243}Am.

EXPERIMENTAL

Apparatus. An internal sample methane proportional counter was used for fission, alpha, and beta counting at voltage settings of 2100, 2900, and 4300, respectively.

A NaI well-type scintillation counter, $1^3/_4 \times 2$ inches, was used for gamma counting.

A silicon diode detector (3 cm^2) coupled to a 256-channel analyzer was used for alpha spectrometry.

A glass tube, 5 mm i.d. and 180 mm in length was drawn to a tip at one end. A small glass wool plug was inserted in the tube to retain the support. To prevent disruption of the column, a small glass wool plug was placed on top of the column.

Reagents. HNO_3, 0.01*M*; HNO_3, 10*M*; and $(NH_4)_2S_2O_8$, 0.5*M* were used.

Zirconium phosphate cation exchange crystals, Bio-Rad ZP-1, 50–100 mesh, hydrogen form is available from Bio-Rad Laboratories, 32nd and Griffith Ave., Richmond, Calif.

(1) R. A. Penneman and T. K. Keenan, "The Radiochemistry of Americium and Curium," NAS-NS-3006 (1960).
(2) F. L. Moore, ANAL. CHEM., **35**, 715 (1963).
(3) H. P. Holcomb, *ibid.*, **36**, 2329 (1964).

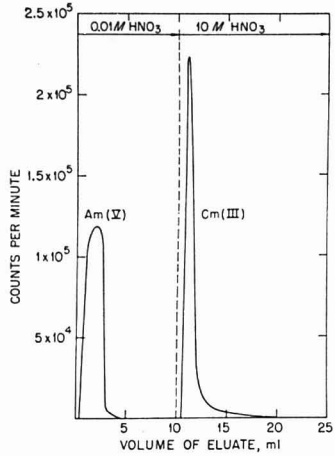

Figure 1. Separation of americium from curium by cation exchange in the zirconium phosphate–nitric acid system

Column: 5 × 30 mm, zirconium phosphate (50–100 mesh), 23° C, flow rate = ~0.3 ml per minute

To 10 grams in a 1-oz screw cap bottle, add 25 ml of 0.1*M* HNO_3. Shake well for about 30 seconds and allow the crystals to settle for about 15 seconds. Pour off the supernatant solution and repeat the procedure five times. This removes most of the fines from the zirconium phosphate crystals. Store in 25 ml of 0.1*M* HNO_3.

Column Preparation. Fill the glass tube with 0.01*M* HNO_3. By use of a medicine dropper, add to the glass tube the slurry of zirconium phosphate exchanger, 5–6 drops at a time. Tap the column after each addition, being careful to eliminate air bubbles. Pack the column to a height of 30 mm and allow the nitric acid to drain to near the top of the column. Do not allow the column to run dry. Condition the column by passing 5 ml of 0.01*M* HNO_3 through it. A flow rate of 7–8 drops per minute (~0.3 ml) is attained.

Procedure. For analytical purposes add to the sample solution an aliquot of a standardized solution of ^{241}Am (5.48 mev) contained in 0.1*M* HNO_3. The alpha radioactivity of the ^{241}Am added should be about one half the estimated alpha radioactivity of the ^{243}Am (5.27 mev) in the sample aliquot.

For general purification purposes omit the above paragraph. Adjust the sample solution to 0.01*M* HNO_3–0.1*M* $(NH_4)_2S_2O_8$. Mix gently by swirling. Oxidize the americium by heating the tube in a water bath at 80–90 °C for 10 minutes. Remove the tube and cool for 5–10 minutes in a beaker of water at room temperature.

Place a 10-ml volumetric flask under the column to collect the americium fraction. Transfer the oxidized solution to the column and elute with 0.01*M* HNO_3 at 7–8 drops per minute until 10 ml are collected. Mix well. Evaporate 100 μl or less on tantalum plates for alpha measurements.

If the curium fraction is desired, elute it from the column with 10 ml of 10*M* HNO_3. Mix well and prepare suitable aliquots on stainless steel plates for alpha measurements.

RESULTS AND DISCUSSION

The conditions used for the oxidation–reduction sequence, Am(III) → Am(VI) → Am(V), were similar to those previously developed (*4*). Ammonium persulfate oxidizes Am(III) to Am(VI) in dilute nitric acid solution. In the absence of a holding oxidant or stabilizing anion, Am(VI) reduces to Am(V). The optimum conditions selected for the preparation of Am(V) are 0.01–0.1*M* nitric acid, 0.05–0.1*M* ammonium persulfate, 10-minute oxidation at 80–90 °C followed by a 5–10 minute cooling period at room temperature.

Early batch type experiments indicated that the large AmO_2^+ ion showed little tendency to sorb on zirconium phosphate from dilute nitric acid; Am(III) and Cm(III) sorbed strongly. The following column conditions were selected for the separation of americium and curium: 5 × 30 mm column of zirconium phosphate (50–100 mesh), room temperature operation at a flow rate of 7–8 drops (~0.3 ml) per minute; eluents, 10 ml of 0.01*M* HNO_3 for Am and 10 ml of 10*M* HNO_3 for Cm.

Typical elution curves are shown in Figure 1. Am(V) elutes rapidly from the column with 0.01*M* HNO_3. If desired, the Cm(III) may be eluted with 10*M* HNO_3. The curium elution curve shows some tailing, a characteristic of inorganic exchangers. However, about 97% of the curium elutes in 5 ml of 10*M* HNO_3; quantitative elution is achieved with 10 ml.

The recovery of americium and its decontamination from curium is excellent. Americium yields average about 90% with curium decontamination factors >2.5 × 10^5. The method requires only about 1½ hours.

Ammonium persulfate concentrations of ≳0.2*M* resulted in slightly premature elution of curium and europium. Presumably, persulfate, sulfate, or bisulfate ions complex the trivalent ions, thereby lowering their distribution coefficients for zirconium phosphate.

Several attempts were made to oxidize Am(III), previously sorbed on the zirconium phosphate column, to the nonsorbable Am(V) oxidation state. Although Am(III) sorbed tightly at 0.01–0.1*M* HNO_3, subsequent yields of Am(V) were very low. In addition, at the elevated temperature required for oxidation, mechanical difficulties associated with gas bubble formation prevented smooth column operation.

Although the major interest in this study was the separation of americium from curium, some observations were made of the behavior of several other metal ions often associated with americium. Table I shows that high decontamination is achieved from these elements. Decontamination factor equals the total amount of element in the feed solution divided by the total amount found in the americium product.

The zirconium phosphate–nitric acid system described affords an impressive separation of americium not only from curium but also from other actinide elements, lanthanide elements, and cesium. The trivalent ions of the transcali-

Table I. Decontamination of Americium in the Zirconium Phosphate–Nitric Acid Method

Element	Decontamination factor
^{137}Cesium	>5.5 × 10^5
$^{152-4}$Europium	>2 × 10^5
^{233}Uranium	3 × 10^2
^{239}Plutonium	8.5
^{244}Curium	>2.5 × 10^5
^{249}Berkelium	2.1 × 10^2
^{252}Californium	>4.5 × 10^5

(4) F. L. Moore, ANAL. CHEM., 40, 2130 (1968).

fornium elements would be predicted to sorb at least as efficiently as californium from 0.01*M* HNO_3. Europium, californium, and uranium elute essentially quantitatively in the 10*M* HNO_3 fraction, as expected for the trivalent and hexavalent ions. The elution curves of Am(III), Cm(III), and Eu(III) are essentially identical.

Plutonium showed the lowest decontamination factor of the actinide elements. The small loss of plutonium to the americium product probably is a reflection of the strong sulfate complexation, which lowers the distribution coefficient for Pu(IV). About 82% of the initial plutonium eluted in the 10*M* HNO_3 fraction.

About 90% of the initial berkelium eluted in the 10*M* HNO_3 fraction.

The separation of cesium from americium is striking. Less than 10% of the cesium added to the column eluted with 10*M* HNO_3. Cesium exhibits a stronger affinity for zirconium phosphate than many multivalent ions. It is noteworthy that no separation of cesium from americium is attained in the extraction chromatographic method (*4*) recently developed.

A number of other elements not evaluated here are known to sorb efficiently from 0.01*M* HNO_3 like curium. Among these elements are strontium, ruthenium, zirconium, niobium, and iron.

APPLICATIONS

The zirconium phosphate cation exchanger for the separation of americium from a number of other elements is valuable both to the analytical and preparative chemist. The column operates at room temperature with relatively high flow rates without the necessity to resort to vacuum or high pressure techniques. The method is simple, fast, and requires few manipulations—advantages for glove box or hot cell work.

Other attractive features of the zirconium phosphate–nitric acid method are that it is considerably less corrosive than the earlier fluoride systems developed (*1–3*), and it is more selective for americium than the lanthanum fluoride (*2*), calcium fluoride (*3*), or extraction chromatographic (*4*) methods.

We have used the new method as a satisfactory tool for the purification and isolation of americium in solutions containing other actinide (III, IV, VI) ions, lanthanide (III, IV) ions, cesium, and various other ions. A practical problem which often arises in the final purification of curium nuclides is the removal of small amounts of contaminating americium. The zirconium phosphate method described here offers a promising approach for achieving that separation.

In process work the most common interferences encountered are chloride ion and α-hydroxyisobutyric acid. These interferences may be eliminated by evaporations with concentrated nitric acid.

ACKNOWLEDGMENT

The author gratefully acknowledges the help of F. Nelson and H. O. Phillips for useful discussions of inorganic exchangers.

RECEIVED for review September 25, 1970. Accepted November 20, 1970. Research sponsored by U. S. Atomic Energy Commission under contract with Union Carbide Corporation.

AIDS FOR ANALYTICAL CHEMISTS

Rapid and Efficient Method for Removing Viscous Polymer Solutions from Nuclear Magnetic Resonance (NMR) Sample Tubes

Alex Jakab

Research Laboratories, The Goodyear Tire & Rubber Co., Akron, Ohio 44316

WE ROUTINELY analyze polymers by NMR and we have found that the use of solvents, strong acids, cleaning solution (*1*) or pyrolysis to clean the sample tubes is not always successful. We have devised a method for removing these viscous polymer solutions from the sample tubes which is simple and relatively rapid, and increases the lifetime of the sample tubes.

We utilize a nonsolvent to precipitate the polymer *in situ*, in conjunction with a stirring rod made from a copper wire formed into a closed-loop on one end. The diameter of the loop is slightly smaller than the diameter of the sample tube. The copper wire facilitates the mixing of the viscous solution and the nonsolvent, and at the same time provides a nucleation site for the precipitation of the polymer.

Our experience has been limited to polybutadienes and polyisoprenes in CCl_4 or benzene, and our procedure is as follows:

The polymer solution usually fills the bottom inch of the cylindrical sample tube. Sufficient methanol is added to fill the sample tube. The copper loop is inserted and the mixture gently agitated by an up-and-down motion of the stirring wire. The precipitated polymer, which adheres to the copper loop, and any polymer clinging to the wall of the tube are removed by lifting the copper wire loop slowly out of the tube. The liquid remaining in the tube now has a much lower viscosity—essentially a CCl_4 (or benzene)—methanol mixture, so it can be poured easily from the sample tube. If the precipitation is incomplete, as indicated by only a slight change in the viscosity of the original sample, the nonviscous upper layer is decanted and fresh methanol re-introduced. A distilled water rinse, followed by a half dozen acetone rinses of both inside and outside of the tube, and drying in an air-oven at 70 °C completes the procedure.

RECEIVED for review August 26, 1970. Accepted October 8, 1970.

(1) N. W. Jacobsen, *J. Chem. Educ.*, **47**, 507 (1970).

Simple Device for Transferring Thin-Layer Chromatographic Fractions for Spectroscopic Examination

Colin J. Clemett

Unilever Research, Port Sunlight Laboratory, Port Sunlight, Wirral, Cheshire, L.62 4XN, U.K.

THIN-LAYER CHROMATOGRAPHY provides a relatively quick method for separating mixtures in amounts of the order of 100 μg. Such quantities are small if spectrometric examination of the fractions is required, so it is necessary to have a means of transferring the fractions as efficiently as possible from the plate into the medium relevant to the particular spectrometric technique.

This can be accomplished using the simple device illustrated in Figure 1. It consists of a disposable Pasteur pipet, the tip of which has been turned in slightly and plugged with glass fiber filter sheet. The wide end is fitted with a bung carrying a capillary tube bent as shown—a Drummond 100-μl Microcap is suitable.

Suction is applied at the plugged end of the pipet (a water pump is adequate) and the mouth of the capillary applied to the spot on the chromatographic plate to be collected. The stationary phase containing the adsorbed material is then efficiently "vacuumed" into the pipet. Alternatively, the plugged Pasteur pipet can be placed inside a side-arm tube, the mouth of which carries a bung holding the capillary. One end of the capillary is arranged to project into the mouth of the Pasteur pipet while the other end is applied to the chromatographic spot, and in this case suction is applied to the side-arm. This method circumvents the restriction caused by the plug in the Pasteur pipet and results in much more rapid pick-up. However, care is required in adjusting the degree of suction applied (very little is necessary), otherwise the material is blown out of the Pasteur pipet and may be lost. The device works extremely well for collecting granular adsorbents such as silica and alumina, but is less successful with some fibrous cellulose adsorbents.

When a fraction has been collected, it is consolidated in the narrow part of the pipet, forming a miniature chromatographic column. This allows the adsorbate to be eluted in a very small volume of a suitable solvent which is important when dealing with only tenths of micrograms of material. Using this technique we have consistently recovered 80 to 90% of 100 μg amounts of an alkyl benzene sulfonate spotted on silica and eluted with 20 μl of water.

Figure 1. Device for vacuum collection TLC fractions

In many cases, the eluate from the Pasteur pipet may be used directly for spectroscopic examination. For mass spectrometry, the eluate is dropped slowly onto the probe tip and the solvent allowed to evaporate. Clean spectra have been obtained from as little as 5 μg of material. Similar success, with 20-μg amounts, has been obtained with infrared spectrometry. In this case the eluate was dropped onto a little KBr powder which was pressed into a microdisk after evaporation of the solvent. For NMR spectrometry, it did not prove possible to transfer the eluate directly into a microcell, as it was generally contaminated with water and the solvents used to develop the chromatogram. This problem was overcome by transferring the eluate into a second Pasteur pipet, the tip of which was sealed. Bridging the neck of this pipet with a drop of solvent prior to adding the eluate confined the latter to the wide portion of the pipet, which facilitated evaporation of the solvent. After evaporation, the tip was broken off and the material remaining washed down into a microcell with the solvent of choice. In this way we have obtained excellent spectra from 100–200 μg amounts (collected from several chromatograms) of a number of compounds, using spectrum accumulation.

ACKNOWLEDGMENT

The mass spectra were obtained by D. N. Forshaw, the infrared spectra by Mrs. E. M. Joyce, and the chromatoplates were prepared by A. Rastrick.

RECEIVED for review August 24, 1970. Accepted October 19, 1970.

Modulated Power Unit for Driving Metal Vapor Discharge Lamps

F. M. Hamm, T. L. Martin, and P. B. Zeeman

Department of Physics, University of Stellenbosch, South Africa

METAL VAPOR DISCHARGE lamps provide convenient light sources for atomic fluorescence spectrometry (*1–3*) because of their high intrinsic brightness and relative narrow lines when driven at suitable current rates, usually somewhat below the factory rated value. Normally these are driven directly from the ac mains, chokes, resistors, or leakage transformers being used to give the necessary current limiting. The light output from a lamp driven in this manner will be interrupted; the intervals of light emission and darkness being unequal in time, see Figure 1, *a*, *b*. This form of modulation is rather unsuitable to be used in conjunction with conventional lock-in detector systems. These systems are widely used in atomic fluorescence and atomic absorption spectrometry because flame emission and flame background can thus be suppressed to the level of their respective noise component determined by the pass band of the amplifier and detector system. In many instruments, *e.g.*, the Zeiss PMQ II spectrophotometer, the frequency of the lock-in detector is the mains frequency. For

(1) R. M. Dagnall, T. S. West, and P. Young, *Talanta*, **13**, 803 (1966).
(2) N. Omenetto and G. Rossi, *Anal. Chim. Acta*, **40**, 195 (1968).
(3) J. D. Winefordner and R. A. Staab, ANAL. CHEM., **36**, 1367 (1964).

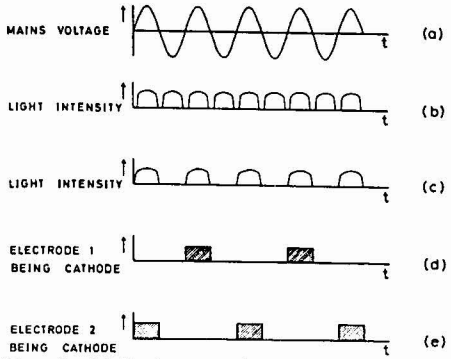

Figure 1. Relation between mains phase, light output, and cathode position of electrodes

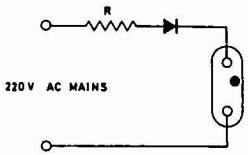

Figure 2. Simple modulation circuit for vapor discharge lamps

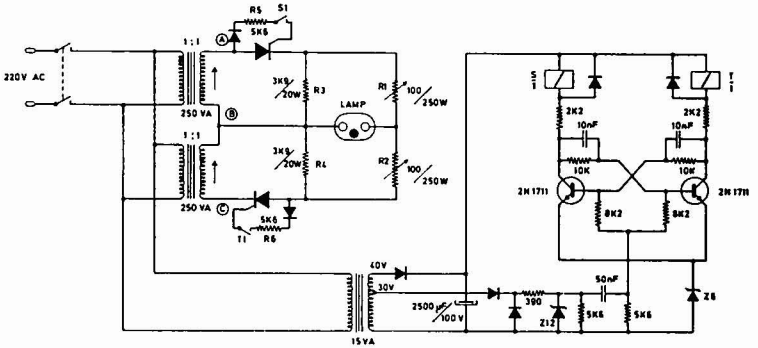

Figure 3. Modulated power unit for driving vapor discharge lamps

All resistors ¼ W if not indicated otherwise. All rectifiers (RCA) 1N-3196

S/1 and T/1 Reed relay driving coils 1000Ω/12–24 V

S1 and T1 Reed Relay contacts (HIVAC XS 2/3)

the vapor discharge lamp, this would mean that they could be driven correctly for instance, by inserting a rectifier in the circuit to suppress one half-period of the mains voltage, see Figure 2. The light output from this arrangement is shown in Figure 1, *a*, *c*. In all such arrangements the actual period of light emission is slightly shorter than the intervals of darkness. This usually does not impair the performance of a lock-in amplifier.

The above method, however, has the following two serious disadvantages: When the lamps are driven from ac mains, the electrodes are alternating anode and cathode, respectively. Consequently the heat generated is equally distributed between the electrodes. In the case of the arrangement shown in Figure 2 for the same average lamp current, one electrode carries almost the total heat generated. This may lead to a shorter lamp life. Second, a marked inhomogeneity of the envelope temperature leads to condensation of metal vapor at the colder sites, sometimes partly blocking the optical path.

The difficulties mentioned above have been overcome by using a lamp modulator, see Figure 3, in which use is still made of suppressing one half-period of the mains voltage, thus providing the correct modulation frequency for the Zeiss instrument for example, but in the conducting phases the electrodes are switched such as to make them anode and cathode alternatively. This is demonstrated in Figure 1, *a*, *d*, *e*.

Referring to Figure 3 a push-pull output is provided at the points *A* and *C* with reference to point *B*. The silicon-controlled rectifiers SCR1 and SCR2 will with either contact S1 or T1 closed at a time, only allow current to flow in say the positive half-period referring to the primary. Now contacts S1 and T1 are driven by the frequency divider circuit in such a way that SCR1 and SCR2 are prepared to conduct alternately in the conduction phases. R1 and R2 are the current limiting resistors for the discharge tube. They should be adjusted for equal light output in both directions of the discharge. This can easily be monitored with an oscilloscope at the amplifier output. R3 and R4 have the function to damp transformer oscillations which occur when the gas discharge extinguishes towards the end of a half-period. R5 and R6 limit the current through the trigger electrodes of the SCR's.

The timing of the relay contacts is not critical, as long as one is closed before the firing voltage is reached and released again before the firing voltage is reached in the following conducting half-period when the same applies to the other contact. These conditions are readily achieved by the circuit without further adjustment.

This modulator has been used successfully in conjunction with the Zeiss PMQ II spectrophotometer. No difficulties should be experienced with the construction of the above circuit even by people not well versed in electronics, whereas changes due to components being at hand may well be done by the more experienced.

RECEIVED for review August 12, 1970. Accepted October 20, 1970. The authors thank the South African Council for Scientific and Industrial Research for a grant in aid of this research.

Simple Continuous Electronic Readout for Rotameter-Type Fluid Flow Measuring Devices Using a Photoelectric Transducer

Seymour Lowell and Stewart Karp

C. W. Post College, Long Island University, Greenvale, N. Y. 11548

ROTAMETER-TYPE FLUID FLOW measuring devices are used extensively in laboratory as well as in engineering applications. In the laboratory, they are found incorporated in such instruments as gas chromatographs, atomic absorption and flame photometers, and many others. Rotameters readily lend themselves to use in a variety of bench experiments involving gas or liquid flow. In many instances a continuous and/or remote readout giving an electronic signal which can be recorded would be desirable. This report describes a simple modification of rotameters which provide such a readout. Other modifications have been suggested to us, but they are not continuous or not so simple (*1*) as the one described here.

Basically, a rotameter consists of a transparent glass tube with a tapered bore vertically positioned with the wide end up. The tube length and bore diameter are chosen in accordance with the nature of the fluid and the flow rate range of interest. A ball or other shaped "float" of appropriate size and density rides up and down the bore as a function of the fluid flow rate. The height of the float in a well designed tube is almost linearly related to the flow rate. Calibration is required, however, for accurate work.

Our modification consists of mounting a light source near one end of the tube so that light rays strike the tube obliquely over its entire length, and mounting a photo-sensitive cell at the other end of the tube. Figure 1 is an example of such a setup.

The device operates as follows: Light entering the tube is refracted and reflected along the bore toward the photocell. The light reaching the photocell is light which entered the tube between the float and the photocell. Light entering on the other side of the float is effectively blocked by the opaque float. For a given geometry and fluid, the amount of light reaching the photocell depends upon float position—hence, upon fluid flow rate.

Most commercially available rotameters can be modified by simply drilling a hole in one of the mounting blocks directly in line with the rotameter tube (see Figure 1) and cementing a photocell over this hole. Light striking the sides of the photocell can be avoided by recessing the cell into the block or simply by blackening it with paint or tape. The light source—generally a convenient 12-V lamp—can be mounted with an insulated clamp or soldered directly to the rotameter casing if the casing can be used as a lead to the bulb. We used a 12-volt bulb powered by a suitable stable power supply.

Electronic output suitable for use with a potentiometric recorder can be achieved with the Wheatstone bridge circuit as shown in Figure 2. If the photocell is mounted at the bottom and the light source near the top of the rotameter tube, the resistance of the cell decreases as flow rate increases. The position of the bulb and photocell can be reversed and in this case, the signal will also be reversed but no less useful.

The optimum position for the light source depends on the geometry of the rotameter tube, but it is usually such that the filament is within $^1/_2$ to 1 cm from the tube. This position

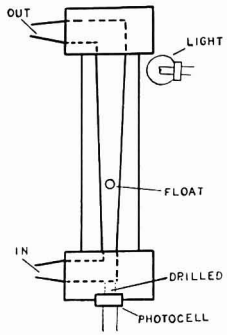

Figure 1. Modified rotameter

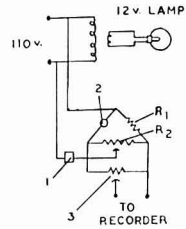

Figure 2. Schematic circuit diagram

1. Full wave rectifier (International Rectifier 18DB4A-C or equivalent). 2. Photo - cell (Clairex CL5M5L or equivalent). 3. Appropriate voltage divider for recorder or meter, R_1 = 5 MΩ, R_2 = 50 kΩ

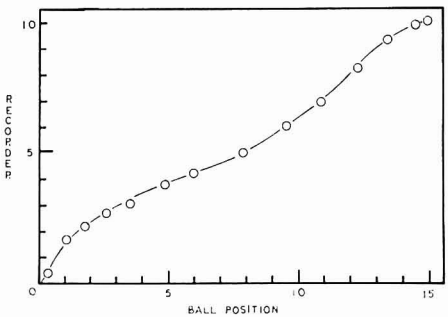

Figure 3. Typical calibration curve

is easily found by moving the bulb until maximum signal is obtained when the float is at some position in the tube.

The relation between output and flow rate or ball position is not linear; therefore, calibration is required. Curves relating ball position to flow rate are usually supplied by the manufacturer for a variety of fluids and pressures. These curves can be used for the modified rotameter, if only a calibration curve relating output with ball position is determined. Hence, usually only a single calibration curve need be determined. Figure 3 shows an example of such a curve.

No change has been observed in the calibration curve of a modified rotameter over a period of a few months.

Rotameters modified as described here have been used in our laboratory to monitor a variety of gases and aqueous solutions, some moderately colored.

It has also been found that extremely low gas (probably low

(1) D. H. Fuller, U. S. Patent 2,912,858 (1959).

liquid) flows can be monitored if the photocell is placed at the bottom of the tube and the light source is placed a centimeter or two from the bottom of the tube. Flows as low as 0.01 cc/min were easily monitored with gas rotameter tubes not designed for such low flows.

In summary, this report describes a simple, inexpensive modification of a basic rotameter-type flow device to provide an electrical signal for monitoring fluid flows.

RECEIVED for review September 21, 1970. Accepted October 29, 1970. This work resulted from a project supported by Quantachrome Corp., Greenvale, N. Y. 11548.

Low Cost Parallel-to-Serial Converter for Digital Instrumentation

Morteza Janghorbani, John A. Starkovich, and Harry Freund

Department of Chemistry, Oregon State University, Corvallis, Ore. 97331

COMMONLY AVAILABLE LABORATORY digital instruments, such as digital voltmeters, typically store information in parallel binary-coded-decimal (BCD) form. Long term storage of such data on paper tape, magnetic tape, or direct processing by a computer frequently requires conversion of the data into a serial form. Typical commercial units may cost between $1000 and $2000, and are usually designed as part of more complex subsystems, with special input–output characteristics that may not be readily compatible with common digital instruments.

A relatively low cost, yet versatile converter, was designed using readily available TTL logic IC's. Specifically, Figure 1 shows a block diagram of the converter employed to interface a chemical instrument supplying parallel BCD data with a teletype requiring serial ASCII Code. The parallel-to-serial converter accepts BCD data from the output of the chemical instrument *via* a DIGIT SELECTOR section. The parallel BCD data are then serialized, encoded, and are outputted *via* the OUTPUT STAGE onto the storage device.

Figure 2 presents a functional diagram of the parallel to serial converter. The heart of the converter consists of three 4-bit static shift registers (Fairchild, U6B930051X) which function both as serializer and ASCII Encoder. The BCD-outputs of the chemical instrument are hard wired to the appropriate inputs IN1 to IN8; IN1 corresponding to the most significant digit. IN9 is wired to generate the BCD representation of an ASCII blank (space). IN1 thru IN9 each contains a quad 2-input AND gate (Motorola, MC3001P) and four high speed diodes (1N662 Jan). The four outputs of each of the quad AND gates are hard wired by means of the diodes to the four inputs of the shift registers P_1 thru P_4, the most significant binary bit (2^4) being connected to P_4. P_0 and P_5 thru P_{11} of the registers (not shown in Figure 2) are hard wired to 1's or 0's to provide the remaining bits of ASCII Code. Figure 3*a* shows the ASCII bit pattern for decimal three.

When the start button is pressed (either manually or automatically) the data available at IN1 are fed to the inputs of registers and are shifted together with P_0 and P_5 through P_{11}, one bit at a time at the clock rate of 9.1 milliseconds per bit to the output. After the 12 bits have been shifted out, the counter-decoder (Fairchild, U6A998979X and Fairchild, U6B930159X) counts up by one, making the contents of IN2 available to the registers and this cycling continues until the contents of IN9 have been serialized and shifted out. In automatic mode, the P-S converter is reset and placed in standby condition awaiting the next start pulse. The start signal (print command) is a 9-volt square wave whose duration is not critical. No stop signal is required. In manual mode, the entire scanning operation repeats continuously, with two temporary contact switches controlling start and stop operations. When the output is connected to a teletype, each cycle results in the print-out of eight digits followed by a space. A

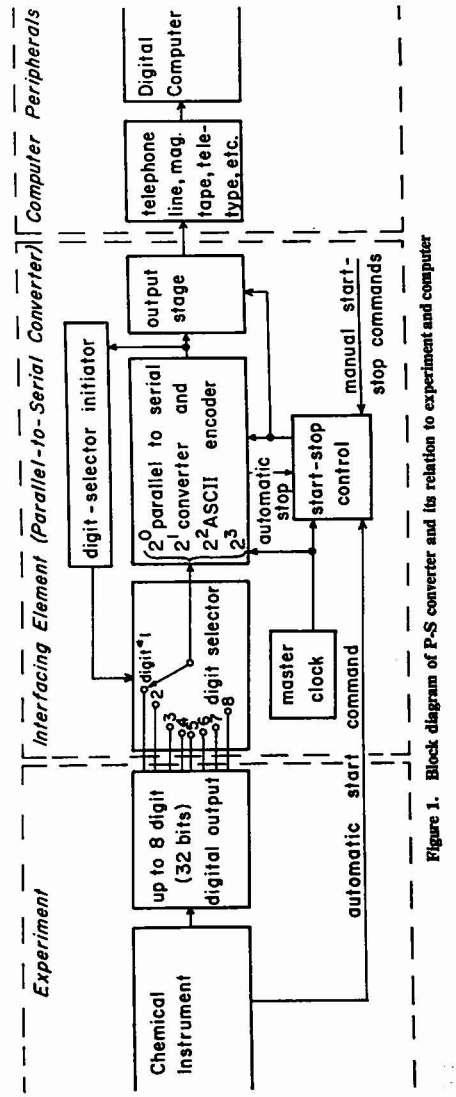

Figure 1. Block diagram of P-S converter and its relation to experiment and computer

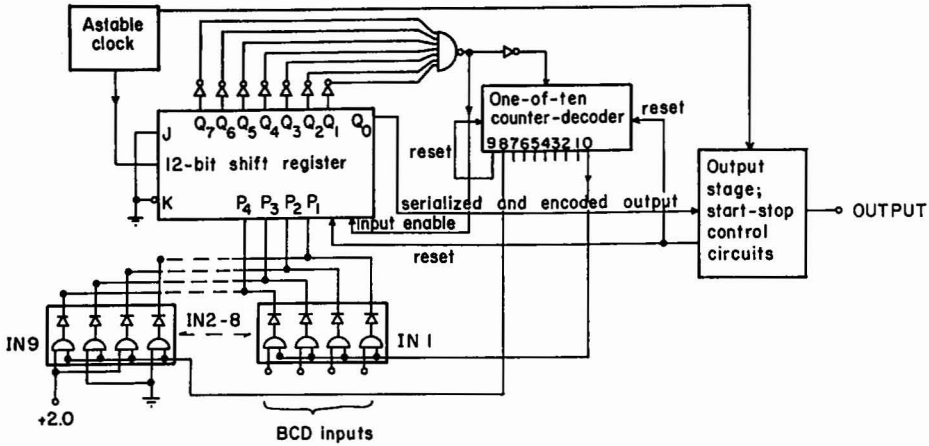

Figure 2. Functional diagram of P-S converter

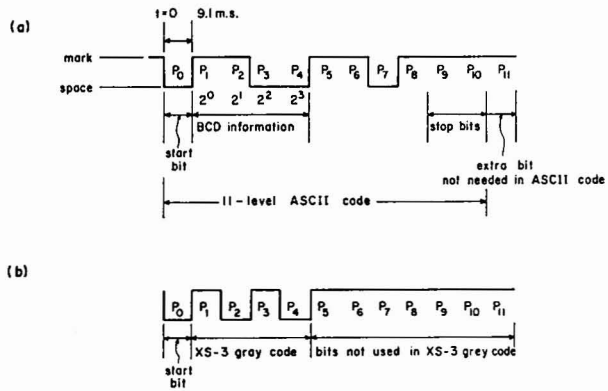

Figure 3. Current wave form for decimal three

a. ASCII Code
b. XS-3 Gray Code with start bit

word length selector switch is available on the front panel which may be used to shorten the output word length to 6 or 4 decimal digits per word.

Figure 4 shows the detailed schematic of the converter. The various blocks are as follows: 1, astable master clock; 2, input; 3, shift registers; 4, digit selector; 5, start, stop synchronization; 6, stop signal generator; and 7, word length selector.

This P-S converter can be adapted readily to much faster data acquisition systems than a teletype by changing the clock rate of the astable master clock. Clock rates up to 1.2 MHz (100,000 12-bit words per second) have been employed successfully. The inexpensive input diodes used in this design determine the upper clock rate, a limitation not considered serious since this clock rate is already 100,000 times faster than the transmission rate of conventional teletypes. Although the instrument was designed primarily for use with data acquisition systems accepting ASCII Code, minor modifications will make it adaptable to other codes if necessary. Figure 3 shows two of many coding systems that may be handled by the instrument. No provision has been made in this design for generation of carriage return and line feed as the teletype is used primarily to provide data acquisition on punched paper tape. However such special characters can be generated but at an increase in cost and complexity that depends on the format desired.

The P-S converter can be built for a total component cost of less than $150 including a well-regulated IC-power supply constructed with Fairchild, U6E7723393 voltage regulator (*1*). The components were assembled on a total of four PC

(1) Fairchild Semiconductor, Mountain View, Calif., Semiconductor Integrated Circuit Data Catalog (1970).

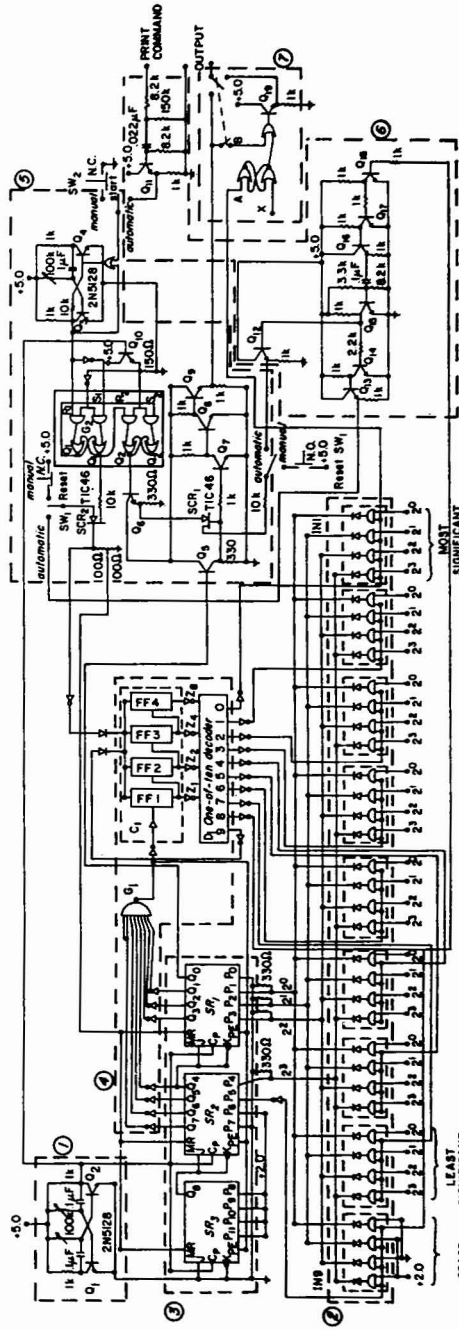

Figure 4. Schematic diagram of parallel-to-serial converter

Boards. The boards are approximately $5^1/_2 \times 7 \times {}^1/_{16}$ inches. The 5-volt power supply for the converter is on a separate circuit board with an edge type connector, so that it can be used interchangeably with other equipment. The circuit boards were mounted in a $7^1/_2 \times 13 \times 9$-inch shadow cabinet box with the necessary switches, indicators, and jacks mounted on the front panel. The complete parts list, as well as copies of the PC masterpositives, are available on request. With master-positives, construction time is estimated to be about 20–25 man-hours.

RECEIVED for review August 24, 1970. Accepted November 20, 1970. Work supported in part by research grant from the Pacific Northwest Pulp and Paper Association.

Ceramic Pressure Device for Preparation of Known Gas Concentrations at the 100 Parts-per-Million Level

Herman D. Axelrod, Ronald J. Teck, and James P. Lodge, Jr.
National Center for Atmospheric Research, Boulder, Colo. 80302

Raymond H. Allen
R. H. Allen Co., Boulder, Colo. 80302

RECENT EMPHASIS on the preparation of known diluted gas streams for the calibration of equipment and the evaluation of analytical techniques has been in the area of 1 ppm (parts per million) and below. O'Keeffe and Ortman (*1*) have described a Teflon (Du Pont) permeation tube for the production of small quantities of gases. Axelrod *et al.* (*2*) have used a gas dosing device for similar purposes. Neither of these systems, however, is useful for concentrations in the 10 to 1000 ppm range. This area is of interest to those who wish to simulate stack sample concentrations. The common technique for the preparation of higher levels has been the use of a mechanically driven syringe to introduce large quantities of the test gas into the sample stream. A complete review of the syringe and other techniques has been presented by Lodge (*3*). An alternate procedure to injection by a syringe is to force gas through a finely drawn capillary from a high pressure tank. Drawbacks to this technique include changes in the capillary due to accumulation of particulate matter, and the capillary's fragility.

Below is described a device which can be used for the production of gases in the 10 to 1000 ppm range. Instead of the capillary, a porous ceramic frit is faced to heavy-wall glass tubing and attached to a high pressure gas cylinder containing the test gas. The pressure behind the frit can be adjusted by a regulator to provide precise flows of test gas. The surface of the frit is swept with a diluting gas, such as nitrogen or air, and the total output can then be passed through a manifold for sampling. This enables the experimenter to produce a variety of gas concentrations in a dynamic system and thus to simulate stack effluences.

Figure 1 shows a model of the dilution system. The ceramic frit can be varied in length to give various flows for a given regulator pressure. The frit material is made of Mullite or Aluminate ceramic, available from the Coors Porcelain Co., Golden, Colo. The device is easy to construct, and, if made with heavy-wall glass, can withstand pressures greater than 20 psig.

Because the device is constructed from glass, there is always a danger of explosion from the pressurization of the test gas. Therefore, the device should be placed in a hood and wrapped with tape or metal gauze or kept behind a safety shield. An alternate precaution would be to place a pressure safety valve in the system with appropriate controls for venting noxious gases. It is, of course, obvious that each device should be pressure tested prior to use.

The diluter is far less expensive than the typical mechanically driven syringe system, and is more reliable than the capillary because the gas is dispersed through many holes in the porous material rather than through one small capillary hole which can become damaged or altered.

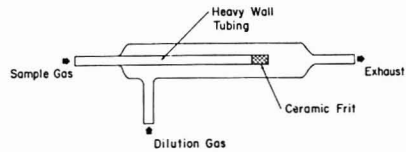

Figure 1. Ceramic gas dilution device

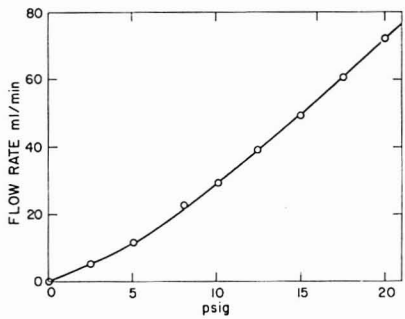

Figure 2. Typical calibration curve for ceramic gas dilution device

The calibration of the flow of test gas through the frit in relation to the regulator pressure can be accomplished through the use of a wet test meter or a soap bubble flow meter. Either of these will give accurate results. Figure 2 shows a typical calibration curve for a hollow Mullite ceramic cylinder section 3 mm long, 6 mm in diameter, and 2-mm-wall thickness. By varying the pressure behind the frit and the flow rate of the diluting gas, the experimenter can produce various concentrations of test gas. Similarly, altering the diameter and thickness of the ceramic frit will also change the flow rate. For an accurate system, a flowmeter would be needed for the diluting gas, but once the frit had been calibrated, further calibration would not be needed.

(1) A. E. O'Keeffe and G. C. Ortman, ANAL. CHEM., 38, 760 (1966).
(2) H. D. Axelrod, J. B. Pate, W. R. Barchet, and J. P. Lodge, Jr. *Atmos. Environ.*, 4, 209 (1970).
(3) J. P. Lodge, Jr., "Air Pollution," Vol. II, 2nd ed., A. C. Stern, Ed., Academic Press, New York, N. Y., 1968, p 465.

RECEIVED for review November 9, 1970. Accepted December 10, 1970. The National Center for Atmospheric Research is sponsored by the National Science Foundation.

AMERICAN CHEMICAL SOCIETY

"Primary Publications on Microfilm"

Your Key to—

- Dramatic savings in archival space and dollars.
- Faster access to needed data.
- Unlimited distribution of copyrighted scientific data.

ACS publications in the program:

JOURNAL OF THE AMERICAN CHEMICAL SOCIETY (1879-1969)
INDUSTRIAL & ENGINEERING CHEMISTRY (1909-1969)
CHEMICAL & ENGINEERING NEWS (1923-1969)
ANALYTICAL CHEMISTRY (1929-1969)
JOURNAL OF PHYSICAL CHEMISTRY (1896-1969)
JOURNAL OF AGRICULTURAL & FOOD CHEMISTRY (1953-1969)
JOURNAL OF ORGANIC CHEMISTRY (1936-1969)
JOURNAL OF CHEMICAL AND ENGINEERING DATA (1956-1969)
CHEMICAL REVIEWS (1924-1969)
JOURNAL OF CHEMICAL DOCUMENTATION (1961-1969)
INDUSTRIAL & ENGINEERING CHEMISTRY—FUNDAMENTALS (1962-1969)
INDUSTRIAL & ENGINEERING CHEMISTRY—PROCESS DESIGN AND DEVELOPMENT (1962-1969)
INDUSTRIAL & ENGINEERING CHEMISTRY—PRODUCT R & D (1962-1969)
BIOCHEMISTRY (1962-1969)
INORGANIC CHEMISTRY (1962-1969)
JOURNAL OF MEDICINAL CHEMISTRY (1959-1969)
CHEMISTRY (1962-1969)
ENVIRONMENTAL SCIENCE & TECHNOLOGY (1967-1969)
ACCOUNTS OF CHEMICAL RESEARCH (1968-1969)
MACROMOLECULES (1968-1969)

For information on "ACS Primary Publications on Microfilm", write or call:

Mr. George Virvan
Special Issues Sales
American Chemical Society
1155 16th Street, N.W.
Washington, D.C. 20036
(202-737-3337)

45.201 grams of priceless information...

...about Mettler's full line of 11 digital readout, high-speed, top-loading balances are contained in our newest catalog. Units that weigh unknowns, batch weigh, checkweigh, weigh-in, and weigh below the balance. Weigh fast—up to 5 items in 60 seconds. Weigh accurately—precision to one part in several hundred thousand. Extremely high reproducibility. Very-easy-to-read digital readout. Available in metric and other calibrations. For a catalog contact Mettler Instrument Corporation, Box 100, Princeton, New Jersey 08540. 609-448-3000.

Mettler

Circle No. 123 on Readers' Service Card

USE
ANALYTICAL CHEMISTRY'S
NEW FOLD-OUT READER SERVICE REPLY CARDS.

YOUR REQUEST FOR FREE DATA IS COMPUTER PROCESSED FOR FAST ACTION.

Analytical Chemistry **MARCH 1971** Valid through MAY 31, 1971

NEW PRODUCTS, CHEMICALS, LITERATURE: 401 402 403 404 405 406 407 408 409 410 411 412 413 414 415 416 417 418 419 420 421 422 423 424 425 426 427 428 429 430 431 432 433 434 435 436 437 438 439 440 441 442 443 444 445 446 447 448 449 450 451 452 453 454 455 456 457 458 459 460 461 462 463 464 465 466 467 468 469 470 501 502 503 504 505 506 507 508 509 510 601 602 603 604 605 606 607 608 609 610 611 612 613 614 615 616 617 618 619 620 621 622 623 624 625 626 627 628 629 630 631 632 633 634 635 636 637 638 639 640

ADVERTISED PRODUCTS: 1 2 3 4 5 6 7 8 9 10 11 12 13 14 15 16 17 18 19 20 21 22 23 24 25 26 27 28 29 30 31 32 33 34 35 36 37 38 39 40 41 42 43 44 45 46 47 48 49 50 51 52 53 54 55 56 57 58 59 60 61 62 63 64 65 66 67 68 69 70 71 72 73 74 75 76 77 78 79 80 81 82 83 84 85 86 87 88 89 90 91 92 93 94 95 96 97 98 99 100 101 102 103 104 105 106 107 108 109 110 111 112 113 114 115 116 117 118 119 120 121 122 123 124 125 126 127 128 129 130 131 132 133 134 135 136 137 138 139 140 141 142 143 144 145 146 147 148 149 150 151 152 153 154 155 156 157 158 159 160 161 162 163 164 165 166 167 168 169 170 171 172 173 174 175 176 177 178 179 180 181 182 183 184 185 186 187 188 189 190 191 192 193 194 195 196 197 198 199 200 201 202 203 204 205 206 207 208 209 210 211 212 213 214 215 216 217 218 219 220 221 222 223 224 225

PRODUCT CAPSULES
(Write in key numbers): _____

Name_____ Position_____

Company_____

Street_____

City_____ State_____ Zip_____

FIRST CLASS
PERMIT NO. 25682
PHILADELPHIA, PA. 19101

BUSINESS REPLY CARD

NO POSTAGE STAMP NECESSARY IF MAILED IN THE UNITED STATES

POSTAGE WILL BE PAID BY

ANALYTICAL CHEMISTRY
P. O. Box #8660
Philadelphia, Pennsylvania 19101

Analytical Chemistry **MARCH 1971** Valid through MAY 31, 1971

NEW PRODUCTS, CHEMICALS, LITERATURE: 401 402 403 404 405 406 407 408 409 410 411 412 413 414 415 416 417 418 419 420 421 422 423 424 425 426 427 428 429 430 431 432 433 434 435 436 437 438 439 440 441 442 443 444 445 446 447 448 449 450 451 452 453 454 455 456 457 458 459 460 461 462 463 464 465 466 467 468 469 470 501 502 503 504 505 506 507 508 509 510 601 602 603 604 605 606 607 608 609 610 611 612 613 614 615 616 617 618 619 620 621 622 623 624 625 626 627 628 629 630 631 632 633 634 635 636 637 638 639 640

ADVERTISED PRODUCTS: 1 2 3 4 5 6 7 8 9 10 11 12 13 14 15 16 17 18 19 20 21 22 23 24 25 26 27 28 29 30 31 32 33 34 35 36 37 38 39 40 41 42 43 44 45 46 47 48 49 50 51 52 53 54 55 56 57 58 59 60 61 62 63 64 65 66 67 68 69 70 71 72 73 74 75 76 77 78 79 80 81 82 83 84 85 86 87 88 89 90 91 92 93 94 95 96 97 98 99 100 101 102 103 104 105 106 107 108 109 110 111 112 113 114 115 116 117 118 119 120 121 122 123 124 125 126 127 128 129 130 131 132 133 134 135 136 137 138 139 140 141 142 143 144 145 146 147 148 149 150 151 152 153 154 155 156 157 158 159 160 161 162 163 164 165 166 167 168 169 170 171 172 173 174 175 176 177 178 179 180 181 182 183 184 185 186 187 188 189 190 191 192 193 194 195 196 197 198 199 200 201 202 203 204 205 206 207 208 209 210 211 212 213 214 215 216 217 218 219 220 221 222 223 224 225

PRODUCT CAPSULES
(Write in key numbers): _____

Name_____ Position_____

Company_____

Street_____

FIRST CLASS
PERMIT NO. 25682
PHILADELPHIA, PA. 19101

BUSINESS REPLY CARD

NO POSTAGE STAMP NECESSARY IF MAILED IN THE UNITED STATES

POSTAGE WILL BE PAID BY

ANALYTICAL CHEMISTRY
P. O. Box #8660
Philadelphia, Pennsylvania 19101

Analytical Chemistry **MARCH 1971** Valid through MAY 31, 1971

NEW PRODUCTS, CHEMICALS, LITERATURE: 401 402 403 404 405 406 407 408 409 410 411 412 413 414 415
416 417 418 419 420 421 422 423 424 425 426 427 428 429 430 431 432 433 434 435 436 437 438 439 440 441 442
443 444 445 446 447 448 449 450 451 452 453 454 455 456 457 458 459 460 461 462 463 464 465 466 467 468 469
470 501 502 503 504 505 506 507 508 509 510 601 602 603 604 605 606 607 608 609 610 611 612 613 614 615 616
617 618 619 620 621 622 623 624 625 626 627 628 629 630 631 632 633 634 635 636 637 638 639 640

ADVERTISED PRODUCTS: 1 2 3 4 5 6 7 8 9 10 11 12 13 14 15 16 17 18 19
20 21 22 23 24 25 26 27 28 29 30 31 32 33 34 35 36 37 38 39 40 41 42 43 44 45 46
47 48 49 50 51 52 53 54 55 56 57 58 59 60 61 62 63 64 65 66 67 68 69 70 71 72 73
74 75 76 77 78 79 80 81 82 83 84 85 86 87 88 89 90 91 92 93 94 95 96 97 98 99 100
101 102 103 104 105 106 107 108 109 110 111 112 113 114 115 116 117 118 119 120 121 122 123 124 125 126 127
128 129 130 131 132 133 134 135 136 137 138 139 140 141 142 143 144 145 146 147 148 149 150 151 152 153 154
155 156 157 158 159 160 161 162 163 164 165 166 167 168 169 170 171 172 173 174 175 176 177 178 179 180 181
182 183 184 185 186 187 188 189 190 191 192 193 194 195 196 197 198 199 200 201 202 203 204 205 206 207 208
209 210 211 212 213 214 215 216 217 218 219 220 221 222 223 224 225

PRODUCT CAPSULES
(Write in key numbers): _____ _____ _____ _____ _____ _____ _____ _____

Name_____ Position_____

Company_____

Street_____

City_____ State_____ Zip_____

FIRST CLASS
PERMIT NO. 25682
PHILADELPHIA, PA. 19101

BUSINESS REPLY CARD

NO POSTAGE STAMP NECESSARY IF MAILED IN THE UNITED STATES

POSTAGE WILL BE PAID BY

ANALYTICAL CHEMISTRY
P. O. Box #8660
Philadelphia, Pennsylvania 19101

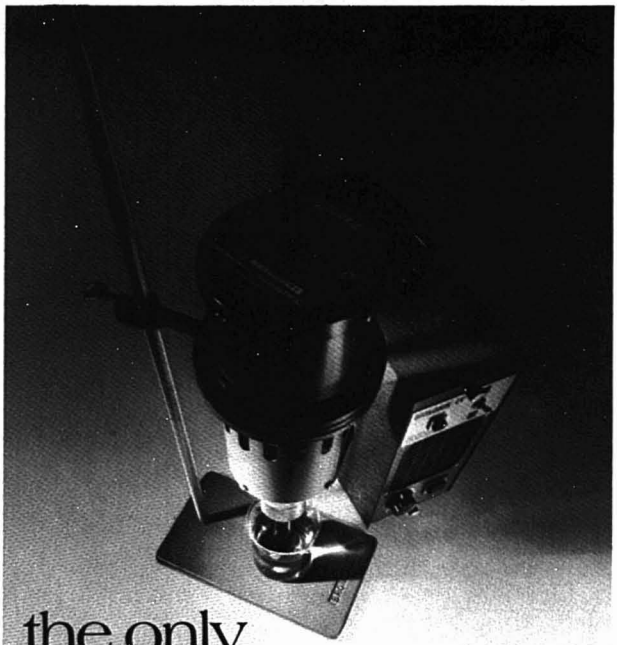

the only space-age ultrasonic probe that keeps its cool!

BIOSONIK® IV **No more overheating** . . . an exclusive internal heat sensing circuit monitors the heat *everywhere*—probe, transducer assembly, even the generator. Automatically shuts generator down if heat exceeds operating parameters . . . while cooling fans operate. Switches back on when circuitry is cooled.

Dual power ranges . . . Hi/Lo power indicators color coded to match the color coded titanium probe tips. No more remembering and playing percentages—use full scale of intensity level dial with either range.

Plus . . . □ 300 watts of acoustical energy □ Power automatically attenuated when probe is separated from media □ Fully automatic tuning for peak performance □ Completely portable—modular construction, advanced miniaturized space-age circuitry, lightweight—so small it occupies negligible lab space □ Up or down probe operation □ Complete selection of tips and cooling accessories. Ask for a demonstration. Call your Bronwill dealer or write:

Bronwill

Bronwill Scientific, Inc.
Box 7824—Rochester, New York 14606

Circle No. 25 on Readers' Service Card

here is the first complete, self-contained Mercury Analyzer System. Coleman Model MAS-50/$875.

It can be used in many scientific fields. Pollution: Air, water, food, soil, tissue. Clinical: Urine, blood, tissue. Industrial Control: Food, metal, soil, fertilizer.

- Sensitivity .01 μg of mercury, equal to or better than A.A.
- Direct reading in μg of mercury
- Hatch and Ott procedure

This compact, self-contained, low-cost system makes determination of mercury in solids and solutions, organic or inorganic, or in air an inexpensive routine procedure. Coleman MAS-50 is so easy to operate, no special training is required. **Call or write today for free bulletin A-350**

PERKIN-ELMER

COLEMAN INSTRUMENTS
42 MADISON STREET
MAYWOOD, ILLINOIS 60153
(312 345-7500)

A DIVISION OF THE PERKIN-ELMER CORPORATION

COLEMAN

"Visit Booths F–19, 20–Federated Meeting"

Circle No. 36 on Readers' Service Card

Potentiometric recorders: here's the picture.

Shown here, a portrait of all there is to know about potentiometric recorders. All from Sargent-Welch. And each deserves its own personality profile:

Model SRG: The basic recorder, distinguished by its advanced performance. Seven pre-calibrated spans. Three chart speeds. Guarded circuits and filtered inputs. Accuracy: ±0.25%. Reproducibility: ±0.1%. Full-scale pen response: Less than one second. Basic price: $1025.

Model DSRG: The SRG times two. That is, a dual-pen recorder, with two linear channels, for recording two time-related variables, side by side or overlapping, on the same chart. Same matchless performance as the SRG, but only a few inches wider. Think of it as a space- and paper-saver. Basic price: $1800.

Model SRLG: The SRG taken one step further, with the addition of a logarithmic function. Eminently suited, therefore, for recording (say) the log of absorbance with a spectrophotometer. Precision, non-circular gears — which do the job much better than electrical approximations to the log function. Basic price: $1325.

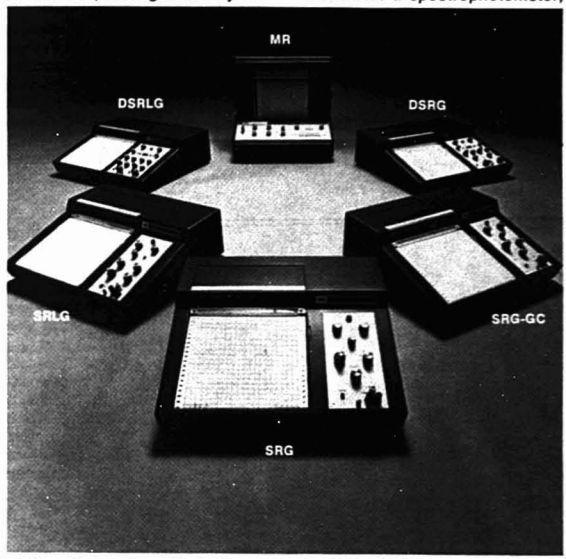

Model DSRLG: Another logical move. Two SRLG's in one dual-pen recorder. Think of what that means if you work with a spectrophotometer, photometer, or densitometer — simultaneous recording of both transmittance *and* absorbance. Or linear/log recording of any two time-synchronized variables. Basic price: $2225.

Model SRG-GC: Something special, for use with a gas chromatograph. Fast response, high AC rejection, floating input, three chart speeds, and continuously variable wide-range spans. Optional integrator for precise measurement of areas under recorded curve. Basic price: $1025 (with integrator, $1820).

Model MR: The ultimate recorder? Perhaps. Few can match it for precision, speed, sensitivity, and versatility. Measures and records (vs. time) any variable that can be translated into voltage or current, *or* that can be time-related by synchronous drive. Twelve ranges, twelve speeds. Basic price: $2850.

As we said, a complete picture of a complete line.

Now read the book.

0-214

Still, in all fairness, one picture and these few words don't do justice to our complete line of recorders. So we've prepared a fully illustrated, 30-page catalog. It's yours, without obligation, for returning the coupon. Do it now.

I'd like a copy of your recorder catalog. I'm especially interested in:

- ☐ Model SRG Recorder
- ☐ Model DSRG Dual-Pen Recorder
- ☐ Model SRLG Linear-Log Recorder
- ☐ Model DSRLG Dual-Pen Linear-Log Recorder
- ☐ Model SRG-GC Recorder for Gas Chromatographs
- ☐ Model MR Multi-Range Recorder

Name _____ Title _____

Organization _____

Address _____

City _____ State _____ Zip _____

Telephone _____ AC

SARGENT-WELCH

Scientific instruments, apparatus, chemicals.
Sargent-Welch Scientific Company
7300 N. Linder Ave., Skokie, Illinois 60076

Chicago/Anaheim/Birmingham/Cincinnati
Cleveland/Dallas/Denver/Detroit
Springfield, N.J./Toronto/Montreal/Vancouver

Circle No. 170 on Readers' Service Card

THE UN-NEW SPECTROPHOTOMETER

The Model 2400-S is the latest result in the continuing development of Gilford UV-Visible Spectrophotometers. And, in keeping with our long-standing practice, it does NOT obsolete existing Gilford equipment. The Model 2400-S is *still* designed around our unique linear absorbance photometer, it is *still* compatible with existing Gilford accessories for gel scanning, thermal denaturation studies, column monitoring, etc. And, it *still* gives you

FLEXIBILITY TO MEET YOUR GROWING NEEDS

gilford®

GILFORD INSTRUMENT LABORATORIES, INC., OBERLIN, OHIO 44074 • GILFORD EUROPE, S.A. • 74 RUE M.S.DEFRESNE • 94 VITRY-SUR-SEINE, FRANCE

See us at Pittsburgh Conference (Booth 608) and FASEB (Booths F & G, 31 & 32)

Circle No. 77 on Readers' Service Card

NEW PRODUCTS

Instruments

Field emission scanning electron microscope, the CWIKSCAN/100 offers better than 200-Å resolution; specimen image is continually displayed at the flicker-free TV scanning rate: 30 picture frames per sec. Useful magnifications range from 12× to 100,000×. Key element of the system is a high intensity field emission electron gun. Price of the system is under $30,000, console mounted. Coates & Welter Instrument Corp. 408-296-3363 **401**

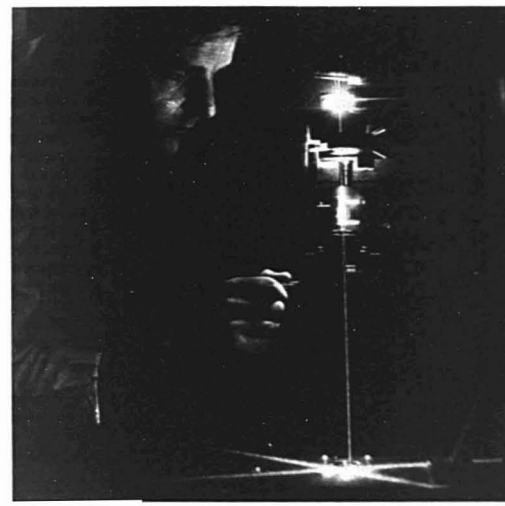

Model 25–400 Raman spectrometer of modular design is a digital laser-Raman instrument. Digital readout in both frequency and intensity makes computerization economical and relatively simple. This high resolution double spectrometer has the longest focal length of any commercially available Raman instrument; focal length is 1.0 meter; effective aperture, f/8.7. Other features include resolution exceeding 0.25 cm^{-1} or 0.1 Å; very low stray light, better than 1×10^{-10}, 15 cm^{-1} from parent line; complete elimination of line-distorting coma; large sample chamber; room for two lasers; and many optional components. Price ranges from $28,000 to $30,000 owing to modular design with many variables. Jarrell-Ash Div., Fisher Scientific Co. 412-391-1330 **402**

Gas chromatography instrument system which frees the analytical chemist from programming and provides high quality data consists of an interface for each chromatograph, a data processor, a teletype terminal, and the manufacturer's prepared software. Capable of handling 1 to 8 gc's, the system can be applied to existing instruments. The basic system in its minimum configuration operates with a 4K memory (expandable to 12K in 4K increments), input/output boards (space for 5, 1 board handles either 1 or 2 gc's or 1 teletype), and the data terminal teletype. Perkin-Elmer programs are stored in the core of the processor; they are prepared in-house at PE in a system which simulates the small processor in a large time-shared computer system. The terminal is equipped with a paper tape reader-punch to output the processed data according to user requirements and to allow the user to communicate with the system in providing the analytical methods. The gc interface converts gc data to digital form at the chromatograph and sends the raw data to the processor. The price of the basic system for use with a single gc is less than $16,000; a system to accommodate 2 gc's can cost less than $18,000; the system can also be leased. The aim of this system is to optimize the processing of gc data in the most economical way. Perkin-Elmer. 203-762-6972 **403**

PRECISION APPARATUS

AND INSTRUMENTS FOR THE ANALYTICAL CHEMIST

460 SERIES ROTAMETERS

These Flowmeters offer:

- Wide angle visibility.
- High accuracy.
- Tubes are easily removed by hand for cleaning or changing flow range.
- Available in stainless steel or aluminum, with or without the control valve.
- Clear plastic shield provided for tube protection and safety.

CHROMATOGRAPHY COLUMNS

- High Pressure columns manufactured of precision bore glass tubing and stainless steel fittings.
- Features:
  On-column sample injection.
  Contamination free construction.
- A complete line of low cost ascending or gravity feed columns with associated sample injection syringes.

"SOLV-SEAL" JOINT

GLASS & QUARTZ JOINTS

Offered in Three Styles

- Standard Taper, Ball & Socket and the patented "Solv-Seal".
- Easy disassembly.
- Interchangeable parts.
- Quartz or Borosilicate glass units in stock.
- Low cost.
- Immediate delivery.

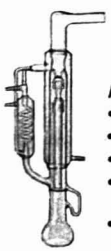

CUSTOM GLASS & QUARTZ

Fabrications to Meet all Analytical Requirements

Mastercraftsmen Glass-Blowers of:

- Condensers.
- Distilling apparatus.
- Extraction apparatus.
- Custom applications & special requirements.
- Guaranteed workmanship.

Lab-Crest / ANDREWS SCIENTIFIC DIVISION FISCHER & PORTER COMPANY

1531 COUNTY LINE RD., WARMINSTER, PA. 18974

Circle No. 82 on Readers' Service Card

from the prime source

HEAVY OXYGEN PRODUCTS

What is in a label? If that label bears the signature "Research Products Division, Miles Laboratories, Inc." the product is from the basic manufacturer, Miles-Yeda Ltd. and you have complete assurance of product integrity and service.

Miles-Yeda Ltd. of the Research Products Division is a *basic* producer of Oxygen-17 and Oxygen-18 products. More than 62 different isotopic oxygen products, in a broad range of enrichments, are available for research. Whatever your needs, consult MILES for these unique stable isotopes.

For a complete listing of isotopes, both stable and radiolabeled, see Catalog B and Supplement 69-B.

MILES

RESEARCH PRODUCTS DIVISION
MILES LABORATORIES, INC.
P.O. BOX 272, KANKAKEE, ILLINOIS 60901 U.S.A.

Circle No. 130 on Readers' Service Card

LEEMA I (low electron energy molecular analyzer) performs both identification of the sample constituents plus quantitative analysis. Applications range from physical chemistry research in elastic and inelastic scattering to routine chemical analysis of unknown mixtures of gases and liquids, monitoring of impurities in gas streams, and ppm trace analysis in air. LEEMA I scans the energy range from 0 to 100 eV at rates from 50 sec per V to 0.1 sec per V; energy resolution of the electron beam scattering cell is better than 0.01 eV; electron energy is stable to better than ±0.01% over 10 hr, not including the contact potential. The oven-mounted inlet system uses septum injection and is heatable to 150°C for vaporization of liquids and volatile solids. The complete instrument costs $24,500. ARIS, Tracor, Inc. 512-926-6130 **404**

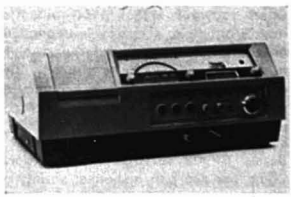

DB-GT ultraviolet spectrophotometer is a double beam replica grating instrument for measuring linear transmittance or absorbance over the 190- to 700-nm range; included is built-in scale expansion and zero suppression. Accuracy is rated at ±0.5% *T* throughout the wavelength range. Other features include a choice of tungsten or deuterium light sources and photometric range to 150% *T* or 3 A using zero suppression. Beckman Instruments, Inc. 714-871-4848 **405**

The Model 50-120 electronics system is designed to operate with any of the company's LEED-Auger electron optics models. These optics systems consist of a source of primary electrons and a 4-grid, hemispherical, retarding field electron energy analyzer. The standard source is an electron gun which provides a beam that is incident normal to the sample surface and is also capable of operation at low energies. The use of the gun and hemispherical energy analyzers allows the same electron optics to be used for both LEED surface structural analysis and Auger spectroscopy surface chemical analysis.

In addition, the company makes a Cylindrical-Auger electron optic system which is able to analyze Auger electrons in the 0- to 2000-eV range with better than 1% resolution and sufficient sensitivity for continuous oscilloscope display. Literature on these systems is available from the company. The Cylindrical-Auger system costs $6950 with coaxial electron gun; LEED-Auger electron optics models range in cost from $4600 to $5000; the Model 50-120 electronics system to be used with these instruments costs $11,500. Physical Electronics Industries, Inc. 612-941-5540 **406**

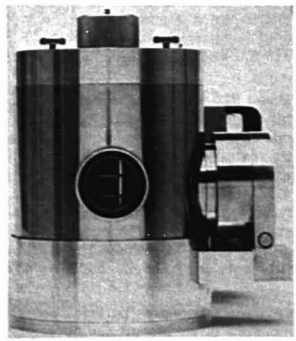

Model 150 field emission electron gun can focus an intense beam of electrons one millionth of an inch in diameter. Although designed for use with scanning electron microscope, other versions of the electron gun are under development for other applications. The electron gun can accelerate electrons up to 20,000 volts and produce a spot size of less than 200 Å; with high quality electron objective lens, spot sizes of less than 10 Å can be obtained. The gun chamber (6 in. in diam and 9 in. high), is an ion getter pumped to better than 5×10^{-9} torr. Model 150 is priced under $20,000. Coates & Welter Instrument Corp. 408-296-3363 **407**

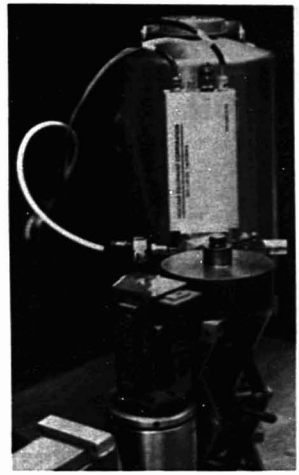

Nondispersive X-ray powder diffractometer based on a new approach to X-ray diffraction permits an analysis time of 1 min and a sample changing time of 15 sec. If data is reduced by on-line computer, reduced data for all elements and compounds are available immediately. The complete system includes an X-ray tube and generator, sample chamber, silicon solid-state detector, multichannel analyzer, and strip chart recorder. Price is less than $20,000. Readout is available on computer-compatible punch paper tape or magnetic tape. Spectrum stripping capability is available, thus unfolding the complex diffraction spectra. Nuclear Equipment Corp. 415-591-8203 **408**

The HR-300 is a 300-MHz nmr system offering the highest performance available in a commercial high resolution spectrometer system. The superconducting magnet used produces a field of 70,500 gauss. This system features: very high sensitivity; field and frequency sweep operation with sweep widths to 20 kHz; increased chemical shift; high stability; large flat-bed recorder; built-in probe positioning device for easy sample interchange; variable temperature capability; and built-in checkout system which simplifies maintenance. It is a modular system and can accept future advances made by the company. Also included is an exceptional Dewar for extremely low cryogenic material loss and a Fourier transform accessory for full compatibility with Fourier transform operation. About $220,000. Varian, Analytical Instrument Div. 415-326-4000 **409**

FEKRUMETER
LOW COST HIGH ACCURACY
DENSITY DETERMINATOR FOR SOLIDS

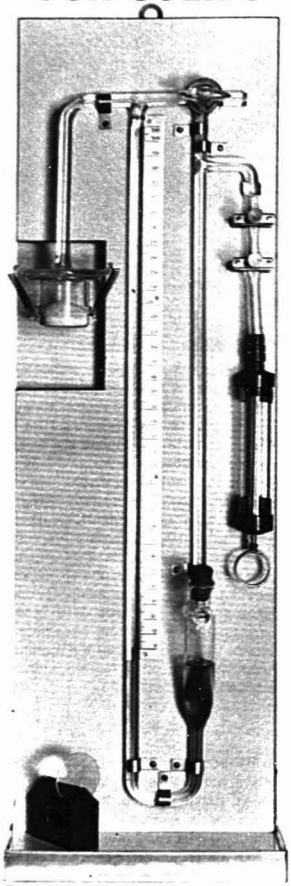

Features:
Determines actual density of sample, not apparent density.
Porous, fibrous, solid, compressed and viscous substances can be measured.
Test sample does not come in contact with liquids.
Accuracy within ±0.3-0.5%
Sample volumes from 0.2-200 ml. can be measured. Porosity can be calculated from test values obtained.
write for technical bulletin

GALLARD-SCHLESINGER CHEMICAL MFG. CORP.
584 Mineola Ave., Carle Place, N.Y. 11514
Telephone: (516) 333-5600 Telex: 126442
TWX: 212-428-0318
Circle No. 76 on Readers' Service Card

Specific Detectors and Monitoring Instruments

Model 460 gas analyzer system for SO_2 and NO_2; full scale range as low as 200 ppm; capable of continuous monitoring; used with company's 400 photometric analyzer and sampling system. $8000, less recorder. E. I. du Pont de Nemours & Co., Inc. 302-774-2358 **410**

Model 461 gas analyzer system for total oxides of nitrogen (NO, NO_2, NO_x) is a source monitor; based on the 400 photometric analyzer and sampling system. $10,500 range. E. I. du Pont de Nemours & Co., Inc. 302-774-2358 **411**

Model 450 liquid analyzer system is used to monitor trace amounts of phenols in water down to low ppb levels; based on the 400 photometric analyzer and sampling system. $9000 range. E. I. du Pont de Nemours & Co., Inc. 302-774-2358 **412**

Models 741 and 742 oxygen analyzers offer full scale sensitivity from 0 to 1% and easy-to-maintain electronic circuitry. Model 741 ($750) is a process analyzer for panel mounting; Model 742 ($795) is for weatherproof field installation. Beckman Instruments, Inc. 714-871-4848 **413**

Model 38D solid-state electronic detector for mercury and other toxic vapors operates on the uv absorption principle; the instrument measures 5 in. × 17 in. × 5 in. and weighs 8 lb; models are available with 50 mV recorder outputs; type of vapor to be monitored must be specified. Price of standard Model 38D is $895. Sunshine Scientific Instruments, Inc. 215-673-5600 **414**

CI-208A laboratory particle counter monitors clean lab air for suspended particles as small as 0.5 micron; the instrument draws in 0.25 ft^3 per min and counts and sizes particles. Less than $4000. Climet Instruments, Inc. 408-736-6950 **415**

Dissolved oxygen analyzer, small enough to hold in one hand, is a temperature-compensated unit; can be calibrated in air, gives instant, continuous, remote readout of dissolved oxygen concentrations. . The Series DOA555 is designed for aeration processes, sewage treatment plants, fisheries, stream pollution measurement, etc. Under $400. BioMarine Industries, Inc. 215-687-2800 **416**

OM322 monitor displays absolute oxygen concentration directly on a 0 to 40% scale; audible alarms are triggered when oxygen level falls below a selected concentration or rises above a certain point; temperature compensation is automatic. Under $400. BioMarine Industries, Inc. 215-687-2800 **417**

Accurate measurements of mercury in solution can be made down to 0.1 ppb with an accessory apparatus for use with the company's atomic absorption instruments. Price for the accessory which is available from scientific supply houses is about $150. The procedure is based on that of Hatch and Ott [Anal. Chem. **40** (14), 2085 (1968)] and is available as a reprint from Perkin-Elmer. "Mercury Package," Perkin-Elmer Corp. 203-762-6972 **418**

New hollow cathode line for atomic absorption, designated WL-22847A, provides superior stability of operation with low noise making. Mercury can be determined down to 10^{-10}-gram level. Prices are in the $115 range each. Westinghouse Electric Corp. 412-255-3322 **419**

Flat-pack infrared detectors, suitable for use uncooled or with thermoelectric cooling, include a spectral response range of 4 to 6 microns; a sensitive area of 230 sq microns. MCT 77°K detectors operate in the 8- to 13-micron region; typical response time at 77°K is 300 nsec. The company, Mullard, Inc., of England, supplied other detectors also. Priced under $750. Optoelectronics, Inc. 707-763-4181 **420**

Recorders and Accessories

Chart recorder Model 8500 potentiometric principle; accuracy is dependent on the potentiometer and the stability of the reference voltage supply. The potentiometer used has an accuracy of ±0.3%. $635. Matheson Gas Products. 201-933-2400 **421**

Series GP702 servographic recorders; 20-in. per sec pen response; variety of chart speeds and full scale spans; total limit of error less than 0.5%; true potentiometric servonull system. $325 to $425. Precision Standards Corp. 714-546-0431 **422**

MP-1027 10-in. potentiometric strip chart recorder includes six electronic speeds (standard 0.1 to 2 in. per min); seven calibrated ranges plus variable range, 10 mV to 1000 mV; error less than ±0.25% with 0.1% repeatability. Standard model is $542. McKee-Pedersen Instruments. 415-937-3630 **423**

Whatman®

This is the table of Contents from the new Whatman Products Catalog.

TABLE OF CONTENTS

Introduction 1
How to Select the Correct Filter Paper 2
General laboratory filtration 2
High efficiency filtration 2
Purity 2
Special properties of filter papers 3
Retention 3
Qualitative Filter Papers 4
Standard filter papers 4
Wet strengthened filter papers 4
Folded filter papers 4
Quantitative Filter Papers 5
Ashless filter papers 5
Hardened ashless filter papers 5
Low ash filter papers 6
Hardened filter papers 6
Glass Fiber Papers 7
General Properties Table 8
Specialties
Absorption accessories 9
Filtering aids 9
Extraction thimbles 9
Phase separating paper 9
Glass fiber filter tube systems 10
Gamma-12 in line filters 10
Laboratory filter tubes 10
Indicator and test papers 11
Papers for Chromatography and Electrophoresis 12
Whatman cellulose chromatography papers 12
Physical properties table 12
Special patterns 13
Paper chromatography sheets and rolls .. 13
Physical properties table 14
Ion exchange papers 14
Adsorbent loaded papers 14
Glass fiber papers 14
Column chromatography products 15
Non-ionic celluloses 15
Cellulose ion exchangers 15
Series I Original fibrous 15
Series II Advanced fibrous 16
Series III Microgranular 16
Whatman precision chromatography columns 17
Thin layer chromatography products 18
Cellulose powders 18
Cellulose ion exchanger for TLC 18

SOLE DISTRIBUTOR IN NORTH AMERICA

reeve angel 9 BRIDEWELL PLACE, CLIFTON, NEW JERSEY 07014

Please send me my free copy of the new Whatman Products Catalog.

Name_____

Institution_____

Address_____

City_____ State_____ Zip_____

Circle No. 159 on Readers' Service Card

®Registered trademark of W. & R. Balston, Ltd., Springfield Mill, Maidstone (Kent), England.

Series 380 X-Y recorders use standard 8½- × 11-in. chart paper; spans from 1 mV to 1 V per inch. $595 to $695. Laboratory Data Control. 203-226-0759 **424**

Model 603-500 oscillocorder has writing speeds of 1, 5, or 10 mm per sec.; vertical sensitivity of 10 V or 2.5 V full scale; linearity of better than 1%. $985. Ultek Div., Perkin-Elmer. 415-321-4117 **425**

Multigraphic recorder can be used with electronic and pneumatic recorders simultaneously; models are available with four or six channels; recording modules (galvanometers or pneumatic) are the same size. Prices vary from $1500 to $3000 depending on how the equipment is used. C. H. Stoelting Co. 312-722-3833 **426**

Portable, self-contained, plug-in, time-base generator produces seven calibrated sweeps from 0.5 sec per in. to 50 (0.25 to 25 sec per cm) for use with the company's Plotamatic X-Y recorders. Accuracy is ±3% full scale; Price is $180. Bolt, Beranek and Newman, Inc. 714-546-5300 **427**

Model 1100 graphic plotter is X-Y recorder which accepts 8-level ASCII code at teleprinter rates, 10 characters per sec or 30 characters per sec; and plots lines up to 3 in. long between points, on a 4-digit absolute coordinate basis; plotting area is 10 × 15 in.; the instrument is compatible with time sharing or direct computer interface. $5500. Brush Div., Gould, Inc. 216-696-0330 **428**

Kipp Micrograph BD-5 offers three knobs to select any one of 24 ranges as sensitive as 20 μV; one of 10 chart speeds, and three input modes; automatic zero suppression feature permits automatic expansion of scale by seven times with no decrease in precision, accuracy, or rapid response time; accessories and other important features are available. $1730. Enraf-Nonius, Inc. 516-741-0430 **429**

Model NSC strip chart recorder uses a rugged galvanometric movement and can be programmed for different input variables easily by changing a printed circuit board; the recorder is programmable for up to six independent variables at one time and has special uses in pollution control, water and air. Single-channel instruments start at $535; six-channel instruments from $635 or $750 for six different inputs. Elnik Instruments, Inc. 201-779-7388 **430**

New toploading balance is fast, accurate...yet RUGGED!

New Torbal ET-1 toploader (160g capacity, 1 mg accuracy) makes accurate weighing easier and more foolproof than ever before.

NEW EASE thanks to complete digital display without the use of optical projections or verniers to read, no estimating.

NEW EASE because the one piece construction of the exclusive Torsion weighing mechanism has no knife edges to chip, wear or collect dust—hence there's no loss in accuracy.

NEW EASE—thanks to the electronic null readout feature, the ET-1 is not affected by sensitivity changes—from temperature or humidity variations or effects of foreign matter or wear. As long as you can see the null needle move for a 1.0 mg weight change, then a difference of 1.0 mg in weight-reading *means* 1.0 mg—today, tomorrow, next month, next year.

NEW EASE because the ET-1's Torsion mechanism is far less affected by *vibration* than optical balances. You can use an ET-1 in conditions other balances can't take.

NEW EASE thanks to out-of-level accuracy. For minor changes in level of the ET-1, *zero point does not change.*

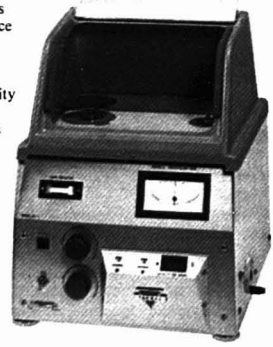

WRITE FOR FREE BROCHURE.

THE TORSION BALANCE CO. Clifton, New Jersey. Sales offices in Chicago, Ill.; San Mateo, Cal.; Pittsburgh, Pa.; Montreal, Quebec; and Windsor, England. Balances manufactured in Waterford, Ireland and Clifton, New Jersey.

TORBAL

Circle No. 175 on Readers' Service Card

Miscellaneous

Linomat quantitative sample streaker for tlc delivers uniform sample application without endpoint retardation; streak width adjustments to 0.5 mm are possible; a stream of nitrogen dries the solvent during sample application. $1495. Camag, Inc. 414-476-7655 **431**

Model RC-9 pH meter is for monitoring pH where a permanent record and control functions are needed; the instrument combines an automatic strip chart recorder and line-operated indicating controller; recorder has double range switch for readings of 2 to 12 pH, or 4.5 to 9.5 pH; readability is 0.02 pH unit ($555). The company also makes a digital pH meter, Model DC-5 ($535) with four-digit Nixie tube readout. This instrument is readable to 0.01 pH from 0 to 14 pH. Industrial and Mill Supply Co. 516-427-4354 **432**

Type 40 pH meter uses a 6-in. meter from 0 to 14 and mV range of ±700 mV; completely battery-operated and portable; accurate to 0.05 pH. Price is $79; with a B-J combination electrode, $99. Chemtrix, Inc. 503-648-1434 **433**

pH Digitrol combines a recording pH meter with two continuous pH records on chart paper; standard range is 2 to 12; other range covers any two-pH scan; an electronic digital pH meter, directly readable to 0.01 pH over the 0- to 14-pH range; and a controlling pH meter with single pole, double throw, adjustable high and low contacts for simple on/off control or alarm. $895. Analytical Measurements, Inc. 201-273-7500 **434**

Model ACM 1 acid concentration meter determines acid strength even in solutions containing buffering salts or metal ions. A semiconductor probe, sensitive to hydrogen ion activity in the presence of fluoride ion, is immersed in a sample treated with fluoride salts. The instrument operates over a standard range of 0 to 0.05*N*. $390. Cedar Grove Operations, Beckman Instruments, Inc. 201-239-6200 **435**

D25D color and color difference meters give instantaneous displays of color and color difference values to the second decimal place; pushbuttons select any of 12 color scales; polarity is included in the five-tube Nixie readout. $4975 to $5850. Hunter Associates Laboratory, Inc. 703-591-5310 **436**

MK-3, new addition to the HAEMACOUNT line of medical instrumentation, in conjunction with the company's MK-DB computer printer will provide four hematological tests in minutes; they are red and white cell counts, and hemoglobin and hematocrit. MK-3 costs $3800; MK-DB, $4500. General Science Corp. 203-377-3784 **437**

Operational computer is a modular scientific computational tool that is patchboard-programmed with standard analog computer techniques yet performs calculations digitally; it is ideal for use in solving differential equations. Denelcor, Inc. 303-892-0987 **438**

MiniAC is a 10-V analog/hybrid computer specifically designed for educational use; outstanding features include modular expansion up to 27 amplifiers, standard digital voltmeter, optional logic expansion, and others. $5000 to $10,000. Electronic Assoc., Inc. 201-229-1100 **439**

Uniflow fiberglass fume hoods now come in 5-ft high models; units are also available in 4- and 6-ft sizes with service fixtures, work surfaces, base cabinets, and venting accessories. About $800 to $1200. Hemco Corp. 816-254-1111 **440**

Model 8430 gas chromatograph uses elution method of separation; instrument's accuracy depends on the temperature controller, sampling valve, two needle valves. Unit weighs only 25 lb and measures 25 × 16 × 12¾ in. $650. Matheson Gas Products. 201-933-2400 **441**

B-20A refrigerated centrifuge offers large volume and high resolution capabilities from 1000 to 20,000 rpm; six heads, including two swinging buckets, zonal rotors, most ultracentrifuge angle rotors, and a broad range of accessories are available; gravities to 45,500 xg; maximum volume, 1500 ml (6 × 250). $3085. Damon Corp. 617-449-0800 **442**

Forced-flow electrophoresis pilot plant, Model 510, can be used for separation and purification of biological materials such as gamma globulin (from horse serum), enzymes (from fermentation broths); also filtration of difficult-to-clarify materials. $16,000. Canalco, Inc. 301-427-1515 **443**

Crystal polishing kit for infrared transmitting crystals, including KRS-5 is supplied with grinding powder compound and Barnsite. $60. Wilks Scientific Corp. 203-838-4537 **444**

Four models of hydrogen purifiers with capacities ranging from 1 to 24 liters per min are available for use in gc, metallurgy, electronics, semiconductors, hydrogeneration, catalytic processes, etc. $710 to $1815. Matheson Gas Products. 201-933-2400 **445**

Automatic composite sampler for liquids collects a composite sample up to two liters over a variety of sampling periods from a positive head of 15 meters to a suction head of 5 meters. Optional accessories include sample temperature control, external trigger facility, depth sampler and probe, and shut-off valve. $850 to $875. Testing Machines, Inc. 516-598-1400 **446**

Models 8287 and 8289 flow controllers adjust and maintain small gas flows for analytical instrumentation; features include a nonrotating needle control valve, bubble-tight O-ring seal shut-off, and integral precision needle valve with nonreversing flow characteristics and high turns-to-lift ratio. Prices are $87 and $175 depending on features. Matheson Gas Products. 201-933-2400 **447**

Model 7000 constant-flow sampler provides flow air sampling in the range of 3 to 6 cfm; useful for sampling airborne contamination in labs, hospitals, clean rooms, and processing areas. $330. Misco Scientific. 415-843-1282 **448**

Model 7670 automatic sampler completely automates measurement of sample volume and injection into the company's gas chromatographs; capable of unattended operation for as many as 36 consecutive samples. Hewlett-Packard, Avondale Div. 215-268-2281 **449**

Two new data acquisition and control subsystems for use with the PDP-8 family of small computers are designed for use where low-level analog signals are encountered or when discrete digital input/output information is required. UDC8 costs $3500+; modules vary from $120 to $480; AFC8 fully implemented with 120 channels costs $13,200. Digital Equipment Corp. 617-897-5111 **450**

CORCO
REAGENT ACIDS

Certified reagent-grade acids available in quantities from pints to tank wagons:

HCl HNO3 H2SO4 NH4OH

Other Corco acids:
Acetic • Fuming Nitric • Fuming Sulphuric • Formic • Hydrofluoric • Perchloric • Phosphoric

• Assured quality
• Prompt delivery

Corco produces only reagent- and electronic-grade chemicals.

Let us know your requirements.

CORCO
CHEMICAL CORPORATION
Manufacturers of Reagent and Electronic Chemicals
Tyburn Road & Cedar Lane, Fairless Hills, Pa. 19030
Phone: (215) 295-5006

Circle No. 37 on Readers' Service Card

Only one company can meet any gas customer's need

MATHESON GAS PRODUCTS
A Division of Will Ross, Inc.
East Rutherford, N.J.; Cucamonga, Calif.; Gloucester, Mass.; Joliet, Ill.; LaPorte, Texas; Morrow, Ga.; Newark, Calif.; Whitby, Ont.

Acetylene, Purified
Air
- Dry
- Ultra Zero
- Zero Gas

Allene
Ammonia
- Anhydrous
- Ultra High Purity

Argon
- High Pressure
- High Purity
- Prepurified
- Research
- Ultra High Purity
- Zero Gas

Arsine
Bis (trifluoromethyl) Peroxide
Boron Trichloride
- C.P.

Boron Trifluoride
- C.P.
- Technical

Bromine Pentafluoride
Bromine Trifluoride
Bromotrifluoroethylene
1,3-Butadiene
- C.P.
- Instrument
- Research

Butane
- C.P.
- Instrument
- Research
- Technical

1-Butene
- C.P.
- Research

cis-2-Butene
- C.P.
- Research

trans-2-Butene
- C.P.
- Research

cis and trans-2-Butene
- C.P.

Calibrating Gas Mixtures
Carbon-14 Gas Mixtures
Carbon Dioxide
- Bone Dry
- Coleman Instrument
- Commercial
- Research

Carbon Monoxide
- C.P.
- Commercial
- Research
- Technical
- Ultra High Purity

Carbonyl Fluoride
Carbonyl Sulfide
Chlorine
- High Purity
- Research

Chlorine Trifluoride
2-Chloro-1, 1-difluoroethylene
Chlorotrifluoroethylene
Cyanogen
Cyclopropane
Deuterium
- C.P.
- Technical

Deuterium Chloride
Deuterium Fluoride
Deuterium Selenide
Deuterium Sulfide
1,2-Dichloro-1, 2-difloroethylene
Difluorodimethylsilane
1,1-Difluoroethylene
1,2-Difluoroethylene
Dimethylamine
Dimethyl Ether
2,2 Dimethylpropane
- C.P.
- Research

Ethane
- C.P.
- Research
- Technical

Ethyl Acetylene
Ethyl Chloride, U.S.P.
Ethylene
- C.P.
- Research
- Technical

Ethylene Oxide
Fluorine
2-Fluoropropene
"Freon-11"
"Freon-12"
"Freon-13"
"Freon-13 B1"
"Freon-14"
"Freon-22"
"Freon-113"
"Freon-114"
"Freon-114 B2"
"Freon-116"
"Freon-C-318"
Geiger Counter Gas Mixtures
"Genetron-21"
"Genetron-23"
"Genetron-115"
"Genetron-142 B"
"Genetron-152A"
"Genetron-1113"
Germane
Helium
- High Pressure
- High Purity
- Matheson Grade
- Research Grade
- Ultra High Purity
- Zero Gas

Heptafluorobutyronitrile
Hexafluoracetone
Hexafluorobutadiene-1,3
Hexafluorobutyne-2
Hexafluorocyclobutene
Hexafluoropropene
Hydrogen
- Extra Dry
- High Pressure
- Prepurified
- Research
- Ultra High Purity
- Zero Gas

Hydrogen Bromide
Hydrogen Chloride
- Electronic
- Technical

Hydrogen Fluoride
Hydrogen Iodide
Hydrogen Selenide
Hydrogen Sulfide
- C.P.
- Technical

Iodine Pentafluoride
Isobutane
- C.P.
- Instrument
- Research
- Technical

Isobutylene
- C.P.
- Research

Krypton, Research
Krypton-85 Mixtures
Manufactured Gas
- Type B
- Type C

Methane
- C.P.
- Commercial
- High Pressure
- Research
- Technical
- Ultra High Purity

Methyl Acetylene
Methyl Bromide
3-Methylbutene-1
- C.P.
- Research

Methyl Chloride
- High Purity

Methyl Fluoride
Methyl Mercaptan
Monoethylamine
Monomethylamine
Natural Gas, Texas
Neon
- Purified
- Research

Neon-Helium Mixtures
Nickel Carbonyl
Nitric Oxide
- Technical

Nitrogen
- Extra Dry
- High Pressure
- High Purity
- Prepurified
- Research

Nitrogen Dioxide
Nitrogen Trioxide
Nitrosyl Chloride
Nitrous Oxide
Oxygen
- Extra Dry
- Research
- Ultra High Purity

Ozone
Pentafluoroethyl Iodide
Pentafluoropropionitrile
Pentafluoropropionyl Chloride
Perfluorobutene-2
Perfluoropropane
Phosgene
Phosphine
Phosphorus Pentafluoride
Propane
- C.P.
- Commercial
- Instrument
- Natural
- Research

Proportional Counter Gas Mixtures
Propylene
- C.P.
- Research
- Technical

Silane
Silicon Tetrafluoride
Sulfur, Dioxide
- Anhydrous
- Commercial

Sulfur Hexafluoride
Sulfur Tetrafluoride
Sulfuryl Fluoride
Trichlorosilane
1,1,1-Trifluoroacetone
Trifluoroacetonitrile
Trifluoracetyl Chloride
Trifluoromethylhypofluorite
Trifluoromethyl Iodide
2-Trifluoromethylpropene
Trifluoronitrosomethane
3,3,3-Trifluoropropene
3,3,3-Trifluoropropyne
Trimethylamine
Trimethylsilane
Vinyl Bromide
Vinyl Chloride
Vinyl Fluoride
Vinyl Methyl Ether
Vinyltrifluorosilane
Xenon, Research Grade

and others in as many as 7 sizes

Write for answers to your gas problems.
Address: Helen, Matheson Gas Products,
P.O. Box 85, East Rutherford, New Jersey 07073.

Matheson, of course

Circle No. 124 on Readers' Service Card

28-70G

NEW CHEMICALS

4-Aminophthalhydrazide

A new reagent for membranous ultrastructural demonstration of certain enzyme activities in electron microscopic techniques is available. Freshly diazotized 4-aminophthalhydrazide is said to represent an advance over previously available reagents since these gave a droplet distribution of enzyme activities which could not be related to underlying ultrastructure in a straightforward manner. The reagent is used as a coupling agent to demonstrate with substrates that yield 4-methoxy-2-naphthylamine or 2-naphthylamine. It produces reddish azo dyes with membranous distribution since 4-aminophthalhydrazide imparts lipophobic properties to the dyes. Polysciences, Inc. 215-343-6488 **501**

Chelating Agents

Unusual complexants for lead: 1,3-diaminopropan-2-ol-tetraacetic acid, *N*-(2-hydroxyethyl)iminodiacetic acid, and nitrilotripropionic acid are new additions for the company's long-range chelate synthesis program. Data and bibliography sheets are available. La-Mont Laboratories. 214-235-4463 **502**

Vapor Deposition Materials

Standard elements and a variety of alloy compositions produced by zone refining or vacuum sublimed to provide low gas content and splatter-free deposition are available. Alkaline earth impurities to 1 ppm or less on most materials (34 in all) are the general rule. Imanco. 914-356-3331 **503**

Ultrapure Metals

Gallium metal and arsenic metal are both now available, 99.9999+% pure. These metals are specifically made for the preparation of gallium arsenide single crystals. Apache Chemicals. 815-877-7858 **504**

Improved Graphite

A new graphite is available in three grades: standard, purified, and spectroscopically pure. This graphite is used for crucibles and resists deterioration with many corrosive reagents at elevated temperatures. It will contain concentrated sulfuric acid for more than two hours at 200°C, boiling concentrated nitric acid, molten sodium peroxide, and lithium tetraborate. Poco Graphite, Inc. 214-526-3430 **505**

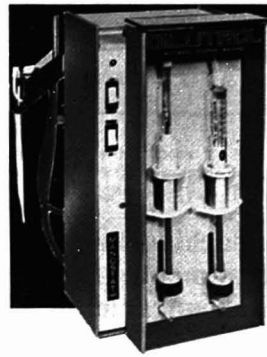

NEW AUTOMATIC dilutrol®

ELECTROMAGNETICALLY CONTROLLED DILUTING MACHINE
safely handles acids, bases, solvents without error, waste, contamination or effort...every time!

Pushbutton-controlled DILUTROL does away forever with cross-contamination and waste of precious sample! Provides precise pickup of adjustable predetermined amount of sample with repeatable accuracy of ±0.3%, continuous diluent delivery with an accuracy ±0.5%. Permits dilution ratio up to 1,000:1. Rinsing action of diluent cleans tip for next cycle! Removable dispensing head rotates through 120 degrees, makes possible operation at distances up to 4 feet. The exclusive electromagnetic check valve assures positive repeatability and provides exclusive airlock between sample and diluent; fluids touch only Teflon and glass. Operates on 115 volts AC. Available either with 4 ML, 1 ML, or .5 ML sample capacity and 10 ML diluent capacity . . . Priced from $495.00.

DILUTROL
AUTOMATIC HAND OPERATION

Available through your laboratory supply dealer

MANOSTAT *DIVISION OF GREINER SCIENTIFIC CORP.*,
20 N. Moore St., Dept. 521, New York, N.Y. 10013, Phone (212) 966-1190

Circle No. 74 on Readers' Service Card

FASTEST GUN IN THE LAB!

Make an instant aerosol with any sprayable liquid! Apply reagents and indicators for thin layer and paper chromatography. Especially useful when reagents must be mixed for immediate or same-day use. Hundreds of everyday uses from sophisticated analyses to aerosol testing—and even touch-up painting.

Quixpray has *POWER!* It has all the power that's needed to produce a true aerosol mist from sprayable liquids. Other sprays, to hold down "flooding" with thin liquids, merely use a lot less pressure. We have a better approach. Each **Quixpray** head is equipped with a full bore dip tube for broad general use. As an accessory we offer a set of two flow regulating dip tubes—(1) Fine, for water-thin liquids and (2) Extra Fine for very thin liquids such as organic solvents. Now—whether you're spraying an alcoholic solution on a paper chromatogram or touch-up paint on a lab bench—you can be sure you're getting the complete dispersion produced by full power.

Quixpray Kit has one complete spray unit with 8 extra jars for storing stock liquids and 6 propellant refills. Also included are the two special flow regulating dip tubes mentioned above.

11160 **Quixpray Kit** $18/kit; 12 kits, $16/each
11175 **Quixpray**, Propellant refills, 15 oz Case of 12 $16.80/case
11170 **Quixpray**, Jars only, 4 oz Case of 12 $4/case
11165 **Quixpray**, Single spray unit (Head, propellant and jar with full bore dip tube) $3.25/unit
11180 **Quixpray**, Flow regulating dip tubes Set of 2 $3/set

PIERCE CHEMICAL COMPANY
P.O. Box 117 Rockford, Illinois 61105 U.S.A.
PHONE 815/968-0747 TWX 910-631-3419

Circle No. 142 on Readers' Service Card

VARIAN'S $5,000 NMR SYSTEM:

the teaching machine that moonlights as a chemical analyst

1.1. Past experience plus new design technology yields EM-300 system. Thanks to the efforts of Varian Anaspect, a moderate performance, 30 megahertz NMR system in the $5,000 price range is now a reality (Fig. 1, below). Varian Anaspect is a natural extension of the fine work carried on by Varian's Analytical Instrument Division, long recognized as a world leader in the design and manufacture of highly sophisticated research instrumentation.

1.2. Inherent value of such a low cost, moderate performance NMR system. A system such as Varian Anaspect's EM-300 serves two important purposes:

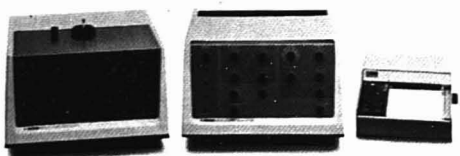

Figure 1. Photograph of Varian Anaspect's new 30 MHz EM-300, a $5,000 moderate performance NMR system designed for both instruction and routine chemical analysis applications. Shown here with optional recorder.

First, as a viable, simply designed and highly dramatic training tool for instruction in both basic chemistry and experimental method, which performs an analysis in less than five minutes (Fig. 2, above); and... Secondly, as a highly stable, minimum-adjustment tool for routine analysis which frees sophisticated machines for more complex chemical problems.

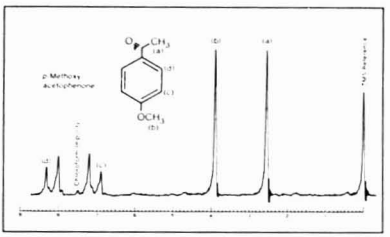

Figure 2. Spectrum for p-methoxyacetophenone shows performance for a typical compound of Varian Anaspect's low cost 30 MHz NMR system, the EM-300.

Understandably, it is no small task to translate the electronics of systems ranging from $20,000 to $100,000-and-up into a moderate performance, low price version such as the EM-300. It requires not only a complete understanding of the technique, but a keen sensitivity for the needs of student, instructor and chemical analyst who will be the end users.

1.3. Spectra, design information available. Complete information on the new EM-300 NMR system as well as typical spectra are yours for the asking. Simply write on your letterhead to: Varian Anaspect, 611 Hansen Way, Palo Alto, California 94303.

varian anaspect

Figure 3. Varian Anaspect, which has made low cost moderate performance instrumentation available to students, instructors and analytical chemists, is a natural extension of the fine work being carried on by Varian's Analytical Instrument Division.

Circle No. 187 on Reader's Service Card

Vital discipline . . .
Vital journal . . .

Biochemistry

The fastest growing journal in the field . . . annually offers over 5400 pages of *original* research in *all areas* of fundamental biology.

Concentrating on manuscripts that generate new concepts and experimental approaches, **Biochemistry** is not merely a depository of scientific data. It is a highly readable and informative publication of the American Chemical Society with an exceptionally clear and well designed format. Color stereophotography is used for illustrative clarity.

Some 30 to 40 papers, biweekly, reflect the strong relationship between chemistry, biochemistry and the other biological sciences.

Subject matter includes enzymes—proteins—carbohydrates—lipids—nucleic acids and their metabolism—genetics—protein biosynthesis—and other rapidly expanding fields.

You'll find **Biochemistry** keeps you current on the most recent research findings. To order your personal subscription, just complete and return the form below.

American Chemical Society
1155 Sixteenth Street, N.W.
Washington, D.C. 20036

Please enter my subscription to **Biochemistry** at the rates checked below.

ACS Members:
- ☐ U.S. $20
- ☐ Canada, PUAS $23
- ☐ Other Nations $23.50

Nonmembers:
- ☐ U.S. $40
- ☐ Canada, PUAS $43
- ☐ Other Nations $43.50

☐ Bill me ☐ Bill employer
☐ Payment enclosed
(Payable to American Chemical Society)

Name

Title

Employer

Address: ☐ Home ☐ Business

City State/Country Zip

Nature of employer's business?
- ☐ Manufacturing or processing
- ☐ Academic
- ☐ Government
- ☐ Other

(Please indicate)

☐ I am an ACS member
☐ I am not an ACS member

Payment must be made in U.S. currency, by international money order, UNESCO coupons, U.S. bank draft; or order through your book dealer.

Note: Subscriptions at ACS Member Rates are for personal use only. K2C

MANUFACTURERS' LITERATURE

Lab Computer Handbook. A 300-page handbook describes hardware and software features and uses of PDP-12 lab computer systems. Digital Equipment Corp., 146 Main St., Maynard, Mass. 01754. 617-897-5111

Photon Counting Catalog. Four pages picture, describe, and price the company's digital synchronous computer; amplifier discriminator; data converter console; power supply console; and PM tube housings. SSR Instruments Co. 213-451-8701 **601**

RI Monitor. Four pages detail a differential refractive index monitor designed for use in liquid chromatography for elution profiles, control process streams, and density gradient composition in labs and industry. Pharmacia Fine Chemicals, Inc. 201-469-1222 **602**

Selection Electrodes. Bull. 7145-A, 10 pages, describes 17 selective ion electrodes for use with expanded-scale lab pH meters. Clinical and research models are covered and typical applications and performance information are given. Beckman Instruments, Inc. 714-871-4848 **603**

Biochemical Research Catalog. Some 1600 products for research, including the life sciences, are listed in a first-edition catalog. Emphasis is on biochemicals such as peptide substrate, chemicals for radioimmunoassay, derivatization reagents for gc analysis of steroids, and other products. Research Plus Laboratories, Inc. 201-627-8800 **604**

Colorimeters for Pollution Testing. A 6-page folder gives information on the company's direct-reading engineer's lab for field testing of water and the DR colorimeter test center which performs 52 different water and wastewater tests. Hach Chemical Co. 515-232-2533 **605**

Laboratory Catalog. A 1176-page catalog contains more than 20,000 items of scientific instruments, apparatus, and lab furniture. It is alphabetically arranged, profusely illustrated, and has both alphabetical and numerical indexes. Curtin Scientific Co. 713-923-1661 **606**

Sputter Ion Gun and Control Unit. Four pages picture, give design features, and specifications for Models 04-131 sputter ion gun and Model 20-005 control unit. Physical Electronics Industries, Inc. 612-941-5540 **607**

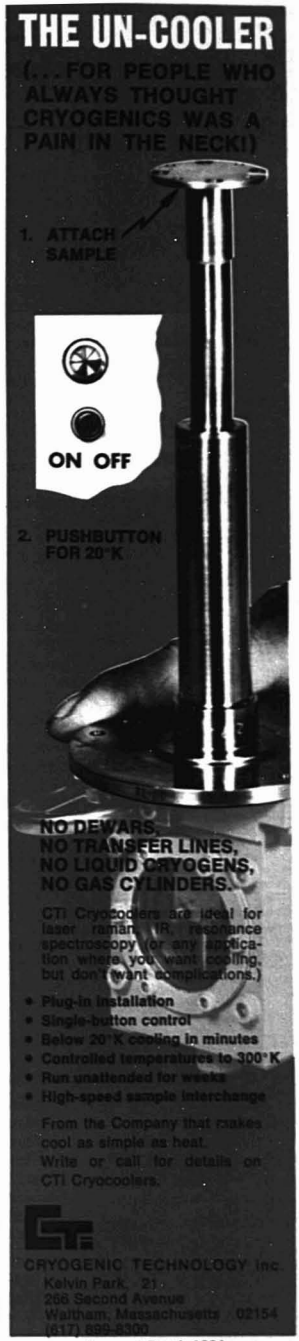

See us at Booth 1624
Pittsburgh Conference
Circle No. 31 on Readers' Service Card

Take new Heath Spectrophotometry for fast, fast relief

These are trying times... especially if you're squeezed between a shrinking budget and expanding equipment requirements. But now there's hope for the most beleaguered... a new, low cost series of Heath modules designed for special industrial, quality control and research use. It offers the same exceptional accuracy & repeatability as our famous "701" system, plus easy user modification. Choose only the modules that suit your requirements... and get a research-quality single beam UV or VIS-near IR system on a budget that even Scrooge would ok.

UV Light Source Modules. The EU-701-91 D_2 Light Source, in conjunction with the EU-45A Power Supply, produces high, constant intensity radiation between 1800 and 4500 Å; optical output stability 0.1%. Mechanical adjustments for precise alignment. Excellent source for high-precision UV spectrophotometry & kinetic studies.

EU-701-91, 3 lbs. $195.00*
EU-45A, 9 lbs. $100.00*

Visible Near IR Light Source Modules. The EU-701-90 Tungsten Light Source and its power supply, the EU-44A, provides constant intensity radiation from 3500 Å to 2 microns. Narrow bands can be maintained to ±0.1% for long periods. Horizontal & vertical adjustments. Excellent for kinetic studies and ordinary absorption measurements.

EU-701-90, 3 lbs. $70.00*
EU-44A, 7 lbs. $70.00*

EU-701-82 Sample Cell Modules. Removable self-aligning cell holder accepts two 1-cm cells. Unique baffle design... light leakage guaranteed less than 1% of photodetector dark current. Readily modified; filter holder & aperture plate included.

EU-701-82, 4 lbs. $75.00*

PM Modules... EU-701-93 PM Housing and EU-42A HV power supply. Supplied with a selected 1P28A tube; others can be used. External programming, 20:1 to 100:1 ratio.

EU-701-93, 4 lbs. $100.00*
EU-42A, 8 lbs. $130.00*

EU-700 Scanning Monochromator. Precision Czerny-Turner optics, 350 mm, f/7, 1180 lines/mm grating. Digital remote scanning, 9 fixed rates to 20 Å/sec. Resolves to better than 1 Å.; tracks within ±1 Å. 70 lbs.... $1275.00*

Choice of readout. Options available include the EU-703-31 Photometric Meter Readout, EU-700-62 Photometric Digital Readout, EU-201V Multi-speed Log/Linear Recorder or EU-20V Multi-speed Servo Chart Recorder.

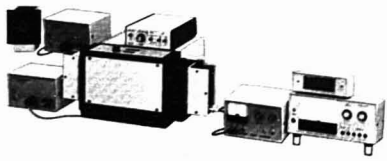

FREE
1971 Heath Scientific Instrumentation Catalog
Describes these and hundreds of other factory assembled instruments and systems...modular digital systems and plug-in logic circuit cards, spectroscopy systems and modules, Heath/Malmstadt-Enke laboratory and instruments, Heath test equipment and much more. Send coupon now or write:
Heath Company
Benton Harbor, Mich. 49022

HEATH
a Schlumberger company

HEATH COMPANY, Dept. 560-01
Benton Harbor, Michigan 49022

☐ Please send free Heath Scientific Instrumentation Catalog

Name_____

Address_____

City_____ State_____ Zip_____

*Mail order prices; FOB factory.
Prices & specifications subject to change without notice.
EK-295

Circle No. 82 on Readers' Service Card

Manufacturers' Literature

Mercury by Electrode. A 4-page reprint from *Newsletter/Specific Ion Electrode Technology*, 1970, 11(9,10)41, describes a method for measuring mercury with a Model 94-53 iodide electrode. The lower limit is 2 ppb Hg^{2+}. Orion Research, Inc. 617-864-5400 **608**

Mercury by Aa. Five pages describe a flameless method of atomic absorption that permits detection of mercury at the 0.2-ppb level. Fisher Scientific Co. 412-391-1330 **609**

Mercury Monitoring. A 9-page bulletin describes mercury pollution monitoring by atomic absorption using a gas cell technique. The article includes figures and 11 references. Instrumentation Laboratory, Inc. 617-861-0710 **610**

Lead in Blood. Six pages detail the atomic absorption spectrometric determination of lead in blood by a solid-phase sampler technique. Data and 3 references are included. Instrumentation Laboratory, Inc. 617-861-0710 **611**

Microscopy and Crystallography Courses. A 6-page catalog details the courses given by McCrone in microscopy and crystallography. McCrone Research Institute. 312-842-7105 **612**

Titrators. A 10-page bulletin describes the company's complete line of titrators, gives specifications, illustrations, and lists 16 applications. Fisher Scientific Co. 412-391-1330 **613**

Lab Apparatus and Glassblowing. A 36-page catalog describes a line of equipment ranging from sophisticated glassworking lathes and ultrasonic machining systems to common bench necessities such as calipers, asbestos, swivels, torches, etc. Wale Apparatus Co. 215-434-6688 **614**

Light Measurement. An 8-page brochure, SF70, describes a modular approach to designing specific light instrumentation needs. A typical system is graphically described; individual units are illustrated, named, and explained. Gamma Scientific, Inc. 714-279-8034 **615**

Uv-Vis Spectrophotometers. A 24-page catalog, 33-6050, illustrated with photographs and charts of typical operating curves, contains information and specifications on the Spectronic 505, 600, and precision spectrophotometers, a reflectance sphere for color specification and matching, and optional attachments. Bausch & Lomb, Inc. 716-232-6000 **616**

Particle Measurement. Eight pages cover the πMC System of specialized modules for automatic measurement of

Now . . . INSTANT
Qualitative Analysis

Both Metallic and Non-Metallic Elements.

Now you can instantly analyze practically any type of sample material. A greatly improved DIRECT VISUAL spectroscopic method is used. There is no need to dissolve sample materials.

The presence or absence of any particular element in sample materials can be determined instantly. Analyses are made using a standard low cost visual type spectroscope in combination with the unique TODD ELEMENTS ANALYZER. Send for full details.

TODD INSTRUMENT COMPANY
Cedars, Penna. 19423 U. S. A.

Circle No. 178 on Readers' Service Card

AVCO LASERS

TUNABLE • VISIBLE • ULTRAVIOLET

SEND FOR YOUR FREE INFORMATION PACKAGE TODAY!

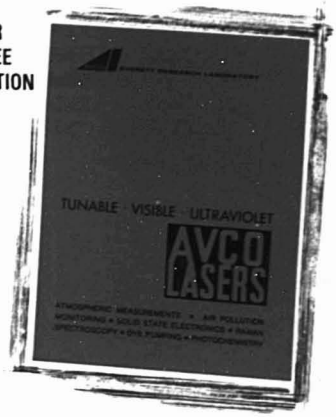

AVCO EVERETT RESEARCH LABORATORY
2385 REVERE BEACH PARKWAY · EVERETT, MASSACHUSETTS 02149

Circle No. 10 on Readers' Service Card

UC-100
Undercounter Laboratory Glassware Washer

All stainless steel, the Forma UC-100 Undercounter Laboratory Glassware Washer features direct spray from double washing arms that clean glassware in both top and bottom wash racks. It offers complete versatility in selection of wash, rinse and drying cycles, with automatic distilled water final rinse. Fits under all laboratory bench tops. Optional prolonged drying. Will operate from distilled water source as low as 2 PSI without booster pump. For complete details write Forma Scientific, Inc., Box 649, Marietta, O. 45750.

Forma Scientific

Circle No. 64 on Readers' Service Card

Perkin-Elmer's new Atomax™ lamps fit any atomic absorption instrument you use.

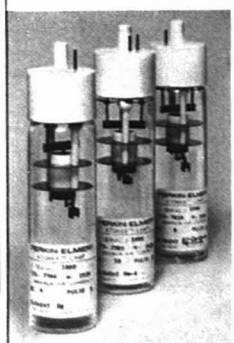

Now, no matter what AA instrument you use, you no longer have to settle for second best in lamps.

Perkin-Elmer introduces Atomax hollow-cathode lamps, directly usable in all makes of atomic absorption equipment.

Perkin-Elmer's Intensitron® lamps have long been distinguished by their brightness, spectral purity, and long life. However, they are too large for many AA's with restricted lamp space. The new Atomax lamps, with a smaller envelope solve the problem.

Atomax lamps are available for every element that can be done by atomic absorption, and also in many multi-element combinations, including the famous seven-element lamp for Ca-Mg-Zn-Cu-Fe-Al-Si.

Free Gift Offer: Send for data now and receive a free Atomax Miniature Broadband Continuum Source, which radiates between 3800 and 8000 A. It also works as a flashlight. Write Instrument Division, Perkin-Elmer Corporation, 702 Main Avenue, Norwalk, Conn. 06852.

PERKIN-ELMER

Circle No. 139 on Readers' Service Card

HAMAMATSU
Multialkali Series
PHOTOMULTIPLIER TUBES

Photomultipliers

Type	Window Type	Spectral Response	Window Material
R446	Side-on	1850～8200	UV glass
R456	Side-on	1600～8200	Quartz
R374	1⅛" Head-on	1850～8500	UV glass
R376	1⅛" Head-on	1600～8500	Quartz
R375	2" Head-on	1600～8500	Quartz

Phototubes

Type	Window Type	Spectral Response	Window Material
R314	Side-on	2000～8500	UV glass
R330	Head-on	2000～8500	UV glass
R424	Head-on	3000～8500	Borosilicate glass

HAMAMATSU offers a really wide range of photomultiplier tubes including side-on or head-on types, standard or miniature versions with photocathodes of Sb-Cs, Ag-Bi-O-Cs, Cs-Te, Bialkali, Multialkali, Au, Cu, Be and Ag-O-Cs.

Our new 1971 brochure, showing the complete line of HAMAMATSU products for modern photometry, is now ready for your approval.

Call or write to:

HAMAMATSU TV CO., LTD.
1126A, Ichino-cho, Hamamatsu-city, Japan.

HAMAMATSU CORPORATION
3000 Marcus Avenue, Lake Success, N.Y. 11040
USA Phone: (516) 354-7121

CALIFORNIA EASTERN LABORATORIES, INC.
1540 Gilbreth Road, Burlingame, Calif. 94010
Phone: 697-6670

Circle No. 84 on Readers' Service Card

particulate materials with the resolution of a microscope and the speed of a computer. Millipore Corp. 617-544-2581 **617**

Scientists' Tools. A 32-page catalog covers hundreds of unusual and hard-to-find tools useful to scientists and researchers. Typical tools are glass pliers, carbide saber-saw blades, plumb and level inclinometers, magnetic work lamps, glass drills, etc. Brookstone Co. 413-785-1551 **618**

Monochromator. Four pages picture, describe, price, and give specifications for the Minimate monochromator, a compact, general-purpose unit for lab applications. Spex Industries, Inc. 201-549-7144 **619**

Magnetic Susceptibility Measurements. A 6-page folder, Bull. 136, explains and illustrates paramagnetism, diamagnetism, and ferromagnetism, defines magnetic susceptibility, and describes the Faraday method of measuring it. Cahn Div., Ventron Instruments Corp. 213-634-7840 **620**

Photometric Log Amplifier. Bull. 57, 2 pages, describes the Model D-131 photometric log amplifier for connecting photomultiplier detectors to a wide variety of readout devices and systems. Durrum Instrument Corp. 415-321-6302 **621**

pH Products. Bull. 4111, 16 pages, covers the company's entire process pH product line and includes information on the Lazaran reference electrode, pH and ORP sensing electrodes, thermocompensators, and the Series 3 flow and submersion assemblies. Beckman Instruments, Inc. 714-871-4848 **622**

High-Purity Reagents. An 8-page reprint from *The Chemist* is titled "High-Purity Reagents for the Analysis of Lunar and Geochemical Samples." J. T. Baker Chemical Co. 201-859-2151 **623**

Pollution and Polarography. A 12-page booklet discusses the use of single-sweep cathode-ray polarography to analytical problems in water and air pollution. Also included are references and detailed procedures for mercury, arsenic, iron, nitrates, and other elements and compounds. Chemtrix, Inc. 503-648-1434 **624**

Demountable Hollow Cathode System. An 8-page brochure describes a low-cost, demountable, hollow cathode system with complete atomic source capabilities that is compatible with all aa spectrophotometers. The GloMax lamp is compared with quick-change cathodes and ordinary sealed lamps. Barnes Engineering Co. 203-348-5381 **625**

Sampling Systems. A 4-page bulletin describes sampling systems for process-type analytical instruments. Systems handle gases or liquids from single point source or multiple locations. Lockwood & McLorie, Inc. 215-675-8718 **626**

Constant Temperature Circulators. Catalog 75, 4 pages, details a full range of immersion, suspension, and reservoir-model, constant-temperature circulators capable of controlling liquid temperatures from −60° to +350°C. PolyScience-Haake, Inc. 312-475-2909 **627**

Camera Microscope. An 8-page booklet demonstrates with 35 photographs the use of the Ultraphot III camera microscope; the use of the unit as a metallograph is also shown. Carl Zeiss, Inc. 212-736-6070 **628**

Company Periodicals

Requests for copies of the following publications should be sent directly to the address shown. Business or professional letterheads are requested.

Aminco Laboratory News. Vol. 26, Nos. 3 and 4, 16 pages, includes an additional 8 pages devoted to clinical laboratory news. Lead article is on water pollution. Other articles deal with new instruments and techniques for both industry and clinical labs. American Instrument Co., 8030 Georgia Ave., Silver Spring, Md. 20910

Analog Dialogue. Vol. 4, No. 2, 16 pages, features a 3-page article on the new 5 pA FET-input IC op amp that uses laser trimming for submillivolt offsets. Other articles deal with application information, circuits, and product insights. Analog Devices, Inc., 221 Fifth St., Cambridge, Mass. 02142

Camag Bibliography Service. Nos. 21 and 22, 44 pages, feature articles on thin layer chromatography and list over 600 tlc articles from technical literature. Camag, Inc., 2855 S. 163rd St., New Berlin, Wis. 53151

Sage Commentary. Pump Report No. 4, 4 pages, includes data on new syringe pumps and an analytical proportioning tubing pump. Sage Instruments, Inc., 230 Ferris Ave., White Plains, N. Y. 10603

Gas-Chrom Newsletter. Vol. 12, No. 1, 8 pages, includes information on O-rings for gc, phenyl-substituted silicone phases, Dexsil 300 (an ultrahigh-temperature stationary phase), diene methyl esters, and galactolipids. Applied Science Laboratories, Inc., 135 N. Gill St., State College, Pa. 16801

PRODUCT CAPSULES

Short "refreshers" on last month's ads. Obtain free information on any of the products or services described by writing in the appropriate key numbers in the "Product Capsules" portion of the reply card preceding this section.

Adsorbents. 32-page book on TLC. **P 153**

Air monitors. Measures SO_2, NO_2, NO_x, H_2S, fluorides, aldehydes, or total oxidants. **P 179**

Amino acid analyzers. Complete line of automatic recording units. **P 157**

Amplifiers. Lock-in unit features many plug-in accessories. **P 56**

Balances. Electric millibalance with built-in digital voltmeter. **P 32**

Baths. 7-1/2 gallon capacity with temp range −20° to 70°C ± 0.02°C. **P 65**

Books. Infrared spectroscopy. **P 5**

Books. Introduction to basic theory and techniques of mass spectrometry. **P 5**

Books. Introduction to quantitative experimental chemistry. **P 5**

Books. 2nd edition of book on quantitative analytical chemistry. **P 5**

Books. First of 5-volume series on nuclear magnetic resonance. **P 5**

Books. Physical methods of chemistry. **P 46**

Books. Components of Scientific instruments. **P 47**

Books. Automatic recording and control, computers in chem research. **P 48**

Books. Organic solvents. **P 49**

Books. Mössbauer effect methodology. **P 149**

Books. Applications of IR spectroscopy. **P 149**

Books. Spectrochemical methods of analysis. **P 192**

Books. Laser raman spectroscopy. **P 194**

Books. Identification techniques in gas chromatography. **P 195**

Books. Organic reaction mechanisms. **P 196**

Books. Progress in separation and purification. **P 198**

Calculators. Programmable unit with 10^{-99} to 10^{+99} range. **P 127**

Calorimeters. Economy-priced unit with precision temperature control. **P 158**

Cells. Literature on precision glass and quartz cells. **P 81**

Cells. Spectrophotometer cells feature fused quartz or glass seams. **P 112**

Chemicals. Data on solvents, reagents, ethers in non-rupturable containers. **P 18**

Chemicals. Price list features ion exchange resins, anion and cation in 44 types and bead sizes. **P 30**

Chemicals. New catalog on lab, prescription, isotopically labeled chemicals. **P 133**

Chromatographs, gas. Free catalog shows model designed for life science studies. **P 19**

Chromatographs, gas. Low-cost, thermal conductivity unit with 4 tungsten-rhenium filaments. **P 72**

Chromatographs, gas. Data processing system substitutes push buttons for operating control. **P 80**

Chromatographs, gas. Automatic cycle unit has digital set control and state-of-the-art circuitry. **P 95**

Chromatographs, gas. Low-cost, dual column isothermal unit. **P 97**

Chromatographs, gas. Engineering report on portable unit for on-site analysis. **P 130**

(*Continued on page 114 A*)

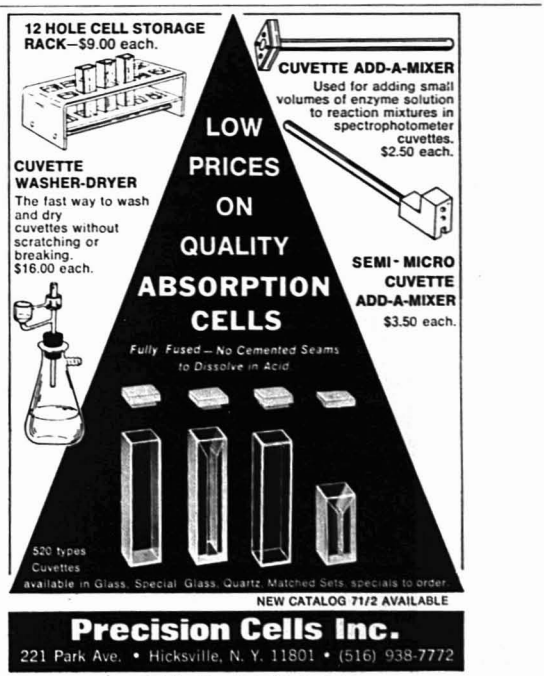

Circle No. 148 on Readers' Service Card

Product Capsules

(*Continued from page 113 A*)

Chromatographs, gas. Brochure describes recent major changes such as direct reading controls, parametric amplifier. **P 145**

Chromatographs, gas. Catalog on computer-compatible unit with built-in flow controls. **P 154**

Chromatographs, gas. Units for routine and research analyses. **P 165**

Chromatography, gas. Automatic unit operates unattended with up to 36 samples. **P 82**

Chromatography, thin layer. Applicator in 10 μl and 50 μl sizes for aqueous solutions or organic solvents. **P 8**

Chromatography, thin layer. Catalog describes plate sizes, coating thicknesses, custom adsorbents. **P 12**

Computers. 640 digital unit with up to 32k of core memory handles up to 64 channels of information. **P 55**

Coulometers. Solid state system includes potentiostat and integrator. **P 123**

Cryogenic units. Details on liquid helium transfer and cooling system. **P 4**

Cryogenic units. Coolers for laser raman, IR, resonance spectroscopy. **P 31**

Desiccants. Dries air and gases to terminal dryness of 0.005 mg per liter of gas. **P 79**

Detectors. New IR unit identifies GC peaks. Scans 2.5μ to 15μ in six seconds. **P 2**

Detectors. Bulletin describes use of ultrasensitive UV photometer in liquid chromatography. **P 39**

Determinators. New sulfur, hydrogen, and carbon units feature solid state design. **P 114**

Dewars. Literature on line of glass and plastic Dewars and accessories. **P 107**

Dilutors. Electromagnetically controlled unit handles acids, bases, solvents. **P 70**

Electronic console. Multipurpose measuring/control system. Plug-ins include amplifiers, electrometers, etc. **P 147**

Electrophoresis. Unit uses direct insertion of sample without paper or starch granules. **P 27**

Enzymes. Carrier-bound, highly active, insoluble enzymes. **P 59**

Evaporators. Variable speed flash unit has controlled heating bath. **P 28**

Evaporators. Magnetic stir-spray principle effects high evaporation rate. **P 176**

Filter papers. Free sampler includes black, white, blue papers and conversion table. **P 167**

Flowmeters. Panel or bench mounted, with or without built-in metering valves. **P 168**

Fraction collectors. Single-unit collector with base, drop detector, timer and digital counter. **P 73**

Fraction collectors. Catalog on unit featuring automatic time delay. **P 93**

Furniture. Literature on complete line from base units to fume hoods. **P 63**

Gases. 104-page catalog on specialty gases and equipment. **P 11**

Gases. Information on complete line of listed gases. **P 121**

Gases. New catalog on high purity gases, mixtures, related equipment. **P 159**

Hot & cold stages. Maintains exact temperature throughout observation. **P 10**

Indicators. 2 models of rapid-reset elapsed time indicators. **P 23**

Instrumentation. Line features calorimeters, thermogravimeters, gas and liquid flowmeters. **P 163**

Instruments. 98-page catalog on shakers, baths, coolers, cathetometers, electro-analysis apparatus. **P 57**

Integrators. Function and its integral recorded simultaneously. **P 86**

Integrators. Digital unit features push button adjustment. **P 98**

Integrators. New GC unit provides integration plus computation. **P 140**

Integrators. Digital unit prints retention time, peak area, and area total. **P 162**

Ion exchangers. Bulletin describes five different ion exchange cartridges. **P 91**

IR accessories. 96-page catalog describes line of IR spectroscopy accessories. **P 147**

Labels. Brochure on permanent, pressure-sensitive microscope slide labels. **P 135**

Lamps. Literature on demountable hollow-cathode unit for use in all makes of AA instruments. **P 16**

Lamps. Data on hollow-cathode units usable in all makes of AA equipment. **P 144**

Lasers. Information on tunable, UV and VIS lasers. **P 9**

Lubricants. Bulletin on greases to stop glassware breakage. **P 29**

Magnets. Free handbook of NMR/EPR/ESR magnets and applications. **P 193**

Melting point apparatus. Kofler unit makes determinations in one minute. **P 10**

Mercury analyzers. Compact, low-cost, self-contained unit. **P 35**

Mercury analyzers. Direct reading in micrograms of mercury and % T. Bulletin. **P 172**

Microscopes. Reichert Thermopan unit has convenient coarse and fine focusing with a single control. **P 10**

Microscopes. Catalog on line that includes all types. **P 197**

Microscopes, electron. Literature on new high resolution unit. **P 151**

NMR standards. Two new proton standards for high temperatures and aqueous solutions. **P 59**

NMR systems. Design info on new, low-cost 30 MHz unit. **P 181**

Oxygen analyzers. Uptake rates of 3 to 300 μl O_2/hr monitored with 1% accuracy. **P 200**

pH indicators. Sticks with dye bound covalently to carrier. **P 59**

pH meters. Data file on meters, accessories, selective ion electrodes. **P 22**

pH meters. Battery operated three-pound unit measures zero to 14 pH. **P 37**

pH meters. Details on six different units. **P 169**

Photomultiplier tubes. Wide range of side-on or head-on types. Brochure. **P 85**

Pipets. Literature on pipets and dilutors to fit any container. **P 113**

Polarographic analyzers. Unit has high P.P.B. sensitivity. **P 139**

(*Continued on page 116 A*)

SOME STRAIGHT TALK ABOUT WILMAD NMR SAMPLE TUBES

- For more than 15 years, Wilmad NMR sample tubes have given investigators performance which has been *consistently problem-free* as sample tubes could be. It is this *experience* and *knowledge* we offer you today.
- The prices of Wilmad NMR sample tubes have remained *consistently the same* for years.
- We *make our own* NMR sample tubes. We have never sold tubes manufactured by someone else and then *blamed them for poor quality*.
- We will match any competitive NMR tubes *at the prices you pay for them*. Then, when you are thoroughly dissatisfied, you'll order the best NMR tubes available . . . Wilmad.
- Wilmad offers the *most extensive* line of NMR *sample tubes* and *peripheral items* available today. One purchase order to one source . . . Wilmad . . . will take care of all your needs.
- In many cases, we have offered to *exchange* poor quality, competitive NMR sample tubes for ours . . . *without cost* . . . to prove the superiority of our tubes. Try us.
- If you haven't received a copy of our latest NMR Catalog, write for it today. We'll send it out by return mail.

WILMAD GLASS COMPANY, INC.

Pioneer in Glassware for NMR Spectroscopy

Route 40 & Oak Road, Buena, N. J. 08310 • Phone: (609) 697-3000

Circle No. 196 on Readers' Service Card

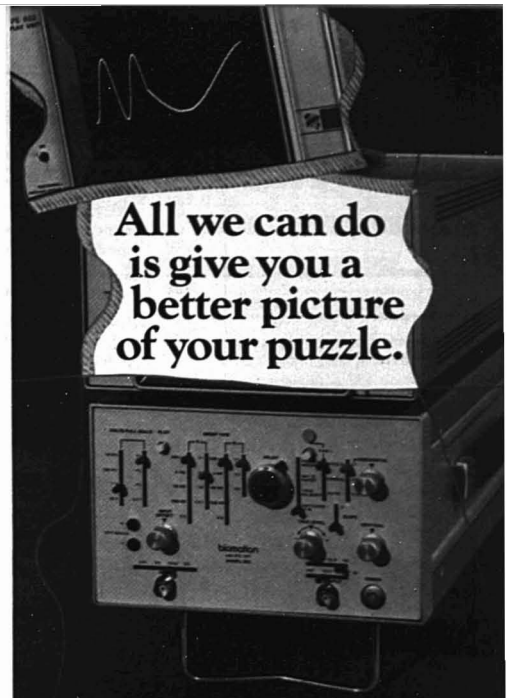

How difficult it is to record a high speed single shot analog signal! And processing the data? It's usually messy, time consuming, inefficient.

But that was before we introduced our Transient Recorders.

With these instruments you can now easily record waveshape (amplitude vs. time) information — even single transient events. This new class of instrument does it all digitally by combining triggering circuits, input amplifier, analog-to-digital converter, digital memory and appropriate readout controls.

You can even record the information preceding your trigger signal — a unique feature called pretrigger recording. That means no more delay lines or tape loops. Output controls let you observe the stored waveshape on a scope, make permanent records on a strip chart or YT recorder, or feed the digital data directly to a computer for analysis.

	Risetime	Resolution	Memory	Cost
Model 610	100 nsec (2.5 MHz bandwidth)	1.5%	128 points	$1750
Model 802	500 nsec (500 kHz bandwidth)	0.4%	1024 points	$2950

Applications? You can measure explosion shock waves; shock tube studies; T-Jump, stop flow and other reaction kinetic chemistry; plasma physics; fluorescent decay studies; automatic test systems for component testing; Lidar and other optics systems; pulsed NMR work; biomedical signal analyses, and many, many more.

Write or call today for full information. Biomation, 1070 East Meadow Circle, Palo Alto, California 94303 (415) 321-9710.

biomation

Circle No. 22 on Readers' Service Card

(Continued from page 114 A)

Potentiostats. New potentiostat/galvonstat has plug-in modules to provide flexibility in readout. **P 138**

Presses. Specs on 6 different sizes of pellet presses. **P 134**

Reagents. Catalog on reagents for TLC. **P 20**

Reagents. Literature on reagents for acrylamide-gel electrophoresis. **P 58**

Recorders. Linear servo motor keeps pen going magnetically. **P 83**

Recorders. Full range of low-cost units with 500 K input. **P 96**

Recorders. Unit provides null-balancing servo-potentiometer recording in minimum panel space. **P 108**

Recorders. Wide-chart readability in a compact case. **P 109**

Recorders. Compact unit has wide selection of ranges. **P 110**

Recorders. Unit provides recording on 5″ × 8″ file cards. **P 111**

Recorders. Unit records the logarithm of absorbance as a function of wavelength. **P 170**

Samplers. Automatic system for AA and emission analysis. **P 92**

Signal averagers. Compensates transformed spectra for frequency-dependent distortions. **P 23**

Solvents. Bulletin describes chemicals distilled in glass. **P 25**

Spectrofluorometers. Catalog on unit for fluorescence analyses. **P 64**

Spectrometers. Bulletin on new photo-electron and Auger unit. **P 3**

Spectrometers. System combines digital readout, teletype printer, and computer. **P 24**

Spectrometers. Data offered on line of 10 new units. **P 26**

Spectrometers. Bulletin on two solid-state NMR units. **P 101**

Spectrometers. Data on analytical Auger unit defines first 3 to 5 layers of a surface. **P 187**

Spectrometers, electron. Reads out binding energies of electrons with high resolution. **P 186**

Spectrometers, NMR. Data on multi-nucleus, easy-to-use unit. **P 182**

Spectrometers, x-ray. Free 17-page application guide on x-ray spectrometry. **P 105**

Spectrometers, x-ray. Info on 4 types of x-ray units. **P 143**

Spectrometers, x-ray. Technical brochures on manual and automated x-ray units. **P 171**

Spectrophotometers. Unit goes from 325 to 925 nm and has digital readout. Catalog. **P 21**

Spectrophotometers. Bulletin on new solid-state digital unit. **P 36**

Spectrophotometers. Brochure on new double beam recording unit. **P 128**

Spectrophotometers. Bulletin on UV-VIS, IR, AA units. **P 165**

Spectrophotometers, AA. Unit changes modes from AA to atomic emission at flip of switch. **P 7**

Spectrophotometers, AA. Analyzes two elements in single sample. **P 62**

Spectrophotometers, IR. New solid-state pneumatic detector has high sensitivity. **P 142**

Spectrophotometers, IR. New unit has solid-state detector circuitry. **P 150**

Spectrophotometers, UV/VIS. Unit for gel scanning, column monitoring, etc. **P 71**

Spectrophotometers, UV/VIS. New, low-cost series of modules for various uses. Free catalog. **P 87**

Spectrophotometers, UV/VIS. 4 models with double monochromators and dual beam photometric systems. **P 184**

Spectrophotometers, UV/VIS. Double-beam recording unit has prism and scale mounted on one unit. **P 199**

Spectroscopy. Literature on complete nuclear spectroscopy systems. **P 131**

Spray kits. Makes an instant aerosol with any sprayable liquid. **P 141**

Stir Plates. Catalog shows units with operating temperatures to 371°C. **P 178**

Stopcocks. Information on units made of Teflon, Viton, and Pyrex. **P 156**

Sulfur analyzers. Dry detection unit works on photometric detection principle. **P 152**

Supports, GC. Bulletin on silane-treated support material. **P 100**

(Continued on page 117 A)

CHEMICAL CAREER OPPORTUNITIES

SECTION HEAD, Analytical Toxicology — $20,000. Central N.J. Area. Ph.D. + practical experience with radioisotopes.

PRINCIPAL SCIENTISTS—$20,000. Phila. suburban area. Ph.D. + exp. in methods development, instrumentation, and familiar with F.D.A. regulations.

ANALYTICAL CHEMIST—$14,000. Central N.J. Area. B.S. Chem + 1-3 yrs. exp. in analysis and Q.C. of pharmaceuticals and cosmetics.

ANALYTICAL/Q.C. ENGINEER — $14,000. Southern Location. B.S. Chem./Ch.E. + 2-4 yrs. exp. in organics. Must know statistics and quality assurance.

To investigate these immediate career opportunities with prestige growth clients, please forward resume in confidence to **Mr. Richard Guerin, Mgr. Chemical Placement Div., EVERETT KELLEY ASSOCIATES, INC., 20th Floor, 121 South Broad Street, Philadelphia, Pa. 19107.** All fees and relocating exp. paid by client companies. (We are Exclusively an Employer FEE PAID Professional Personnel Placement Service.)

Circle No. 57 on Readers' Service Card

Product Capsules

(*Continued from page 116 A*)

Surface area analyzers. Determinations within the 0.1 to more than 2,000 m^2/gm range. **P 41**

Surface area units. Literature and technical info on instruments for characterizing physical properties of materials. **P 129**

Syringes. New high pressure (up to 300 atmospheres) GC syringe. **P 84**

Test sets. Designed to check performance of spectrophotometers and colorimeters. **P 88**

Thermal analyzers. Technical paper on thermal analysis flame ionization detector. **P 34**

Thermal analyzers. Bulletin on applications of DTA, DSC, TMA, and TGA methods. **P 45**

Thermal analyzers. Info on system featuring scanning calorimeter, TGA, and TMA. **P 146**

Thermal analyzers. Micro DTA and TGA systems from −150°C to 1500°C. **P 165**

Thermal analyzers. Basic modular DTA design provides for expansion. **P 175**

Timers. Viscosity unit starts and stops automatically, is accurate to .02% ± seconds. **P 190**

Titrators. Analyzes for ppm amounts of N, S, or halogen. **P 94**

Titrators. 6-unit instrument is completely modular with interchangeable accessories. Catalog. **P 122**

Titrators. Brochure on new six-module automatic unit. **P 125**

Titrators. Automatic Karl Fischer unit with direct readout. **P 136**

Traps, filter. Dries and filters gas stream in pressurized flow system. **P 33**

Tubing. 74 sizes of flexible, clear, nonoxidizing tubing. **P 132**

Tubing. Standard vinyl tubing cut to 15-inch lengths and color-coded wishbone bridges. **P 54**

Ultrasonic unit. Produces pilot plant data that duplicates effects of production equipment. **P 161**

Valve-minder. Data on new unit that automates GC valves. **P 38**

Valves. 3-way, 4-way, and 5-way ball valves with color coded directional handles. **P 191**

Vessels, decomposition. Stainless steel 23 ml bomb for sample dissolution. **P 61**

Voltmeters. Digital microvolt multimeter sensitive to 1 μV. **P 106**

Hamamatsu Quality in Hollow Cathode Lamps

Researchers in atomic analysis can now rely upon the high-wavelength purity and stability of Hamamatsu Hollow Cathode Lamps. In the Model L233, for instance, a special base metal in the cathode reduces the "clean-up phenomenon" of the Neon filler gas to insignificance. Background level is extremely low, and an excellent, flat curve of high accuracy is producible with comparatively low current. When your research in atomic absorption spectroscopy calls for a light source that is completely dependable, specify Hamamatsu. All popular, widely-used elements are available. Off-the-shelf delivery. Exclusive retail distributorship in the U.S.A.

Write or call Dept. HC-3AC

OCLI INSTRUMENTS

132 Water St / So Norwalk / Conn / 06854 / (203) 853-2224

Circle No. 133 on Readers' Service Card

LABORATORY SUPPLY CENTER

CABLE ADDRESS: SACTEX — PROMPT SHIPMENT

POLAROGRAPHIC SPECIALTIES

Quaternary ammonium compounds.
Highly purified salts and solutions.
Cells designed for use above -2.0 volts.

SOUTHWESTERN ANALYTICAL CHEMICALS
BOX 485 — AUSTIN, TEX
AREA 512 444-3626
—literature on request

PCR ANALYTICAL SERVICE
CHN DSC IR UV
RATE SCHEDULE ON REQUEST
PCR, INCORPORATED
P.O. BOX 1466 / GAINESVILLE, FLORIDA 32601
(904) 376-7522

ELECTRON MICROSCOPY ▲ MICROANALYSIS
SCANNING — TRANSMISSION — REPLICATION
ELECTRON MICROPROBE — X-RAY DIFFRACTION — ELECTRON DIFFRACTION
METALLOGRAPHY ▲ FRACTOGRAPHY ▲ FAILURE ANALYSIS
ERNEST F. FULLAM, INC. — *Scientific Consultants*
P.O. BOX 444 SCHENECTADY, N. Y. 12301 518-785-5533

Manufacturers Representative
We cover the key area of N.J., N.Y. and Eastern Pennsylvania and are looking for additional lines of laboratory instruments and equipment.
United Scientific Co.
P.O. Box 142
Cedar Knolls, N.J. 07927
(201) 241-9898

NOCHROMIX
"DICHROMATE" SUBSTITUTE
METAL ION FREE
GLASS CLEANING REAGENT
1 Box (makes 10 x 9 lb. with H_2SO_4)... $12.50
GODAX LAB., 6 VARICK ST., N. Y. 10013

MASS SPECTROMETRY
Instantaneous Scanning of Gas Chromatographic Effluent
Direct Solids Introduction
Mass Range 2-2000
Resolution 3000
GOLLOB ANALYTICAL SERVICE INC.
Write for brochure
46 Industrial Road, Berkeley Heights, N. J. 07922 · 201-464-3331

Forty Six Distilled in Glass Solvents

BURDICK & JACKSON LABORATORIES, INC. 616 722 2310
MUSKEGON, MICHIGAN 49442

FINALLY!!

A logical method for selecting columns for gas chromatography.
No more . . .
1. Lists of **polar** columns
2. Duplication of columns
3. Wasted time on obviously incorrect columns
4. Use of **obsolete** columns

But . . .
1. A list of numerically classified columns
2. A method for selecting columns based on structure of sample
3. **Examples** showing how system works

IT'S Free . . . and described in our 1971 catalog and in our column classification chart. Write for both. Self-addressed envelopes will speed up delivery.

SUPELCO, INC.
Supelco Park
Bellefonte, Pa. 16823
Phone (814) 359-2732

NMR SOLVENTS

Chloroform-d,	99.8% D	100g	$14.00
Acetone-d_6,	99.5% D	10g	$10.00
DMSO-d_6,	99.5% D	10g	$10.00

Request Catalog EJ-71

STOHLER
Stohler Isotope Chemicals
49 Jones Road
Waltham, Mass 02154
Tel: 617 891-1827-8

MASS SPECTROMETRIC ANALYSIS
Thin films-solid state materials.
Bulk and trace analysis of all solid materials.
Concentration gradients of diffused impurities.
Resolution 5000.
Sensitivity to parts per billion.
GCA Technology Division, division of GCA Corporation, Bedford, Mass., Tel. (617) 275-9000.
Attn: Director of Marketing

REFRACTOMETER SALES SERVICE
For over 50 years VALENTINE has provided fast expert repair service on ALL refractometer types, and at fair prices.
SEVEN Precision Refractometers to choose from.
ALL DIRECT READING, no conversion tables required.
VALENTINE INSTRUMENT COMPANY
2188 Primrose Avenue
Vista, California 92083 (714) 727-0839

LaMotte Chemical
Chestertown, Maryland 21620
Manufacturers of chemical testing equipment and accessories since 1919
Write Dept. AC for free catalog

p-Aminohippuric Acid • α-Benzoin Oxime • α-Bromonaphthalene
tert.-Butyl Methyl Ether • 2(4-Chlorophenoxy)ethanol • Cochineal
α-Chloropropionic Acid • 1,2-Diethoxyethane • Diethyl Adipate
Ethyl Pyruvate • Hippuric Acid • Iminodiacetic Acid Disodium Salt
3-Indoleacetic Acid • Maltose • α-Naphthoic Acid • Neocuproine
Phenoldisulfonic Acid • D-Ribose • Salicin • DL- & L-Serine
Sodium Dihydroxytartrate • Sodium Dithionate • Sodium Pyruvate
Thionalide • Trisodium Pentacyanoamineferroate • Xylitol • Xylose

Write for list K-69 of other chemicals
Tel: 201 696-1700 TWX: 710 988-5831 Zip Code 07440

EASTERN CHEMICAL CORPORATION BOX K PEQUANNOCK, N. J.

Rates Available on Request

Analytical Chemistry

Penelope Mallach, Production Manager

142 East Ave.

Norwalk, Conn. 06851

203-853-4488

INDEX TO ADVERTISERS IN THIS ISSUE

ACS Publications 75A–78A
***Academic Press** 31A
Flamm Advertising
A.E.I. Scientific Apparatus Ltd. 74A
Streets Provinces
Airco Industrial Gases 80A
Fred Wittner Company
***Air Products—Specialty Gas** 41A
Rumrill-Hoyt, Inc.
Allen-Bradley Company 46A
Hoffman-York, Inc.
Alpha Metals, Inc. 65A
Steven Wynn Communications
***American Instrument Company** 1A
Industrial Advertising Associates
American Optical Corporation 26A
Fuller & Smith & Ross, Inc.
***Applied Science Laboratories, Inc.** 120A
Media Services, Ltd.
***Avco** 111A
John F. Norris & Co., Inc.

***Bausch & Lomb—Analytical Systems Div.** 30A
Wolff Associates, Inc.
***Beckman Instruments, Inc. (SID)** ... 7A
N.W. Ayer/Jorgensen/MacDonald, Inc.
***Beckman Instruments, Inc. (Cedar Grove)** 50A
Lescarboura Advertising, Inc.
Biomation 115A
Hal Lawrence, Inc.
Brinkmann Instruments, Inc. ..... OBC
The Shaller-Rubin Co., Inc.
***Bronwill Scientific, Inc.** 96A
Wolff Associates
Bruker Scientific, Inc. 47A
Schweitzer Advertising
***Buchler Instruments Div., a Sub, of G. D. Searle & Co.** 68A, 81A
Selvin & Jaffee

***Carle Instruments, Inc.** 43A
Cochrane Chase & Co., Inc.
***Fred S. Carver, Inc.** 81A
Scott Inc., Advertising
Clay Adams 22A
Cummins, MacFail & Nutry, Inc., Advertising
***Coleman Instruments Corporation** ... 96A
Mandabach & Simms, Inc.
Corco Chemical Corporation 105A
Charles D. Karlsruher
Corning Glass Works 33A
Rumrill-Hoyt, Inc.
Cryogenic Associates, Inc. 83A
Bell-Catterlin & Hedgcock Advertising, Inc.
Cryogenic Technology, Inc. 109A
Julian Brightman Company

Eastman Kodak Company 23A
Rumrill-Hoyt, Inc.
Everett Kelley Associates, Inc. 116A
Philip J. Perlman Associates, Inc.

Fabri-Tek Instruments, Inc. 12A
Towell & Timmons, Inc.
***Fischer & Porter Company** 100A
Furlong Promotions, Inc.
***Fisher Scientific Company** 82A
Tech-Ad Associates
***Forma Scientific** 111A
O-Val Advertising Services, Inc.

Gallard-Schlesinger 102A
Tobias Associates, Incorporated
***Gilford Instrument Laboratories, Inc.** 98A
Carpenter, Lamb & Hernick, Inc.
***Gow-Mac Instrument Company** 59A
Kenyon Hoag Associates
Greiner Scientific Corporation 107A
Fairfax, Inc.

***Hamamatsu TV Co., Ltd.** 112A
Kairyusha Advertising Ltd.
***Hamilton Company** 54A
Swain, Mealer & Emerson, Inc.
Heath Co. 110A
Advance Advertising Service
***Hewlett-Packard** 34–35A
Richardson, Thomas & Bushman, Inc.
***Holt, Rinehart & Winston, Inc.** 68A
Swayhoover, Barbini & Pesce, Inc.

***Instrumentation Specialties Company** 61A
Graham Printing & Advertising
Ithaco, Incorporated 66A
Hart-Conway Co., Inc.

Jeolco (U.S.A.) Inc. 92A
Kenyon Eckhardt Inc.
Johnston Laboratories 69A
Cahn Avis Gerard Advertising

***Laboratory Data Control** ..... IFC
A. B. W. Toft & Co.
Leeds & Northrup 25A
Schaefer Advertising Inc.

MC & B Mfg Chemists 84A
Cooper, Strock, Scannell
***Matheson Gas Products** 52A, 73A, 106A
Cooper, Strock, Scannell
Meloy Laboratories 14A
Gerardi Associates, Inc.
E. Merck 79A
Deutsche Anzeigen GMBH
***Merck & Co., Inc.** 27A
Rumrill-Hoyt, Inc.
***Mettler Instrument Company** 10A, 95A
Harris D. McKinney, Inc.
Micromeritics 44A
George & Glover
Miles Laboratories 100A
Dick Loew & Associates

***Nester/Faust** 38A
deMartin-Marona & Associates
***Nuclear-Chicago, a Sub. of G. D. Searle & Company** 28A
Sidney Clayton Associates, Inc.

***O.C.L.I.** 117A
A.B.W. Toft & Company

***Packard Instrument Company** 63A
Ross Llewellyn, Incorporated
Parr Instrument Company 65A
F. Willard Hills
***Perkin Elmer** 20–21A, 64A, 85A, 111A
Gaynor & Ducas, Inc.
Philips Electronic Instruments 32A
J & M Condon, Inc.
***Photovolt Corporation** 5A
Michel-Cather, Inc.
***Pierce Chemical Company** 107A
Advertising Design
***Precision Cells, Incorporated** 113A
Co-Art Associates, Inc.
***Precision Scientific Company** ..... IBC
Tri-State Advertising Co., Inc.
***Princeton Applied Research Corporation** 16A
Mort Barish Associates, Incorporated

Qanta/Metrix Corporation 49A
Murphy Advertising, Incorporated

Redlake Labs, Incorporated 70A
Murphy Advertising, Inc.
Reeve Angel 103A
Arthur Eckstein & Associates, Inc.

***Sargent-Welch Scientific Company** .9A, 97A
Sidney Clayton Associates, Inc.
SciChem Co. 71A
Los Angeles Addressing and Mail
***Scientific Glass Apparatus Co., Inc.** .. 56A
Setaram, France 88A
Agency Havas
Siemens Corporation 18A
Ries Cappiello Colwell, Inc.
Spectrametrics 8A
The Strayton Corporation

Technicon 29A
Mediad Incorporated
***Thermolyne Corporation** 60A
E. R. Hollingsworth & Associates

***Arthur H. Thomas Company** 94A
Todd Instrument Company 111A
***The Torsion Balance Co.** 104A
Michel-Cather, Inc.
G. K. Turner Associates 6A
Frank Haylock

***Varian Aerograph** 86–87A
Chiat/Day, Inc.
***Varian AID** 70A, 108A
Chiat/Day, Inc.
Varian Cary 24A
Chiat/Day, Inc.
Vidar Corporation, Autolab Division .. 48A
Bill Fisher Advertising

***Waters Associates** 53A
Thomas R. Sundheim, Inc.
Wave Energy Systems Incorporated .. 40A
John W. Tynacz Co.
Wescan Instruments 58A
Harris and Associates
Wilmad Glass Co., Inc. 115A
Walsh Advertising Agency

▼ ▼ ▼

Laboratory Section 118A
Burdick and Jackson Laboratories, Inc.
Eastern Chemical Corporation
Ernest F. Fullam, Incorporated
GCA-Technology Division
Godax Laboratories
Gollob Analytical Service
LaMotte Chemical Products Company
PCR, Inc.
Southwestern Analytical Chemicals
Stohler Isotope Company
Supelco, Incorporated
United Scientific Company
Valentine Instrument Company

Advertising Management for the American Chemical Society Publications

CENTURY COMMUNICATIONS CORP.

Edward P. Blanchard, President, Thomas N. J. Koerwer, Executive Vice President, 142 East Avenue, Norwalk, Connecticut 06851 (Area Code 203) 853-4488

ADVERTISING SALES MANAGER
Thomas N. J. Koerwer

SALES REPRESENTATIVES

Chicago 60601 . . . Eugene Eldridge, Century Communications Corp., 307 North Michigan Avenue, 312-641-0890.

Cleveland 44113 . . . Michael Hayes, Century Communications Corp., 75 Public Square, 216-523-1930.

Dallas 75207 . . . Parker Harris, Roy McDonald Asso., 714 Stemmons Tower West, 214-637-2444.

Denver 80203 . . . Robert H. Heidersbach, Roy McDonald Asso., Inc., 846 Lincoln Street, 303-825-3325.

Houston 77006 . . . Frank N. Vickrey, Richard Clothier, Roy McDonald Asso., Inc., 3130 Southwest Freeway, 713-529-6711.

Los Angeles 90045 . . . Clay S. Holden, The Connecticut Century Communications Corp., Airport Arcade Bldg., 8820 S. Sepulveda Blvd., Suite 215, 213-776-0552

Norwalk 06851 . . . Don Davis, Richard Feary, Century Communications Corp., 142 East Avenue, 203-853-4488.

Philadelphia 19034 . . . James A. Byrne, Century Communications Corp., 535 Pennsylvania Avenue, Fort Washington, Pa., 215-643-2586.

Great Britain and Western Europe . . . Brayton Nichols, The American Magazine Group, 44 Conduit Street, London, W.1, England, Telephone Regent 4714.

Japan . . . Sumio Oka, International Media Representatives, Ltd., 1 Shiba-Kotohiracho, Minatoku, Tokyo.

PRODUCTION DEPARTMENT
Production Director
Joseph P. Stenza

Advertising Production Manager
Penelope Mallach

**See ad in ACS Laboratory Guide*

FUTURE ARTICLES

Gas Chromatographic Analysis of Phenol and Substituted Methyl Phenol Using Open Tubular Columns
J. Hrinvnak and J. Macák

Thin Layer Electrochemistry. Minimization of Uncompensated Resistance
G. M. Tom and A. T. Hubbard

Solvent Effects on Protonation Constants: Ammonia, Acetate, Polyamine, and Polyaminocarboxylate Ligands in Methanol-Water Mixtures
D. B. Rorabacher, W. J. MacKellar, F. R. Shu, and M. Bonavita

Dynamics of Continuous Segmented Flow Analysis
R. D. Begg

Continuous Electrochemical Determination of Cyanide. Application to Cyanogenic Glycosides in Sudan Grass
D. B. Easty, W. J. Blaedel, and L. Anderson

Computer Acquisition of Frontal Analysis Chromatographic Data for Surface Area Determination
M. F. Burke and D. C. Ackerman, Jr.

Radioisotope Derivative Procedure for the Determination of Epinephrine or Norepinephrine
W. J. Blaedel and T. J. Anderson

Instrumental Peak Distortion. III. The Analysis of Overlapping Curves
I. G. McWilliam and H. C. Bolton

Optimum Parameters for Flame Emission Spectroscopy with the Nitrous Oxide–Acetylene Flame
G. D. Christian and F. J. Feldman

Further Investigation of the Colorimetric Reaction between Aromatic Isocyanates and Peroxy Compounds
R. F. Layton and L. A. Knecht

Colorimetric Determination of Traces of Zinc in Zinc Oxide
J. M. Kruse

Determination of Dissolved Oxygen Using Photoreduced Leuco Phenothiazine Dyes
P. A. Hamlin and J. Lambert

Quantitative Determination of Dialkyl Phosphates and Dialkyl Alkylphosphonates by Gas–Liquid Chromatography
E. J. Quinn and D. H. Ahlstrom

Polarimetric Studies of Alkali Metal Ion Complexes of D-Propylenediaminetetraacetic Acid
J. D. Carr and D. G. Swartzfager

New Approach to the Microdetermination of Fluoride Adsorption-Diffusion Technique
P. Venkateswarlu and P. Sita

Thin-Layer Densitometry of Certain Malto-Oligosaccharides
C. T. Mansfield and H. G. McElroy

Some Anomalies of the Gibbs Reaction
J. C. Dacre

Gas Chromatographic Determination of Polycyclic Aromatic Hydrocarbons
K. Bhatia

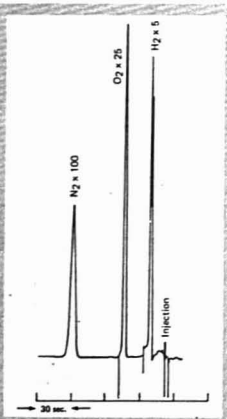

Separation of H_2, O_2 and N_2. Column: 6' x 1/8" copper P. W. MOLECULAR SIEVE 5A 60/80. He carrier, 15 psig. at 18 ml/min. Col. temp. 24°C. Thermistor detector at 10 ma with sensitivities as shown.

another 1st in Gas Chromatography

PRETESTED

MOLECULAR SIEVES

Now the standard material for GC analysis of O_2 and N_2 is available with assurance of quality.

Proper preparation and pretesting of the finished product guarantees these molecular sieves for excellent performance.

Each batch is supplied with test results showing the O_2/N_2 separation under specific operating conditions. See example at left.

Available in all mesh sizes:
PT MOLECULAR SIEVE 5A - for trace analyses
PT MOLECULAR SIEVE 13X - for speed analyses

For more details, write for the March/April GAS–CHROM NEWSLETTER.

Applied Science Laboratories, Inc.

Post Office Box 440 / State College, Pennsylvania 16801 / 814-238-2406

Circle No. 7 on Readers' Service Card

Precision Auto-Aquatrator™ for fast, accurate KF titrations automatically

Time saving is the single most important feature of this instrument for many users. Time is money, and the Auto-Aquatrator will pay for itself in speed, accuracy and reproducibility. You can rapidly determine the moisture content of any organic or inorganic sample submitted, using standard Karl Fischer reagent. Simply add the sample, record the initial burette reading, and press the "start" button. This compact, self-contained unit performs the entire titration. When the end point is reached, the titrant feed circuit is de-energized and the pilot light indicates the titration is completed. The operator merely notes the final burette reading and calculates the moisture content.

Looks easy to operate and it is!

And this new model has been improved by the addition of a positive burette filling valve to replace the original plunger filling system. The new valve directs air pressure from the internal vacuum pressure pump through the drying tubes. This pressurizes the reagent bottles to force the reagent up into the burettes. To learn more about the Auto-Aquatrator, consult your Precision Scientific Dealer or write us. Precision Scientific Co., 3737 W. Cortland St., Chicago, Illinois 60647.

PRECISION SCIENTIFIC

SUBSIDIARY OF GCA CORPORATION

Circle No. 149 on Readers' Service Card

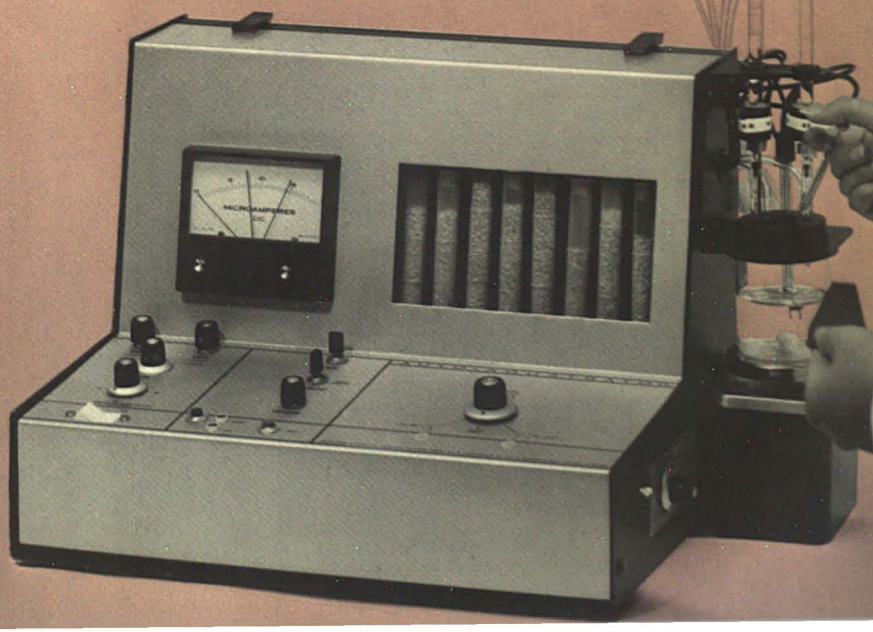

Believe it.

Some like it cool (down to −10°C). Some like it hot (up to +150°C). *Everybody* likes the unbeatable price tag of $595.

The Lauda K-2/R Refrigerated Constant Temperature Circulator is ideal for accurate tempering of jacketed instruments and a variety of other laboratory applications. Especially where control precision, wide temperature range and trouble-free ruggedness are the real measure of value.

Need it cooler, or a little more bath space? The new Lauda K-4/R operates down to −30°C and has a larger, easy-access immersion chamber that accommodates standard 4x8″ test tube racks.

Both compact models feature all-stainless steel construction, solid-state electronic system, continuously variable heater wattage control, an exclusive, extra-sensitive thermoregulator, liquid flow control and drain valves, and a reading thermometer at no extra cost.

Still an unbeliever? Write for a convincing catalog with information about all of our constant temperature baths and circulators for operation in ranges from −120° to +330°C.

LAUDA Circulators

A DIVISION OF BRINKMANN

In U.S.: Lauda Circulators, Division of Brinkmann Instruments, Cantiague Rd., Westbury, N.Y. 11590.
In Canada: Brinkmann Instruments (Canada) Ltd., 50 Galaxy Boulevard, Rexdale (Toronto), Ontario.

Circle No. 18 on Readers' Service Card

-16 W.A. 2514